Holocene on the High Country: A multiproxy interrogation of paleoenvironmental sensitivity along an elevational transect of high-altitude Australia

THE UNIVERSITY OF SYDNEY

James Bakis

School of Geosciences
Faculty of Science
University of Sydney

A thesis submitted to fulfil the requirements of the degree of Doctor of Philosophy

2026

Statement of originality

This is to certify that the content of this thesis is my own work. This thesis has not been submitted for any other degree or purpose. I certify that the intellectual content of this thesis is the product of my own work, and that all assistance received in preparing this thesis and all sources have been acknowledged.

James Bakis

Authorship attribution statement

This thesis contains published work and work submitted for publication. Chapters 2–4 are published articles or are submitted and, at the time of writing, under review. These chapters have been reformatted for inclusion in this thesis. The details of these works are presented below, including the contributions of all authors.

Chapter 2 of this thesis is published as:

Bakis, J., Penny, D., Hamilton, R., Hua, Q., Barry, L. & Gadd, P. 2026. Asymmetric sensitivity of lake catchments to climate and land use change on the Monaro Tablelands, southeastern Australia: A multiproxy, multisite synthesis of postglacial lacustrine records. *Quaternary Science Reviews,* 373, 109729. https://doi.org/10.1016/j.quascirev.2025.109729.

James Bakis designed the study, performed field and laboratory methods, analysed the data, generated figures, and wrote the drafts of the manuscript. Dan Penny assisted with research design, field methods, data interpretation and manuscript editing. Rebecca Hamilton assisted with data analysis and manuscript editing. Quan Hua performed radiocarbon dating and assisted with manuscript editing. Linda Barry performed stable carbon isotope analysis and assisted with manuscript editing. Patricia Gadd performed μXRF analysis.

Chapter 3 of this thesis is submitted for publication (under review) as:

Bakis, J., Penny, D., Hamilton, R., Hua, Q., Barry, L. & Gadd, P. 2025. Thresholds in montane sensitivity to climate and land use change over the late Holocene: Multiproxy evidence from Snowy Mountains peat records, southeastern Australia. *Palaeogeography, Palaeoclimatology, Palaeoecology***.**

James Bakis designed the study, performed field and laboratory methods, analysed the data, generated figures, and wrote the drafts of the manuscript. Dan Penny assisted with research design, field methods, data interpretation and manuscript editing. Rebecca Hamilton assisted with data analysis. Quan Hua performed radiocarbon dating and

assisted with manuscript editing. Linda Barry performed stable carbon isotope analysis and assisted with manuscript editing. Patricia Gadd performed μXRF analysis.

Chapter 4 of this thesis is submitted for publication (under review) as:

Bakis, J., Penny, D., Hamilton, R., Hua, Q., Barry, L. & Gadd, P. 2025. Spatiotemporal divergences in alpine and subalpine sensitivity to Holocene climate and land use change: Paleoenvironmental insights from the Snowy Mountains, southeastern Australia. *Quaternary Science Reviews.*

James Bakis designed the study, performed field and laboratory methods, analysed the data, generated figures, and wrote the drafts of the manuscript. Dan Penny assisted with research design, field methods, data interpretation and manuscript editing. Rebecca Hamilton assisted with data analysis and manuscript editing. Quan Hua performed radiocarbon dating. Linda Barry performed stable carbon isotope analysis. Patricia Gadd performed μXRF analysis.

James Bakis

As supervisor for the candidature upon which this thesis is based, I can confirm that the authorship attribution statements above are correct.

Dan Penny

Generative Artificial Intelligence (AI) attribution statement

During the preparation of this thesis, the author used the generative AI tool ChatGPT to assist with the refinement and optimisation of R language code to produce and improve figures using existing data. No generative AI was used in the generation, direct analysis or interpretation of data, nor to produce or modify text in this thesis. The author confirms that, where generative AI was used to amend code, the output was independently reviewed for errors and/or inaccuracies. The author takes full responsibility for the submitted thesis, confirms the work is their own, and has used generative AI in accordance with University guidelines and policies.

Abstract

High-altitude landscapes are among the most sensitive environments to climate and land use change. However, paleoscientific determinations of high-altitude sensitivity are disproportionately informed by paleoecological reconstructions from mountains *sensu stricto*. These biases limit constraints on broader 'systemic' (i.e., biotic and abiotic) sensitivity across entire high-altitude complexes (i.e., mountains and highlands). This thesis applies multiproxy analyses to thirteen sedimentary sequences along an elevational transect of the High Country, a vulnerable mountain-highland complex in southeastern Australia, to reconstruct paleoenvironmental changes since ~13,900 cal yr BP. By comparing these data with independent records of climate and land use change, the systemic sensitivity of the High Country is resolved at the site, zonal and regional scale.

This study demonstrates that regional systemic variability was primarily dictated by hydroclimate over most of the Holocene until ~2600 cal yr BP, when there was a synchronous cross-altitudinal increase in moisture availability despite declining precipitation and warming. This signal is argued to reflect a threshold shift in sensitivity towards an intensified El Niño Southern Oscillation, albeit through regionally bifurcated mechanisms. Regardless of specific climatic forcings, mountain catchments appear to have been consistently more sensitive to climate change than highland catchments over the Holocene.

A similar mountain-highland dichotomy is exhibited in the context of European-era land use change, suggesting mountains are also more sensitive to such. European-era instability for both domains is unprecedented since at least ~3200 cal yr BP, confirming the High Country has been more perturbed by European land use change than any climatic perturbation over this interval. Reconstructions suggest that future disequilibrium will be exacerbated by ongoing climate and land use change. Regional responses to anthropogenic disturbance are anticipated to involve catchment drying, peatland desiccation and amplified erosional and fire regimes, though to varying degrees along the elevational profile.

“On those who enter the same rivers, ever different waters flow”

— Heraclitus, Fragment B12 (trans. Barnes, 1982)

Acknowledgements

While this thesis bears one name, it is a product of the contributions of many individuals and organisations. Unrivalled among them is my primary supervisor, Prof Dan Penny, to whom my gratitude cannot be overstated. First supervising me as a green Honours student, Dan has, over the years, endowed me with skills that have congealed my passion for paleoscience into something useful. Even as that passion ebbed, as it does during the tempest that is a PhD, Dan's unwavering encouragement inspired me to stay the course. In these regards, Dan is both an exceptional supervisor and scientist, who I am honoured to have worked with.

I also express profound appreciation to my auxiliary supervisor, Dr Rebecca Hamilton, who, while dragged into the maelstrom relatively late, was invaluable in developing my research methods and the substance of my thesis. Many thanks must also be extended to those members of the Australian Nuclear Science and Technology Organisation (ANSTO) – namely Dr Quan Hua, Linda Barry and Patricia Gadd – who oversaw ^{14}C dating and $\delta^{13}C$ and μXRF analyses and made intellectual contributions to the manuscripts.

I am also indebted to the University of Sydney (USYD) School of Geosciences technical staff – Dr Ann Ling, Dr Nick Proschogo, Dr Tiago Passos and Dr Bern Antonio – for their tireless coordination of laboratory and field logistics. Also recognised are David Eddy and Dr Lachlan Ingram, who devoted substantial time, effort and expertise to supporting fieldwork on the Monaro Tablelands. In the Snowy Mountains, fieldwork was facilitated by a long list of members from the NSW National Parks and Wildlife Service, under a NSW Government Department of Planning, Industry and Environment Scientific License (SL 102697).

This research was supported by an Australian Government Research Training Program (RTP) Scholarship. I also acknowledge the significant financial support provided by a 2022 NSW-Department of Planning and Environment Memorandum of Understanding Partner Grant, and several ANSTO Research Portal projects (AP17584, AP18304, AP19492, AP20786). Noted also are the ^{14}C dating services provided by DirectAMS and the CHRONOS ^{14}Carbon-Cycle Facility, University of NSW.

I am forever grateful to my family, and especially to Steph, for enthusiastically and/or begrudgingly assisting me with fieldwork, always having a keen interest in my research,

and keeping me anchored through it all. You have all relentlessly supported me since long before this PhD, which I could never have completed without you.

Finally, to the High Country itself, a place which has been an enduring constant throughout my life. In many ways, the landscape I remember no longer exists – the snows return ever thinner, the fires burn ever hotter, the dieback spreads ever further. Of course, the High Country was never immutable but is, like all features of the natural world, always in transition. Universal transience underpins Heraclitus' doctrine of flux, which is summarised by the epigraph, a nod to the aphorism *πάντα ῥεῖ* ('everything flows'). Flux arises as a motif throughout this thesis, and is a truth that has been understood for millennia by the region's Traditional Owners – chiefly the Ngarigo people – whose deep connection to Country is also acknowledged here. To appreciate the High Country's ephemerality is to appreciate that this thesis is as much a farewell to a bygone landscape as it is a bracing for one that is perpetually emerging.

Ever different waters flow here.

Table of contents

List of figures

List of tables

List of abbreviations

AA	**A**ustralian **A**lps
aCAR	**A**pparent **c**arbon **a**ccumulation **r**ates
ANSTO	**A**ustralian **N**uclear **S**cience **T**echnology **O**rganisation
BMI	**B**ulk **m**ineral **i**nflux
C/N	**C**arbon/**n**itrogen
CHAR	**C**harcoal **a**ccumulation **r**ates
ENSO	**E**l **N**iño–**S**outhern **O**scillation
GEC	**G**lobal **e**nvironmental **c**hange
LIA	**L**ittle **I**ce **A**ge
MA	**M**oisture **a**vailability
MWP	**M**edieval **W**arm **P**eriod
NSW	**N**ew **S**outh **W**ales
OM	**O**rganic **m**atter
RoC	**R**ate-**o**f-**C**hange
SAM	**S**outhern **A**nnular **M**ode
SHWW	**S**outhern **H**emisphere **W**esterly **W**inds
SM	**S**nowy **M**ountains
TEC	**T**hreatened **e**cological **c**ommunity
TN	**T**otal **n**itrogen
TOC	**T**otal **o**rganic **c**arbon
µXRF	**M**icro-**X**-Ray **f**luorescence

Chapter 1

Introduction and literature review

1.1. Chapter summary

High-altitude environments (mountains and highlands) are extremely vulnerable to global environmental change. As this chapter highlights, a unique nexus of physiography, climate and ecology amplifies biophysical sensitivity to perturbation. As such, these environments are rapidly deteriorating under ongoing climate and land use change, threatening the persistence of hosted ecological communities and the provision of critical ecosystem services. However, it is argued here that research into high-altitude change remains disproportionately informed by ecological metrics, a limitation that also manifests in paleoscience through the preferential interrogation of biotic sediment-hosted proxies. This entrenches an ecological bias in constraints on long-term 'systemic' sensitivity, which considers the role of not only biotic but also abiotic agents in dictating macroscale sensitivity. This chapter demonstrates that a paleoscientific application of this 'geoecological' rationale is critical for attaining more representative insights into the long-term response behaviour of high-altitude environments on centennial to millennial timescales. Following a uniformitarian logic, such insights permit more accurate projections of future environmental change under anthropogenic forcing.

The knowledge gap arising from preferential ecological research remains particularly vast in a high-altitude region of southeastern Australia known as the High Country, a mountain-highland complex comprising the Snowy Mountains and Monaro Tablelands. This chapter demonstrates that, attributable to its low elevation, relief and prolonged history of anthropogenic degradation, the High Country is especially vulnerable to changes in climate and land use. However, consistent with the global convention, paleo-research on the High Country has historically been concerned with reconstructing changes in vegetation and fire from pollen and charcoal records, which are representative of neither systemic variability nor sensitivity. Moreover, a review of the spatial distribution of these records reveals that the existing corpus of research is significantly skewed towards the Snowy Mountains and away from the Monaro Tablelands. This is emblematic of the global tendency to prioritise mountains for environmental research over highlands, which appends significant uncertainty to the long-term sensitivity of the latter. This is problematic given highlands are often more modified by land use change and thus predisposed to further destabilisation.

In view of the knowledge gaps inherited from these conceptual (ecological) and spatial (mountain) biases, this thesis conducts a multiproxy interrogation of natural archives

across an altitudinal transect of the High Country, with the prevailing objective of constraining the long-term systemic sensitivity of its constituent mountain and highland components. By assessing sensitivity at the process, catchment, zonal and regional scale, this study predicts environmental responses to climate and land use change as both stressors continue to accumulate over the 21st century. Thesis findings will constitute a critical reference frame through which conservation and land management strategies can be tailored to specific environments, with a long-term and system-scale consideration of sensitivity. Implementation of such knowledge can improve the resilience of high-altitude systems and, in turn, their dependent ecologies and people.

1.2. High-altitude environments as sentinels of global environmental change

1.2.1. The necessity for a geoecological approach in addressing global environmental change in mountains and highlands

High-altitude environments are vulnerable to climate and land use change, the two facets of global environmental change (GEC) (Schmeller et al., 2018). GEC is defined by Goudie (2002) as encompassing multiscalar changes in, *inter alia*, climate, land use and cover, ice cover and biogeochemical cycles, as well as their implications for the broader ecosystem. The term 'ecosystem' was itself first employed by Tansley (1935) to describe "the whole *system*, … including not only the organism-complex, but also the whole complex of physical factors forming what we call the environment" (p. 299). In view of these definitions, researching the impacts of GEC on ecosystems inherently necessitates a 'systemic' scope, which is defined in this thesis as considering not only the biotic but also abiotic phenomena constituting an 'ecosystem'. A systemic approach is especially pertinent to mountains, where GEC is subclassified by Becker and Bugmann (2001) into a) changes affecting environments at global scales, and b) changes generated by local processes but which are becoming globally pervasive; these are synonymous with climate and land use change, respectively.

The sensitivity of mountains to these two expressions of GEC is attributable to the distribution and functioning of their constituent ecosystems (*sensu lato*, as defined above) being prescribed by topography and climate (Fort, 2015, Schmeller et al., 2022). High

elevation and relief yields steep gradients in temperature and precipitation, the former universally decreasing upslope and the latter generally increasing but also often exhibiting low- to mid-elevational maxima, particularly in tropical-subtropical mountains (Roe, 2005, Parish, 2014, Körner, 2021). This climatic gradient is replicated ecologically as a cross-altitudinal succession of narrow environmental envelopes ('bioclimatic zones') delimited by stepped transitions in faunal and especially floral assemblages ('ecotones'), where beta diversity is highest (Beniston, 2003, Grabherr et al., 2010, Körner et al., 2011, Loeffler et al., 2011). The high lateral density of these zones – with increasing elevation: the montane, subalpine and alpine – is without parallel in any other setting, with the closest analogue being the hemispheric-scale gradient of biomes dictated by latitudinal climate zones (Diaz et al., 2003, Beniston, 2016).

Climate is evidently the first order of control on the ecological stratification of mountains, which are hence exhibiting among the most rapid and dramatic responses to climate change. This is most ubiquitously observed as a vertical displacement of zones in response to warming, though this is often complicated by land use (Beniston, 2003, Diaz et al., 2003, Fort, 2015). Mountains therefore serve as invaluable sentinels of GEC, with their bioclimatic gradients frequently being exploited to assess ecological sensitivity (Hall et al., 2009, Tito et al., 2020). As such, the preponderance of mountain research is represented by empirical metrics of biological and ecological change, namely rates and magnitudes of ecotonal migration, biodiversity loss, physiological adaptations and phenological dissociations (e.g., Harsch et al. (2009), Elumeeva et al. (2013), Öztürk et al. (2015), Inouye and Wielgolaski (2025)).

While these measures are essential for determining species- to community-level sensitivity to GEC and predicting future ecological changes, consultation of ecological data *in vacuo* inherently biases our understanding of systemic (i.e., abiotic *and* biotic) sensitivity and risks over- or underestimating future systemic change (Körner, 2021, Schmeller et al., 2022). Of course, this is not to insinuate that research into abiotic functioning is absent from mountain research. On the contrary, there is an expansive pool of knowledge pertaining to the sensitivity of predominantly inorganic ecosystem components such as erosion, fire, edaphic cycling, hydrology and cryology (e.g., Schumacher et al. (2006), Hagedorn et al. (2010), Deline et al. (2015), Huss et al. (2017)). The last of these is the subject of increasingly intensive research given the salient role of snow and ice in modulating mountain hydrology, as well as the significance of mountains

as global 'water towers' for humanity (Messerli et al., 2004). However, abiotic research remains not only eclipsed by studies emphasising the life sciences but also lacks integration with ecological metrics within a systemic framework.

In recognition of this dearth of interdisciplinarity, systemic thinking has been increasingly advocated for under the conceptual framework of 'geoecology', first consolidated as a theory by Troll (1971). Geoecology, directly building on Tansley's (1935) 'ecosystem' definition, is founded on the *a priori* assumption that "biotic and abiotic aspects [are] equals in an interdependent relationship" (Ives, 2019, p. 9). As such, geoecology aims to suture the gulf between geosciences and life sciences (Ives, 2012). Despite its conceptual maturity and utility in especially natural resource management, geoecology only observed substantial research uptake between 1990–2000, declining thereafter (Baiping, 1995, Gordon et al., 2002, Kumar and Deshmukh, 2015, Webber, 2019, Kumar et al., 2021). This is concerning given geoecology represents the only avenue through which the sensitivity of inorganic and organic processes, and their combined impacts on systemic sensitivity, can be fully appreciated.

As such, the limited uptake of geoecology as a method of enquiry risks reversion to more parochial approaches that reduce the mechanistic complexity of ecosystems to simplistic, ecologically biased models. These reductive methodologies do not adequately consider the reverberative potential of climate and land use on the broader biophysical (and thus human) domain (Kumar and Deshmukh, 2015, Webber, 2019). Indeed, the inseparability of biotic and abiotic processes means exogenous disturbance to any single component can propagate throughout the biophysical system. This is being expressed for an increasing number of high-altitude ecosystems through 'state shifts', which result from the system being forced out of its basin of attraction towards a critical transition (Scheffer et al., 2012).

Such bifurcation events are often heralded by early warning signals such as 'flickering', 'skewness' and 'critical slowing down' in systemic variability (Scheffer et al., 2009, Wang et al., 2012, Bauch et al., 2016). Examples of recent high-altitude critical transitions include the regime shift from alpine meadow to woody shrubland across Northwest Yunnan Province due to climate-land use-vegetation feedbacks (Brandt et al., 2013), and fire-driven forest collapse across western North America (Coop et al., 2020). As apparent from these two examples alone, however, high-altitude critical transitions are

typically appreciated through an ecological and specifically floristic lens, with an insufficient consideration of their systemic implications.

Alongside a lack of geoecological scope, a second knowledge gap emerges in the tendency for high-altitude research to prioritise mountains *sensu stricto* over other elevated terrains known variously as plateaux, tablelands, uplands and hills, but which may be collectively labelled as 'highlands'. Highlands are defined here as being any low-relief region with a minimum elevation of 500 m ASL and an average elevation beneath the montane zone, if it is present. Some terrains that satisfy this definition include the Meseta Central, Armenian Highlands, Central Otago and Tibetan Plateau (Fig. 1.1). The hitherto omission of highlands from this introduction is testament to their poor recognition in the literature, which, as intimated, is almost exclusively concerned with mountains due to their complex topography and thus ecology.

These factors render mountains ideal 'natural laboratories' for assessing ecological responses to disturbance (Tito et al., 2020). Mountains are hence often assigned higher conservation and research priority than highlands, which are usually attached to or even circumscribe mountains, but are geomorphically discrete in that they are of lower relief and elevation. This results in highlands having insufficient bioclimatic zonation to

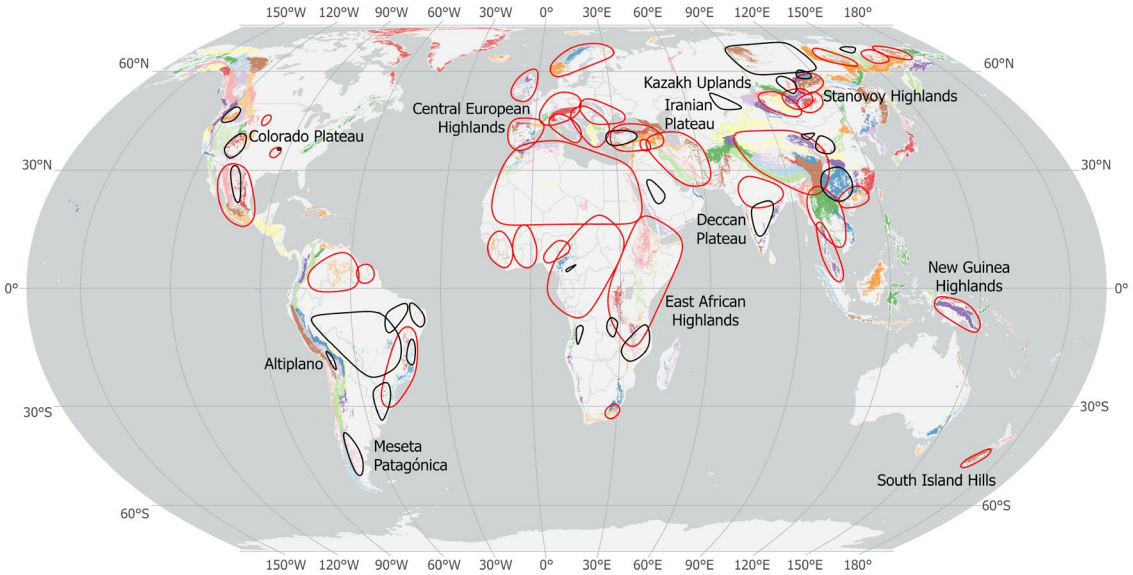

Figure 1.1. World map of mountain and highland systems (randomly coloured polygons), according to the Global Mountain Biodiversity Assessment (Snethlage et al., 2022). Systems outlined black are those classified as highlands, while red outlines denote systems that are classified as mountains but possess names including 'Highland' or terms typically reserved for highlands (i.e., 'Plateau', 'Tablelands', 'Upland', 'Hill').

warrant intensive research into ecological changes that are more relevant to mountains (e.g., ecotonal displacements) (Jung et al., 2021). A dichotomy in biodiversity is apparent along many mountain-highland gradients such as the Southern Andes-Patagonian Plateau and the Himalaya-Tibetan Plateau (Fig. 1.2a) (Beniston, 2016, Hughes et al., 2021).

Aside from their distinct geomorphology, highlands exhibit minimal commonality in terms of area, elevation, geology, climate or macroecology. As such, they are rarely addressed in high-altitude research as a 'zone' discrete from mountains, which in contrast possess globally replicable topographies and zoned ecologies. Indeed, conceptual models of the high-altitude elevational profile often dismiss the area underlying the montane zone with inconsistent, nebulous terms such as 'submontane', 'foothills' or even 'low mountains' (Beniston, 2016, Sayre et al., 2018). Moreover, where the term 'highlands' is employed, it is often liberally applied to any large, elevated area with generally low relief, but which often contain mountains. Examples of such systems include the Ethiopian Highlands, Scottish Highlands and the Central Highlands (Tasmania) (Fig. 1.1) (Mani and Giddings, 2012).

A lack of both conservation value and a standardised definition is problematic given highlands are, owing to their geomorphology, more accessible than mountains for human dispersal and are thus exposed to more intensive primary land uses such as pastoralism (Hughes et al., 2021). Consequently, a substantially smaller proportion of many highlands (e.g., Highveld and Armenian Highlands) is legally protected relative to their abutting mountains (the Drakensberg and Caucasus, respectively) (Fig. 1.2b) (World Database on Protected Areas, 2025). The economic value of highlands is often augmented by their proximity to mountains, rendering them valuable 'bases' for the exploitation of mountain resources such as rivers and montane forests. Selective human development on highlands is evidenced by many being dominated by land use classes (i.e., rangeland, cropland and pasture) instead of 'natural' land cover classes (i.e., grassland, shrubland and forest) that still dominate most mountains (Fig. 1.2c) (Jenkins et al., 2013, Winkler et al., 2020).

The concentration of land use impacts such as overgrazing, soil nutrient enrichment and land clearing has resulted in severe deterioration of highland ecosystems, many of which occur within the rain shadows of mountains and are thus already operating near their thresholds of ecological tolerance under marginal (cold and dry) conditions. As such, highlands have generally witnessed greater biodiversity loss and soil degradation than mountains, as is apparent between, for example, the Great Plains and Rocky Mountains

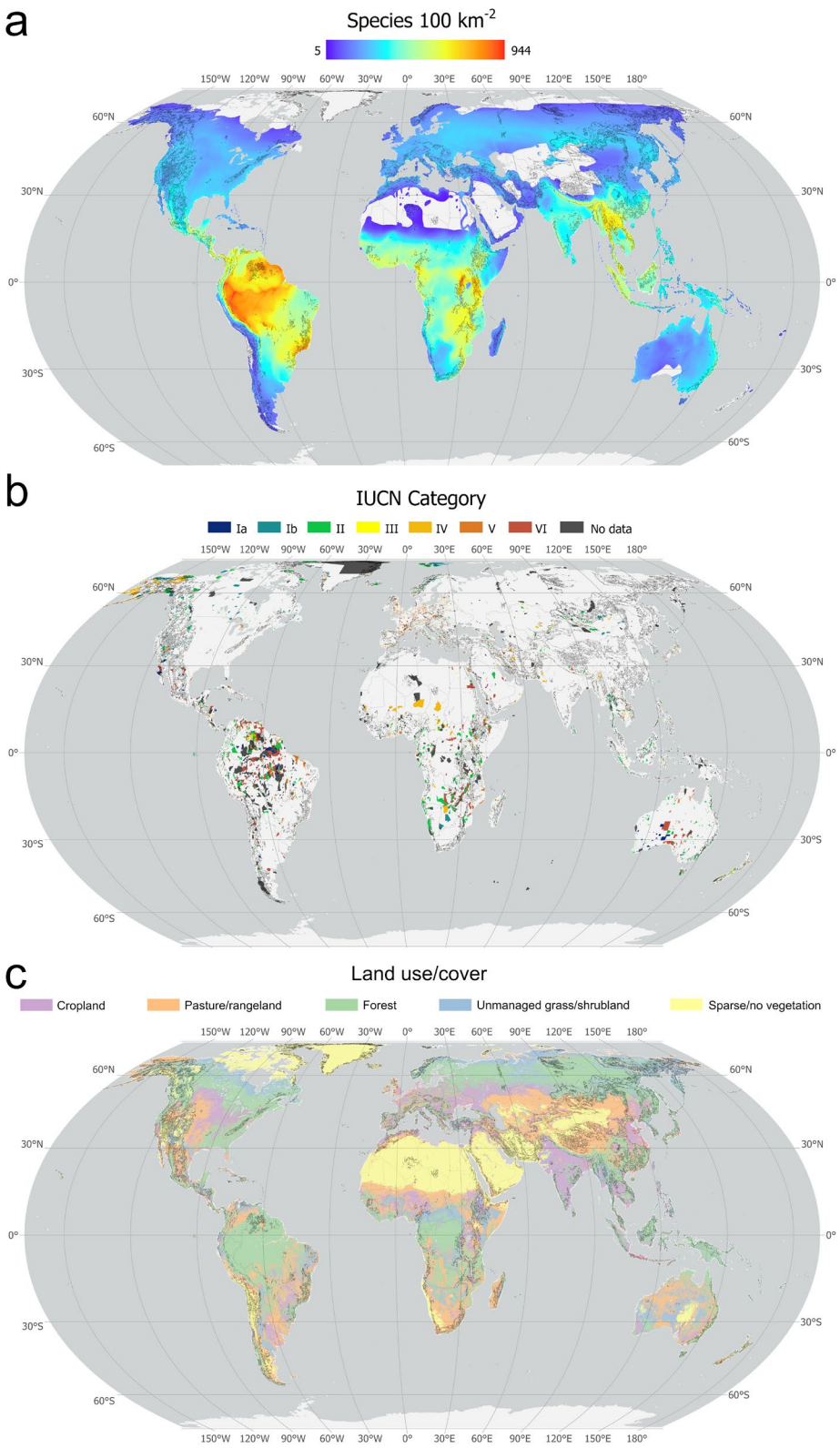

Figure 1.2. World maps of mountain and highland systems (see Fig. 1.1) overlain with data for **a)** total mammal, bird and amphibian species richness (Jenkins et al., 2013), **b)** IUCN protected areas (World Database on Protected Areas, 2025), and **c)** land use and land cover in 2019 (Winkler et al., 2020).

(Fisher and van Velthuizen, 2002, Newbold et al., 2016). Therefore, while their suppressed relief and ecological zonation diminishes their value as sentinels of climate change relative to mountains, highlands are arguably more valuable sentinels of land use change. Despite this, sparse highland research means future impacts of GEC remain poorly constrained from an ecological let alone geoecological perspective. This embeds significant uncertainty in likely future trajectories of highland environments and the viability of various ecosystem services on which large industries and populations depend.

Constrained by the two knowledge gaps identified here – a lack of systemic research and highland emphasis – much of the subsequent literature review is inevitably limited to discussion of high-altitude characteristics and change in an ecological and mountain context. While unrepresentative of high-altitude systems from both a geoecological and geographical perspective, this pool of knowledge constitutes a valuable reference frame through which high-altitude sensitivity and responses to GEC can be consolidated, and from which the necessity for filling the above gaps becomes clear.

1.2.2. High-altitude environments: global characteristics, vulnerabilities and change

As intimated in the previous subsection, geomorphology is a key determinant of highland and mountain sensitivity to climate and land use change. In highlands, lower elevation and relief is conducive to human degradation but also produces a relatively monotonous biophysical system that is not strongly prescribed by climate, resulting in these terrains being more sensitive to land use than climate change. This is in stark contrast to mountains, whose high elevation and relief not only restricts land use but also forces self-differentiation into bioclimatic zones. Each zone is climatically prescribed, rendering mountains – and especially the alpine zone – more sensitive to climate than land use change.

1.2.2.1. Bioclimatic zonation

Representing ~21.5% of global mountain area, the alpine zone is the uppermost and most floristically distinct bioclimatic zone. Alpine vegetation is defined by an absence of trees due to wind exposure and growing seasons being shortened by both cold summers

and snow and/or ice cover (Körner, 2004, Holtmeier, 2009, Grabherr et al., 2010, Körner et al., 2011, Körner, 2021). The alpine zone can be subdivided into 'true alpine' and 'nival', the former typified by a mosaic of herbfield, heathland, grassland, bogs and fens ('alpine meadow'), and the latter by sparse feldmark to no vegetation ('alpine desert'). Alpine desert is produced by extreme winds and a supra-snowline position, which lowers growing season temperatures to <3.5 ºC (Grabherr et al., 2001, Beniston, 2003, Grabherr et al., 2010, Körner et al., 2011, Körner, 2021).

The alpine and nival subzones are also pedologically discrete. Although the entire alpine zone is mantled by thin, poorly developed soils because of low productivity and supply-limited conditions, the highest nival summits are the most soil-depleted. Here, ridges are blanketed by either a shallow veneer of lithosols, regosols or leptosols, or simply bedrock exposed by extreme aeolian and cryological erosion (Poulenard and Podwojewski, 2006, Parish, 2014, Beniston, 2016). Conversely, on the lower slopes and saddles of the alpine zone proper, soil profiles are often deeper and more organic, ranging from poorly drained gleysols to clayey cambisols. These arise from a) high rates of organic matter (OM) production, and b) low rates of microbial metabolisation due to low temperatures and high soil moisture supplied by high rainfall and persistent meltwater from snow and ice (Poulenard and Podwojewski, 2006).

Indeed, the alpine zone is unique in that it is the only environment outside of polar regions where the cryosphere is the primary moderator of hydrological cycling. Of greatest consequence to alpine hydrology is the cryosphere's status as a long-term (seasonal to perennial) reservoir of precipitation, regulating the downslope transfer of water through retention in cooler months and steady release upon warm-season melting (Huss et al., 2017). This has myriad implications for alpine biota and soils, providing subnivean (sub-snowpack) habitat for aestivating/hibernating fauna, sustaining moisture for vegetation growth and OM preservation, and generating unique landforms such as solifluction terraces, cirques and moraines, which promote geodiversity (Aitchison, 2001, Poulenard and Podwojewski, 2006, Jonas et al., 2008). Critically, the regulating capacity of the alpine cryosphere also reduces the erosivity of runoff, thereby stabilising alpine slopes and streams, reducing turbidity and lowering downslope flooding risk (Beniston, 2003, Huss et al., 2017).

The alpine zone is demarcated from the underlying subalpine zone by the treeline ecotone, the elevation of which generally decreases with latitude in pursuit of the growing

season isotherm of ~6.4–6.7 ºC. However, due to local heterogeneities in slope, aspect, soils and arboreal composition, as well as anthropogenic stressors such as deforestation and grazing, the treeline is rarely a sharp isothermal marker but more often diffuse and/or fragmented (Körner, 2004, Loeffler et al., 2011, Körner et al., 2017). The underlying subalpine zone is characterised by open, low-lying woodland or forest due to growth being stunted by marginal temperatures, though they are generally warm enough to support a dense understorey. Warmer conditions also accelerate soil microbial activity, which results in lower OM content compared to alpine soils (Schinner, 1982, Körner, 2013, Siles et al., 2017). While the base of the subalpine zone usually coincides with the snowline, it is often not floristically distinct enough to be distinguished from the underlying montane zone. In these cases, it is often recognised as an 'upper montane' subzone (Slatyer, 2010, Körner, 2021).

Where it is pronounced, however, the subalpine-montane ecotone is generally expressed as a transition to tall, wet forest due to higher temperatures extending the growing season and reducing frost exposure. This facilitates higher productivity and OM deposition via leaf litter production, resulting in montane soils typically being both deeper and more organic than the overlying two zones (Körner, 2004, Körner et al., 2017, Körner, 2021, Mehmood et al., 2024). However, high biomass also increases fuel loads, meaning the montane zone usually observes the highest fire activity. Fire therefore impacts large tracts of mountain environments, given the montane zone is usually the largest mountain zone. This is especially true for mountains with a hypsometric peak at low-middle elevations; these are respectively coined 'pyramid' and 'diamond' systems by Elsen and Tingley (2015), who recognise that these two morphologies represent 71% of mountains.

Ecology is evidently the principal criterion in distinguishing the alpine, subalpine and montane zones, with there being minimal literature assessing how abiotic functions such as soil, fire and erosion vary along the mountain transect. The salience of ecology diminishes, however, across the transition from the montane zone to highlands which, though clear from a geomorphological standpoint, are far less globally replicable in an ecological sense. Indeed, while many highlands are distinguishable from the montane zone by a forest-grassland ecotone (e.g., Patagonian Plateau), highlands can also be expressed as a transition to scrub forest (e.g., Deccan Plateau) or even desert and xeric shrubland (e.g., Colorado Plateau) (Dinerstein et al., 2017). Inconsistency in highland ecology is due to low elevation and relief introducing climatic conditions more hospitable

to a wider variety of generalist taxa, reducing the role of temperature as a primary ecological control over abiotic factors such as lithology and especially precipitation.

Indeed, a feature shared by most highlands is limited precipitation, which is due to many being on the leesides of mountains and escarpments (e.g., the Great Plains, Central Highlands (Madagascar)). This subjects highlands to foehn winds and thus a rain shadow effect, inducing aridity or semi-aridity (Peel et al., 2007, Sharples, 2020). Orographically limited precipitation, in concert with low temperatures, results in many highlands being sparsely vegetated, which is the only shared characteristic of the ecoregions listed above. Indeed, despite floristic disparities, most highlands are categorised at the biome level as steppe, savannah or montane grassland and shrubland, which are of low biodiversity (Dinerstein et al., 2017, Critical Ecosystem Partnership Fund, 2024).

This is not the case for mountains, whose densely zoned ecologies endow them with substantially higher biodiversity than is predicted based on area alone (Körner, 2000, Körner, 2004, Beniston, 2016). In fact, mountains represent 18 of the 36 global biodiversity hotspots, hosting 85% of mammal, bird and amphibian diversity despite only accounting for 12.3% of non-Antarctic land area (Fig. 1.2a) (Guisan et al., 2019, Tito et al., 2020, Pereira et al., 2022, Schmeller et al., 2022, Critical Ecosystem Partnership Fund, 2024). Generally, biodiversity decreases upslope due to reduced available area and higher representation of fewer specialist species. However, due to ecotonal diffusion of species, this decline in biodiversity is often nonlinear until the treeline, and in many cases observes a mid-elevational peak in the montane or subalpine zones (e.g., fern diversity on Mount Kilimanjaro) (Grabherr et al., 1995, Hemp, 2002, Körner, 2004).

Mountains also exhibit high rates of endemism which, unlike biodiversity, often increases with altitude due to isolated alpine and subalpine summits obstructing lateral species migration, thereby functioning as habitat ‘islands’ that restrict floral and faunal gene flow (Beniston, 2003, Körner, 2004, Guisan et al., 2019). An alpine-subalpine confluence of island biogeography, cold temperatures, cryology and topographic complexity yields an abundance of microclimates and -habitats. This array of evolutionary niches promotes speciation of isolated biota, in some instances down to the catchment scale (Pickering, 2007, Albrich et al., 2020, Körner, 2021, Schmeller et al., 2022).

1.2.2.2. Ecotonal migration

The coupling of mountain biogeography with climate means even moderate climatic deviations in can trigger dramatic ecological reconfiguration, especially along ecotones. The most globally reproducible example of this is the upslope migration of biota in pursuit of their ranges of thermal tolerance under global warming (Diaz et al., 2003, Frei et al., 2010, Fort, 2015, Schmeller et al., 2022). This has been equated to the poleward migration of latitudinal biomes, the key corollary being the global retraction of the polar biome and alpine zone due to both being at their northernmost and uppermost limits, respectively (Elsen and Tingley, 2015). Ecotonal displacement is most starkly apparent along the treeline, for which there is abundant evidence of advance in especially North America and Eurasia since the late 20th century (Moiseev and Shiyatov, 2003, Harsch et al., 2009). Recent global analysis of 142 sites by Hansson et al. (2021) found that 66% of treelines have migrated upslope, though such observations remain skewed towards Northern Hemisphere mountains due to longer records and a larger sample population.

Despite this hemispheric bias, it remains true for all non-Antarctic continents that alpine-subalpine habitat islands are effectively 'sinking' within a rising 'sea' of montane forest (Slatyer, 2010). While intracommunal dynamics in the alpine zone have exhibited relative insensitivity to climate change thus far, treeline advance poses a major threat to alpine biota due to its capacity to introduce competition with lower-elevation species buoyed by warming (Grabherr et al., 2003, Gehrig-Fasel et al., 2007, Grabherr et al., 2010, Körner, 2021). While mountains with a nival zone (e.g., European Alps) offer temporary refugia for vertical evasion of warming in the form of uncolonised alpine desert, lower ranges (e.g., Atlas Mountains) lack such a buffer zone. In the latter case, biota will be reliant on microtopographic refugia such as valleys with cooler and/or moister aspects. Irrespective of local variability, extinction rates are expected to increase with altitude given the upslope increase in endemism and decrease in functional redundancy, as well as the inherency of mountain summits as biogeographic 'cul de sacs' (Egan and Price, 2017, Albrich et al., 2020).

While highland taxa are not challenged by topographic isolation, warming in highlands poses its own unique threat in that rising isotherms cover much larger areas per unit time due to lower relief. The opposite is true for mountains; Loarie et al. (2009) observe that biomes associated with mountains rank lowest in terms of 'climate change velocity', defined as the velocity of temperature change by biome. Higher climate change velocities

for highlands mean that ecosystems adjusted to their uniquely cool conditions are experiencing a loss of thermally hospitable land area at a rate exceeding that of potential upslope migration. Moreover, many highland ecosystems cannot evade warming as they are not adapted to wetter and steeper montane slopes, where forests can additionally act as a barrier to migration if it is resilient to warming or even migrating downslope, as has recently been observed in the northern Appalachian Mountains (Foster and D'Amato, 2015). However, for some highland ecosystems such as on the Tibetan Plateau, precipitation appears to be a more important control on biogeography, complicating biogeographic shifts (Wang et al., 2022).

Beyond conservation, ecotonal migration has implications for carbon storage in mountains especially; studies suggest treeline rise and concomitant forest expansion will increase aboveground biomass and produce more soil carbon (e.g., Field et al. (2007)) However, it has been counterargued that elevated productivity, lowered water tables, more oxidised soils and accelerated OM decomposition in forests results in atmospheric loss of belowground carbon at a rate exceeding aboveground retention (Hartley et al., 2012, Parker et al., 2015). This implies less efficient gross carbon sequestration in forests relative to alpine meadow, in turn portending reduced overall sequestration for mountains experiencing treeline rise (Wilmking et al., 2006, Hansson et al., 2021). These conflicting projections of carbon storage are emblematic of a broader uncertainty regarding changes in abiotic functions such as pedogenesis and fire. This uncertainty arises from the inability to directly apply the simple ecological model of upslope migration to these abiotic processes, which in addition to lagging behind vegetation changes are also dictated by immutable controls such as lithology, slope and aspect.

The prognosis for migrating mountain ecologies is further deteriorated by elevation-dependent warming. This describes the positive correlation between the rate of warming and elevation, which translates to amplified warming in mountains relative to surrounding highlands and lowlands (Pepin et al., 2015). While its precise forcings remain nebulous, elevation-dependent warming appears to be a positive feedback of warming-driven modifications to mountain snow and ice albedo, aerosols, soil moisture, cloud cover and water vapour (Kotlarski et al., 2012, Rangwala and Miller, 2012, Abbas et al., 2024). Though globally variable in its intensity, this relationship has been observed in mountains across the Tibetan Plateau (Liu et al., 2009) and western United States (Diaz and Eischeid, 2007) and is projected to intensify in the near future. Owing to this mechanism, models

predict temperature increases of 3–5 ºC in mountains by 2100, significantly higher than the global average projection of 2.2–3.5 ºC (Nogués-Bravo et al., 2007, Intergovernmental Panel on Climate Change, 2023).

Although recent studies argue that elevation-dependent warming is not observable when altitudinal differences are globally averaged, nor for sites within the same latitudinal belt (except for Australia and New Zealand), there is strong evidence for it at local scales, more so for temperate and polar zones than the tropics (Fig. 1.3a) (Nogués-Bravo et al., 2007, Guisan et al., 2019, Pepin et al., 2022b). Elevation-dependent warming threatens the migratory capacity of mountain plants, many of which are already failing to keep pace with rising isotherms especially along the treeline and in temperate regions, where rainfall decline already lowers dispersal rates. Additionally, many taxa lack the ability to migrate altogether (due to barriers such as substrate type or summits), and/or do not possess the phenotypic plasticity to adapt to warming *in situ*, elevating their extinction risk (Frei et al., 2010, Rehm and Feeley, 2016, Tito et al., 2020, Freeman et al., 2021, Lu et al., 2021).

1.2.2.3. Causes and impacts of hydrological change

While warming is universally projected for high-altitude regions, precipitation changes will be less spatially uniform (Fig. 1.3b). Although increases of between 5–20% are anticipated for the Hindu Kush, Himalaya and Ethiopian Highlands, models simultaneously project decreases for the Southern Andes and Mediterranean (Hock et al., 2019). Discrepancies are also expected in the seasonality, altitude and intensity of precipitation changes, though there is an emerging consensus that there will be winter increases at higher elevations and decreases at lower elevations, with some exceptions such as the Rocky Mountains (O'Gorman, 2014, Rajczak and Schär, 2017, Hock et al., 2019, Ferguglia et al., 2024).

Increased cool-season precipitation may encourage snowfall in higher altitude/latitude mountains. However, at lower altitude/latitudes this will manifest as an increase in the frequency of extreme precipitation by 15% per degree of warming in the Northern Hemisphere, due to a phase shift from solid- to liquid-state precipitation (Kapnick and Delworth, 2013, Ombadi et al., 2023). Declining precipitation at lower elevations is, in synergy with warming, increasing fire severity and frequency in especially montane forests due to large dry-fuel loads, as evident across the lower Sierra Nevada (Stephens

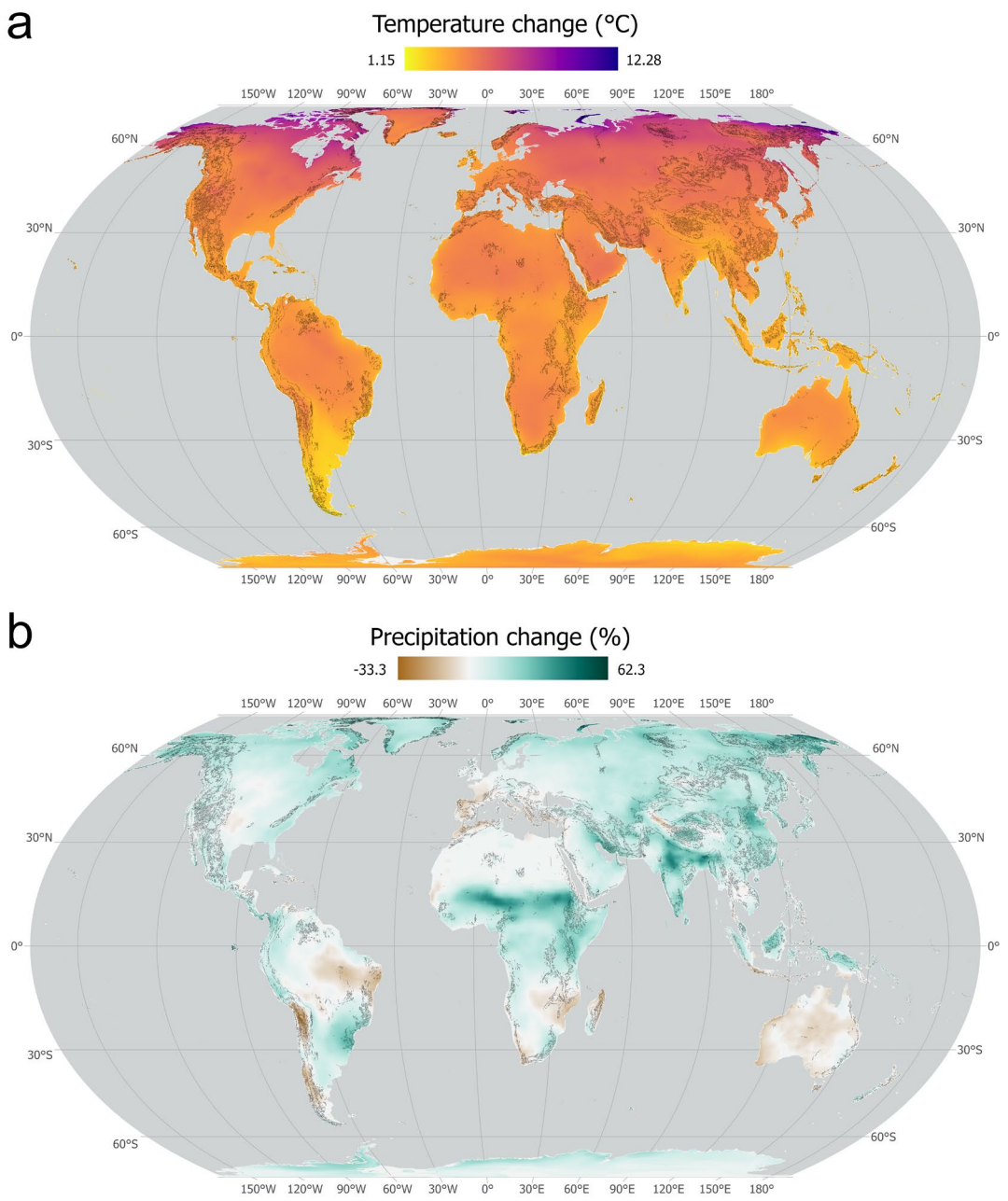

Figure 1.3. World maps of mountain and highland systems (see Fig. 1.1), overlain with gridded data for projected changes in **a)** annual mean temperature and **b)** annual precipitation. Projections are for 2081–2100 relative to the 1970 –2000 baseline under SSP2-4.5, using the ACCESS-CM2 model variant of CMIP6 (Eyring et al., 2016, Fick and Hijmans, 2017).

et al., 2018). There is no consensus on future precipitation changes in highlands, though drying in some regions threatens grassland ecosystems, given these are already moisture-limited biomes where precipitation is the prevailing climatic control (Wesche et al., 2016).

Changing precipitation seasonality and a decline in the snow-to-rain ratio has severe implications for the mountain cryosphere, which is contracting globally. In higher

altitude/latitude mountains, contraction is plainly apparent as glacier retreat, which is projected to be especially rapid for mid-latitude systems such as the subtropical Andes and European Alps, where ice volume loss will approach 80% and 84%, respectively, by 2100 (Huss et al., 2017). In lower-altitude systems lacking glaciers (e.g., Drakensberg Mountains), cryospheric collapse is instead manifesting as a decline in snow cover. This has already been observed for 78% of mountains between 2000–2018, with a global mean decline of ~7.8% between 1984–2024 (Notarnicola, 2020, Blau et al., 2024). As for treeline rise, snow decline is most rapid in mid-elevational areas and coastal mountains, where temperature is the dominant control on snow cover (Brown and Mote, 2009).

Reduced snow cover threatens the ecological and hydrological functioning of all mountains exceeding the local snowline, given the aforementioned role of snowpack in hydrological modulation. Ecologically, reduced snowfall and earlier spring melting is expected to trigger phenological dissociations between snow-dependent flora, fauna and climate, and facilitate an extirpation of meltwater-dependent groundcover, enabling invasion of generalists into areas of former snowpatch cover (Stewart, 2009, Slatyer et al., 2022). Reduced seasonal snow cover also has implications for edaphic features such as freeze-thaw cycles, nutrient fluxes, soil pH and moisture and OM decomposition (Edwards et al., 2007, Kosolapova and Altshuler, 2024).

At this interface between ecology and soil are mountain bogs and fens and their peaty substrates, which Millar et al. (2017) argue to be among the most vulnerable ecological communities to hydrological change. This position was informed by observations that lower-altitude bogs and fens are less productive (i.e., accumulate less peat), which they attribute to reduced snowpack, earlier snowmelt and thus lower water tables. Indeed, the primary criterion for peat formation is subsoil anoxia, which inhibits decomposition by detritivores and permits net accumulation of dead OM. Anoxia arises from saturation of the soil matrix, which in alpine bogs and fens is primarily dependent on water infiltration from snowmelt at a rate that exceeds drainage (Moore, 1987, Pickering, 2007, French et al., 2016, Garisoain et al., 2024).

Declining snow cover is thus concerning from a carbon storage perspective given peatlands are the largest terrestrial carbon sink on the planet, storing 30% of global soil carbon despite occupying 3% of global land area (Minasny et al., 2024). Reduced productivity caused by snow decline therefore threatens to convert many peatlands from CO_2 and CH_4 sinks to sources, with evidence that this is already occurring in the Pyrenees.

Here, peatland desiccation due to drought resulted in peatlands emitting 31 g C m^{-2} yr^{-1} between 2017–2022, though this value increased by 77% once punctuated fluvial export of carbon via erosion was accounted for (Garisoain et al., 2024), a process that is itself being exacerbated by increased snowmelt runoff. If this critical transition is realised across mountains globally, peatlands will contribute significantly to a positive warming feedback, undermining climate mitigation (De Jong et al., 2010).

Reductions in snow cover are also reinforcing the impact of more extreme rainfall on runoff, which itself is contributing to the physical removal of snowpack, forming another positive feedback. Rapid melting and more frequent high-intensity rainfall impair infiltration of water into soils, increasing the volume and thus erosive capacity of especially warm-season runoff (Somers and McKenzie, 2020). Elevated erosion rates not only threaten high-altitude slope instability but are increasing the occurrence of flooding events in adjacent highlands and lowlands (Nearing et al., 2004, Haque et al., 2019, Davenport et al., 2020, Hotovy et al., 2024). The hydrological impacts of melting and rainfall will be most severe across the mountains of central Asia and western North and South America, where snowmelt is the dominant control on streamflow, placing their catchments at the highest risk of flooding and landslides (Adam et al., 2009, Stewart, 2009). These hydrogeomorphic events are destructive to terrestrial and aquatic habitats and threaten an increasingly large proportion of the human population that inhabits mountains and their peripheries in pursuit of this very same water supply (Schmeller et al., 2022).

1.2.2.4. Human-environment interactions

Mountains sustain ~50% of the world's river systems and thus over half the global human population, much of this being around the Tibetan Plateau where mountain water supply is already considered 'essential but vastly insufficient' (Beniston, 1999, Messerli, 2000, Adler et al., 2023). Propinquity is key to the access of mountain water resources for irrigation, hydropower and consumption; as such, 14% of the globe resides in mountains and adjacent highlands, two-thirds of this in urban settings (Ehrlich et al., 2021). Despite its exploitational advantage, proximity to mountains in the context of changing precipitation regimes and a depleted cryosphere is increasing human vulnerability to periods of low discharge (and water stress) punctuated by flooding and landslides. These

hazards decimate infrastructure and reduce water quality due to sediment influx, which also infills critical reservoirs (López-Moreno et al., 2004, Schaefli et al., 2007, Wulf et al., 2010, Rajczak and Schär, 2017).

Acutely vulnerable to these hazards are populations with low adaptive capacity, namely the 90% of high-altitude communities residing in developing countries, landslide-prone tropical regions and arid to semi-arid regions. In the latter, mountains can be responsible for up to 90–100% of water supply, though their rivers are more inclined to flash flooding (Diaz et al., 2003, Viviroli and Weingartner, 2004, Romeo et al., 2015, Adhikari et al., 2018, Pereira et al., 2022). Hydrological hazards are ubiquitous around the Tibetan Plateau and Andes in particular, which together account for almost all of the global population at high or very high risk of future changes in mountain water resources (Adler et al., 2023).

This is concerning given population growth is also rapid across much of central and southern Asia, whose total population is surpassed only by eastern and southeastern Asia (Gu et al., 2021). The large populations of these regions and their exponential growth contribute strongly to projections that the proportion of the global lowland population dependent on mountain runoff resources will increase by 17% to 1.5 billion people by 2050 (relative to 1960) elevating demand on mountain services and exposing more people to hydrogeomorphic hazards (Viviroli et al., 2020). Unsurprisingly, mountains assigned the highest 'water tower index' (water-supplying value) by Immerzeel et al. (2020) were also identified as having the potential to impact up to 1.9 billion people living within them or directly downstream.

While mountains therefore threaten high-altitude communities, the inverse is also increasingly true, with 60% of mountains being under intense human pressure (Elsen et al., 2020). The resource-driven occupation of high-altitude regions is not a novel demographic pattern, spanning millennia in many regions (e.g., Europe and Australia). However, post-industrial intensification and exponential population growth are amplifying land use impacts (Parish, 2014, Li et al., 2019). For mountains in developing nations (e.g., Himalaya, Ethiopian Highlands), traditional agricultural methods such as seasonal cropping and transhumant grazing remain the dominant land use. Though less intensive than modern agriculture, these practices are becoming increasingly destructive due to a lack of regulation, improved accessibility, disproportionate population growth, and a post-globalisation shift towards cash crop monocultures (Nogués-Bravo et al., 2007,

Beniston, 2016, Li et al., 2019, Romeo et al., 2021). Although such practices have largely been abandoned across mountains in developed countries (e.g., Pyrenees, Rocky Mountains), this has been in favour of more intensive industries. These include commercial grazing, mining, forestry, abstraction of water for hydroelectricity and irrigation, and 'hard tourism', including hiking and snowsports (MacDonald et al., 2000, Grabherr et al., 2001, Nogués-Bravo et al., 2007, Beniston, 2016).

In both developing and developed contexts, agriculture has been the dominant agent of degradation in mountains but especially highlands. Overexploitation in both terrains is associated with carbon, nutrient and biodiversity loss due to tilling and livestock grazing via soil exposure and channel and sheet erosion (West et al., 2014, Zhou et al., 2020, Pereira et al., 2022). Agriculture has also driven massive inputs of limiting nutrients (N and P) into catchments via agrochemicals and livestock. Excessive nutrient enrichment is disturbing biota adapted to often nutrient-poor soils and is exacerbating eutrophication events in high-altitude lakes and streams (Ho et al., 2019, Li et al., 2021). The contribution of agriculture to erosion and pollution can be compounded within certain catchments by mining, which alters streamflow and injects toxic trace elements (e.g., As, Hg, Cu, Zn) into soils and waterways to levels exceeding those acceptable for wildlife and humans (Wohl, 2006, Korpak, 2017, Le Roux et al., 2020, Schmeller et al., 2022).

Agriculture is also, second to timber production, a major vector of high-altitude deforestation, which fragments forests and forces migration of the treeline (e.g., Shandra et al. (2013)). While logging has traditionally targeted native stands, a novel stressor emerging from modern forestry is the deliberate sowing of exotic arboreal genera (*Pinus* and *Eucalyptus*, in many regions), which outcompete their native equivalents, intensify fire regimes and reduce soil quality and carbon storage (Fahey and Jackson, 1997, Hofstede et al., 2002, Nunes, 2012, Cifuentes-Croquevielle et al., 2020). Non-native invasions are also being inadvertently facilitated by agriculture (e.g., seed dispersal via herded stock and contaminated composts) and touristic activities such as biking, which translocate exotic flora along trails and roads (Hemp, 2008, Liedtke et al., 2020).

In mountains, many of the above land uses are exacerbating the effects of climate change, hindering ecotonal migration particularly along lower montane slopes, where impacts are often most pervasive (Elsen et al., 2020). This downslope coalescence of stressors continues exponentially into highlands, where prolonged exposure to grazing in particular has significantly modified grassland-dominated environments. However,

highland responses are variable given global disparities in biophysical conditions and the duration/intensity of pastoralism (Butterbach-Bahl et al., 2011, Wesche et al., 2016).

1.3. The High Country: biophysical setting and impacts

1.3.1. Physical, climatic and ecological setting of the Snowy Mountains

The necessity for a geoecological assessment of high-altitude sensitivity to the climatic and land use manifestations of GEC described above is most pertinent to regions that are limited in extent and are therefore impacted over proportionately larger areas (Mooney et al., 1997). This is the case for high-altitude Australia, which exists within the broader Australasia-Southeast Asia zone recognised by Blyth (2002) as having the largest percentage area affected by multiple anthropogenic stressors (see Section 1.3.3 and 1.3.4). In Australia, this is due to an extremely restricted high-altitude area, with only 0.87% of the continent exceeding 1000 m ASL and a mere 0.15% existing above the snowline (Williams and Wahren, 2005, Pickering, 2007, Geoscience Australia, 2014). On the mainland, all of this alpine and subalpine habitat is confined to a region of southeastern Australia known historically as the High Country, which encompasses the Australian Alps (AA) and much of the South Eastern Highlands bioregions under the Interim Biogeographic Regionalisation for Australia framework (Fig. 1.4a) (Sahukar et al., 2003).

The AA straddles the states of Victoria and New South Wales (NSW) and is accordingly partitioned into the Victorian Alps and Snowy Mountains (SM) subregions, though the latter also extends slightly into Victoria (Fig. 1.4b). The SM represents the largest contiguous body of alpine, subalpine and montane habitat in Australia, despite occupying only 0.09% of continental area (Sahukar et al., 2003, DCCEEW, 2020). The SM is not only biogeographically but also geomorphically discrete, being a remnant feature of prolonged, discontinuous period of orogenesis also responsible for forming the broader Great Dividing Range, which, spanning the eastern continental margin, is one of the longest cordilleras in the world. The Great Dividing Range is the product of three geologic phases: 1) cyclic continental accretion commencing in the Neoproterozoic to form a complex of sutured orogenic belts (the Tasmanides), 2) intraplate thermal uplift and rifting in the mid-Cretaceous to -Cenozoic, and 3) sporadic hotspot volcanism until the late Cenozoic (Bishop, 1988, Veevers et al., 1994, Glen, 2013, Müller et al., 2016). The second phase of intermittent dynamic uplift under one province of the Tasmanides –

the Lachlan Orogen – is responsible for the high elevation of the AA, and especially the SM. In fact, the SM represents the most elevated segment of the Great Dividing Range and indeed Australia, despite its highest summit Mount Kosciuszko being a globally modest 2228 m ASL (Fig. 1.4b) (Sahukar et al., 2003, Müller et al., 2016).

Owing to its low elevation, SM experiences a limited seasonal snow regime. An area of only 1200 km^2 observes ≥60 annual days of snow cover, with the snow season peaking within a relatively narrow window between July and August (Pickering, 2007). The timing, duration and volume of snowfall in the SM, and precipitation for southeastern Australia more broadly, is moderated by semi-regular variability in teleconnections, chiefly the El Niño–Southern Oscillation (ENSO) and Southern Annular Mode (SAM), which together modulate hydroclimate for southern and eastern Australia (Fig. 1.4a) (Theobald et al., 2016). ENSO is the primary control on the volume of spring rainfall on interannual timescales, with oscillations between the El Niño and La Niña phases being associated with lower and higher than average rainfall, respectively. ENSO is also a significant determinant of temperature; El Niño is correlated with positive temperature anomalies across southeastern Australia, particularly in summer and autumn (Fierro and Leslie, 2014, Lieber et al., 2023). This is significant given the warm season witnesses peak annual snowmelt discharge, meaning ENSO intensity can determine the timing and duration of flows.

Conversely, SAM is more influential on summer and winter rainfall, dictating the latitudinal position of the moisture-laden Southern Hemisphere Westerly Winds (SHWW) across southern Australia, which are obstructed by the AA (Mason and Williams, 2013a, Raut et al., 2014, Tozer et al., 2023). Orographic interception results in the SM observing the highest annual rainfall in southern Australia (~1700 mm yr^{-1}), which peaks slightly in winter in accordance with a seasonal poleward relaxation of the SHWW (Xu and Hutchinson, 2013, Slattery, 2015, Theobald et al., 2016, Bureau of Meteorology, 2025b). These influences on precipitation inherently extend to snowfall, with Pepler et al. (2015) identifying that El Niño and positive SAM phases are associated with reduced winter and spring snow cover in the SM. However, they also note that temperature is the primary control, with the low area and volume of annual snowfall being ascribed to low elevation and thus marginal temperatures for snow persistence.

The low elevation of the SM is a product of near-continuous tectonic stability following an Eocene termination of uplift, which has permitted peneplanation to present.

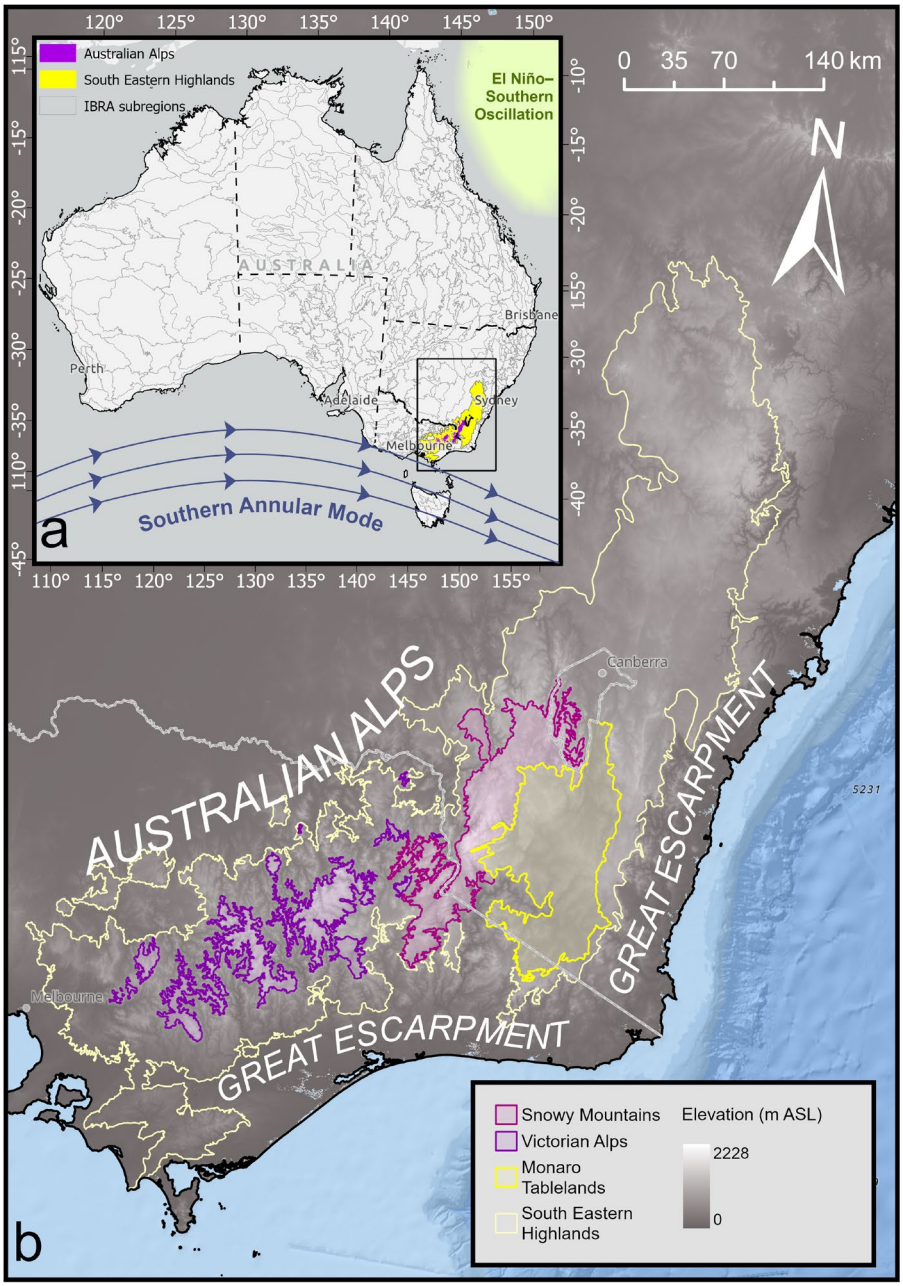

Figure 1.4. Regional setting of the High Country in southeastern Australia, with relevant climate drivers and bioregions highlighted. 'Monaro' biogeographic subregion has been clipped to the Snowy Monaro Local Government Area, consistent with the in-text regional definition (Department of Customer Service Spatial Services, 2020). Digital elevation model sourced from Gallant et al. (2009). Bioregion data sourced from DCCEEW (2020).

Prolonged denudation has reduced the SM to a low-lying orogenic root geomorphically analogous to the Appalachian Mountains, with a steep western and shallow eastern gradient (Fig. 1.7d) (Kohn et al., 1999, Costin, 2000, Kirkpatrick, 2002, Webb, 2017). Tectonic quiescence has encouraged fluvial erosion of the range by major perennial systems (e.g., Snowy, Thredbo and Jacob Rivers) to form deeply incised valleys.

Protracted weathering of the predominantly granitoid and metasedimentary bedrock is also responsible for the genesis of a well-developed mantle of soil of 0.6–1 m thickness (Fig. 1.7f, g). This is deep by global standards, considering most mountains are supply-limited due to high relief (Stromsoe et al., 2016, Wilson et al., 2022).

Preservation of this regolith can thus be explained by low relief (and thus a transport-limited regime) but also low elevation, which has suppressed Cenozoic glaciation due to high temperatures limiting snowpack consolidation. As such, the only instances of Quaternary Period glaciation in the SM, and in fact mainland Australia, were localised to only the highest modern alpine peaks of the Main Range (see Section 1.4.2) (Costin, 1955, Costin and Polach, 1971, Colhoun and Peterson, 1986, Costin, 1989). Suppressed glaciation limited the area exposed to processes such as plucking and abrasion, permitting the accumulation of regolith as well as its conversion to highly organic alpine humus by colonising alpine groundcover, which now occupies 99% of the alpine zone (Costin, 2000, Barrows et al., 2001, Kirkpatrick, 2002, Wilson et al., 2022).

Alpine meadow evidently dominates the alpine zone, akin to other alpine environments globally (Fig. 1.7b). Specifically, 62% of alpine area is occupied by tall alpine herbfield due to the abundance of its preferred landforms, namely well-drained slopes and low, sheltered ridges on the easterly aspects of the Main Range (Mason and Williams, 2013c, Pickering and Venn, 2013). The remaining alpine area is mostly a mosaic of heath (25%), alpine bogs and fens (5.8%), short alpine herbfield (0.9%) and feldmark (1.9%) (Pickering and Venn, 2013). Heath generally occurs on middle to upper slopes in settings similar to tall alpine herbfield, while short alpine herbfield is confined to areas downslope of the most persistent snowpatches, where gradual snowmelt infiltration sustains soil moisture late into or even throughout the warm season (Fig. 1.5) (Costin, 2000, Mason and Williams, 2013c, Pickering and Venn, 2013).

Unlike underlying zones, where soil type is controlled by parent material, alpine pedology is strongly dependent on vegetation type and, in turn, climate and topography (Wilson et al., 2022). Herbfield and heath communities are almost always associated with alpine humus (‘organosols’), which, while varying from shallow and stony on upper slopes to loamy on lower slopes, is always OM-rich. This is not the case for feldmark, which is confined to the highest summits of the Main Range where winds are strongest, temperatures lowest and frosts most severe. Here, ground-hugging species are established on thin, infertile lithosols, except on the most inhospitable ridges, where bedrock remains

Figure 1.5. Looking towards a segment of the Snowy Mountains Main Range forming the western interfluve of the Blue Lake cirque. Short alpine herbfield (foreground) is sustained by meltwater from upslope snowdrifts (background), which in this instance have persisted to late summer (8 February 2023). Personal photograph, 2023.

alpine desert (Mason and Williams, 2013c, Mason and Williams, 2013b, Pickering and Venn, 2013).

Other than exposed ridgelines, the only other alpine areas where organosols do not occur is under bogs and fens, where peat instead develops (Fig. 1.7b) (Mason and Williams, 2013c). Bogs and fens are identified by Hope et al. (2012) as 'mires', which describes any peat-accumulating wetland. The authors also recognise that mires can be hydrologically subdivided according to whether they a) develop either along topographic lows such as valley floors and saddles, where drainage is impeded and the water table is high ('topogenous'), or b) along hilltops or hillsides, where moisture is almost exclusively delivered via precipitation ('ombrogenous'). SM mires are overwhelmingly topogenous, while the ombrogenous minority is exclusively constituted by bogs. This is because bogs are capable of accumulating peat well above the water table such that vegetation becomes hydrologically perched (Moore, 1987, Hope et al., 2009b, Hope et al., 2012, Mooney et al., 2021).

Bogs and fens can also be distinguished by surficial ecology; bogs are characterised by stagnant water or ombrotrophic conditions and accordingly comprise a complex

mosaic hosting the keystone moss species *Sphagnum cristantum*. Conversely, fens typically possess open and sometimes running water, and as such are minerotrophic and typified by simpler sedge-rush associations, with *Carex gaudichaudiana* as the keystone species (Fig. 1.6) (Sahukar et al., 2003, Hope et al., 2012). While disparate, both mosaics are extremely effective at trapping sediment, while the high porosity of the fibrous upper peat unit (acrotelm) enables large amounts of runoff, snowmelt and rainfall (up to 92% by volume) to be sequestered in the underlying peat (catotelm) (Hope et al., 2012, Loisel and Yu, 2013). Retention of sediment and water is essential for filtering flows, sustaining mire vegetation during drought and fire, and moderating outflow such that the erosivity of runoff is buffered (Good et al., 2010, Hope et al., 2012).

In addition to these regulating ecosystem services, mires are also highly efficient carbon stores. Hope et al. (2012) estimate a total of 3.55 Mt of carbon is sequestered across SM peatlands, though only ~13% of this occurs in the alpine zone, with over thrice as much (42%) in the underlying subalpine zone (Fig. 1.7b). This is surprising given downslope increases in temperature and decreases in rainfall (Fig. 1.7c, 1.8) mean peat-growing conditions begin to approach their climatic limits in the subalpine zone (Kirkpatrick, 2002, Hope and Nanson, 2015). The size of this subalpine reservoir is made

Figure 1.6. Foreground: A topogenous montane fen envelopes Delaneys Creek along a frost hollow, northern Snowy Mountains. Even in the montane zone, snow cover can be substantial during winter (left; 29 July 2024), though montane fens are more dependent on runoff and groundwater for most of the year (right; 2 April 2024). Background: *E. delegatensis* stands still recovering almost five years after crown scorching during the 2019–2020 fire season, permitting prolific shrub growth. Personal photograph, 2024.

more curious given that mires are increasingly represented by a third hydrogeomorphic class – moors – which host much shallower, more slowly accumulating peats. Moors are also the most dependent on surface flows for moisture and nutrient inputs, and are thus defined by a simple association of drier sedge-rush shrubland with *Empodisma minus* as the keystone species (Hope et al., 2012). Although the subalpine emergence of moorland is laterally abrupt, the true diagnostic feature of the alpine-subalpine ecotone is, as for all alpine-hosting mountain ranges, the treeline (Mason and Williams, 2013c)

In the SM, the treeline corresponds to the 10 ºC mid-summer isotherm at ~1800 m ASL and is defined by a transition to low-growing, open woodland almost exclusively represented by snow gum (*Eucalyptus pauciflora*), with a dense understorey of snowgrass (*Poa* spp.), heath and herbs (Fig. 1.7, 1.8) (Mooney et al., 1997, Mason and Williams, 2013c). The treeline is rarely sudden, usually being overlain by 'tree-limit ribbons' trending parallel to the prevailing winds and which can extend up to several hundred metres into the alpine zone proper, where topographic microclimates are marginally hospitable (Green and Venn, 2012). Below the treeline, floristic heterogeneity is exhibited within the tree stratum itself; on the eastern flanks, subalpine woodland is fragmented by treeless valleys of cold air drainage ('frost hollows'), which are essentially inverted tree lines operating as quasi-alpine refugia (Sahukar et al., 2003, McDougall et al., 2005). Here, valley floors are dominated by sod-tussock associations, while low relief enables the water table to rise to a sufficiently shallow depth to permit the establishment of mire assemblages and the accumulation of peat (Sahukar et al., 2003, Kemp and Hope, 2014). Outside of these frost hollows, subalpine soils are less organic due to accelerated OM decomposition under drier and warmer conditions. Zonal pedology is thus more directly prescribed by the granitic and sedimentary bedrock that underlies most of the SM, and which weathers to gley podsols (Geoscience Australia, 2012, Wilson et al., 2022).

Descending the altitudinal profile, mires reach their greatest abundance in the montane zone, not due to climatic conditions but rather this being the largest zone (Fig. 1.6, 1.8). Indeed, the montane zone represents 74% of SM area due to its low relief and valley dissection (Fig. 1.7d). As such, it hosts 44% of the range's total peat carbon despite only representing 25% of total peatland area, due to most montane mires being wide but shallow moors (Gallant et al., 2009, Hope et al., 2012). Floristically, the montane zone is signalled by a replacement of open woodland at ~1500 m ASL by tall, wet sclerophyll forest with a sparse understorey of ferns and small trees, due to higher mean annual

temperatures (6–9 ºC) and moderate annual rainfall (1100–1600 mm) (Fig. 1.7, 1.8) (Mason and Williams, 2013c, Xu and Hutchinson, 2013, Slattery, 2015). This temperature-precipitation optimum supports the highest rates of OM production in the SM, which is implicated in the development of extensive podsols and clay loams. These are surprisingly fertile and thick (>1 m) considering the parent material and the fact that the montane zone occupies the steepest segment of the altitudinal profile, which promotes colluviation (Sahukar et al., 2003, Mason and Williams, 2013b, Mason and Williams, 2013c).

Deep soils and a favourable climate also support high vertical growth of the canopy, which is dominated by *Eucalyptus* but exhibits significant intracommunal variation with elevation and aspect. In wetter, sheltered areas (i.e., southerly/easterly aspects and the upper montane zone) there is an alliance of moisture-demanding alpine ash (*E. delegatensis*), brown barrel (*E. fastigata*) and *E. pauciflora*. Meanwhile, drier, more exposed areas (i.e., westerly/northerly aspects and the lower montane zone) exhibit associations of drought-tolerant candlebark (*E. rubida*), ribbon gum (*E. viminalis*), blue gum (*E. globulus*) and narrow-leaved peppermint (*E. radiata*) (Costin, 2000, Sahukar et al., 2003, Mooney, 2004, Mason and Williams, 2013c, Slattery, 2015). High woody fuel loads and the abundance of pyrophytic *Eucalyptus* promote the most energetic fire regime of all three zones. Particularly influential in intensifying fire activity is the keystone species *E. delegatensis*, which, despite being intolerant of burning, is also an obligate seeder and thus germinates after fire (Fig. 1.6) (Zylstra, 2018).

Figure 1.7. (next page) Biophysical dimensions of the High Country (Snowy Mountains and Monaro regions, as defined in Fig. 1.4). **a)** Sentinel-2 L2A true colour image (30 October 2024) of the High Country (Copernicus Data Space Ecosystem, 2025) and major perennial rivers (State Government of NSW Spatial Services, 2025), with mountain-highland boundary denoted by dashed line. **b)** Major vegetation groups in the (NSW portion only) (DCCEEW, 2016a). **c)** Mean annual temperature and annual precipitation for 1976–2005 (NSW portion only) based on ANUCLIM v.6.1 (Xu and Hutchinson, 2013). **d)** Digital elevation model with major bioclimatic/physiographic zones outlined (Gallant et al., 2009). **e)** Land use and land cover (secondary classification) in 2023 (Australian Bureau of Agricultural Resource Economics Sciences, 2024). **f)** Major soil types, following the Australian Soil Classification (Searle, 2021). **g)** Major lithological groups (Geoscience Australia, 2012) and locations of all lakes documented by Benson and Jacobs (1994) (DCCEEW, 2015b).

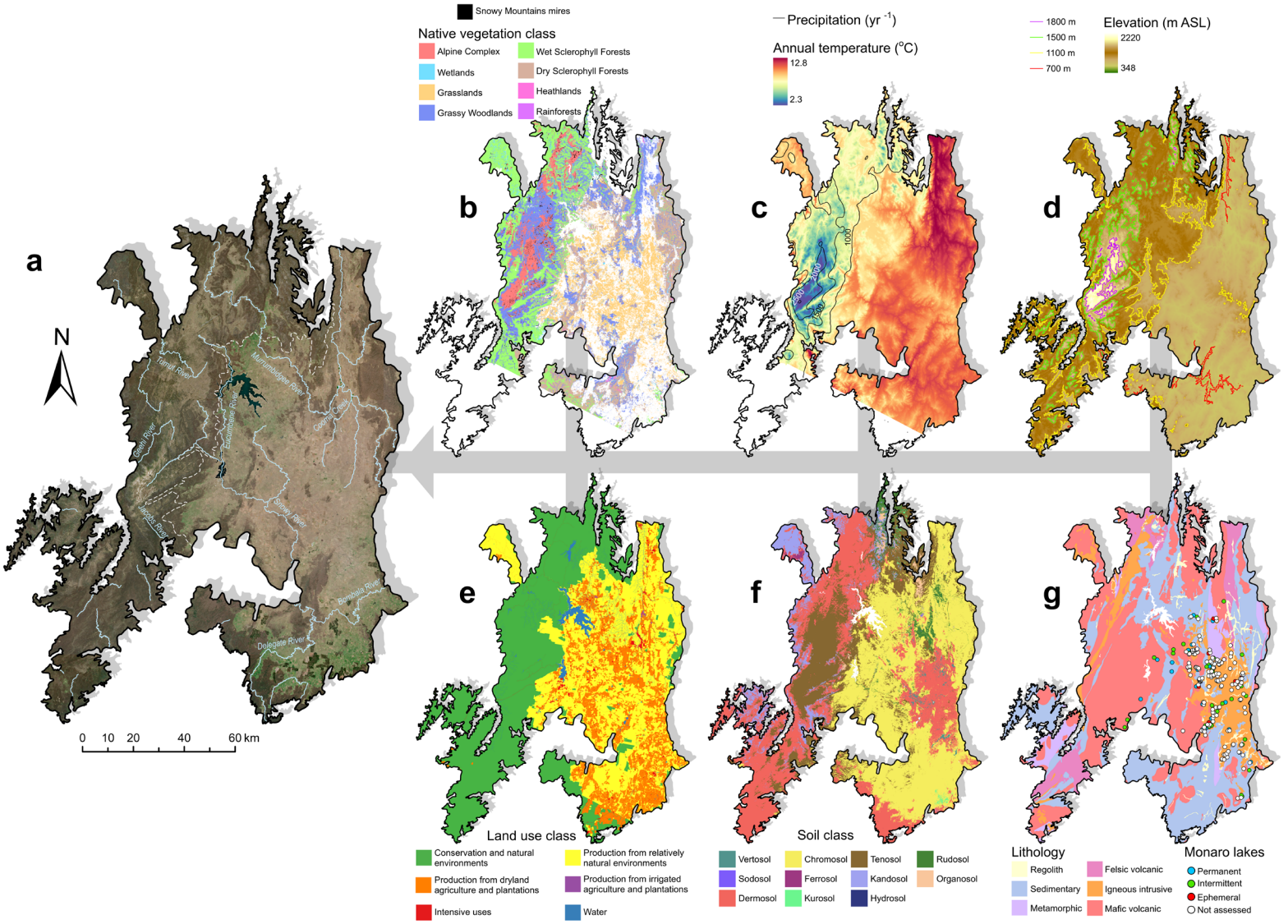
a
b
c
d
e
f
g
N
0 10 20 40 60 km
Tantawangalo Creek
Bendoura Creek
Brown River
Bemboka River
Delegate River
Snowy Mountains mires
Native vegetation class
Alpine Complex
Wetlands
Grasslands
Grassy Woodlands
Wet Sclerophyll Forests
Dry Sclerophyll Forests
Heathlands
Rainforests
Precipitation (yr -1)
Annual temperature (°C)
12.8
2.3
1800 m
1500 m
1100 m
700 m
Elevation (m ASL)
2220
348
Land use class
Conservation and natural environments
Production from relatively natural environments
Production from dryland agriculture and plantations
Production from irrigated agriculture and plantations
Intensive uses
Water
Soil class
Vertosol
Chromosol
Tenosol
Rudosol
Sodosol
Ferrosol
Kandosol
Organosol
Dermosol
Kurosol
Hydrosol
Lithology
Regolith
Felsic volcanic
Sedimentary
Igneous intrusive
Metamorphic
Mafic volcanic
Monaro lakes
Permanent
Intermittent
Ephemeral
Not assessed

1.3.2. Physical, climatic and ecological setting of the Monaro Tablelands

The base of the montane zone at ~1000 m ASL delineates the SM as a biogeographic subregion, marking the limit of wet sclerophyll forest (Fig. 1.7b, 1.8). On the eastern flanks only, this ecotone also demarcates the SM as a mountain range, coinciding with an abrupt shallowing of relief to a broad plateau known as the Monaro Tablelands ('Monaro') (Fig. 1.4b, 1.7d) (Sahukar et al., 2003, Wilson et al., 2022). While the Monaro as a biogeographic subregion of the South Eastern Highlands extends as north as Goulburn (Fig. 1.4), from a physiographic perspective it is more restricted. Specifically, the Monaro more appropriately describes the ~8000 km^2 peneplain east of the SM, which slopes southward to a minimum elevation of ~800 m ASL slightly south of the NSW-Victoria border (Fig. 1.4b) (Sahukar et al., 2003, DCCEEW, 2020). It is bounded to the north by the Brindabella and Tinderry Ranges, to the northeast by the Kybeyan Range

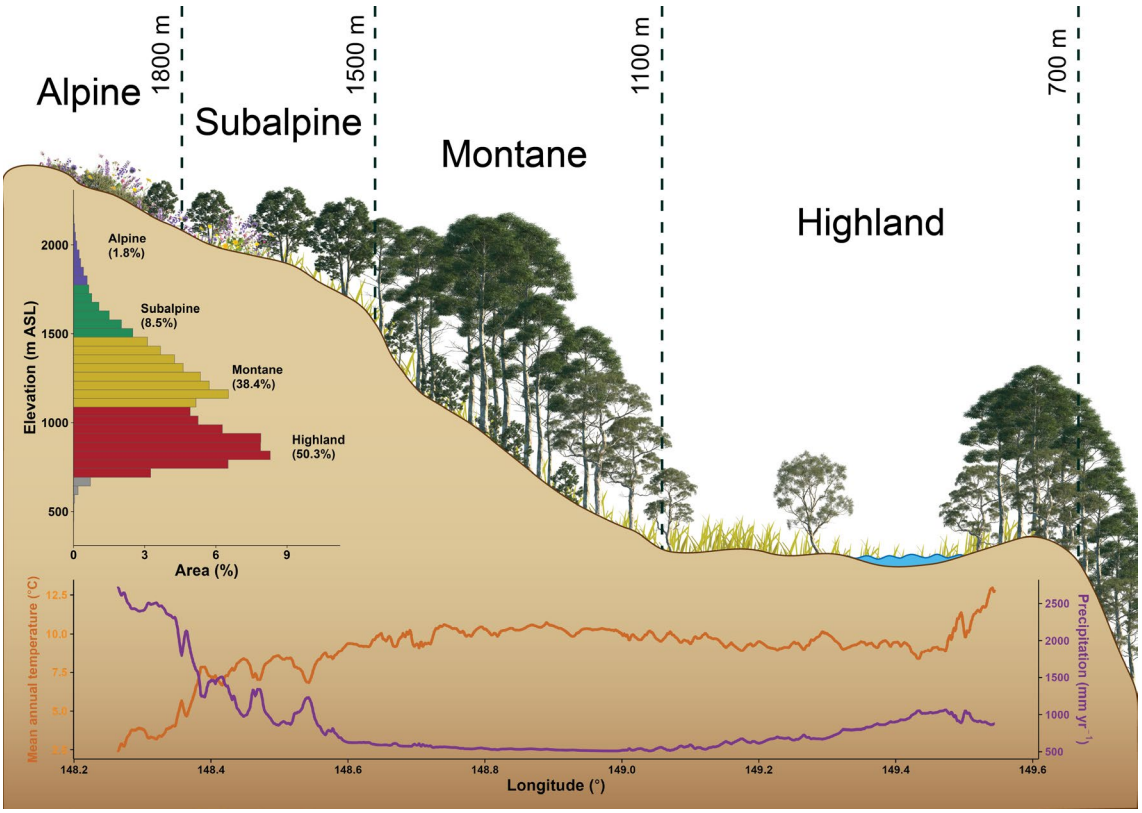

Figure 1.8. Conceptual model of a west-east cross-section of the High Country, highlighting the key climatic, topographic and floristic features defining each bioclimatic/physiographic zone. Hypsometric profile informed by elevation data from Gallant et al. (2009) for the High Country, as defined in Fig. 1.7. Temperature and precipitation profiles were derived from latitudinal transects of the climate rasters presented in Fig. 1.7c (Xu and Hutchinson, 2013), which were drawn eastwards from the latitude of Mount Kosciuszko (36.456° S).

and to the east and south by the Great Escarpment, the latter being a product of post-uplift pediplanation of the Great Dividing Range (Ollier, 1982, Taylor and Roach, 2003).

Underlain by the Lachlan Orogen, the Monaro shares a common basement with the SM, though is more extensively represented by folded and faulted Ordovician to Lower Silurian metasediments than the Upper Silurian batholiths which define the western Monaro and SM (Fig. 1.7g) (Costin, 1954, Geoscience Australia, 2012). In terms of surface geology, however, the dominant feature is the Monaro Volcanic Province, a ~4200 km^2 mafic lava field extruded by intraplate volcanism onto the Paleozoic paleosurface over a minimum 25-million yr interval from the Eocene to Oligocene (Brown, 1994, Roach et al., 1994, Roach, 1999). Draping the central and eastern Monaro, this lava field is the largest in the South Eastern Highlands and mostly comprises a series of basalt units known as the Monaro Volcanics, which reach at least ~400 m thickness in areas where flows flooded paleovalleys (Brown et al., 1992).

Affected by the same prolonged period of Cenozoic tectonic stability that enabled SM denudation, the Monaro Volcanics have also been pervasively weathered to form profiles of smectite clay grading to saprolite over a depth of 55 m (Brown et al., 1992, McQueen, 1994). At the surface, the original stepped basaltic terraces have been reduced to undulating plains of smectitic, highly fertile chocolate soils and black chernozems, the latter being the only example of such in mainland Australia (Costin, 1954). Due to the geologically recent eruption of the Monaro Volcanic Province, the plateau is only weakly dissected, though the exposed Paleozoic substrate in the west has been deeply incised by the Snowy and Murrumbidgee Rivers. These systems respectively flow eastward and westward, being diverted around the lava field and having their catchments bisected by the northwest-trending Monaro Range, a chain of eruption sites constituting a segment of the Great Dividing Range (Fig. 1.7a, d) (Taylor and Roach, 2003, Sharp, 2004). While generally flat and continuous, the Monaro Volcanic Province is in places interspersed with rocky hills corresponding to either volcanic plugs or exhumed Paleozoic substrate. In the latter case, granitic and sedimentary bedrock yields leached podsols and lithosols, respectively (Costin, 1954, Taylor and Roach, 2003).

The Monaro is also climatically unique in that it is the only subregion of the South Eastern Highlands to be impacted by the SM's interception of the SHWW (Slattery, 2015). The eastward descent of foehn winds over the leeward Monaro means the region experiences the driest conditions in Australia east of the Great Dividing Range, with

annual rainfall ranging between 450–700 mm (Fig. 1.7c), dramatically less than that the SM alpine zone. This orographic effect is strongest in the central-western Monaro around the locality of Arable and deteriorates both westward towards the SM and eastward towards the coast (Sahukar et al., 2003, Pickering and Venn, 2013, Xu and Hutchinson, 2013). The rain shadow also peaks in intensity during winter and autumn, when the SHWW reach their northernmost extent, while their poleward retraction in summer and spring facilitates an inland incursion of southeasterly humid air from the Tasman Sea (Brereton et al., 1995). This warm-season wind reversal imposes a second, albeit weaker, easterly rain shadow due to maritime systems being obstructed by the Kybeyan Range (Slattery, 2015). This seasonal orographic 'seesaw' reinforces the Monaro's moderately arid climate which, in combination with relatively cold annual temperatures (-1–11 ºC), produces marginal growing conditions (Taylor and Roach, 2003).

The region is consequently characterised by a savannah-like mosaic of open grassland and grassy woodland (Fig. 1.7, 1.8) (Costin, 1954). This ecology has presumably defined the Monaro for several million years, as Cenozoic paleozoological and palynological evidence indicates the rain shadow has persisted since at least the Miocene (Taylor and Walker, 1986, Ride et al., 1989, Sahukar et al., 2003, Dorrough et al., 2004). The prolonged existence of this ecosystem is reflected in the geographic name itself, which is a European adaptation of that used by the Ngarigo people, the Traditional Owners of much of the region (Maneroo, meaning 'big plain') (Sydney Morning Herald, 1858). While therefore predating human occupation, it is likely that this savannah has been expanded by Indigenous landscape opening (see Section 1.4.4). Regardless, this macroecology is not monotonous, being complicated by lithological and thus pedological heterogeneity.

Specifically, where mafic clay soils prevail, these typically support tussock grassland comprising an alliance of *Poa siberiana*, kangaroo grass (*Themeda australis*), wallaby grass (*Danthonia* sp.) and spear grass (*Austrostipa scabra*). These species collectively define an ecological community known as Natural Temperate Grassland of the South Eastern Highlands ('Temperate Grassland') (Fig. 1.7, 1.9a) (Costin, 1954, Sahukar et al., 2003, Department of the Environment and Energy, 2016). Conversely, the shallow podsols and lithosols overlying Paleozoic bedrock are generally associated with grassy woodland hosting an association of *E. viminalis*, *fastigata*, *globulus, rubida* and *pauciflora* (Fig. 1.7). The latter two species are keystone members of another community

known as Monaro Tablelands Cool Temperate Grassy Woodland ('Grassy Woodland') (Fig. 1.9b) (Costin, 1954, Sahukar et al., 2003, NSW TSSC, 2019).

Another unusual product of the Monaro's unique climate and geology is its 215 lenticular lakes ('the Monaro lakes') (Fig. 1.9c), 90% of which are emplaced partially or exclusively on the Monaro Volcanics (Benson and Jacobs, 1994) (Fig. 1.7). This strong spatial correlation has been attributed to solution weathering of the basalt regolith and aeolian excavation of the resultant basins. The significance of wind as an erosional agent is supported by ~65% of lakes being emplaced on the interfluve or flanks of the Monaro Range (Pillans and Walker, 1995, Taylor and Roach, 2003, DCCEEW, 2015b). Those lakes occurring on basalt are thus situated on heavy smectite that effectively impedes

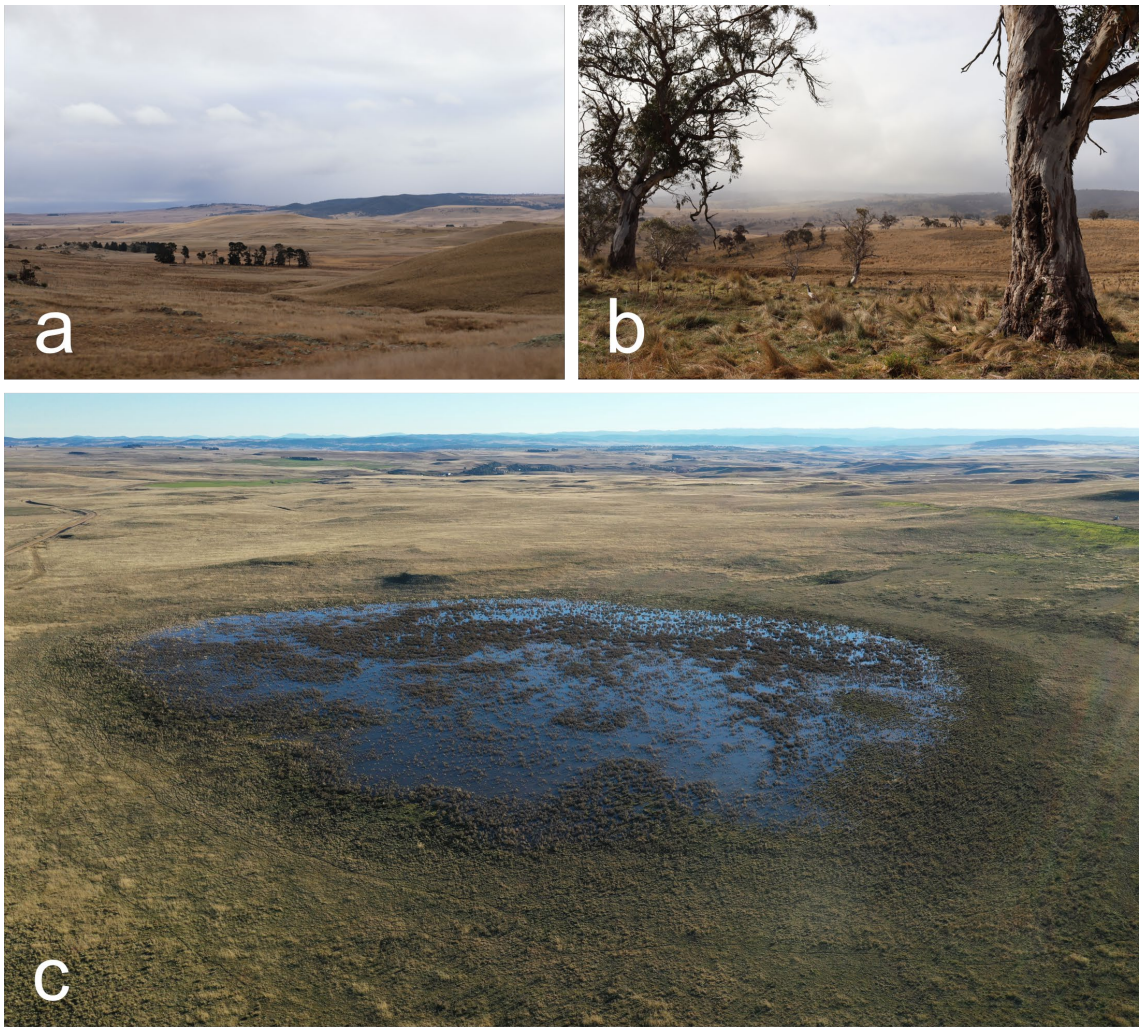

Figure 1.9. The main ecological components of the Monaro, each corresponding to a threatened ecological community. Displayed are **a)** tussock grassland on the basaltic terraces of the central Monaro (personal photograph, 2022), **b)** eucalypt grassy woodland in the eastern Monaro (personal photograph, 2022), and **c)** Boundary Lake, an archetypal example of the Monaro lakes (photograph by Lachlan Ingram, 2021).

groundwater seepage. Lakebed impermeability, in conjunction with endorheic drainage, renders the Monaro lakes pluvial and thus hydrologically seasonal given the highly variable and limited orographic rainfall regime (Benson and Jacobs, 1994, Hobbs et al., 2016).

However, the Monaro lakes vary widely in their degree of hydrological permanence, which refers to the duration and continuity of lake inundation. This is largely a function of basin depth, with deeper basins tending to be more perennial due to their capacity to retain larger volumes of water less vulnerable to evapotranspiration, which buffers the effects of drought. Benson and Jacobs (1994), surveying 64 of the Monaro lakes, classify each as either permanent (rarely dry), intermittent (seasonally dry) or ephemeral (frequently dry), finding each class to be associated with specific floral assemblages (Fig. 1.7g). As such, lake permanence is a major control on basin ecology. While permanent basins tend to host algae and deepwater macrophytes, intermittent and ephemeral systems are typified by shallow sedge-herb-grass associations, due to these latter two classes being shallower and more prone to drying and terrestrial plant encroachment (Benson and Jacobs, 1994).

Irrespective of these floristic differences, all lakes constitute a subgroup of an ecological community known as the Upland Wetlands of the New England Tablelands and the Monaro Plateau ('Upland Wetlands') (Department of the Environment and Heritage, 2005). The Monaro lakes also support a diversity of diatom flora owing to their moderate to high alkalinity (pH 7.4–9.6), a rare geochemical feature in Australian lakes and one attributable to leaching of $NaHCO_3$ (sodium bicarbonate) from the alkali basalt (Williams et al., 1970, Pillans and Walker, 1995, Richardson and Caldwell, 2002). While the composition of these diatom communities varies substantially between lakes, being richer in less turbid, more permanent lakes, they are surprisingly cosmopolitan and comparable to analogous alkaline lake ecologies globally, despite their remoteness (Richardson and Caldwell, 2002).

1.3.3. Impacts of historical and contemporary climate and land use change on the Snowy Mountains

As demonstrated in Section 1.3.1, the high bio- and geodiversity of the SM is attributable to a fragile nexus of climate, topography and ecology, the inextricability of

which risks systemic destabilisation upon perturbation to any one component. For the SM, human agency is the unequivocal propagator of such destabilisation, manifesting historically as European pastoralism (and prehistorically as Indigenous occupation; see Section 1.4.4) and being perpetuated by inherited and novel stressors, including climate change.

The subdued elevation of the SM is foundational to its heightened biophysical sensitivity as it results in highly restricted zones. This is most apparent for the alpine zone, which occupies just 0.0001% (~1286 km^2) of continental area and, as such, is one of the smallest alpine areas globally (Costin, 2000, Pickering, 2007, Gallant et al., 2009). Low elevation also means alpine biota are functioning near their maximum temperature thresholds and are therefore disproportionately threatened with extinction under anthropogenic warming (Pickering et al., 2008). This is compounded by the absence of a nival zone and deep valley dissection of the alpine and subalpine zones, which respectively prevent the altitudinal and lateral retreat of taxa to climatic refugia (Williams and Wahren, 2005, Mason and Williams, 2013c). Especially vulnerable are alpine endemics and species confined to the eastern flanks of the SM, the gentler relief of which translates to higher climate change velocity.

Consistent with the continental average, the SM warmed by 1.4 ºC between 1950–2024, at a rate of 0.2 ºC per decade (Grose and Hennessy, 2024). This is concerning given warming of even 3 ºC would be sufficient for a total conversion of alpine to subalpine conditions (Green et al., 1992). With warming of up to 2.6 ºC and 5 ºC projected for the alpine zone by 2050 and 2100, respectively, total disappearance of a true alpine climate is likely within 50 years, irrespective of a business-as-usual or even limited mitigations scenario (Hennessy et al., 2008, Harris et al., 2016, Hoffmann et al., 2019). However, the shift to a subalpine climate is not anticipated to be replicated ecologically, at least not instantaneously. Converse to many Northern Hemisphere mountain taxa, 91% of SM alpine plants have not physiologically adapted to warming since 1890 (Soudzilovskaia et al., 2013, Sritharan et al., 2021).

Inertia is also apparent along the SM treeline, which has not observed any considerable upslope advance in the historical period (Wearne and Morgan, 2001). This is in contrast to observations by Harsch et al. (2009) and Hansson et al. (2021) that treeline rise is apparent across most mountains globally. Ecotonal stability is surprising, given global warming has already rendered the lower 100 m of the alpine zone climatically suitable

for the establishment of subalpine vegetation (Green and Venn, 2012). Treeline stasis has been ascribed to low upslope dispersal rates of *E. pauciflora* due to a lack of dispersal methods, and increased burning under warming and drying (Green, 2009, Slatyer, 2010, Naccarella et al., 2020).

These stressors are being superimposed on widespread dieback of *E. pauciflora* occurring since 2017 due to outbreaks of the wood-boring longicorn beetle (*Phoracantha mastersi*) (Fig.1.10a), which consumes the woody stem of its host as deep as the inner phloem. While the catalyst of these infestations remains enigmatic, current hypotheses implicate warming and drought stress, the former being of particular concern given the upslope expansion of outbreaks is currently inhibited by colder temperatures (Ward-Jones, 2021, Brookhouse et al., 2024, Bryant et al., 2024). Due to these barriers to treeline migration, it has been observed that *E. pauciflora* is instead encroaching at an increasing rate into frost hollows, where alpine microclimates are disappearing (Fig. 1.10b) (Wearne and Morgan, 2001, Pickering, 2007).

Figure 1.10. *E. pauciflora* dieback is pervasive across the subalpine and upper montane zones (**a, b**; background) but not significant in the montane zone proper (**a**; foreground), where fire is the predominant stressor due to high postcolonial eucalypt density). Frost hollows such as Diggers Creek (**b**) are potentially at risk of downslope treeline advance. Personal photograph, 2023, 2024).

The impacts of treeline stability on abiotic functions such as soil formation, hydrology and fire are complex, given these factors are dependent not solely on vegetation but also climate, which is changing despite the treeline. However, the trajectories of such biophysical processes along the alpine-subalpine ecotone remain unexplored to date. In lieu of a treeline 'vanguard', it is anticipated that the upslope invasion of vegetation will instead be pioneered by introduced weed species, which were numbered at 175 by Johnston and Pickering (2001). Critically, 83% of invasive plants surveyed by McDougall et al. (2005) are thermally confined to beneath the snowline at the subalpine-montane ecotone. This implicates snow cover as the limiting factor in the ascent of alien flora, which will thus be enabled by its projected decline.

Indeed, assuming a high-emissions trajectory to 2050, climate models anticipate a 97% reduction in the area observing ≥60 days of snow cover yr^{-1}, a reduction in total snow volume by 62% and a vertical displacement of the snowline by up to 570 m. Declining snow cover is ascribed to both a reduction in annual precipitation (up to 40 mm by 2060–2079) and the shift to a rainfall-dominated regime (Hennessy et al., 2003, Hennessy et al., 2007, Love et al., 2019). Snow decline represents a continuation of historical trends, with spring thaw already occurring on average two days earlier per decade since 1954 (Hennessy et al., 2007). This is partially due to an 18% reduction in cool-season rainfall between 1980–2011 alone, which Fiddes and Pezza (2015) relate to a southward displacement of the SHWW and an intensification of the subtropical ridge. A consequential reduction in precipitation and thus snowfall has already significantly impacted mountain hydrology; Theobald et al. (2016) calculate that the number of precipitation days capable of contributing flows to SM catchments decreased by an average of 1.4 days per decade between 1958–2012.

Future snowfall declines will increase the area above the present snowline hospitable to exotic flora, 92% of which germinate from seed and are thus dispersing rapidly (Johnston and Pickering, 2001). While there is no evidence that climate change has enabled upslope migration of invasive plants anywhere in the AA, this is probable as warming accelerates (McDougall and Broome, 2007, Slattery, 2015). Invasion will exacerbate competition with native plants, the most vulnerable among which are those dependent on snow for summer moisture (e.g., short alpine herbfield) (McDougall et al., 2005, Pickering, 2007, Pickering et al., 2014). The synergy of warming, drying, snow cover decline and weed invasion are recognised as paramount agents of decline in alpine

communities. Two such communities – Snowpatch Herbfield and Windswept Feldmark in the Australian Alps Bioregion – have thus been state-listed as critically endangered Threatened Ecological Communities (TECs) in the last decade (NSW TSSC, 2015, NSW TSSC, 2018).

Due to it being closer to its thermal limit of tolerance, as well as the frontline of exotic invasion, the Snowpatch Herbfield TEC has observed particularly steep decline in recent decades. As such, it is argued by Bergstrom et al. (2021) to be one of 13 Australian terrestrial ecosystems undergoing ecological collapse, which the authors define as a "potentially irreversible change to ecosystem structure, composition and function" (p. 2). Given the vast majority of invasive plants in the SM are annual or biennial forbs, their replacement of alpine perennials will facilitate extensive exposure of soils due to annual to interannual die-off (McDougall et al., 2005). This will exacerbate hillslope erosion, which is already projected by to increase by up to 18% by 2060–2079 due to more intense rainfall and snowmelt events alone (Zhu et al., 2020). Erosion, in turn, threatens to reduce the carbon storage capacity of alpine organosols, which endowed the SM with among the highest pre-clearing soil organic carbon stocks in NSW (Gray et al., 2016).

The abundance of exotic flora in the SM is attributable to European introductions, both deliberate and inadvertent, since colonisation in the 1820s (Mooney et al., 1997, Costin, 2000). From this time, squatters began driving stock from into the SM from the adjacent Monaro to graze sheep and cattle (Hancock, 1972, Slattery, 2015). While this was initially for relief from drought on the Monaro, grazing quickly became seasonal in the SM, with warm-season herding of stock penetrating into high alpine areas by the 1860s and remaining completely unregulated until 1889 (Hancock, 1972, Scherrer and Pickering, 2001, Mooney, 2004). Despite grazing being policed after this time through the issuing of 'snow leases', sheep and cattle were still freely ranged at high stocking rates (reaching ~550,000 head in drought years), which accelerated weed dispersal along stock routes (Newman, 1954, King, 1959).

While weed proliferation was rapid, it was the more immediate impacts of sheet and channel erosion, initiated by livestock grazing, trampling and pugging, that prompted the termination of leases above ~1400 m in 1958, 14 years after the founding of Kosciuszko State Park (King, 1959, Clark, 1992). Grazing was progressively restricted until complete prohibition two years after the establishment of Kosciuszko National Park in 1967, the boundaries of which initially excluded much of the montane zone on account of its

commercially viable stands of *E. delegatensis* (Costin, 1954, Bryant, 1971, Mosley, 1989). Abolishment was highly effective at stabilising slopes, with Stromsoe et al. (2016) calculating erosion rates of 60 ± 220 t km^{-2} yr^{-1} during the late- to post-grazing period (1915–2015), dramatically below peak grazing rates of 460 ± 220 t km^{-2} yr^{-1} computed by Costin et al. (1960). Erosion mitigation yielded obvious benefits for soil and ecological rehabilitation, though grazing prohibition was less motivated by conservation interests so much as alpine catchment stabilisation for construction of the Snowy Mountains Hydroelectric Scheme in 1949 (Costin, 1957, Clark, 1992, Good, 1992). A lack of conservation emphasis is encapsulated by the deliberate planting of 23 invasive species as part of rehabilitation efforts, selected for their high adaptability to SM climate. This trait has resulted in 20% of invasive plants becoming naturalised in the region (Clothier and Condon, 1968, Johnston and Pickering, 2001, McDougall et al., 2005).

Despite 80 years elapsing since the cessation of grazing in Kosciuszko National Park, a diversity of exotic fauna persist as feral mammal populations inherited from colonial-era introductions, the most detrimental being rabbits, foxes, pigs, deer and especially horses (Pickering, 2007, Slattery, 2015). Present in the AA since 1843, and established as a feral species since the 1890s, the horse (*Equus caballus*) is the salient active faunal stressor in the bioregion, continuing the legacy of livestock by removing riparian and terrestrial vegetation and reactivating erosion even in rehabilitated catchments (Dyring, 1990, Worboys and Pulsford, 2013, Scanes et al., 2021). As large ungulates, horses are particularly damaging to mires, which are an attractive source of water and palatable vegetation (e.g., *C. gaudichaudiana*) (Robertson et al., 2019). In pursuit of these resources, horses strip groundcover, sink into and dislodge peat, and collapse streambanks (Fig. 1.11a) (Worboys and Pulsford, 2013, Robertson et al., 2019, Wilson et al., 2022).

The outcome of this is the reduced hydraulic conductivity of, and increased outflow from, peatlands. More punctuated flows exacerbate the erosivity of downstream runoff, thereby increasing turbidity and sedimentation in rivers, lakes and reservoirs (Worboys and Pulsford, 2013, Robertson et al., 2019). Within peatlands, stream incision lowers the water table and encourages desiccation already initiated by warming, drying and amplified burning (Fig. 1.11b) (Worboys and Pulsford, 2013, McDougall et al., 2023). Drying is also reinforced by exposure of the peat surface, which accelerates decomposition and compromises the carbon-storing capacity of the peatland (Treby and Grover, 2024). This threatens to convert many mires from carbon sinks to sources, a

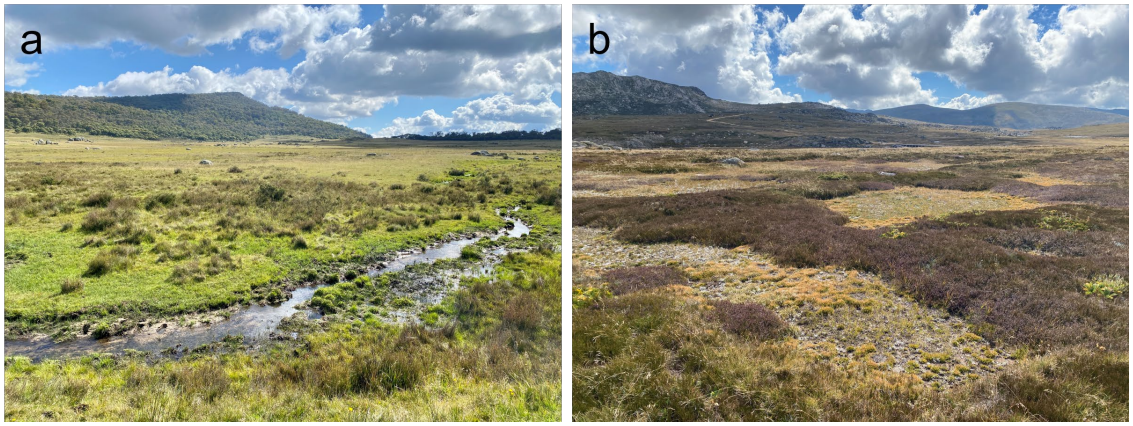

Figure 1.11. a) A montane *Empodisma* moor on Botherum Plain, which has been heavily grazed and pugged by feral horses. **b)** A desiccated ombrotrophic *Sphagnum* bog near the headwaters of the Snowy River, showing relict, terrestrialised pond-and-hummock features. Personal photograph, 2023, 2024.

transition already being realised for many horse-impacted sites. Treby and Grover (2023) observe that carbon emissions from bogs with peat surfaces exposed by horses were up to 91% higher than those retaining *Sphagnum* coverage. In addition to direct removal, horses also impact mire vegetation though inputs of N and P via excrement, which can exceed the tolerance thresholds of native oligotrophs (Treby and Grover, 2024). Excess nutrients are beneficial for many exotic weeds and thus encourages their encroachment, which is simultaneously enabled through the translocation of seeds by traversing horses (Pickering et al., 2010).

These impacts are worsening in spite of piecemeal attempts to reduce horse populations in Kosciuszko National Park, which have increased by an average of 23% yr^{-1} since 2003 to ~18,814 individuals in 2023 (Office of Environment and Heritage, 2023). Damage to peatland ecology and structure has been so pervasive that recovery is anticipated to require decades and millennia, respectively, given slow vegetation and peat growth rates. However, this prognosis assumes a stable climate, and so damage to many mires is deemed irreversible considering climate change (Good et al., 2010, Driscoll et al., 2019, Robertson et al., 2019, Wilson et al., 2022). Due to the impacts of historical and contemporary grazing, SM peatland area has declined by 30% over the European era (French et al., 2016). All mires are thus recognised as endangered under the federal TEC listing of the Alpine Sphagnum Bogs and Associated Fens community (TSSC, 2008).

Alongside erosion and species invasions, the third prevailing impact of colonial-era grazing was the indiscriminate burning of vegetation by snow lessees (Newman, 1954).

Pastoral ignition was particularly prevalent in the montane zone, where intense 'hot burns' were annually applied to eucalypt forests in summer and autumn to thin the tree stratum, drain mires and produce 'green pick' palatable to livestock (Banks, 1989, Zylstra, 2006). This resulted in rapid and widespread dieback of mature stands of *E. delegatensis* (Byles, 1932, Zylstra, 2006). However, the abrupt termination of burning after the cancellation of leases from 1969 permitted extensive regeneration of even-aged stands of *E. delegatensis*, with postcolonial fire suppression increasing forest density relative to the precolonial baseline (Fig. 1.10a) (Mooney, 2004).

Densified forest has exacerbated the montane fire regime, with closer trees enabling a more effective passage of fire. This is being reinforced climate change and the high flammability of the post-fire coloniser *E. delegatensis*. Zylstra (2018) observes that juvenile stands are eight times more likely to burn than mature stands, but less likely to survive repeated fire due to the increased risk of crown death. A warmer and drier climate is therefore inducing a self-reinforcing trend of more frequent fire, leading to widespread dieback of juvenile *E. delegatensis*, which require 20 years without fire to reach reproductive maturity. A critical transition is in turn expected to be crossed, whereafter forest will be replaced by open grassy shrubland (Bowman et al., 2014, Bassett et al., 2015, Zylstra, 2018). This is already being observed in certain areas, where fire is too severe for mature stands to survive and recurrence intervals are too short for juvenile stands to mature (Hoffmann et al., 2019).

While the decline of Ash-type montane forest has not prompted any formal TEC listing, it is recognised together with subalpine woodland as another collapsing ecosystem by Bergstrom et al. (2021). This positive flammability feedback has contributed to unprecedented fire extent, frequency and severity across the AA; 85% of the bioregion burned between 2002–2013 alone, with some areas burning up to three times during this period (Bowman et al., 2014). Such rapid fire return intervals represent a dramatic departure from the precolonial baseline of one or two events per century (Williams et al., 2008). Fire weather will intensify under continued climate change, with the number of spring 'Very High Fire Danger' days expected to increase by 250% under a high-emissions trajectory, by 2100 (Jacobs and Anderson, 2016).

Since the conclusion of pastoralism in the SM, the major industry has been tourism, which wavers seasonally between hiking, camping and mountain biking in summer and snowsports in winter (Pickering et al., 2003a). There are four snowsports resorts in the

SM, all of which are mostly in the subalpine zone. As such, the construction and expansion of ski runs and infrastructure (e.g., roads, accommodation, etc.) necessitates the clearing of large tracts of grassy woodland, fragmenting it into isolated refugia with heightened vulnerability to aforementioned stressors (e.g., fire and *Phoracantha*-induced dieback). The disposal of untreated human waste from ski resorts and villages has also resulted in nutrient enrichment of soils and waterways, reinforcing horse impacts (Good, 1995, Pickering and Hill, 2003). However, summer activities more directly degrade soils, with compaction and erosion arising from even moderate off-track hiking and camping (Pickering et al., 2003b, Growcock, 2006). Such practices also negatively impact plant ecology, with evidence of reduced groundcover height, coverage and biodiversity in subalpine areas exposed to hiking and biking (Pickering et al., 2011).

1.3.4. Impacts of historical and contemporary climate and land use change on the Monaro Tablelands

Converse to the SM, the Monaro has remained a predominantly pastoral district since European settlement, consequently experiencing a more prolonged history of European land use change. Following colonisation in 1823, the Monaro was rapidly populated by illegal squatters from Sydney seeking to graze the vast open downs (Currie, 1825, Lhotsky, 1835). An unregulated land and stock boom ensued until the 1840s, by which time most of the Ngarigo had been forcibly removed and the seasonal transhumance of stock into the SM was well established (Hancock, 1972, Slattery, 2015). Given the tablelands' climatic unfavourability for cropping or dairying, livestock products, particularly wool, became increasingly central to the regional economy, with paddocked, high-intensity grazing commencing from the 1870s (Hancock, 1972, Lawrence and Davies, 2011, Cook, 2021).

Due to its agricultural significance, the Monaro is not afforded the same conservation protections provided by the national park listing of the SM (Fig. 1.7e), hosting seven reserves totalling only 39 km^2 (Environment and NSW, 2008). As such, most of the highland has been continuously grazed for two centuries and exposed to myriad associated stressors. Principal among these was clearing of grassy woodland through hot burning and ringbarking, which was advocated for by the Department of Agriculture as an inexpensive means of expanding pasture (Hancock, 1972). Eyles (1977) implicates

ringbarking, burning and grazing in the widespread channel entrenchment of chains of 'scour' ponds once abundant across the broader South Eastern Highlands, which have converted to permanent streams and erosion gullies. Costin (1954) also observed widespread gullying on the Monaro specifically, attributing it to the same land uses.

Intensive non-rotational grazing has also engendered severe ecological decline. Selective consumption of the seed heads and flowers of native grasses by domestic stock has initiated population decline in Temperate Grassland (Dorrough and Ash, 2003). This has been compounded by the deliberate sowing and livestock dispersal of exotic grasses, herbs and legumes, which, facilitated by artificial nutrient enrichment, have outcompeted native species in many areas. Native intolerance of these stressors under even mild grazing regimes explains the positive correlation between the ratio of exotic to native taxa and grazing intensity (Dorrough et al., 2004). Grazing relies on a patchwork of intact Temperate Grassland and an increasing proportion of 'modified pasture', defined as comprising a significant exotic component and now representing one third of the Monaro's grazing land (Fig. 1.7e) (Dorrough and Ash, 2003, Australian Bureau of Agricultural Resource Economics Sciences, 2024). In modified pasture, replacement by alien flora has reduced not only native species richness but also aboveground biomass and soil carbon stock (Orgill, 2016, Brown and Ingram, 2021).

The precolonial distribution of intact Temperate Grassland has retract by >90% during the European era, existing now as fragments rarely exceeding 0.1 km^2; it is therefore federally recognised as a critically endangered TEC (TSSC, 2016). Grazing has also severely degraded the Upland Wetlands community, which is state-listed as an endangered TEC (NSW TSSC, 2005). This listing recognises grazing, trampling and weed competition as the prevailing stressors (Fig. 1.12), though other impacts are emerging as agriculture intensifies, notably the in-wash of herbicides and fertilisers and the draining of lakes such as the largest Beards Lake (Benson and Jacobs, 1994).

Similar threats are also recognised for the Grassy Woodland community, which as of 2019 had been reduced to only 5% of its precolonial area (NSW TSSC, 2019). While this is predominantly due to ringbarking and burning, retraction is being perpetuated by ongoing browsing of the ground stratum by livestock and smaller herbivores such as rabbits. This has inhibited regeneration of the tree stratum and facilitated replacement of the tussock understorey with exotic taxa, particularly in smaller refugia where edge

Figure 1.12. Livestock grazing occurs down to the strandline even during wet phases for the Monaro lakes, as apparent at Racecourse Lake (**a**). This results in in heavily pugged shorelines, as evidenced at Lake Jillamatong (**b**). Personal photograph, 2023.

effects are stronger. Grassy Woodland is therefore state-listed as a critically endangered TEC (NSW TSSC, 2019).

Another threatening process identified in the listings of all three described TECs is climate change. While the broader South East and Tablelands district warmed on average by ~0.8 ºC by 2014 relative to 1990–2009, the Monaro specifically observed no significant change in rainfall between 1980–2011 (Fiddes and Pezza, 2015, DCCEEW, 2024a). However, future changes in these variables will be more perceptible; the Monaro is projected to observe 3.5–3.7 ºC warming by 2100 under a high-emissions scenario, accompanied by a decline in annual rainfall (DCCEEW, 2024b). Drying is anticipated to be spatially and seasonally variable; while winter decreases are predicted for the entire Monaro, these will be greatest in the southeast (≤-36%), which will also observe summer declines despite mild increases (≤7%) elsewhere (DCCEEW, 2024b). Changes in precipitation amount and seasonality are largely ascribable to future increases in the frequency and amplitude of ENSO (exacerbating drought) and an increasingly positive SAM (reducing winter rainfall), with the geographic discrepancies in rainfall change

being a product of the orographic effect (Lim et al., 2016, Deng et al., 2022, Lieber et al., 2024, Thirumalai et al., 2024).

The number of severe fire weather days will also increase across much of the Monaro due to warming, drying and increased warm-season rainfall, the latter increasing fuel loads (DCCEEW, 2024a). This threatens flammable remnants of Grassy Woodland, especially given much of the TEC persists in the more mesic southeast, where drying will most severe. This is problematic given recent dieback of the keystone *E. viminalis*, which expanded to 2000 km^2 within eight years of detection in 2005 (Ross and Brack, 2015). While the proximal cause of dieback has been identified as infestations of and defoliation by the eucalyptus weevil (*Gonipterus* sp.), it has been proposed that colonial pasture 'improvement' and fire suppression, in concert with increasing drought length and frequency, are lowering *E. viminalis* resilience to *Gonipterus* outbreaks. Infestations themselves worsen when water-stressed trees replace consumed foliage with more palatable young growth, killing the tree (Ross and Brack, 2015, Upper Snowy Landcare, 2015, Jurskis, 2016). In view of decline in all three TECs, the Monaro has been identified by Bergstrom et al. (2021) as a third and final collapsing ecosystem on the High Country.

1.3.5. Socioeconomic impacts of environmental change on the High Country

As a biophysically unique region of Australia, the High Country is a vital source of ecosystem services, many of which are rare on the continent. This means the socioeconomic impacts of environmental decline are likely to be disproportionately high. Arguably the most valuable of the High Country's ecosystem services is its provisioning of water to southeastern Australia, with the AA alone contributing ~29% of flows to the Murray-Darling Basin and $9.6 billion to the national economy (2011 values) (Worboys and Roger, 2011, Worboys, 2015).

Much of this monetary value is attributable to the Snowy Mountains Hydroelectric Scheme, which supplies a significant proportion of the east coast's renewable energy (32% in 2018) and diverts flows for irrigated agriculture in the Murrumbidgee and Murray River catchments (Sahukar et al., 2003, National Museum of Australia, 2024). Most water used by the scheme is sourced from snowmelt and groundwater from organosols and peatlands, which filter out sediments and limiting nutrients (Wilson et al., 2022).

Decreased precipitation and snow cover, alongside an increase in the number of deteriorating catchments (n. 42 in 2015), is poised to significantly reduce the utility of the SM and broader AA as a water tower for southeastern Australia (Worboys, 2015).

As intimated, SM peatlands are also one of the most effective archives of carbon on the continent, storing more soil organic carbon than even alpine organosols (Wilson et al., 2022). The impending regional shift in peatlands from carbon sinks to sources therefore threatens to reinforce the positive global greenhouse feedback, undermining Australia's emissions reduction targets (Grover et al., 2005, Grover and Baldock, 2012, Hope and Nanson, 2015). Impaired carbon sequestration is also the greatest socioeconomic repercussion of subalpine dieback and montane megafires, which will increase emissions via combustion, soil erosion OM decomposition (Tulau and McInnes-Clarke, 2015). However, current and potential greenhouse emission contributions from the decline of SM peatlands, soils and forests collectively have not yet been quantified.

Environmental degradation is also expected to disrupt the AA tourism industry, which is valued at $40 billion and is foundational to local businesses (Pickering, 2007). The most obvious impact on tourism is declining snow cover, which is projected to reduce ski season length by 100 days under the worst-case scenario by 2050 (Pickering, 2007). This will adversely impact winter tourism revenue, 70% of which is contributed by snowsports (Morrison and Pickering, 2013). While snowmaking can buffer the short-term impacts of reduced snowfall, this will not be feasible by the end of the 21st century (Hennessy et al., 2008). Many businesses are therefore pivoting towards summer activities such as hiking and mountain biking (Toomey et al., 2024). However, intensification these activities is itself likely to reinforce soil contamination, weed dispersal and soil erosion, compromising the summer amenity of the region that attracts tourists.

On the Monaro, socioeconomic trajectories are more ambiguous, given grazing is increasingly reliant on exotic perennials for pasture and may therefore be somewhat insensitive to Temperate Grassland decline. In fact, modelling by Cullen et al. (2009) for southern Australia projects increases in pasture production for regions predicted to warm and dry, when the additional effects of CO_2 fertilisation are considered. If applicable to the Monaro, this would imply an increase in the profitability of wool and livestock production, which contributed to 84% of the region's gross agricultural value in 2020–2021 (.idcommunity, 2023).

However, the increases modelled by Cullen et al. (2009) are minor and are only anticipated for the study's 2030 scenario, with decreases of 19% modelled for the 2070 scenario as continued warming and drying offset the positive impacts of CO_2 fertilisation. This is more consistent with recent modelling of pasture growth rates near the southern Monaro locality of Bungarby by Alcock (2012), which projects declines in summer growth for 2030 due to warming and drying. Reduced productivity of the pastoral sector will be reinforced by hydrological changes such as reduced flows of major snowmelt-fed rivers and more frequent and prolonged drying of the Monaro lakes, especially shallower ephemeral systems. Given most of the Monaro lakes occur on private landholdings or travelling stock reserves, they represent an indispensable terrestrial water resource for watering livestock in an otherwise moderately arid highland (Benson and Jacobs, 1994).

1.4. Paleoenvironmental research on the High Country: value and a review of existing records

1.4.1. The utility of paleoscience in constraining the environmental sensitivity of the High Country

The preceding two sections demonstrate that the High Country, like all high-altitude environments, is extremely sensitive to external perturbation and, as such, is experiencing severe deterioration under GEC. However, it must be recognised that the historical record documenting climate and land use change on the High Country spans only two centuries corresponding to European occupation. While critical for investigating European land use impacts, this short observational record is limited to constraining environmental variability on up to decadal timescales. As such, it fails to capture longer-term (i.e., centennial- to millennial-timescale) responses to disruption, which are generally higher in amplitude.

A paucity of long-term data is remedied by reconstructing paleoenvironmental change from natural archives, particularly those accumulating detritus from the surrounding catchment. These materials possess environmentally sensitive geochemical and sedimentological properties that serve as proxies for various abiotic and biotic processes operating within and around the depositional locus (Gornitz, 2008). Lakes and peatlands are particularly instrumental as they offer a compromise between millennia-long

timespans (unlike tree rings and coral skeletons) and centennial to sub-centennial resolutions (unlike marine and coastal sediments) (Ruddiman, 2001, Cohen, 2003). As such, they represent the vast majority of terrestrial archives informing global paleo-research (i.e., paleoenvironmental and paleoclimatic research) (Kaufman et al., 2020).

This skew towards lake and peatland sediments is replicated for the High Country, which harbours the densest concentration of paleo-research in Australia but is almost exclusively represented by tarn and peat records (Fig. 1.14). This is due to its abundance of such archives, which are rare elsewhere on the continent due to prolonged aridity, low relief and restricted Quaternary glaciation being unfavourable to their formation. Nonetheless, the volume of Australian paleo-research has increased exponentially over the last 50 years, bridging the temporal gap between historical and long-term records (Dixon et al., 2017). On the High Country, this has allowed the paleoclimatic and paleoecological history of the region to be robustly constrained for the Holocene epoch, which spans to 11,700 years Before Present (yr BP). Synonymous with the present interglacial, the Holocene, despite its relative climatic stability, represents a valuable case study for appraising environmental sensitivity under a climate analogous to the precolonial baseline, with which the modern high-altitude environment was equilibrated (Bradley, 2008).

While the Holocene spans several millennia, the high resolution of peat and lake records on the High Country permits the abrupt impact of Europeans to be detected, rendering the Holocene the only period wherein both climate and land use impacts can be reasonably compared. A minority of High Country records also extend further into the Late Pleistocene, transgressing deglaciation, and as such offer a rare insight into environmental sensitivity to rapid climate change. This is critical in the context of contemporary GEC, especially given ecological change in Australia over the 21st century is anticipated to equal or exceed that experienced during the deglaciation, despite its rate already being unprecedented in the last several million years (Steffen, 2009). Despite the epoch's analogue potential, most studies reconstructing the Holocene on the High Country are primarily concerned with palynological or charcoal variability indicative of past vegetation and fire dynamics. This is reminiscent of the global ecological bias detailed in Section 1.2.1, which is applicable to paleoenvironmental as well as contemporary environmental research. For example, in 'Temp12K', the most extensive

database of Holocene paleotemperature proxies (Kaufman et al., 2020), pollen data represent 86% of the proxies derived from peat and lake sediment records.

Overreliance on such data is problematic in that it extends ecological bias to millennial timescales. Specifically, if biotic proxies are consulted in isolation under the assumption that they are more reliable than other proxies, large/small changes can imply high/low ecosystem sensitivity, when this may not be accurate (Birks and Birks, 2006). For example, a multiproxy study by Hamilton et al. (2019) for a Sulawesi lake record deduces biome-scale resilience to glacial-scale climate change, which undermines the pre-existing consensus of high forest sensitivity informed by leaf wax isotope data alone. Ecological biases such as these risk misinforming projections of environmental change under a uniformitarian framework. There is thus a necessity to apply a geoecological rationale to paleoscience such that biotic and abiotic changes are investigated simultaneously to achieve a more representative insight into millennial-timescale systemic sensitivity.

Indeed, Nogués-Bravo et al. (2007) recognise that, even in a contemporary context, discrete biophysical mechanisms exhibit different responses to climate change, a disparity that is likely to be more extreme on larger timescales. The dearth of geoecological praxis in paleoscience can be rectified through multiproxy analyses, which triangulate between proxies sensitive to abiotic and biotic processes, namely hydrology, erosion, productivity, pedogenesis and fire. Reduced dependence on any singular proxy permits a more holistic reconstruction of systemic variability and in turn sensitivity, if catalysts of change are known (Birks and Birks, 2006). While high-altitude paleoscience has gravitated towards multiproxy analysis in recent years (e.g., Schroeter et al. (2020), Zhang et al. (2024), Rostami et al. (2024)), it remains a chasmic knowledge gap on the High Country, with Hope et al. (2012) recognising that the preponderance of pollen and charcoal records (Fig. 1.14) is incomprehensive, advocating for incorporation of greater variety of proxies.

However, this recommendation was made only in the context of the SM, where the vast majority of available records are already clustered for reasons described above. While other proximal ranges such as the Tinderry and Kybeyan Ranges also host important (mostly peat) records, there is a paucity of data from the Monaro (Fig. 1.14). This geographic bias is resonated by Mooney et al. (1997), who argue that the current distribution of records is not only sparse but uneven, and so unrepresentative of regional geodiversity. This argument is upheld several decades later and reflects the global skew of contemporary and paleoenvironmental research towards mountains, which tend to

harbour a higher proportion of high-altitude records relative to highlands (Williams et al., 2018, National Centers for Environmental Information, 2025). At the global scale, insufficient interrogation of highlands is presumably due to their a) ecological homogeneity, b) poor record preservation conditions and c) dearth of millennial-timescale natural archives. All factors except the third are also applicable to the Monaro which, as discussed in this section, hosts viable Holocene archives.

The maldistribution of High Country records risks interpretations of millennial-timescale systemic sensitivity for the SM being extrapolated over the Monaro. Such mountain-centric generalisations fail to account for the markedly disparate climatic, physiographic and ecological conditions of the Monaro. Moreover, due to more pervasive pre- and post-European exploitation of the Monaro, much of the highland is classed as modified to highly modified, potentially predisposing it to rapid and dramatic systemic change at least in response to continued land use change (Cresswell et al., 2021). As such, there is an urgent need to constrain the long-term sensitivity of the Monaro specifically. Despite the above conceptual and spatial knowledge gaps, the available pool of paleo-data from the High Country provides a valuable reference frame through which the climatic and ecological history of the region can be understood, and against which more comprehensive insights can be contextualised.

1.4.2. Late Pleistocene to Holocene environmental history of the Snowy Mountains

While the SM was the only region of mainland Australia to have been glaciated during the Quaternary, ice cover was extremely restricted by global standards due to the range's low elevation, which placed it at the thermal limit of cryological processes (Martin, 1986b, Colhoun and Barrows, 2011). Peak ice cover during the Last Glacial Maximum – constrained by cosmogenic exposure dating to between 20,000–17,000 yr BP in Australia – is inferred to have encompassed an area of just 13 km^2 in the SM, equating to 0.3% of the area above the modern snowline. This is estimated to have comprised 13 cirque glaciers along the sheltered southeasterly aspects of the Main Range, and one short valley glacier in the upper Snowy River valley (Galloway, 1963, Colhoun and Peterson, 1986, Barrows et al., 2002). This is in stark contrast to Tasmania, where two ice caps rooted by ~450 cirque glaciers appear to have blanketed Central Plateau and West Coast Ranges.

This was due to Tasmania's higher latitude and maritime setting resulting in greater exposure to the humid SHWW. Favourable geography also explains the oldest known glacial advance in Tasmania being assigned a minimum age of 1,000,000 years ago (yr) (Colhoun and Barrows, 2011).

This well precedes the earliest evidence of glacial advance in the SM from terminal moraines, which exposure dating constrains to ~53,300 yr (Snowy River Advance). This first advance was also the most extensive in the SM, being succeeded by three progressively restricted advances occurring at 32,000 yr (Hedley Tarn Advance), 19,100 yr (Blue Lake Advance) and 16,800 yr (Mount Twynam Advance) (Barrows et al., 2001) (Fig. 1.15a). This stepped cryological deterioration culminated in abrupt deglaciation and ice-free conditions from ~15,800 yr, well preceding that for Tasmania (~14,200 yr) due to more marginal SM glaciers rapidly transgressing their climatic thresholds of permanence (Barrows et al., 2001, McMinn et al., 2008, Colhoun and Barrows, 2011).

Deglaciation exposed the only five tarns in mainland Australia: Club Lake, Lake Albina, Lake Cootapatamba, Blue Lake (Fig. 1.13a) and Hedley Tarn. All are cirque lakes except Hedley Tarn, which is instead a moraine-dammed segment of Blue Lake Creek (Fig. 1.13b, c). Perhaps due to this unique hydrogeomorphology, Hedley Tarn is the only tarn which has not been the subject of any paleo-research to date, with all others yielding among the oldest and highest resolution lacustrine sequences in Australia, as confirmed by numerous studies (e.g., Raine (1974), Martin (1986b), Dodson et al. (1994), Stanley and De Deckker (2002), Burdick (2022), Thomas et al. (2022), Mickelson (2024)).

Highly localised SM glaciation permitted periglacial conditions down to 1000 m ASL during the last glacial period. This is evidenced by widespread remnant features including fossil solifluction terraces, slope deposits, frost-shattered bedrock and blockstreams with exposure ages clustering between 23,000–16,000 yr, overlapping with the Blue Lake Advance (Colhoun and Peterson, 1986, Galloway, 2003, Barrows et al., 2004, Williams et al., 2009a). Presence of these features led Costin and Polach (1971) to infer that mean annual temperatures 8–10 ºC cooler than present would have been necessary for their genesis. This suggests subalpine conditions prevailed down to at least the base of the contemporary montane zone during the Last Glacial Maximum. This is consistent with earlier inferences from cirque floor elevation data by Galloway (1963) that the snowline was 600–700 m lower than present during this time.

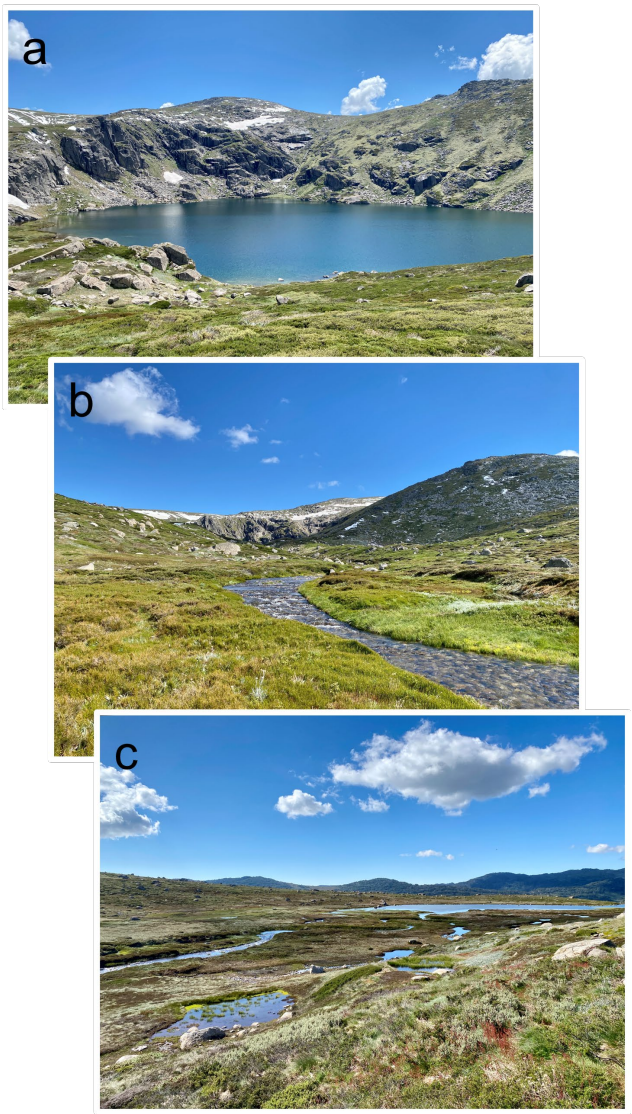

Figure 1.13. Hydrological segments of the upper Blue Lake catchment, comprising **a)** the Blue Lake cirque, **b)** the Blue Lake blockstream and fringing bogs, and **c)** the bog complex emplaced on the alluvial fan at the inlet of Hedley Tarn, dammed by a terminal moraine (background). Personal photograph, 2023.

More recent research by Barrows et al. (2022) reveals that periglacial features (scree slopes, alluvial fans and valley fills) dating to 13,000–66,000 yr are in fact ubiquitous across the broader South Eastern Highlands. This indicates that subalpine conditions defined the entirety of the High Country earlier in the last glacial cycle. An even larger area was probably subalpine over most of the Quaternary, given Slee and Shulmeister (2015) observe older periglacial deposits as north as ~30° S. In the SM, widespread periglacial deposits are theorised to have constituted the substrate on which alpine coloniser (i.e., feldmark and mire) vegetation first established following a period of rapid postglacial climatic amelioration, estimated by Raine (1974) to have occurred between 17,000–13,000 yr BP. A subsequent expansion of mires is particularly well supported by

the fact that most peat deposits cored from the SM overly inorganic gravels, sands and clays, which are interpreted as periglacial colluvial and alluvial deposits (Hope et al., 2012).

While waterlogging is a predeterminant of peat formation, low temperatures are an important secondary control as they slow rates of decomposition. Marginal satisfaction of both criteria allow peat to accumulate at rates of 2–5 cm 100 yr^{-1} in the modern AA, significantly slower than Northern Hemisphere averages (Grover et al., 2005, Hope and Nanson, 2015, Swindles et al., 2024). However postglacial amelioration permitted an optimum of sufficiently warm conditions to elevate mire productivity and sufficiently cool conditions to limit decomposition, such that peat accumulation rates were higher than present. This was facilitated by the earlier establishment of alpine communities such as feldmark, herbfield, heath and tussock grassland, which stabilised catchment slopes. A concomitant buffering of erosion enabled mire species to establish first on river flats, where saturated conditions slowed decomposition of plant litter (Hope et al., 2012). Once deglaciation was sufficient to completely terminate periglacial activity, mires expanded from these drainage lines to less topographically favourable hillsides and eventually ridgelines, initiating peatland expansion (Hope et al., 2012).

Early radiocarbon (^{14}C) dating of peats from the cirque catchments around Carruthers Peak and the upper Snowy River conveys peat initiation from as early as 17,000 yr BP, clustering around 15,000–14,000 yr BP (Fig. 1.15b) (Costin, 1972, Martin, 1986b). However, a post-deglaciation timing for initiation has since been revised with the advent of more accurate ^{14}C dating and the analysis of new records down to the montane zone, which corroborate that peat development in the SM was actually most widespread between ~11,000–8000 yr BP (Fig. 1.15b) (Martin, 1999, Marx et al., 2011). The lack of a correlation between altitude and initiation timing suggests the entire SM became suitable for peat development relatively simultaneously, probably owing to its low elevation and relief (Hope et al., 2012). An early Holocene timing for initiation has been argued to be a response to mean summer temperatures in the alpine zone surpassing the minimum threshold of mire vegetation growth (≤10 ^{o}C) several millennia after deglaciation was complete (Martini and Glooschenko, 1985, Marx et al., 2011). This new consensus is also more temporally consistent with the commencement of alpine pedogenesis between 12,000–7000 calibrated (cal) yr BP (Fig. 1.15b) (Stromsoe et al., 2016).

Postglacial amelioration is corroborated by abundant pollen records from peat as well as tarn sequences. This is true even for earlier studies arguing for Late Pleistocene peatland genesis; the first palynological investigation by Raine (1974) of a sediment core from Blue Lake concludes that nival conditions on the Main Range terminated from ~17,000 yr BP with the appearance of herbfield and feldmark taxa. These communities appear to have stabilised after a second amelioration phase from 13,000–8700 yr BP (Fig. 1.15b), following which time Raine (1974) infers treeline rise to its modern elevation based on a massive increase in pollen abundances. A two-phase model for plant colonisation is consistent with pollen analysis of records from the neighbouring Pounds Creek and Club Lake by Martin (1986a) and Martin (1986b), who determine the earliest phase of vegetation change to be colonisation of alpine desert by sparse feldmark from ~15,700–10,600 yr BP, with a dramatic increase in pollen from ~11,700 yr BP suggesting widespread nival recruitment of herbfield. This colonisation period is concluded by an apparent total replacement of feldmark by associations of grassland, herbfield and heath until ~7000 yr BP. At this point Martin (1986b), converse to Raine (1974), argues that the treeline, while rising, was probably still beneath its present elevation.

Early Holocene treeline ascent is supported by a record from Caledonia Fen, which preserves an increase in *Eucalyptus* pollen at ~11,000 yr BP and a steep decline in *Poaceae* thereafter until ~7000 yr BP (Kershaw et al., 2007). These changes are argued to reflect transgression of the treeline across the site's elevation (1280 m ASL), resulting in a replacement of subalpine grassland (Kershaw et al., 2007). As Caledonia Fen is currently in the core of the montane zone, this implies continued treeline rise well afterwards, consistent with the chronologies proposed by Raine (1974), Martin (1986a) and Martin (1986b). These changes logically postdate treeline advance to ~1000 m ASL by ~11,800 BP for the montane Micalong Swamp, which subsequently transitioned from subalpine woodland to wet forest and thus integrated into the montane zone by ~10,000 yr BP (Kemp, 1993).

Ecotonal shifts are further communicated by a record from Rennix Gap, which preserves an increase in *Eucalyptus* pollen at ~10,600 cal yr BP, coeval with the frost hollow itself transitioning from climax alpine herbfield to a subalpine bog-fen-grassland mosaic (Fig. 1.15c) (Hope et al., 2019). While treeline changes are also interpreted for the adjacent subalpine bog of Diggers Creek, this is interpreted to have occurred substantially later at ~7000 yr BP, with stability of *E. pauciflora* pollen from ~6580 yr BP

possibly indicating treeline stabilisation from this time (Martin, 1999). Curiously, the treeline shift at Diggers Creek is coincident with increased representation of the shrub genus *Pomaderris*, a typical understorey element of mesic forest. The subsequent stability of *Pomaderris* until ~4000 yr BP therefore indicates a sustained increase in moisture that is obviously too late to be attributed to postglacial amelioration (Martin, 1999). While not as dramatic as postglacial signals, this expansion of mesic taxa is replicated by many other pollen records across the SM, suggesting this was a regionally significant hydroclimatic event.

Indeed, the timing of these wetting signals overlap with a global climatic phase known as the Holocene Hypsithermal ('hypsithermal), so termed as it manifests in many Northern Hemisphere records as a period of elevated temperature due to a hemispheric peak in summer solar insolation (Fig. 1.15a) (e.g., Rossignol-Strick (1999)). However, the precise magnitude of such warming is disputed, with models estimating global temperatures were anywhere between 0.2–0.7 ^{o}C above the 19th century average (Kaufman et al., 2020). In southeastern Australia, and the Southern Hemisphere more generally, the hypsithermal appears to have manifested more strongly as a precipitation than a thermal optimum (Fig. 1.15a). Many regional pollen and lake-level records indicate an epochal maximum in rainfall between 8200–5500 yr BP (Fig. 1.15b) (De Deckker, 2022, Clerke, 2023).

In the SM alpine zone, the hypsithermal is expressed in the Club Lake and Pounds Creek records of Martin (1986b) as a replacement of pure alpine grassland by mixed grass-sedge alliances at ~7000 yr BP, attributable to increased precipitation. Martin (1986b) also observes an increase in *Pomaderris* until 4400 yr BP, overlapping with increases of the same genus by Raine (1974) at Blue Lake (Fig. 1.15c). *Pomaderris* is no longer observed around either cirque; therefore, its detection suggests a significant but transient deviation of the treeline above its modern position until the late Holocene. In addition to pollen, the hypsithermal also manifests as a reduction in charcoal at subalpine sites such as Rennix Gap (Fig. 1.15e) and Cotter Source Bog, indicating suppressed fire activity presumably due wetter vegetation being less flammable (Hope and Clark, 2008, Hope et al., 2019).

This '*Pomaderris* interval', so coined by Martin (1986b), is succeeded in the author's Club Lake record by an increase in local sedge and distal *Eucalyptus* pollen, suggesting an expansion of dry taxa above and below the treeline, respectively. This is consistent

with a late Holocene drying trend that has been reconstructed for southeastern Australia more broadly, and which is widely ascribed to a strengthening of the Walker Circulation and thus ENSO variability across the Pacific, inducing a mean El Niño-like state (Rein et al., 2005, Donders et al., 2006, Black et al., 2007, Perner et al., 2018). Post-hypsithermal climatic deterioration is also expressed at Blue Lake, which shows an abrupt decline in total pollen abundances (i.e., vegetation) after ~6000 yr BP (Raine, 1974). However, these patterns are contradicted by some subalpine records such as Diggers Creek and Rennix Gap, which convey late Holocene increases in some wet taxa (Martin, 1999, Hope et al., 2019). This elevational discrepancy may suggest that late Holocene ENSO amplification was not sufficiently pronounced at lower elevations and/or was within the tolerance ranges of less moisture-demanding plants, which may have been more responsive to the increased interannual variability than reduced amount of precipitation.

ENSO intensification appears to manifest more consistently in sedimentological than palynological proxies. This is true for micro-X-ray fluorescence data from a Blue Lake core obtained by Burdick (2022), who attributes post-6000 cal yr BP increases in Rb/Sr and K/Ti to reduced chemical weathering in the cirque under declining precipitation. ENSO is also implicated as an erosional forcing in an independent Blue Lake record from Stanley and De Deckker (2002), who quantify Holocene grain size variability in aeolian quartz. The authors identify coarsening following an interval of reduced grain size between ~7600–5500 cal yr BP (overlapping with the hypsithermal), which they interpret to be a product of an ENSO-induced aridification of the continental interior and an intensification of wind strength. Inland aridity is supported by dust flux data obtained by Marx et al. (2011) from an upper Snowy River valley peat record, which reveals a large increase in deposition from the interior after ~2000 cal yr BP (Fig. 1.15d). This is argued to reflect a poleward displacement of moisture-bearing SHWW fronts across southeastern Australia due to ENSO intensification.

ENSO forcing is perceptible in peat stratigraphy itself, with many SM records possessing lenses of sand which cap laminated peaty silts and date to ~3500–2700 yr BP. This has been argued to reflect catchment destabilisation due to poor vegetation cover as a result of increased drought and fire (Hope et al., 2012). While this inference of drying is apparently contradicted by subsequent rapid fibrous peat accumulation (and peat initiation in younger peatlands), this may in fact be reflective of a late Holocene temperature- rather than precipitation-driven shift to more favourable peat-growing

conditions, considering post-hypsithermal neoglacial cooling (Hope et al., 2012, Stromsoe et al., 2016). This supported by palynological indications of mid-late Holocene cooling, such as an apparent transient reversion to subalpine woodland at the now-montane Micalong Swamp between 4000–1900 cal yr BP (Kemp and Hope, 2014). However, such evidence is sparse and not replicated across all zones.

Late Holocene records instead corroborate two positive temperature anomalies, the first indicated by a lipid biomarker record from Club Lake to have occurred between 1500–1100 cal yr BP, involving a ~2 ºC rise in mean summer air temperature (Fig. 1.15f) (Thomas et al., 2022). This warm period has been related to intensified El Niño and temporary SHWW strengthening. The intensity of this alpine warming interval is supported by large spikes in charcoal accumulation rates (Fig. 1.15e) and the ratio of arboreal to non-arboreal pollen, indicative of increased fire activity and treeline rise, respectively (Thomas et al., 2022). Increased burning during this time is substantiated by coarsening and low OM content between ~2500–1100 cal yr BP at Lake Albina, which has been attributed to vegetation removal and erosion of exposed slopes (Mickelson, 2024). This warm period does not appear to have been confined to the alpine zone, with a record from the montane mire of Brooks Ridge Fen revealing increased charcoal influx but, conversely, reduced arboreal pollen between 1600–1300 yr BP (Mooney et al., 1997). This is inferred by the authors to reflect a diminished tree stratum due to amplified fire, which permitted an expansion of herbaceous elements and thus forest opening.

This warm period appears to have been succeeded by a second milder warming event during the last millennium, with the same Club Lake temperature record from Thomas et al. (2022) indicating warming of <1ºC between 800–400 cal yr BP. This is corroborated by a speleothem temperature record from Yarrangobilly Caves, which conveys temperatures ~0.7 ºC above the 1961–1990 mean between ~700–400 yr BP, and which is argued by McGowan et al. (2019) to have been the warmest interval in the northern SM for the last ~2100 yr. McGowan et al. (2019) reconstructs reduced snow cover during this time, though this constitutes one segment of a highly oscillatory long-term signal which suggests no long-term change in snow cover over the Common Era, despite sustained warming conveyed by Thomas et al. (2022) (Fig. 1.15f).

Both the Thomas et al. (2022) and McGowan et al. (2019) temperature records support modelling interpretations by Gergis et al. (2016) that the period from 800–400 yr was the warmest in Australasia in the millennium preceding the industrial period, with Lorrey et

al. (2008) implicating an intensification of the southwestern Pacific northeasterlies. While this second warm period appears therefore to have been a continental-scale event, it does not appear to have significantly influenced fire activity nor vegetation. Indeed, alpine sites such as Blue and Club Lake, down to montane sites Brooks Ridge Fen, Micalong Swamp and Cotter Source Bog, all suggest stable fire activity and modern floral assemblages persisting until European colonisation (Raine, 1974, Kemp, 1993, Dodson et al., 1994, Mooney et al., 1997, Hope and Clark, 2008).

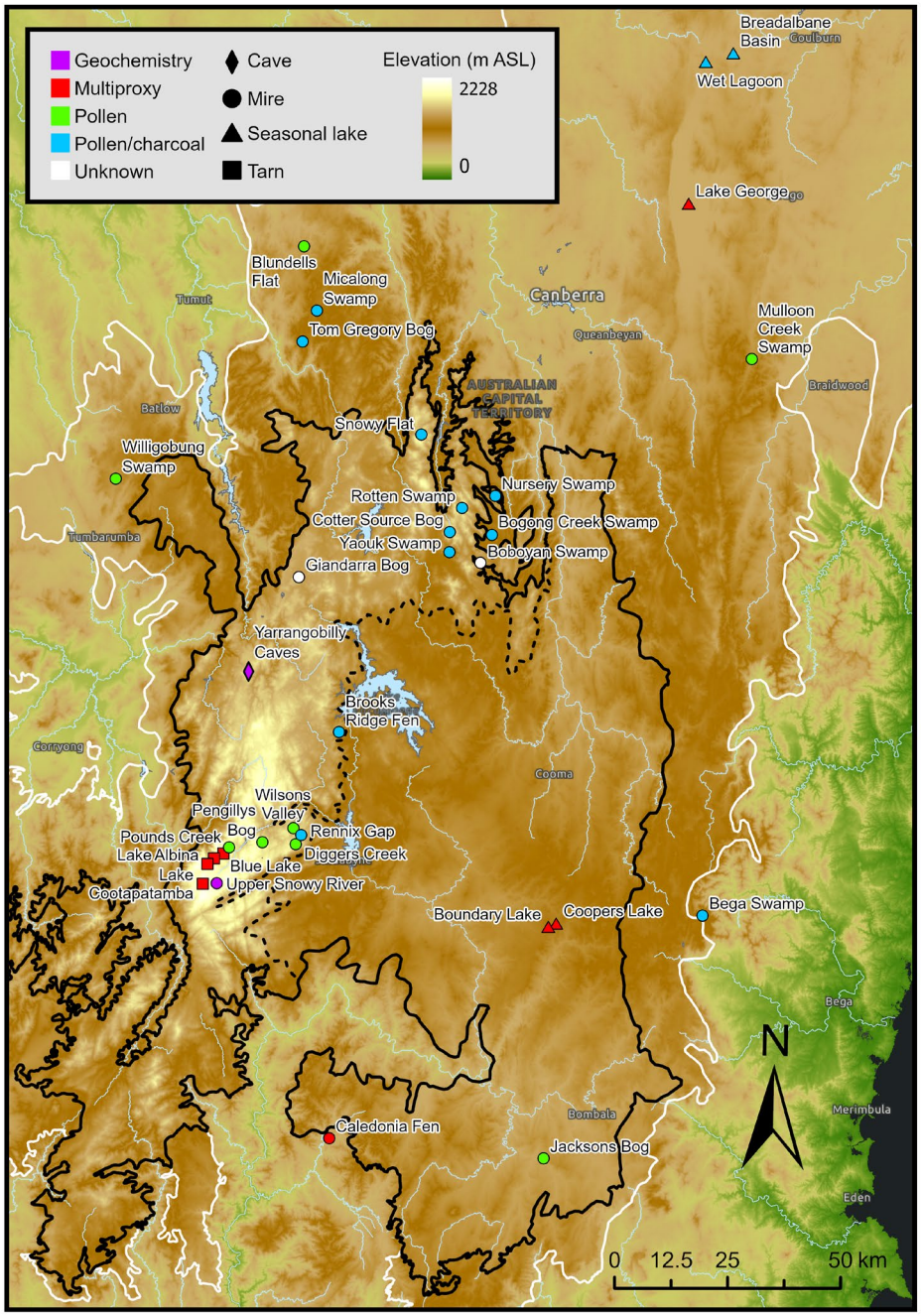

Figure 1.14. Distribution of important paleo-studies discussed in the text, distinguished by archive type and proxies investigated, based on available information.

Figure 1.15. (next page) Time-series stack of paleorecords mentioned in the text or of major relevance to this study. **a)** July solar insolation for 30° N (Laskar et al., 2004) and surface temperature data from EPICA Dome C (Jouzel et al., 2007). Black bars indicate the ^{10}Be age uncertainties of the Blue Lake and Mount Twynam Advances, with the diamond denoting the onset of ice-free conditions in the Snowy Mountains (Barrows et al., 2001). **b)** Modelled lake-level trends for Australian lakes (Clerke, 2023; Appendix A) and relative abundance of upland herb pollen for Blue Lake (Raine, 1974). Coloured bars denote the windows for the onset of Snowy Mountains alpine herbfield colonisation (blue) (Raine, 1974, Martin, 1986a, Martin, 1986b), alpine pedogenesis (brown) (Stromsoe et al., 2018) and peatland initiation (red) (Hope et al., 2012). **c)** Relative abundances of *Pomaderris* pollen for Blue Lake (Raine, 1974) and *Eucalyptus* pollen for Rennix Gap (Kemp, 1993). **d)** Dust flux for Upper Snowy River (Marx et al., 2011) and relative abundance of *Eucalyptus* pollen for Bega Swamp (Hope et al., 2004). **e)** Total charcoal counts for Rennix Gap (Kemp, 1993) and charcoal accumulation rates for Club Lake (Thomas et al., 2022). **f)** Mean summer air temperature from Club Lake (Thomas et al., 2022) and snow cover from Yarrangobilly Caves (McGowan et al., 2019). Solid vertical line denotes the approximate onset of exponential human population growth in Australia (Johnson and Brook, 2011), and dashed vertical line denotes the timing of European colonisation of the High Country (1820 CE; 130 cal yr BP). Shaded coloured intervals denote the timing of important climatic phases on the High Country specifically, these being the Last Glacial Maximum (GM), postglacial amelioration (PA), the Holocene Hypsithermal (HH), the onset of ENSO intensification (EO), and the first and second warm periods (W1 and W2) reconstructed by Thomas et al. (2022).

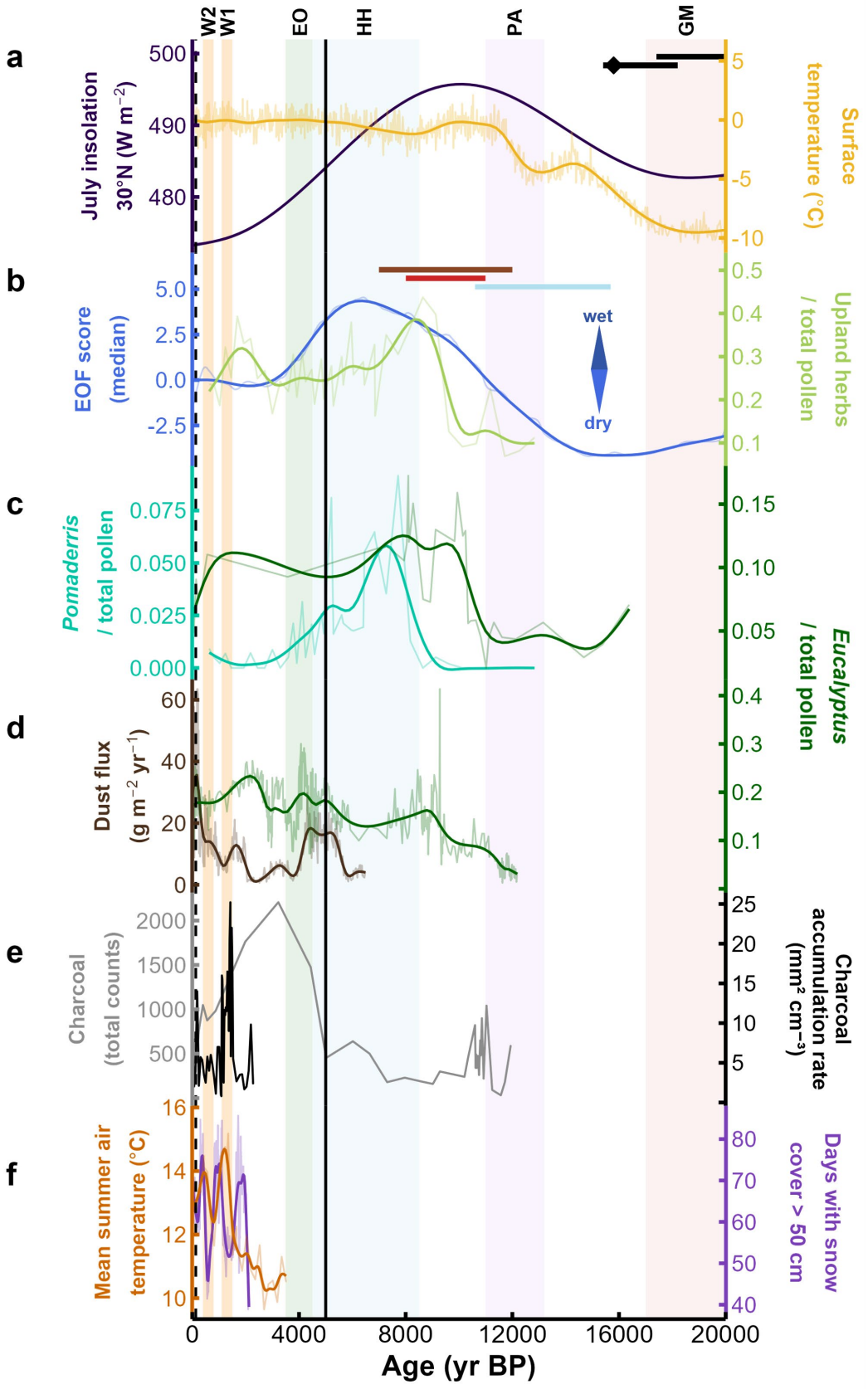
W2
W1
EO
HH
PA
GM
a
July insolation 30°N (W m⁻²)
500
490
480
Surface temperature (°C)
5
0
-5
-10
b
EOF score (median)
5.0
2.5
0.0
-2.5
wet
dry
Upland herbs / total pollen
0.5
0.4
0.3
0.2
0.1
c
Pomaderris / total pollen
0.075
0.050
0.025
0.000
Eucalyptus / total pollen
0.15
0.10
0.05
0.4
0.3
0.2
0.1
d
Dust flux (g m⁻² yr⁻¹)
60
40
20
0
e
Charcoal (total counts)
2000
1500
1000
500
Charcoal accumulation rate (mm² cm⁻³)
25
20
15
10
5
f
Mean summer air temperature (°C)
16
14
12
10
Days with snow cover > 50 cm
80
70
60
50
40
0
4000
8000
12000
16000
20000
Age (yr BP)

1.4.3. Late Pleistocene to Holocene environmental history of the Monaro Tablelands and South Eastern Highlands

It is evident, even from the inexhaustive review of paleorecords above, that the SM has been the subject of comprehensive paleo-research, resulting in a well-constrained Holocene paleoclimatic and paleoecological history. As intimated in Section 1.4.1, however, this is not true for the adjacent Monaro, which harbours very few studies of postglacial environmental change, all save one (Southern, 1982) being concerned with macroscale hydrogeomorphic change (Fig. 1.14). This is curious given one such study by Pillans and Walker (1995) validates the Monaro lakes as viable Holocene-spanning natural archives. However, it should be recalled from the previous subsection that the bulk of data obtained from the SM is palynological. This is not coincidental; climatically prescribed vegetation and good conditions for pollen preservation render the SM an optimal case study for investigating long-term vegetation dynamics. In contrast, a relatively monotonous highland ecology and poor preservation in the frequently dry and oxidised Monaro lakes means that paleo-research, consistent with its ecological bias, is redirected upslope.

Analysis of Monaro lake sediments by Pillans and Walker (1995) was motivated by the preliminary surveying of Pillans (1987), who observed that many lakes occurring on the Monaro Volcanics are accompanied by ~50 cm-thick, sheet-like deposits on their leeward margins. Pillans (1987) recognised that these 'lake shadows' are compositionally identical to their adjacent lake floors, both being composed of black smectite. However, analysis also revealed a marked disparity in grain size between lake shadow and floor deposits, with the upper horizons of the former and latter comprising silt-sized clay aggregates and gravels, respectively. This observation, supported by anecdotal evidence that the lake shadows accumulate during phases of drought, led Pillans (1987) to hypothesise that lake shadows are aeolian deposits genetically akin to lunettes, being produced by the deflation and downwind deposition of lake floor clays during lake exposure, which leaves a coarser lag deposit *in situ*.

Deflation is foundational to the lake evolution model subsequently developed by Pillans and Walker (1995), who attribute lake genesis to aeolian excavation of solution-weathered natural depressions in the basalt terrain. Recognising, however, that deflation is minor during modern droughts, the authors argue that more appreciable climate change must be required to sufficiently strip weathered regolith such that basins can become

hydrologically active and initiate sedimentation. This hypothesis was supported by exploratory ^{14}C dating of sequences cored from five lake floors, all of which yielded Holocene basal ages, while a lake shadow from Coopers Lake produced a maximum age of ~22,660 yr BP (Pillans and Walker, 1995). In view of these Holocene lake floor and glacial lake shadow ages, Pillans and Walker (1995) theorise that lake deflation is most severe during cold, dry glacial maxima and terminates upon amelioration to interglacial conditions. Interglacial sedimentation commences in freshly excavated basins due to the emergence of a depocenter and enhanced runoff. While deflation events do occur on interglacial timescales, these are usually minor due to lakebed exposure being too brief or localised alone lake margins, where strandlines are less vegetated and are prone to both aeolian and lacustrine remobilisation (Fig. 1.16).

Figure 1.16. Lakebed exposure is common along the strandlines of lakes such as Boundary Lake **(a)** and Racecourse Lake **(b)**. Personal photograph, 2023.

This 'solution-deflation' model for lake maturation is supported by further sampling of two lake floors by Bakis (2021), which also obtained Holocene basal ages. Importantly, this study concludes that one of these basins – Boundary Lake (Fig. 1.9c) – experienced prolonged lake floor exposure between 9000–7200 cal yr BP, resulting in pedogenesis and highly variable moisture, productivity and sedimentation. While this is incoherent with hypsithermal onset, Bakis (2021) does infer a subsequent lake filling interval peaking at ~6000 cal yr BP, consistent with the apex of the hypsithermal (Clerke, 2023). The results from Pillans and Walker (1995) and Bakis (2021) serve as proof of concept that the Monaro lakes are archives of intact sedimentary records with Holocene coverage, establishing the Monaro as an invaluable source of natural archives whose abundance is unusual among highlands globally. While the study by Bakis (2021) represents the first attempt to reconstruct basin-scale Holocene environmental variability, no other attempts have yet been made at utilising these archives to reconstruct paleoenvironmental change, rendering the Monaro a 'missing piece' in the literature.

As such, the remainder of this subsection reviews proximal paleoenvironmental studies from the South Eastern Highlands, given its comparable climate, elevation, relief and vegetation. The closest and most widely cited among these is Bega Swamp, a topogenous mire situated on the Great Escarpment ~15 km east of Nimmitabel. Here, palynological data from Hope et al. (2004) indicate an expansion of forest elements from 10,500 yr BP, probably reflecting an amelioration-induced transition from subalpine to montane conditions. This is followed by increased representation of wet ferns, heath and shrubs (including *Pomaderris*) from ~7500 yr BP, which are indicative of more mesic conditions typical of the hypsithermal. Given the proximity and equivalent elevation of Bega Swamp to the Monaro, Pillans and Walker (1995) propose that the early Holocene subalpine-montane shift at Bega Swamp implies subalpine conditions (and thus *Poa*-dominated grassland) also prevailed on the Monaro before 10,000 yr BP.

The mid-Holocene dominance of wet taxa at Bega Swamp is abruptly terminated by a dramatic increase in *Eucalyptus* pollen, indicating a transition to modern dry woodland, after ~4500 yr BP (Fig. 1.15d). This suggests a delayed response to post-hypsithermal climatic deterioration relative to SM records, with subsequent stability from ~1700 yr BP also indicating a higher degree of floristic resilience to ENSO amplification (Green et al., 1988, Hope et al., 2004, Donders et al., 2007). These mid-late Holocene trends are resonated in the only other peripheral study site of Jacksons Bog, a valley fen bordering

the southern Monaro. Here, pollen analysis by Southern (1982) indicates *Eleocharis*-type swamp sedge was abundant until ~4000 yr BP, suggesting moist conditions persisted until the late Holocene. After this time, the record indicates rapid replacement by dry *Epacris* heath and surrounding *Eucalyptus* woodland, aligning with ENSO intensification.

Farther afield in the South Eastern Highlands, another notable study site is Lake George which, despite hosting the oldest terrestrial Quaternary deposit in Australia, has been subject of only two studies addressing Holocene environmental change specifically. The earliest of these, by Singh and Geissler (1985), interprets from pollen and charcoal records that Lake George filled following ephemeral conditions during the last glacial period. The lake may have also experienced higher rainfall than present between 10,000–7700 yr BP and 6000–5000 yr BP, in moderate agreement with amelioration and the hypsithermal, respectively. This timing of amelioration is corroborated by later research from Fitzsimmons and Barrows (2010), who infer that permanent lake conditions prevailed from 10,000–8000 yr. The authors also reconstruct highstands between 6000–2400 yr BP and 700–300 yr, theorising the former to be related to the hypsithermal but offering no strong explanation for the latter.

Hydrological trends at Lake George are supported by similar patterns at nearby Breadalbane Basin and Wet Lagoon, which indicate hypsithermal-related lake-level maxima between 7400–2700 yr BP and 5000–2000 yr BP, respectively, and ephemeral conditions over the Common Era (Dodson, 1986). Interestingly, however, these lake-level changes are not accompanied by any major deviations in the pollen and charcoal data, which are highly volatile and incomparable. This indicates a higher degree of sensitivity to local variability than regional climate change, at least in the northern South Eastern Highlands.

Pollen trends are instead more congruent with early- to mid-Holocene paleoclimate among more southerly sites such as Willigobung Swamp, the only highland site on the windward flanks of the SM. Here, organic fen sedimentation is interpreted by Kemp and Hope (2014) to have commenced at ~11,800 cal yr BP. This is contemporaneous with peat formation at the overlying montane site of Micalong Swamp (see Section 1.4.3), suggesting that the earlier argument of peat initiation being simultaneous at all elevations of the SM extends to the highland domain (Kemp and Hope, 2014). A subsequent expansion of wet forest is reconstructed between ~9900–7500 cal yr BP, though it is unclear whether this is a response to amelioration or the hypsithermal, given it is

succeeded by an increase in charcoal indicative of drying from ~5900 cal yr BP. This sequence is contradicted by palynological trends on the leeward side of the SM at Mulloon Creek Swamp, which curiously records a decline *Eucalyptus* but large increase in *Cyperaceae* after ~3600 cal yr BP, conveying a wetting trend that contradicts ENSO intensification (Hope et al., 2009a).

Further disagreement with late Holocene paleoclimate is also apparent for the final highland record of Blundells Flat, which expresses late Holocene stability in charcoal and modern pollen assemblages (Hope et al., 2006). Despite conflicting chronologies, these studies corroborate a regional mosaic of *Eucalyptus* woodland, grassland and swamps that still defines the South Eastern Highlands. This macroecology likely also persisted on the Monaro until colonisation, though this presumption demands palynological verification from the Monaro itself (Starr et al., 1996, Wasson et al., 1998). It is hitherto apparent that there are major paleoenvironmental disparities between the mountain and highland domains, biotic and abiotic proxies and even proximal sites. This reinforces the necessity for a cross-elevational investigation of systemic change for this complex high-altitude system.

1.4.4. Pre-European anthropogenic influences on High Country paleoenvironmental records

It is obvious that the preceding review does not address the influence of Indigenous Australians on Holocene paleoenvironmental change on the High Country. This omission is testament to archaeological evidence for such being extremely scarce, often equivocal and generally not exceeding 1000 m ASL or ~4000 yr (Flood, 1980, Aplin et al., 2010). As such, it is difficult to confidently attribute apparent paleoenvironmental changes to human activity.

In the SM, this paucity of evidence has been partially ascribed to poor preservation of artefacts and ecofacts in the granite-derived acidic regolith. However, a more widely cited explanation is that the AA were simply not inhabited until deglaciation, owing to permanent snow and ice cover and a lack of game, with habitation for many millennia thereafter being seasonal (Costin, 2000). Such patterns of habitation are replicated for Tasmania, where Indigenous communities were confined to below the limit of periglaciation until the Holocene (Cosgrove, 1989, Porch and Allen, 1995, Allen, 1996,

Way et al., 2025). Evidence for the Holocene peopling of the SM derives from Cave Y259, emplaced at 1100 m ASL in the northern SM, where artefacts have a maximum age of ~9700 cal yr BP (Aplin et al., 2010). This age conveys that amelioration facilitated mountain occupation, despite alpine conditions still prevailing above 1000 m ASL during this time, according to paleorecords (see Section 1.4.2).

Indeed, there is a consensus that amelioration enabled many groups – the Ngarigo, accompanied by the Jaitmathang, Ngunawal, Walgalu and Djilamatang – to undertake summer pilgrimages to the SM from the abutting highlands, western slopes and coastal plains (Argue, 1995, Zylstra, 2006, Slattery, 2015). The timing of this seasonal movement appears to have been dictated by the annual warm-season migration to the SM by the Bogong moth (*Agrotis infusa*), which was an important summer food source and foundational to large mountain corroborees (Flood, 1980, Sahukar et al., 2003). This is evidenced by cooked *Agrotis infusa* remains from Cloggs Cave, as well as colonial accounts of mass gatherings in the SM, the latter confirming these festivals persisted until the mid-19th century (Stephenson et al., 2020).

Evidence of SM occupation appears to significantly predate the consensus for abrupt mid-late Holocene population growth and sedentism across Australia (Black et al., 2007, Johnson and Brook, 2011, Portenga et al., 2016a, De Deckker, 2022). Interestingly, there is a particularly obvious absence of mid-Holocene evidence for occupation for sites such as Cave Y259, which appears to have been abandoned after 9120 yr BP (Aplin et al., 2010). This hiatus is postulated to reflect reduced mountain accessibility due to an expansion of dense montane forest during the hypsithermal (Theden-Ringl, 2016).

Inferences of seasonal occupation commencing in the Holocene have also been made for the Monaro. While there is sparse, tentative evidence for inhabitation of the plateau and broader uplands as early as 25,000 yr, the most conclusive for the Monaro derives from a burial site near Cooma dating to ~7000 yr (McQueen, 1994, Young, 2005, Way et al., 2025). This lends credence to the argument that the Monaro was at least seasonally visited by nomadic groups from the early Holocene. Despite evidence of occupancy throughout the Holocene, human activity remains difficult to isolate from the reviewed proxy records, probably due to Indigenous presence being predominantly nomadic until the late Holocene (Prosser, 1990, Portenga et al., 2016a, Theden-Ringl, 2016). Large-scale Indigenous modification persisted from at least this time until the colonial era, as

confirmed by settler observations of widespread, continuous burning across the South Eastern Highlands by Indigenous groups (Zylstra, 2006).

In addition to the effect of nomadism on human traces, Indigenous land use practices such as burning are also typically low in frequency, size or severity. Therefore, it is often challenging to disentangle associated proxy signals from natural variability. It has for these reasons been argued that proxy variability in High Country paleorecords is likely more reflective of climatic and stochastic environmental variability than human agency over most of the Holocene (Mooney et al., 1997, Thomas et al., 2022). However, such a claim requires verification through targeted analyses of robust human proxies to precisely quantify the magnitude of anthropogenic ecosystem modification over the Holocene.

1.5. Research approach

From this review of high-altitude research emerge two motifs, these being a disproportionate emphasis on a) ecological change and b) those occurring in mountains *sensu stricto*. In the context of High Country paleoscientific literature, these lacunae are manifested through widespread interrogations of pollen and charcoal variability, with a clustering of such records in the SM. This is not to dismiss the importance of such research, which has established robust constraints on the paleoclimatic and paleoecological history of the SM, whilst also contextualising the magnitude of European ecological disturbance relative to the late Holocene baseline. However, a review of these data reinforces the critiques of Hope et al. (2012) and Mooney et al. (1997) that the sparse network of existing records is methodologically biased and does not account for the diversity of landscape types on the High Country. These limitations in turn impair our capacity to project systemic high-altitude responses to GEC.

This project aims to remedy these knowledge gaps by reconstructing postglacial environmental variability along an altitudinal (highland-to-mountain) transect of the High Country. This will be achieved through multiproxy analyses of sedimentary sequences from the alpine, subalpine, montane and highland zones, reconstructing catchment-scale changes in key abiotic and biotic processes. For each zone, cores from multiple mire and/or lake sites will be sampled and analysed to representatively reconstruct zonal changes. Site selection will prioritise lakes and mires in catchments where contemporary

observations indicate substantial ecological deterioration, such as those hosting TECs, as these are where constraints on systemic sensitivity to GEC are most urgently required.

Sensitivity itself will be ascertained by comparing synthesised proxy records with independent records of climate and land use. Specifically, magnitudes, directions, rates and lags of multiproxy change will be compared with those determined from paleoclimate and historical records to evaluate the responsivity of the biophysical system to these perturbations. This study will constitute the most methodologically and geographically comprehensive investigation of paleoenvironmental change on the High Country to date and will be vital for inferring how sensitivity varies not only between discrete processes, sites and zones but also relative to other high-altitude environments globally. Following a uniformitarian framework, these interpretations can be employed to more confidently project environmental responses to anthropogenic GEC. It is anticipated these findings will constitute a critical resource informing existing conservation and land management strategies on how actions and resources can more effectively address and reduce systemic sensitivity.

1.6. Research objectives

Specifically, this project will satisfy the following objectives:

1. Evaluate downcore variability in environmentally sensitive proxies (magnetic susceptibility, elemental geochemistry, mineral grain size, total organic carbon and nitrogen, $\delta^{13}C$ and macrocharcoal abundances) from the sedimentary records of mire and lake sites cored across the alpine, subalpine, montane and highland zones.

2. Reconstruct, for each site, variability in key abiotic and biotic processes (hydrology, erosion, primary productivity, nutrient availability and fire) through triangulation between individual proxy records appended to a robust chronological model.

3. Synthesise multiproxy data to reconstruct systemic paleoenvironmental change at the site, zonal and regional scale.

4. Assess, through comparisons of paleoenvironmental records with independent records of paleoclimate and European land use change, biophysical sensitivity to these stressors at the site, zonal and regional scale.

5. Consult interpretations of systemic sensitivity to make qualified prognoses of future environmental change at the zonal scale in the context of projected climate and land use change.

1.7. Thesis structure

This thesis comprises six sections: this integrated introductory and literature review chapter (Chapter 1); three independent research papers presenting original data obtained for the highland zone (Chapter 2), montane zone (Chapter 3) and subalpine and alpine zones (Chapter 4); a discussion synthesising data from the results chapters (Chapter 5); and a conclusion summarising the key findings and appraising the project's satisfaction of the above research objectives (Chapter 6). Each results chapter follows the methodology outlined in Section 1.5 and are concluded by afterword sections that review findings and offer a conceptual bridge to the following chapter.

Chapter 1 (this chapter) reviews the literature pertaining to high-altitude environments at both the global scale and that of the High Country. For both, it summarises high-altitude climatic and environmental (abiotic and biotic) attributes, considers how these affect sensitivity to climate and land use change, and explores the contemporary impacts of both these stressors. It then reviews the current pool of knowledge pertaining to the paleoclimatic and paleoenvironmental history of the High Country specifically. This chapter identifies two prevailing research problems: that high-altitude research places disproportionate emphasis on ecological change and on mountains specifically. It argues that an insufficient consideration of systemic and highland variability impairing interpretations of high-altitude sensitivity. This chapter represents a combined introduction and literature review, given the scope of the study and the research objectives were inductively informed by a review of the literature itself, which deductively confirmed knowledge gaps.

Chapter 2 investigates postglacial environmental change on the Monaro, and as such is the only independent research chapter to address both knowledge gaps. Multiproxy analysis of five Monaro lake records indicate that the Monaro is more sensitive to decreases than increases in moisture availability. It is also determined that lake basins themselves are highly sensitive to ENSO and exhibit hysteretic hydrological change under such. Unprecedented European-era systemic instability suggests the biophysical

system is more sensitive to European land use change than any climatic perturbation since deglaciation.

Chapter 3 employs a revised method from Chapter 2 to two mire peat records from the SM montane zone to reconstruct late Holocene systemic variability. It is asserted that the montane zone experienced sudden hydrological recovery due to increased snowmelt inflow resulting from changing ENSO-SHWW interactions. Catchment rewetting suggests montane catchments experienced a threshold shift whereby they became more sensitive to temperature than precipitation. Rewetting is associated with increased peatland productivity (especially in moisture-limited complexes), erosion and fire, while the European era is not associated with any systemic departure from the late Holocene baseline.

Chapter 4 reapplies the revised method of Chapter 3 to six mire peat and tarn records from the SM alpine and subalpine zones. This study reproduces the late Holocene rewetting signals (and associated systemic responses) identified in Chapter 3 – suggesting this was a mountain-wide event – and offers potential evidence implicating ENSO. It is determined that subalpine catchments have been more significantly perturbed by ENSO intensification and European-era land use change, implying greater subalpine sensitivity to both climate and land use change.

Chapter 5 compares the zonal reconstructions developed in Chapters 2–4 to evaluate cross-altitudinal differences in zonal sensitivity. Zonal records are also aggregated to approximate regional paleoenvironmental change and sensitivity to Holocene climate and land use change. High Country interpretations are then contextualised within the global literature to assess the replicability of regional findings.

Chapter 6 reviews thesis findings, satisfaction of the research objectives and identifies potential directions of future research.

Chapter 2

Asymmetric sensitivity of lake catchments to climate and land use change on the Monaro Tablelands, southeastern Australia: A multiproxy, multisite synthesis of postglacial lacustrine records

2.1. Abstract

Paleoenvironmental research in vulnerable high-elevation environments is skewed towards paleoecological analysis, biasing our understanding of broader systemic (i.e., both abiotic and biotic) environmental sensitivity. Moreover, paleorecords from mountains are overrepresented relative to adjacent highlands, which is problematic given the latter's greater agricultural value and thus more acute degradation. Here, we present a multiproxy, multisite assessment of regional paleoenvironmental change since 13,900 cal yr BP for the Monaro Tablelands of southeastern Australia, a highland terrain in the rain shadow of the Snowy Mountains. We find that, while regional hydrological change is effectively contemporaneous with temperature and hydroclimate, local dynamics appear to be equally influential on catchment moisture availability, implying only mild hydrological sensitivity to climate.

Principal among these intrinsic controls is poor substrate permeability, which is responsible for: a) late Holocene wetting signals despite climatic deterioration, and b) hysteresis in basin hydrology, whereby lakes and their ecological communities become increasingly resilient to moisture availability as permanence increases. Asymmetric sensitivity extends to catchment-scale rates of change, which observe a positive, albeit weak, correlation with drying over wetting. European-era rates of change are unprecedented for the entire study period, suggesting higher systemic sensitivity to land use than any major climatic perturbation since deglaciation. Continued biophysical deterioration is anticipated for the Monaro as land use impacts are augmented by projected warming, drying and increased rainfall variability across southeastern Australia, while changes in lake permanence are expected to be geographically bifurcated. These projections implicate adverse outcomes for endemic threatened ecological communities.

2.2. Introduction

High-elevation environments (i.e., mountains and highlands) are highly vulnerable to external perturbations due to their biogeographic isolation, bioclimatic zonation and/or low ecological redundancy, compounded by elevational amplification of climate change and concentration of land uses (Beniston, 2003, Pepin et al., 2015, Guisan et al., 2019). As such, they exhibit among the most dramatic responses to climate and land use change globally (Fort, 2015, Schmeller et al., 2022), impacting the viability of conservation, the

intensity and frequency of natural hazards, and the provision of critical environmental services. However, assessments of anthropogenic environmental change at high elevations are predominantly informed by ecological indices such as biodiversity and endemism, tree line elevation and phenology (e.g., Harsch et al. (2009), Elumeeva et al. (2013), Inouye and Wielgolaski (2024)).

Though critical for gauging the sensitivity of high-elevation ecosystems, these metrics embed an inherent ecological bias in our understanding of broader 'systemic' sensitivity, which we define as pertaining to the entire biophysical system, comprising both abiotic and biotic phenomena. Importantly, a systemic methodology considers the sensitivities of discrete biophysical processes and their role in buffering or amplifying macroscale sensitivity. While this 'geoecological' framework is recognised as vital for preserving high-elevation resilience in conservation and land management spheres (Gordon et al., 2002, Kumar and Deshmukh, 2015), it remains underused in paleoscience. Indeed, high-elevation paleo-research remains disproportionately represented by palynological studies (e.g., Razjigaeva et al. (2017), Zhang and Feng (2018), Han et al. (2019)), which risks under- or overestimating systemic sensitivity and hampers the utility of paleoenvironmental analogues in constraining future responses to stress. This can be remedied through multiproxy analysis, wherein cross-validation of parameters permits a more representative reconstruction of systemic change from which sensitivity can be ascertained through comparison with known disturbances (Birks and Birks, 2006, Gornitz, 2008).

Across high-elevation regions globally, paleoenvironmental research is also generally sparser in highlands (here denoting plateaus, tablelands and uplands) than in mountains *sensu stricto*, owing to the former's paucity of well-preserved, high-resolution natural archives (i.e., glaciers, tarns and mires) (National Centers for Environmental Information, 2025). Moreover, the lower relief of highlands reduces ecotonal steepness, attenuating climatic influence on paleoecological signals. Subdued topography also contributes to a downslope reduction in the availability of ecological niches, manifesting as a decline in biodiversity and endemism along many mountain-to-highland ecological gradients (e.g., Himalaya-Tibetan Plateau, Southern Andes-Patagonian Steppe) (Beniston, 2016, Hughes et al., 2021). Highlands are therefore often assigned lower conservation and thus research priority than adjacent mountains, further skewing the imbalance of paleoenvironmental knowledge (Jung et al., 2021). Ironically, it is owing to their lack of conservation, as well

as their proximity to mountain-specific environmental services (e.g., water supply), that highlands typically host larger populations and more intensive agriculture than less accessible mountains. Indeed, most highlands are now overwhelmingly represented by agricultural land use classes (i.e., pasture, rangeland and cropland) rather than 'natural' land cover classes (i.e., grassland, shrubland and forest) (Jenkins et al., 2013, Winkler et al., 2020). The accumulation of local stressors not limited to land clearing, species invasions, grazing and excess nutrient inputs has contributed to many highlands experiencing greater biodiversity loss than mountains (e.g., North American Great Plains versus Rocky Mountains), eroding their ecological resilience to climate change (Newbold et al., 2016). Despite this, a dearth of multiproxy paleo-research entrenches uncertainty in projecting long-term systemic change and thus conservation, land management and industry in these economically significant regions.

Here, we present multiproxy records collated from lacustrine sequences from the Monaro Tablelands of southeastern Australia, a highland terrain that has been severely modified by European pastoralism since the early 19th century. We evaluate downcore variability in environmentally sensitive sedimentological and geochemical parameters to reconstruct changes in erosion, hydrology, primary productivity, fire and biogeochemistry over the Holocene and most of the postglacial Late Pleistocene. Synthesising these data through multivariate analysis, directions, magnitudes, rates and lags of systemic change are compared with known climatic and European influences. In so doing, we constrain sensitivity to these external stressors at the process, catchment and regional scale to make qualified projections of systemic responses to anthropogenic pressures over the 21st century.

2.3. Regional setting

The Monaro Tablelands ('Monaro') is a ~8000 km^2 plateau undulating between 800–1100 m ASL within a broader high-elevation region of southeastern Australia known historically as the 'High Country'. Perched immediately east of the Snowy Mountains, it is bounded to the north by the Tinderry and Brindabella Ranges, and to the south and east by the Great Escarpment (Fig. 2.1) (Taylor and Roach, 2003). Geomorphically, the region is a peneplain underlain in the centre and east by the Monaro Volcanic Province, an extensive lava field composed of basalt units ('Monaro Volcanics') extruded onto the pre-

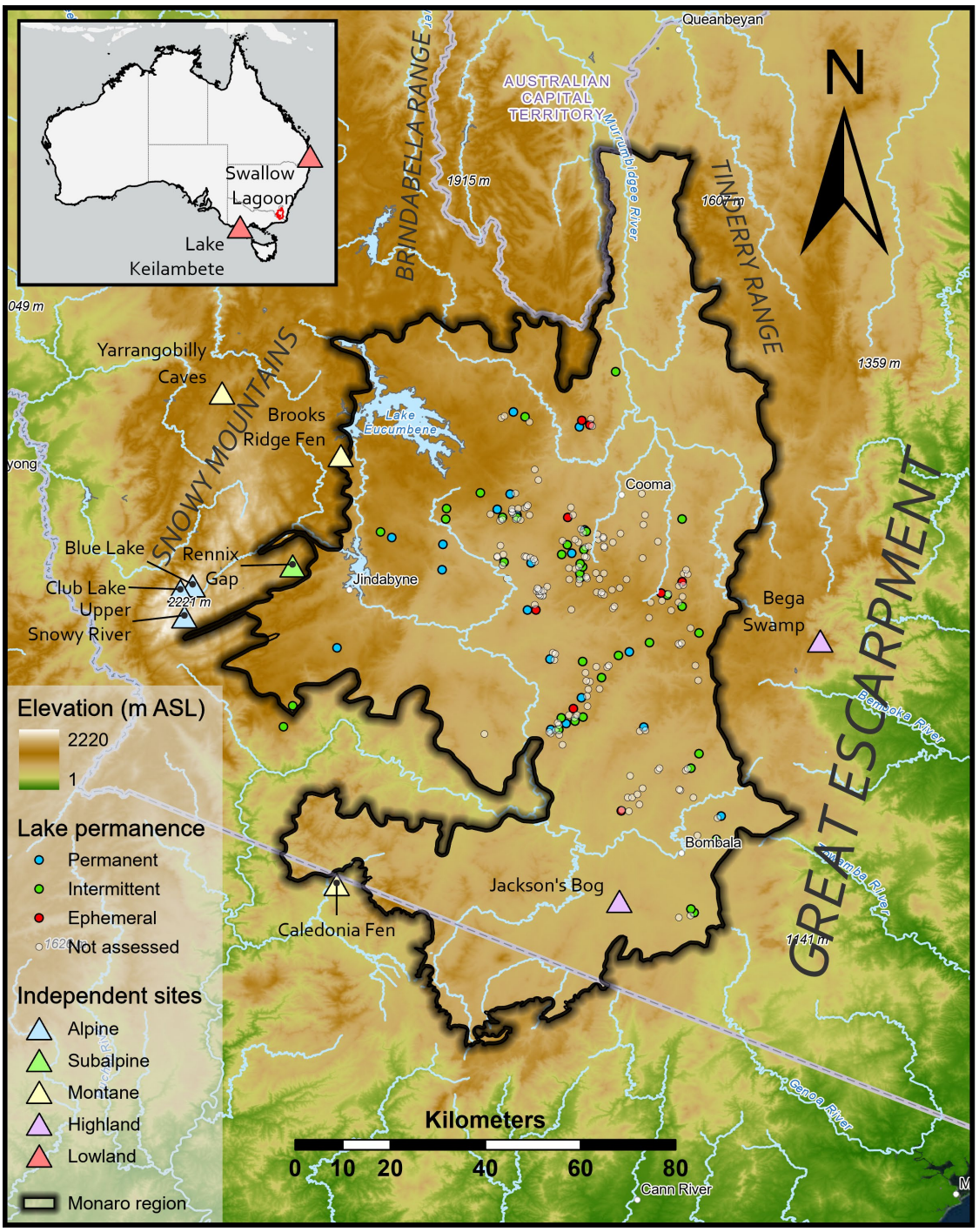

Figure 2.1. Elevation and hydrography map of the Monaro and surrounds (back outline, red in inset; DCCEEW (2023)), with constituent lakes (circles coloured by permanence; Benson and Jacobs (1994), DCCEEW (2015b)) and surrounding sites that have been the subject of independent studies mentioned in-text (triangles coloured by bioclimatic/physiographic zone). Elevation data obtained from Geoscience Australia (2008) and hydrography data from State Government of NSW Spatial Services (2025). 'Monaro' boundary synthesised by clipping the Monaro bio-subregion (DCCEEW, 2020) to the Snowy Monaro Local Government Area (Department of Customer Service Spatial Services, 2020).

existing paleosurface during the Eocene and Oligocene (Fig. 2.2) (Brown et al., 1992, Roach et al., 1994). This basement, still exposed in the west and south, is dominated by Silurian to Devonian granitoid intrusions and moderately deformed to metamorphosed sedimentary units constituting the Lachlan Orogen (Sahukar et al., 2003). Protracted, post-eruptive denudation of the Monaro has permitted deep fluvial incision by major rivers (Snowy and Murrumbidgee) and intense chemical weathering and pedogenesis on all surface lithologies. On the Monaro Volcanics, this has generated a thick mantle of fertile black earths (chocolate soils and chernozems), while granitic and sedimentary bedrock units are overlain by leached podsols and lithosols, respectively (Costin, 1954, Jenkins and Morand, 2002, Sahukar et al., 2003).

Attributable to its position leeward of the Snowy Mountains, the Monaro is impacted by a rain shadow resulting from the range's orographic obstruction of the prevailing westerly winds, a major source of precipitation for southeastern Australia (Taylor and Roach, 2003, Fogt and Marshall, 2020). Consequently, the plateau exhibits the driest conditions in Australia east of the Great Dividing Range; mean annual rainfall ranges from ~450–700 mm from the central to eastern Monaro in accordance with the eastward decay of the rain shadow, significantly lower than the Snowy Mountains (~1800–2600 mm) and adjacent coastal plain around Bega (~750–1200 mm) (Xu and Hutchinson, 2013). Moderately arid conditions, in concert with cold winters and mild summers generated by the tablelands' high elevation, prescribe marginal plant growing conditions, yielding a savannah-like mosaic of grassland and open woodland spatially dictated by lithology and thus pedology (Costin, 1954).

Specifically, dense, clayey mafic soils tend to support associations of grass species, chiefly snowgrass (*Poa siberiana*), kangaroo grass (*Themeda* spp.), spear grass (*Austrostipa* spp.), red grass (*Bothriochloa macra*) and wallaby grass (*Danthonia* spp.). These represent keystone species of the Natural Temperate Grassland ('Temperate Grassland') community that extends over much of the broader South Eastern Highlands bioregion (Fig. 2.2), of which the Monaro is a subregion. Natural Grassland is also federally recognised as a threatened ecological community (TEC) due to overgrazing and replacement by exotic weeds; while this listing is designed to enhance the resilience of the TEC, it remains threatened to present (Benson, 1994, Department of the Environment and Energy, 2016). On infertile podsols and lithosols, vegetation is typically grassy eucalypt woodland represented by *Eucalyptus viminalis, E. fastigata, E. globulus, E.*

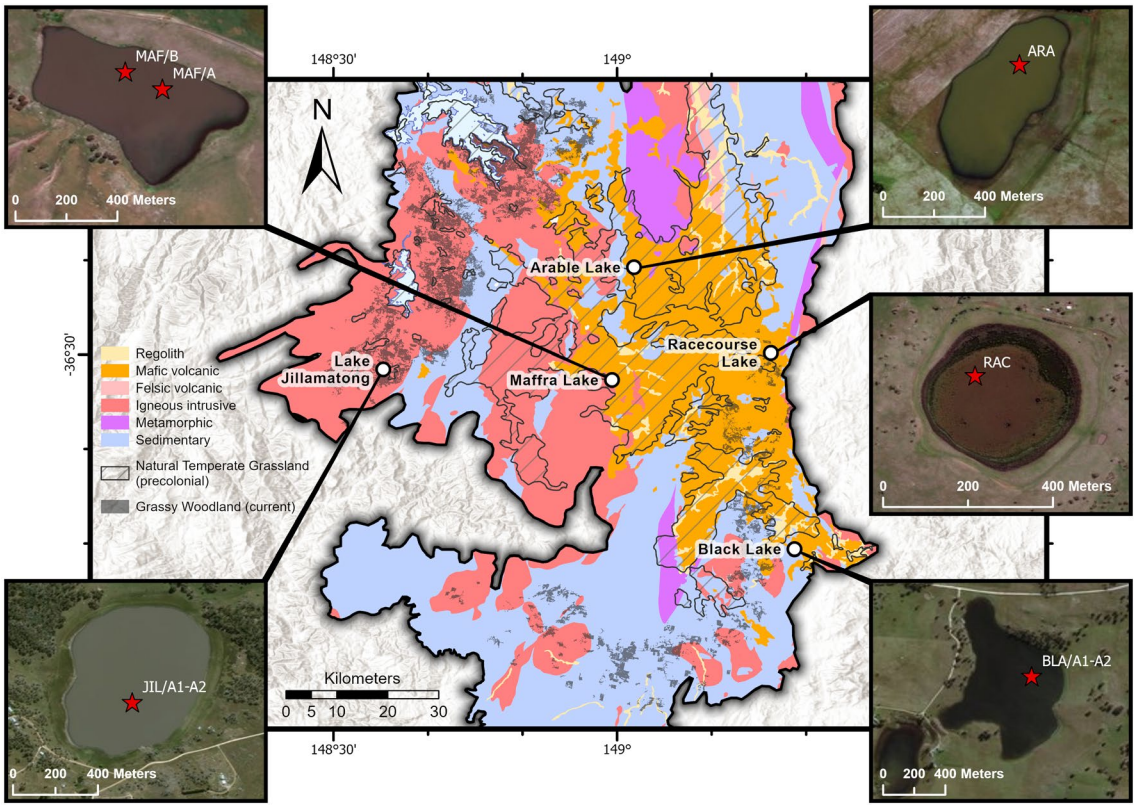

Figure 2.2. Partial map of the Monaro with locations of sampled lakes (white circles), underlain by the distributions of terrestrial TECs and simplified lithology. Insets identify coring locations (red stars) for each lake. Geological data adapted from Geoscience Australia (2012). Temperate Grassland data obtained from DCCEEW (2015a) and Grassy Woodland data from DCCEEW (2019).

rubida and *E. pauciflora*. The latter two species dominate the tree stratum of the Monaro Tablelands Cool Temperate Grassy Woodland ('Grassy Woodland') community, listed as threatened at the state level in recognition of extensive land clearing leaving only 5% of its indigenous distribution remaining (Fig. 2.2) (DCCEEW, 2019). Decline of these TECs is evidently an outcome of prolonged European occupation of these uniquely treeless plains, which were considered a boon to pastoralists arriving on the tablelands from the 1820s CE in pursuit of open grazing land (Costin, 1954, Hancock, 1972, Eyles, 1977). Agriculture remains a major component of the regional economy (Snowy Monaro Regional Council, 2018), with associated land use pressures engendering ecological decline of such severity that Bergstrom et al. (2021) lists the Monaro as one of 17 mainland ecosystems currently experiencing macroecological collapse.

Lithology controls the distribution of not only flora but also the region's ~215 alkaline, endorheic lakes ('the Monaro lakes'), 85% of which are emplaced exclusively on the Monaro Volcanics (Williams et al., 1970, Richardson and Caldwell, 2002). This strong

spatial correlation is attributed by Pillans and Walker (1995) to solution weathering of random depressions in the basalt terrain only under ameliorated climates, explaining the absence of pre-Holocene ^{14}C ages obtained from lacustrine sedimentary sequences by these authors (see also Bakis (2021)). The smectitic composition of the lakebeds impedes effective drainage and groundwater recharge, rendering them claypans that are hydrologically pluvial and hence seasonal due to limited rainfall (Pillans, 1987, Benson and Jacobs, 1994, Hobbs et al., 2016). However, the Monaro lakes' degree of permanence is geographically variable, being largely a function of basin depth.

Deeper basins are rarely dry (termed 'permanent' by Benson and Jacobs (1994)) and support deepwater macrophyte and algal associations, while shallower basins tend to be seasonally dry ('intermittent') or frequently dry ('ephemeral') and host sedge-herb-grass associations. Regardless of ecology, all lakes are constituents of the Upland Wetlands of the New England Tablelands and Monaro Plateau ('Upland Wetlands'), a federally listed TEC. This listing ascribes decline to weed invasions, erosion and nutrient inputs associated with agriculture around these basins, which are a rare terrestrial water source on private landholdings and travelling stock reserves (Department of the Environment and Heritage, 2005).

Despite their known preservation of Holocene-age natural archives, we are not aware of any further utilisation of the Monaro lakes for paleoenvironmental research. Moreover, research across the broader High Country has historically targeted tarn and mire records from the Snowy Mountains, with Hope et al. (2012) recognising that its population of paleorecords is overwhelmingly represented by palynological and charcoal reconstructions. Nonetheless, the literature derived from the High Country (Fig. 2.1) constitute a valuable reference frame for constraining Holocene paleoclimate, within which our results can be contextualised to assess systemic sensitivity. There is a consensus among these records that the commencement of the Holocene on the High Country is marked by rapid amelioration between ~10,800–10,000 yr ^{14}C yr BP (conventional ^{14}C age) subsequent to deglaciation of southeastern Australia from 20,000–15,000 ^{14}C yr BP (conventional ^{14}C age) (Barrows et al., 2001, Barrows et al., 2002). This is expressed as a widespread shift towards more moisture-demanding vegetation at sites including Club Lake and Pound's Creek (Martin, 1986a), Rennix Gap (Hope et al., 2019) and Bega Swamp (Green et al., 1988, Donders et al., 2007) (Fig. 2.1). Given the peripheral

location of Bega Swamp to the Monaro, Pillans and Walker (1995) deduce that the latter must too have experienced a subalpine climate before 10,000 ^{14}C yr BP.

While this has not yet been substantiated by any Monaro-specific evidence, subalpine conditions would imply suitability for human occupation, given higher elevation archaeological evidence of the seasonal presence of the local Ngarigo people under colder alpine conditions from at least ~9700 cal yr BP (Aplin et al., 2010, Slattery, 2015, Theden-Ringl, 2016). In view of this age, postglacial peopling of the more hospitable Monaro presumably occurred by this time at the latest, though unequivocal evidence of habitation is currently limited to a single ~7000 cal yr BP-old burial site near Cooma (Young, 2005). Regardless, the Monaro has likely experienced modification by the Ngarigo over most of the Holocene, which regional evidence suggests was predominantly characterised by an intensification of fire regimes (Black et al., 2007). However, evidence from the South Eastern Highlands suggests burning was too infrequent, localised and/or low impact to significantly alter background erosion rates (Portenga et al., 2016a). Considering therefore the opaqueness of indigenous human traces and the lack of targeted research into such on the Monaro, the impact of Holocene land use change remains unconstrained.

Following amelioration, early-middle Holocene increases in precipitation are inferred from a stronger representation of wet-adapted plant taxa at sites such as Bega Swamp (Green et al., 1988, Hope et al., 2004), coincident with a global interval of elevated temperature and moisture known as the Holocene Hypsithermal ('hypsithermal') which occurred in southeastern Australia between ~8200–5500 yr (De Deckker, 2022). On the High Country, paleorecords generally convey a termination of the hypsithermal from slightly later, with drying commencing between ~4500–3500 cal yr BP; this is widely attributed to the intensification of the El Niño–Southern Oscillation (ENSO) (Southern, 1982, Donders et al., 2007). There is a consensus from South Pacific records of increasing El Niño amplitude and frequency over the late Holocene (Moy et al., 2002, Rein et al., 2005, Donders et al., 2008, Hagemans et al., 2022), overlapping with two warming periods on the High Country. Reconstructing temperature variability to 3690 cal yr BP, Thomas et al. (2022) interpret warming in the Snowy Mountains between 1500–1100 cal yr BP, coeval with inferred tree line advance as well as increased alpine to montane fire activity (Mooney et al., 1997). A second, milder warm period is also reconstructed for the Snowy Mountains by both Thomas et al. (2022) and McGowan et al. (2018) between ~800–400 cal yr BP.

2.4. Materials and methods

2.4.1. Site selection, sampling and observations

Five lakes were selected for sampling following the site selection method outlined in Appendix A1. Given the Monaro lakes are mostly small, shallow and closed, they possess a simple lenticular bathymetry with minimal cross-basin variation in lakebed stratigraphy (Pillans and Walker, 1995). The basin depocenter was thus targeted for sampling as it was likely representative of the whole facies. Depocenters were located by superimposing historical shoreline contours using historical satellite imagery. Following Bakis (2021), cores were sampled by hammering a steel collar attached to a 5 cm interior diameter polyvinyl chloride core barrel into the lakebed until refusal. If replicate cores were collected, the longest was selected for analysis on the presumption it possessed an older basal age. Following retrieval, cores were split longitudinally and lithostratigraphic observations were immediately recorded. Each core was scanned for volume magnetic susceptibility at 0.5 cm resolution using a Bartington MS3 meter fitted with a MS2E sensor, following Dearing (1999a). This was done for core correlation and the identification of episodes of pedogenesis, detrital sedimentation and redox variability associated with fluctuating lake hydrology (Mullins, 1977, Oldfield et al., 1983, Dearing, 1999b, Thompson, 2012). Core surfaces were subsampled into contiguous 0.5 cm slices by cutting perpendicular to the inferred bedding plane. Samples were stored at 3 °C at the University of Sydney (USYD).

2.4.2. Sample analyses

2.4.2.1. Dating and chronological modelling

Based on age observations by Pillans and Walker (1995) and Bakis (2021), all cores were anticipated to possess Holocene-age material; accordingly, AMS ^{14}C was the most appropriate dating method. Dating was performed at the Australian Nuclear Science and Technology Organisation (ANSTO; Hua et al. (2001), Fink et al. (2004)), DirectAMS and the CHRONOS ^{14}Carbon-Cycle Facility at the University of New South Wales (NSW) (Turney et al., 2021). Bulk sediment samples were first submitted to constrain maximum ages and verify appropriateness for further dating (full preparation method in Appendix A2). Detailed dating targeted sporopollenin (‘pollen’) as this fraction was expected to

provide reliable chronological control while also being relatively coherent with underlying bulk sediment samples. ^{14}C ages (yr BP ± 1σ), reported in BP, were calibrated using the R software BACON (v. 3.3; Blaauw and Christen (2011), R Core Team (2020)). Age calibration was performed using the Southern Hemisphere calibration curve (SHCal20) (Hogg et al., 2020) and age-depth models were generated. All ages are expressed as 'cal yr BP', i.e., calibrated years Before Present (with present set at 1950 CE by convention).

2.4.2.2. X-Ray fluorescence

Scanning micro-X-ray fluorescence (μXRF) analysis was performed on all cores to evaluate downcore geochemical variability (Last and Smol, 2002, Croudace and Rothwell, 2015, Davies et al., 2015), which we anticipated to be highly variable given seasonal lake hydrology and thus volatility of allochthonous (i.e., elements indicative of detrital flux) and autochthonous (i.e., pH- and redox-sensitive elements) processes. Cores were scanned at ANSTO at 0.1 cm resolution using an Itrax XRF core scanner fitted with a Mo tube. Raw concentrations for 33 major, minor and trace elements were reported as relative counts per second. A subset of optimal (i.e., environmentally relevant, high signal/noise, infrequent zero values) elements were cleaned and normalised to a conservative variable to identify areas of genuine compositional change by removing closed sum effects. Ti was selected for normalisation due to its environmental abundance, high detectability and insensitivity to biogeochemical processes (Kylander et al., 2011, Davies et al., 2015). To decompose statistical complexity and identify multivariate relationships, principal component analysis was performed using the R package 'FactoMineR' (Lê et al., 2008, McKillup and Dyar, 2010, R Core Team, 2020).

2.4.2.3. Mineral grain size

Mineral grain size analysis was conducted for all cores to constrain variability in clastic influx and/or lakebed deflation (Pillans, 1987). Samples were taken at 2 cm resolution and subjected to chemical treatments to isolate siliciclastics (full method in Appendix A3). Samples were analysed at USYD using a Malvern Mastersizer 3000 laser diffractometer equipped with a Hydro LV dispersion unit. Triplicate blue light measurements were taken per sample to calculate a mean grain size distribution, which

was then decomposed into summary statistics using the GRADISTAT Excel package (v.8; Blott and Pye (2001)).

2.4.2.4. Total organic carbon and total nitrogen

The mass percentages of total organic carbon (TOC) and total nitrogen (TN) (TOC-TN), and their atomic ratio (C/N) are important indices for paleoproductivity and paleoecology (Meyers and Teranes, 2001, Schittek et al., 2016). In the Monaro lakes, TOC-TN is anticipated to primarily reflect the production and deposition of organic matter (OM) by hydrophytes and algae, which is positively correlated with lake permanence. C/N was investigated as low (<10) and high (>12) values are associated with N-rich algae and N-poor terrestrial plants, respectively, rendering it a proxy for lake basin ecology (Meyers, 1994, Meyers and Teranes, 2001, Turner et al., 2015, Lone et al., 2018). A standard wet volume (2 cm^3) of material was subsampled at 2 cm resolution and dried to calculate moisture content and dry bulk density prior to acid digestion of inorganic carbonates (full method in Appendix A4). Dried, pre-treated and homogenised samples were loaded in tin capsules for analysis using a VELP Scientifica CN 802 Carbon Nitrogen Analyser at USYD.

2.4.2.5. Stable carbon isotopes

The ratio of the two stable isotopes of carbon ($\delta^{13}C$), provides a critical secondary dimension for reconstructing paleoecology. In cases where C/N indicates a terrestrial source for OM, $\delta^{13}C$ permits differentiation between the C_3 (-26 to -30 ‰) or C_4 (-17 to -9 ‰) plant pathway groups (Meyers, 1994, Lamb et al., 2006). C_3 plants are the dominant floristic component of the contemporary grassland-woodland mosaic but also lake macrophyte associations (Benson, 1994, Benson and Jacobs, 1994), and so interpreting C_3 signals demands multiproxy triangulation. Meanwhile, the C_4 minority is solely represented by *Themeda* spp. and *Bothriochloa macra*, both major constituents of the Temperate Grassland TEC (Sahukar et al., 2003). As such, a positive deviation in $\delta^{13}C$ towards C_4 values may reflect turnover in the catchment from a woodland- to grassland-dominated state and/or lakebed terrestrialisation by grasses (Hamilton et al., 2024). For $\delta^{13}C$ analysis, unused TOC-TN material was retained, and duplicate samples were loaded into tin capsules to verify uniformity; mass ranges were determined from TOC results

(Section 2.4.2.4). Samples were analysed with an Elementar VarioISOTOPE Elemental Analyser coupled with an Elementar PrecisION Isotope Ratio Mass Spectrometer at ANSTO to measure relative isotopic abundances of C, reporting $\delta^{13}C$ as ‰.

2.4.2.6. Macroscopic charcoal

The abundance of macroscopic charcoal (macrocharcoal; >125 μm) in sediments is reflective of local to regional fire activity (Whitlock and Larsen, 2001). On the Monaro, increased macrocharcoal abundances are presumed to reflect an expansion of woody vegetation given grasses typically produce particles <120 μm (Leys et al., 2017). In targeting macrocharcoal, therefore, we approximate the prevalence of not only local fires but of forest and shrub communities, which we anticipate is positively correlated with humidity due to increased biomass. While charcoal production is certainly also influenced by indigenous burning, we interpret it as a predominantly paleoclimatic signal following conclusions by Mooney (2012) that charcoal records across Australasia are correlated with climate rather than low-impact burning. Two cores, from sites representing the western and eastern Monaro, were selected for analysis to identify any spatial discrepancies in paleofire associated with eastward orographic deterioration. Subsamples with a volume of 1 cm^3 were taken from contiguous 0.5 cm slices, from which macrocharcoal was isolated through dispersion and sieving partially adhering to the method of Stevenson and Haberle (2018) (full method in Appendix A5). Samples were counted for macrocharcoal fragments with a Zeiss Stemi 305 Stereo Microscope, and raw counts were converted to charcoal accumulation rates (CHAR; particles/cm^2/ yr).

2.4.3. Statistical analyses

2.4.3.1. Hydrological and ecological reconstructions

The most critical dimension of environmental change in a lake catchment is moisture availability (MA), which is a product of inputs and outputs via precipitation, groundwater, evaporation and transpiration. In the pluvial, seasonal Monaro lakes, directions and magnitudes of hydrological change are expected to be pronounced under even modest changes in temperature and rainfall, offering an insight into hydrological sensitivity to climate. To ascertain directionality of site hydrology, proxies presumed to be most

sensitive to moisture were inverted where necessary such that positive deviations corresponded to 'wetting' and negative to 'drying'. To ensure comparability, proxies were Z-score standardised, and the median of all proxies was calculated for each depth interval to generate a composite record of wetting and drying. Importantly, this record is not a 'pure' signal of basin or catchment hydrology, but an aggregate of both.

While useful for inferring directionality, dimensionless standardisation removes absolute constraints from the record and thus comparability of magnitudes of change between sites. We address this by consulting the relationship between $\delta^{13}C$ and C/N, which defines bivariate domains in which OM from different photosynthesising sources (e.g., freshwater algae, C_3 and C_4 terrestrial plants) typically fall (Meyers, 1994, Lamb et al., 2006). Given their seasonality, it is reasonable to expect that the Monaro lakes transitioned between the three hydrological states identified by Benson and Jacobs (1994) in response to millennial-scale fluctuations in Holocene paleoclimate.

Such shifts should manifest in the bivariate data as migration between the C_3/algal and C_3/C_4 domains, indicating frequent (permanent), seasonal (intermittent) or rare (ephemeral) lakebed inundation. To compile a regional hydrological record, site chronologies were fixed to a standardised timescale. Following Hamilton et al. (2024), we performed 10,000 Monte Carlo iterations on each site record, where for each an age was randomly generated within the defined minimum and maximum age bounds, and values were linearly interpolated onto a fixed 100-yr time grid. For each time interval, a median Z-score was calculated from all iterations. Time-standardised records were subjected to a second round of Monte Carlo sampling, wherein random values were generated 1000 times within the confidence limits of each record, and a single Z-score was calculated for each bin as the median of all site Z-scores across all iterations.

2.4.3.2. Paleoclimate reconstructions and cross-correlation analysis

A simplified version of the above standardisation approach was employed to reconstruct synthesis records of paleoclimate for southeastern Australia and relevant surrounding regions, against which our regional hydrology curve could be compared to gauge sensitivity to climate (see Appendix A6 for data details and visualisations). Paleoclimate records were prioritised if they a) exhibited significant temporal overlap with our regional record, b) derived from southeastern Australia (defined here as being

south of 23.5° S and east of 130° E), and c) quantitatively reconstructed hydroclimate or temperature. These criteria significantly reduced the number of records that could be collated, forcing inclusion of some records that did not satisfy all three criteria (see Appendix A6 for justifications).

Paleoclimate data were cleaned (truncated to the maximum age in our model and zero values removed) and direction-standardised such that positive values consistently reflected increased moisture or temperature. As age uncertainties were not available for all datasets, records were simply interpolated onto a common 100-yr time grid from the original chronologies without age resampling. From this, a median value was calculated per 100 yr to ensure temporal comparability with our regional hydrology record. Records were then Z-score standardised, and a composite trend was produced by calculating the median Z-score across all records at each timestep. To estimate lead/lag between hydrology and climate, cross-correlation was performed using the R 'stats' package (R Core Team, 2020), which calculated at which lag time (i.e., number of 100-yr timesteps) the correlation between hydrology and both hydroclimate and temperature was highest.

2.4.3.3. Rate-of-change reconstructions

Rate-of-change (RoC) analysis assesses how rapidly a system changes when perturbed, with higher values indicating a more unstable system. To reconstruct systemic RoC over time, the complete suite of proxy data – capturing all major catchment processes – were analysed using the R-Ratepol package (v 1.2.3; Mottl et al. (2021b)) in R (R Core Team, 2020). As far as we are aware, this is the first application of this method to multiproxy data without a paleoecological emphasis. Prior to analysis, data were linearly interpolated to the maximum proxy resolution (i.e., 0.1 cm; μXRF) to avoid sampling gaps resulting in artefactual pulses in RoC between actual values. In R-Ratepol, data were binned into working units of 150 yr using the moving window approach, which involved calculating RoC between consecutive bins, migrating the bin forward by a timestep of 30 yr and recomputing RoC, repeating this until the end of the record. This was repeated 10,000 times, with the final RoC for each bin calculated as the median of all iterations. Points of rapid change (peak-points; >2σ in model) were also isolated for each record. Regional RoC was calculated as the median of all sites per 100-yr bin.

2.5. Results

2.5.1. Core sampling, stratigraphy and chronological modelling

The following five sites were sampled in November 2023: Arable Lake, Black Lake, Lake Jillamatong, Maffra Lake and Racecourse Lake (Fig. 2; see Appendix A7 for site details). Coring was performed within depocenters (Fig. 2; see Appendix A8 for core details and optical scans) but repeatedly encountered high resistance due to heavy lakebed clay content. This resulted in a degree of compaction for all cores, though substantial water columns and diffuse sediment-water interfaces at all sites meant compaction could not be accurately constrained. Nonetheless, due to downcore homogeneity, relative sedimentation changes are presumed to have been preserved. Magnetic susceptibility was found to be invariable for all cores and so was not utilised for core correlation or multiproxy analysis.

The Arable Lake core (ARA; 28 cm length) was compositionally homogenous, comprising a single unit of massive black mud. ^{14}C dates at 16 cm and 28 cm yielded similar raw ages of 541 ± 66 yr BP and 575 ± 25 yr BP (Table 2.1). The basal age was unexpectedly young and the mean sedimentation rate it implies is inconsistent with those reconstructed by Pillans and Walker (1995). Observation of pollen slides sampled at ultra-low resolution showed no exotic *Pinus* pollen at depths assigned post-European ages by a test chronology incorporating only the basal age. On this basis, it was concluded that the basal age was likely a product of clay desiccation cracking and illuviation of younger material. The basal age was thus disregarded and an age-depth model was generated by extrapolating below the 16 cm age, yielding a median basal age of 1115 (95% confidence interval: 782–1618) cal yr BP (see Appendix A9) (Blaauw, 2010, Lacourse and Gajewski, 2020). While this introduces significant uncertainty into the sub-16 cm section of ARA, this chronology produced a more realistic mean sedimentation rate of 25 cm/1000 yr, though this value and those for other cores are likely to have artificially increased by coring compaction.

The Black Lake core (BLA; 28.5 cm) also possesses a single unit of massive black mud. Age-depth modelling produced a median basal age of 1468 (1240–2040) cal yr BP (see Appendix A9). Modelled sedimentation rates decrease from 60–15 cm/1000 yr from core base to top, punctuated by a sharp decline between ~1400–1250 cal yr BP. The Lake Jillamatong core (JIL; 38 cm) exhibits two units; Unit 1 (0–32 cm) is composed of

Table 2.1. ^{14}C dating results for all cores. Asterisks denote samples that were not incorporated into the final chronological models due to either a 'Modern' result, or a date / major age reversal that was already ignored by the model or implied a dramatic hiatus that was improbable given no chronostratigraphic evidence of such (i.e., no unit boundary nor coarsening diagnostic of a lag deposit; Fig. 2.3). 'OZBY', 'D-AMS' and 'UNSW' Lab IDs are for samples analysed at ANSTO, Direct AMS and the University of NSW, respectively. ^{14}C ages calibrated using CALIB program (v. 8.2) with SHCal20 (Stuiver and Reimer, 1993, Hogg et al., 2020).

Lab ID	Core ID	Depth (cm)	Material	Radiocarbon age (yr BP ± 1σ)	Median age (cal yr BP)	2σ range (cal yr BP)
OZBY51	ARA	16	Pollen	541 ± 66	527	333 to 648
UNSW-3566*	ARA	28	Bulk sediment	575 ± 25	539	509 to 623
OZBY35	BLA	11.5	Pollen	924 ± 25	778	728 to 902
OZBY36	BLA	19.5	Pollen	1518 ± 22	1352	1310 to 1406
D-AMS 054014	BLA	28.5	Bulk sediment	1375 ± 15	1241	1179 to 1295
OZBY37	JIL	15.5	Pollen	498 ± 56	503	327 to 623
OZBY38	JIL	27	Pollen	1397 ± 59	1264	1106 to 1368
OZBY39*	JIL	32	Pollen	1087 ± 60	948	798 to 1063
D-AMS 054015	JIL	38	Bulk sediment	3230 ± 20	3409	3365 to 3450
OZBY44	MAF	8.5	Pollen	Modern	-66	-69 to -5
OZBY45	MAF	19.5	Pollen	83 ± 86	111	-6 to 279
OZBY46	MAF	27.5	Pollen	424 ± 98	413	151 to 623
OZBZ34*	MAF	41	Bulk sediment	1786 ± 71	1657	1483 to 1865
D-AMS 054017	MAF	47.5	Bulk sediment	5280 ± 25	5996	5921 to 6177
OZBY40	RAC	7.5	Pollen	224 ± 58	189	0 to 430
OZBY41	RAC	15	Pollen	7498 ± 61	8273	8051 to 8399
OZBY42	RAC	20.5	Pollen	9374 ± 80	10539	10262 to 10745
OZBY43	RAC	26	Pollen	10,674 ± 70	12651	12485 to 12741
D-AMS 054016*	RAC	29	Bulk sediment	9100 ± 30	10255	10178 to 10273

massive black mud and transitions across a clear boundary to the massive olive black mud of Unit 2. Chronological modelling yielded a basal median age of 3272 (2357–3441) cal yr BP (see Appendix A9). Sedimentation rates increase from 0.5–30 cm/1000 yr from core top to bottom, with a marked acceleration between ~1200–400 cal yr BP. The Maffra Lake core (MAF; 47.5 cm) comprises a single unit, though there is a decreasing abundance of vertically oriented olive black mottling from 17–37 cm in a matrix of massive grey mud. The modelled chronology produced a median basal age of 5964 (5720–5964) cal yr BP (see Appendix A9). Sedimentation rates fluctuate between 2–8 cm/1000 yr until ~580 cal yr BP, when there is a precipitous increase to ~65 cm/1000 yr at present.

The Racecourse Lake core (RAC; 29 cm) is the most stratigraphically heterogeneous of all cores, hosting four lithostratigraphic units. Unit 1 (0–9 cm) is composed of massive black mud and shows a clear transition to Unit 2 (9–21.5 cm), also massive black mud but observing the emergence of alternating light-dark, ~0.2 cm-thick laminae. Unit 2 transitions abruptly to Unit 3 (21.5–27 cm), defined by massive black mud that also preserves laminations, albeit with lower contrast. At the base of Unit 3 there is another abrupt boundary with Unit 4, composed of massive olive black mud and preserving the most contrasting laminations. A large age reversal is observed between the lowermost pollen age at 26 cm and the underlying bulk sediment basal age at 29 cm. As for ARA, the age reversal was assumed to be an artefact of illuviation; the basal sample was therefore rejected, and extrapolation over the lower 3 cm indicated a median basal age of 13,907 (12859–16268) cal yr BP (see Appendix A9). Sedimentation rates vary between ~1–3 cm/1000 yr until ~350 cal yr BP, when there is a dramatic increase to ~20 cm/1000 yr at core top.

It is apparent from Table 2.1 that some cores exhibit age reversals as well as age discrepancies between proximal samples that might be interpreted as hiatuses. While some of these ages have been removed from the age-depth models on the basis of there being no chronostratigraphic evidence for a hiatus and/or an indication these ages are outliers, it is certainly possible that hiatuses are occurring, especially for MAF and RAC. Indeed, while Pillans and Walker (1995) suggest that significant deflation events and hiatuses are unlikely for the Monaro lakes during interglacial periods, there is widespread evidence that southeastern Australian lakes have been subject to hiatuses over the Holocene (Fitzsimmons and Barrows, 2010, Wilkins et al., 2013, Woodward et al.,

2014a). While the possibility of hiatuses in our sampled cores can therefore not be dismissed, low dating resolutions and a lack of chronostratigraphic support means hiatuses can also not be identified with confidence and so have not been manually forced in the chronological model. It should also be recognised that age-depth discrepancies apparent in Table 2.1 may also be a product of age bias towards pollen and/or bulk sediment samples. Specifically, these different fractions are impacted by processes such as argilloturbation and catchment soil erosion, which can promote downcore translocation of young carbon in pollen as well as deposition of old carbon in bulk sediment, complicating core chronologies (Vandergoes and Prior, 2003, Cadd et al., 2022), De Deckker et al. (2023). However, verification of bias towards older or younger ages is not possible in this case given the dating strategy employed (i.e., no dating of multiple sample fractions).

2.5.2. Multiproxy analyses

The dominant multiproxy trend for ARA (Fig. 2.3) is a marked deviation in many values around ~500 cal yr BP. For mean grain size, this manifests as a transition from fine silt to medium silt due to an increase in the silt/clay ratio. This is contemporaneous with changes in TOC-TN and $\delta^{13}C$, which achieve their respective minima and maxima before increasing and decreasing to present. This ~500 cal yr BP trough in previously stable TOC-TN also coincides with elevated C/N, which reaches an absolute maximum at ~450 cal yr BP before declining to present at a rate comparable to $\delta^{13}C$. Principal component analysis for ARA – and indeed all other cores – finds Principal Components (PC) 1 and 2 to be contributed to by different combinations of elements that derive from multiple sources (see Appendix A10).

Because these combinations vary across sites, these PCs cannot be interpreted consistently as proxies for any specific processes and so are presented here to simply describe bulk trends across the elemental suite. For ARA, PC1 and 2, explaining 41% and 19% of elemental variance, respectively (see Appendix A10), exhibit no shift at ~500 cal yr BP. Instead, both PCs are dominated by a dramatic pulse at ~260 cal yr BP, whereat values increase by a factor of two to three. The only elements to adhere to the ~500 cal yr BP transition are Ca/Ti and Mn/Ti (and thus Mn/Fe), which achieve their absolute maxima and minima around this time before recovering and stabilising to present.

The BLA proxy data (Fig. 2.3) reveal an interval of abrupt change between ~1300–1200 cal yr BP, during which time there is a rapid decline in sedimentation rates. This is coincident with increasing mean grain size due to elevated silt contributions. TOC-TN increase after ~900 cal yr BP and both C/N and $\delta^{13}C$ deviate positively before stabilising. This transitional phase is also one of the dominant features in the μXRF data, preserved as a major change in both PC1 and PC2 (explaining 45% and 33% variance, respectively) (see Appendix A10). Both PCs also express an unprecedented increase commencing from ~50 cal yr BP, which coincides with a negative deviation in $\delta^{13}C$ and slightly elevated sedimentation rates.

The proxy data for JIL (Fig. 2.3) capture a multivariate transition occurring over the period from ~2200–1800 cal yr BP, overlapping with the modelled age of the sole unit boundary (1943 (1282–2740) cal yr BP). While sedimentation rates are relatively unresponsive during this period, mean grain size displays fining towards the lower boundary of the medium silt class due to a dramatic increase in the relative proportion of clay, which is entirely absent prior to ~2350 cal yr BP. TOC-TN stabilise at high values following an increase from an absolute minimum at ~3000 cal yr BP, while C/N remains unaffected and $\delta^{13}C$ stabilises in a broad trough which persists until ~1000 cal yr BP. CHAR is especially responsive to this transition, observing a sevenfold increase over a narrow window between ~2100–1900 cal yr BP. PC1 (explaining 49% variance) declines markedly over this period (see Appendix A10).

MAF preserves some of the highest magnitude changes of all five records and shows large inconsistencies across the proxy suite (Fig. 2.3). Sedimentation rates exhibit the largest absolute increase of all cores at ~700 cal yr BP, increasing by a factor of 20 from this time to present. This is not reflected by any change in mean grain size, which shows only minor fining within the medium silt class to present, though this may be an artefact of unknown instrumental complications resulting in the clay fraction not being properly registered for this core, despite replacement samples being analysed. TOC-TN are also stable throughout the sequence until a tenfold increase commencing from ~450 cal yr BP

Figure 2.3. (next page) Multiproxy diagrams for each core, displaying age-plotted sedimentation rates as well as results for sedimentological (yellow), paleoecological (green), geochemical (purple) and paleofire (black) proxy data. These are accompanied by the median Z-score data (blue). Black dashed lines denote the timing of colonisation of the Monaro (i.e., 1820 CE; 130 cal yr BP) and red solid lines indicate the depth and corresponding age of a stratigraphic boundary.

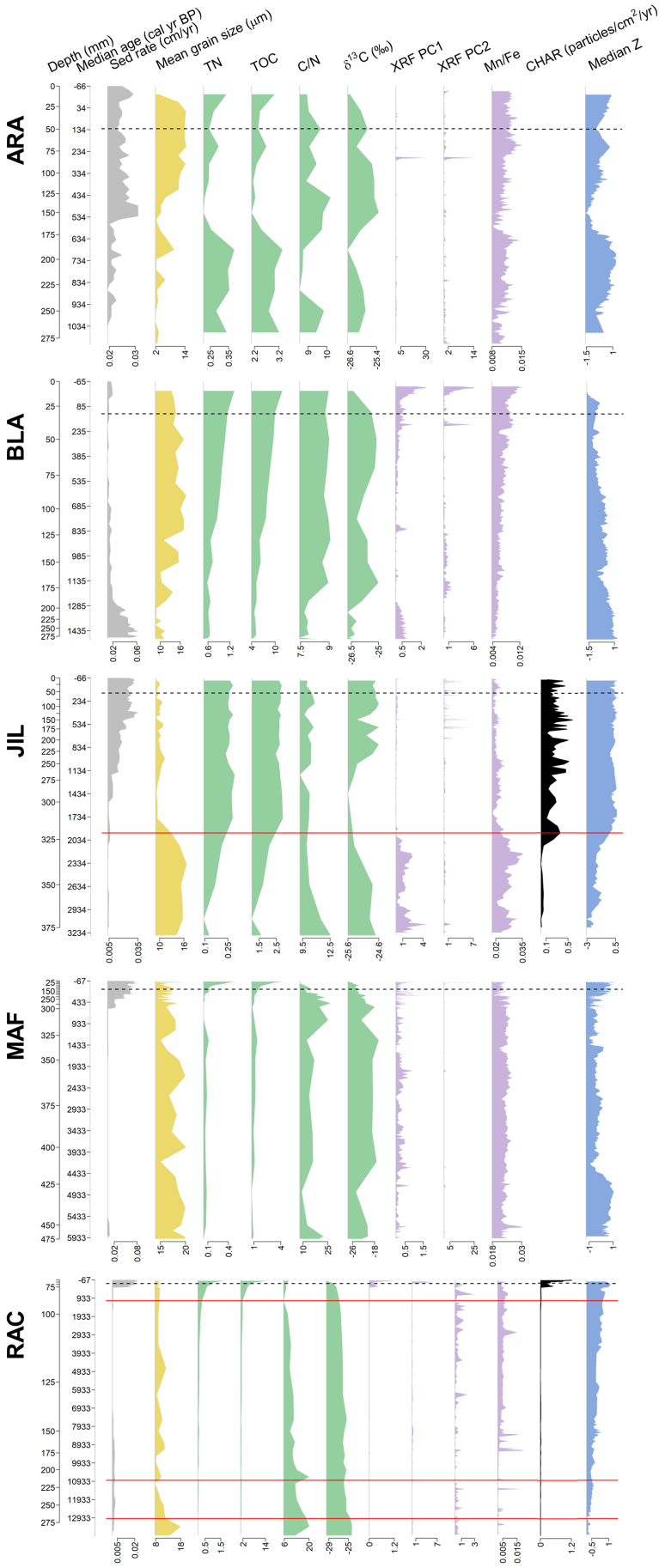
Depth (mm)
Median age (cal yr BP)
Sed rate (cm/yr)
Mean grain size (µm)
TN
TOC
C/N
δ13C (‰)
XRF PC1
XRF PC2
Mn/Fe
CHAR (particles/cm2/yr)
Median Z
ARA
BLA
JIL
MAF
RAC

to present. This is coeval with rapid negative excursions in both C/N and $\delta^{13}C$, which both exhibit the highest magnitude variability of all five records. Despite paleoecological volatility, the μXRF data are remarkably stable for most of the sequence, with PC1, explaining 37% variance, oscillating mildly throughout the record (see Appendix A10).

The RAC proxy data also exhibit low multivariate coherence (Fig. 2.3). Sedimentation rates remain low for most of the sequence, declining mildly after ~7000 cal yr BP and stabilising before a precipitous 20-fold increase from ~350 cal yr BP to present. However, mean grain size does not appear to respond to this change, remaining stable within the medium silt range after marked fining ending at ~11,000 cal yr BP, coincident with the modelled age of the base of Unit 2. TOC-TN remains low and stable until an exponential increase from ~1000 cal yr BP, though C/N exhibits no such uptick, instead showing high volatility prior to ~10,000 cal yr BP. While $\delta^{13}C$ also undergoes large magnitudes of change, relative variance is low, following a linear negative trend throughout the record. CHAR is also low until ~350 cal yr BP, when there is a 62-fold increase from this point to present, tracking sedimentation rates. While PC1 (explaining 45% variance) captures a core-top pulse from ~130 cal yr BP (see Appendix A10), elemental abundances are stable for the rest of the record. Mn/Fe is a notable exception, displaying eight major positive excursions, seven of which occur before 8000 cal yr BP.

2.5.3. Statistical analyses

A summary of proxies used in the site-specific hydrological reconstructions, together with their hydrological interpretations and plausible justifications for these, is presented in Table 2.2. Time series records of the output hydrological reconstructions are presented for each site in Fig. 2.4, accompanied by whole-suite RoC. The degree to which the hydrological records are representative of whole-suite trends is quantified by principal component analysis of these same input proxies in Appendix A11, which demonstrates the level of agreement between the dominant mode of variability and the hydrological signals. Also presented are composite records of hydrology and RoC across all sites (Fig. 2.5a), and hydroclimate and temperature (Fig. 2.5b). Note that composite hydrological data post-400 cal yr BP has been removed due to obvious anthropogenic modification, rendering it useless for inferring natural hydrology. Cross-correlograms between composite hydrology and both hydroclimate and temperature are shown in Fig. 2.5c.

Table 2.2. Summary of input proxies for each site hydrological reconstruction, indicating where inversions were applied to ensure consistent directionality across proxies. Proxies expected to be negatively correlated with wetting (N) were inverted, while those expected to be positively correlated with wetting (P) were retained in their original orientation. Interpretations are accompanied by justifications outlining possible hydrological mechanisms, based on site-specific multiproxy triangulation and/or field observations. Note that interpretations are reductive and do not list all potential influencing processes; rather, they offer the most plausible mechanistic relationship with moisture availability based on available evidence.

Proxy	Correlation with MA	Justification
		Arable Lake
Mean grain size	P	Wetting increases clastic influx – deflation unlikely in a permanent lake over a 1000 yr interval. Evidence of streams on southeastern margin.
TOC	P	Wetting increases lake level and thus gross algal productivity.
C/N	N	Wetting increases lake level and thus algal dominance.
$\delta^{13}C$	N	Wetting increases lake level and thus algal dominance.
Ca/Ti	N	Wetting increases lake level and inhibits carbonate precipitation. Likely precipitative rather than detrital given Ti-normalisation, PC alignment with Mn/Ti, and a weak correlation between raw Ca and Ti counts.
Mn/Fe	P	Wetting increases lake level and mixing, permitting oxygenation.
		Black Lake
Mean grain size	P	Wetting increases clastic influx – deflation unlikely in a permanent lake over a 1000 yr interval.
TOC	N	Wetting increases lake level and reduces light penetration in such a deep, turbid lake, suppressing gross algal productivity.

C/N	N	Wetting increases lake level and thus proportional algal dominance relative to terrestrial inputs, despite declines in gross algal productivity.
$\delta^{13}C$	N	Wetting increases lake level and thus algal dominance relative to terrestrial inputs, despite gross declines in algal productivity.
Ca/Ti	N	Wetting increases lake level and inhibits carbonate precipitation. Likely precipitative rather than detrital given Ti-normalisation, PC alignment with Mn/Ti, and a weak correlation between raw Ca and Ti counts.
Mn/Fe	N	Wetting raises lake levels and limits bottom-water oxygenation. Clay swelling reduces sediment oxygenation.
		Lake Jillamatong
Mean grain size	N	Wetting suppresses deflation – higher correlation between mean grain size and silt/clay ratio (consistent with lag deposit formation). Such lag deposits are likely to correspond to minor, seasonal (drought-related) deflation events that do not produce measurable hiatuses.
TOC	P	Wetting increases lake level and thus gross algal productivity.
C/N	N	Wetting increases lake level and thus algal dominance.
$\delta^{13}C$	N	Wetting increases lake level and thus algal dominance.
Ca/Ti	N	Wetting increases lake level and inhibits carbonate precipitation. Likely precipitative rather than detrital given Ti-normalisation, PC alignment with Mn/Ti, and a weak correlation between raw Ca and Ti counts.
Mn/Fe	N	Wetting increases lake levels and limits bottom-water oxygenation. Clay swelling reduces sediment oxygenation. Increased algal productivity permits more eutrophic, reducing conditions.
CHAR	P	Wetting increases woodland fuel loads.
		Maffra Lake
Mean grain size	P	Wetting increases clastic influx - no lake shadow observed during 2019 drought. Evidence of streams on southwestern margin.
TOC	N	Wetting reduces terrestrial inputs. Terrestrial plants are abundant, and algae not observed in field – former is presumed to dominate OM inputs.
C/N	N	Wetting increases lake level and thus algal dominance relative to terrestrial inputs.

$\delta^{13}C$	N	Wetting increases lake level and thus algal dominance relative to terrestrial inputs.
Ca/Ti	N	Wetting increases lake level and inhibits carbonate precipitation. Likely precipitative rather than detrital given Ti-normalisation, PC alignment with Mn/Ti, and a weak correlation between raw Ca and Ti counts.
Mn/Fe	N	Wetting raises lake levels and limits bottom-water oxygenation. Clay swelling reduces sediment oxygenation. Increased algal productivity permits more eutrophic, reducing conditions.
		Racecourse Lake
Mean grain size	N	Wetting suppresses deflation – higher correlation between mean grain size and silt/clay ratio (consistent with lag deposit formation). Such lag deposits are likely to correspond to minor, seasonal (drought-related) deflation events that do not produce measurable hiatuses.
TOC	P	Wetting increases lake level and thus gross algal productivity.
C/N	N	Wetting increases lake level and thus algal dominance.
$\delta^{13}C$	N	Wetting increases lake level and thus algal dominance.
Ca/Ti	N	Wetting increases lake level and inhibits carbonate precipitation. Likely precipitative rather than detrital given Ti-normalisation, PC alignment with Mn/Ti, and a weak correlation between raw Ca and Ti counts.
Mn/Fe	P	Wetting increases lake level and mixing, permitting oxygenation.
CHAR	P	Wetting increases woodland fuel loads.

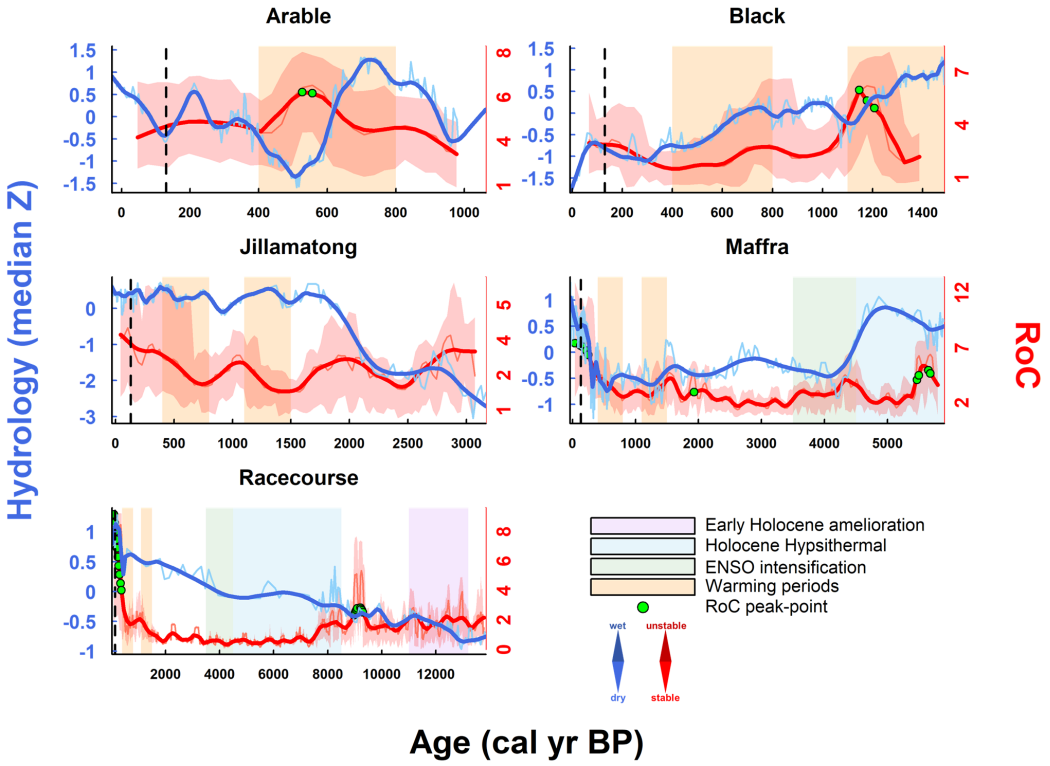

Figure 2.4. Time series reconstructions of catchment moisture availability and RoC for each site. Pale curves represent raw data, and dark curves represent loess-smoothed trends. Red envelopes correspond to 95% uncertainty ranges. Relevant paleoclimatic phases, inferred from southeastern Australian paleorecords discussed in-text, are indicated by coloured intervals. Dashed vertical lines correspond to European colonisation of the Monaro.

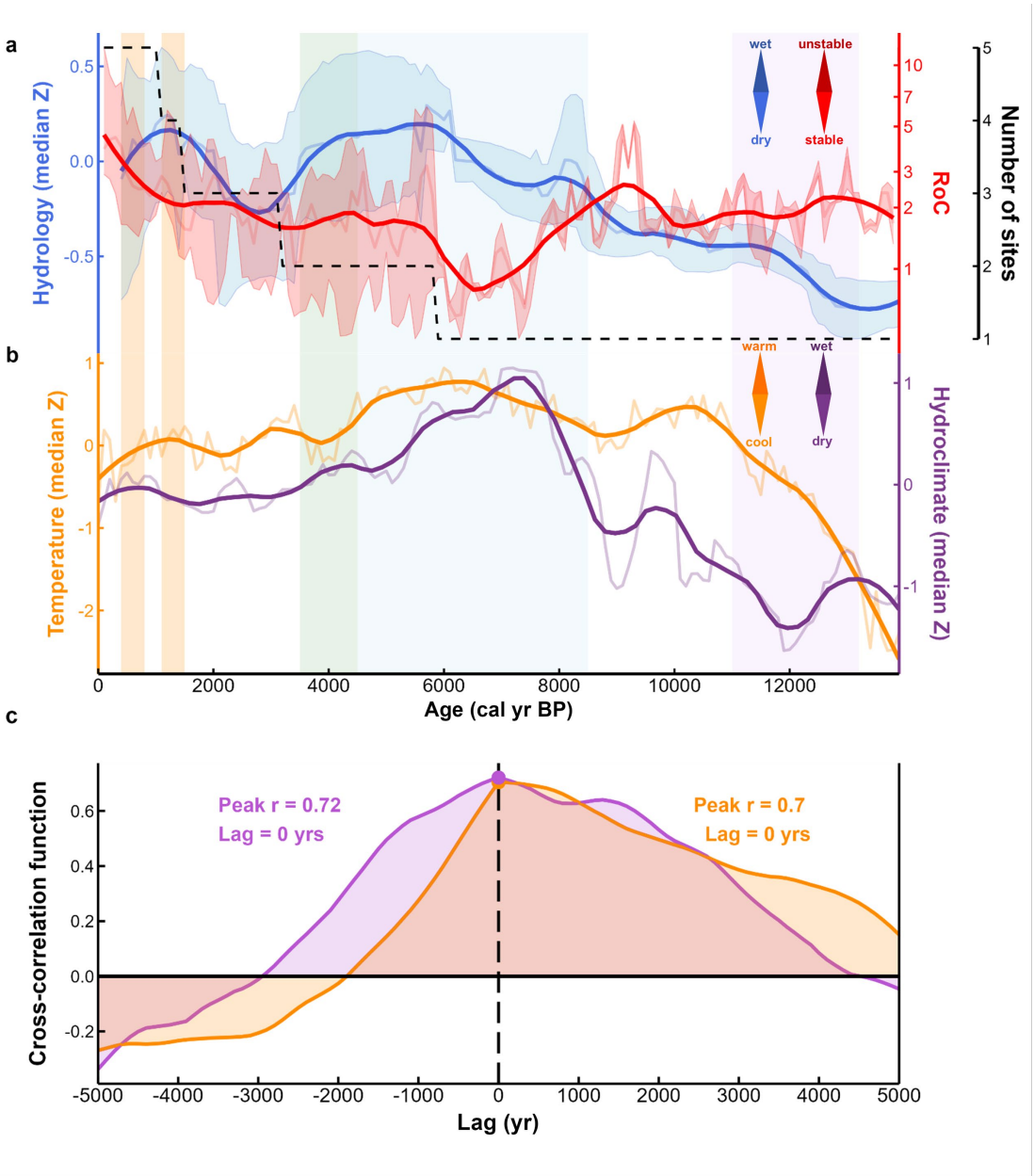

Figure 2.5. Reconstructions of **a)** regional hydrology and RoC for the Monaro with 95% uncertainty ranges (shaded envelopes), and **b)** paleotemperature and paleo-hydroclimate trends for southeastern Australia and the South Pacific. Dark curves are loess-smoothed trends for the raw data (pale curves) and coloured intervals reflect the same paleoclimatic phases described for Fig. 2.4. Presented in **c)** are hydrology cross-correlograms for southeastern Australian and South Pacific hydroclimate (purple shading) and temperature (orange shading).

2.6. Discussion

2.6.1. Systemic variability at the catchment scale

2.6.1.1. Arable Lake (1115 cal yr BP to present)

Consistent with the multiproxy structures observed for ARA, the dominant pattern in the Arable Lake hydrology reconstruction is a pronounced drying interval centring on ~500 cal yr BP (Fig. 2.4). The record initially indicates wetter than average conditions approaching peak MA at ~700 cal yr BP, at which stage there is abrupt drying to a minimum at ~500 cal yr BP. This is immediately succeeded by partial recovery stabilising by ~350 cal yr BP until present, indicating no detectable colonial influence on the input proxies. While mid-millennium drying is pronounced, the relationship between C/N and $\delta^{13}C$ (Fig. 2.6) communicates that it was insufficient to result in any true shift in ecology and thus hydrological state. Indeed, the system has remained in the algal range of values for the entire record, save for a transient C_3-directional departure between ~500–400 cal yr BP. Though coincident with drying, this excursion is too brief and mild to suggest a genuine state transition. A more realistic interpretation is that this reflects a mild reduction in the ratio of algal to terrestrial OM due to lake level lowering and strandline encroachment of sedges and grasses.

Reviewing independent paleorecords from the High Country, we find a surprisingly strong correlation between this record and temperature, apparently implicating evaporation as the driving mechanism for lake-level lowering. The strongest evidence arises from the speleothem paleotemperature record reconstructed by McGowan et al. (2018) for Yarrangobilly Caves (Fig. 2.1), which chronicles pronounced warming between ~800–400 cal yr BP. Despite the low chronological certainty of the Arable Lake record, maximum drying around the position of the sole date (where there is greatest chronological confidence) occurs during the peak of this warm period (see Appendix A12). Specifically, the Yarrangobilly Caves record indicates that temperatures achieve a maximum since ~2100 cal yr BP (~0.7 ºC above the mean for 1961–1990 CE) at 557 yr BP. The regional significance of this warm period is articulated by correlation with the Club Lake (Fig. 2.2) temperature record from Thomas et al. (2022), which conveys a transient ~2.8 ºC increase mean summer temperature between 817–435 cal yr BP.

This event appears to have been not only regional but continental in influence; climate modelling by Gergis et al. (2016) confirms that the period from 800–600 yr BP was the

warmest in Australasia in the millennium preceding the preindustrial period. Warming has been ascribed to strengthening northeasterly winds in the southwestern Pacific, suggesting strong maritime influence even within the rain shadow (Lorrey et al., 2008). Reconstructing systemic RoC for Arable Lake (Fig. 2.4) finds that values increase from a minimum to a single peak-point cluster at ~550 cal yr BP, before declining and stabilising to present. This RoC peak coincides with the drying segment of the hydrology curve; the absence of a peak during the subsequent and commensurate recovery phase, as well as the pre-maximum wetting interval, suggests greater systemic destabilisation during periods of drying than wetting. RoC is unresponsive during the European period, indicating minimal systemic disturbance.

2.6.1.2. Black Lake (1470 cal yr BP to present)

We find no evidence of a mid-millennium drying event for Black Lake (Fig. 2.4), which instead follows a more linear drying trajectory throughout the record, punctuated by a brief trough between ~1250–1050 cal yr BP and another negative deviation from ~70 cal yr BP to present. The timing of the latter excursion indicates post-European anthropogenic confounding of the data. This is supported by positive deviations in sedimentation rates, μXRF PC1 and PC2, and Mn/Fe (Fig. 2.3), suggesting colonial modifications of runoff and catchment geochemistry but apparently not ecology. The C/N-δ^{13}C relationship (Fig. 2.6) conveys that the basin has been dominated by algal inputs – and has therefore remained permanent, as currently classified by Benson and Jacobs (1994) – since at least ~1500 cal yr BP. This suggests that drying was, as for Arable Lake, insufficient to induce a lacustrine transition, merely lowering lake level. Linearity in drying receives weak support from higher elevation records; while the Thomas et al. (2022) reconstruction does record another higher magnitude warm event between ~1500–1100 cal yr BP, temperature oscillations are far more volatile than our hydrological record.

Drying at Black Lake is instead more congruous with hydroclimatic trends inferred from Bega Swamp, the most proximal independent site, which communicates a persistent albeit mild increase in dry taxa from ~3500 cal yr BP to present, attributed to ENSO intensification and thus increased drought frequency (Green et al., 1988, Donders et al., 2007). This is corroborated by evidence further afield, with a mean annual rainfall reconstruction from Swallow Lagoon revealing gradual drying commencing from ~3200

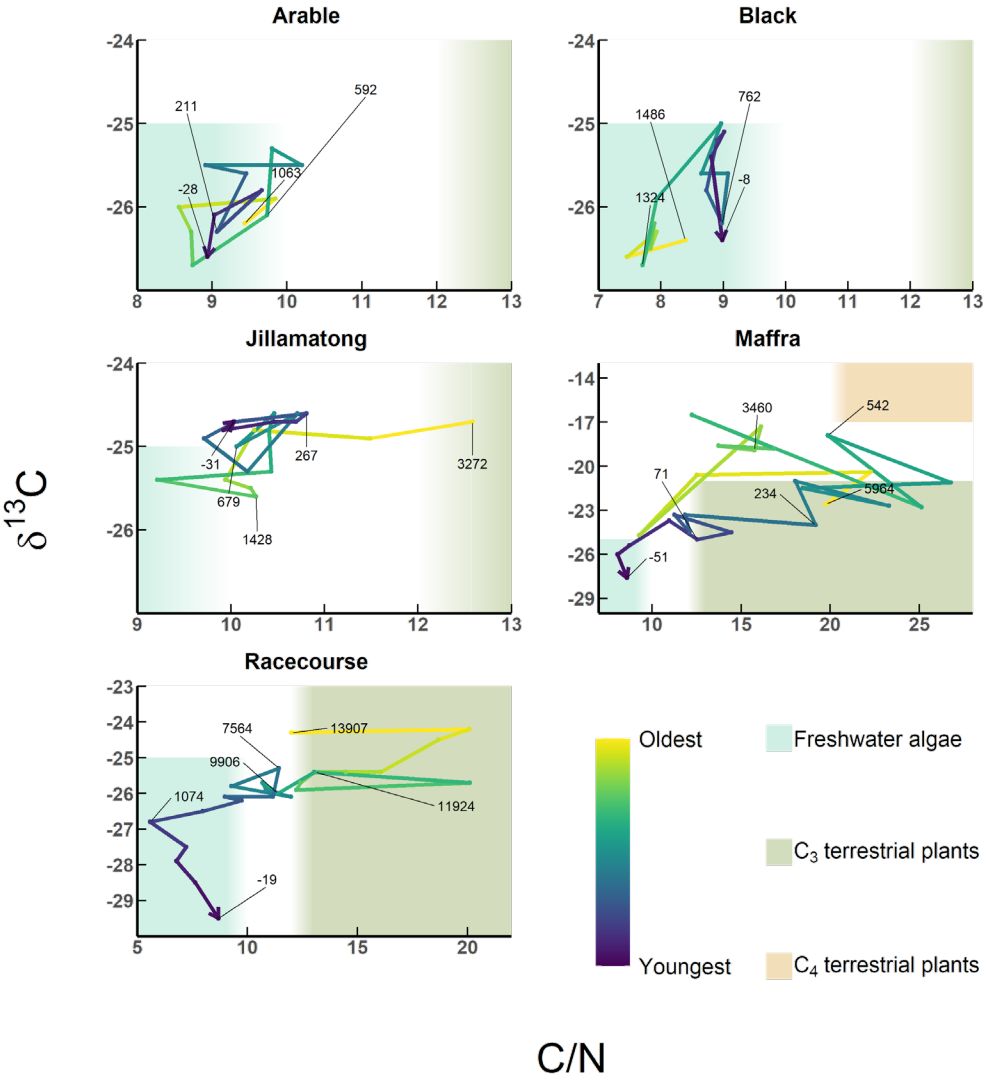

Figure 2.6. Reconstructed basin ecological changes visualised through the C/N-δ^{13}C bivariate space. Vectors denote trajectories to present, coloured according to the record-specific chronological model. Blurred regions delineate the value ranges typical for OM produced by algae (blue), C_3 plants (green) and C_4 plants (orange), derived from Lamb et al. (2006). The oldest, youngest and random intervening calibrated ages are labelled to assist in comparison of record timescales.

cal yr BP, attributable to strengthening El Niño (Barr et al., 2019). The RoC record for Black Lake displays a single cluster of peak-points at ~1200 cal yr BP, during which time RoC triples. As for Arable Lake, this peak is coeval with the negative component of the minor drying trough, again indicating more pervasive systemic destabilisation under drying than wetting, an inference supported by a coeval collapse in sedimentation rates. Despite continued drying to present, however, RoC quickly recovers to pre-peak values; this suggests systemic stability under gradual but not rapid drying. RoC is only mildly

elevated during the European period, indicating greater disequilibrium in response to drought than land modification.

2.6.1.3. Lake Jillamatong (3270 cal yr BP to present)

The dominant feature in the Lake Jillamatong hydrology reconstruction is a relatively dramatic increase in moisture balance from ~3200 until 1800 cal yr BP, whereupon there is an abrupt stabilisation for the remainder of the record (Fig. 2.4). Reviewing the C/N-$\delta^{13}C$ trajectory (Fig. 2.6), we find that the system existed in the C_3 domain for the first century of the record and entered the algal domain from ~2200 cal yr BP, persisting in this state until present. This suggests that basin ecology transitioned relatively early in the catchment wetting phase, which accelerates after this time. Given Benson and Jacobs (1994) classify Lake Jillamatong as permanent, consistent with the modern algal signature, we infer the basin has been permanent for the last ~2200 yr and was ephemeral at the beginning of the record. An ecological shift preceding major wetting implies abrupt community reorganisation following a minor input of moisture into the ephemeral basin, with subsequent algal stability suggesting ecological stasis under more dramatic increases in MA. While independent paleorecords appear to align strongly with inferred hydrological trends at Lake Jillamatong, attributed mechanisms do not. The most proximal evidence corroborating late Holocene increases in MA derives from peat sequences from the Namadgi Ranges and Snowy Mountains, which convey accelerated accumulation between ~3500–2500 cal yr BP; however, this is ascribed to cooling and reduced fire activity, and so does not explain contemporaneous wetting at Lake Jillamatong (Costin, 1972, Hope et al., 2009b, Stromsoe et al., 2016).

The strongest correlation derives from Lake Keilambete in western Victoria, for which Bowler and Hamada (1971) and Bowler (1981) reconstruct an increase in lake level commencing at ~2500 yr after a variable Holocene minimum at ~3000 yr, with a subsequent stabilisation from ~1900 yr (conventional ^{14}C age). Correlation between variable, low lake levels at Keilambete and increased aeolian volatility inferred by Stanley and De Deckker (2002) for Blue Lake is attributed by the authors to ENSO amplification. While this mechanism explains dry conditions early in the Lake Jillamatong record, it is contradicted by subsequent wetting both there and at Keilambete despite increasing El Niño frequency (Moy et al., 2002, Donders et al., 2008). In fact,

most southeastern Australian lake records convey drying over the late Holocene associated with the shift to a mean El Niño-like state (Marx et al., 2011, Barr et al., 2019, Clerke, 2023).

However, it must be recognised there has also been an increase in a) the amplitude of ENSO and b) the frequency of multiyear events over the late Holocene, with multiyear La Niña becoming more common than multiyear El Niño (Donders et al., 2008, Carré et al., 2021, Lu et al., 2025). The implication of this is, despite the increased dominance of El Niño, La Niña has also become more intense and is lengthening at a faster rate. Given the catchment and lakebed of Lake Jillamatong – and indeed all study sites – is composed of highly impermeable smectite, it is likely that longer, more intense La Niña phases have impaired effective claypan drainage during intervening El Niño and neutral phases, irrespective of the increased frequency and intensity of El Niño. This reduction in hydrological recovery time would translate to net basin inundation despite decreased humidity, consistent with the wetting trend reconstructed for Jillamatong. The validity of this hypothesis is supported by the lake filling signal at Keilambete, for which a heavy clay substrate is also observed (Bowler and Hamada, 1971). However, this model does not explain the post-1800 cal yr BP plateauing of hydrology at Lake Jillamatong, which may reflect competing effects of the two superimposed warming periods.

Reconstructing RoC reveals an oscillatory signal devoid of peak-points, though the highest values occur at ~3800 and ~100 cal yr BP. The first maximum aligns with the onset of a minor wetting pulse between ~3000–2700 cal yr BP prior to the main transition phase, which itself coincides with a significantly milder RoC increase. This indicates that, as for ecology, systemic instability is highest after initial wetting, though the relationship is weak. Record-maximum RoC at ~100 cal yr BP appears to be a continuation of a much longer increase commencing from ~600 cal yr BP and so cannot be confidently ascribed to colonial activity.

2.6.1.4. Maffra Lake (5960 cal yr BP to present)

The hydrological reconstruction for Maffra Lake (Fig. 2.4) is characterised by high moisture balance prior to an abrupt drying event between ~4600–4400 cal yr BP, which itself is succeeded by relative stability until a dramatic positive deviation from 361 (180–612) cal yr BP to present. This final pulse occurs in the absence of any major paleoclimatic

change and is coincident with an unprecedented sedimentation spike; we therefore interpret this as another confounding colonial signal, with the ~210 yr offset probably attributable to low dating resolution. The C/N-$\delta^{13}C$ relationship (Fig. 2.6) experiences the most extreme and chaotic trajectory of all sites, possibly an artefact of degradational and diagenetic modifications of OM due to poor matrix preservation (Meyers and Teranes, 2001). Nonetheless, the data generally express that, prior to ~4600 cal yr BP drying, the basin existed on the high-$\delta^{13}C$ periphery of the C_3 domain, migrating in the C_4 direction afterwards. Maffra Lake remained in the C_3-C_4 buffer zone for most of the record until ~800 cal yr BP, at which time it returned to the C_3 domain and adopted a rapid trajectory toward the algal domain, which it only entered at -10 cal (-63–113) yr BP.

This abrupt, post-800 cal yr BP transition is unrealistic as a hydrological event and almost certainly an artefact of European enhancement of algal productivity, probably due to nutrient influx. Given Benson and Jacobs (1994) recognise Maffra Lake as permanent and dominated by C_3 sedges and aquatic herbs, we infer C_3 values prior to ~4600 cal yr BP to reflect a dominance of this deepwater community rather than terrestrialisation, in view of increased MA. The ensuing C_4-directional shift coincident with drying is concluded to be an expression of elevated contributions from C_4 grasses. We thus interpret the C_4 signal to reflect the expansion of Temperate Grassland, which must have persisted for the remainder of the Holocene, given Costin (1954) recognises the central Monaro was within the pre-colonial distribution of this TEC (DCCEEW, 2015a).

Drying at ~4600 cal yr BP overlaps with the generally established termination of the hypsithermal on the High Country; Raine (1974) infers a decline in moist flora at Blue Lake from 6500 yr BP, while the proportion of southeastern Australian lakes exhibiting peak levels decreases after ~5500 yr BP (conventional ^{14}C age) (Harrison, 1993, Clerke, 2023). Although the rate of drying is disproportionate to the more gradual profile of hypsithermal deterioration, our record displays a moderate negative correlation with a record of Murray-Darling Basin dust flux from Marx et al. (2011), where a similarly abrupt decline in flux occurs a few hundred yr after drying at Maffra Lake (see Appendix A12). The authors attribute decreased flux to ENSO intensification resulting in contradictorily wetter rather than drier conditions west of the continental divide; reasonable corroboration between this record and Maffra Lake therefore suggests the latter was highly responsive to the ENSO onset. As for Lake Jillamatong, RoC does not strongly agree with the major phase of hydrological change (Fig. 2.4), for which RoC is

elevated but has no peak-points. Surprisingly, a peak instead occurs under relatively stable and high MA from ~5700–5500 cal yr BP, which we cannot explain. RoC increases exponentially after ~400 cal yr BP coincident with the hydrological anomaly, with record-maximum modern values indicating unprecedented systemic disequilibrium at present.

2.6.1.5. Racecourse Lake (13,910 cal yr BP to present)

The Racecourse Lake hydrological reconstruction registers a curiously linear increase in MA despite capturing almost the entire post-deglacial period (Fig. 2.4). It is punctuated by only two positive excursions, the first occurring at ~8500–8000 cal yr BP, driven solely by a cluster of Mn/Fe oxidation peaks. The second occurs at 350 (136–1505) cal yr BP, coinciding with a dramatic increase in sedimentation rates and therefore presumed to be another colonial signature, again with chronological offset. Decomposing the input proxy data reveals that the wetting signal prior to the first oxidation pulse is mainly contributed to by TOC, C/N, $\delta^{13}C$ and CHAR, suggesting a stronger ecological response to initial increases in moisture, as with Lake Jillamatong. Precursory ecological change is supported by the C/N-$\delta^{13}C$ pathway (Fig. 2.6), which indicates the system existed in the C_3 domain until 10,000 cal yr BP and entered the algal domain from ~8000 cal yr BP. Stability ensued until an acceleration towards increasingly algal values from ~2500 cal yr BP. As Racecourse Lake is presently intermittent (Benson and Jacobs, 1994), these trends denote ephemeral conditions before 10,000 cal yr BP and intermittence after 8000 cal yr BP, with an increase in algal productivity from ~2500 cal yr BP. This progression explains oxidation pulses only occurring before 8000 cal yr BP, which are likely a product of frequent lakebed exposure episodes typical of an ephemeral basin.

Initial wetting is consistent with postglacial amelioration over the Pleistocene-Holocene boundary apparent from ecological changes at higher elevation sites such as Rennix Gap (Hope et al., 2019). The shift to intermittence also coincides with hypsithermal onset, as implicated by rapid peat accumulation at many Snowy Mountains sites between ~8600–8500 cal yr BP (Costin, 1972, Hope et al., 2012). Unexpectedly, however, hydrology is unresponsive during the hypsithermal itself, resuming wetting from ~4000 cal yr BP following termination. This cannot be reasonably attributed to any specific mechanism, but does suggest some local muting effect given evidence of the

hypsithermal is preserved in the pollen records of Bega Swamp only ~20 km to the east (Green et al., 1988, Donders et al., 2007).

Post-hypsithermal wetting is also curious given increased El Niño from this time. However, considering the easterly position of Racecourse Lake and its greater exposure to precipitation and ENSO, it is possible this trend again reflects increased permanence due to claypan impermeability and increased La Niña intensity and multiyear frequency, via the same mechanism proposed for Lake Jillamatong. This may also explain increased algal productivity after ~2500 cal yr BP, which postdates the algal transition at Lake Jillamatong by only ~300 yr and therefore may also be a product of more continuous inundation at Racecourse Lake. Despite this agreement, an ENSO-intensification hypothesis for increased permanence at these two sites is apparently contradicted by post-hypsithermal drying to present at Maffra Lake, which is also emplaced on clay and should therefore exhibit similar wetting. However, it should be recalled that Maffra Lake is emplaced in the driest zone of the rain shadow; we therefore attribute this confliction to an orographic muting of this effect in the central Monaro.

Unlike other records, RoC agrees strongly with hydrology, suggesting a coupling between systemic stability and MA over longer timescales. Consistent with the linearity of amelioration, RoC is elevated but stable during the Late Pleistocene and early Holocene. This indicates increased landscape variability due to moisture stress (as for Maffra Lake and Lake Jillamatong) but not systemic reorganisation, suggesting amelioration was sufficiently gradual for systemic change to 'keep pace' with wetting. RoC declines to a minimum during the hypsithermal, conveying transgression of some hydrological threshold permitting systemic stability through to the late Holocene despite ENSO intensification. The European-era increase in RoC is unprecedented for the entire record, suggesting European land use has resulted in record-maximum systemic disequilibrium.

2.6.2. Systemic variability at the regional scale

Due to the incomparability of Z-score values between site hydrology records, relative magnitude (i.e. Z-score) in the regional composite record (Fig. 2.5a) can only be assessed prior to 6000 cal yr BP, as this marks the youngest bin informed by a single record (i.e., Racecourse Lake). Values after 6000 cal yr BP represent the median of at least two

records, meaning Z-score values after this time can only be compared with other times in terms of directionality and relative magnitude. Despite this limitation, it is apparent from our hydroclimate reconstruction (Fig. 2.5b) that southeastern Australia and the South Pacific observed lower precipitation in the Pleistocene than during the Holocene. On this basis, it is reasonable to infer that minimum hydrological values between 13,900–12,800 cal yr BP actually reflect record-minimum MA. This period is succeeded by increasing moisture until 6100 cal yr BP, accelerating between 12,800–11,500 cal yr BP. The timing of such amelioration – which is of course also defined by warming – is supported by palynological changes at Caledonia Fen (tree line rise by 11,000 cal yr BP; Kershaw et al. (2007)) and Mt Kosciuszko (herbfield replacement of feldmark from 10,600 cal yr BP; Martin (1986a)).

Stabilisation of hydrology at 6100 cal yr BP suggests maximum regional MA for the hypsithermal; this is consistent with the timing of peak lake levels in southeastern Australia (Clerke, 2023), though it lags behind peak precipitation in the hydroclimate reconstruction by ~1600 yr. Lag is also observed in the context of post-hypsithermal drying, which is pronounced between ~4500–3000 cal yr BP despite the hydroclimate curve plateauing during this time. This may not necessarily represent a delayed response but rather a stronger response to strengthening El Niño from ~4500 cal yr BP than the earlier post-hypsithermal decline in gross precipitation. However, this inference is again contradicted by subsequent wetting of unknown magnitude from ~3000 cal yr BP, which is not replicated in our hydroclimate record. This unexpected inflection may reflect a sudden switch in the dominant climatic control from increased ENSO intensity to frequency, which postdates the former (Clement et al., 2000, Donders et al., 2008). Specifically, increased frequency of multiyear La Niña may have resulted in increased permanence for at least Lake Jillamatong and Racecourse Lake (and perhaps Arable and Black Lakes), due to reduced hydrological recovery time. As such, we interpret this component of the regional record to be more reflective of basin hydrology than catchment MA, which probably declined during this time due to El Niño intensification and poor rain infiltration into soils.

Hydrological stabilisation and resurgence of drying from ~1500–400 cal yr BP suggest the emergence of another opposing influence. The coincidence of this drying trend with the two discussed warming periods may suggest that warming during a post-maximum decline in ENSO frequency forced a return to drier basin and catchment states (Moy et

al., 2002, Hagemans et al., 2022). Despite case-specific lags, peak cross-correlation with both hydroclimate (r = 0.72) and temperature (r = 0.7) at a lag of 0 (Fig. 2.5c) implies that, on average, regional hydrological responses to climate occur within 100 yr. While this indicates rapid response times, which is unsurprising for pluvial claypans and their impermeable catchments, R^2 values are low for both hydroclimate (0.52) and temperature (0.5). This indicates that climate is only responsible for ~50% of inferred hydrological variability, while an unconstrained combination of intrinsic factors (i.e., stochastic variability, feedbacks and anthropogenic influences) are almost equally influential on hydrology.

Reconstructing regional RoC (Fig. 2.5a) finds that values are stable during the Pleistocene and early Holocene, consistent with linear amelioration and suggesting a strong coupling between systemic stability and MA during this time. After ~9000 cal yr BP, RoC declines to an absolute minimum at ~6200 cal yr BP despite continued catchment wetting, indicating the regional landscape was approaching a quasi-equilibrium state. RoC increases again during late-hypsithermal drying and continues increasing over the remainder of the Holocene. This conveys systemic destabilisation in response to both declining catchment MA and amplified ENSO variability, which would have translated to more dramatic and frequent reconfiguration of system interactions. RoC increases dramatically after 500 cal yr BP, almost doubling to present, which we attribute to embedded colonial signals. Modern RoC – and indeed that of the entire European period – achieve record-maximum values, suggesting greater biophysical disequilibrium at present than any time since ~13,900 cal yr BP. Unprecedented biophysical instability supports ecosystem collapse inferred by Bergstrom et al. (2021) and suggests destabilisation is not purely ecological but systemic in scale.

2.6.3. Interpreting systemic sensitivity

At the basin scale, it appears that ephemeral lakes are most sensitive to hydroclimatic change, being more prone to increased permanence than basins already in an intermittent or permanent state. This is apparent in the case of Lake Jillamatong and Racecourse Lake, which are the only two sites conveying not only early ephemeral conditions but later increases in permanence. Critically, these state shifts are not succeeded by any further instances of such, despite subsequent paleoclimatic perturbation. Evidence of

hydrological shifts are absent for Arable, Black and Maffra Lakes, all of which record permanent conditions for the entirety of their records, and the latter site being of sufficient age to invalidate the argument that a lack of evidence at these sites is an artefact of short temporal coverage. These observations imply some hysteresis behaviour in lake hydrology, whereby basins are more likely to experience a state change if they are ephemeral but are more resilient to reduced MA once they have entered a permanent or intermittent state. This is logical, given their propensity to rapidly inundate due to low substrate permeability and display increasingly high retention times as humidity increases. The negative relationship between permanence and sensitivity corroborates findings by Meerhoff et al. (2012) that shallow lakes (maximum depths <5 m) and those with lower hydrological residence times are most sensitive to climate change.

Asymmetric hydrological sensitivity also extends to basin ecology, which appears to be not only more sensitive to hydrological change than abiotic processes but is more sensitive to such when ephemeral conditions prevail. At the two sites that preserve a state shift, ecology responds to increased moisture well in advance of other abiotic processes such as erosion and lake geochemistry. Specifically, the algal transitions at both Racecourse Lake and Lake Jillamatong coincide with relatively mild wetting that precedes more appreciable hypsithermal- and ENSO-driven wetting, during which ecology remains unresponsive. Stability is also observed along the ecological trajectories of Arable and Black Lakes (Fig. 2.6), both of which are permanent.

This indicates that, as for permanence, basin ecology is highly sensitive to mild increases in moisture balance but is less so to subsequent wetting once permanence is achieved. This is realistic, given even slight inundation of the lake floor would be sufficient to replace C_3 sedge-grass associations with an aquatic, algal-dominated community. Lake Jillamatong and Racecourse Lake also register stronger ecological fluctuations prior to their respective shifts. This may represent 'flickering' before a critical transition (Wang et al., 2012), which in this context probably reflects increased competition between terrestrial and aquatic contributions until inundation is sufficiently continuous to force ecology toward a new basin of attraction. Ephemeral volatility is typical of shallow lakes, which may possess multiple ecological stable states (Vitense et al., 2018), while post-shift stability supports observations by Fuentes and Petrucio (2015) that lake level stability due to high retention times increases algal productivity.

Expanding from the basin scale, we deduce that moisture-stressed catchments are generally more sensitive to climate change than those in mesic regions beyond orographic influence, regardless of the permanence of their constituent lake. This is especially evident in the rain shadow-affected catchment of Arable Lake, which despite hosting a permanent basin is the only system for which we confidently interpret a lake-level response to warming. The absence of such behaviour in the similarly aged Black Lake record undermines the counterargument that preservation of this signal at Arable Lake is simply a product of high sampling resolution. Maffra Lake, also permanent but located in the core of the rain shadow, not only indicates abrupt drying highly disproportionate to the gradual deterioration of the hypsithermal but is also the only site whose catchment expresses major community turnover to grassland. The driest sites, Arable and Maffra Lakes, also possess the highest mean rates of change for all five sites (Fig. 2.4), indicating frequent systemic instability. In comparison, the more mesic Black and Racecourse Lakes show not only lower RoC but also remarkably linear hydrological trajectories over time, while Lake Jillamatong shows a very stable hydrology after its lake becomes permanent, suggesting a quasi-equilibrium of catchment interactions under higher MA. We ascribe this dichotomy between dry and wet catchments to precipitation at the latter being sufficiently high and persistent that climate variability is attenuated (see warming periods at Black Lake; hypsithermal at Racecourse Lake). These catchments are thus less sensitive to climate than more arid sites, where variability in already limited moisture is amplified, triggering a proportionately larger systemic response.

While the relationship between catchment hydrology and RoC is negative, it is also weak, suggesting low systemic sensitivity to MA. This is especially applicable to Lake Jillamatong and Maffra Lake, which preserve RoC peaks that do not align with their respective wetting and drying events, as well as Black Lake, for which RoC peaks during a very mild drought episode but is unresponsive to long-term drying. These observations convey that RoC must be highly sensitive to unassessed factors (e.g., feedbacks, stochastic variability, human activities) working to suppress, amplify and/or delay the impacts of hydrological change. However, in instances where there is some coupling of RoC and hydrology, this usually manifests as elevated RoC during periods of drying or drier than average conditions.

This is documented in cases such as mid-millennium drying at Arable Lake, the brief drying trough at Black Lake, post-3000 cal yr BP drying at Maffra Lake and ephemeral

conditions at Lake Jillamatong and Racecourse Lake. We therefore interpret that, despite low overall sensitivity to MA, systemic disequilibrium is more likely during drying than wetting. This asymmetry is ascribed to drying having a greater capacity than wetting to destabilise moisture-sensitive processes such as terrestrial vegetation growth, erosion, pedogenesis and lake productivity, presumably due to moderately arid conditions placing these systems close to their lower thresholds of tolerance. This is coherent with conclusions by Yao et al. (2021) that dryland ecosystems, especially those modified by pastoral land use, are more vulnerable under drier than wetter conditions, at least in an ecological context.

The significance of internal factors in prescribing systemic behaviour is resonated at the regional scale, where paleoclimate can only explain half of hydrological variability. We thus interpret that endogenous controls are equally influential on landscape hydrology, conveying only moderate regional sensitivity to climate. Nonetheless, where responses to climate are apparent, they occur on average within a century, implying hydrological change is effectively coeval with climate in cases where the latter is sufficiently pronounced to outcompete local noise. This contemporaneity is exemplified in the case of Racecourse Lake, which must have been so sensitive to incipient postglacial amelioration that it inundated and activated sedimentation from as early as ~13,900 cal yr BP, under what Pillans and Walker (1995) presume to have been subalpine conditions.

Hydrological synchroneity with climate is likely attributable to the low permeability of clay soils conducive to rapid runoff and basin inundation. Critically, poor drainage results in conversely high lake buffering capacity upon inundation, recalling our hysteresis model. The negative relationship between catchment RoC and drying/dry conditions is replicated at the regional scale for most of the record, with RoC being elevated under dry early Holocene conditions despite amelioration, declining to a minimum during the hypsithermal and increasing again upon its deterioration. Post-3000 cal yr BP increases in RoC are unsurprising given late Holocene decreases in catchment MA; however, these values are substantially higher than during much drier early Holocene conditions, which we attribute to superimposed ENSO variability. We therefore propose that catchments are more sensitive to the interannual variability than gross availability of moisture, probably due to more extreme, rapid oscillations in system processes (e.g., vegetation growth, fire, erosion events). This likely contributes to the poor correlation observed between RoC and MA.

Sensitivity to European land use is spatially variable, with no obvious colonial signal manifesting at Arable Lake or Lake Jillamatong, and only a weak, abiotic marker at Black Lake. This cannot be attributed to a lack of forcing, given the pervasive modification in all five catchments (see Appendix A7), nor to any other characteristic unique to the two sites that do preserve an exponential pulse. While we cannot provide a reasonable explanation for this disparity, decomposing the proxy data reveals colonial excursions are always associated with increased sedimentation, and sometimes by increased algal contributions, productivity and/or redox changes. We therefore conclude that erosion is the most diagnostic symptom of colonial land use change in these catchments, suggesting high vulnerability to soil exposure driven by grazing and cropping. Increased algal dominance and productivity also suggests that the Monaro lakes are prone to eutrophication resulting from influx of limiting nutrients by livestock and fertilisers; these are in turn recognised in the Upland Wetlands recovery plan as facilitating weed encroachment (NSW TSSC, 2005). Unprecedented European-era RoC suggests the Monaro is more sensitive to land use change than any major climatic disturbance since deglaciation. This is consistent with global paleoecological RoC analysis by Mottl et al. (2021a), who conclude that human impacts on ecosystems exceed those of any postglacial climatic perturbation, for all continents, though it is important to recall that we are unable to account for pre-European anthropogenic influences.

2.6.4. Implications for future anthropogenic biophysical change

The most recent climate projections for NSW (NARCliM2.0) forecast 3.5–3.7 ºC warming for the Monaro by 2100 CE (2080–99 window relative to 1990–2009 baseline), under the IPCC's medium- to high-emissions pathway (SSP3-7.0) (Intergovernmental Panel on Climate Change, 2023, AdaptNSW, 2024). Projected trends in precipitation are more geographically variable; while annual rainfall is anticipated to decline across the region, much larger decreases (-10 to -17%) are expected for the southeastern Monaro than elsewhere (-2 to -10%). Furthermore, although increases (0 to +7%) in summer-autumn rainfall (Fig. 2.7) and decreases (-11 to -22%) in winter-spring rainfall are projected for most of the region, the southeastern Monaro is anticipated to dry across all seasons, especially in winter (up to -36%) (AdaptNSW, 2024).

Decreased annual and increased warm-season precipitation is largely ascribable to projected changes in the behaviour of ENSO and the Southern Annular Mode (SAM), respectively, the latter being the dominant control on the latitudinal position of the moisture-laden westerlies (Meneghini et al., 2007). A positive SAM is associated with a poleward retraction of the westerlies and a concomitant increase and decrease in summer and winter rainfall, respectively, in southeastern Australia. Analysis of historical data reveals the SAM has shifted towards a mean positive state since 1950 CE, with modelling predicting this will continue over the 21st century, exacerbating the seasonal imbalance in precipitation (Lim et al., 2016, Deng et al., 2022). Changes are also identified for ENSO, the amplitude of which has increased by 10% since 1950 CE; oscillations are anticipated to not only intensify over the coming decades but also become more frequent (Cai et al., 2023, Thirumalai et al., 2024). Furthermore, Lieber et al. (2024) conclude that regions experiencing wet or dry conditions during El Niño or La Niña are likely to observe an

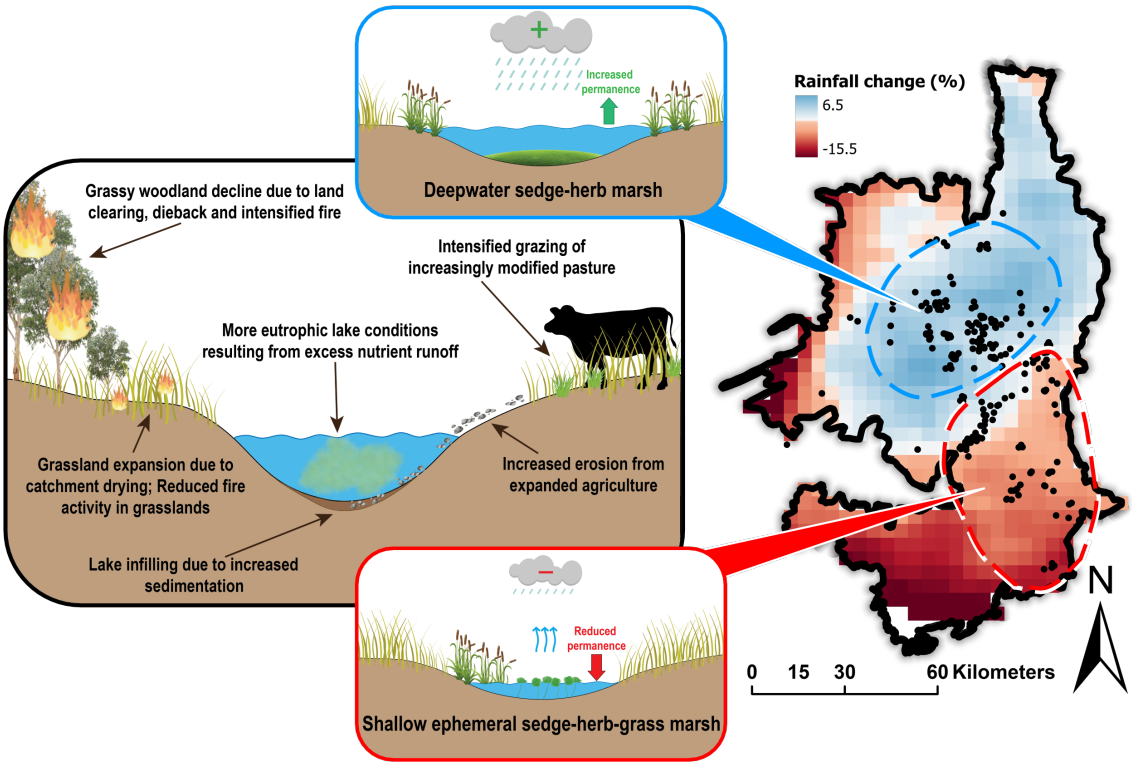

Figure 2.7. Projected rainfall trends and expected biophysical outcomes for the Monaro. Map grid values reflect the mean percentage change in warm-season (summer-autumn) rainfall for 2080–2099 CE relative to 1990-2009 CE, under SSP3-7.0 (NARCliM2.0) (DCCEEW, 2024b). Dashed regions demarcate the subpopulations of lakes likely to observe increased permanence (north) or decreased permanence (south), with ecological implications summarised in the top and bottom inset, respectively. Large centre inset depicts major biophysical changes anticipated for all basins and catchments.

amplification of these conditions, implicating more severe El Niño and thus drought for southeastern Australia. Consistent with late Holocene trends, multiyear instances of both phases are also likely to increase in the future (Ding et al., 2022, Geng et al., 2023).

The Monaro currently exhibits maximum and minimum rainfall in summer and winter, respectively (Bureau of Meteorology, 2025a); lake basins are thus dependent on warm-season rainfall for replenishment and persistence through the drier cold season. As such, despite projected warming and reduced annual and cold-season precipitation, we anticipate that the complementary SAM-related shift towards warm-season rainfall – in concert with more intense and frequent multiyear La Niña – will result in increased lake retention time in parts of Monaro projected to receive increased summer rainfall. This deduction is informed by reconstructed late Holocene basin wetting attributed to intensified ENSO. We therefore expect an increase in the relative proportion of permanent lakes over much of the rain shadow-affected central and northern regions (Fig. 2.7) and increasingly resilient basin hydrology and ecology thereafter, following the hysteresis behaviour reconstructed for these sites. This is unlikely to be the case in the south and east, however, where we expect the nexus of warming and year-round precipitation declines will force a widespread downgrading of many basins to ephemeral states. While resilient permanent lakes such as Black Lake may persist in such a state for longer, we expect sooner shifts to ephemeral conditions for intermittent systems such as Racecourse Lake.

These spatially bifurcated trajectories have significant implications for the conservation of the Upland Wetlands TEC, which we predict will become increasingly represented by deepwater herbs at the expense of floating-attached and emergent macrophytes, due to the regional expansion of permanent basins. In contrast, systems deteriorating into an ephemeral state are likely to see increased characterisation by shallow sedge-herb-grass marsh, an archetypal ephemeral assemblage (Benson and Jacobs, 1994) (Fig. 2.7, small insets). More frequent and protracted lakebed terrestrialisation by colonising grasses may encourage an encroachment of grazing onto lake floors, given ephemeral sites are the most severely pugged on the Monaro, and are assigned lowest conservation value (Benson and Jacobs, 1994). If realised, these patterns will translate to a long-term extirpation of the Upland Wetlands in the south and east. Ecological shifts are also likely to precede systemic instability, given higher ecological than abiotic sensitivity. Increased representation of Upland Wetlands in rain shadow-

emplaced basins may demand a reprioritisation of these sites as high-value refugia, ensuring more successful conservation outcomes. Given most lakes are on private landholdings, conservation of emerging permanent lakes would be most feasible through establishment not of nature reserves but travelling stock reserves – as is already the case for Maffra Lake – which are subject to low stocking rates and 81% of which possess medium to high conservation value on the Monaro (Department of Regional New South Wales, 2017).

In contrast to dichotomous basin trajectories, we anticipate warming and annual rainfall declines will result in universal drying of surrounding catchments, given poor infiltration capacity. The macroecological implications of catchment drying will likely include increased prevalence of drought-tolerant grasses and thus regional grassland expansion analogous to that reconstructed for post-hypsithermal Maffra Lake. This will be facilitated by novel stressors (i.e., grazing, severe fire weather, land clearing and eucalypt dieback), perpetuating the decline of the Grassy Woodland TEC (Ross and Brack, 2015, DCCEEW, 2024a). Retraction may ironically act to suppress regional fire activity, which is exacerbated by woody eucalypt vegetation, the growth of which appears to be correlated with higher rather than lower humidity (Fig. 2.7).

However, grassland expansion may not translate to positive conservation outcomes for the Temperate Grassland TEC either, given recent decline of this community especially in the central and southern Monaro due to overgrazing and supplanting by naturalised weed species (Garden et al., 2001, Dorrough and Ash, 2003). Moreover, modelling of native pasture growth rates on the Monaro by Alcock (2012) projects declines for 2030 CE due to warming and drying. We thus anticipate grassland expansion will be pioneered not by pure Temperate Grassland but hybridised native-exotic assemblages constituting modified pasture (Fig. 2.7). This may benefit the grazing industry – a third of the area of which is already dependent on modified pasture – particularly in the rain shadow, which represents the nucleus of present grassland coverage, and where emerging permanent lakes may bolster livestock watering capacity (Australian Bureau of Agricultural Resource Economics Sciences, 2024).

The above ecological changes will form only one facet of broader systemic destabilisation, which is likely to increase beyond modern unprecedented levels given the positive correlations between RoC and both drying and ENSO intensification, both of which are projected for 2100 CE. This is especially pertinent to rain shadow-affected

subregions poised to remain the driest areas of the Monaro despite increases in warm-season rainfall (AdaptNSW, 2024), which itself may exacerbate dissociation of system processes due to increased seasonal asymmetries. However, recognising that RoC is often insensitive to MA, systemic destabilisation will also be strongly dictated by a suite of local processes, particularly those identified as sensitive to land modification (i.e., erosion and trophic status). Specifically, land use change is likely to increase soil exposure and erosion due to a) overgrazing, trampling and diminution of native species due to exotic competition, and b) eutrophication of lakes due to enhanced nutrient influx associated with increased stocking rates. Rapid sedimentation may also threaten shallower basins (e.g., Maffra Lake) with infilling, counteracting the positive effect of increased permanence and 'artificially' inducing ephemeral conditions (Fig. 2.7).

2.7. Conclusions

Here we have constrained the systemic sensitivity of the Monaro to climate and land use from multiproxy reconstructions of five lacustrine sedimentary sequences. We find that, although the region shows short average response times to hydroclimatic and temperature changes, these are only responsible for approximately half the hydrological variability in the landscape. This implies only moderate hydrological sensitivity to climate, and that magnitudes and directions of hydrological change are equally determined by intrinsic catchment processes. Of salient influence among these endogenous actors is the uniquely impermeable pedology of the lake catchments, which forces rapid transfer of moisture from slopes to basins. This mechanism explains the post-3000 cal yr BP wetting signal in regional MA despite post-hypsithermal climatic deterioration, an idiosyncrasy that is attributed to more intense and frequent multiyear La Niña and reduced hydrological recovery time due to poor drainage. These late Holocene trends also suggest higher hydrological sensitivity to interannual climatic variability than gross moisture variability. Impermeability also explains inferred hysteresis in lake hydrology, namely the tendency for lakes to remain permanent/intermittent once they depart an ephemeral state. In upgrading basins, the corresponding shift from a terrestrial to aquatic ecology occurs early during wetting, preceding many abiotic changes and remaining stable despite subsequent increases in MA. It is therefore concluded that

permanent/intermittent systems and their ecological communities are less sensitive to MA than ephemeral basins.

We also infer that moisture-stressed catchments are more hydrologically sensitive to climate change than those in mesic areas, probably attributable to the former already existing near their thresholds of systemic stability. Catchment sensitivity to drying is replicated by changes in RoC, which is more frequently associated with lower rather than higher moisture. Despite this asymmetry, moisture appears to only weakly influence RoC, reinforcing the significance of endogenous interactions in governing systemic sensitivity. Internal attributes must also have some influence on catchment sensitivity to European land use change, the impacts of which are not manifested in every record. Nonetheless, unprecedented RoC after colonisation indicates the Monaro is more sensitive to the impacts of pastoralism than any major climatic perturbation since deglaciation.

In the context of projected warming, drying and changes to climate drivers, we propose the Monaro will observe an increase in the proportion of permanent lakes within the rain shadow, where warm-season increases in rainfall are forecasted, while the south and east may be increasingly represented by ephemeral basins due to annual rainfall deficits. These trends threaten the Upland Wetlands with floristic simplification and retraction. In surrounding catchments, we expect universal drying due to warming and decreased annual rainfall, which, in concert with increased annual to interannual rainfall variability, is likely to amplify systemic disequilibria, with poor conservation outcomes for both Temperate Grassland and Grassy Woodland. Biophysical destabilisation due to climate change will be exacerbated by land use change, namely increased stocking rates on savannised catchments and ephemeral lake floors, threatening catchments with erosion and basins with eutrophication and infilling.

2.8. Afterword

This chapter has addressed the biases of high-altitude research outlined in Chapter 1 by investigating the systemic paleoenvironmental sensitivity of the Monaro through multiproxy analysis of five lake sequences. While difficulties in ^{14}C dating resulted in poorly resolved core chronologies, multisite synthesis has elucidated several spatiotemporal asymmetries in highland sensitivity to climate and land use change. Despite lake catchments being moderately sensitive to postglacial changes in

hydroclimate, the Monaro lakes themselves have been more sensitive to the interannual variability than gross amount of precipitation.

This is evidenced by lake hydrological recovery from ~2600 cal yr BP despite declining precipitation, a discrepancy attributed to an increase in the frequency, intensity and duration of La Niña phases and thus reduced drainage capacity. Hydrological recovery translated to increased permanence for at least Lake Jillamatong and Racecourse Lake. These lakes have become more hydrologically and ecologically resilient since their departure from an ephemeral state, which in both cases have been heralded by major ecological reorganisation. Further asymmetries emerge in lake catchments being more sensitive to drier than wetter conditions; drier catchments such those hosting Arable and Maffra Lake are more unstable under and responsive to climatic forcing than more mesic catchments. Moreover, systemic instability for all catchments is negatively correlated with MA.

However, the weakness of these correlations indicate postglacial systemic stability has also been strongly prescribed by intrinsic mechanisms such as stochastic variability, internal feedbacks and precolonial land use. The latter of these factors may be particularly significant given European-era instability is unprecedented for the entire record, implying higher highland sensitivity to land use than climate change. Despite these generalisations, there exists substantial site variability in systemic responses to disturbance, which confirms that highland sensitivity is spatially heterogeneous and suggests that future responses to GEC will also be regionally complex. Indeed, reviewing these reconstructions, future changes are likely to include, *inter alia*, geographically bifurcated transitions in lake permanence and a shift towards frequent, low-intensity fires as geographically peripheral woodland is replaced by modified pasture.

To assess the degree to which highland sensitivity deviates from that of adjacent mountains, Chapter 3 endeavours to apply a comparable multiproxy approach to the overlying montane zone of the SM. The montane zone is investigated independently in this thesis as it is the most extensive zone in the SM and in fact most mountains globally, rendering it geographically representative of mountain environments, change and sensitivity.

Chapter 3

Thresholds in montane sensitivity to climate and land use change over the late Holocene: Multiproxy evidence from Snowy Mountains peat records, southeastern Australia

3.1. Abstract

Mountains are extremely vulnerable to anthropogenic disturbance, with degradation of the montane zone being globally consequential. However, mountain responses to exogenous perturbations are often ecologically framed, skewing interpretations of systemic (i.e., abiotic *and* biotic) sensitivity. In a paleoscientific context, this impairs accurate reconstructions and thus projections of long-term biophysical change. Here, we present, from two peat records, a comprehensive multiproxy reconstruction of montane paleoenvironmental change in the Snowy Mountains, southeastern Australia. Reconstructing systemic variability since ~3200 cal yr BP, we interpret an early decline in catchment moisture availability contemporaneous with intensification of the El Niño-Southern Oscillation (ENSO). Abrupt systemic change during this time implies threshold sensitivity to precipitation.

Curiously, we reconstruct a later recovery in moisture availability – associated with increased erosion, fire and peatland productivity – contemporaneous with ENSO-related warming, which we ascribe to enhanced warm-season inflow of snowmelt into montane catchments. The centrality of ENSO to declining precipitation and warming implicates it as the salient forcing on late Holocene montane dynamics. However, the temporal shift in climatic influence on our records from precipitation to temperature suggests transgression of some threshold in systemic sensitivity towards the latter. Threshold sensitivity is also inferred for peatlands, with moisture-stressed complexes appearing less resilient to climate and land use change. Despite reconstructed increases in moisture availability under warming and low overall sensitivity to colonial-era degradation, we project substantial drying and destabilisation of montane catchments under accelerating climate change. Our records suggest systemic instability will be characterised by peatland deterioration and intensified erosional and fire regimes.

3.2. Introduction

Mountains are among the most sensitive terrestrial environments to global environmental change. High elevation and relief manifest restricted areas and steep climatic gradients that produce bioclimatic zones near their thresholds of instability (Gordon et al., 2002, Beniston, 2003, Guisan et al., 2019). Such characteristics predispose these zones (alpine, subalpine and montane) to dramatic destabilisation under climate

change, impairing their provision of environmental services to industries that, in turn, exacerbate environmental stress (Grabherr et al., 2001, Hock et al., 2019, Pepin et al., 2022a, Pereira et al., 2022, Ombadi et al., 2023). These compounding stressors have initiated historically unprecedented biophysical changes surpassing those in most other environments (Fort, 2015, Schmeller et al., 2022).

While relevant across the entire mountain transect, changes occurring in the lowermost montane zone are of global consequence, as it is often the largest zone and thus most representative of mountain environments worldwide (Körner et al., 2017). Due to an elevational optimum of temperature and precipitation, montane environments are typified by elevated productivity, pedogenesis, fire activity and erosion (Körner, 2004, Körner et al., 2011, Mehmood et al., 2024). Climatic intensification of these interactions is propelling many montane ecosystems towards tipping points (e.g., Albrich et al. (2020), Bush (2020), Das et al. (2024)). This is concerning in the context of warming-driven ecotonal advance, which is facilitating expansion of montane forest in the 62% of mountains exhibiting a mid-elevational peak or trough in area, such as the Rocky Mountains, Himalaya and Australian Alps (Elsen and Tingley, 2015). The implication of this is that the global mountain environment will become increasingly represented by the montane zone and its unique anthropogenic transformations, which are not only climatically but also locally driven (Elsen and Tingley, 2015). Indeed, the montane zone lies on the altitudinal 'frontline' of land use changes imposed by industries encroaching from adjacent highlands and lowlands (Allan, 1986, Hall et al., 2009, Armenteras et al., 2011).

Although anthropogenic perturbations reverberate throughout the entire biophysical system, they are primarily assessed through ecological metrics such as ecotonal, phenological and biodiversity changes (e.g., Harsch et al. (2009), Pauchard et al. (2009), Grabherr et al. (2010), Elumeeva et al. (2013), Inouye and Wielgolaski (2025)). An emphasis on ecological sensitivity (i.e., reactivity to stimuli) biases our understanding of 'systemic' sensitivity, that is, pertaining to the entire landscape as the sum of biotic and abiotic components. This core tenet of geoecology remains underappreciated in paleoscience, which in mountains is disproportionately informed by palynological, charcoal and tree-ring studies (Kumar and Deshmukh, 2015, Razjigaeva et al., 2017, Zhang and Feng, 2018, Han et al., 2019, Ives, 2019). Reliance on such data risks extending ecological bias to millennial timescales, impairing the utility of paleo-

analogues in accurately projecting systemic environmental change to better inform conservation and land management (Birks and Birks, 2006, Gornitz, 2008).

This knowledge gap is being remedied by multiproxy studies (e.g., Cheng and Ye (2019), Rostami et al. (2024), Zhang et al. (2024)), which involve triangulation between abiotic and biotic proxies to achieve a more representative reconstruction of long-term systemic variability. Through comparison of multiproxy reconstructions with independent records of paleoclimate and land use, variability can be translated to sensitivity, strengthening predictions of catchment-scale responses to anthropogenic disturbance. Despite its global uptake, multiproxy research is sparse in the Snowy Mountains (SM) of southeastern Australia, which remains dominated by pollen and charcoal records (Hope et al., 2012). Here, we present multiproxy paleoenvironmental reconstructions from two new montane peat records from the SM. Incorporating a range of biotic and abiotic proxies, we constrain sensitivity at the process, catchment and zonal scale to make qualified prognoses of future environmental change in an extremely sensitive montane environment.

3.3. Regional setting

Straddling the border of New South Wales and Victoria, the SM constitutes the largest contiguous body of montane, subalpine and alpine habitat in Australia, despite representing 0.09% of continental area (Fig. 3.1a) (Sahukar et al., 2003, DCCEEW, 2020). Cenozoic denudation has reduced the SM to a low-relief and -elevation plateau with an areal peak in the montane zone (~1000–1500 m ASL), which spans 74% of the range (Fig. 3.1a) (Kohn et al., 1999, Costin, 2000, Elsen and Tingley, 2015). While its altitudinal range is defined by that of wet sclerophyll forest, the montane zone is also geomorphically discrete; on the eastern flanks, abrupt changes in slope demarcate it from the Monaro Tablelands below and alpine-subalpine zones above (Sahukar et al., 2003, Mooney, 2004, Mason and Williams, 2013c).

Although the montane zone occupies the steepest segment of the mountain profile, sufficiently high annual temperatures (~9–6 ºC) and rainfall (~1000–1600 mm) accelerate organic matter decomposition such that deep (>1 m), relatively fertile clay loams and podsols are widespread despite the heavily leached granite and sandstone bedrock (Geoscience Australia, 2012, Mason and Williams, 2013b, Xu and Hutchinson, 2013,

Slattery, 2015, Wilson et al., 2022). This thick soil mantle supports tall open forest dominated by Ash-type *Eucalyptus* associations that vary with aspect and the orographic decline in rainfall downslope (Costin, 2000, Sahukar et al., 2003, Mooney, 2004, Mason and Williams, 2013c, Slattery, 2015). Montane floristics are further complicated by the intercalation of open valleys facilitating the drainage of both cold air and water, rendering them low-elevation refugia for mires (Fig. 3.1b) (Mooney et al., 1997, Sahukar et al., 2003, Hope et al., 2012, Kemp and Hope, 2014). In the montane zone, these mires are predominantly topogenous, minerotrophic fens (inundated sedge-rush mires) and moors (sedge-rush shrubland) (Grover et al., 2005, Hope et al., 2012, Wilson et al., 2022).

Fire regimes are also most intense in the montane zone, attributable to high biomass production and the prevalence of pyrophytic eucalypts which promote fire but are also

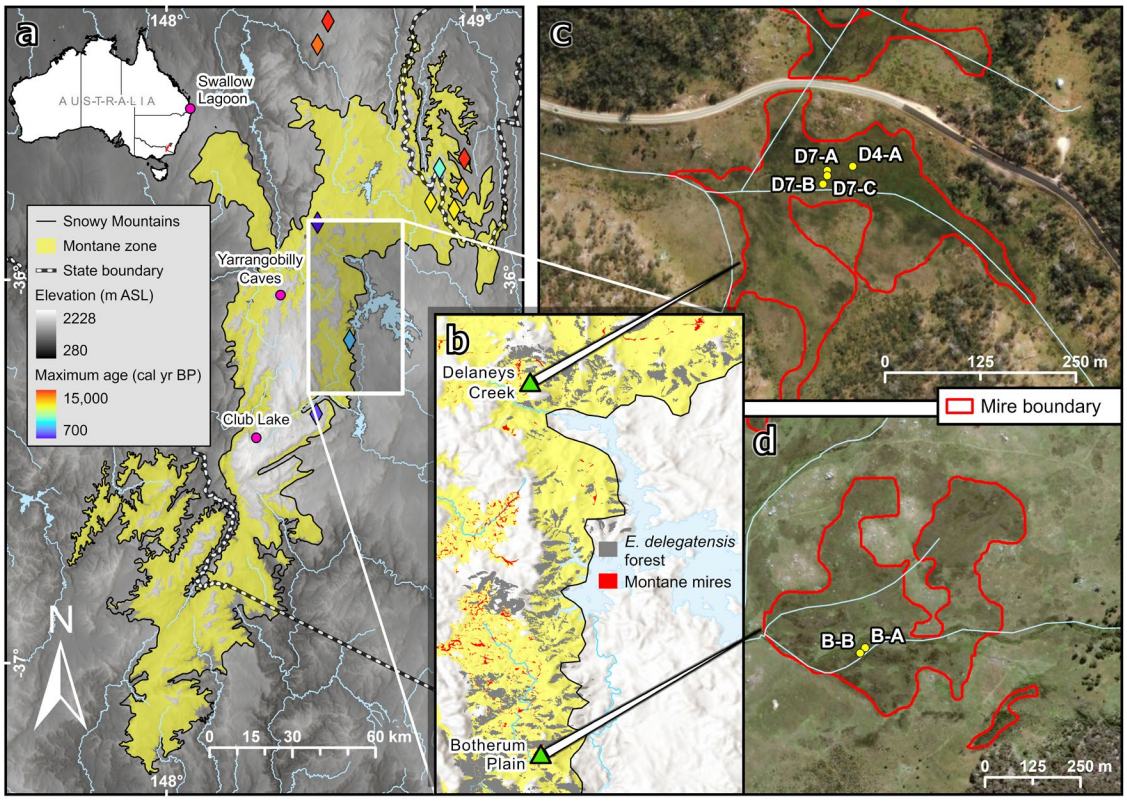

Figure 3.1. Maps displaying **a)** the Snowy Mountains biogeographic subregion, including location in Australia (red region in inset) and independent montane records (diamonds), **b)** locations of mires sampled in this study and of relevant ecological communities, and locations of cores at **c)** Delaneys Creek, and **d)** Botherum Plain (yellow points). Pink markers denote mainland paleoclimate studies relevant to this study; non-mainland sites are not mapped. Data obtained from DCCEEW (2020) (Snowy Mountains subregion), Gallant et al. (2009) (digital elevation model), State Government of NSW Spatial Services (2025) (hydrography), DCCEEW (2016b) (montane mires), DCCEEW (2016a) (*E. delegatensis* forest) and Hope et al. (2012) (ages and locations of independent montane records).

sensitive to high fire return intervals (O'Dowd and Gill, 1984, Boland, 2006, Williams et al., 2009b, Zylstra, 2018). Consequently, montane forests have been significantly modified by the indiscriminate application of fire by European pastoralists from the 1830s, which marked a dramatic departure from the precolonial baseline of low-intensity burning sustained in part by the Indigenous Ngarigo people (Hancock, 1972, Mooney, 2004). Over a century of annual 'hot' burning, followed by prohibition from 1958 and ongoing fire suppression, has encouraged the post-fire proliferation of colonising eucalypts, increasing the density of the modern tree stratum (Wimbush and Costin, 1979, Mooney et al., 1997, Zylstra, 2006).

This is problematic in the context of global warming and concomitant changes to the El Niño-Southern Oscillation (ENSO) and Southern Annular Mode (SAM), the two dominant regional climate drivers (Slattery, 2015). Resultant warming and drying are amplifying fire weather, which drove the burning of 85% of the broader Australian Alps from 2002–2013 alone (Hennessy et al., 2008, Pickering and Venn, 2013, Bowman et al., 2014). Intensified fire is being reinforced by the increased postcolonial density of montane forest, which burns more readily and facilitates the growth of more flammable juvenile stands. A positive flammability feedback has evidently emerged whereby forests are becoming younger and sparser, approaching a critical transition to grassy woodland (Bowman et al., 2014, Zylstra, 2018, Bergstrom et al., 2021). While Bergstrom et al. (2021) hence argue montane forests are collapsing, the systemic implications of ecological change have not yet been investigated systematically.

In the montane zone, the corpus of paleoenvironmental data derives exclusively from mires, whose underlying peats are the only available natural archives of Holocene paleorecords (Fig. 3.1a). This is concerning given montane peatlands are not only threatened with physical destruction by fire but also by feral horses, with peatland recovery from the latter requiring millennia even without the superimposed effects of climate change (Hope and Clark, 2008, TSSC, 2008, Lawrence et al., 2009, Driscoll et al., 2019, Treby and Grover, 2024). The increasing rarity of these natural archives underscores the urgency of applying multiproxy analyses to their records to reconstruct both their sensitivity and that of surrounding catchments. However, interrogation of montane peat records to date has been limited to reconstructing vegetation and fire histories, with minimal systemic contextualisation of such changes (e.g., Mooney et al. (1997), Hope et al. (2009b), Kemp (1993)).

3.4. Materials and methods

3.4.1. Site selection and sampling

Sampling sites were selected from the population of montane mires documented by Hope et al. (2012) (Fig. 3.1b) based on their topographic setting, with the authors demonstrating that valley-floor complexes are associated with deeper, older sequences. Mires were also prioritised based on proximity to *E. delegatensis* forest (Fig. 3.1b), given the species' keystone status and thus central role in contemporary ecological 'collapse' (Bergstrom et al., 2021). Following these criteria, we selected a fen on Delaneys Creek ('Delaneys'; Fig. 3.1b, c) and a moor on Botherum Plain ('Botherum'; Fig. 3.1b, d) (Appendix B1). Cores were recovered using a Russian peat sampler along a cross-mire transect to characterise lateral changes in the depositional facies, following which they were placed into polyvinyl chloride liners, stratigraphically logged, subsampled and refrigerated.

3.4.2. Dating, chronological modelling and multiproxy analysis

Basal samples were submitted first for AMS ^{14}C dating to verify core suitability for analysis. Detailed dating was subsequently conducted for the oldest core at each site only, targeting a combination of bulk sediment and sporopollenin samples with minimal discrepancy in accuracy expected between these fractions (Appendix B2). Conventional ^{14}C ages in yr BP were calibrated, and age-depth models in calibrated yr BP (cal yr BP) were constricted using the R software BACON (Blaauw and Christen, 2011, R Core Team, 2020) and the SHCal20 calibration curve (Hogg et al. (2020).

Cores with detailed chronologies were subjected to downcore analysis of sedimentological and geochemical parameters with known sensitivity to key abiotic and biotic processes (Appendix B3–6). Whole cores were scanned for volume magnetic susceptibility to identify intervals of peat humification and/or influx of eroded soils (Mullins, 1977, Dearing, 1999b, Dearing, 1999a, Thompson, 2012). Scanning micro-X-ray fluorescence (μXRF) was also performed to assess geochemical variability associated with clastic influx, which we anticipated would be clearly expressed in these organic deposits (Last and Smol, 2002, Croudace and Rothwell, 2015, Davies et al., 2015). Lithogenic elements were thus expected to contribute significantly to the first Principal Component (μXRF PC1) generated by Principal Component Analysis of the μXRF data.

After subsampling, we analysed mineral grain size to supplement our μXRF erosional indices with a qualitative measure of fluvial energy, given both sites are emplaced on drainage networks (Fig 1c, d). To augment these predominantly abiotic proxies, we also quantified total organic carbon (TOC) and total nitrogen (TN) (TOC-TN) and their ratio (C/N), which are overwhelmingly influenced by peat preservation and decomposition prescribed by moisture balance (Kuhry and Vitt, 1996, Anderson, 2002, Charman et al., 2013, Loisel and Yu, 2013, Yang et al., 2023, Treby and Grover, 2024). To further constrain productivity, bulk $\delta^{13}C$ was measured; while this can be influenced by bog-fen transitions, such transitions are rare in Australian peat records (Cristea et al., 2014, Mooney et al., 2021, Yang et al., 2023). Moreover, $\delta^{13}C$ is predominantly controlled by decomposition, and is thus regarded as a proxy for such (Drollinger et al., 2019, Yang et al., 2025). Macrocharcoal (>125 μm) abundances were measured to reconstruct local fire variability. Given saturated peat does not readily burn and macrocharcoal derives from woody vegetation, we consider it a proxy for forest rather than mire burning (Whitlock and Larsen, 2001, Mooney and Tinner, 2011).

3.4.3. Statistical syntheses

To reconstruct the systemic variability of both catchments, we evaluated magnitudes, directions, rates and lags of change across the proxy suite. Using modelled sedimentation rates and dry bulk density calculations, we computed three simple ‘magnitudes’ of change: bulk mineral influx, apparent C accumulation rates and macrocharcoal accumulation rates (Appendix B7); these respectively append absolute constraints to erosional yield, peatland productivity and fire activity. Apparent C accumulation rates are of particular interest, as they remain understudied in Australian peatlands (Gaffney et al., 2025). To assess directions of change, we standardised these absolute metrics and aggregated them with other standardised, qualitative proxies to reconstruct relative moisture availability (Appendix B8). This is the most relevant variable for which directionality should be constrained as it is presumed to be the salient control on multiproxy variability. This is in view of a) the mesic conditions of the montane zone, and b) a consensus that hydroclimate, not temperature, has been the dominant forcing on southeastern Australian Holocene records (Harrison, 1993, Quigley et al., 2010, De Deckker, 2022, Clerke, 2023).

Following Hamilton et al. (2024), proxies were directionally standardised such that all were positively correlated with 'wetting', based on *a priori* presumptions on the relationships between their corresponding processes and moisture availability (Appendix B8). Rate-of-Change analysis was also performed on the proxy suite (Appendix B9) to approximate how rapidly the system adjusts to perturbation, with higher values indicating greater instability (Mottl et al., 2021b). To reconstruct 'zonal' variability, all above composite records were binned or interpolated to 100 yr intervals (the maximum resolution ensuring multisite data for each interval) and averaged across both sites (Appendix B7–9). Zonal records were subject to simple Pearson correlation with independent reconstructions of temperature, precipitation and climate drivers to qualitatively gauge climatic sensitivity (see Section 3.5.3; Appendix B10). Zonal Rate-of-Change was also cross-correlated with temperature and precipitation, using the 'stats' package in base R (R Core Team, 2020), to assess any lead/lag relationships between systemic and climatic destabilisation.

3.5. Results

3.5.1. Core sampling, stratigraphy and chronological modelling

Three rounds of site sampling between 2023 and 2024 obtained six short cores from Delaneys (Fig. 3.1c) and two from Botherum (Fig. 3.1d) (Appendix B11). For Delaneys, D7-A (length 49 cm) was selected for dating and multiproxy analysis due to it capturing a downcore transition from sapric black peat to dark greyish brown silt. This transition was also observed in the upper 10 cm of D4-A2, which underlies D7-A but is situated 27 m downslope. Below 10 cm, D4-A2 grades to yellowish-brown sand which could not be dated due to low TOC. By stratigraphically correlating the upper 10 cm of D4-A2 and lower 10 cm of D7-A, ^{14}C dates from D4-A2 were transferred to their equivalent depth in D7-A (Appendix B12). This yielded a median basal age of 3261 (95% confidence interval 2922–6771) cal yr BP for D7-A (Appendix B13). Both Botherum cores, B-A and B-B, were of similar length (35 cm and 41 cm, respectively) and visually identical, comprising a unit of black peat with a fibrous upper subunit. Basal ^{14}C samples were therefore analysed for both B-A and B-B, which were respectively dated to 1781 ± 25 yr BP and 1851 ± 24 ^{14}C yr BP (Table 3.1). The older B-B was prioritised for detailed dating, producing a median basal age of 1620 (1229–1800) cal yr BP (Appendix B13).

Table 3.1. ^{14}C dating results for all dated cores. Asterisks indicate removal from age-depth modelling due to a 'Modern' result or a major age reversal presumably relating to 'young' C influencing pollen samples. Lab ID 'OZBY' is for samples analysed at the Australian Nuclear Science and Technology Organisation (Hua et al., 2001, Fink et al., 2004). Lab ID 'D-AMS' is for samples analysed at DirectAMS (Tate et al., 2023). Sampled depths indicate core-specific depths, while true depths indicate depths relative to ground level.

Lab ID	Core ID	Sampled depth (cm)	True depth (cm)	Material	^{14}C age (yr BP ± 1σ)
OZCF88*	D7-A	14		Pollen	Modern
OZCF89	D7-A	35.5		Bulk sediment	2806 ± 25
OZBY49	D7-A	36		Pollen	1774 ± 82
OZBZ36	D7-A	49		Bulk sediment	7032 ± 75
OZCF90*	D4-A2	0.5	39.5	Bulk sediment	Modern
OZBZ35	D4-A2	6	45	Bulk sediment	2990 ± 63
OZCF92	D4-A2	10	49	Bulk sediment	2739 ± 29
D-AMS 050595	B-A	41		Bulk sediment	1781 ± 25
D-AMS 050596	B-B	19		Bulk sediment	721 ± 19
OZBQ19*	B-B	25		Pollen	680 ± 51
OZBQ20	B-B	28		Pollen	787 ± 55
D-AMS 050597	B-B	35		Bulk sediment	1851 ± 24

3.5.2. Multiproxy analysis

D7-A can be subdivided into three multiproxy phases corresponding to lithostratigraphic units (Fig. 3.2a). The earliest spans until ~2700 cal yr BP, overlapping with the sub-peat unit, and exhibits intermediate $\delta^{13}C$ and maxima in sedimentation rates, mean grain size, C/N and μXRF PC1, 77% of its variance being contributed to by lithogenic elements (Appendix B14). This phase also records minima in TOC-TN and macrocharcoal counts. While $\delta^{13}C$, TOC-TN and macrocharcoal counts at the start of this phase well exceed average sub-10 cm values in D4-A2, grain size, magnetic susceptibility and C/N are substantially lower (Appendix B12). Magnetic susceptibility is the only proxy to remain unresponsive into the second phase, which coincides with the transition to peat and is signalled by abrupt deviations in all proxies then stability until ~1900–1600 cal yr BP. Stability is apparent in low sedimentation rates, minimum grain size, PC1 and C/N, maximum $\delta^{13}C$ and gradual increases in TOC-TN and macrocharcoal. The third phase is marked by increasingly negative $\delta^{13}C$ and increased TOC-TN, grain size, PC1,

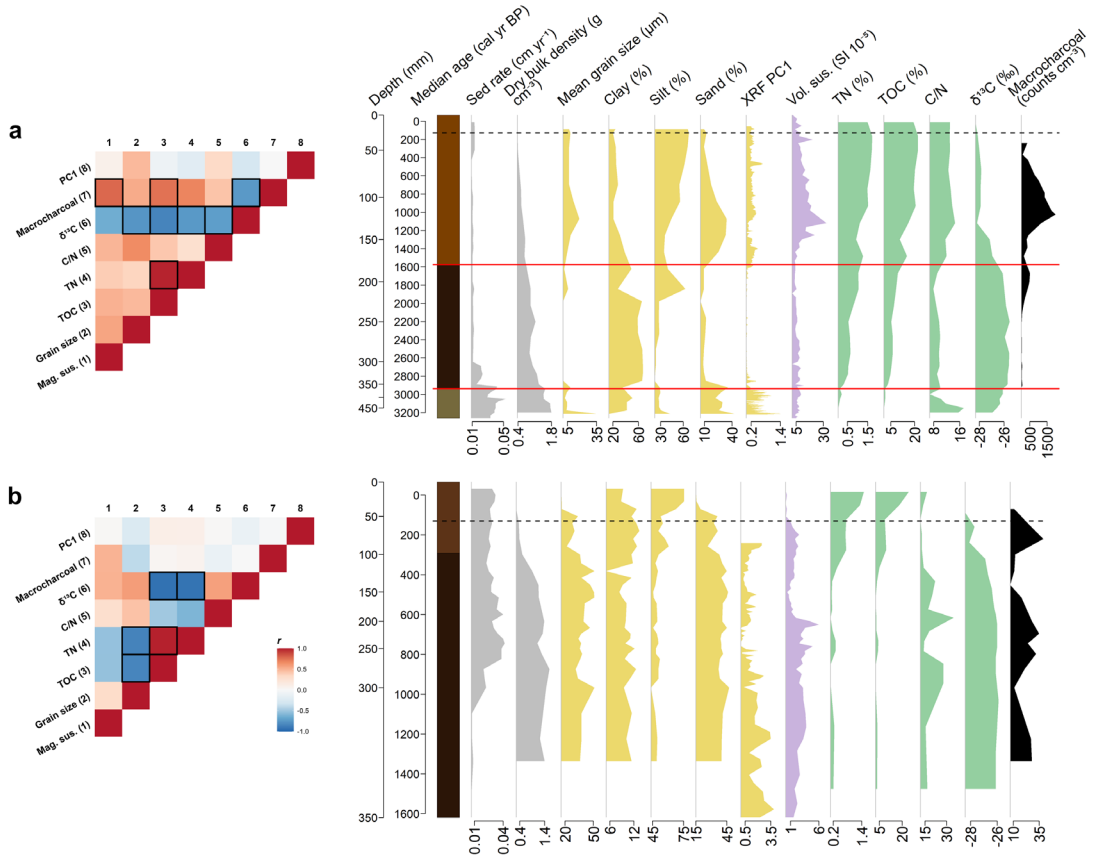

Figure 3.2. Correlation matrices and records for key proxies from the D7-A **(a)** and B-B **(b)** cores. Outlined matrix cells highlight strong correlations with $|r| \geq 0.7$. Solid red and dashed black lines on proxy diagrams reflect unit/subunit boundaries and the timing of European colonisation (130 cal yr BP; 1820 CE), respectively. Proxies are coloured according to their predominant relevance to sedimentation (grey), erosion (yellow), soil formation (purple), peatland productivity (green) or fire (black).

magnetic susceptibility and macrocharcoal. All proxies then plateau except for magnetic susceptibility and macrocharcoal, which have maxima at ~1100 and ~1000 cal yr BP, respectively. $\delta^{13}C$ is negatively correlated with every proxy except magnetic susceptibility (Fig. 3.2a).

Consistent with a lack of stratigraphy, no multiproxy 'phases' are observed for B-B (Fig. 3.2b). Sedimentation rates increase significantly between ~1100–700 cal yr BP, though the abruptness of this change may be artificially elevated by a clustering in the depth distribution of ^{14}C ages (Table 3.1). Grain size oscillates moderately until fining from ~400 cal yr BP into the European period, attributable to an unprecedented decrease in the sand/silt ratio. μXRF data from B-A, transferred to B-B via sequence slotting, reveal a general decline in PC1 values (63% lithogenics; Appendix B14) until a minimum at ~700 cal yr BP, followed by a partial recovery. Magnetic susceptibility is more variable,

increasing gradually until a pulse from ~700–600 cal yr BP, subsequently exhibiting a two-step decline to present. TOC-TN and $\delta^{13}C$ are low and high, respectively, until inverse deviations at ~400 cal yr BP, and are thus the most strongly correlated across the proxy suite (Fig. 3.2b). C/N is extremely volatile, but like $\delta^{13}C$ is more positive before ~400 cal yr BP. CHAR is also variable but demonstrates two pronounced troughs between ~1200–800 and ~500–300 cal yr BP.

3.5.3. Statistical syntheses

Time series records of moisture availability, Rate-of-Change, bulk mineral influx, C and macrocharcoal accumulation rates are presented for each site in Fig. 3.3. Composite 'zonal' records of these data are shown in Fig. 3.4 (a, b) alongside aggregated pollen and charcoal records from independent montane studies (c; Appendix B15) and reconstructions of paleoclimate (d, e, f). All paleoclimate records represent the closest available reconstructions to our study region that entirely overlap our records. Fig. 3.4e and 4f reconstruct key metrics pertaining to ENSO and SAM, respectively; in the absence of any southeastern Australian records for these, models were used as well as records from South America, given the region's exposure to ENSO and SAM via hemispheric teleconnections.

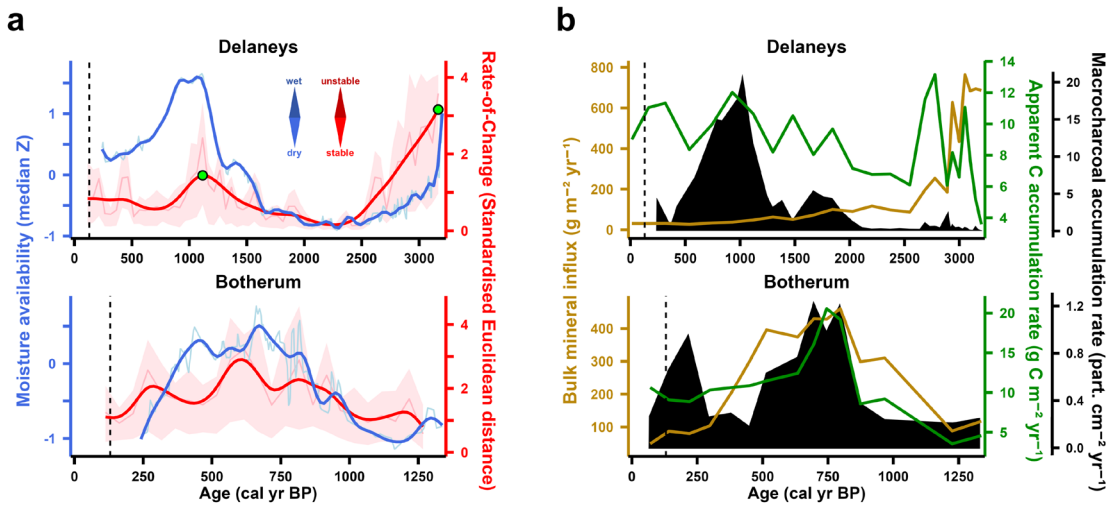

Figure 3.3. Time series records of site **a)** moisture availability and Rate-of-Change, and **b)** bulk mineral influx, apparent C accumulation rates and macrocharcoal accumulation rates. For a), dark curves represent smoothed trends of the raw data series (pale curves). Red envelope represents 95% confidence interval for Rate-of-Change. Dashed vertical lines denote the timing of European colonisation.

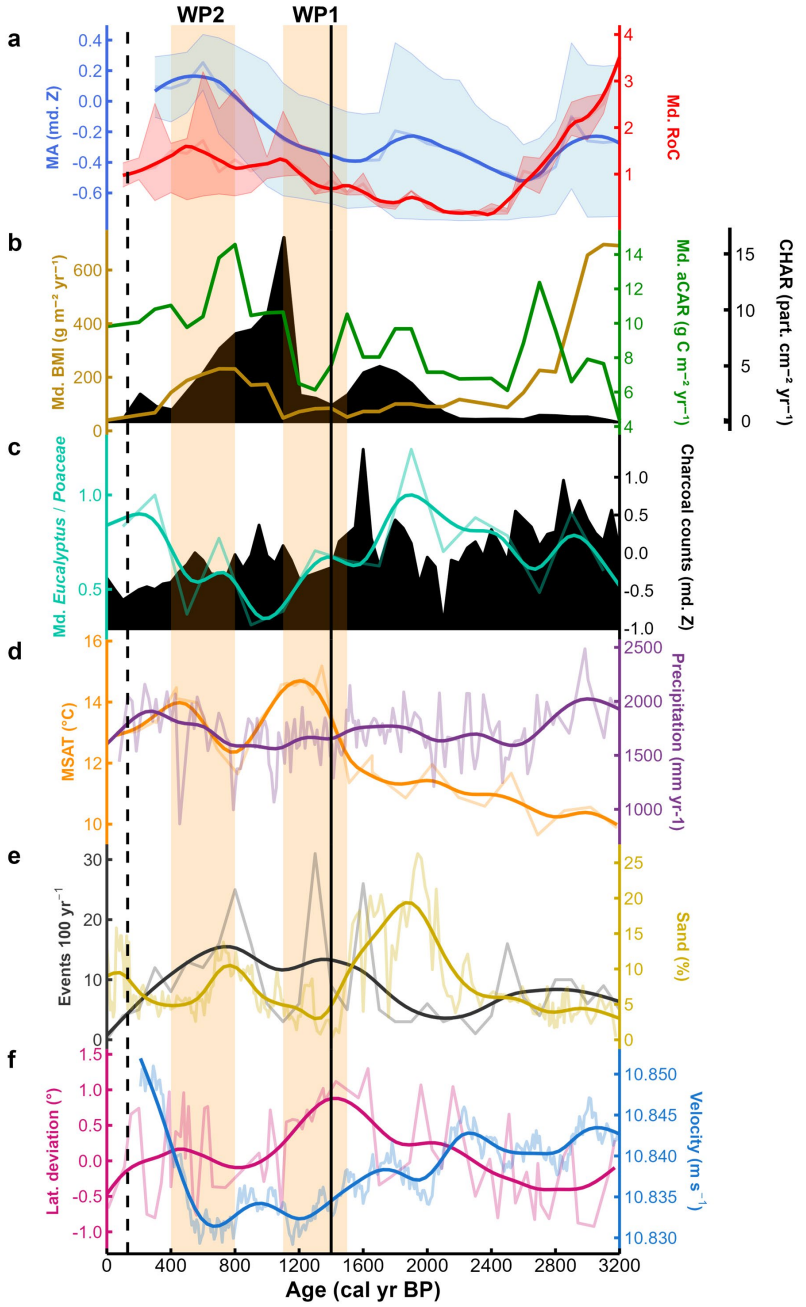

Figure 3.4. Time series records of montane and climatic variability. **a)** Zonal moisture availability and Rate-of-Change. **b)** Zonal bulk mineral influx, apparent C accumulation rates and macrocharcoal accumulation rates. **c)** Averaged pollen ratios and charcoal counts from independent SM montane records (Hope et al., 2012). **d)** mean summer air temperature from Club Lake (Thomas et al., 2022) and annual precipitation from Swallow Lagoon (Barr et al., 2019). **e)** ENSO frequency from Lake Palcacocha (Moy et al., 2002) and sand content (indicating El Niño intensity) from El Junco Lagoon (Conroy et al., 2008). **f)** latitudinal deviation of the Brazil-Malvinas Confluence relative to the modern position (indicating SHWW latitude) from the western South Atlantic (Voigt et al., 2015) and simulated SHWW velocity (Wan et al., 2025). Shaded envelopes in a) represent 95% confidence intervals. Solid vertical line denotes the oldest rounded 100 yr age of Botherum. Orange intervals denote the first and second warm periods (WP1 and WP2) reconstructed by Thomas et al. (2022).

3.6. Discussion

3.6.1. Reconstructing systemic variability

3.6.1.1. Variability at the catchment scale

Concurrent with the earliest multiproxy phase in D7-A, the hydrological reconstruction for Delaneys (Fig. 3.3a) indicates abruptly declining moisture availability (MA) until ~2700 cal yr BP. High MA at the start of the record is associated with maximum and minimum bulk mineral influx (BMI) and apparent C accumulation rates (aCAR), respectively (Fig. 3.3b). While minimum aCAR seemingly contradicts the expected positive correlation between MA and peatland productivity (Perrier et al., 2022), low values correspond to the sub-peat silt unit and so probably reflect mire colonisation of the paleo-floodplain. This is supported by the largest increase in aCAR postdating the largest decreases in BMI and grain size, suggesting that, by ~2700 cal yr BP, MA had declined to some optimum between being a) sufficiently low to suppress fluvial erosion of peat, and b) sufficiently high for peat accretion to outpace decomposition. Macrocharcoal accumulation rates (CHAR) are marginally higher during this time, implying a negligible intensification of Ash-type forest burning. Consistent with multiproxy volatility, Rate-of-Change (RoC) is highest at the start of this phase and preserves a 'peak-point' (RoC >2σ) at 3166 (time bin 3141– 3191) cal yr BP, suggesting unparalleled systemic instability.

Following this drying trend is a broad MA minimum persisting until ~2000 cal yr BP, associated with a collapse in BMI but only a moderate trough in aCAR. This is curious given the C/N and $\delta^{13}C$ data convey maximum peat decomposition during this time; we interpret this to reflect organic matter inputs still being high enough to offset metabolisation encouraged by desiccation. CHAR declines to a minimum during this dry phase, conveying reduced forest fuel loads. Stability in these parameters contributes to a minimum for RoC, which increases again during the subsequent period of dramatic wetting from ~1600 cal yr BP, coincident with a final peak-point at 1116 (1091–1141) cal yr BP. RoC declines as MA stabilises at a maximum between ~1100–800 cal yr BP, which is associated with a 6.5-fold increase in CHAR and a continued increase in aCAR, but no change in BMI. While CHAR collapses to pre-peak values alongside later drying, RoC increases negligibly into the European period, partly due to continued inertia in aCAR and BMI.

Despite extending to only 1337 (889–1716) cal yr BP, the Botherum MA reconstruction also preserves a late-record maximum (Fig. 3.3a), albeit at ~800–400 cal yr BP, slightly later than Delaneys. RoC for Botherum is also marginally higher than for Delaneys over the overlapping period and displays a broad increase during the MA maximum before declining in tandem with post-peak drying. BMI, aCAR and CHAR (Fig. 3.3b) are all strongly positively correlated with the wetting peak, recording coeval maxima between ~800–700 cal yr BP. While aCAR and especially BMI record subsequent declines, CHAR exhibits a second pulse at ~200 cal yr BP. RoC and aCAR increase marginally after European colonisation, while BMI and CHAR decline.

3.6.1.2. Variability at the zonal scale

Replicating the Delaneys record from which the period 3200–1800 cal yr BP is solely derived, the zonal MA record (Fig. 3.4a) preserves drying to minimum MA by ~2600 cal yr BP. This is followed by wetting – with an artefactual jump at the record join – accelerating from ~1100 cal yr BP to maximum MA at ~600 cal yr BP, with high values until at least ~300 cal yr BP. MA records a weakly positive (r = 0.33) correlation with RoC, indicating montane catchments are generally more unstable under wetter than drier conditions. This is apparent from the two largest RoC peaks coinciding with the early wet phase and MA maximum, the latter itself occurring slightly after peaks in BMI, aCAR and CHAR between ~1100–800 cal yr BP (Fig. 3.4b). Although these magnitudes represent the average of two records for time bins <1400 cal yr BP – biasing inferences of absolute change relative to older values – they indicate the aCAR and CHAR pulses are unprecedented for the last ~3200 cal yr. BMI instead shows a maximum at ~3100 cal yr BP, precursory to peat initiation. After their final peaks, BMI and CHAR decline significantly into the European era, while aCAR declines to intermediate values.

3.6.2. Interpreting the systemic sensitivity of the montane zone

3.6.2.1. Sensitivity to climate change

Comparing our zonal indices with independent paleoclimatic reconstructions (Fig. 3.4) yields mostly weak correlations (Fig. 3.5). Even accounting for statistical artefacts, these data suggest low systemic sensitivity to any single climate metric, and perhaps greater sensitivity to the superimposition of multiple metrics as well as the

attenuating/amplifying effects of intrinsic feedbacks and stochastic variability. Human agency is also likely influencing apparent trends, given evidence of montane habitation by the Ngarigo people from at least ~9700 yr BP and increased high-altitude burning and erosion following a late Holocene shift to sedentism (Prosser, 1990, Aplin et al., 2010, Portenga et al., 2016a, Theden-Ringl, 2016). However, Mooney et al. (1997) argue these changes were relatively low impact and should be considered a secondary environmental forcing relative to climate.

While the average explanatory power of the climate indices is weak, several moderate and marginally moderate correlations emerge. Most surprising among these is that of MA and mean summer air temperature (MSAT), as reconstructed by Thomas et al. (2022) from the SM tarn Club Lake (Fig. 3.4d). This is not only the strongest climatic correlation for MA but is also positive, implying that MA increases with warming. Indeed, both indices increase gradually prior to sharp Common Era deviations, with wetting accelerating upon the termination of the first and warmest of two warm periods (~1500–1100 cal yr BP) and peaking during the second, milder warm period (~800–400 cal yr BP). Thomas et al. (2022) recognise that both warm periods coincide with episodes of SHWW intensification (Turney et al., 2016) and also note the known teleconnection between the SHWW and ENSO (Wanner et al., 2008, Dätwyler et al., 2020). However, more recent, quantitative simulations of SHWW velocity by Wan et al. (2025) suggest late Holocene weakening (Fig. 3.4f), with both warm periods being more temporally aligned with increased El Niño frequency as reconstructed by Moy et al. (2002) (Fig. 3.4e). While Schneider et al. (2018) determine this reconstruction to be inconclusive as an El Niño signal, it is still correlated with late Holocene increases in ENSO intensity (Fig. 3.4e) (Conroy et al., 2008) and model-based simulations of ENSO frequency (Clement et al., 2000). Stronger temporal agreement between MSAT and ENSO implicates the latter as a more acute catalyst of warming than the SHWW.

ENSO intensification is difficult to mechanistically reconcile with wetting given its positive role in warming (and evapotranspiration) and the tendency for El Niño to lower rainfall in southeastern Australia (Tozer et al., 2023, Lieber et al., 2024). Indeed, ENSO has been implicated by Barr et al. (2019) in a late Holocene decline in rainfall reconstructed from Swallow Lagoon (Fig. 3.4d), with ~3200 cal yr BP (i.e., the start of our record) marking an abrupt shift to a drier, more variable precipitation regime. Despite warming and drying, a Yarrangobilly Caves speleothem record from McGowan et al.

(2019) (Fig. 3.1a) indicates no long-term change in SM snow cover over the Common Era. It is possible that snow cover stability is also superimposed on a late Holocene increase, given an equatorward migration of the SHWW (Fig. 3.4f), which on interannual timescales enhances SM winter precipitation under SAM (Meneghini et al., 2007, Voigt et al., 2015, Fogt and Marshall, 2020).

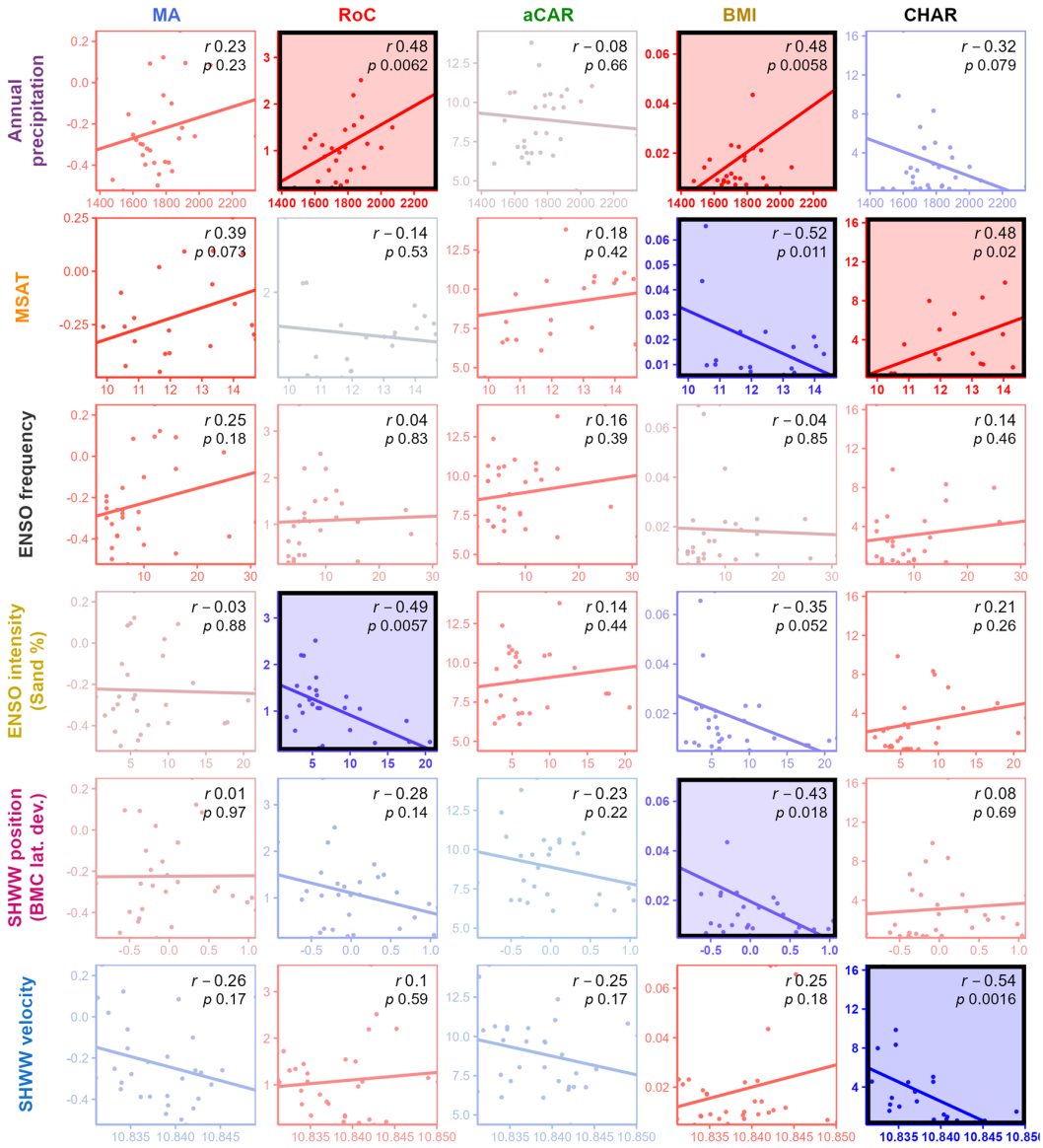

Figure 3.5. Grid of scatter plots visualising the relationships between this study's zonal (columns) and independent climate (rows) parameters presented in Fig. 3.4., with regression trendlines and *r* values annotated. Colour gradient is scaled between minimum and maximum *r* for the entire population of correlations, with darker and paler colours indicating stronger and weaker |*r*|, respectively. Negative correlations are coloured blue and positive correlations red. Shaded plots depict correlations that are at least moderate in strength (i.e., |*r*| 0.4). Plots outlined black depict correlations that are statistically significant at $p \leq 0.05$.

While the McGowan et al. (2019) record is too brief to confirm any such increase in snow cover, even stability under warming would promote earlier and more intense spring discharge of alpine-subalpine snowmelt, which contributes at least 39% of annual inflows into SM catchments (Bilish et al., 2020). Although more punctuated flows should translate to net drying, we note that montane catchments host 44% of the SM peat reservoir, the high hydraulic conductivity of which enables long-term snowmelt retention and flow regulation (Good et al., 2010, Hope et al., 2012). It is thus plausible that higher warm-season runoff into montane peatlands during the warm periods increased MA despite higher evapotranspiration and lower precipitation, possibly explaining higher MA sensitivity to MSAT than to precipitation.

In fact, coupling between MA and precipitation only occurs during the 3200–2700 cal yr BP wet phase; this overlaps with a period of high rainfall from 3500–3000 cal yr BP ascribed by Barr et al. (2019) to a transient La Niña-like mean state. This reinforces hydrological sensitivity to ENSO and may also partially explain late Holocene wetting, which is contemporaneous with an increase in the frequency of multiyear La Niña events despite increasing El Niño dominance (Donders et al., 2008, Carré et al., 2021, Lu et al., 2025). As MA and precipitation are only related during this high-rainfall period, we infer threshold behaviour in hydrological sensitivity whereby precipitation must be sufficiently elevated and/or persistent to override MSAT as the dominant control on MA.

Threshold sensitivity to precipitation is reverberated by maximum RoC during this time, which reflects major systemic reorganisation associated with peatland genesis at Delaneys. This RoC maximum explains its strongest positive correlation being with precipitation, suggesting the balance of biophysical interactions is not only most sensitive to precipitation but also deteriorates under elevated precipitation. Interestingly, RoC is even more strongly correlated with precipitation ($r = 0.52$) at a lag of 200 yr when both records are cross correlated (Appendix B16), indicating a brief delay in biophysical response times. While no lead/lag relationship is observed with MSAT, RoC does gradually decouple from precipitation after peat initiation and moves into phase with MSAT as precipitation falls, reinforcing threshold sensitivity to the latter. Taking peak RoC and thus peat initiation to be precipitation-driven, this event must be related to the cessation of the La Niña-like mean state, recalling that the Delaneys peat unit overlies silts indicative of even higher streamflow and hence precipitation.

A ~3000 cal yr BP timing for peat initiation is very late relative to other montane records, whose maximum ages cluster between 10,000–14,500 yr BP (Fig. 3.1a), implicating postglacial amelioration (Hope et al., 2012). Despite this, initiation at Delaneys displays a remarkable coincidence with the ages of sand lenses (~3500–2700 cal yr BP) observed in several such records. These have been postulated to reflect increased erosion due to sparser vegetation cover under ENSO-driven drying (Cohen and Nanson, 2007, Hope et al., 2012, De Deckker, 2022). This is supported by palynological data from these records (Fig. 3.4c), which convey grassland dominance preceding peat initiation. Peat sand lenses are overlain by rapidly accumulated peats suggestive of increasing productivity probably due to stabilised catchments, an inference supported by the landscape closing signal in the pollen data (Hope et al., 2012). These trends lend credence to our hypothesis that peat initiation was a critical transition relating to an ENSO-driven decline in precipitation and fluvial discharge sufficient to permit mire establishment.

Despite this initial role of precipitation in enhancing productivity, aCAR is most strongly positively correlated with MSAT, peaking at the start of the second warm period. This conveys another threshold shift whereby productivity was augmented by elevated snowmelt supply. This reinforces sensitivity to ENSO, which is substantiated by aCAR being positively correlated with both ENSO metrics and more strongly negatively correlated with both SHWW metrics, congruent with reduced SHWW influence during peak aCAR. Although the aCAR maximum of 14.6 g C m^{-2} yr^{-1} is relatively high, it is low by global standards, with long-term mean aCAR for high-altitude peatlands worldwide generally ranging between ~11 and 47 g C m^{-2} yr^{-1} (Gaffney et al., 2025, Yang et al., 2025).

We thus interpret that both sites have functioned as weak carbon sinks over their records, implying marginal conditions for SM peat growth during the late Holocene; this is consistent with observations that SM peatlands currently operate near their climatic limits (Hope et al., 2012, Hope and Nanson, 2015). The aCAR maximum itself is derived primarily from the Botherum record, with lower, more stable aCAR at Delaneys suggesting differences in mire sensitivity, potentially due to contrasting hydrogeomorphic conditions. Specifically, it is likely that fens such as Delaneys are more resilient to disturbance due to more continuous inundation and thus hydrological buffering capacity. Conversely, moisture-limited moors such as Botherum are inherently closer to their thresholds of instability and thus more sensitive to hydrological perturbations (e.g.,

snowmelt supply). This aligns with observations that moisture-depleted mires are less resilient to ongoing drying (Harris et al., 2020, Lees et al., 2021).

Like MA, BMI is most correlated with MSAT, albeit negatively. This is likely due to maximum BMI coinciding with the pre-peat wet phase despite low MSAT, which is consistent with major catchment erosion associated with high but falling precipitation and more sparsely vegetated slopes. This event drives an almost equal but negative correlation with precipitation, reinforcing higher initial sensitivity to such. We interpret a third moderate relationship with SHWW latitude to be a spurious correlation driven by the early erosional event, with no similarities observed thereafter. Peak BMI exceeds maximum late Holocene soil mass accumulation rates in the SM (220 g m^{-2} yr^{-1}) by 218%, indicating a supply-limited regime in the montane zone upon ENSO intensification (Stromsoe et al., 2016).

Low CHAR during this time suggests that sparse vegetation early in the record was characterised by sparser Ash-type forest. While averaged montane charcoal abundance instead shows maximum values (Fig. 3.4c), this record incorporates both micro- and macrocharcoal data and therefore likely captures distal grassland burning during this period of opening. Curiously, our later CHAR maximum is inconsistent with minimum canopy dominance and declining charcoal abundances. One explanation for this may be that, in contrast to the early precipitation-driven decrease in vegetation cover, landscape opening during our CHAR peak was driven by burning, rather than vice versa.

The coincidence of maximum CHAR with the first warm period implicates the latter in a severe intensification of the montane fire regime, which is supported by MSAT having the strongest positive correlation with our CHAR record. As for MA, RoC and aCAR, this conveys a threshold shift in sensitivity from precipitation early in the record to temperature once warming accelerated. This transition also explains the increase in BMI during the second warm period, which is consistent with enhanced snowmelt runoff and erosion, although burning-driven landscape opening may also be a contributor. Despite sensitivity to temperature, CHAR is even more strongly and negatively correlated with SHWW velocity, with maximum CHAR coinciding with minimum velocity. This suggests burning is also enhanced by SHWW weakening and thus precipitation in winter, when the SHWW contribute their most (79%) to seasonal precipitation (Chubb et al., 2011).

3.6.2.2. Sensitivity to land use change

Relatively low RoC at the 100-cal yr BP bin, which incorporates data up to ~88 cal yr BP (~1862 CE), suggests systemic stability even during the period of unregulated European pastoralism. Stability cannot be ascribed to a lack of disturbance, as both sites were situated along arterial corridors of livestock transhumance from the Monaro Tablelands (Hancock, 1972, NSW Parks and Wildlife Service, 1991). Low RoC must therefore indicate genuine catchment resilience to at least the early impacts of European land use change. This is reinforced by no significant deviations in zonal BMI, which incorporates data up to ~1937 CE and remains an order of magnitude lower than the grazing era erosion rate of 460 g m^{-2} yr^{-1} determined by Costin et al. (1960), though their calculation does consider total soil. Interestingly, the CHAR record, terminating at ~1880 CE, demonstrates a marked decline after colonisation, suggesting a reduction in catchment burning that contradicts the uptick apparent in independent charcoal records.

While aCAR also declines after colonisation until at least ~1937 CE, this change is negligible, which is inconsistent with the widespread degradation of montane peatlands following colonisation (Grover et al., 2005, Worboys and Pulsford, 2013, Treby and Grover, 2024). More surprising is a slight increase in aCAR for Botherum, which we had anticipated to record decreased productivity given its high apparent climatic sensitivity. While we are therefore inclined to dismiss this increase as an artefact of young peat preservation (Charman et al., 2013, Loisel and Yu, 2013, Young et al., 2019, Young et al., 2021), it is accompanied by other proxy changes indicative of actual environmental change. Specifically, increased aCAR overlaps with decreased BMI and abrupt grain size fining, which again conflicts with a known exacerbation of erosion by grazing and burning (Stromsoe et al., 2016). While we have no mechanistic explanation for these deviations, they certainly indicate marked hydrological disturbance; this probably relates to channel modification by grazing and land clearing, as has been recorded across high-altitude Australia (Wasson et al., 1998, Scanes et al., 2021). While minor, these changes in aCAR, BMI and grain size at Botherum are more appreciable than at Delaneys, perhaps reinforcing lower sensitivity thresholds in moors than fens.

3.6.3. Implications for future systemic responses to anthropogenic perturbation

Current climate change modelling for New South Wales (NaRCliM2.0) projects significant warming and drying for the SM (DCCEEW, 2024a). Under the IPCC's medium- to high-emissions pathway (SSP3-7.0), annual temperatures are projected to rise by ~3.5–3.9 ºC by 2100, with greater warm-season increases, while annual precipitation is expected to decrease by 8–19%, with larger winter declines (Intergovernmental Panel on Climate Change, 2023, DCCEEW, 2024b). These patterns are due to global warming and its perpetuation of late Holocene trajectories in climate drivers. Specifically, ENSO will continue to both shift towards an El Niño-like mean state and observe increased amplitude and multiyear instances of both phases (Ding et al., 2022, Cai et al., 2023, Geng et al., 2023, Lieber et al., 2024, Thirumalai et al., 2024). Meanwhile, SAM is expected to continue to shift towards a mean positive state, facilitating a decline in winter precipitation (Voigt et al., 2015, Lim et al., 2016, Deng et al., 2022).

While montane MA appears to have been positively impacted by MSAT and thus ENSO intensification over the last ~3200 yr, we recognise sustained snow cover as being fundamental to this relationship. Given observations and projections of dramatic snow cover decline under global warming, intensified El Niño and a more positive SAM, we expect this positive relationship between montane MA and MSAT has already deteriorated. In fact, climate change has not only reduced winter snow cover but also promoted earlier, more rapid spring melting (Hennessy et al., 2003, Hennessy et al., 2007, Love et al., 2019), with the McGowan et al. (2019) record indicating that snow cover is already at a minimum for the last ~2000 yr. This is reducing the status of snowpack as a reliable source warm-season moisture supply to montane catchments, exacerbating catchment drying under declining precipitation. Indeed, Theobald et al. (2016) calculated that the number of precipitation days capable of delivering flows to SM catchments decreased by 1.4 days per decade between 1958–2012.

Declining MA will lower the productivity of mires and, in turn, their thresholds of resilience to land use change as implied by our aCAR reconstructions (Worboys and Pulsford, 2013, McDougall et al., 2023). This is already initiating a positive feedback wherein reduced hydraulic conductivity of less productive peatlands is reinforcing catchment drying (Morrison and Pickering, 2013, Robertson et al., 2019). Desiccation threatens to also convert many peatlands to carbon sources, given marginal productivity

even under a more optimal late Holocene climate. Indeed, damaged SM peatlands are already emitting significantly more CO_2 than intact complexes (Treby and Grover, 2023). Collapse of moors is likely to precede that of fens given the higher apparent sensitivity of Botherum to climate and land use change.

While we interpret systemic stability to have been relatively insensitive to warming and reduced under wetting, this relationship appears to have been strongly driven by the peat initiation stage, which occurred in the context of higher humidity and lower temperatures. Given the unprecedented severity of warming, precipitation declines and land use change, we anticipate significant systemic disequilibria across montane catchments. Our reconstructions indicate that biophysical reorganisation will be characterised by increased catchment erosion as a result of more intense snowmelt runoff and rainfall and sparser Ash-type forest, exacerbated by feral horse grazing. Forest opening will itself be facilitated by an intensification of fire activity by both warming and winter precipitation declines.

3.7. Conclusions

Here, we have reconstructed paleoenvironmental variability in the SM montane zone through multiproxy synthesis of two peat records, inferring systemic sensitivity to perturbations over the last ~3200 yr. Paramount among our findings is high systemic sensitivity to MSAT, with two pronounced warm periods between ~1500–400 cal yr BP coinciding with catchment wetting and instability, the latter characterised by large increases in erosion, peatland productivity and forest fire. We attribute maximum MA during these warm periods to an increased transfer of snowmelt from alpine-subalpine to montane catchments, where abundant peatlands may have retained such water for protracted intervals. While this explains augmented productivity and catchment erosion, intensified burning of Ash-type forest was likely a direct consequence of warming and reduced winter precipitation.

Precipitation itself appears to have been a secondary environmental forcing to temperature, except during the period of high but declining MA and maximum systemic instability from ~3200–2700 cal yr BP. Such disequilibrium is associated with peatland initiation, which we interpret to have been a critical transition linked to the intensification of ENSO and a consequential decline in precipitation. This would have reduced stream

discharge and increased forest cover such that there was a sufficient decline in transport energy to permit mire colonisation of montane valleys. The coincidence of a) high MA with a La Niña-like mean state, and b) subsequent drying with El Niño intensification implicates ENSO as the prevailing climatic control on late Holocene montane variability, which is reinforced by the later shift in sensitivity from precipitation to ENSO-driven warming. This shift itself implies greater biophysical sensitivity to temperature and threshold sensitivity to precipitation, with systemic responses to the latter occurring on average within ~200 yr of perturbation.

Higher systemic instability for Botherum suggests that moisture-stressed moors are more sensitive to climatic perturbation than fens such as Delaneys. This is substantiated by European-era deviations, which are more pronounced for Botherum and indicate marked hydrological changes. However, changes post-colonisation are generally minor, conveying high thresholds of resilience to colonial land use change. Such thresholds are likely to have been already exceeded, however, under modern feral horse grazing, intensified ENSO, declining precipitation and especially warming, which will continue to reduce catchment MA. Such stressors threaten to convert many mires (and especially moors) to carbon sources and intensify erosional and fire regimes, potentially translating to systemic collapse across the montane zone this century, according to reconstructed biophysical lag.

3.8. Afterword

Although this chapter assesses SM montane sensitivity within a similar methodological framework as Chapter 2, it adopts a revised method that is more relevant to terrestrialised montane catchments. Specifically, magnitudes of biophysical change are constrained by several measures of flux pertaining to peatland productivity, erosion and fire. Additionally, this chapter assesses systemic lag by consulting RoC instead of MA. It also conducts a more quantitative assessment of sensitivity to climate (i.e., Pearson correlation) for a larger suite of paleoclimatic indices than Chapter 1.

Application of this revised method to two montane peat records reveals that late Holocene catchment drying is interrupted by hydrological recovery from ~2600 cal yr BP. This rewetting signal is associated with increases in peatland productivity, erosion and fire (summing to elevated systemic instability), and is in temporal agreement with a

regional warming trend driven by ENSO intensification. Despite warming being contemporaneous with a concomitant decline in precipitation, it is also superimposed on Common Era stability in snow cover. It is therefore argued that rewetting was caused by increased snowmelt inflow into peatlands, suggesting a decoupling from precipitation, which appears to have previously dictated systemic behaviour from ~3200–2700 cal yr BP. Indeed, peatland initiation at ~3000 cal yr BP is attributed to a decline in streamflow caused by declining precipitation rather than warming.

While this warming-snowmelt mechanism for rewetting diverges significantly from that proposed in Chapter 2 for the Monaro, rewetting in both the montane and highland zones is synchronous and evidently ascribed to ENSO, implicating this climate driver as the prevailing control on systemic dynamics at low to middle elevations. However, highland-montane similarities deteriorate during the European era, which is not characterised by montane disequilibrium, indicating systemic resilience. Despite this, Chapter 3 proposes that compounding expressions of GEC are likely to initiate widespread degradation of peatlands (especially moors), catchment erosion and forest fire. Desiccation of moisture-limited moorland is resonant of that projected for seasonal lakes in drying subregions of the Monaro, reinforcing that similar biophysical outcomes (i.e., preferential deterioration of moisture-limited systems) can manifest across zones despite different mechanisms.

While the montane zone is geographically representative of the SM, large highland-montane dichotomies highlight the importance of performing zone-specific appraisals of sensitivity. This is pertinent to the alpine and subalpine zones, which are the most climatically and biophysically unique of the high-altitude transect. Chapter 4 completes the cross-altitudinal assessment of high-altitude sensitivity by reapplying this analysis on alpine-subalpine records.

Chapter 4

Spatiotemporal divergences in alpine and subalpine sensitivity to Holocene climate and land use change: Paleoenvironmental insights from the Snowy Mountains, southeastern Australia

4.1. Abstract

The alpine and subalpine (alpine-subalpine) zones represent the most vulnerable components of the mountain transect. However, contemporary and paleoenvironmental alpine-subalpine responses to perturbation are often ecologically assessed, biasing inferences of systemic (i.e., abiotic *and* biotic) sensitivity to perturbation and thus projections of biophysical change. Here, we perform a multiproxy, multisite synthesis of new peat and lake sediment records from the alpine-subalpine complex of the Snowy Mountains, southeastern Australia, reconstructing paleoenvironmental changes since ~10,600 cal yr BP to interpret systemic sensitivity to climate and land use change. While we determine hydroclimate to be the dominant control on alpine-subalpine variability over millennial timescales, we infer a late Holocene switch in sensitivity to temperature.

Specifically, we implicate ENSO-related warming in a recovery of catchment moisture availability from ~2600 cal yr BP, implemented by snowmelt inflow into peatlands. Despite this precipitation-to-temperature sensitivity switch, ENSO is recognised as the prevailing forcing on Holocene climatic and systemic variability. This is especially apparent for the subalpine zone, for which we infer greater instability under the late Holocene ENSO-dominated climatic regime than the alpine zone. While we also interpret greater subalpine sensitivity to European land use change, postcolonial instability for the entire alpine-subalpine complex is unprecedented since at least ~3700 cal yr BP, conveying higher systemic sensitivity to land use change than any climatic perturbation since this time. These reconstructions prognose adverse outcomes for alpine and especially subalpine catchments, which we anticipate will experience drying, peatland collapse, ecotonal migration and intensified erosion and fire under accelerating anthropogenic stress.

4.2. Introduction

Mountains are regarded as ‘sentinels’ of global environmental change due to the unique interaction between climate and topography in these terrains (Fort, 2015, Schmeller et al., 2018, Schmeller et al., 2022). High elevation and relief yield steep temperature and precipitation gradients prescribing a dense altitudinal succession of bioclimatic zones (Beniston, 2003, Parish, 2014, Körner, 2021). These are, with decreasing elevation, the alpine, subalpine and montane zones, each being defined by

distinct floral assemblages that transition abruptly along stepped, isothermal 'ecotones', namely the treeline and forest line (Diaz et al., 2003, Körner et al., 2011, Loeffler et al., 2011). The climatic sensitivity of these zones means all are responding rapidly to climate change, which is being exacerbated by land use change (Diaz et al., 2003, Beniston, 2016, Egan and Price, 2017, Schmeller et al., 2022, Ioan et al., 2025).

Most vulnerable to these compounding manifestations of global environmental change are the alpine and subalpine (alpine-subalpine) zones. Circumscribed by montane forest, alpine-subalpine complexes are disproportionately threatened by climate change due to their restricted areas and topographic isolation (Beniston, 2003, Slatyer, 2010). This is concerning for the 71% of mountains globally with hypsographic tails (i.e., proportionally small land areas) towards their summits, such as the Rocky Mountains, Zagros Mountains and Australian Alps (Elsen and Tingley, 2015). In such regions, upslope ecotonal migration has dire implications for alpine-subalpine ecosystems, which are confined to these retracting refugia and exhibit the highest rates of mountain endemism (Beniston, 2003, Körner, 2004, Schmeller et al., 2022). As such, many alpine-subalpine taxa are at risk of extinction as they lack both avenues of escape and the phenotypic plasticity to adapt to disappearing niches, particularly those generated by snow and ice (de Villemereuil et al., 2018, Guisan et al., 2019, Tito et al., 2020).

Indeed, the alpine-subalpine complex is the only non-polar environment where the cryosphere dominates the hydrological regime, with it regulating flows, sustaining microclimates and constituting specialist habitat (Huss et al., 2017). Snow and glacial retreat are therefore reinforcing the more direct effects of climate change on mountain hydrology, elevation-dependent warming and phenology (Aitchison, 2001, Jonas et al., 2008, Pepin et al., 2015). Downslope, cryospheric collapse is increasing the frequency, duration and severity of hydrogeomorphic hazards (e.g., landslides and flooding) and periods of reduced streamflow, threatening the 1.9 billion people dependent on mountains as 'water towers' for runoff resources (Messerli et al., 2004, Immerzeel et al., 2020, Adler et al., 2023). More locally, alpine-subalpine responses to climate change are further complicated by land use changes that modify hydrology, exacerbate catchment erosion, introduce native species and pollute soils and waterways (Wohl, 2006, Korpak, 2017, Elsen et al., 2020, Schmeller et al., 2022).

The characterisation of mountain environments and their anthropogenic transformation is largely ecological given their bioclimatic stratification, which renders

them optimal 'natural laboratories' for investigating floral and faunal responses to perturbation (Chape et al., 2005, Hall et al., 2009, Silveira et al., 2019, Tito et al., 2020). As such, understanding mountain sensitivity to stimuli remains overwhelmingly informed by ecological metrics such as ecotonal advance, biodiversity loss and phenological dissociations (e.g., Harsch et al. (2009), Öztürk et al. (2015), Inouye and Wielgolaski (2025)).

These measures are critical for gauging ecological change but inherently bias inferences of systemic sensitivity – that is, pertaining to that of the entire biophysical system as the sum of both biotic and abiotic phenomena (Bakis et al., 2026). The geoecological rationale of empirically addressing systemic change lies in obtaining a more representative insight into biophysical sensitivity (Ives, 2019). This is pertinent to the alpine-subalpine complex given its retreat risks the disappearance of not only endemic biota but also endemic biophysical processes (e.g., low-intensity fire, meltwater discharge from snow and ice and retention in peatlands, etc.). Constraining the sensitivity of such processes permits more comprehensive projections of future environmental change, better informing conservation and management of alpine-subalpine landscapes and their dependent biota, industries and communities (Gordon et al., 2002, Kumar and Deshmukh, 2015, Webber, 2019, Kumar et al., 2021).

The ecological emphasis apparent in contemporary research emerges also in paleoscience, which in mountains is disproportionately informed by palynological and charcoal studies (Williams et al., 2018). This limited scope is being remedied through multiproxy analyses (e.g., Schroeter et al. (2020), Zhang et al. (2024), Rostami et al. (2024)), which minimise bias inherited from individual proxies and permit robust reconstructions of systemic variability. Multiproxy research remains underutilised in the Snowy Mountains (SM) of southeastern Australia, which harbours one of the most restricted and climatically marginal alpine-subalpine complexes on the planet (Pickering, 2007).

Alpine-subalpine processes such as bog and snowpack formation are thus already operating near their climatic limits and so are poised to deteriorate rapidly as projected warming and drying exceed boundary conditions (Pickering, 2007, Hope and Nanson, 2015). While change in the SM is well understood in an ecological context, the long-term systemic implications for the alpine-subalpine complex are yet to be constrained by the current corpus of paleoenvironmental data (Hope et al., 2012), with this only being

systematically attempted by Bakis et al. (2025) for the montane zone. Here, we synthesise multiproxy data obtained from six bog and tarn cores sampled across the SM alpine-subalpine complex, in order to produce a systemically and geographically representative reconstruction of Holocene paleoenvironmental variability. Through comparison with independent records of paleoclimate and land use, we constrain sensitivity at the process, catchment, zonal and complex scale to make qualified prognoses of systemic change.

4.3. Regional setting

The SM describes a mountain range and biogeographic subregion bestriding the state borders of New South Wales and Victoria. Despite constituting the highest terrain in the Australian Alps bioregion and indeed Australia, the SM has a maximum elevation of only 2228 m ASL at Mount Kosciuszko (Fig. 4.1a) (Sahukar et al., 2003). Low elevation is attributable to prolonged tectonic quiescence and Cenozoic denudation of the broader cordillera, which has reduced the SM to a low-relief, highly dissected plateau representing only 0.09% of continental area. Of this, a mere 3.5% (~128,560 ha) and 18% (~25,280) ha) is alpine and subalpine, respectively, with the majority of this being confined to Kosciuszko Massif at the range's core (Fig. 4.1b) (Kohn et al., 1999, Costin, 2000, Gallant et al., 2009, Webb, 2017, DCCEEW, 2020, Wilson et al., 2022).

Consistent with the floristic characterisation of mountain environments globally, the alpine zone of the SM is demarcated from the subalpine zone by the treeline ecotone, which occurs at ~1800 m ASL in accordance with the mid-summer isotherm of 10 ºC (Fig. 4.1b) (Sahukar et al., 2003, Mason and Williams, 2013c). Above the treeline is a mosaic of feldmark, herbfield, heath and bogs ('alpine herbfield'). Except for on exposed feldmark-dominated ridges, where thin lithosols prevail, the alpine zone is underlain by humic organosols and peats due to the preservation of organic matter by low temperatures and persistent moisture supply from high rainfall and snowmelt (Sahukar et al., 2003, Mason and Williams, 2013b, Pickering and Venn, 2013, Wilson et al., 2022).

Beneath the treeline, alpine meadow abruptly transitions to open *Eucalyptus (E.) pauciflora* woodland with a dense understory (Sahukar et al., 2003, Mason and Williams, 2013c). Higher temperatures and lower rainfall sufficiently accelerate metabolisation of organic matter such that pedology is less informed by climate than parent material (i.e., granites and metasediments) (Geoscience Australia, 2012, Mason and Williams, 2013b,

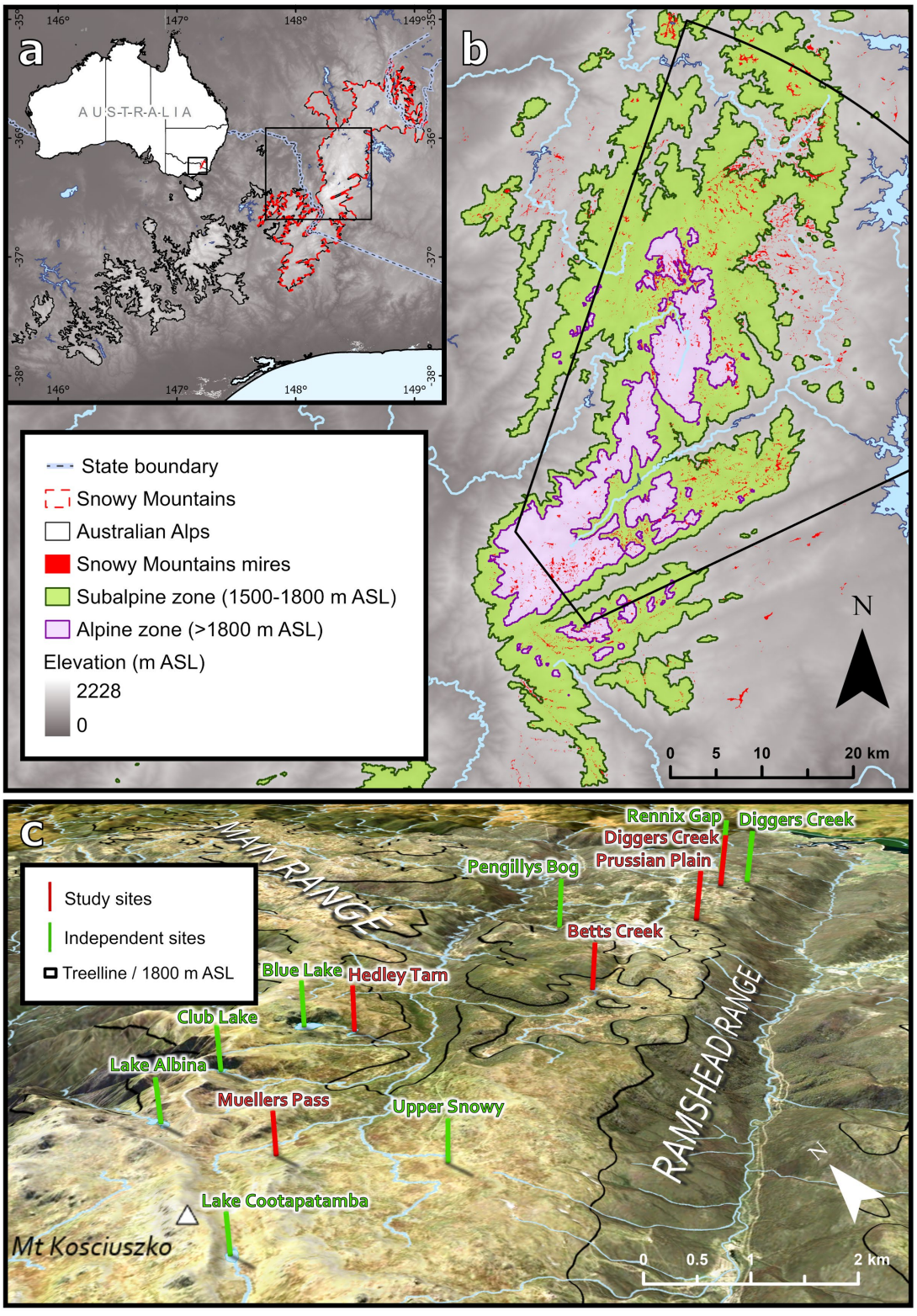

Figure 4.1. Maps depicting **a)** the Snowy Mountains and its location in the broader Australian Alps bioregion and Australia (DCCEEW, 2020), **b)** the Kosciuszko Massif and its constituent alpine-subalpine zones and mires (DCCEEW, 2016b), and **c)** locations of the sites targeted in this study as well as of major independent paleoenvironmental studies in the alpine-subalpine complex of the Kosciuszko Massif. Extent indicators denoted by black boundaries. DEM data obtained from Gallant et al. (2009) and hydrography data from State Government of NSW Spatial Services (2025).

Slattery, 2015). As such, infertile gley podsols dominate subalpine slopes except along the valley floors of treeless 'frost hollows'. These are alpine refugia where cold air drainage yields an inverted treeline and, in concert with an elevated water table, supports peat growth in bogs, fens and moors (collectively 'mires') (Sahukar et al., 2003, McDougall et al., 2005, Hope et al., 2012, Wilson et al., 2022).

The low relief of the SM threatens rapid alpine-subalpine retreat under global warming. With alpine warming of up to 5 ºC projected by 2100 CE, the SM will witness a total disappearance of alpine conditions in the 21st century, with the lower 100 m of the alpine zone having already become climatically subalpine (Green et al., 1992, Hennessy et al., 2008, Green and Venn, 2012, Harris et al., 2016, Hoffmann et al., 2019). However, warming is not being replicated ecologically; converse to global trends, the SM treeline is not advancing upslope due to poor seed dispersal and worsening dieback due to beetle infestations stimulated by climate change.

Moreover, 91% of alpine plants, unable to migrate in the absence of a nival buffer zone, are not adapting to warming (Wearne and Morgan, 2001, Pickering, 2007, Soudzilovskaia et al., 2013, Naccarella et al., 2020, Hansson et al., 2021, Sritharan et al., 2021, Ward-Jones, 2021). Ecological inertia threatens *in situ* extinction of endemics due to warming and the concomitant disappearance of niches associated with declining snowpack area, duration and volume. In addition to warming, snow cover declines are being accelerated by falling annual and especially cool-season precipitation, attributable to changes in two major climate drivers. These are the El Niño–Southern Oscillation (ENSO) and Southern Annular Mode (SAM), the latter dictating the latitudinal position of the moisture-bearing Southern Hemisphere Westerly Winds (SHWW) (Hennessy et al., 2007, Fiddes and Pezza, 2015, Lim et al., 2016, Love et al., 2019, Deng et al., 2022, Lieber et al., 2024).

While climatic impacts on alpine-subalpine biota are well constrained, implications for the broader biophysical system are usually extrapolated as a unidirectional outcome of climate change, with minimal consideration for internal abiotic-biotic feedbacks (Pickering and Venn, 2013). However, many biophysical features (e.g., slope stability and edaphic cycles) are inextricable from not only climate but also ecology. As such, recent changes in one of these controls (climate) and stasis in the other (ecology) is predisposing the alpine-subalpine complex to unexpected systemic change. Additionally, the ecological model of altitudinal advance is not relevant to many biophysical processes, which are also

dictated by immutable factors such as lithology, slope and aspect. Systemic trajectories of change are made more uncertain by ongoing European degradation since the regional establishment of pastoralism in the 1820s CE (Mooney et al., 1997, Costin, 2000). Colonial land use was heralded by the seasonal transhumance of sheep and cattle from the adjacent Monaro Tablelands into the SM until the cancellation of pastoral leases above ~1400 m in 1958 CE (King, 1959, Clark, 1992, Mooney, 2004).

While its prohibition was motivated by the necessity to reduce catchment erosion ahead of the establishment of the SM Hydroelectric Scheme, pastoralism also introduced other stressors including intense annual burning and exotic flora and fauna (Costin, 1957, Clark, 1992, Good, 1992). Ironically, dispersal of alien plants was itself accelerated by deliberate sowing during these slope stabilisation efforts (Johnston and Pickering, 2001, McDougall et al., 2005). Many exotic plants are now therefore naturalised in the SM; McDougall et al. (2005) recorded 128 exotic species across the Australian Alps, thought critically 83% of these were confined to warmer conditions below the treeline. In lieu of an advancing treeline, therefore, subalpine replacement of alpine natives is instead likely to be pioneered by weeds, the seasonal die-off of which is already exacerbating soil erosion (McDougall et al., 2005).

Since the establishment of Kosciuszko National Park in 1967, feral horses and tourism have supplanted pastoralism as the main vectors of local degradation (Mosley, 1989). These stressors not only perpetuate weed dispersal but also contaminate soils and streams, encourage sheet and channel erosion and destroy mires (Pickering et al., 2003b, Pickering et al., 2010, Pickering et al., 2011, Worboys and Pulsford, 2013, Robertson et al., 2019). The compounding of climate and land use change has engendered such pervasive destruction of alpine mires, feldmark and herbfield that all three are considered threatened, with the latter now undergoing ecological collapse (TSSC, 2008, NSW TSSC, 2015, NSW TSSC, 2018, Bergstrom et al., 2021). While these threatened listings are ecologically framed and thus not diagnostic of systemic environmental status, the listing of mires is of particular concern given their underlying peats are excellent archives of not only carbon but also paleorecords (Hope et al., 2012).

4.4. Materials and methods

4.4.1. Site selection and sampling

Due to their alpine-subalpine abundance (Fig. 4.1b) and known utility as Holocene-spanning natural archives (Hope et al., 2012), several *Sphagnum* bogs were targeted for coring and multiproxy analysis of their peat records (Fig. 4.1c). Bogs were selected from a population of sites along the two major ranges of the Kosciuszko Massif, the Main and Ramshead Ranges, which mostly span the alpine and subalpine zones, respectively (Fig. 4.1c). We prioritised sites in high-relief, topogenous hydrogeomorphic settings free of major fluvial incision and anthropogenic disturbance (Moore, 1987, Hope et al., 2012, Hope and Nanson, 2015).

Three subalpine bogs (Diggers Creek, Prussian Plain and Betts Creek) and two alpine bogs (Hedley Tarn and Muellers Pass) met these criteria. In addition to its fringing bog, the lakebed of Hedley Tarn was targeted given proximal tarns host postglacial sequences (Fig. 4.1c) (Appendix C1) (e.g., Raine (1974), Martin (1986b), Burdick (2022), Mickelson (2024)). We recovered 2–6 cores across each bog using a Russian peat sampler (50 cm monolith chamber; driven into peat until refusal) to identify any lateral changes in the depositional facies. The lakebed of Hedley Tarn was cored using a 5 cm interior diameter polyvinyl chloride core barrel, which was driven into the lakebed until refusal using a collar-and-hammer system, following Bakis (2021). Peat cores were placed into polyvinyl chloride liners while lakebed cores were capped, sealed and later longitudinally split. All cores were stratigraphically logged, subsampled and stored at 3 ºC.

4.4.2. Laboratory and statistical methods

AMS ^{14}C dating of a combination of bulk sediment and sporopollenin samples was performed on selected cores at three laboratories (Appendix C2). Raw ^{14}C ages were reported in years before present (yr BP ±1σ) and were calibrated using the R software BACON (Blaauw and Christen, 2011, R Core Team, 2020) using the Southern Hemisphere calibration curve (SHCal20) (Hogg et al., 2020). Calibrated ages (cal yr BP) were used to generate Bayesian age-depth models in BACON. Dated cores were subject to downcore analysis of a suite of sedimentological and geochemical indicia identified by Bakis et al. (2025) as being sensitive to key abiotic and biotic catchment processes in

mountain environments. These were dry bulk density, magnetic susceptibility, elemental abundances (evaluated with μXRF), mineral grain size, total organic carbon (TOC) and nitrogen (TN) and their ratio (C/N), $\delta^{13}C$ and macrocharcoal (>125 μm) abundances (Appendix C3–6). Collectively, these are indicia for catchment hydrology, erosion, pedogenesis, productivity, organic matter decomposition and fire, which constitute the main components of a biophysical system (see Bakis et al. (2025)).

To infer systemic variability from these individual processes, proxies were statistically synthesised to assess magnitudes, directions and rates of change across the proxy suite, again following Bakis et al. (2025). Magnitudes of change calculated were bulk mineral influx (BMI), apparent carbon accumulation rates (aCAR) and macrocharcoal accumulation rates (CHAR) (Appendix C7); these respectively constrain absolute changes in erosion, peatland productivity and fire, which are the three alpine-subalpine functions arguably most dramatically perturbed by modern anthropogenic change in the SM. Quantifying long-term aCAR is especially important given it remains vastly understudied in Australian peatlands, which cover a significant proportion of alpine-subalpine catchment areas (Gaffney et al., 2025). aCAR was also reconstructed for the Hedley Tarn lakebed record as the site is entirely fringed by bogs, which are thus the major vector of organic matter to an otherwise oligotrophic system.

Indeed, given their vast alpine-subalpine coverage, productivity of peatlands serves as a proxy for broader catchment moisture availability (MA), which is the net balance of hydrological inputs and outputs prescribed by temperature, precipitation, runoff and groundwater flows (Clymo, 1984, Hope et al., 2012, Charman et al., 2013, DCCEEW, 2016b, Yang et al., 2025). As older peats are more decomposed and thus possess lower TOC, aCAR is prone to artefactual increases with decreasing depth, and as such can be an unreliable indicator of long-term peat productivity, particularly in the oxic acrotelm where TOC increases exponentially (Charman et al., 2013, Loisel and Yu, 2013, Young et al., 2019, Young et al., 2021). However, long-term accumulation rates of SM peatlands have been very slow (Hope et al., 2012), we anticipate very thin acrotelms and thus only short artefactual changes to aCAR, which is therefore likely to serve as an accurate proxy for millennial-timescale peatland productivity.

Alpine-subalpine MA is presumably the dominant control not only on peatland productivity but in fact the entire biophysical system, given Holocene climate change in southeastern Australia has been defined by marked deviations in temperature but

especially precipitation; this is consequential for the alpine-subalpine complex given its mesic, snowfall-dominated precipitation regime (Harrison, 1993, Quigley et al., 2010, De Deckker, 2022, Clerke, 2023). MA is therefore anticipated to be expressed strongly across the entire proxy suite; as such, our three absolute metrics were aggregated with all other qualitative proxies to approximate relative hydrological change (i.e., wetting and drying). Input proxies were first directionally rescaled where necessary such that all proxies were positively correlated with wetting, based on multiproxy triangulation, *a priori* presumptions and field observations. Proxies were then standardised and averaged to produce a dimensionless record approximating hydrological change at each site, following Hamilton et al. (2024) (Appendix C8). To supplement these hydrological records, Rate-of-Change (RoC) was also computed as an aggregated metric for the proxy suite to infer changes in systemic stability (Mottl et al., 2021a, Mottl et al., 2021b) (Appendix C9).

To estimate macroscale systemic variability across the alpine-subalpine complex, we time-standardised and averaged all site records described in this subsection (Appendix C7–9) except for CHAR, due to major floristic and thus pyrological disparities between the alpine and subalpine zones. Specifically, macrocharcoal abundance in a subalpine record is more likely to reflect local fire dynamics in both the canopy and understorey, while a record from the treeless alpine zone is presumed to be a mixed signal of subalpine fire activity and treeline proximity. Statistical incomparability is also inherent between aCAR for the Hedley Tarn lakebed record and all other bog records, given the the mechanisms driving organic matter inputs into an oligotrophic tarn (allochthonous) differ substantially from that of bogs (autochthonous).

As such, aCAR data for the Hedley Tarn lakebed record were omitted from multisite aggregation for time bins overlapping with or between data from bog records. To interpret climatic sensitivity from these alpine-subalpine records, we quantified Pearson correlation with independent reconstructions of regional temperature and precipitation, as well as of metrics relevant to the major climate drivers ENSO (event frequency and intensity) (Moy et al., 2002, Conroy et al., 2008) and Southern Annular Mode (SHWW latitude and velocity) (Voigt et al., 2015, Wan et al., 2025). Sensitivity to land use change was evaluated by reviewing proxy, site and multisite records relative to the timing of European pastoralism and conservation within the alpine-subalpine complex.

4.5. Results

4.5.1. Core sampling, stratigraphy and chronological modelling

Multiple cores were recovered from each site during three rounds of fieldwork in 2023 and 2024 (Appendix C10). The core with the oldest basal ^{14}C age and/or the most confident chronological model was selected for multiproxy analysis (Table 4.1). For Diggers Creek, the selected core DA4 (48 cm) comprises a single unit of fibrous black peat with no discernible acrotelm (see Appendix C11 for core optical scans) and was modelled to have a median basal age of 4641 (95% confidence interval between 4083–4817) cal yr BP (Appendix C12 for chronological models).

For Prussian Plain, the core PB (50 cm) consists of sapric peat with no clear acrotelm but a root-rich upper unit (0–7 cm); this is underlain by a unit of black gravelly peat that grades to a basal unit of dark brown peat at 43 cm, the base of which yielded a median age of 4263 (3928–4991) cal yr BP. For Betts Creek, the core BA (76 cm) was synthesised from two 50 cm cores (BA1 and BA2) sampled 10 cm apart with a 24 cm depth overlap, both being composed of black fibrous peat with no visible acrotelm. Based on their overlap, ^{14}C ages from both cores were combined to synthesise the BA chronology, which produced a median basal age of 2501 (1408–2688) cal yr BP. Multiproxy data from the upper 26 cm of BA1 was appended to the top of BA2 to synthesise a full multiproxy record for BA.

For Hedley Tarn, the selected mire core HD2 (32 cm) exhibits an acrotelm (0–3 cm) that was more fibrous than the underlying two units of sapric peat. These two units are discernible at 22 cm from an increased abundance of micaceous clasts, with the lowermost unit producing a median basal age of 510 (405–636) cal yr BP. For the Hedley Tarn lakebed, the core HA (92 cm) displays an upper unit of organic sandy silt (0–7 cm), a second unit of moderately organic gravelly sand (7–38 cm), a third unit of highly organic gravelly sand (38–49 cm), a fourth unit of inorganic gravelly sand (49–61 cm), a fifth unit of inorganic sand with biotitic laminae (61–86 cm), and a sixth unit of inorganic sandy silt. Due to low TOC in the lower three units, only Units 1–3 could be ^{14}C-dated, with Unit 3 yielding a median basal age of 10,624 (9005–10,999 cal yr BP). For Muellers Pass, the core MB1 (39 cm) comprised a fibrous acrotelm (0–5.5 cm), a second unit of sapric black peat (5.5–34 cm) and a third unit of sapric brown peat enriched with gravel and with a median basal age of 3267 (2445–3417) cal yr BP.

Table 4.1. ^{14}C dating results for all analysed cores. Lab ID 'OZBY' is for samples analysed at the Australian Nuclear Science and Technology Organisation (Hua et al., 2001, Fink et al., 2004). Lab ID 'D-AMS' is for samples analysed at DirectAMS (Tate et al., 2023). Lab ID 'UNSW' is for samples analysed at the University of New South Wales (Turney et al., 2021). Sampled depths indicate core-specific depths, while true depths indicate depths relative to ground level (relevant to BA only).

Lab ID	Core ID	Sampled depth (cm)	True depth (cm)	Material	^{14}C age (yr BP ± 1σ)
D-AMS 050599	DA4	20		Bulk sediment	1003 ± 22
OZBQ30	DA4	24		Sporopollenin	1135 ± 42
OZBQ31	DA4	36		Sporopollenin	1801 ± 21
D-AMS 050600	DA4	48		Bulk sediment	4215 ± 26
OZCF85	PB	9		Sporopollenin	160 ± 22
OZCF86	PB	27		Sporopollenin	846 ± 29
OZCF87	PB	48		Sporopollenin	3758 ± 25
OZCF81	BA	12		Sporopollenin	336 ± 24
OZCF82	BA	27		Sporopollenin	1171 ± 25
OZCF83	BA	1	27	Sporopollenin	53 ± 20
UNSW-3564	BA	50		Bulk sediment	1190 ± 20
OZCF84	BA	25	51	Sporopollenin	835 ± 23
UNSW-3565	BA	50	76	Bulk sediment	2540 ± 20
D-AMS 050612	HD2	25		Bulk sediment	387 ± 25
OZBQ25	HD2	28		Sporopollenin	202 ± 28
D-AMS 050613	HD2	32		Bulk sediment	518 ± 32
OZCK51	HA	4		Bulk sediment	736 ± 37
OZCK52	HA	7		Bulk sediment	1408 ± 36
OZCK53	HA	11		Bulk sediment	2525 ± 42

OZCK54	HA	14	Bulk sediment	7980 ± 52
OZCK55	HA	18	Bulk sediment	4801 ± 39
OZCK56	HA	30	Bulk sediment	8328 ± 45
OZCK58	HA	40	Bulk sediment	8000 ± 37
OZCE31	HA	43	Bulk sediment	8125 ± 42
OZCK59	HA	44	Bulk sediment	8014 ± 29
OZCK60	HA	47	Bulk sediment	7965 ± 40
OZCK61	HA	49	Bulk sediment	9496 ± 43
OZBQ21	MB1	24	Sporopollenin	1114 ± 25
OZBQ22	MB1	30	Sporopollenin	1990 ± 52
D-AMS 050614	MB1	39	Bulk sediment	3155 ± 24

4.5.2. Multiproxy analyses

Reviewing multiproxy trends for DA4 (Fig. 4.2), we observe a large decrease in mean grain size ('grain size') from the sand to silt range by ~3200 cal yr BP, driven by a significant reduction in the sand/mud ratio. Values then oscillate within the coarse silt range for the remainder of the record. Performing principal component analysis on the µXRF data for selected elements, we find the first principal component (PC1) to be dominantly (70%) contributed to by lithogenic elements (see Appendix C13 for Principal Component Analysis results of cores). While volatile, PC1 exhibits a general increase until ~2000 cal yr BP, after which time it declines before increasing again from ~400 cal yr BP. Magnetic susceptibility oscillates within 2σ until a brief peak centring on European

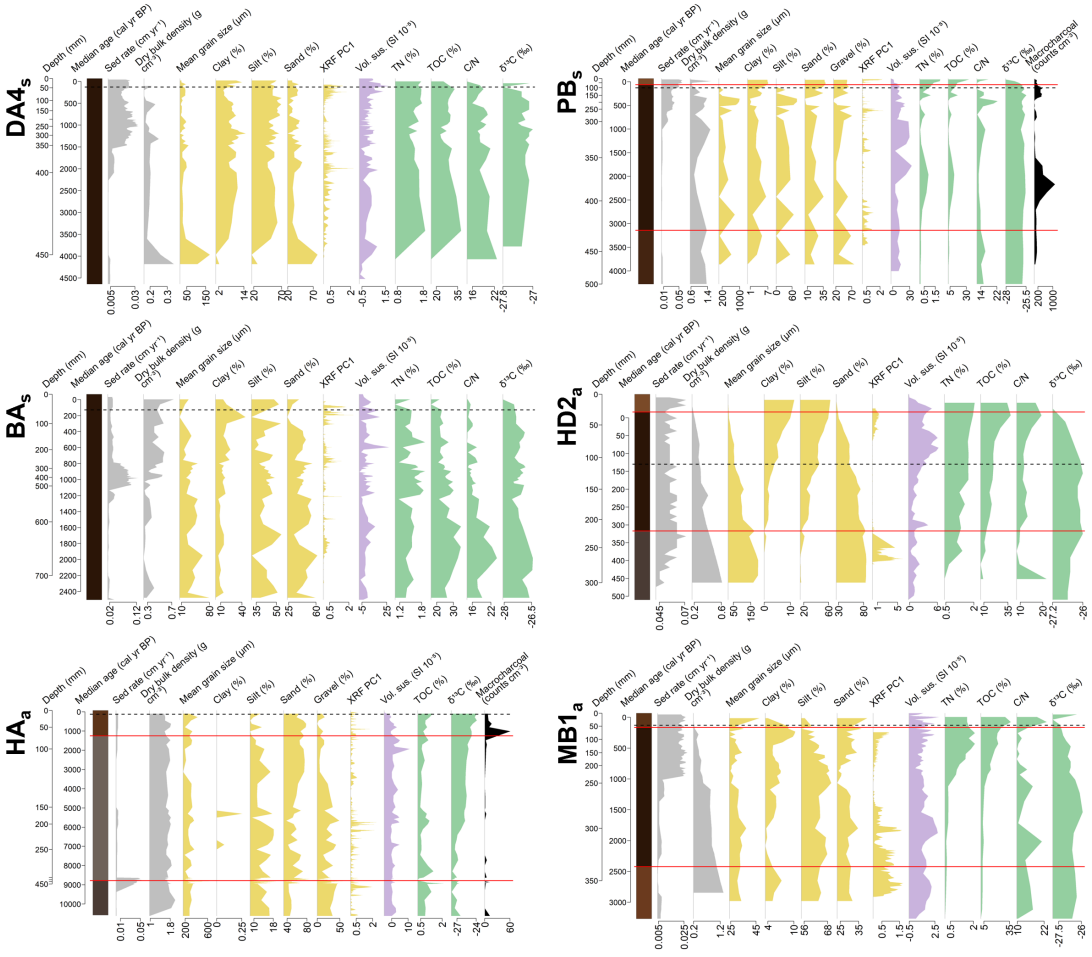

Figure 4.2. Lithostratigraphic and proxy time series diagrams for all alpine ($_a$) and subalpine ($_s$) cores. Solid red and dashed black lines reflect boundaries of sedimentary units (described in text) and the timing of European colonisation (130 cal yr BP; 1820 CE), respectively. Variable data series are coloured according to significance as proxies for sedimentation (grey), erosion (yellow), humification/soil erosion (purple), peatland productivity (green) and fire (black).

colonisation ('colonisation'). Coincident with the early decline in grain size, TOC and TN increase dramatically until ~3400 cal yr BP, displaying a slight trough centring on ~1200 cal yr BP before recovering. Relative stability is observed in both C/N and $\delta^{13}C$.

Due to the abundance of gravel in PB (Fig. 4.2), grain size lies in the sand range until colonisation, after which it decreases into the silt range due to a relative increase in clay. PC1 (59% lithogenics) is volatile but displays a sustained decline between ~2600–1500 cal yr BP. Magnetic susceptibility is low and stable until ~2300 cal yr BP, at which time it becomes more variable and elevated before gradually declining from ~800 cal yr BP. Coinciding with the period of low PC1 values is a broad maximum in TOC and TN following a period of low and stable values; TOC and TN subsequently falls between ~2000–400 cal yr BP before increasing dramatically. C/N exhibits inverse behaviour to TOC and TN, while $\delta^{13}C$ remains stable until a large decrease at core top. These pronounced deviations coincide with the acrotelm and so are more likely to be artefacts of such than environmental signals. Macrocharcoal counts are dramatically elevated between ~2900–1600 cal yr BP and increase slightly again at ~400 cal yr BP before declining for the remainder of the record.

For the core BA (Fig. 4.2), grain size declines irregularly through the record from the sand-silt boundary into the coarse silt range, driven by a long-term increase in the proportion of clay. Fining is accompanied by a long-term increase in PC1 (73% lithogenics), though it also increases during brief periods of lower sand content and displays an unprecedented spike around colonisation. While magnetic susceptibility and TN show no sustained trend, TOC undergoes a long-term decline, reaching a broad maximum between ~2100–1400 cal yr BP. Maxima also occur around this time for C/N and $\delta^{13}C$, which also decline thereafter. Similar to BA but over a much briefer timespan, HD2 (Fig. 4.2) also displays a long-term fining in grain size, which declines from the fine sand to medium silt range due to a gradual decline in the sand/mud ratio. PC1 (72% lithogenics) displays a dramatic decline until ~300 cal yr BP, subsequently remaining low and stable until an uptick commencing at 66 cal yr BP (c.1884 CE). Magnetic susceptibility is also stable until an increase peaking at c.1866 CE. TOC and TN show long-term increases, though TN increases sharply at c.1577 CE; as such, C/N displays a trough at this time, before also increasing. $\delta^{13}C$ exhibits a broad maximum between ~350–150 cal yr BP, declining again after colonisation.

Grain size for HA (Fig. 4.2) displays long-term stability, oscillating with in the medium sand range with an interval of slight fining into the fine sand range between ~3100–1800 cal yr BP associated with a transient increase in the proportion of silt. PC1 (81% lithogenics) also displays no strong trend, but is more elevated prior to ~5000 cal yr BP. Magnetic susceptibility is low and stable throughout the record, though shows higher values between ~2000–1200 cal yr BP. TOC also remains stable but shows periods of slightly elevated values centring on ~8800 and ~5500 cal yr BP, with a sustained increase from ~1800 cal yr BP. Due to TN consistently being below the limit of detection, both it and C/N could not be quantified. $\delta^{13}C$ is more negative prior to ~7500 cal yr BP, after which time it becomes increasingly positive.

Macrocharcoal counts are very low until ~1600 cal yr BP, when there is a large increase and subsequent decline to moderately elevated values. While remaining in the coarse silt range for the entire record, grain size for MB1 (Fig. 4.2) shows relative stability prior to ~1100 cal yr BP before declining abruptly to a minimum by ~900 cal yr BP, attributable to a large decline in the sand/mud ratio. Grain size then recovers before exhibiting unprecedented coarsening into the European period due to a large increase in the sand/mud ratio. PC1 (68% lithogenics) is elevated prior to ~1500 cal yr BP, displaying a subsequent trough from until 700 cal yr BP before increasing for the remainder of the record. Magnetic susceptibility oscillates throughout the record but does preserve a maximum at ~1800 cal yr BP that is coincident with spikes in grain size and PC1. TOC and TN increase dramatically from ~1200 cal yr BP, while C/N is extremely volatile. $\delta^{13}C$ increases until ~1600 cal yr BP, decreasing for the remainder of the record.

4.5.3. Statistical syntheses

Time series records of MA, RoC, aCAR, BMI and CHAR are shown for each site in Fig. 4.3. Aggregated multisite alpine-subalpine records are presented in Fig.4 (a, b) for each of these metrics except CHAR, and omitting HA from bog aCAR (see Section 4.4.2 for justifications). European-era changes in MA and aCAR data are not discussed in this study, as they are respectively modified by anthropogenic activities and acrotelm artefacts and so are not indicative of actual hydrological or environmental change. Also shown in Fig. 4.4 are aggregated independent records of alpine-subalpine charcoal and pollen abundances (c; Appendix C14) and paleoclimate variability (d–g) with which we assess

correlative strength in Fig. 4.6 (Appendix C15). Due to the selected quantitative records of temperature and precipitation only spanning part of our multisite records (Fig. 4.4e), we perform correlation analysis for the Holocene and late Holocene, separately. Holocene analysis instead incorporates dimensionless composite records of hydroclimate and temperature synthesised by Bakis et al. (2026) from relevant independent records (Fig.

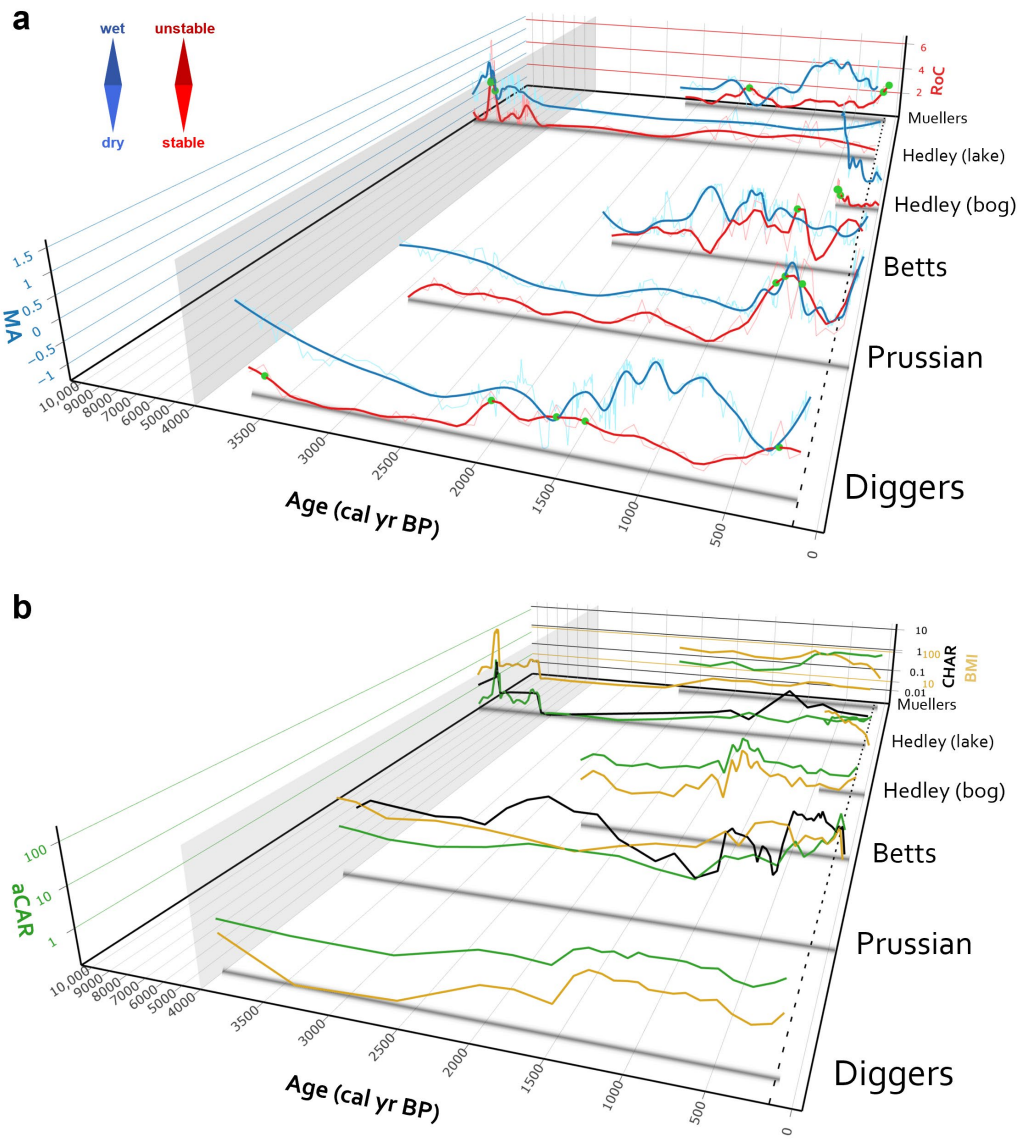

Figure 4.3. Site time series records of **a)** moisture availability (MA; median Z) and Rate-of-Change (RoC; Euclidean distance), and **b)** $\log_{10}$ scaled apparent carbon accumulation rates (aCAR; g C m^{-2} yr^{-1}), bulk mineral influx (BMI; g m^{-2} yr^{-1}) and macrocharcoal accumulation rates (CHAR; particles cm^{-2} yr^{-1}). Green spheres denote RoC 'peak-points' (i.e., ≥2σ). Grey vertical panel highlights an axis break at 4000 cal yr BP. RoC for Hedley bog has been resampled at a higher (5 yr) resolution here for visualisation but retains a standard cross-record resolution for multisite aggregation (Fig 4a).

4.4d; Appendix C16). Holocene correlation analysis excludes the CHAR and multisite aCAR records, while late Holocene analysis addresses the CHAR record from PB only (see Section 4.4.2 for justifications).

Figure 4.4. (next page) Time series records of aggregated alpine-subalpine and paleoclimatic variability. **a)** Alpine-subalpine moisture availability (MA) and Rate-of-Change (RoC), with shaded envelopes representing 95% confidence intervals. **b)** Alpine-subalpine bulk mineral influx (BMI) and apparent carbon accumulation rates (aCAR), the latter excluding Hedley Tarn lakebed for timesteps younger than the base of the oldest bog datum (i.e., 4279 cal yr BP; solid vertical line). Dotted aCAR segment indicates interval informed solely by Hedley Tarn lakebed. **c)** Composite pollen and charcoal record synthesised from independent Snowy Mountains alpine-subalpine records (Hope et al., 2012). **d)** Composite Z-score records of regional temperature and hydroclimate. **e)** mean summer air temperature from Club Lake (Thomas et al., 2022) and mean annual precipitation from Swallow Lagoon (Barr et al., 2019). **f)** ENSO frequency from Lake Palcacocha (Moy et al., 2002) and sand content (indicating El Niño intensity) from El Junco Lagoon (Conroy et al., 2008). **g)** Latitudinal deviation of the Brazil-Malvinas Confluence relative to the modern position (indicating SHWW latitude) from the western South Atlantic (Voigt et al., 2015) and simulated SHWW velocity (Wan et al., 2025). Shaded time intervals denote the timing of the following climate phases: the Holocene Hypsithermal (HH), the time window for ENSO onset (EO) and the first and second warm periods (W1 and W2) reconstructed by Thomas et al. (2022). An arrow is used to indicate the timing of postglacial amelioration (PA), which manifests in independent SM records prior to the start of our record (13,200–11,000 cal yr BP; see main text).

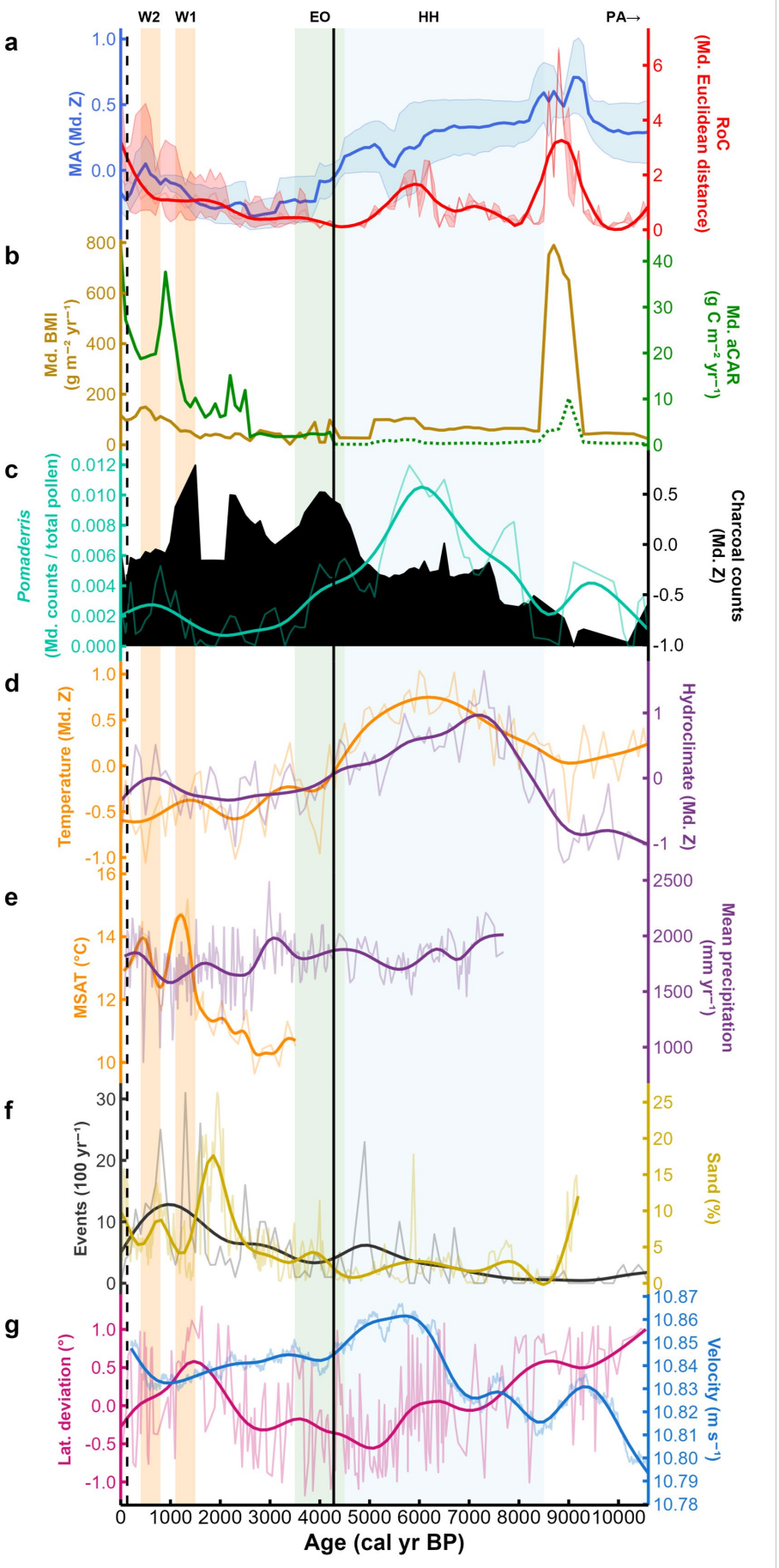
W2
W1
EO
HH
PA→
a
MA (Md. Z)
RoC (Md. Euclidean distance)
b
Md. BMI (g m⁻² yr⁻¹)
Md. aCAR (g C m⁻² yr⁻¹)
c
Pomaderris (Md. counts / total pollen)
Charcoal counts (Md. Z)
d
Temperature (Md. Z)
Hydroclimate (Md. Z)
e
MSAT (°C)
Mean precipitation (mm yr⁻¹)
f
Events (100 yr⁻¹)
Sand (%)
g
Lat. deviation (°)
Velocity (m s⁻¹)
Age (cal yr BP)

4.6. Discussion

4.6.1. Reconstructing systemic variability

4.6.1.1. Variability at the catchment scale

Reconstructing relative hydrological change for Diggers Creek ('Diggers') (Fig. 4.3a), we interpret drying to minimum MA between ~3800–2200 cal yr BP, followed by an inflection to maximum MA by ~900 cal yr BP. This is succeeded by a brief trough centring on ~400 cal yr BP, with partial hydrological recovery by colonisation. In tandem with initial drying, RoC declines to a minimum at ~3000 cal yr BP before increasing abruptly at ~2000 cal yr BP, tracking rewetting. RoC declines again during the MA maximum before increasing sharply to peak values across the drying trough. While RoC is very weakly correlated with MA (r = 0.14), its sign implies greater systemic instability under wetting than drying.

This is apparent when both signals are decomposed into aCAR and BMI (Fig. 4.3b) which are low and stable during the MA minimum and increase precipitously at ~1500 cal yr BP, alongside rewetting. These trends indicate both peatland productivity and catchment erosion were minimally impacted by early drying but significantly so by rewetting. The abruptness of these increases, their lag with wetting and high values thereafter suggest a permanent state shift relating to the exceedance of some MA threshold. After colonisation, RoC increases negligibly from already high values, indicating a European-era perpetuation of already unprecedented instability. This minor increase can be partially attributed to a 60% increase in BMI by c.1845 CE, indicating an intensified erosional regime.

The hydrological reconstruction for Prussian Plain ('Prussian') (Fig. 4.3a) also indicates initially wetter conditions followed by drying to an MA minimum between ~2700–2000 cal yr BP, coincident with Diggers. However, unlike Diggers, rewetting is gradual until ~800 cal yr BP, when there is a pulse to maximum MA at ~500 cal yr BP followed by abrupt drying to pre-peak values. RoC oscillates at relatively low values until ~900 cal yr BP, at which time it spikes alongside peak MA. The RoC-MA correlation is moderately positive (r = 0.57), again suggesting greater systemic disequilibrium under wetting. This is clear from trends in BMI especially (Fig. 4.3b), which displays a 135-fold increase from minimum to maximum MA, declining upon drying. aCAR does not increase until ~1000 cal yr BP and peaks well after maximum MA, indicating peatland

productivity was less perturbed by rewetting than erosion. While CHAR peaks during the MA maximum, it also observes a period of high values between ~2800–1700 cal yr BP, during peak drying. This suggests amplified burning of subalpine woodland under both wetting and drying, but more so under the former. RoC displays a 2.8-fold increase to a maximum between c.1899–1959 CE, implying unprecedented instability after colonisation. This can be partially explained by early colonial maxima in CHAR and especially BMI followed by large declines, suggesting a two-phase intensification and attenuation of the subalpine fire and erosional regime.

While the MA record for Betts Creek ('Betts') is too brief to verify the presence of an early wet phase as communicated by the Diggers and Prussian records, it does capture another MA minimum centring on ~2000 cal yr BP (Fig. 4.3a). While this is again succeeded by wetting, maximum MA is achieved much earlier and is more protracted that in the preceding two records, spanning from ~1400–900 cal yr BP. RoC is low until a large increase at ~1300 cal yr BP, though extreme volatility thereafter indicates cyclic alternations between stability and instability. Nonetheless, an overall increase conveys greater instability under wetting, as supported by another positive, albeit weak, MA-RoC correlation (r = 0.28). This is clear from trends in aCAR and BMI (Fig. 4.3b), which are low and stable until precipitous pulses at ~1200–800 cal yr BP, occurring during but towards the end of the MA maximum. These lagged spikes suggest another MA threshold transgression like Diggers, with higher post-pulse values again indicating a state shift characterised by accelerated peatland productivity and erosion. RoC declines negligibly after colonisation, reinforcing minimal systemic disturbance conveyed by Diggers. Despite this, BMI increases by 117% between c.1818–1951 CE, mirroring trends at Diggers and Prussian.

MA for the Hedley Tarn bog record ('Hedley bog') declines from c.1540 CE with stability emerging from colonisation (Fig. 4.3a), though European-era trends may not accurately reflect hydrology. Precolonial drying appears to replicate post-peak MA declines in all previous records but is only in temporal agreement with that for Prussian. RoC strongly tracks MA, declining until stabilisation from colonisation; RoC and MA for Hedley bog are therefore the most strongly correlated for all sites (r = 0.62). This correlation not only reinforces the subalpine narrative of instability under wetting but suggests even greater positive coupling on sub-centennial timescales. While this is supported by aCAR (Fig. 4.3b), which exhibits an abrupt 87% increase between c.1577–

1540 CE under wetter conditions, BMI instead increases linearly throughout the record. This implies a persistent decline in detrital influx from the Blue Lake blockstream, with a concomitant reduction in fluvial erosivity perhaps explaining the stepped increased in productivity along the river mouth bog complex. This is the only instance of a whole-record negative relationship between aCAR and both MA and BMI. Uninterrupted declines in BMI after colonisation indicate no major perturbation to catchment erosion – supported by grain size inertia – despite minor systemic instability implied by elevated RoC.

Trends in MA for the Hedley Tarn lakebed ('Hedley lake') record chronicle relatively dramatic wetting until a maximum at ~9100 cal yr BP cal yr BP (Fig. 4.3a). This is followed by lower but high MA until ~6000 cal yr BP, at which time there is abrupt drying to a minimum at ~2000 cal yr BP. This is coincident with all subalpine records, indicating that ~2000 cal yr BP marks a minimum in alpine-subalpine MA for the last ~10,600 yr. While subsequent rewetting is also apparent for Hedley lake, it is relatively minor, suggesting that the Common Era MA maxima apparent in all preceding records were negligible relative to Holocene-scale trends. RoC for Hedley lake is surprisingly low during the initial wetting phase but displays an abrupt maximum under peak MA, declining again before another minor peak during the ~6000 cal yr BP drying event.

RoC then approaches a broad minimum until a stepped increase at ~2000 cal yr BP alongside Common Era rewetting. RoC is again positively but most weakly correlated of all sites with MA (r = 0.14), suggesting instability under wetting is maintained even at the Holocene scale, albeit less so. This is plainly apparent from the aCAR and BMI data (Fig. 4.3b), which dramatic maxima at ~8900 and ~8700 cal yr BP, respectively coinciding with peak MA but lagging long-term wetting, similar to Betts. The aCAR and BMI pulses correspond to the most organic horizon in the HA core and are driven by a dramatic spike in sedimentation rates but no increase in grain size. Coarsening is instead driven by the appearance of gravel 11 cm below the base of the dated core section, which itself is marked by the emergence of organic matter, presumably from Hedley bog.

This stratigraphy suggests a three-stage environmental history defined by 1) a significant increase in catchment instability following deglaciation of the Blue Lake cirque (Barrows et al., 2001) (undated gravel emergence), 2) a stabilisation of the erosional regime and bog colonisation around Hedley Tarn (basal organic matter emergence), and 3) increased MA permitting bog expansion but also massive sediment

influx (aCAR and BMI spikes). Following their pulses, aCAR and BMI stabilise slightly above pre-pulse values – again similar to Betts and thus suggesting a permanent state shift – before minor troughs between ~4500–2500 cal yr BP, coincident with minimum MA.

Both variables increase steadily thereafter, preceding rewetting by ~500 cal yr BP. Average CHAR is dramatically lower for Hedley lake than Prussian; this is expected given the former's distance from the subalpine zone, which is the primary source of macrocharcoal due to an abundance of woody vegetation. That said, relative trends for Hedley lake reveal an increase during the Holocene MA maximum, suggesting wetting was an alpine-subalpine-scale event and was associated with increased or more proximal burning. CHAR falls to a minimum by ~5000 cal yr BP before spiking at ~1000 cal yr BP. Excluding an anomalous earlier pulse calculated from a single macrocharcoal grain, the ~1000 cal yr BP pulse is the only instance of CHAR for Hedley lake being higher than Prussian, which preserves a trough at the same time.

The Muellers Pass (Muellers) reconstruction, similar to all subalpine bogs, indicates an initial interval of lower MA with a trough at ~1800 cal yr BP (Fig. 4.3a), after which time there is precipitous wetting to peak MA at ~800 cal yr BP. RoC maintains few similarities with MA, showing elevated values alongside both minimum and maximum MA, with an abrupt maximum just prior to colonisation. Accordingly, RoC and MA are very weakly but once again positively correlated (r = 0.19). The early RoC peak is not captured by aCAR nor BMI (Fig. 4.3b), which are both relatively stable until sharp increases at ~1100 cal yr BP, coincident with peak MA. While BMI declines after a maximum at ~1000 cal yr BP, aCAR peaks at ~700 cal yr BP and remains high; such inverse behaviour evokes that observed for Hedley bog over the overlapping period, suggesting alpine erosion and bog productivity have behaved inversely over most of the last millennium. RoC does not increase after colonisation but does remain high, indicating a continued instability. This is partly driven by a sustained decline in BMI, replicating the post-European decrease in erosion inferred for Hedley bog.

4.6.1.2. Variability at the zonal to complex scale

There are clear precolonial disparities in RoC, aCAR and BMI (Fig. 4.5) between the alpine and subalpine population of records. Specifically, RoC for subalpine sites is 17% higher than for alpine sites and possesses more extreme upper outliers (Fig. 4.5a),

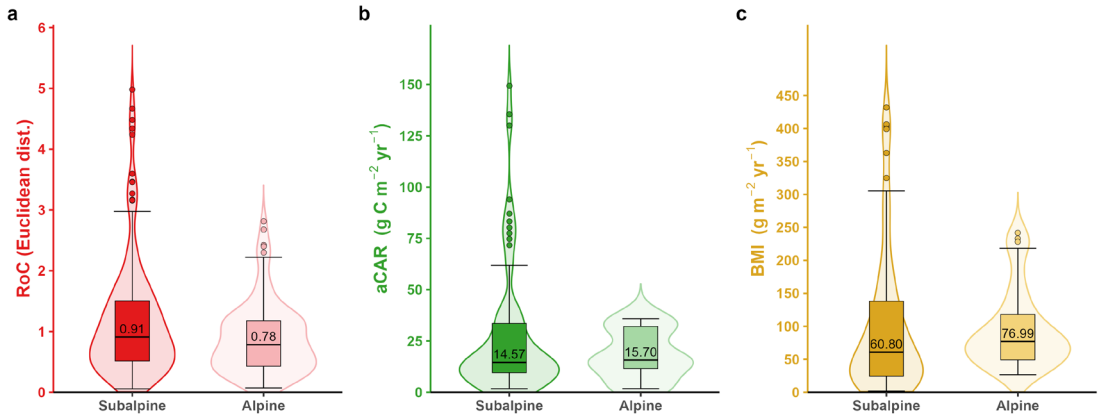

Figure 4.5. Violin plots comparing aggregated subalpine and alpine data for the precolonial late Holocene (i.e., from the base of the oldest bog record to the youngest precolonial data point). Median lines annotated.

suggesting that subalpine catchments have not only been more variable over the late Holocene but are more prone to episodic reconfiguration, as evidenced by the critical transitions in peatland productivity and erosion at Diggers and Betts. One explanation for this is the more climatically and biophysically transitional environment of the subalpine zone, which places it closer to thresholds of instability than the more climatically stable alpine core, rendering the former a more dynamic system (Mason and Williams, 2013a, Holtmeier and Broll, 2018).

We find median aCAR to be comparable between the subalpine and alpine zones but slightly higher in the latter (Fig. 4.5b). Unsurprisingly, this implies that alpine peatlands are marginally more productive than subalpine peatlands, probably due to more continuously favourable climatic conditions known to be conducive for mire maturation into a bog, which is the most productive growth form and dominates the alpine zone (Hope et al., 2012, Ronkainen et al., 2014, Yang et al., 2023). Alpine records also possess substantially (26%) higher BMI (Fig. 4.5c), reflecting a higher-yield erosional regime perhaps attributable to more acute alpine exposure to snowmelt runoff, frost weathering and gelifluction (Barrows et al., 2001, Mason and Williams, 2013c, Reinfelds et al., 2014, Wilson et al., 2022). That said, it should also be recognised that the upper quartiles and outliers for BMI are markedly higher for the subalpine zone, diagnostic of more unstable catchments with a greater propensity for extreme erosional events that also contribute to its higher subalpine RoC. This may be due to a more rainfall-dominated precipitation regime (contributing to more erosive runoff and stream discharge) and thicker soils

mantling higher-relief catchments (increasing the likelihood of mass wasting events) (Bilish, 2020, Wilson et al., 2022).

Aggregating all site records, we approximate Holocene variability across the alpine-subalpine complex (Fig. 4.4a, b). Adhering to the Hedley lake record from which the first ~6800 yr is solely inherited, the multisite records preserve extreme Holocene maxima in MA, RoC, aCAR and BMI between ~9500–8000 cal yr BP. This event ('the Hedley Tarn event') is followed by collapses and prolonged stability in RoC, aCAR and BMI as MA gradually declines until ~4500 cal yr BP. Drying accelerates from ~4500–3900 cal yr BP as bog records are incorporated. RoC is low and unresponsive during this time, increasing only following rewetting from ~2600 cal yr BP after an MA minimum. Rewetting culminates in a final MA peak at ~500 cal yr BP, with RoC remaining stable until post-peak drying, and almost tripling over the European era. RoC at present is highest for all times except the pulse during the Hedley Tarn event and thus represents the only point at which systemic instability can be confidently inferred to be unprecedented for all alpine-subalpine sites. Consistent with every site record, precolonial alpine-subalpine RoC is weakly positively correlated with MA (r = 0.22).

The increase in aCAR at ~4200 cal yr BP is an artefact of the transition from the Hedley lake data to the bog data. However, we still infer extremely low bog aCAR (median 2.2 g C m^{-2} yr^{-1}) from at least this time until ~2500 cal yr BP; such low values suggest alpine-subalpine peatlands were probably carbon sources prior to rewetting. After ~2500 cal yr BP, there is an almost sevenfold increase in aCAR coinciding with rewetting. While aCAR stabilises at substantially higher values after this time until ~1300 cal yr BP (8.3 g C m^{-2} yr^{-1}), these are still very low relative to high-altitude peatlands globally (Gaffney et al., 2025), indicating marginal conditions for alpine-subalpine peat growth over most of the late Holocene. Low productivity is terminated by a 4.5-fold spike to 37.6 g C m^{-2} yr^{-1} at ~900 cal yr BP, subsequently stabilising at 19.5 g C m^{-2} yr^{-1} until acrotelm artefacts are incorporated.

Stabilised values are towards the lower end of the global range (Gaffney et al., 2025), indicating alpine-subalpine peatlands have been continuously moderately productive for only ~1100 yr prior to colonisation. Overlap with rewetting suggests that enhanced productivity is related to increased MA. This is also true for catchment erosion; BMI oscillates at low values after the Hedley Tarn event before increasing from ~1500 cal yr BP, lagging the first aCAR pulse by ~1000 yr. From this time, BMI triples to a peak of

~149 g m^{-2} yr^{-1} at ~500 cal yr BP, coinciding with the final MA peak, and declines slightly before a final increase after colonisation that is ~21% lower than the ~500 cal yr BP peak. Peak BMI at ~500 cal yr BP therefore represents the only definite maximum in alpine-subalpine sediment yield, indicating an even more intense erosional regime under peak late Holocene MA than European land use change.

4.6.2. Interpreting the systemic sensitivity of the alpine-subalpine complex

4.6.2.1. Sensitivity to Holocene climate change

Comparing Holocene trends in MA, RoC and BMI with independent reconstructions of paleoclimate yields mostly weak to non-existent correlations (Fig. 4.6), implying low to no systemic sensitivity to any single climate metric. As Bakis et al. (2025) speculate for the montane zone, weak relationships are probably attributable to the unconstrained influences of multiple superimposed climatic indices, Indigenous land use changes, stochastic variability and biophysical feedbacks amplifying and/or attenuating extrinsic forcings. The latter of these is especially significant at the Holocene scale, with the Hedley Tarn event dramatically weakening correlations paleoclimatic correlations particularly with MA. In fact, MA is not correlated with hydroclimate but becomes strongly positively correlated (r = 0.7) once the Hedley Tarn event and preceding period is omitted from the calculation. That said, MA possesses all four of the only moderate correlations between any alpine-subalpine and climate metric, all of which are statistically significant; this suggests that MA has been more sensitive to Holocene climate change than catchment erosion and the biophysical stability of the complex itself.

While the negative correlation between MA and SHWW velocity is seemingly contradictory given these moisture-laden frontal systems are a major source of precipitation for southeastern Australia (Fogt and Marshall, 2020), it should be realised that maximum SHWW velocity in the mid-Holocene coincides with – and is in fact a product of – a poleward retraction of the belt to its southernmost extent (Fig. 4.4g) (Voigt et al., 2015, Tamhane et al., 2023, Wan et al., 2025). As observed during positive Southern Annular Mode phases, southward displacements of the SHWW are associated with reduced annual and especially cool-season rainfall across southeastern Australia (Meneghini et al., 2007, Raut et al., 2014, Fogt and Marshall, 2020); this is supported by

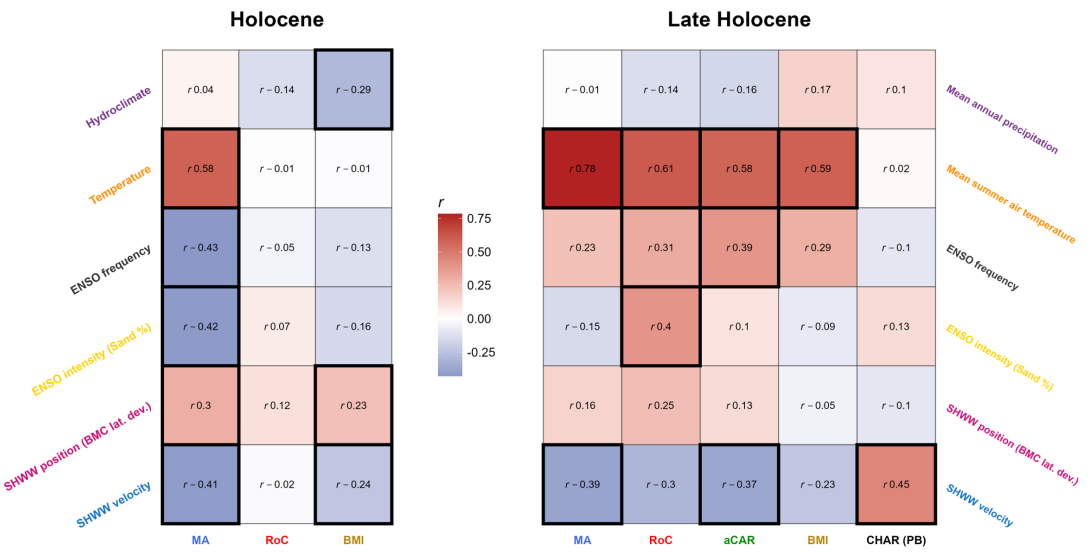

Figure 4.6. Grids presenting correlative strength and sign between various multisite alpine-subalpine (columns) and paleoclimate (rows) metrics shown in Fig. 4.4 for the Holocene and precolonial Late Holocene. Plots outlined black highlight correlations that are statistically significant at $p \leq 0.05$. Note that MSAT data is not available for Late Holocene timesteps ≤3500 cal yr BP, and so *r* values are only based on a shorter period.

MA being negatively correlated with SHWW latitude. As such, the negative relationship between MA and SHWW strength is probably a spurious correlation driven by poleward deflection resulting in peak velocity. Regardless, stronger correlations with both ENSO frequency and intensity imply higher direct sensitivity to ENSO than the SHWW, with negative relationships with both ENSO metrics indicating that alpine-subalpine catchments become drier under more frequent and intense ENSO activity. This is clear in high MA after the Hedley Tarn event overlapping with Holocene minima in both ENSO frequency and intensity.

Suppressed ENSO-type variability during the early-middle Holocene is responsible for the Holocene Hypsithermal ('hypsithermal'), which manifests in proximal high-altitude records as an interval of elevated precipitation between ~8500–4500 yr BP. This has been attributed to an insolation-driven weakening of the Pacific Walker Circulation and concomitant shift to a La Niña-like mean state (Southern, 1982, Donders et al., 2007, Koutavas and Joanides, 2012, Carré et al., 2014, White et al., 2018, De Deckker, 2022). The emergence of such a state across the alpine-subalpine complex is clear from independent palynological records, which reveal a surge in the relative proportion of pollen for *Pomaderris* – a wet understorey element – coeval with the onset of the

hypsithermal, with peak abundance lagging maximum hydroclimatic intensity by ~1500 cal yr (Fig. 4.4c) (Hope et al., 2012).

This *'Pomaderris* interval', as it is termed by Martin (1999), is also associated with elevated charcoal abundances (Fig. 4.4c), indicating an intensification of fire due to increased fuel loads under peak precipitation but probably also temperature, which presumably extended growing seasons (Hope et al., 2012). The hypsithermal explains high MA until ~6300 cal yr BP and the positive relationship between MA and temperature, which is the strongest of all correlations but is likely another spurious correlation relating to warming being a secondary confounding feature of the hypsithermal (Cohen and Nanson, 2007, De Deckker, 2022, Lowry and McGowan, 2024). However, the MA pulse during the Hedley Tarn event (Fig. 4.4a) is inconsistent with peak hydroclimatic intensity – which occurs later at ~7300 cal yr BP (Fig. 4.4d) – but is also too late to be ascribed to postglacial amelioration (Martin, 1986a, Kershaw et al., 2007). Instead, organic matter emergence at ~10,624 cal yr BP, indicating mire establishment around Hedley Tarn, is in better agreement with postglacial amelioration, as constrained by reconstructed peatland and herbfield colonisation of the periglacial terrain over the Pleistocene-Holocene transition (Costin, 1972, Raine, 1974, Martin, 1986a, Martin, 1986b, Martin, 1999, Marx et al., 2011).

Regardless, the coincidence of mire establishment and the MA pulse with postglacial amelioration and hypsithermal onset, respectively, convey rapid responses and thus sensitivity to hydroclimate. This is reinforced by the profile of the MA pulse itself, which is disproportionately steep relative to hydroclimate and is therefore posited to reflect some dramatic critical transition immediately triggered by hypsithermal onset. Specifically, the associated spikes in aCAR and BMI (Fig. 4.4b) could reflect a rapid acceleration of bog productivity and sediment yield, respectively, in response to increased precipitation. The absence of coarsening despite the BMI spike suggests a massive increase in sediment yield was not accompanied by heightened erosivity for at least the Blue Lake blockstream.

Stanley and De Deckker (2002) similarly do not observe any increase in grain size for Blue Like itself during hypsithermal onset, confirming stability in transport energy also applied to the cirque headwaters. One reason for this discrepancy between yield and erosivity may be that the hypsithermal was defined in southeastern Australia by more persistent but not more intense precipitation, given suppression of ENSO variability (Barr et al., 2019, De Deckker, 2022, Clerke, 2023). Dramatically elevated influx but not

erosivity may explain why Hedley bog was also able to become so extremely productive during this time, with stable streamflow permitting *in situ* preservation of organic matter at the river mouth of Blue Lake Creek. In fact, presumable progradation of the alluvial fan due to increased yield may have even accelerated bog expansion by increasing subaerial but saturated area optimal for paludification.

The post-peak collapse in BMI may reflect slopes becoming stabilised due to increasing catchment coverage by colonising alpine meadow (Hope et al., 2012). Meanwhile, the collapse in aCAR might be explained by Hedley bog accreting so rapidly that it had sufficiently raised itself above the influence of the water table to transition from a nutrient-rich minerotrophic to nutrient-poor – but more productive – transitional complex. This is consistent with the conventional model of bog maturation and would explain aCAR collapsing but still being higher than under the drier pre-hypsithermal climate (Moore, 1987, Anderson, 2002, Swindles et al., 2025). As such, the apparent decline in MA over the course of the hypsithermal probably does not reflect genuine drying but may instead be an artefact of the biophysical system stabilising in its new basin of attraction and thus becoming more insensitive to hydroclimate (Scheffer et al., 2012).

This is supported by the overall decline in RoC for the remainder of the hypsithermal. While both RoC and BMI are most strongly and negatively correlated with hydroclimate, these correlations are very weak and appear to be artefacts sustained by their spikes during the Hedley Tarn event, with minimal agreement observed with hydroclimate thereafter. Hydrological sensitivity to ENSO is reinforced by dramatic drying at ~4500 cal yr BP, synchronous with the termination of the hypsithermal due to ENSO intensification and the shift to a drier El Niño-like mean state (Fig. 4.4f) (Donders et al., 2008, Marx et al., 2009, Barr et al., 2019, Hagemans et al., 2022). This is confirmed by a large decrease and increase in alpine-subalpine *Pomaderris* pollen and charcoal abundance, respectively, conveying a drying of vegetation and thus increased burning (Hope et al., 2012). Notably, this mechanism (i.e., fuel desiccation) for intensified burning differs from that proposed for the early Holocene (i.e., increased fuel loads), with the continued post-hypsithermal increase in macrocharcoal suggesting neoglacial cooling and drying was a more effective driver of alpine-subalpine burning than the hypsithermal.

4.6.2.2. Sensitivity to late Holocene climate change

Comparing trends in late Holocene alpine-subalpine and paleoclimatic variability under a quasi-modern (i.e., ENSO-dominated) climate, we again observe mostly weak to no correlations (Fig. 4.6). While MA no longer emerges as the most climatically sensitive metric, it is by far the most strongly correlated with mean summer air temperature (MSAT) as reconstructed by Thomas et al. (2022) from the SM tarn Club Lake (Fig. 4.1c). Despite this, all other alpine-subalpine metrics except CHAR are also most strongly and positively correlated with MSAT. Comparatively, the annual precipitation record reconstructed by Barr et al. (2019) from Swallow Lagoon, North Stradbroke Island, possesses a very weak to no correlation with all alpine-subalpine metrics. These relationships imply that, at least under a climatic regime analogous to present, MA, systemic stability, peatland productivity and catchment erosion were considerably more sensitive to MSAT than annual precipitation, with all tending to increase under warming. Indeed, MA, RoC, aCAR and BMI increase alongside MSAT over the late Holocene (Fig. 4.4e), with all except RoC peaking during or between two warm periods reconstructed between ~1500–1100 and 800–400 cal yr BP, the regional significance of which are verified by other paleotemperature reconstructions (Mooney et al., 1997, Gergis et al., 2016, McGowan et al., 2019).

Consistent with its strongest correlation, MA tracks MSAT particularly well, increasing from the onset of the first and warmest warm period and peaking during the second, milder warm period. However, catchment rewetting under warming is curious given both a presumable increase in evapotranspiration and the intensification of ENSO, the latter having already been implicated in abrupt catchment drying from ~4500 cal yr BP, as well as by Barr et al. (2019) in the late Holocene decline in precipitation for Swallow Lagoon. This contradictory MA-MSAT relationship is also recognised by Bakis et al. (2025), who reconstruct their own MA peak for the montane zone only ~100 yr prior to that reconstructed in this study, which they attribute to increased snowmelt inflow into montane peatlands (McGowan et al., 2019).

Bakis et al. (2025) implicate higher snowmelt runoff during these warm periods in intensified erosion and peatland productivity, which we also observe. Given these similarities and the fact that snowmelt constitutes an even larger source of flows into alpine-subalpine catchments (Bilish, 2020, Bilish et al., 2020), we propose that warming-driven increases in snowmelt supply also stimulated our own late Holocene increases in

MA, aCAR and BMI and thus RoC, driving their strongest and positive MSAT correlations. Higher alpine-subalpine MA during these warm periods is verified by an uptick in the abundance of *Pomaderris* at this time, as well as inferences by both Raine (1974) and Vernon (2017) that the Blue Lake catchment has experienced wetting since ~1500 yr BP.

Bakis et al. (2025) relate warming to the intensification of ENSO and posit that a concurrent northward shift in the SHWW resulted in not only stable but increased snow cover such that ENSO and thus MSAT could switch from a negative to positive forcing on MA. In our record, this mechanism reconciles ~4500 cal yr BP drying concurrent with ENSO onset (and poleward SHWW) with rewetting during peak ENSO (and equatorward SHWW), while also explaining post-500 cal yr BP drying coinciding with a return to suppressed ENSO (and poleward SHWW) (Moy et al., 2002, Conroy et al., 2008, Voigt et al., 2015). While Vernon (2017) speculates that wetting at Blue Lake may relate to inland incursions of the SHWW as reconstructed by Marx et al. (2011), the author considers only the effect of increased precipitation. Along with Barr et al. (2019), higher precipitation is not corroborated by many lower high-altitude sites with negligible to no snowmelt inflow, such as Brooks Ridge Fen, Jackson's Bog and Bega Swamp (Southern, 1982, Hope et al., 2004). This suggests a substitutive mechanism for rewetting, such as that proposed by Bakis et al. (2025), must have been present at higher altitudes only.

ENSO as a mechanism for rewetting and thus systemic change would explain RoC being the only metric to possess statistically significant correlations with both ENSO metrics. The link between ENSO and warming is moderately supported by wavelet analysis of the Prussian and Betts μXRF PC1 data (Fig. 4.7a, b) (Appendix C17). These are the only two records with sufficiently high-resolution chronologies to investigate ENSO-range (2–7 yr) periodicity in the PC1 data. The large lithogenic contributions to both PC1 records render these potential proxies for erosional events whose frequency and intensity are presumably positively correlated with ENSO (Moy et al., 2002, Conroy et al., 2008). Although no pronounced band of statistical significance emerges in the ENSO range for either record, we observe that its median spectral power increases after ~1800 cal yr BP for Prussian and at least ~2300 cal yr BP for Betts (Fig. 4.7c).

Interestingly, median power for Prussian and Betts achieve precolonial maxima at ~800 cal yr BP and ~600 cal yr BP, respectively, with statistical significance also emerging from this time. These maxima coincide with the second warm period and high

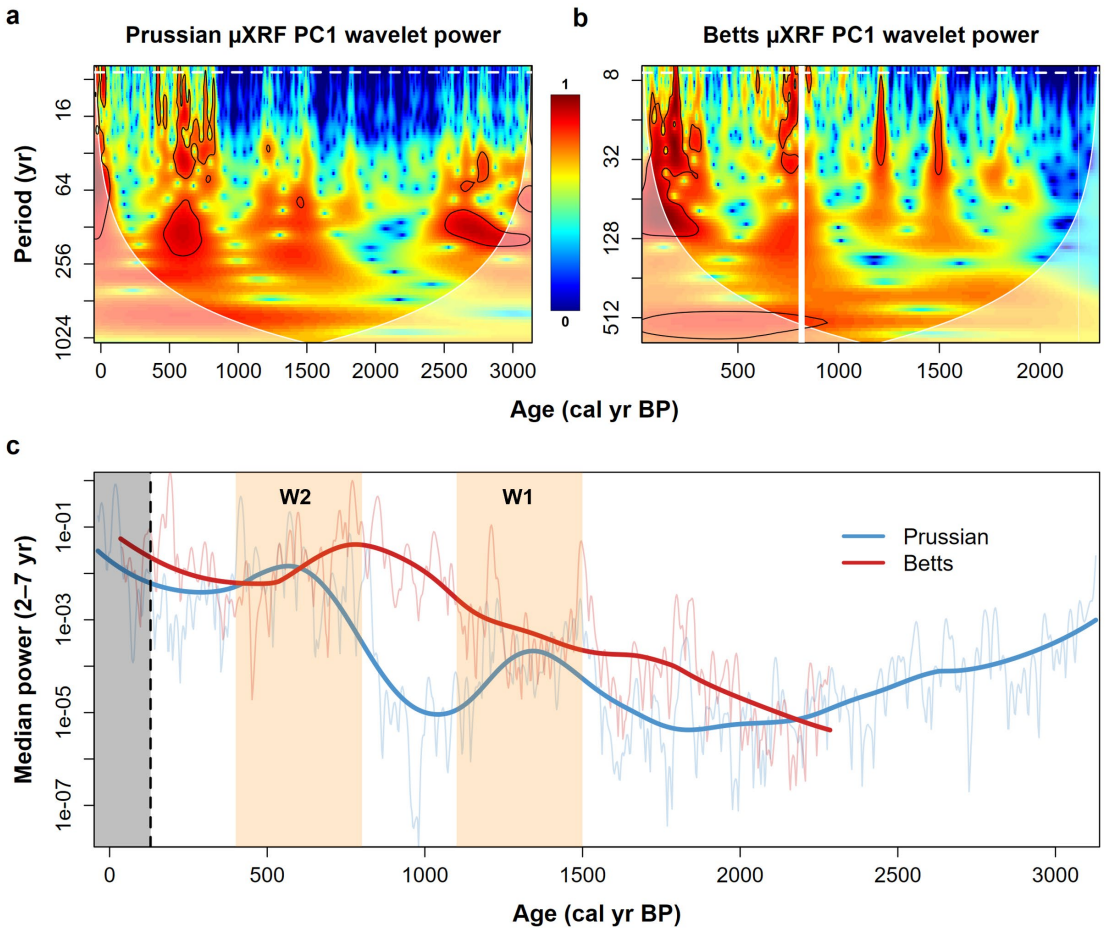

Figure 4.7. Outputs of wavelet analysis of the µXRF PC1 data for **a)** Prussian Creek and **b)** Betts Creek. White dashed line in wavelet power plots denote the periodicity of 7 yr. Black contours delineate time-period regions where power exceeds the 95% significance level. Shaded peripheries demarcate the cone of influence. White intervals indicate sampling gaps due to material removal for ^{14}C dating. **c)** Median spectral power value for every timestep in the 2–7 yr periodicity range. Grey region denotes the European era, during which time data is unequivocally modified by land use changes and therefore should not be consulted.

ENSO intensity and frequency. While this temporal agreement does not, of course, directly implicate ENSO in the observed spectral power trajectories, it does support our hypothesis, and that of Bakis et al. (2025), that warming and thus rewetting was ENSO-related. ENSO as a positive MSAT forcing is supported by modern observations that surface air temperature anomalies in southeastern Australia are positively correlated with El Niño, especially in summer and autumn (Fierro and Leslie, 2014, Lieber et al., 2023).

If late Holocene systemic behaviour can therefore be predominantly ascribed to ENSO, then higher RoC in the subalpine than alpine zone suggests greater ENSO-driven instability beneath the treeline ecotone than above it. Indeed, increased frequency and intensity of drought and high rainfall events under ENSO constitute reasonable

mechanisms by which the more extreme, episodic increases in subalpine RoC (i.e., systemic reorganisation) and BMI (i.e., slope failure) might occur, consistent with contemporary observations by Nyman et al. (2019). Higher alpine aCAR and BMI also suggests that ENSO-driven rewetting more effectively increased peatland productivity and erosion in the alpine than subalpine zone, despite erosional events being less common and/or extreme. It should also be noted that warming likely constituted an important secondary positive forcing on productivity in both zones, given it is capable of extending growing seasons and accelerating growth of *Sphagnum* groundcover and thus peat, but only if it does not also drive a net decline in MA (Charman et al., 2013, Loisel et al., 2014).

ENSO variability may also explain changes in the treeline itself; the brief increase in Hedley lake CHAR above that of Prussian at ~1000 cal yr BP implies a subalpine-equivalent fire regime at least at the elevation of Hedley Tarn, within ~100 cal yr of the termination of the first warm period. As such, and given the treeline is MSAT-delimited, we hypothesise a transient rise in the treeline to at least ~60 m above its modern position to Hedley Tarn in response to warmer/longer growing seasons during the first and warmest warm period. This is moderately supported by Club Lake records, with Thomas et al. (2022) reconstructing a pulse in both CHAR and the woodland/alpine ratio only ~150 yr earlier, and Martin (1986b) postulating treeline rise throughout the late Holocene.

While the Prussian CHAR record cannot directly confirm this hypothesis, the fact that the Hedley lake pulse coincides with a trough for Prussian eliminates the possibility that the former is a product of intensified fire activity and so must reflect some other mechanism, the most plausible being treeline rise. CHAR for Prussian itself is most strongly and positively correlated with SHWW velocity, with both increasing dramatically over the last ~500 yr. While Wan et al. (2025) do not explain anomalous SHWW strengthening, this is probably a result of its aforementioned poleward retraction over the last millennium. An associated decline in winter precipitation might explain the precipitous increase in burning conveyed by Prussian (Chubb et al., 2011, Fogt and Marshall, 2020), though there is curiously no evidence for such in independent charcoal records. The earlier CHAR increase at ~2100 cal yr BP for Prussian may also relate to a more poleward SHWW, which we have already implicated alongside ENSO in the Holocene MA minimum for the alpine-subalpine complex at this time.

4.6.2.3. Sensitivity to European land use change

The European era represents a RoC maximum for the time period informed by both alpine and subalpine records (i.e., after ~3700 cal yr BP). This conveys that systemic instability after colonisation is unprecedented for this interval, and thus that alpine-subalpine catchments are more sensitive to European land use change than any climatic forcing under an established, ENSO-dominated climatic regime. While European-era RoC is certainly being artificially increased by acrotelm artefacts, these are very unlikely to account for such a precipitous increase in RoC, which is informed by deviations in many other independent proxies.

Salient among these is BMI, which increases dramatically during the grazing era for Diggers, Prussian and Betts, implying a departure from the late Holocene baseline prior to prohibition of alpine-subalpine grazing. Notably, all three of these sites are subalpine, with no European-era increases in BMI being preserved in the alpine records. This zonal discrepancy cannot be ascribed to a lack of perturbation in the alpine zone given historical evidence of seasonal grazing up to the Main Range (King, 1959, Hancock, 1972, Scherrer and Pickering, 2001, Slattery, 2015), with Costin et al. (1960) calculate massive soil loss during this time. Moreover, De Deckker et al. (2023) show that erosional responses to grazing were effectively immediate in the Blue Lake cirque, with sedimentation rates exceeding the precolonial baseline by 18-fold at the end of the grazing period.

Despite these contradictions, our data are concordant with conclusions by Stromsoe et al. (2016) that grazing induced minimal erosion in more vegetated catchments, and that extensive alpine meadow coverage is responsible for reduced erosion relative to lower elevations. As such, erosional impacts appear to be highly catchment-dependent in the alpine zone, with dense groundcover and lower relief in our sampled alpine catchments probably explaining higher apparent alpine tolerance to land use change (Costin, 2000, Wilson et al., 2022). This is also consistent with narrower distributions in late Holocene alpine RoC and BMI compared to the more dynamic subalpine zone, reinforcing the notion of subalpine catchments being closer to thresholds of instability. Post-European stability in alpine BMI does not necessarily imply an absence of erosional perturbation, however, with Muellers recording an unprecedented increase in grain size after colonisation. The mechanism driving coarsening but not increased yield is unclear but does confirm major erosional disturbance on even alpine summits.

Substantial European-era coverage by the Prussian record in particular divulges a two-stage erosional history for the site, characterised by a pulse in BMI at the end of the grazing period followed by a 75% decline after prohibition. This pulse may reflect massive erosion around this time that was the very impetus for the termination of snow leases (Costin, 1957, Clark, 1992, Good, 1992), which itself may be responsible for the post-pulse decline in erosion (Stromsoe et al., 2016). A two-stage sequence is also apparent for CHAR, which while superimposed on a dramatic precolonial increase, rises an additional 56% during the early colonial period to a maximum, indicating an initial intensification of burning such that unprecedented late Holocene burning was achieved.

Following this pulse, however, CHAR declines precipitously into the postcolonial period, with the record terminating at values comparable to prior to the late Holocene peak. While the timing of this decline seemingly contradicts the notion of annual, high-intensity firing by pastoralists, it may in fact reflect major opening of subalpine woodland, with a diminished tree stratum reducing the flux of macrocharcoal to the valley floor (Newman, 1954, Mooney, 2004, Zylstra, 2006). Longer-term declines, however, are more likely to be a product of the abolishment of grazing and establishment of conservation measures characterised by revegetation and the suppression of both European and Indigenous burning (Good, 1992, Mooney, 2004, Good and Johnston, 2019).

Renewed collapse of the canopy under contemporary *E. pauciflora* dieback may also be contributing to declines over the final part of the record (Ward-Jones, 2021). Regardless, precipitous increases then decreases in BMI and CHAR suggest rapid erosional and pyrological responses to an early intensification and then relaxation of European land use practices. The abruptness of these adjustments reinforces late Holocene inferences of high subalpine sensitivity to stimuli and explains unprecedented European-era systemic disequilibrium in the multisite record.

4.6.3. Implications for future systemic responses to anthropogenic perturbation

The most recent climate modelling for New South Wales (NaRCliM2.0) projects universal warming and precipitation declines across the SM (DCCEEW, 2024b). By 2100 CE, under the IPCC's medium- to high-emissions pathway (SSP3-7.0), the alpine-subalpine complex is anticipated to experience warming of 3.6–3.9 ºC and precipitation

declines of 12–19%, with larger changes expected for the warm season and alpine zone (Intergovernmental Panel on Climate Change, 2023, DCCEEW, 2024b, DCCEEW, 2024a). This is due to global warming and associated changes in ENSO and the Southern Annular Mode, which, in a continuation of late Holocene trends, are shifting toward an El Niño and positive mean state, respectively (Lim et al., 2016, Deng et al., 2022, Cai et al., 2023, Lieber et al., 2024, Thirumalai et al., 2024).

While we implicate late Holocene ENSO intensification and resultant warming in catchment rewetting since ~2600 cal yr BP, this model assumes at least stability in snow cover over the Common Era, as conveyed by McGowan et al. (2019). However, due to anthropogenic warming and declining precipitation, this same record indicates snow cover is now at a minimum for the last ~2000 yr. Moreover, the area observing ≥ 60 annual snow cover days is projected to decline by 97% by 2050 CE under a high-emissions pathway (Pickering and Green, 2009, Chubb et al., 2011, Theobald et al., 2016). While Reinfelds et al. (2014) find that precipitation declines and shifts to earlier peak discharge have been more appreciable for the alpine zone since the mid-20th century, annual runoff has declined more substantially for lower elevation catchments due to larger decreases in snow cover. This is consistent with higher reconstructed subalpine sensitivity to climate change due to more marginal climatic conditions and confirms that any positive late Holocene association between MSAT and MA has already deteriorated, especially at lower elevations. While temperature has evidently reverted from a positive to negative forcing on MA, it is likely to remain the dominant control on systemic variability, in view of its maximum correlative strength with MA, RoC, aCAR and BMI over the late Holocene.

Sustained significance of warming is demonstrated by the increasingly widespread desiccation of alpine-subalpine peatlands, which is being driven by not only declining hydrological recharge but also increasing evapotranspiration under warming, particularly in summer (Hope and Nanson, 2015). Desiccation is in turn initiating a positive drying feedback whereby the declining hydraulic conductivity of increasingly unproductive peatlands is impairing their capacity to sequester flows, thereby increasing the rate of downslope water transfers already being directly accelerated by earlier, more abrupt spring thaw (Grover, 2006, TSSC, 2008, Grover et al., 2012, French et al., 2016). This feedback is likely to be more severe for subalpine peatlands, which may cross thresholds of tolerance sooner than alpine complexes due again to more marginal climatic

conditions, which we have implicated in lower subalpine productivity over the late Holocene.

Elevational differences in peatland sensitivity are confirmed by contemporary observations that, of those alpine-subalpine peatlands that are recovering from European degradation, most are situated at higher elevations (Hope et al., 2012). This zonal disparity is being reinforced by ongoing degradation by feral horses, which are more populous and thus detrimental in the subalpine zone (Dyring, 1990, Worboys and Pulsford, 2013, Robertson et al., 2019, Office of Environment and Heritage, 2023). Climatic and feral horse destruction of peatlands is inhibiting not only their retention of runoff but also carbon, with many damaged complexes now emitting rather than sequestering CO_2 across the Kosciuszko Massif (Treby and Grover, 2023, Treby and Grover, 2024). In view of these stressors, as well as their already unproductive to marginally productive conditions over the late Holocene, we anticipate a near-future mass conversion of alpine and especially subalpine peatlands from carbon sinks to sources. In fact, an apparent carbon-source status prior to ~2500 cal yr BP during the MA minimum demonstrates that alpine-subalpine are capable of achieving such a state under far milder climatic changes than those projected.

More punctuated surface discharge due to peatland degradation will also increase the erosivity of runoff events. This will be further augmented by earlier spring snowmelt, which has been implicated in higher catchment erosion at ~500 cal yr BP than during even the European era. Indeed, increased spring snowmelt alone is projected to increase the erosivity of rainfall by up to 24% by 2040 CE relative to the 1990–2009 CE baseline, though this effect is expected to collapse to 1% by 2080 CE as snowmelt contributions become negligible (Zhu et al., 2020). Even after this occurs, catchment erosion will be sustained by the shift from a solid- to liquid-state precipitation regime under warming and amplified oscillations between drought and high-intensity rainfall associated with more frequent and intense multiyear instances El Niño and La Niña (Ding et al., 2022, Lieber et al., 2024). Amplification of ENSO is particularly concerning given we have identified this as the ultimate climatic forcing on systemic destabilisation over the late Holocene.

Catchment erosion is also likely to be worsened by an increasingly positive Southern Annular Mode (Lim et al., 2016), given we have implicated a poleward SHWW and concomitant decline in winter precipitation in an unprecedented late Holocene increase in woodland burning. Intensified subalpine fire will accelerate soil exposure already made

ubiquitous by proximal stressors such as weed invasion, feral horse grazing and summer tourism (Pickering et al., 2003b, Pickering et al., 2011, Worboys and Pulsford, 2013, Scanes et al., 2021, Ward-Jones, 2021). All mechanisms will sum to an intensified erosional regime, especially for the subalpine zone, which we have interpreted to have been more prone to extreme erosional events under both late Holocene climate change and European land use change.

Interpreting the ~1000 cal yr BP pulse in CHAR for Hedley lake to genuinely reflect a temporary alpine incursion of the treeline suggests that an increase in MSAT to ~15 ºC during the first warm period was sufficient for a conversion of at least the lowermost ~60 m of the alpine zone to subalpine woodland. This is concerning given summer temperatures are projected to surpass the modern MSAT range of 10–12 ºC by 3.8–4.2 ºC by 2100 CE, exceeding that achieved during the first warm period by up to 1.2 ºC (Love et al., 2019, DCCEEW, 2024b). While treeline rise to above Hedley Tarn thus appears inevitable, we note that the Hedley lake CHAR pulse postdates the apex of the first warm period by ~300 yr and its termination by <100 yr, implying centennial-scale lags in treeline advance. This is consistent with historical observations of treeline stasis due to poor dispersal capacity compounded by modern dieback and an intensified fire regime (Green, 2009, Naccarella et al., 2020, Ward-Jones, 2021). Historical and reconstructed lags in ecotonal migration thus suggest that an appreciable encroachment of the subalpine zone is unlikely this century, with Naccarella et al. (2020) arguing that lag with warming is likely to be prolonged in areas of persistent disturbance.

Near-future treeline inertia does not necessarily preclude the alpine zone from more immediate systemic change. Despite higher apparent alpine stability under late Holocene climate change and colonial land use change, the inferred critical transition during the Hedley Tarn event suggests an alpine propensity for rapid biophysical reorganisation in response to even mild perturbation. While this event occurred within the context of climatic amelioration, we still, as discussed, anticipate increased catchment erosivity under contemporary climatic deterioration. This may exaggerate the negative relationship between peatland productivity and erosion that has emerged in the alpine zone over the last millennium, as conveyed by the Hedley bog and Muellers records. This may translate to incision or burial of alpine peatlands more so than desiccation as expected for the warmer and drier subalpine zone. Indeed, increased sediment influx into and incision of alpine mires is already ubiquitous across the SM (Good et al., 2010). Regardless of

specific zonal mechanisms, alpine responses to ongoing degradation are likely to manifest at the macroscale later than for the more unstable subalpine zone, considering higher inferred alpine resilience. However, once such unconstrained thresholds are transgressed, critical transitions analogous in severity (but not necessarily direction) to the Hedley Tarn event may become more frequent and widespread, manifesting as a systemic tipping point across the alpine zone even in advance of delayed treeline encroachment.

4.7. Conclusions

Performing multiproxy analysis on a suite of peat and lake sediment records, we have reconstructed paleoenvironmental changes across the alpine-subalpine complex of the SM since ~10,600 cal yr BP, offering critical insights into systemic sensitivity to perturbation. While catchments universally appear to be more unstable under higher MA, regardless of timescale, systemic sensitivity to climate appears to vary with timescale and altitude. At the Holocene scale, rapid responses to hydroclimate (i.e., peatland initiation during postglacial amelioration, the Hedley tarn event during hypsithermal onset and declining MA during ENSO onset) implicates precipitation as the dominant forcing on systemic variability over millennial timescales. However, shorter late Holocene trends indicate a switch in sensitivity to temperature in the Common Era, with MA, systemic instability, peatland productivity and erosion all appearing to be positively impacted by warming despite long-term declines in precipitation. This supports conclusions by Bakis et al. (2025) that the late Holocene marked a threshold shift in catchment sensitivity from precipitation to temperature, which we too hypothesise relates to changing interactions between ENSO intensity and SHWW latitude permitting a warming-driven increase in snowmelt inflow into catchments.

Despite this sensitivity shift, a recognition of ENSO as the dominant mechanism for both Holocene and late Holocene climatic and systemic variability suggests alpine-subalpine catchments have been most sensitive to this climate driver over the Holocene. This is particularly true for the subalpine zone, which we have reconstructed as being more unstable with a higher propensity for dramatic and permanent changes in peatland productivity and erosion. In contrast, the alpine zone appears to have been more resilient to climate change under ENSO, a discrepancy we attribute to a more stable microclimate and lower catchment relief. ENSO appears to have also driven changes in the

configuration of these two zones themselves, with Common Era warming possibly triggering a temporary but substantial incursion of the treeline into the alpine zone. Below the treeline, however, warming is not associated with an intensification of the fire regime. Rather, subalpine burning appears to be more sensitive to latitudinal shifts in the SHWW, intensifying during periods of southward displacement and possible declines in annual and winter precipitation.

Zonal disparities also emerge during the European era, during which subalpine catchments appear to have been more sensitive to the early intensification then relaxation of colonial grazing and burning. Regardless, biophysical instability for the alpine-subalpine complex at present is unprecedented since at least ~3,700 cal yr BP and possibly longer, suggesting greater systemic sensitivity to land use change than any climatic forcing over the late Holocene. Deducing ENSO and thus MSAT to have already reverted to negative forcings on catchment MA under anthropogenic climate change, we anticipate future catchment drying that will result in – and be reinforced by – desiccation of mires. Peatland collapse, in concert with an intensified fire regime and local anthropogenic stressors, will also exacerbate and be adversely impacted by catchment runoff and erosion. While our records suggest more rapid and severe systemic changes should be anticipated for the subalpine zone, they also reveal that the alpine zone is also prone to instances of dramatic biophysical reorganisation (i.e., the Hedley Tarn event and treeline rise), albeit over long timescales, with minimal warning and with some degree of lag.

4.8. Afterword

The method in Chapter 3 has here been replicated for six bog and tarn cores from the SM alpine-subalpine complex, thereby completing the cross-altitudinal analysis endeavoured in this thesis. However, this chapter differs slightly in that it involves comparisons between these two zones prior to statistical aggregation. It also investigates climatic sensitivity at two different timescales (Holocene and late Holocene) due to uneven data coverage.

Chapter 4 concludes that, as for the highland zone, hydroclimate has been the prevailing forcing on alpine-subalpine MA and systemic variability over the Holocene, as evidenced by the Hedley Tarn event coinciding with hypsithermal onset. However, late Holocene trends reveal yet another rewetting signal commencing at ~2600 cal yr BP –

synchronous with the highland and montane zones – which is again attributed to ENSO-driven warming and increased snowmelt. As for the montane zone, concomitant biophysical changes include increased peatland productivity, erosion and burning, expressed at the macroscale as systemic destabilisation. Importantly, these changes are more pronounced for the subalpine zone, which has hosted less productive peatlands and has been more prone to systemic reorganisation and slope erosion. This is attributed to a more marginal climate and a transitional biophysical setting, reaffirming inferences from previous chapters that such environments (e.g., drier highland catchments, moorlands) are more dynamic and sensitive to climate change. This is reinforced in the context of land use change, with the subalpine zone recording more pronounced European-era erosion and systemic instability than the alpine zone.

These reconstructions substantiate existing projections that alpine-subalpine catchments will dry as snowmelt supply diminishes under GEC. In the interim, however, more rapid and punctuated runoff from warm-season snowmelt will exacerbate catchment erosion already being accelerated by amplified burning and peatland deterioration, especially in the subalpine zone. Peatlands are also likely to be impacted by erosion itself, contributing to a positive feedback that will result in many converting to carbon sources. Treeline rise is also likely to manifest under warming, though according to alpine reconstructions will probably exhibit some centennial-timescale lag.

While it is clear from this chapter that alpine-subalpine sensitivity observes both similarities and differences with that of montane and highland catchments, this has been neither qualitatively nor quantitatively resolved through direct zonal comparisons. Chapter 5 compares and synthesises zonal records in order to assess cross-altitudinal patterns in sensitivity, as well as the macroscale sensitivity of the High Country itself relative to high-altitude regions globally.

Chapter 5

Discussion

5.1. Chapter summary

This chapter discusses the findings of Chapters 2–4 to constrain the systemic sensitivity of the High Country from an interzonal, regional and global perspective. This discussion will compare the zonal records synthesised in each of the preceding chapters and, considering the conclusions of these chapters, assesses zonal disparities in sensitivity to climate and land use change (Section 5.2). It is noted that the alpine and subalpine zones are not compared here, as they have already been discretely addressed in the preceding chapter. They are hereafter acknowledged as a single 'alpine-subalpine' complex, unless stated otherwise. While BMI was not reported for the Monaro (hereafter 'highland') record in Chapter 2 due to later revision of the method, it is interpreted here for the purpose of zonal comparability. aCAR remains unreported for the Monaro as it is presumed to be a mixed signal of terrestrial and aquatic productivity and so is not useful for gauging ecological sensitivity. Similarly, CHAR for the Hedley lake record is not revisited as it has been interpreted as a combined intensity/treeline proximity signal and so should not be integrated with more confident CHAR records.

To reconstruct the paleoenvironmental variability of the High Country as a single physiographic unit, this discussion also aggregates all zonal records to synthesise a regional record of postglacial changes in MA, systemic stability, mountain peatland productivity, catchment erosion and fire (Section 5.3). This method follows that outlined in Chapters 2–4 to produce the zonal records. Qualitative and quantitative comparisons (time-series overlay, Pearson correlation and cross-correlation) between these metrics and paleoclimate and land use records for the late Holocene (i.e., ~3200–0 cal yr BP; the only period with complete multizonal temporal overlap) support confident interpretations of cross-zonal sensitivity. This chapter concludes with a review of findings relative to high-altitude environments globally, to assess the global replicability, or lack thereof, of High Country interpretations (Section 5.4).

To maximise comparability with this Australian case study, thesis findings are qualitatively reviewed against paleo-studies from temperate high-altitude analogues (comprising mountains and leeward highlands) fringing the Pacific Ocean, where ENSO is the dominant mode of interannual climatic variability (Moy et al., 2002, Conroy et al., 2008, Carré et al., 2014, Le, 2017). Specifically, this review targets mountain-highland complexes from the New Zealand South Island (Southern Alps-Central Otago), Patagonia (Southern Andes-Patagonian Plateau) and western North America (Sierra Nevada-Great

Basin). Consistent with the first knowledge gap identified in Chapter 1 (Section 1.4.1), and as will become apparent in Section 5.4, there is a lack of geoecological emphasis in the literature from these three regions, where studies are disproportionately represented by palynological and charcoal records.

Excluding CHAR and aCAR, which are widely quantified, data presented in this thesis are limited in their comparability with this trans-Pacific corpus of proxy data, given the systemic scope of the study's methodology. This is potentially problematic given preceding chapters have demonstrated that paleoecological and systemic responses to perturbation can diverge on sub-centennial timescales (e.g., an absence of floristic reorganisation during the hypsithermal onset events). However, there is also evidence that paleoecological and systemic behaviour is more harmonic on longer timescales (e.g., the *Pomaderris* interval aligning with high hypsithermal MA). As such, and acknowledging this caveat, the global literature is still useful for comparing long-term environmental sensitivity between high-altitude environments at a superficial level.

5.2. Resolving zonal sensitivity across the High Country

5.2.1. Zonal disparities in sensitivity to Holocene climate change

Due to inconsistencies in zonal record timespans (Fig. 5.1), robust comparisons of Holocene-timescale sensitivity to climate are only possible between the highland and alpine-subalpine records for most metrics, including MA (Fig. 5.1a). While highland MA indicates wetting until ~6100 cal yr BP, postdating the apex of the hypsithermal by ~1600 yr, alpine-subalpine MA peaks much earlier at ~9100 cal yr BP. Alpine-subalpine MA conveys relatively persistent drying from ~8500 cal yr BP, aligning approximately with hypsithermal onset (De Deckker, 2022). In Chapter 2 (Section 2.6.2) it is posited that the early-middle Holocene highland pattern may reflect a genuine hydrological lag with hydroclimate, perhaps due to greater sensitivity of the impermeable lake catchments to climatic variability than annual precipitation, which were respectively suppressed and elevated during the hypsithermal (Leonard et al., 2016, Chen et al., 2019, De Deckker, 2022).

In contrast, the early MA peak in the alpine-subalpine record has been equated in Chapter 3 to systemic reorganisation during the Hedley Tarn event (Section 4.6.2.1) rather

than an actual pulse in MA. This was affirmed by the spike in alpine-subalpine RoC from ~9200–8600 cal yr BP indicating dramatic destabilisation (Fig. 5.1b). These mountain-highland divergences imply large differences in hydrological sensitivity to hydroclimate. While the highland lag indicates low sensitivity to early-middle Holocene hydroclimate, the coincidence of the Hedley Tarn event with hypsithermal onset suggests alpine-subalpine catchments are not only more hydrologically responsive to hydroclimatic change but are predisposed to destabilisation under such. This disparity is attributable to differences in both geomorphology and climate, which Chapter 1 establishes as the two main criteria distinguishing mountains and highlands (Section 1.2.1). Specifically, in addition to preferential highland sensitivity to rainfall variability, the low relief of the Monaro generates strongly transport-limited conditions that are inconducive to spikes in sedimentation such as that which defines the Hedley Tarn event, which occurred downstream of a supply-limited cirque.

Indeed, while Chapter 4 concludes alpine catchments to be less prone to slope instability than subalpine catchments (Section 4.6.1.2), higher local relief, a more mesic climate and snowpack contributions to runoff mean the alpine zone is still more geomorphically unstable than the Monaro. This is supported by early-middle Holocene BMI (Fig. 5.1d), which is lower and more stable for the highland than alpine-subalpine record, implying no major erosional disturbances on the Monaro for most of the postglacial period. However, excluding the Hedley Tarn event, median BMI for both records is comparable until the late Holocene, suggesting that, while the alpine-subalpine complex experienced a more unstable erosional regime over most of the Holocene, sediment yield was ultimately equivalent to the Monaro. This is again attributed to transport-limited conditions in both terrains relative to the interjacent montane zone, which occupies the steepest segment of the altitudinal transect and has presumably exhibited more extreme erosional events over the postglacial period. While this is supported by dramatically elevated BMI preceding peatland initiation at Delaneys Creek (‘the Delaneys Creek event’), the montane record is of insufficient length to confirm this hypothesis at the Holocene scale.

Although the Hedley Tarn event validates higher alpine-subalpine sensitivity to hydroclimate than the highland zone in an erosional context, it must be recalled this event was also marked by paludification of Hedley bog, partially due to deltaic progradation under elevated sedimentation itself (Fig. 4.3; Section 4.6.3.2). This is clear from the

coeval alpine-subalpine pulse in aCAR (Fig. 5.1c), for which highland data is not presented given the absence of peatlands in the catchments of the five sampled Monaro lakes. This absence is emblematic of a broader dearth of peatlands across the Monaro save for its escarpment and montane ecotonal peripheries, which represent mesic refugia for mires in a semi-arid landscape (NSW TSSC, 2004, Hope et al., 2012). Instead, Monaro catchments were dominated by Temperate Grassland, which is more resilient to and can even proliferate under drying (Costin, 1954, Department of the Environment and Energy, 2016).

This is supported by reconstructed grassland expansion across the driest Maffra Lake catchment during late Holocene drying (Section 2.6.1.4). Low catchment MA on the Monaro also accelerates the post-depositional decomposition of any terrestrial OM due to soil desiccation and frequent grassfire (Marchin et al., 2018). As such, not only is ecosystem productivity on the Monaro presumably less responsive to wetting than in mountain peatlands, but any responses are likely to be removed from or muted in the sedimentary record. This is supported by the low signal/noise ratio of the C/N-$\delta^{13}C$ trajectory for Maffra Lake (Fig. 2.6), from which possible grassland expansion was inferred. Notwithstanding preservation effects, the highland domain can therefore be considered to be less sensitive to hydroclimate than the mountain domain in terms of productivity as well as erosion, possibly explaining both the lack of any highland MA pulse at hypsithermal onset and MA lagging peak Holocene hydroclimatic intensity.

However, lower highland sensitivity to hydroclimate does not necessarily preclude all components of highland catchments from destabilisation under changes in such. Indeed, the highland RoC record reveals a precipitous early Holocene pulse indicating biophysical reorganisation (Fig. 5.1b). As detailed in Chapter 2 (Section 2.6.1.5), this pulse is inherited from a cluster of Mn/Fe spikes from Racecourse Lake reflecting oscillations between lakebed exposure and inundation, precursory to a critical transition from an ephemeral to intermittent lake ('the Racecourse Lake event'). Contemporaneity between these oxidation spikes and high ecological volatility inferred from the C/N-$\delta^{13}C$ trajectory (Fig. 2.6) were inferred to be symptomatic of biogeochemical 'flickering' prior to an upgrading of lake permanence (Section 2.6.3). Crucially, the corresponding RoC pulse spans from ~9400–9100 cal yr BP, overlapping substantially with the Hedley Tarn event. Although the Racecourse Lake and Hedley Tarn events are mechanistically incomparable, hypsithermal onset has been implicated in both.

Given Racecourse Lake and Hedley Tarn respectively bracket the lower and upper limits of the altitudinal transect, coevality in their RoC maxima suggests that hypsithermal onset induced a period of major systemic disequilibrium across the High Country. Specifically, it is argued that hydroclimatic transgression of some positive MA threshold induced dramatic change for both endorheic and exorheic basins between ~9400–9000 cal yr BP. This implies lake-hosting catchments were more sensitive to wetting associated with the hypsithermal than with deglaciation, though of course the former is a continuation of the latter and so destabilisation may actually be a lagged response to amelioration (Kaufman et al., 2020, Clerke, 2023). Indeed, the Pleistocene portion of the highland RoC record indicates high systemic instability argued to reflect systemic equilibration with climate change. Similarly, the Hedley lake record indicates several major biophysical events preceding the Hedley Tarn event, including increased fluvial erosivity and later peatland establishment at 10,624 (95% confidence interval 9005–10,999) cal yr BP, the latter falling within the ~11,000–8000 yr BP basal age range of independent peat sequences (Hope et al., 2009b, Hope et al., 2012).

Generalising from the above catchment-specific observations, it might be argued that the High Country was already unstable even prior to the hypsithermal, which may have simply represented a tipping point for lake catchments. That said, pre-peak instability is only apparent for the highland RoC record, with the alpine-subalpine record instead showing very low values prior to the Hedley Tarn event. This suggests increased fluvial energy and peatland colonisation were not systemic events. This absence of pre-event instability for alpine-subalpine record results in its relative RoC increase from pre-peak to peak values being 4.3 times higher than for the highland record. This implies more appreciable perturbation to the alpine-subalpine complex than the Monaro, reaffirming greater alpine-subalpine sensitivity to hydroclimate.

Chapters 2 (Section 2.6.1.5) and 4 (Section 4.6.1.1) also articulate that the Racecourse Lake and Hedley Tarn events are succeeded by permanent state shifts – sudden transitions to an intermittent lake and a higher yield/ombrotrophic regime, respectively – conveying stabilisation of both systems in new basins of attraction. Stabilisation is quantitatively confirmed for the highland record by the post-peak decline in RoC culminating in a minimum at ~6200 cal yr BP. While post-peak alpine-subalpine RoC does not achieve a minimum, values also decline precipitously relative to the Hedley Tarn event. These trends indicate relative stability across the High Country during the hypsithermal but,

more importantly, that the first two to three millennia succeeding these state shifts were characterised by high stability and systemic resilience to ongoing amelioration.

Post-shift resilience may explain the artefactual hypsithermal-era drying trend in the alpine-subalpine MA record and the lagged MA peak in the highland record. However, although the highland record conveys lower post-peak RoC than the alpine-subalpine record, it also does not achieve minimum RoC until ~300 yr after its peak, in contrast to ~200 yr for the alpine-subalpine record. This indicates that, while systemic reorganisation achieved greater stability in the highland domain, the alpine-subalpine complex restabilised more rapidly. It is therefore inferred that highlands require much longer to restabilise but become more stable once a new equilibrium is achieved.

Mountain-highland disparities in hydrological sensitivity to hydroclimate reemerge during post-hypsithermal ENSO intensification. Specifically, rapid drying in the highland MA record does not commence until ~3500 cal yr BP, which marks the end of the ~1000 yr window within which ENSO onset is usually identified in independent High Country records. Conversely, rapid alpine-subalpine drying initiates at ~4500 cal yr BP, at the start of this window. This reaffirms that alpine-subalpine hydrology was more responsive to hydroclimatic change. However, this mountain-highland lead-lag relationship deteriorates in the late Holocene, during which time the alpine-subalpine, montane and highland MA records indicate synchronous hydrological recovery from ~2600 cal yr BP. While different zonal mechanisms have been proposed for late Holocene rewetting – namely warming-driven increases in snowmelt in the mountain zones and upgraded lake permanence in the highland domain – all are ascribed to ENSO intensification.

Remarkable contemporaneity of rewetting across the entire altitudinal transect suggests that ~2600 cal yr BP marks the time when hydroclimatic variability had sufficiently amplified to offset the effects of declining precipitation, enabling ENSO to switch from a negative to positive MA forcing across the High Country regardless of zonal mechanisms. Alongside this universal MA inflection, the late Holocene is also characterised by gradual increases in RoC for all three zones commencing between ~2500–2000 cal yr BP, alongside incipient rewetting. While montane destabilisation cannot be evaluated in a Holocene context, median RoC for the precolonial late Holocene in the alpine-subalpine and highland zones is respectively 72% and 36% higher than their overlapping pre-late Holocene medians. Although this suggests greater late Holocene

instability for both the SM and Monaro, it also conveys a more dramatic departure from the Holocene baseline for the former than the latter.

Implicating ENSO intensification in late Holocene destabilisation, as in rewetting, this implies greater mountain than highland sensitivity its amplification. A larger relative increase in alpine-subalpine RoC is resonant of the same behaviour during hypsithermal onset, suggesting alpine-subalpine catchments have consistently been more prone to climatogenic destabilisation than highland catchments over the Holocene. Importantly, however, the overlapping precolonial Holocene durations of the alpine-subalpine and highland record reveal the latter to have a median RoC 177% higher than the former. This indicates that highland catchments have been more unstable than mountain catchments over the Holocene, despite being less perturbed by hypsithermal and ENSO onset. However, such a generalisation requires further validation, given it does not account for the montane zone, which is most spatially representative of the mountain environment (Section 3.3) and is clearly susceptible to systemic reorganisation (see the Delaneys Creek event).

Holocene-median trends in MA and RoC reveal both metrics to be weakly positively and even more weakly and negatively correlated for the alpine-subalpine and highland zones, respectively (Fig. 5.2). It is therefore interpreted that Holocene alpine-subalpine instability has not only been more strongly prescribed by MA but is also more likely under wetting, while highland instability is more independent of MA but tends to be associated with drying, as demonstrated in Chapters 2 (Section 2.6.3) and 4 (Section 4.6.2). Reviewing magnitudes of change, it is apparent that elevated RoC over the Common Era is being partly driven by rapid deviations in aCAR, BMI and CHAR (Fig. 5.1c–e). Increases in aCAR have been interpreted to reflect improved peatland productivity due to snowmelt inflow across all mountain zones. Late Holocene increases are also observed for the mountain BMI records, reinforcing snowmelt runoff as a contributor to increased erosion.

Interestingly, an increase is also apparent for the highland record, though this cannot be attributed to snowmelt given the lack of seasonal snow cover on the Monaro and the endorheic drainage of lake catchments. However, the contemporaneity of the highland BMI increase with those in the mountain records does appear to also implicate ENSO. Notwithstanding single-record bias for the earlier portion of the record, the highland BMI peak is highest for the entire postglacial period, which might suggest an unprecedented

increase in sedimentation. Finally, the late Holocene is also characterised by increases in alpine-subalpine, montane and highland CHAR, translating to a universal intensification of burning across the High Country over the last two to three millennia. As for BMI, albeit again with single-record bias, late Holocene highland CHAR is unparalleled for the postglacial period, potentially indicating an unprecedented intensification of burning on the Monaro as a result of ENSO intensification.

5.2.2. Zonal disparities in sensitivity to late Holocene climate change

As identified above, late Holocene hydrological recovery on the High Country is coeval across the altitudinal transect, though subsequent MA patterns diverge between records, indicating disparities in hydrological sensitivity to centennial-scale climate change. Specifically, highland rewetting culminates in peak late Holocene MA at ~1200 cal yr BP, much earlier than the montane and alpine-subalpine zones, whose MA maxima are more temporally aligned at ~600 and ~500 cal yr BP, respectively (Fig. 5.1a). Chapter 2 concludes from the C/N-δ^{13}C trajectories (Fig. 2.6) that the Monaro lakes experienced hydrological stabilisation during the Common Era following upgraded permanence. As such, plateauing of highland MA from ~2000 cal yr BP probably does reflect genuine hydrological stabilisation and suggests further post-permanence lake inundation was negligible until peak MA. It can therefore be inferred that MA not only peaked up to ~700 yr earlier on the Monaro but also stabilised up to ~1500 yr before the SM peak.

As intimated above, earlier plateauing of highland MA is ascribed to hysteretic limnology, which results in fundamental differences in the mechanisms and ENSO sensitivity of claypan versus peatland hydrology. While the preceding subsection deduces ENSO to be the dominant forcing on both late Holocene drying and rewetting across the

Figure 5.1. (next page) Stacked time-series overlay of zonal metric records, and corresponding violin plots for the precolonial late Holocene (3200–200 cal yr BP). Darkest, medium and lightest time-series records and violin plots correspond to the highland, montane and alpine-subalpine (ASA) records, respectively. Alpine-subalpine aCAR data for >3500 cal yr BP (dotted segment) is derived solely from the Hedley lake record. Shaded time intervals correspond to relevant paleoclimatic intervals, these being postglacial amelioration (PA), the Holocene Hypsithermal (HH), onset of ENSO intensification (EO), and the first and second warm periods (W1 and W2). Dashed vertical line across time-series stack corresponds to the timing of European colonisation of the High Country (1820 CE; 130 cal yr BP). Dotted lines and crosses on violin plots respectively denote the range and median of European-era values.

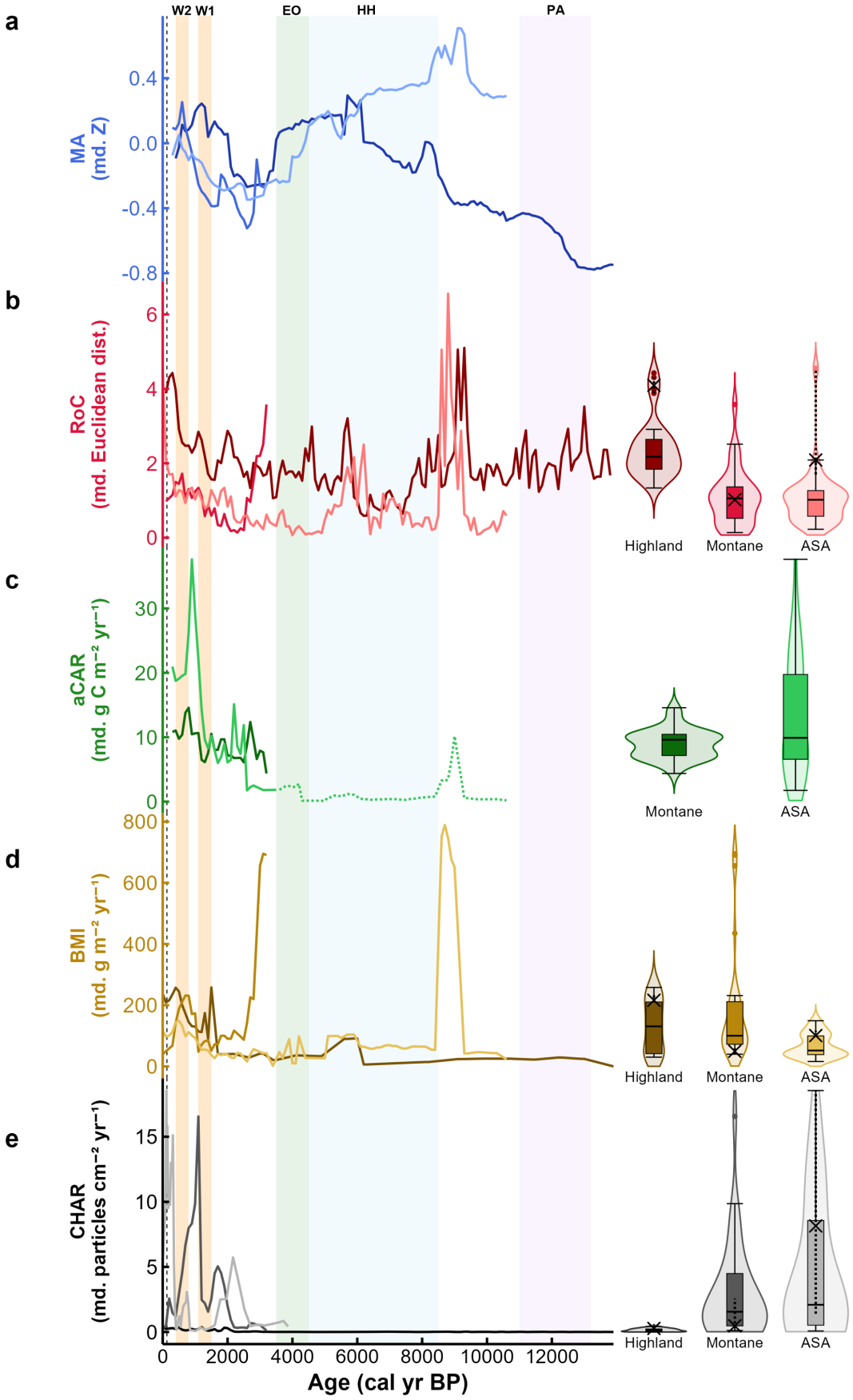
a
b
c
d
e
W2
W1
EO
HH
PA
MA (md. Z)
0.4
0.0
-0.4
-0.8
RoC (md. Euclidean dist.)
6
4
2
0
aCAR (md. g C m⁻² yr⁻¹)
30
20
10
0
BMI (md. g m⁻² yr⁻¹)
800
600
400
200
0
CHAR (md. particles cm⁻² yr⁻¹)
15
10
5
0
Highland
Montane
ASA
0
2000
4000
6000
8000
10000
12000
Age (cal yr BP)

High Country, Chapter 2 concludes that highland rewetting reflects reduced hydrological recovery times of the Monaro lakes under longer, more frequent and more intense La Niña phases. In contrast, Chapters 3 and 4 ascribe mountain rewetting to elevated snowmelt inflow as a result of ENSO-related warming. In view of these contrasting mechanisms, the earlier peak in highland MA may not reflect any lag in mountain hydrology, but simply a mountain-highland dichotomy in hydrological sensitivity to different expressions of ENSO. Indeed, increased multiyear La Niña frequency is reconstructed by Lu et al. (2025) to have commenced from as early as ~7000 cal yr BP with a moderate acceleration between ~4000–3000 cal yr BP, synchronous with ENSO intensification more broadly. In contrast, ENSO-related warming is only pronounced between ~1500–400 cal yr BP (Thomas et al., 2022), overlapping with peak alpine-subalpine and montane MA and postdating highland MA stabilisation by ~500 yr. The timing of intensified multiyear La Niña and warming are respectively more consistent with mountain and highland rewetting and therefore explain the temporal offset in peak MA between both domains.

Mountain rewetting is also much more gradual than highland rewetting. This does not necessarily undermine the previous Holocene-timescale inference that SM catchments were more hydrologically sensitive to climate, but rather reinforces it, given mountain rewetting is actually coincident with incipient warming in the Club Lake record. In contrast, while highland rewetting is coeval with and more rapid than mountain rewetting, it still lags the acceleration in multiyear La Niña frequency by at least ~600 yr. This reaffirms highland catchments as being less hydrologically responsive to climate, despite average postglacial lag with climate being 0 yr (Fig. 2.5), which is proposed to reflect lead and lags cancelling out at the record scale.

Rapid but lagged highland rewetting probably reflects an abrupt but delayed critical transition in response to the transgression of an MA threshold, specifically the sudden increases in permanence for several lakes (i.e., Lake Jillamatong and Racecourse Lake). This is consistent with the lake hysteresis model proposed in Chapter 2, which would also reconcile stabilisation for the ~800 yr after rewetting, despite ongoing increases in multiyear La Niña frequency. Specifically, the model posits that the Monaro lakes were more hydrologically insensitive to continued wetting after their critical transitions, which explains prolonged MA stability until its peak. Post-shift hydrological resilience is not relevant to SM catchments (which lack claypan hydrogeomorphology), resolving the

absence of MA plateauing for the montane and alpine-subalpine records prior to their late Holocene maxima.

While the previous subsection identifies the late Holocene to be a period of elevated systemic instability across the High Country, more acute statistical interrogation reveals spatiotemporal disparities in destabilisation. Although the Delaneys Creek event inflates late Holocene RoC for the montane zone such that its precolonial median is 14% higher than that of the alpine-subalpine record, highland RoC is still 106% higher than even the montane zone (Fig. 5.1b). This suggests an exponential increase in systemic instability downslope, with the Monaro being more persistently unstable than SM catchments under an ENSO-dominated climatic regime. This is not to dismiss the significance of the Delaneys Creek event, which results in the montane record having the only precolonial upper outlier of all three records. It is thus proposed that montane catchments have been the most prone to systemic reorganisation over the late Holocene due to delayed peatland initiation (Section 3.6.2.1). However, this interpretation relies on Delaneys Creek being representative of montane catchments.

The regional typicality of Delaneys Creek is indeed supported by maximum ages of the closest independent montane peat records (i.e., Giandarra Bog, Wilsons Valley and Brooks Ridge Fen), which all date to the late Holocene (Thomas, 1991, Mooney et al., 1997, Martin, 1999). This suggests a late Holocene pulse in mire establishment across the lower montane zone, much later than alpine-subalpine and high-montane systems, which all indicate genesis during postglacial amelioration (Hope et al., 2009b, Hope et al., 2012). Delayed lower montane establishment is presumably due to higher temperatures and lower MA. These constraints likely rendered frost hollows such as the that hosting Delaneys Creek only hospitable for mires in the late Holocene, by which time sufficient neoglacial cooling and streamflow declines had occurred to permit colonisation of valley floors (Donders et al., 2007, Kemp and Hope, 2014, Barr et al., 2019). The Delaneys Creek event can therefore be confidently inferred to reflect abrupt systemic reorganisation for at least the lower montane zone, despite the highland zone being more consistently unstable over the late Holocene.

Reviewing the relationship between MA and RoC reveals these variables to be positively correlated for all three zones over the precolonial late Holocene, albeit strongly for only the alpine-subalpine complex and weakly for the montane and highland zones (Fig. 5.2). This implies that, under ENSO, high-altitude catchments are more unstable

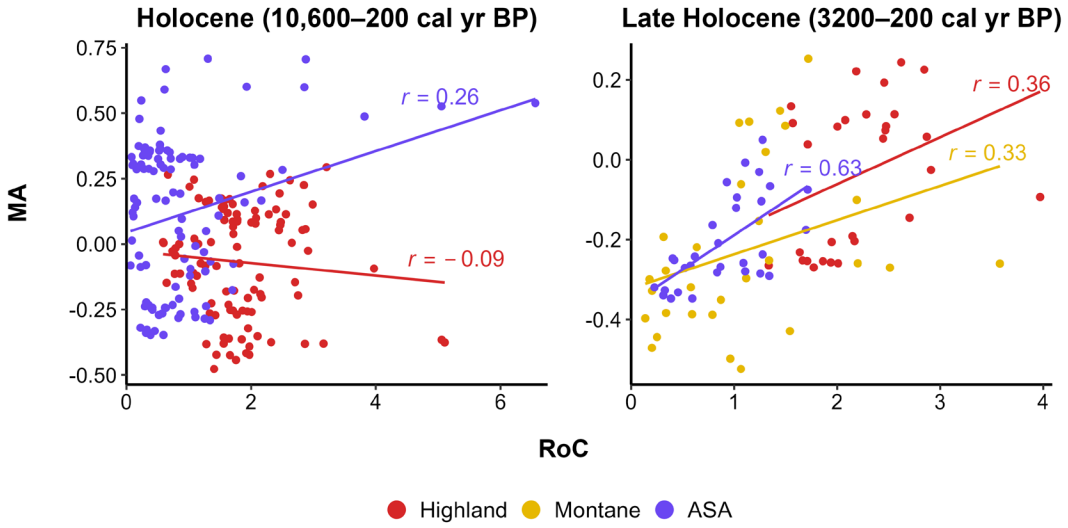

Figure 5.2. MA-RoC scatterplots for the overlapping precolonial Holocene (left) and late Holocene (right) periods of each zonal record.

under wetting, though instability only increases somewhat linearly with MA for the alpine-subalpine complex. A weaker montane correlation is again probably due to the occurrence of the Delaneys Creek event. As such, it does not actually indicate lower sensitivity to MA but rather the opposite, with high but declining MA in fact triggering this event. While state shifts may also be weakening the MA-RoC correlation in the highland record, evidence suggests this could only be introduced by increased lake permanence at ~2000 cal yr BP, which does not manifest clearly in site RoC records due to this being a lake- rather than catchment-scale event. More likely is that this weak highland relationship genuinely reflects low systemic sensitivity to MA, due to competing factors described in Chapter 2 (Section 2.6.3).

Another factor possibly contributing to late Holocene MA-RoC decoupling in the highland and montane zones is occupation by the Ngarigo and neighbouring peoples, whose populations became larger and more sedentary across southeastern Australia after ~5000–3000 yr BP (Black et al., 2007, Johnson and Brook, 2011, Portenga et al., 2016a). A concomitant intensification of land use – namely high-frequency, low-intensity burning – in the more accessible montane and highland zones is almost certainly influencing the RoC data and may be artefactually weakening apparent systemic coupling with MA. However, it is not feasible to quantify the proportional contribution of Indigenous practices to reconstructed RoC trends given the lack of targeted interrogation of such in this study. It should also be recalled that late Holocene vegetation and fire changes have

widely been ascribed to climate (specifically, ENSO) more so than land use, due to the environment purportedly having achieved equilibrium with the latter by this time (Shulmeister, 1999, Dodson and Mooney, 2002, Black et al., 2007).

In contrast to the highland and montane zones, the alpine-subalpine complex a) is dominated by processes more inextricable from MA (e.g., snowpack formation, gelifluction, frost weathering, peatland formation) (Costin, 2000, Wilson et al., 2022), and b) has experienced a briefer period of less intensive/continuous human occupation over the Holocene (Dodson et al., 1994, Zylstra, 2006). It is therefore reasonable to propose that alpine-subalpine biophysical processes have more tightly covaried with late Holocene MA changes, which have been relatively low in magnitude even considering snowmelt surpluses (Stromsoe et al., 2018). This explains the alpine-subalpine complex having the strongest MA-RoC correlation and lowest median RoC of all records for the late Holocene. Stronger MA-RoC coupling replicates what has been observed at the Holocene scale, suggesting alpine-subalpine stability has been more proportional to MA than downslope over almost the entire Holocene. This is reaffirmed by the more rapid, stepped increase in alpine-subalpine RoC upon rewetting than in the highland record, which conversely remains high but invariable.

Despite the lower apparent sensitivity of the Monaro to MA on both Holocene and late Holocene timescales, the late Holocene MA-RoC correlation for the highland record diverges from the Holocene in that it becomes positive. This conveys that the Monaro has behaved more similarly to the SM over the late Holocene in that it has converted to a system that is more unstable under elevated MA, in contrast to earlier behaviour (e.g., maximum stability during the hypsithermal). As such, while the Monaro did not destabilise during ENSO onset, ongoing ENSO intensification may be responsible for a reversal of highland sensitivity to MA, reasons for which are unclear. Importantly, the late Holocene is also characterised by a strengthening of the MA-RoC correlation relative to the Holocene median for both the highland and alpine-subalpine records. These strengthened correlations imply that the development of a modern climatic regime also resulted in increased systemic sensitivity to MA, despite the emergence of potentially weakening variables (e.g., intensified land use).

Deconstructing zonal records into aCAR, BMI and CHAR (Fig. 5.1c–e), reasons for the late Holocene increase in RoC for all zones become clear. While both alpine-subalpine and montane aCAR corroborate a late Holocene increase in SM peatland productivity, the

former does not increase until ~2500 cal yr BP. In fact, alpine-subalpine aCAR is low and stable between ~3500–2500 cal yr BP, indicating no pronounced peatland response to ENSO as a negative MA forcing but a rapid response to it as a positive forcing, within ~100 yr of rewetting. In contrast, the emergence of peat at ~3000 cal yr BP in the Delaneys Creek record indicates a montane peatland response to ENSO ~500 yr prior to the alpine-subalpine complex. However, it must be recalled that peatland initiation at Delaneys Creek was a product of declining rather than increasing MA, consistent with ENSO still being a negative MA forcing during this time. Indeed, montane aCAR does not increase until ~1900 cal yr BP, suggesting this marks the actual time when ENSO positively impacted montane peatlands. This increase postdates that for alpine-subalpine peatlands by ~600 yr, indicating that, while the montane zone responded earlier to ENSO as a negative MA forcing, it responded much later to it as a positive forcing.

Attributing increased productivity to elevated snowmelt, the lagged montane response may reflect lower snowmelt discharge into a zone where inflow would also presumably need to be even higher to offset more marginal conditions for peat growth. In comparison, a more optimal alpine-subalpine climate and acute exposure to snowmelt constitute reasonable factors by which a more rapid alpine-subalpine increase in productivity would occur under rewetting. Despite this montane lag, an earlier montane response to ENSO overall is consistent with interpretations from Chapters 3 and 4 that moisture-limited systems (moors and subalpine bogs, respectively) are more sensitive to hydrological change than those in more favourable settings (fens and alpine bogs, respectively). This explains the Delaneys Creek event occurring at a time when alpine-subalpine aCAR is unresponsive, given the sampled alpine-subalpine peatlands probably established much earlier (likely following deglaciation, according to the Hedley lake and independent records) and are thus less topogenous due to greater vertical accretion (Hughes, 2000). Additionally, a more mesic alpine-subalpine climate may have been sufficient to buffer ENSO-related drying, keeping peatlands active but unproductive until rewetting.

In fact, alpine-subalpine aCAR is even lower than montane aCAR prior to rewetting, having a pre-rewetting median of only ~1.8 g m^{-2} yr^{-1}. Such values are not reconstructed for high-altitude or even low-altitude peatlands globally, at neither Holocene nor recent timescales (Loisel et al., 2014, Gaffney et al., 2025). It is therefore argued that, while alpine-subalpine conditions prevented total mire deterioration under low MA, drying was still sufficient to severely desiccate peatlands such that they were almost certainly carbon

sources until ENSO switched to a positive forcing. As mentioned, declining MA during this time instead positively impacted montane peatlands by reducing fluvial erosivity while simultaneously providing saturated conditions, such that peatlands remained carbon sinks from genesis. This explains montane aCAR exceeding alpine-subalpine aCAR for several millennia until rewetting had fully manifested. Regardless of the forcing status of ENSO and greater montane sensitivity to such, it can be confidently concluded that ENSO impacted all SM peatlands from at least ~3500–3000 cal yr BP but did not enhance productivity until ~2500–1900 cal yr BP.

Supporting the warming-snowmelt hypothesis, aCAR for both zones spikes during the pronounced warm periods reconstructed by Thomas et al. (2022), when inflow was presumably highest. However, consistent with a lagged initial increase, montane aCAR peaks at ~800 cal yr BP, ~100 yr later than peak alpine-subalpine aCAR, which is also 158% higher. This reinforces that more optimal alpine-subalpine conditions resulted in stronger, more abrupt increases than in marginal, distal montane peatlands. Higher alpine-subalpine sensitivity to snowmelt proven for a final time during the post-peak aCAR decline, which is far more dramatic for alpine-subalpine than montane peatlands. This reaffirms higher alpine-subalpine dependency on snowmelt for growth, though much higher post-peak alpine-subalpine values convey more favourable conditions persisted even after snowmelt inflow diminished.

While both records are similar in that post-peak aCAR remains higher than pre-peak aCAR, this is unlikely to represent a permanent state shift in growth form (i.e., ombrotrophication) for most systems given all are currently topogenous except for Betts Creek. That said, higher post-peak values may reflect reduced dependency on (but not total isolation from) groundwater following rapid accretion. Zonal similarity is also observed in late Holocene aCAR medians, which are essentially equal despite much larger Common Era increases for alpine-subalpine peatlands. This is due to lower alpine-subalpine than montane aCAR until ~2500 cal yr BP and higher alpine-subalpine aCAR thereafter effectively cancelling out, implying comparable productivity across the SM when centennial-scale fluctuations are ignored. Although post-peak alpine-subalpine aCAR is within the typical range of high-altitude peatlands globally, montane aCAR oscillates at the minimum end of this range (Gaffney et al., 2025), conveying that even increased snowmelt was insufficient for montane peatlands to become productive. In fact, median late Holocene aCAR for both zones is outside the typical global range (Gaffney

et al., 2025), indicating that SM peatlands have been very weakly productive and thus poor carbon sinks at least under an ENSO-dominated climate.

As intimated previously, the late Holocene is also defined by increased clastic sedimentation across the altitudinal transect. Excluding the extreme BMI values associated with the Delaneys Creek event (which represent all montane upper outliers), the BMI profiles for the montane and alpine-subalpine records are most similar, respectively peaking at ~700 and ~500 cal yr BP. The coevality of these peaks, which coincide with the second warm period, is unsurprising given increased erosion across the SM has been attributed in Chapters 3 and 4 to snowmelt additions to streamflow and runoff. Importantly, however, peak montane BMI exceeds peak alpine-subalpine BMI by 55%, suggesting that the erosional impact of snowmelt was more significant for the montane zone despite it being less influential on montane productivity. The most realistic explanation for this apparent contradiction is the montane zone having greater local relief as well as an unusually thick soil mantle (Mason and Williams, 2013b, Wilson et al., 2022), which together render slopes more unstable.

This represents a downslope continuation of conclusions made in Chapter 4 for the subalpine zone, which was determined to be more prone to extreme erosional events over the late Holocene than the lower-relief alpine zone (Section 4.6.2.2). However, Chapter 4 also finds that total sediment yield was higher in the alpine zone (Fig. 4.5), again perhaps due to lower relief. As such, while slope instability more likely in the steeper subalpine and montane zones, yield is higher in the alpine and montane zone due to low relief and deep soils, respectively. These factors translate to higher slope instability in the lower two mountain zones due to higher relief but lowest yield in the supply-limited subalpine zone, where soils are thin. The satisfaction of both criteria (high relief and deep soils) explains the montane zone having much higher median late Holocene BMI than the alpine-subalpine complex, as well as a wider BMI distribution owing to the Delaneys Creek event. Interestingly, both the alpine-subalpine and montane records are similar in that their BMI peaks postdate their aCAR peaks by 200–300 yr, indicating centennial-scale lags in erosional responses to snowmelt runoff, relative to peatlands.

A synthesis of Northern Hemisphere pollen records by Williams et al. (2002) shows that initial vegetation responses to climate for all groups (trees, shrubs, herbs and mosses) occur within <100 yr, with a median and maximum response time of 60 yr and <200 yr, respectively. Sub-centennial response times are consistent with observations here that

alpine-subalpine mire productivity increased within ~100 yr of rewetting. Moreover, the observation by Williams et al. (2002) of consistent lag across mire and terrestrial groups means alpine-subalpine mire response times might be considered somewhat indicative of that of proximal groundcover. As such, the more immediate response of peatlands to rewetting relative to erosion may reflect higher responsivity of groundcover more generally. Increased vegetation coverage for both mires and slopes is a known mechanism by which erosion is offset on centennial timescales (Shuttleworth et al., 2015, Francke et al., 2019). However, the later increase in BMI suggests that this buffering mechanism eventually deteriorates as runoff exceeds the capacity for vegetation to entrain loose regolith. Nonetheless, the data presented here imply that the moderating effect of vegetation cover is effective for several centuries.

While highland BMI also increases during the Common Era, this manifests as two pulses peaking at ~1500 and ~400 cal yr BP, bracketing the warm periods with a trough spanning the warm periods themselves. This mismatch is unsurprising given snowmelt cannot have contributed to Monaro lake catchment erosion. The BMI pulse from ~1500 cal yr BP is instead more temporally coherent with the upgraded permanence of lakes – namely Lake Jillamatong and Racecourse Lake – between ~2000–1500 cal yr BP, with all basins being permanent or upgraded by at least ~1100 cal yr BP. In view of this overlap with the BMI pulse, it is plausible that upgraded permanence resulted in more extensive lake transgression. Lake-level rise would have remobilised exposed, loosely consolidated strandline soils and, in larger lakes with wind/wave action and granitic and sedimentary bedrock (e.g., Black Lake and Lake Jillamatong), fine littoral sands (Fig. 1.16). Redeposition of margin sediments in depositional loci would have translated to increased, albeit autochthonous, detrital influx.

Lake margin reworking is likely to have been the dominant agent of lake sedimentation given extremely low catchment relief, dense grass coverage above the strandline and the paucity of perennial or even ephemeral drainage lines, which together limit erosion via runoff or streamflow. Lake-level driven re-entrainment and -deposition of shoreline sediments is a common feature across many seasonal lakes in semi-arid regions analogous to the Monaro, such as the Kenyan Rift Valley (Renaut and Owen, 2023). Importantly, this mechanism would not rework sediments cored from the depocenter, given this would be the site of most persistent inundation, especially post-permanence. This hypothesis implies that lacustrine sediment reworking was a far more effective driver of

sedimentation than snowmelt runoff in the SM, given the highland record possesses the highest peak and median precolonial late Holocene BMI of all three records. Of course, the highland record must realistically incorporate some lesser allochthonous component, which may have been contributed by fire given synchroneity between the first BMI and CHAR pulses.

Indeed, the highland CHAR record divulges a 33-fold increase between ~2300–1900 cal yr BP, slightly preceding the increase in BMI and thus communicating an intensification of fire followed by erosion. Taking increased CHAR to reflect intensified burning of Grassy Woodland (rather than Temperate Grassland), it is reasonable to postulate that more frequent/intense burning resulted in a decline of the grassy understorey but not the canopy, simply due to a lack of woody protection (Dzwonko et al., 2018). A sustained canopy is supported by CHAR being consistently high to present, which confirms a persistence (i.e., survival or at least rapid regeneration) of woody but not necessarily herbaceous fuel loads. A fire-driven sparsening of the ground stratum would have translated to more exposed and hydrophobic topsoils susceptible to erosion (Doerr et al., 2006) The minor lag between the CHAR and BMI pulses perhaps reflects slow creep of these eroded soils into lake basins given low relief. Despite the massive Common Era intensification of woodland burning, median late Holocene highland CHAR is still extremely low relative to montane and subalpine values, which also display much larger ranges of variability. Expectedly, this conveys that late Holocene burning was far more frequent/intense for the sub-treeline SM than the Monaro, presumably due to more abundant fuel loads (Fraser et al., 2016).

The earliest surges in montane and subalpine CHAR well exceed the earliest highland surge and also bracket it, occurring at ~1700 and ~2200 cal yr BP, respectively. General coevality between all surges is particularly curious when it is recalled that highland burning was a response to higher MA cyclicity under ENSO (increasing biomass), while mountain burning was a more direct response to ENSO-driven warming and SHWW-driven precipitation declines (desiccating biomass). However, ENSO as a common factor to both mechanisms suggests that it was sufficiently amplified by ~2000 cal yr BP to trigger a precipitous intensification of burning across the High Country. This timing for an ENSO response postdates those identified for MA and aCAR but predates that for SMI BMI, indicating vegetation responses to MA both precede and trigger pyrological responses, which, in turn, precede and trigger erosion.

Following their initial pulses, both montane and subalpine CHAR decline again only to experience unprecedented increases at the end of the first and second warm periods, respectively. These second spikes have thus been related to warming but especially to a coeval poleward migration of the SHWW (Section 3.6.2.1; 4.6.2.2), with elevated but invariable highland CHAR during this time indicating that the Monaro remained more sensitive to ENSO. This is perhaps attributable to its rain-shadow emplacement; orographic interception of the SHWW may have muted the impact of reduced frontal activity on highland precipitation during this time. As such, the highland fire regime may have been more sensitive to less obstructed maritime rain-bearing systems related to Pacific synoptic systems (e.g., East Coast Lows) and teleconnections (e.g., ENSO) (Taylor and Roach, 2003, Slattery, 2015). Mountain and highland fire regimes can hence be deduced to have possessed fundamentally different climatic sensitivities, despite Common Era burning for both being dramatically elevated relative to earlier in the late Holocene.

5.2.3. Zonal disparities in sensitivity to European land use change

Isolating zonal RoC data postdating European colonisation ('colonisation'; 130 cal yr BP) elucidates that, while alpine-subalpine and highland values have increased, montane values continue a linear decline apparent since its late Holocene MA maximum at ~600 cal yr BP (Fig. 5.1b). This results in mean European-era RoC for the montane zone being equal to that of the late Holocene, suggesting no systemic departure from the long-term baseline. As articulated in Chapter 3, this is curious given the montane zone is known to have been more pervasively modified by pastoralism than the alpine-subalpine complex (King, 1959, Mooney, 2004, Slattery, 2015), for which the data instead convey unequivocal European disturbance.

More unexpected is the decline in montane RoC itself, conveying not only a lack of disturbance but in fact increased stability. Chapter 3 therefore concludes that the montane zone exhibits some degree of resilience to land use change such that destabilisation did not occur during at least the colonial period, where the RoC data terminates (specifically, 1861 CE). The reason for such resilience remains unclear and is inverse to interpretations that the montane zone was more unstable under ENSO than the alpine-subalpine complex, in fact observing the most extreme instance of late Holocene destabilisation on the High

Country (i.e., the Delaneys Creek event). While this inconsistency cannot be mechanistically reconciled, it certainly implies greater montane sensitivity to climate than land use change.

Opposite to the montane record, alpine-subalpine and highland RoC show precipitous European-era spikes which achieve values unparalleled for their entire records save for their respective, site-specific events at hypsithermal onset. Indeed, all late Holocene upper RoC outliers for these two records derive from the European era, suggesting profound systemic reorganisation. Chapter 2 identifies that, while the highland spike commences prior to colonisation, this is almost certainly an artefact of low chronological certainty and a product of European impacts, namely increased erosion and lake eutrophication. As determined in Chapters 2 and 4, unprecedented multisite RoC for the highland and alpine-subalpine records indicate greater sensitivity to land use change than late Holocene climate change. Critically, while mean European-era highland RoC is 23% higher than alpine-subalpine RoC, the relative alpine-subalpine increase from colonisation to present is 167%, while for the highland zone it is only 48%. Therefore, although the Monaro has continued to be more unstable than all mountain zones, the alpine-subalpine complex has experienced a far more dramatic departure from its precolonial state, suggesting greater perturbation to the latter. This replicates the alpine-subalpine response to hypsithermal onset.

Given late Holocene – and indeed Holocene – highland RoC is much higher than alpine-subalpine RoC, it might be speculated that lower highland sensitivity to European land use change is in fact a product of a more unstable baseline state. Specifically, it is plausible that a landscape such as the Monaro, which is naturally more variable due to flexible biophysical boundary conditions, is less prone to destabilisation than a landscape more strictly prescribed by climate and topography, such as the alpine-subalpine complex. Alpine-subalpine systems have narrower ranges of tolerance and are thus more susceptible to state shifts if stability basins are reconfigured (Scheffer and Carpenter, 2003, Scheffer et al., 2012). This implies that systems constantly oscillating within wider basins of attraction (i.e., the Monaro) are thus less sensitive to land use change than more 'specialised' systems that are usually more stable but rapidly reorganise when their stricter bioclimatic limits are exceeded.

Indeed, many alpine-subalpine mechanisms endemic to this complex (e.g., snowmelt runoff, bog and organosol development, low-intensity surface fires) are dependent on

niche bioclimatic criteria which, if altered or removed by land use, trigger dramatic environmental changes (Pickering, 2007, Pickering et al., 2014, Slattery, 2015, Wilson et al., 2022). In contrast, highland environments such as the Monaro already observe a wider array of climatic and geomorphic conditions that support more generalised (as opposed to specific) processes (e.g., pedogenesis on various lithologies), summing to a more variable environment that is less constrained to a specific equilibrium state (Costin, 1954, Taylor and Roach, 2003).

Greater highland resilience to European disturbance may also be attributable to longer and more continuous human habitation. The Monaro is asserted to have been occupied by the Ngarigo and neighbouring peoples from much earlier in the Holocene; ergo, it has been more pervasively modified by various land uses, namely ignition for hunting and vegetation management (Flood, 1980, Young, 2005, Theden-Ringl, 2016). Such influences, while unconstrained here, have been posited to have altered late Holocene RoC for the Monaro especially, and have likely enabled the highland to effectively 'coevolve' with and 'adapt' to human disturbance well in advance of colonisation, resulting in a dampened European impact (Dodson and Mooney, 2002). This mountain-highland discrepancy in land use sensitivity evokes that already inferred for climatic sensitivity. It is therefore deduced that the SM has been consistently more sensitive to Holocene hydroclimate, late Holocene ENSO intensification and European pastoralism.

Montane land use resilience is reinforced when BMI data are separated from the bulk RoC signals (Fig. 5.1d). Chapter 3 observes that montane BMI continues to decline after its MA maximum in the second warm period, with no marked acceleration or deceleration of this decline occurring after colonisation. This culminates in a montane BMI minimum at the end of the record, suggesting maximum relaxation of montane erosion after colonisation. Conversely, the alpine-subalpine and highland records display European-era increases of comparable magnitude, though in both cases these do not exceed their Common Era peaks.

As identified in preceding chapters, this indicates that, while alpine-subalpine and highland erosion has been more sensitive to land use change, European-era erosion across all zones has not been as extreme as during their earlier snowmelt- and permanence-driven peaks. It is therefore argued that ENSO-induced climate change has been a more effective driver of erosion than European land use change. While a European-era minimum in montane BMI suggests a full recovery of the erosional regime after the peak

MA runoff phase, the alpine-subalpine and highland upticks are, though minor, still very high relative to the Holocene median. This implies that alpine-subalpine and highland erosion rates are currently well above the long-term baseline due to these being superimposed on a partial recovery of the erosional regimes.

European-era CHAR trends vary markedly between zones (Fig. 5.1e), confirming disparate fire histories due to contrasting floristics. Curiously, however, the highland CHAR record preserves the only instance of a sustained increase over the European era, which is inherited entirely from the Racecourse Lake record. Given European-era CHAR is unprecedented in the Racecourse Lake record, it is possible that peak CHAR in the highland record reflects peak fire activity on the Monaro since ~13,900 cal yr BP, though it should also be noted that no such pattern is observed for Lake Jillamatong. This dichotomy between the eastern and western records may reflect the situation of Lake Jillamatong along the precolonial montane-highland ecotone (DCCEEW, 2025). As such, the site probably observed quasi-montane fire dynamics before an artificial mountainward retreat of this ecotone under European clearing. This would explain the Lake Jillamatong

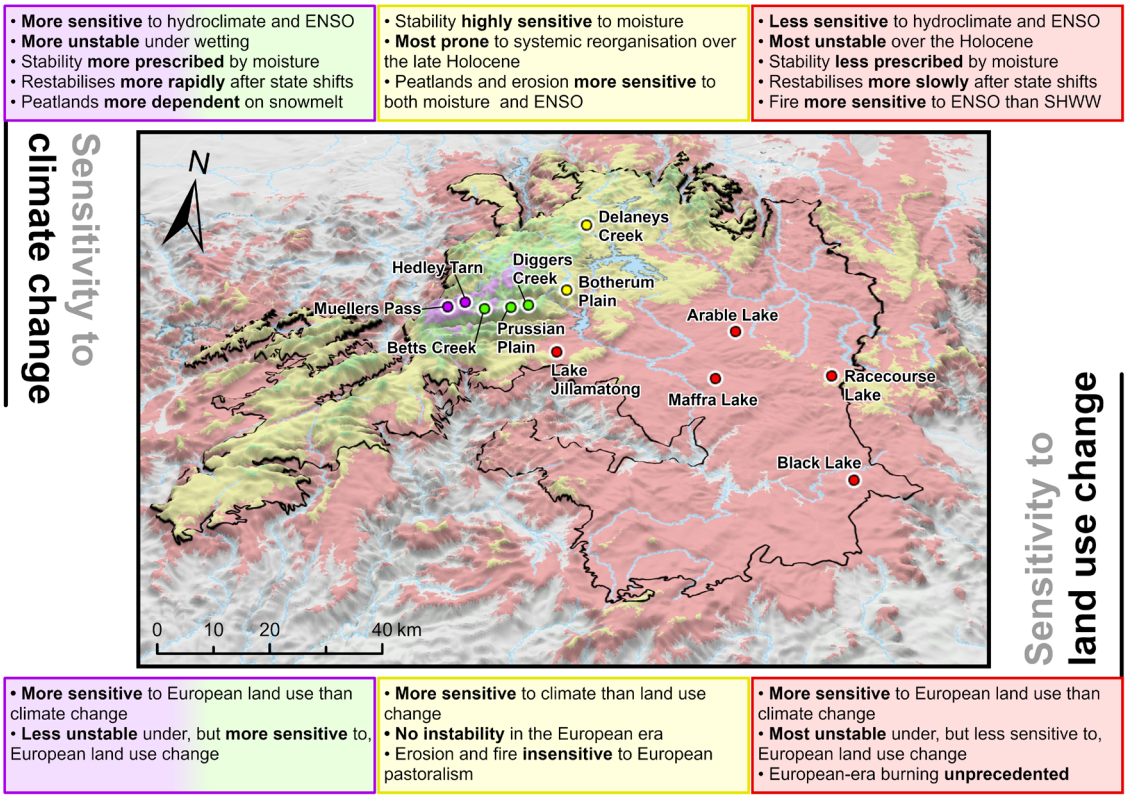

Figure 5.3. Summary of the main discussed findings on systemic sensitivity for the alpine-subalpine (purple-green), montane (yellow) and highland (red) zones in relation to climate (top) and land use change (bottom).

CHAR record being comparable to the montane record in that both lack a European-era spike. In fact, all mountain records indicate long-term declines in fire activity during the European era despite widespread pastoral firing, indicating these are catchment-specific exceptions from the regional regime shift.

Despite declines in the alpine-subalpine and montane records, it should be noted that median European-era CHAR for the former is over an order of magnitude higher than the latter, which is instead equivalent to highland values. This suggests that, despite European-era declines in mountain burning, subalpine burning has remained much more frequent and/or intense than in the montane zone, which has in contrast experienced a decline in fire activity to a state comparable to the highland zone. Greater subalpine burning is again unexpected given pastoral firing was most severe in the montane zone, although it must be recognised that subalpine CHAR has declined towards montane values over the European period. This conveys that high subalpine fire activity at colonisation is a residual response to precolonial drying under a southward SHWW shift, which has been implicated in the final subalpine CHAR spike (Section 4.6.2.2). As interpreted for erosion, this implies European disturbance to a fire regime that had not completely recovered from earlier climatic perturbation.

5.3. Constraining the sensitivity of the High Country

5.3.1. High Country sensitivity to climate change

Aggregating all zonal MA records to approximate hydrological change across the High Country (Fig. 5.4a), it is clear that ~13,900–8300 cal yr BP was a period of relatively persistent wetting. This is consistent with continual postglacial amelioration of global and regional climate (Clark et al., 2012, Petherick et al., 2013, Clerke, 2023). MA stabilisation at the end of this period – conveyed by more frequent wet-dry oscillations – are also coherent with hypsithermal onset across southeastern Australia (De Deckker, 2022), though its ~600 yr lead of peak hydroclimatic intensity is probably an artefact of systemic desensitisation after reorganisation (see Section 5.2.1). Despite this discrepancy, persistent drying from ~4500 cal yr BP is in high agreement with ENSO intensification. This suggests high hydrological sensitivity to ENSO, revalidating it as the primary forcing on regional MA.

ENSO-driven drying terminates with rewetting from ~2600 cal yr BP, apparent from increasingly persistent wetting values until a final Common Era MA peak at ~600 cal yr BP. Hydrological recovery from ~2600 cal yr BP is of high chronological certainty given all three zonal records show rewetting from this time (see Section 5.2.1). Peak MA and post-peak drying are also in temporal agreement with Common Era peaks in ENSO intensity and especially frequency (Moy et al., 2002, Conroy et al., 2008). Coherence with ENSO frequency results in MA being most strongly correlated with it than any other High Country metric over the precolonial late Holocene. In contrast, no correlation emerges with ENSO intensity due to the volatility of this signal, despite long-term trends also agreeing.

Consistent with the Racecourse Lake record from which the earliest ~3300 yr of the regional composite is informed, regional RoC declines until ~9500 cal yr BP (Fig. 5.4b), which as discussed probably reflects gradual biophysical equilibration with a nascent interglacial climate. Relative stability is briefly achieved before an unparalleled pulse spanning ~9400–8400 cal yr BP, terminating approximately at hypsithermal onset. This is inherited from the Hedley Tarn and Racecourse Lake events, which together indicate a period of hypsithermal-induced instability that is potentially unprecedented for the Holocene on the High Country, notwithstanding poor record coverage. Hypsithermal onset is succeeded by rapid recovery to a long-term RoC minimum at ~6700 cal yr BP, within ~1000 yr of the apex of the hypsithermal, reaffirming maximum systemic stability shortly after (and probably as a result of) reorganisation. RoC witnesses a subsequent increase until ~5700 cal yr BP, the reason for which is unclear. RoC then stabilises intermediate values until ~300 cal yr BP, indicating no major destabilisation due to ENSO-driven drying or rewetting.

This implies decoupling between systemic stability and MA since the middle Holocene. Indeed, while regional RoC and MA are already weakly negatively correlated for the precolonial postglacial period (r = -0.32; $p < 0.001$), an even weaker relationship is observed for the precolonial late Holocene (r = 0.3). While the late Holocene correlation seems to imply a reversal in sensitivity, it is not statistically significant (p = 0.097) and bears no visual relationship with the MA time series. A weakened and insignificant late Holocene correlation suggests that, although High Country catchments were more sensitive to MA during the early-middle Holocene such that they were more stable during wet phases (i.e., the hypsithermal), systemic functioning became more

insensitive to MA as ENSO intensified. While this does not necessarily implicate ENSO in such decoupling, it is reasonable that a more volatile climate would attenuate the influence of MA as a sole biophysical forcing relative to more frequent and extreme interannual fluctuations between factors such as productivity, erosion and fire. Interestingly, a weakened late Holocene MA-RoC correlation is inverse to individual observations for the alpine-subalpine and highland zones in Section 5.2.2, reinforcing high zonal heterogeneity in systemic sensitivity to MA.

Importantly, while late Holocene regional RoC is higher than for the hypsithermal, it does not display any long-term trend. Late Holocene non-directionality is suggestive of a system that was moderately unstable but not increasingly so, indicating no thresholds of instability were exceeded during this period. Rather, it is logical that ENSO imposed constant but mild biophysical stress such that the High Country became more dynamic but that this state was maintained. RoC non-directionality is clear when the rewetting period is bisected into the 'wetting' phase (i.e., 3200–1600 cal yr BP) and the 'peak MA' phase (i.e., 1500–200 cal yr BP) (Fig. 5.4.b), which show negligible differences in RoC. While the peak MA phase is associated with two upper outliers, these derive from timesteps immediately prior to colonisation, which incorporate European-era artefacts from the highland record. It is therefore unlikely these outliers are precolonial. Despite ENSO being implicated in RoC non-directionality, it is this same plateauing that results in no ENSO-RoC correlation over the late Holocene.

Converse to RoC, SM aCAR certainly demonstrates a sustained trend for the late Holocene, the only period with multisite coverage (Fig. 5.4c). aCAR is stable but extremely low (median 2.4 g C m^{-2} yr^{-1}) from at least ~4200 cal yr BP until an increase commencing at ~3000 cal yr BP. This reaffirms that, while SM peatlands were extremely unproductive carbon sinks (sources, in fact) during ENSO-driven drying, they were did not undergo irreversible decline. While the stepped increase from ~3000 cal yr BP appears to be an artefact of the inclusion of the montane record, subsequent trends indicate increasing productivity until ~1100 cal yr BP, reinforcing the beneficial impact of snowmelt. However, a median aCAR of only 6.6 g C m^{-2} yr^{-1} during the wetting phase suggests that SM peatlands were still unproductive even despite increasing MA. Low productivity is finally terminated by a precipitous increase from ~1100 cal yr BP (the end of the first warm period), which culminates at a maximum of 26.8 g C m^{-2} yr^{-1} at ~900 cal yr BP. While aCAR dips following this peak, the decline is relatively minor and still

within the typical range of high-altitude peatlands globally (Gaffney et al., 2025). This confirms that SM peatlands have been moderately productive for only the last ~1000 yr, excluding the European era.

Median aCAR during the peak MA phase is 165% higher than during the wetting phase, suggesting that wetting by this time had exceeded an MA threshold facilitating a massive increase in productivity. High aCAR even during post-peak drying conveys a permanent state shift in SM peatlands following the transgression of this MA threshold, whereby they became both more productive and insensitive to ongoing hydrological change. This evokes state shifts observed across other systems (e.g., sustained Monaro lake permanence from ~2000 cal yr BP) and timescales (e.g., ombrotrophication after the Hedley Tarn event). While peak MA values are again too low to indicate ombrotrophication – except for Betts Creek, the only modern raised bog – permanently elevated aCAR for several sites (i.e., Diggers Creek and Botherum Plain) suggests a regional regime shift such that SM mires became less dependent on runoff/groundwater. As such, the post-900 cal yr BP decline in aCAR probably reflects a transition to a less but still productive state, rather than MA reverting to a negative productivity forcing. Such threshold behaviour is probably partially responsible for late Holocene aCAR being more weakly (but still positively) correlated with ENSO metrics than MA itself.

Holocene-timescale trends in BMI reveal a gradual increase over the postglacial period until a pulse characterising the Hedley Tarn event (Fig. 5.4d). BMI then stabilises at slightly higher values during the middle-late Holocene until a second cluster of pulses corresponding to the Delaneys Creek event. Values restabilise until a final increase from

Figure 5.4. (next page) Time-series records and precolonial late Holocene violin plots of aggregated zonal metrics (timestep median, weighted by number of sites) **(a–e)**, and time-series records of ENSO frequency from Laguna Palcacocha (Moy et al., 2002) and sand content (ENSO intensity) from Laguna El Junco (Conroy et al., 2008) **(f)**. *r* values in each time-series plot indicate Pearson correlation between that regional metric and each paleoclimatic metric in (**f**), denoted by the same colour. Coloured horizontal bar in **a)** denotes the direction of hydrological change between each consecutive timestep, where dark and light respectively indicate wetting and drying. Coloured horizontal bars in **b)** denote the aggregated sum of RoC peak-points across all input zonal records (weighted by number of sites) for each timestep, where darker indicates a higher sum. Shaded stepped lines plotted on secondary y-axes of each time-series plot denote number of sites informing each timestep. Due to incomparability of zonal floristics and thus fire regimes, zonal CHAR records were Z-score standardised prior to aggregation in order to assign equal influence to all records regardless of magnitude.

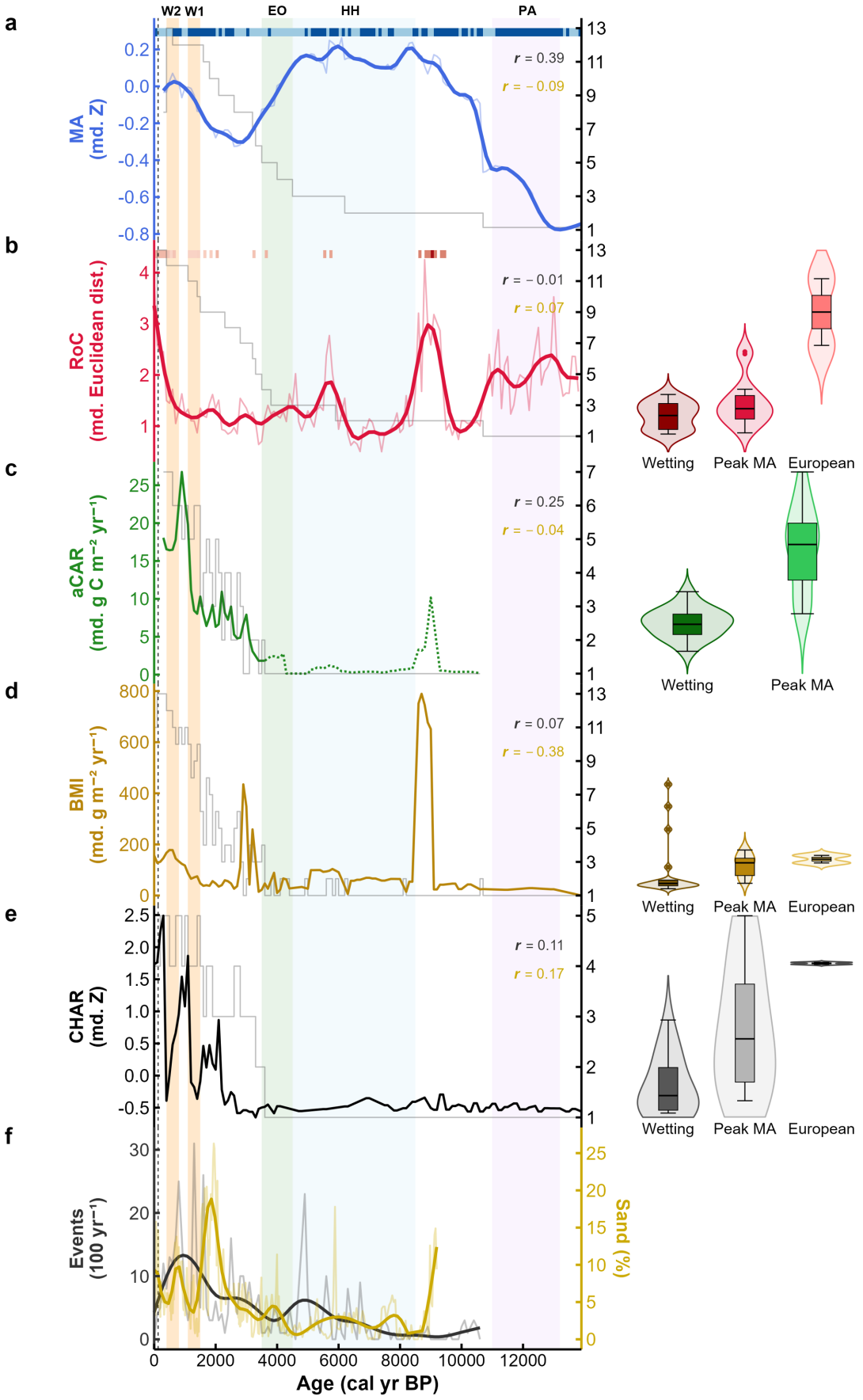
a
b
c
d
e
f
W2 W1
EO
HH
PA
MA (md. Z)
r = 0.39
r = −0.09
RoC (md. Euclidean dist.)
r = −0.01
r = 0.07
aCAR (md. g C m⁻² yr⁻¹)
r = 0.25
r = −0.04
BMI (md. g m⁻² yr⁻¹)
r = 0.07
r = −0.38
CHAR (md. Z)
r = 0.11
r = 0.17
Events (100 yr⁻¹)
Sand (%)
Age (cal yr BP)
Wetting
Peak MA
European

~1500 cal yr BP, coinciding with the onset of the first warm period. This suggests that High Country erosion was relaxed prior to the Common Era, with the only perturbations reflecting site- rather than regional-scale events, though it is reiterated that pre-late Holocene coverage is extremely poor. From ~1500–500 cal yr BP, BMI increases by 272% to 178 g m^{-2} yr^{-1}. Given this value is informed by all three zonal records, it confirms unprecedented erosion for at least the last ~3200 yr. While the wetting phase possesses all late Holocene upper outliers, these are derived from the Delaneys Creek event and so are not regionally representative.

Importantly, late Holocene BMI exhibits lag with other metrics; both its initial increase and peak postdate those of MA and aCAR. These lags reaffirm a delayed response to MA that substantiates the hypothesis presented in Section 5.2.2 that erosional responses to runoff were buffered for several centuries by increased vegetation cover in the SM, or a transport-limited regime on the Monaro. In contrast to aCAR, decreased but high post-peak BMI probably reflects regional erosion slowly recovering from peak ENSO activity rather than any state shift. Of all regional metrics, BMI possesses the strongest, albeit negative, correlation with ENSO intensity. This might be driven by peak BMI postdating peak ENSO intensity by ~1500 yr, reinforcing erosional lag.

Despite the composite CHAR record showing low and stable values until the late Holocene (Fig. 5.4e), most of the Holocene is informed solely by the Racecourse record and cannot be assumed to reflect regional fire regimes. Nonetheless, the multizonal portion of the record still conveys low, stable values until ~2200 cal yr BP, suggesting that, similar to SM peatlands, High Country burning was unresponsive to early ENSO intensification. A ~2300–1300 yr lag with ENSO onset cannot realistically reflect any delayed response in fire, which responds to climate change instantaneously on centennial timescales (Marlon et al., 2009). As such, the lag must reflect genuine pyrological insensitivity to ENSO intensification.

CHAR subsequently displays three dramatic peaks spanning ~2100–1600 cal yr BP, ~1100–600 cal yr BP and ~300 cal yr BP until colonisation. The timing of the first of these peaks reaffirms the deduction from Section 5.2.2 that the start of the Common Era marks the first regional response to ENSO, irrespective of zonal mechanisms (i.e., biomass production or desiccation). This first uptick coincides with peak ENSO intensity rather than frequency, suggesting that stronger rather than more frequent La Niña and/or El Niño phases were particularly important for amplified burning. This is supported by

CHAR being the second most strongly correlated variable with ENSO intensity after BMI. The initial uptick postdates the earliest positive response times for regional MA (~2600 cal yr BP) and mountain aCAR (~3200 cal yr BP) but predates the BMI (~1400 cal yr BP). This indicates that, while fire responses to ENSO lag those of MA and peatland productivity, they lead catchment erosion.

While no climatic explanation can be offered for the first trough in CHAR, the coincidence of the second pulse with the first, most severe warm period implicates it as its primary forcing. This peak eclipses the first and, given it coincides with peak ENSO activity, suggests it was a product of such. However, this second peak is again surpassed by the third and final peak, which has been related to warming but also SHWW changes. Given the third peak represents maximum fire activity for the late Holocene, it might be argued that the regional fire regime was more sensitive to the combined effect of SHWW and ENSO than ENSO alone.

As highlighted in Section 5.2.2, while these late Holocene patterns are presumably altered by Indigenous burning, it has been argued that cool burns were insignificant relative to climate change, and are therefore difficult to feasibly isolate from charcoal records (Mooney, 2004, Mooney and Tinner, 2011). Moreover, it is known that Indigenous burning is not independent of climate but can often be dictated by it (Theden-Ringl et al., 2023). For example, it has been proposed that fire suppression was conducted in the Sydney Basin in response to increased fire risk under amplified ENSO (Black et al., 2007). It is therefore reasonable that natural and anthropogenic pyrological responses to ENSO may have reinforced each other rather than cancelling out (e.g., increased biomass intensifying natural burning and Indigenous understorey burning).

Performing cross-correlation analysis on all five regional records for the precolonial late Holocene (Fig. 5.5), it is possible to approximate lead-lag relationships during rewetting. As expected, MA consistently leads all other metrics and thus possesses the greatest median lead, validating it as an independent variable on systemic change. While RoC of course comprises the aCAR, CHAR and BMI signals, it still lags the first two of these magnitudes. Indeed, aCAR possesses the second greatest median lead after MA, indicating peatlands are the most responsive biophysical component to hydrological change. CHAR follows aCAR in the lead-lag ranking but shows a median of 0 yr due to it leading, lagging and covarying with various metrics, individually. This large spread implies that, while changes in fire lag MA, they are on average contemporaneous with

broader systemic change. This is reinforced by the direct RoC-CHAR correlation also being 0 yr.

While RoC itself possesses a greater median lag than CHAR, this value incorporates lag with the independent MA and so does not necessarily imply that systemic change lags fire. However, a significantly greater median and direct RoC lag with aCAR implies that vegetation changes are often precursory to – and could possibly be considered early warning signals of – broader systemic destabilisation. This is unsurprising, considering high-altitude flora are known to be highly responsive to contemporary climate change, which as explicated in Section 1.2.1 is a reason for the bias towards ecological research in high-altitude regions (Beckage et al., 2008, Loeffler et al., 2011, Tito et al., 2020). Short ecological response times have also been communicated in Chapter 2, with changes in vegetation sources of OM in the Monaro lakes often occurring in advance of shifts in permanence and lake geochemistry.

While the cross-correlation results convey lower systemic than ecological sensitivity, RoC still possesses a lower median lag than BMI. As the lowest ranked variable, BMI

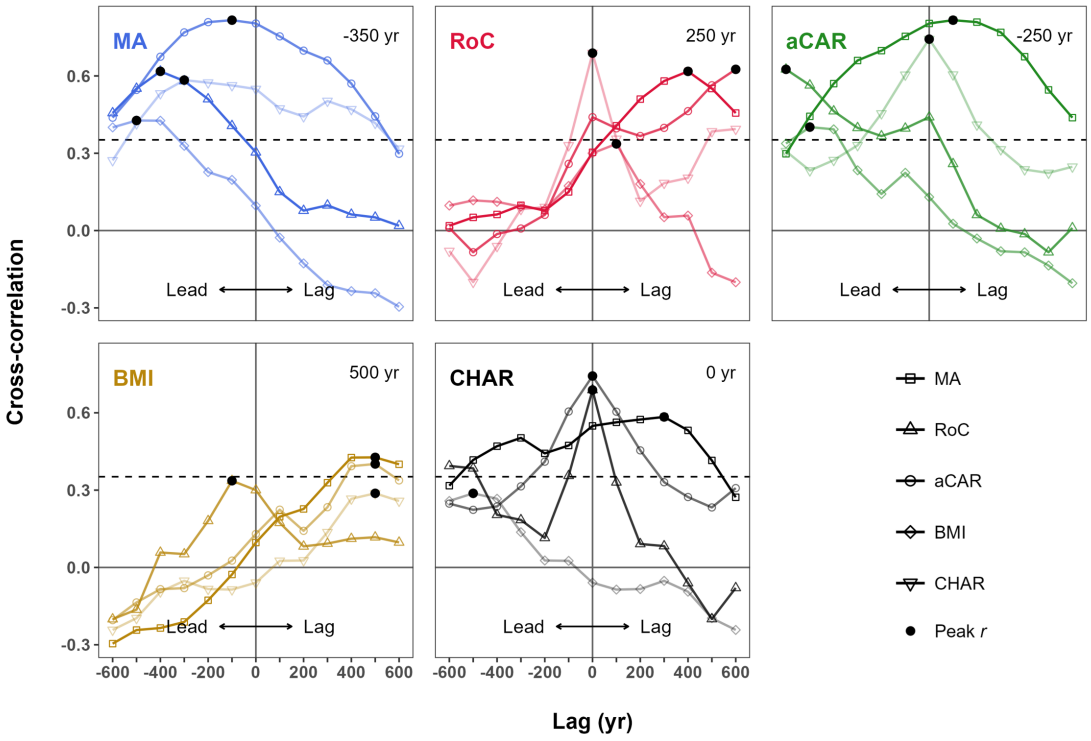

Figure 5.5. Cross-correlograms for and between each regional metric for the precolonial late Holocene. Annotated value in top right of each panel denotes the median lag value for all peak *r* values of each metric, where negative and positive values indicate a median lead and lag, respectively. Horizontal dashed lines correspond to the approximate 95% significance bounds.

appears to be the least responsive to perturbation, lagging systemic change itself. This suggests that catchment erosion is relatively insensitive to climate, with erosional responses tending to signal the end of systemic destabilisation. As supported by a median BMI lag greater than aCAR and to a lesser amount CHAR, long erosional response times are probably due to initial buffering by vegetation cover and later promotion by burning and soil exposure. This is consistent with what has been proposed for the wetting and peak MA phases. In sum, cross-correlation analysis indicates that changing MA on the High Country triggers delayed systemic responses that are a) heralded by changes in peatland productivity, b) contemporaneous with changes in fire, and c) concluded by changes in erosion.

5.3.2. High Country sensitivity to European land use change

Inherited from highland and alpine-subalpine trends, median regional RoC for the European era is 2.5-fold higher than the postglacial median, with values at present (i.e., 0 cal yr BP; -50–50 cal yr BP) being unparalleled by any preceding event save for at hypsithermal onset (Fig. 5.4b). European-era instability may therefore be unprecedented on the High Country for most of the postglacial period, and is certainly unprecedented for at least the last ~3200 yr. As identified for the highland and alpine-subalpine zones, and notwithstanding major record bias, these data imply greater high-altitude sensitivity to the impacts of European pastoralism than any climatic perturbation since the hypsithermal. Importantly, RoC at present is also 50% higher than the preceding 100 cal yr BP timestep, which itself is only 7% higher than the oldest precolonial timestep (200 cal yr BP). This suggests far greater postcolonial- than colonial-period disturbance despite impacts generally being more severe in the latter (Costin, 1957, King, 1959, NSW Parks and Wildlife Service, 1991, Clark, 1992).

Greater postcolonial instability conveys multidecadal lag in the regional response to European land use change. It might therefore be argued that the High Country exhibited some degree of resilience whereby the landscape was able to absorb the colonial impacts of land use change, only destabilising in the postcolonial period when ongoing degradation had finally exceeded this threshold of tolerance. As detailed throughout this thesis, postcolonial continuation of stress is obvious across the high-altitude transect. Modern stressors inherited from the colonial period are not limited to feral horses

perpetuating earlier livestock degradation of peatlands (Dyring, 1990, Robertson et al., 2019, Scanes et al., 2021), weed expansion reactivating erosion on formerly grazed slopes (Carr et al., 1992, Johnston and Pickering, 2001) and a lack of fire management increasing the fire activity due to a densified tree stratum (Mooney et al., 1997, Zylstra, 2006). Legacy effects and systemic lag also support the hypothesis in Section 5.3.2 that the lack of European-era deviatory behaviour in the montane record may be due to insufficient temporal coverage.

Also consistent with the highland and alpine-subalpine records, regional BMI increases during the European era, though again does not occur until the postcolonial period and is only 23% higher than during the colonial period (Fig. 5.4d). This indicates relatively minor postcolonial intensification of the erosional regime. Lagged erosional changes are also consistent with conclusions from the preceding subsection that erosion responds slowly to perturbation, confirming this applies to land use as well as climate change. A delayed erosional response to land use change is resonant of observations by Portenga et al. (2016b), who find that, while burial ages of European-era alluvium across the South Eastern Highlands are highly variable, multiple sites possess maximum ages postdating colonisation as much as ~50–110 yr. This indicates site resilience resulting in delayed gully erosion despite a known intensification of grazing (Meredith, 1844). While the regional BMI increase in this study is minor, it should be recognised that it is an inflection superimposed on the declining limb of the Common Era peak. As a result, the European era possesses a higher mean BMI than the wetting and even peak MA phases of the late Holocene, despite the latter observing maximum BMI. This reinforces the narrative of anthropogenic perturbation to catchments that had not yet stabilised after peak MA.

European-era regional CHAR is notably lower than the period immediately prior to colonisation (Fig. 5.4e). Indeed, there is a clear European-era decline in CHAR, reflecting similar trends in all records except Racecourse Lake. However, median European-era CHAR exceeds both the wetting and peak MA periods, due to the decline occurring relative to the precolonial SHWW-driven spike. As for the erosional regime, this conveys European modification of a fire regime that was still equilibrating with a climatic shift. Continued climatic forcing after colonisation, in concert with the competing effect of hot burning amidst catchment-specific declines, may be responsible for the European-era decline being relatively minor. The decrease in CHAR also commences in the colonial

period, preceding the postcolonial uptick in BMI. This is consistent with findings in the preceding subsection that fire tends to respond to disturbance in advance of catchment erosion.

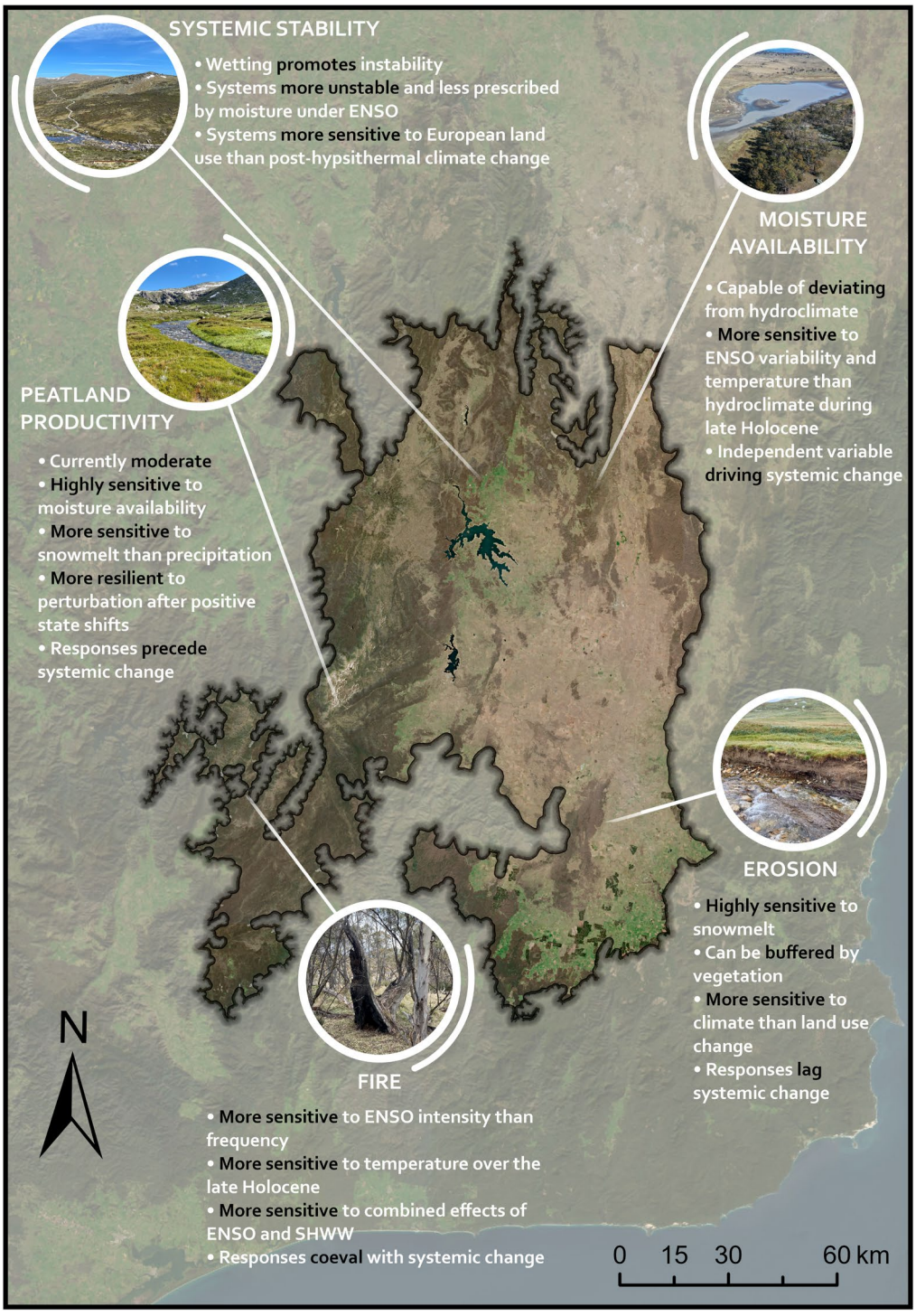

Figure 5.6. Summary of the main discussed findings on regional systemic sensitivity to climate and land use change, framed by the five key metrics explored in this discussion.

5.4. Reviewing High Country sensitivity in a global high-altitude context

5.4.1. Moisture availability

A salient finding of this study is that hydroclimate has been a dominant and positive forcing on High Country MA for most of the postglacial period. Given the global relevance of glacial-interglacial hydroclimatic changes, it is unsurprising that this inference is replicated for many global high-altitude paleorecords, albeit mainly through palynological and charcoal proxies. Paleorecords are particularly abundant in Patagonia, where there is a corroboration of abundant steppe vegetation during the late-glacial period prior to postglacial amelioration (Whitlock et al., 2006, Bamonte et al., 2025). While some argue steppe prevalence during this time to be due to low temperatures given reconstructed humidity (e.g., McCulloch and Davies (2001), Villa-Martínez and Moreno (2007)), most cite both cold and especially arid conditions as driving this floristic state (de Porras et al., 2014, Bamonte et al., 2025). Subsequent increases in MA under postglacial amelioration are communicated by an expansion of mesic arboreal elements, namely *Nothofagus*, with woodland and closed forest expanding across the highland and mountain domains, respectively (Villa-Martínez and Moreno, 2007, Mansilla et al., 2018).

Foresting of Patagonia appears to be interrupted by declining MA during the hypsithermal, given the inverse expression of a mean La Niña-like state in the eastern Pacific and a weakening of the SHWW. Consequently, studies argue for a resurgence of steppe elements and another mountainward retreat of the forest-steppe (i.e., mountain-highland) ecotone during the hypsithermal (Huber and Markgraf, 2003, Sottile et al., 2012, Marcos et al., 2025). Despite this consensus, many studies counterargue continued or even maximum forest dominance, with most of these deriving from sites in the high or windward Southern Andes (Whitlock et al., 2006, Villa-Martínez and Moreno, 2007, Echeverria et al., 2014). This indicates major mountain-highland disparities in MA that are also apparent from this thesis' comparison between the alpine-subalpine and highland records in Section 5.2.1, underscoring the necessity to address these terrains as discrete subsystems. Patagonian changes in MA remain inverse to the High Country into the late Holocene, when records indicate increasing MA due to the shift towards a mean El Niño-like state and equatorward SHWW migration. Higher humidity is evidenced by increases

in peatland MA and an eastward readvance of the forest-steppe ecotone towards its present position (Whitlock et al., 2006, Iglesias et al., 2012, Markgraf et al., 2013).

While deglacial and early Holocene MA patterns for Patagonia are replicated for high-altitude New Zealand, late Holocene changes for this region are more aligned with initial drying on the High Country, given the relatively consistent expression of ENSO across Australasia (Allan, 1986). Late Holocene records from the Southern Alps indicate an expansion of dry forest taxa alongside a lowering of water tables, coincident with bog drying and an opening of scrubland to grassland in the leeward Central Otago (McGlone and Moar, 1998, Wilmshurst et al., 2002, Walker et al., 2003). Importantly, drying appears to have been more severe and geographically consistent across Central Otago than the Southern Alps, where some studies, particularly from the windward Fjordland, instead indicate late Holocene wetting, implicating SHWW changes (Knudson et al., 2011).

This is resonant of the mountain-highland disparity in MA variability intimated by the above Patagonian studies, with orographic obstruction of the SHWW being a common factor. Orography as a driver of bifurcated mountain-highland MA responses aligns with the hypothesis that Maffra Lake was the only lake to definitely not upgrade permanence in the late Holocene due to it being situated in the core of the SM rain shadow (Section 2.6.1.5). Specifically, Chapter 2 proposes the central Monaro may have remained dry enough to mute the positive impacts of intensified multiyear La Niña registered by less orographically impacted lakes. Regardless of zonal hydroclimate-MA discrepancies, all above studies implicate hydroclimate as a paramount forcing on postglacial MA variability, consistent with the High Country.

Also in agreement with thesis findings, many studies recognise ENSO as a major control on MA, though many also identify SHWW activity as a more significant driver, especially for lower latitude regions such as Patagonia. Regardless, climatic variability becomes more clearly expressed in many late Holocene records than precipitation amount, coherent with thesis interpretations that MA became more strongly prescribed by ENSO frequency/intensity. In the Southern Alps, an ENSO-dominated climate is inferred by Wilmshurst et al. (2002) from amplified wet-dry oscillations in floristic elements despite contemporaneous declines in precipitation, indicating selective sensitivity to the interannual variability of hydroclimate. Downslope in Central Otago, the authors also determine from a bog sequence intensified late Holocene drought and increasingly variable surface wetness (i.e., MA).

In the Southern Andes, Nanavati et al. (2019) reconstruct increased late Holocene variability in the abundance of *Nothofagus* following an earlier mid-Holocene increase. The authors therefore interpret wetter late Holocene conditions owing to a northward expansion of the SHWW but also attribute accelerated floristic alternations to an intensification of ENSO and SAM. At lower elevations along the forest-steppe ecotone, Loisel et al. (2023) infer increased centennial-scale variability in peatland MA superimposed on a late Holocene increase, which they similarly ascribe to changes in ENSO and the SHWW.

Decreased late Holocene sensitivity to precipitation amount is reproduced in Northern Hemisphere records, though not necessarily due to ENSO nor on millennial timescales. Specifically, a record from the highland terrain of the Great Basin indicates that, while steppe changes (i.e., *Poaceae* expansion) were related to hydroclimate during the warmer Medieval Climate Anomaly (MCA), vegetation and lacustrine geochemistry became more directly prescribed by catchment-scale fire events rather than hydroclimate during the later Little Ice Age (LIA) (Cooper et al., 2021). While this shift in sensitivity from hydroclimate to internal factors is driven by temperature changes between the MCA and LIA, it evokes the longer-timescale, ENSO-driven decoupling of High Country MA from hydroclimate by ~2600 cal yr BP, at which time local mechanisms (i.e., claypan impermeability and snowmelt inflow) became the new direct controls on high-altitude MA.

While there is therefore global evidence that high-altitude hydrology can disassociate from hydroclimate, few studies corroborate hydrological recovery in spite of climate, as argued for the High Country. For example, a Patagonian study of the western Andes by Echeverria et al. (2014) reconstructs a decline in their MA index around the time of ENSO onset and hydrological recovery peaking at ~570 cal yr BP. This MA profile is in remarkable agreement with late Holocene drying followed by peak MA at ~600 cal yr BP on the High Country. However, Echeverria et al. (2014) attribute the initial decline in MA to a weakening of the SHWW, hydrological recovery to the MCA and a final return to drier conditions to the LIA. As such, no decoupling from hydroclimate is argued for. A lack of global support for High Country rewetting suggests the mechanisms of such are regionally specific. This underpins the premise that high-altitude environments are unique terrains host to biophysical interactions that are rarely globally or even regionally replicable.

5.4.2. Biophysical stability

As discussed, the early and late Holocene is characterised by high climatic and thus MA variability across Pacific high-altitude regions. This, in turn, often translates to environmental destabilisation in paleorecords, though relatively few studies express this quantitatively through RoC, as endeavoured in this thesis. One such study for the Sierra Nevada by Anderson et al. (2022) finds that the period of postglacial amelioration is generally defined by high or maximum pollen RoC and is followed by a decline to minimum RoC by the early-middle Holocene. While there is no evidence of any abrupt destabilisation at hypsithermal onset, postglacial instability and mid-Holocene stability is coherent with interpretations made for the High Country.

Similarly, Iglesias et al. (2018) observe slightly elevated RoC for vegetation assemblages across the Southern Andes during the early Holocene and a prolonged period of RoC equal to zero over the middle Holocene. Given the global replicability of postglacial amelioration, it can be determined that High Country instability during this time is indicative of a global high-altitude adjustment to amelioration. These trends are corroborated by more qualitative studies for the same region, where Nanavati et al. (2019) reconstruct forest expansion during the late-glacial and early Holocene periods and stable forest and fire regimes in the middle Holocene.

While mid-Holocene stability is also coherent with High Country reconstructions, and therefore seemingly supports the negative MA-RoC regional correlation, it should be recalled that the hypsithermal for these eastern Pacific high-altitude regions is broadly characterised by lower rather than higher precipitation (Benson et al., 2002, Minckley et al., 2007, Hermann et al., 2018). Agreement in mid-Holocene stability despite inverse MA expressions suggests that hypsithermal stability on the High Country is more likely to reflect resilience after a state shift than a positive linear response to MA. Iglesias et al. (2018) also reconstruct mid-Holocene stability for the Southern Andes (where conditions were locally wetter), though they also note two RoC pulses during this time relating to transient expansion of shrubs and bogs. This again suggests that there is no globally replicable positive MA-RoC correlation, though it does indicate that high-altitude catchments are prone to sudden destabilisation in response to increased MA, as is apparent from the High Country hypsithermal onset events.

Importantly, the aforementioned Sierra Nevada study by Anderson et al. (2022) also observes large site variability in late Holocene RoC, with evidence of both declines and increases in response to shorter timescale events such as the MCA and LIA. Despite site inconsistency, responses to these temperature-related events even in the context of late Holocene increases in regional precipitation (Wahl et al., 2015) reaffirm decoupling of environmental stability from MA and towards temperature. Anderson et al. (2022) also do not identify any late Holocene increase in RoC, confirming High Country interpretations that, despite increased climatic variability, this was insufficient to force high-altitude environments into new stable states. This is not a universally supported interpretation, however, with Villa-Martínez and Moreno (2007) computing for southwestern Patagonia a pronounced spike in RoC associated with vegetation changes and pulse in fire activity at ~2700 cal yr BP. However, the authors observe this to be the only instance of such for the late Holocene, with these events being more common in the mid-Holocene. This supports thesis inferences that dramatic events were more likely under higher magnitude climatic changes earlier in the Holocene (i.e., hypsithermal onset).

It should also be noted that the site targeted by Villa-Martínez and Moreno (2007) is situated at the forest-steppe (i.e., montane-highland) ecotone. As such, late Holocene instability supports the proposition that more transitional, marginal zones are more dynamic over centennial timescales, as interpreted for the SM subalpine and especially montane zones. While late Holocene destabilisation is not globally reproducible, where such trends are observed, these are often ascribed to ENSO and SAM. Indeed, Patagonian studies such as Nanavati et al. (2019) and de Porras et al. (2012) implicate these two climate drivers in enhanced variability in floristic composition and fire regimes across both the mountain and highland domains, regardless of how MA was expressed for either. Iglesias et al. (2018) also reconstruct a sharp late Holocene increase in RoC corresponding to a departure of forest and bog vegetation from their Holocene mean state, which the authors relate to ENSO and SAM.

In addition to intensified climate drivers, human agency is recognised as an increasingly significant contributor to elevated RoC towards present. Iglesias et al. (2018) argue that human occupation of the Southern Andes is likely contributing to higher RoC from the start of the Common Era. Importantly, however, RoC is high but non-directional until the European era, a period marked by an unprecedented increase in RoC evocative

of unparalleled European-era destabilisation on the High Country. This supports the High Country consensus that, while land use change is not a novel high-altitude stressor, Indigenous impacts are often more opaque than European-era impacts. Indeed, the unprecedented European-era spike in RoC in the Iglesias et al. (2018) records suggests at least some high-altitude systems have been more sensitive to European activity than any Holocene climatic forcing.

Many other records communicate a similar narrative, with Iglesias and Whitlock (2014) interpreting greater human modification of vegetation-fire regimes in the European than precolonial periods in Patagonia. Interestingly, in the Southern Alps, McWethy et al. (2010) infer more appreciable vegetation-fire responses to European land use in more easterly, rain-shadow impacted sites than western, mesic sites. This suggests moisture-limited mountain environments are more sensitive to human disturbance, which is inconsistent with European-era resilience of the SM montane zone. As such, while European impacts are often more appreciable than pre-European impacts, discrepancies in mountain zonal sensitivity to such are not necessarily globally translatable.

Zonal disparities in stability are also apparent at late Holocene as well as European timescales, with Markgraf and Huber (2010) interpreting from Patagonian records an agreement in vegetation dynamics between high- and low-elevation sites during the early Holocene, but a divergence in the late Holocene. Specifically, the authors interpret that lower-elevation stability became more strongly prescribed by precipitation but higher-elevation sites became increasingly sensitive to temperature. As well as disparities in zonal sensitivity, this reaffirms a diminished influence of hydroclimate on environmental variability during the late Holocene.

Zonal inconsistencies are replicated elsewhere in Patagonia, with Marcos et al. (2025) determining that highland records generally indicate consistent, stable steppe vegetation over the late Holocene with only internal ecological shifts. This is contrasted by dramatic alternations in vegetation assemblages across the forest-steppe ecotone in during humid-arid shifts. As concluded for the High Country, this suggests highland environments are less prone to state shifts than more transitional and climatically prescribed mountain zones, despite (and perhaps due to) the former being more persistently unstable due to higher biophysical plasticity.

5.4.3. Peatland productivity

This thesis proposes that peatland productivity in the SM was positively impacted by ENSO-driven warming commencing from ~2500–1900 cal yr BP. However, as for MA, there is no global evidence for any late Holocene 'switch' in ENSO from a negative to positive forcing on peatland productivity, reinforcing the dependence of such mechanisms on local bioclimatic conditions. Regardless, MA is certainly corroborated by independent studies as the primary positive control on peatland productivity. For example, McGlone and Moar (1998) identify a cessation of bog growth at ~5000 yr BP in Central Otago as being coincident with forest opening, attributing both to increased drought.

This suggests that, despite low peatland productivity in the SM for most of the late Holocene, local conditions for peat growth were still more favourable than in warmer, semi-arid highland environments such as the Monaro and Central Otago, where peatlands have become less common. In fact, even along marginally alpine refugia of Central Otago such as the Old Man Range, where peatlands persisted after lower highland systems deteriorated, peat accumulation became very slow and episodic by the late Holocene due to drier summers (McGlone et al., 1997). Such reconstructions are consistent with High Country observations that more elevated, less moisture-stressed mires are more productive and thus less susceptible to hydrological perturbation. These studies also substantiate the argument that many SM peatlands were carbon sources prior to rewetting.

McGlone and Wilmshurst (1999) ultimately implicate ENSO in late Holocene peatland decline, recognising that multiannual episodes of wet winters associated with El Niño would have been essential for transient recovery of surviving highland bogs due to the development of bog pools, permitting their persistence until present. Therefore, while ENSO may not have undergone any late Holocene reversal as an MA forcing, Central Otago reconstructions imply that it was capable of fulfilling a dualistic role in peatland persistence, simultaneously desiccating bogs on millennial-centennial timescales and sustaining them on sub-decadal timescales. This validates the capacity for ENSO to operate as both a negative and positive productivity forcing, albeit in a different context to the SM.

Despite the inverse eastern Pacific expression of ENSO, a positive MA-productivity relationship is maintained. In Patagonia, Huber et al. (2004) date ombrotrophication in the montane zone to ~5500 cal yr BP, consistent with the development of mesic conditions

(Heusser, 1998) and roughly coinciding with ENSO-driven peatland decline in Central Otago (McGlone and Moar, 1998). Patagonian ombrotrophication is also ~2500 yr earlier than peatland genesis at the montane analogue Delaneys Creek, at least ~3000 yr earlier than the increase in SM productivity and ~4500 yr earlier than possible ombrotrophication of Betts Creek. This lead with all SM responses implies there was an earlier satisfaction of peat-growing conditions much even on lower Andean slopes than anywhere in the SM, reinforcing marginal conditions across the latter. However, Huber et al. (2004) also infer that Holocene MA was never high enough to induce ombrotrophication along the drier montane-highland ecotone of Patagonia despite optimal growing temperatures, reaffirming that MA is a more important determinant of peatland productivity than temperature.

While there is no global evidence of snowmelt-driven increases in peatland productivity despite warming for the late Holocene, this interaction has been recorded on recent decadal timescales. In the Southern Alps, Fewster et al. (2025) date peat formation in an alpine valley to ~1949 CE, with moss development from ~1963 CE. The authors identify poor catchment drainage, high meltwater supply and the shift to a rainfall-dominated regime as likely mechanisms driving peatland formation despite/due to anthropogenic warming. However, recognising meltwater availability as a critical control, Fewster et al. (2025) anticipate that this mechanism is not regionally generalisable and is highly dependent on local factors, namely catchment drainage patterns. This reinforces the argument in this thesis that enhanced peatland productivity is possible even under warming, but only if an alternative source of moisture (i.e., snowmelt or an increased rain/snow ratio) is sufficient to offset increased evapotranspiration and/or decreased precipitation. Catchment-specific dependence of this process may explain why it does not emerge as a common feature in late Holocene peat records globally.

Local constraints on peatland productivity are also communicated by Loisel and Bunsen (2020), who reconstruct a widespread Patagonian fen-bog transition at ~4200 cal yr BP. While a volcanic eruption is implicated in the timing of this transition, this is interpreted as a tipping point superimposed on late Holocene hydroclimatic deterioration due to ENSO and SAM intensification. Specifically, more frequent drought is argued to have accelerated decomposition such that basal peats hardened and isolated fens from the water table, forcing ombrotrophication. This ‘dry route’ to bog development differs vastly from the ‘wet route’ of enhanced flows postulated for SM raised bogs such as Hedley bog

and Betts Creek, while the Patagonian transition again precedes positive SM responses by several millennia. Nonetheless, the model of Loisel and Bunsen (2020) does lend credence to the argument that declining MA can augment productivity, as proposed for Delaneys Creek, whose establishment was permitted by declining streamflow.

Interestingly, Loisel and Bunsen (2020) also find that those Patagonian fens that did convert to bogs had a median late Holocene aCAR of 19 g C m^{-2} yr^{-1}, equal to peak SM aCAR during the late Holocene MA maximum but 130% higher than the precolonial late Holocene median. In contrast, median aCAR for sites that remained fens was only 5 g C m^{-2} yr^{-1}, comparable to SM values prior to ENSO-driven rewetting at ~2600 cal yr BP. Of these 'persistent' fens that did not convert, a large proportion are situated on the Patagonian Plateau, where highland MA was never sufficient to induce a fen-bog transition. This is consistent with the discussed interpretations of Huber et al. (2004). These data confirm that SM productivity over the late Holocene has been very low relative to high-altitude peatlands in climatically comparable high-altitude regions.

The highland emplacement of most of the persistent Patagonian fens identified by Loisel and Bunsen (2020) also validates this thesis' argument that poor SM peatland productivity was largely a function of low elevation and thus marginal peat-growing conditions. Recalling that Betts Creek is the only study site that is currently ombrotrophic, and that it possesses the highest median aCAR, it is deduced that a marginal SM climate prevented a mass fen-bog transition like that reconstructed by Loisel and Bunsen (2020). Consequently, many SM mires have persisted as less productive topogenous systems even in the alpine zone, despite the recent contributions of snowmelt. Huber et al. (2004) also identify a late Holocene increase in mean annual precipitation to 600 mm yr^{-1} as responsible for Patagonian ombrotrophication. It can therefore be inferred that snowmelt contributions in the SM must have been high enough to simulate at least this much precipitation and trigger ombrotrophication at Betts Creek, despite net MA declines from evaporation and declining precipitation.

5.4.4. Catchment erosion

The preceding sections of this discussion articulate a cross-zonal intensification of erosion during the Common Era, attributable to ENSO and concomitant increases in snowmelt runoff, fire and lake permanence. While this section has shown that such

mechanisms are regionally rather than globally relevant, independent records strongly corroborate a positive correlation between high-altitude erosional and MA. In the Southern Alps, a sediment core from Lake Ohau preserves varves produced by clastic influx relating primarily to warm-season inflow and flood events (Roop et al., 2016). Given snowmelt contributes 21% of mean annual inflow to Lake Ohau (Kerr, 2013), and a much larger proportion of warm-season inflow, varves confirm a positive association between snowmelt and slope erosion, validating it as a mechanism for the SM BMI peaks.

Additionally, the findings of Roop et al. (2016) indicate that, irrespective of the hydrological source of such runoff, the warm season is the period of greatest sediment influx into Lake Ohau. This supports the notion that increased erosion for at least the SM reflects runoff during the warm season, when snowmelt inflow is highest (Bilish et al., 2020). A positive association between MA and mountain erosion is reverberated in other regions such as Patagonia; a study of Laguna Meseta by Franco et al. (2024) divulges a mid-Holocene shift from biogenic to allochthonous minerogenic sedimentation due to increased fluvial erosion. The authors in turn relate increased streamflow to elevated precipitation and glacial advances during a period of intensified SHWW. This substantiates the thesis' argument that meltwater, in conjunction with precipitation, exacerbates catchment erosion.

In fact, despite glaciers now being absent from the catchment of Laguna Meseta, snowmelt still contributes a significant proportion of basin inflow. This confirms that snowmelt can remain a major MA source even under warmer conditions, as postulated for the SM during the warm periods. Importantly, the transition from autochthonous to allochthonous sedimentation inferred by Franco et al. (2024) also highlights that even mature lake systems are capable of abrupt shifts in their sedimentation regimes. While the direction and hydrological catalyst of this shift are incomparable to the Common Era shift to autochthonous sedimentation in the Monaro lakes, both cases are ultimately due to wetting, validating MA as an important mechanism for shifts in lacustrine sediment provenance.

Many studies also recognise the frequency and intensity of climatic oscillations as being the dominant driver of sediment influx into basins over the late Holocene, as inferred for the High Country in the context of ENSO. This is especially apparent from lakes on leeward flanks of the Sierra Nevada such as June Lake, from which a sediment core displays detrital layers corresponding to runoff pulses during late Holocene wet

phases, similar to Lake Ohau (Roop et al., 2016, Lyon et al., 2020). Curiously, Lyon et al. (2020) also observe that some wet phases (e.g., the LIA) are not associated with any such pulses, a discrepancy they attribute to increased vegetation coverage in the catchment under elevated MA, which is presumed to have stabilised slopes. This reinforces the recurring argument that there was a deterioration of a simple linear relationship between MA and hydroclimate over the late Holocene.

It also reaffirms that increased vegetation cover can suppress or delay catchment erosion, resulting in an attenuated response, as proposed for the SM. As such, floristic changes can regulate mountain erosion. This mechanism is not limited to mountains, with Leslie and McGlone (1973) concluding for the Central Otago highlands that grassland expansion after postglacial amelioration protected periglacial regolith from erosion that was severe earlier in the last glacial cycle, when regolith was exposed. Interestingly, both the Lyon et al. (2020) study of June Lake and a study of the adjacent Fallen Leaf Lake by Noble et al. (2016) deduce that, while lake sedimentation is positively correlated with MA, it is less sensitive to aridity.

Moreover, Noble et al. (2016) recognise that erosional responses to drought are more pronounced in lake records from the semi-arid Great Basin. Indeed, a study of Mono Lake on the mountain-highland boundary of the Sierra Nevada and Great Basin reveals that lake-level changes themselves, rather than catchment erosion, were responsible for increased variability in grain size and authigenic carbonate deposition over the late Holocene (Zimmerman et al., 2021). A separate study of this site by Hodelka et al. (2020) demonstrates that lake-level changes were responsible for shoreline reworking and thus remobilisation and redeposition of sedimentation, such that drought became an important control on lakebed facies.

These observations reinforce greater hydrological sensitivity to climatic variability than precipitation amount and suggest that moisture-stressed basins are more prone to shifts between allochthonous and autochthonous inputs. Both interpretations are again coherent with, albeit mechanistically unrelated to, the ENSO-driven shift in the magnitude and provenance of sedimentation in the Monaro lakes, which like Mono Lake are also seasonal highland systems. The relative erosional stability of the aforementioned Sierra Nevada lakes during dry but not wet phases is also resonant of the asymmetric sensitivity of the Monaro lakes and their catchments, with more mesic lakes being less

responsive to climatic events, and the Monaro as a whole being more unstable under drying than wetting.

Impacts on erosion by highland lakes rather than their catchments are also asserted by a study of Lago Cardiel on the Patagonian Plateau, where lake turbulence and lake-level lowering are implicated in increased deposition of sand and inorganic carbon, respectively (Markgraf et al., 2003). These hydrological changes are in turn attributed to deviations in ENSO and the SHWW. This indicates high highland lake sensitivity to these climate drivers and a predominantly autochthonous sedimentation regime, again consistent with the Monaro lakes. The above case studies therefore suggest that moisture-limited basins in highland terrains often possess erosional regimes that are more sensitive to climate change and autogenic controls (i.e., lake-level changes) than mesic mountain basins, which are instead more resilient to climate and more sensitive to allogenic controls (i.e., runoff).

Despite these discrepancies, there is a global consensus that land use change has exacerbated erosion across both mountains and highlands. Curiously, however, Southern Alps records indicate that Māori deforestation initiated greater erosion than European activities (Woodward et al., 2014b), counter to independent observations that Indigenous impacts on High Country erosion have been relatively small (Prosser, 1990, Portenga et al., 2016a). Importantly, Woodward et al. (2014b) also conclude that Southern Alps lakes themselves cannot return to their pre-human baseline states due to permanent changes in hydrological regimes by erosion, reinforced by internal feedbacks (e.g., persistent wind-induced resuspension of eroded nutrients). This indicates hysteretic lake sensitivity resonant of the Monaro lakes, though as pertaining to land use rather than climate change.

Anthropogenic erosion is also communicated for the adjacent highland domain, with Thorburn (1974) ascribing increased sedimentation in Central Otago to high-intensity burning by squatters in the mid-19th century, which promoted soil erosion. This also supports thesis inferences that increased burning, while climatogenic rather than anthropogenic, may have constituted an important secondary driver of Monaro lake sedimentation in the Common Era. Colonial European burning is also implicated in increased soil erosion on the Patagonian Plateau (Mayr et al., 2005). In conjunction with the two New Zealand studies (Thorburn, 1974, Woodward et al., 2014b), this implies that fire has contributed significantly to European-era erosion. It also reaffirms that European impacts on erosion are often more pronounced than Indigenous impacts in highland

terrains, where land use change was more intensive and occurred earlier than in less accessible mountains.

5.4.5. Fire activity

The global abundance of high-altitude charcoal studies means the sensitivity of fire to climate as well as land use change – as intimated above – is particularly well constrained. Such studies validate High Country interpretations that fire activity in transitional mountain (i.e., subalpine and montane) zones has been far greater than on highlands, not merely over the late Holocene but the entire postglacial period. Indeed, Huber et al. (2004) identify burning to have been most severe in Patagonia just above the forest-steppe ecotone, attributing this to a balance of intermediate MA and high fuel loads, as is the case for SM montane forest. As such, Huber et al. (2004) ascribe a mid-late Holocene decline in fire to the emergence of a wetter climate promoting an expansion of mesic rainforest-moorland at the expense of xeric woodland, with the former not being dry enough to promote widespread burning.

In addition to wet Andean forest, low fire activity is also inferred for the Patagonian Plateau (Iglesias et al., 2012, Iglesias and Whitlock, 2014), with Sottile et al. (2012) ascribing low burning in the early to mid-Holocene to patchier shrub and grass coverage. This is consistent with other highlands such as the Great Basin, where Mensing et al. (2006) reconstruct lower fire activity in the sagebrush-dominated valleys of the Basin and Range Province than at the woodland-sagebrush ecotone along intercalated ranges. Interestingly, Sottile et al. (2012) along with others (e.g., Iglesias et al. (2018)) deduce that the late Holocene in the Southern Andes is also marked by an increase in fire activity for steppe despite the downslope decrease in MA and thus fire.

While this mountain-highland divergence contradicts universal increases in burning across the High Country, it is consistent with thesis interpretations that fire in each terrain possesses an inverse sensitivity to the same climate driver. Specifically, it has been argued that burning on the Monaro was intensified by increased fuel loads, whereas in the SM burning was facilitated by fuel desiccation. This dichotomy is replicated elsewhere; in the Great Basin, Mensing et al. (2006) identify that highland burning was dependent on fuel loads rather than desiccation, and as such was respectively intensified and suppressed when sagebrush proliferated during wet phases and declined during dry phases.

Contrastingly, Huber and Markgraf (2003) posit that fuel desiccation was the limiting factor for forest fire in the Southern Andes, and as such was attenuated under higher precipitation producing moister foliage.

Another disparity that emerges in the literature is the causal relationship between fire and vegetation changes. While some studies attribute landscape opening/closing to increases/decreases in fire, others argue the opposite, instead implicating fire as a mechanism rather than an outcome of canopy density. This aligns with conclusions from Chapter 3 that an early decline in SM montane burning during the ~2700 cal yr BP MA minimum resulted from a diminished tree stratum, while landscape opening during the later warm periods was conversely an outcome of intensified burning itself (Section 3.6.2.1). Global examples of fire as a consequence rather than a driver of vegetation change are abundant; in the Great Basin, Minckley et al. (2007) propose that fires were unlikely to have been a mechanism for vegetation changes, and in Patagonia Iglesias et al. (2012) assert that forest incursion into steppe resulted in an increase in fire activity, rather than vice versa. In contrast, fire as an agent of vegetation change is considered by studies such as Huber and Markgraf (2003), who conclude that increased fire frequency during drier early Holocene episodes were a major cause of steppe expansion across Patagonia due to burning of the tree stratum. The authors also argue that wetting and suppressed fire during the late Holocene caused the development of closed forest, rather than being an outcome of it. Moreover, in Central Otago, McGlone and Moar (1998) propose that late Holocene grassland expansion across the highland is largely attributable to increased burning.

Irrespective of precise configuration of the MA-fire-vegetation nexus, there is an agreement that ENSO and/or SHWW changes commanded late Holocene deviations in fire activity, consistent with what has been determined for the High Country. Returning to the McGlone and Moar (1998) study, the authors implicate ENSO-driven drought in the late Holocene intensification of fire across Central Otago. This is corroborated by Nanavati et al. (2019), Iglesias et al. (2016) and Whitlock et al. (2006) for Patagonia, where a shift to frequent surface-level fires is also ascribed to ENSO intensification. Other studies such as de Porras et al. (2012), Jara et al. (2019) and Martel-Cea et al. (2024) argue the SHWW to be an even more significant fire forcing than ENSO intensification. This is in contrast to the High Country, where SHWW changes have been speculated to only have been a dominant influence over the last several hundred years of the late

Holocene, and perhaps never for the orographically sheltered Monaro. This disagreement with Patagonian records may be a product of the higher latitudinal position of Patagonia and thus greater exposure to SHWW storm tracks (Kilian and Lamy, 2012).

Charcoal trends over the last millennium also indicate ongoing or reactivated changes in fire activity as a result of European and pre-European land use change, but to varying degrees depending on regional histories. McWethy et al. (2010) identify that Polynesian occupation drove increased burning in the Southern Alps over the last few centuries, indicating higher pyrological sensitivity to land use than climate change. Interestingly, McWethy et al. (2010) also deduce that forests on the wetter western flanks were more resilient to human ignition than orographically moisture-stressed eastern forests. This supports independent conclusions described above relating to fire being less sensitive to climate in wetter mountain areas, suggesting this is upheld in the context of land use change.

However, higher sensitivity of drier forests is in conflict with unresolved lack of a SM montane response to European burning and a dramatic response in the more mesic subalpine zone. Greater agreement with thesis findings is instead found in Central Otago, where McGlone and Wilmshurst (1999) conclude that Māori burning and a concomitant removal of the residual tree stratum was facilitated by an already dry, fire-conducive late Holocene climate. As argued in Section 5.3.1 for Indigenous land use, this conveys that human disturbance can be reinforced by climatic conditions. It also aligns with inferences that high European-era burning in the SM subalpine zone was at least partially inherited from an intensified precolonial fire regime established by SHWW changes. This is supported by Huber et al. (2004), who postulate that Indigenous burning in Patagonia was concentrated in the highly flammable steppe biome, despite limited biomass rendering a naturally attenuated highland fire regime.

Importantly, McGlone and Wilmshurst (1999) also posit that human occupation resulted in fire transitioning to an agent of vegetation change rather than an outcome of it, again supporting the notion that fire can alternate between these roles. This supports arguments by McGlone and Moar (1998) that even in already open highland settings, Māori burning resulted in a further replacement of scrubland with grassland. While Indigenous burning is pronounced in New Zealand records, Patagonian records such as those presented by Iglesias and Whitlock (2014) indicate that prehistoric occupation was

not signalled by any profound change in the high-altitude fire regime, with vegetation-fire dynamics instead coevolving with climate until major change in the European area.

Additionally, Huber et al. (2004) argue that, because Indigenous burning was focused in already fire-conducive environments, human and climatic influences are difficult to partition, as argued by independent High Country studies. The global inconsistency in pyrological responses to humans underscores the uncertainty entrenched in generalisations of high-altitude fire regime sensitivity to land use as well as climate change. This is especially pertinent to the High Country, where human impact is notably ambiguous but cannot be dismissed.

Chapter 6

Conclusions

This study was conceived out of recognition, from a review of the available literature, that high-altitude paleoscience is a) methodologically skewed towards constraining paleoecological (as opposed to systemic) sensitivity, and b) geographically skewed towards mountains (as opposed to highlands). As explicated in Chapter 1, these biases and their inherited knowledge gaps are exaggerated for the High Country of southeastern Australia (comprising the SM and Monaro), which also serves as a microcosm of the challenges faced by high-altitude systems globally under GEC. This thesis has empirically addressed the above knowledge gaps by applying multiproxy analyses to cores obtained from thirteen study sites along an elevational transect of the High Country, which have informed reconstructions of cross-altitudinal paleoenvironmental change. In so doing, this thesis has constrained the systemic sensitivity of the High Country in relation to postglacial climate change and European land use change. This concluding chapter reviews thesis findings, assesses their satisfaction of the research objectives listed in Section 1.6, and makes recommendations for future research.

6.1. Thesis findings and satisfaction of research objectives

The first objective of this study was to "evaluate downcore variability in environmentally sensitive proxies (magnetic susceptibility, elemental geochemistry, mineral grain size, total organic carbon and nitrogen, $\delta^{13}C$ and macrocharcoal abundances) from the sedimentary records of mire and lake sites cored across the alpine, subalpine, montane and highland zones". This was successfully accomplished for all sites, though zonal changes in archive availability meant different deposits were sampled for the highland (seasonal lakes) and mountain (mires and tarns) domains. This resulted in certain proxies being less statistically informative for some zones than others. For example, magnetic susceptibility exhibited a low signal/noise ratio for all Monaro lake records but not the peat sequences, and μXRF PCA data also observed much lower site consistency for the former than the latter. Another limitation of this study is the uneven number and spatial distribution of sites investigated across the altitudinal transect, which was a result of zonal changes in the availability of sites that satisfied site selection criteria, or which yielded viable records. This unevenness limits the geographical representativeness of zonal reconstructions.

The second objective of this study was to "reconstruct, for each site, variability in key abiotic and biotic processes (hydrology, erosion, primary productivity, nutrient availability and fire) through triangulation between individual proxy records appended to a robust chronological model". Due to the substantial site variability observed in multiproxy relationships (see above), process-level interpretations were only feasible by supporting multiproxy triangulation with *a priori* assumptions and direct site observations of catchment-scale variability. Poor site reproducibility in multiproxy relationships highlight the significance of endogenous processes in governing site-level systemic change. Translating multiproxy data to temporal records was also complicated by most core chronologies having high temporal uncertainty. This was due to a) a sparse distribution of ^{14}C samples along most cores, and b) dating of a combination of bulk sediment and sporopollenin samples. The former impaired accurate identification of the timing of specific multiproxy deviations (e.g., apparent European signals with precolonial modelled ages), while the latter hindered discernment of age reversals and outliers.

The above statistical and chronological uncertainties were partially accounted for by satisfying the third research objective, which was to "synthesise multiproxy data to reconstruct systemic paleoenvironmental change at the site, zonal and regional scale". Site-level multiproxy synthesis involved reconstructing directions, rates, magnitudes and lags of systemic change through various metrics. Multisite synthesis for the Monaro (Chapter 2) reveals that highland MA increased from ~13,900 cal yr BP until the middle Holocene and declined thereafter, before abruptly recovering from ~2600 cal yr BP. Consultation of geochemical data indicates this rewetting signal represents a lake- rather than catchment-scale transition, namely upgraded lake permanence. This is associated with an increase in lake sedimentation that is predominantly autochthonous but also possibly contributed to by a coeval intensification of woodland burning. These biophysical changes sum to elevated systemic instability during rewetting, though this is eclipsed by European-era destabilisation, which is unprecedented for the record and characterised by catchment erosion, lake eutrophication and woodland burning.

While the long-term paleoenvironmental histories of the montane, subalpine and alpine zones (Chapters 3 and 4) diverge markedly from the highland domain, one curious commonality is that they also record catchment rewetting from ~2600 cal yr BP, suggesting this was a regionally significant event. Hydrological recovery across SM catchments is associated with increases in peatland productivity, erosion, fire and,

possibly, treeline elevation, which sum to elevated systemic destabilisation for the subalpine zone in particular. While mountain instability during rewetting is pronounced, it is not unprecedented; in fact, it is well exceeded by systemic reorganisation during the Hedley tarn and Delaneys Creek events, which are both associated with high MA.

European-era instability for the alpine-subalpine complex is unprecedented for at least the late Holocene, and possibly longer. Post-European instability is defined by changes in fire and erosion that are again most pronounced for the subalpine zone but are surprisingly absent from the montane zone. Despite these elevational disparities, zonal aggregation reveals that European-era destabilisation is unprecedented on the High Country for at least the last ~3200 yr, and possibly since hypsithermal onset. Assessing regional relationships between major biophysical components, it is determined that changes in MA, regardless of sign, generally trigger delayed systemic responses that are heralded by ecological changes, coeval with pyrological changes and concluded by erosional changes.

With these multiscalar reconstructions established, the fourth objective of this study was to "assess, through comparisons of paleoenvironmental records with independent records of paleoclimate and European land use change, biophysical sensitivity to these stressors at the site, zonal and regional scale". Consulting independent records, it is apparent that highland and mountain hydrological changes have been relatively harmonic with hydroclimate over most of the Holocene. However, regional rewetting from ~2600 cal yr BP represents the first and only instance of a sustained cross-altitudinal deviation from hydroclimate, specifically declining precipitation under late Holocene ENSO intensification. Hydrological decoupling from hydroclimate is in fact ascribed to ENSO itself and suggests a regional threshold shift in systemic sensitivity from hydroclimatic intensity to variability, which enabled ENSO to effectively switch from a negative to positive forcing on MA.

However, this sensitivity switch is attributed to vastly different mechanisms for the highland and mountain domains. Specifically, rewetting on the Monaro is ascribed to an increase in the duration, frequency and intensity of La Niña; this likely impaired effective drainage of these impermeable claypans, forcing a widespread upgrading of lake permanence. In contrast, SM rewetting is argued to be a product of an ENSO-driven warming interval which, superimposed on long-term snow cover stability, may have increased snowmelt inflow into, retention within, and gradual outflow from peatland-

dominated mountain catchments. Rewetting in both terrains appears to have influenced other major biophysical processes but not fire activity, whose regional intensification is proposed to have been a more direct response to ENSO. In particular, amplified burning on the Monaro is related to increased woodland fuel loads under more volatile ENSO oscillations, while in the SM it is attributed to fuel desiccation under warming.

Upgraded lake permanence on the Monaro is heralded by increasing algal dominance – indicating high biotic sensitivity to MA – and is followed by hydrological stability and thus resilience to further climatic perturbation. Beyond this hysteretic lake behaviour, further asymmetric highland sensitivities are observed in catchment instability being weakly but positively associated with drying phases. Preferential sensitivity to drying is reinforced by drier lake catchments being more unstable than those in more mesic settings. Late Holocene rewetting in the SM is more abrupt relative to its domain-specific ENSO forcing than Monaro rewetting, indicating mountain catchments are more sensitive to climate than highland catchments.

This is also true at the Holocene scale, with alpine-subalpine MA exhibiting no lag with hypsithermal nor ENSO onset – unlike the Monaro – and the Hedley Tarn event itself suggesting major biophysical reorganisation in response to hypsithermal onset. Alpine restabilisation after hypsithermal onset is also more rapid than for the Monaro, suggesting mountain catchments are more effective at reorganisation than less climatically prescribed highland catchments. Indeed, the more generalised biophysical composition of the Monaro may explain why it has remained consistently more variable over the Holocene and also less responsive to hydroclimate and MA, as evidenced by a lack of systemic destabilisation upon rewetting. Conversely, mountain rewetting is accompanied by a stepped increase in instability, which is also characterised by more pronounced relative increases in peatland productivity and absolute increases in erosion for the subalpine and montane zones. This indicates that more marginal, transitional mountain zones are more sensitive to climatic disturbance than the alpine nucleus of the SM.

This is partially upheld in the context of European-era land use change, which is associated with more dramatic increases in erosion and peatland productivity for the subalpine zone, though the lack of a montane response implies zonal resilience. European-era destabilisation for the alpine-subalpine complex is more appreciable than for the highland domain, suggesting at least upper mountain catchments are more sensitive to land use as well as climate change. European-era instability for the High

Country as a whole is surpassed only by the hypsithermal onset events, suggesting greater high-altitude sensitivity to European land use change than any major Holocene climatic perturbations save for hypsithermal onset. The above interpretations are corroborated to varying degrees by global high-altitude records, suggesting the High Country is not representative of high-altitude systems globally.

The final objective of this study was to "consult interpretations of systemic sensitivity to make qualified prognoses of future environmental change at the zonal scale in the context of projected climate and land use change". For the Monaro, reconstructions suggest that future environmental responses to GEC will be defined by catchment drying, facilitating an expansion of modified pasture at the expense of Grassy Woodland and Temperate Grassland. This will also induce a shift from high-intensity, infrequent fires to low-intensity, frequent fires. Responses of the Monaro lakes themselves will be more spatially complex; rain shadow-emplaced systems are anticipated to become more permanent under projected increases in warm-season rainfall. This may render central Monaro lakes refugia for the Upland Wetlands TEC, which is likely to experience extirpation outside the rain shadow where year-round rainfall declines will force most lakes to downgrade to ephemeral states. Grassland expansion and lake desiccation may enhance the productivity of agriculture, which will exacerbate catchment erosion and lake eutrophication.

SM reconstructions indicate future systemic change is also likely to encompass catchment drying and intensified erosion under ongoing climate change, snowmelt declines, weed proliferation and feral horse grazing. Drying and erosion may reinforce a positive feedback with mountain peatlands and force many to convert to carbon sources. Data suggest that erosion and peatland decline will be most severe in the subalpine and montane zones, where relief is higher, soil mantles are thicker, mire productivity is lower, weeds are abundant, and grazing persists. Erosion and peatland degradation will also be exacerbated by amplified subalpine and montane burning, which will impact an increasingly larger proportion of the SM as the treeline advances, albeit with a multi-centennial lag.

6.2. Recommendations for future research

The previous section has noted several challenges encountered through implementation of the research objectives, which illuminate avenues for future research. Firstly, it was noted that there was high site variability in multiproxy relationships. While this inconsistency is argued be reflective of genuine differences in endogenous controls and site-level sensitivity, it is also probably an outcome of multiproxy sampling resolutions, which are low and inconsistent for most proxies/cores. This may be resulting in common environmental changes not being consistently registered between proxies and sites. Future research should therefore prioritise higher-resolution multiproxy analyses in order to more confidently assess site differences in responses to shared perturbations. This is especially critical for resolving sensitivity to European-era land use change, which for most records was limited to a simplistic pre- and postcolonial framework. This prevented insights into sensitivity to decadal to sub-decadal events such as the onset and termination of grazing and the implementation of various conservation strategies (e.g., TEC recovery plans).

It has also been acknowledged that there is large cross-altitudinal unevenness in the number and distribution of sites targeted in this study. This should be rectified through the analysis of a larger, more widespread population of records particularly for the montane zone, which despite being the largest zone, was investigated using the lowest number of records (n. 2). As for multiproxy analysis, the resolution of ^{14}C dating should also be significantly increased to improve the chronological confidence of records and the timing of discrete perturbations such as the hypsithermal onset events and European colonisation. Dating should also resolve issues surrounding sample fraction biases by either targeting a single fraction or, more ideally, multiple fractions for each sample. This will permit verification of any systemic younging or ageing arising from the analysis of bulk sediment or sporopollenin, as has been speculated in this study but remains unverified. This would, in turn, enable identification of whether age reversals, outliers or hiatuses are genuine which, in combination with a dense downcore dating, will strengthen age-depth models.

As has been intimated throughout Chapters 2–4, systemic reconstructions presented in this thesis can both diverge from and align with known paleoecological changes on short and long timescales, respectively. However, this conclusion is informed by comparisons with independent records from different locations and with different chronologies,

removing a common control variable necessary to validate systemic-ecological comparisons. It is therefore critical that future research performs both systemic and paleoecological analyses on the same records, which would enable a more direct and confident appraisal of the coherence, or lack thereof, between system- and species/community-scale changes.

This approach would be particularly impactful if applied to other mountain-highland complexes globally, such as those discussed in Section 5.3, which host a wealth of paleoecological data but lack geoecological emphasis. A global employment of coupled systemic-ecological empirical assessments would establish more universal constraints on the value of the methodology promoted in this thesis, rather than being relevant to a single region. That said, application of this systemic-ecological assessment on the High Country alone would still likely yield valuable information for stakeholders on long-term systemic-biotic interactions, which would be instrumental in the formulation of land management and conservation strategies aimed at increasing TEC resilience.

Finally, it is clear that there has been an inadequate investigation of precolonial land use impacts on the paleoenvironmental reconstructions presented here. This biases inferences of land use sensitivity to a European context, while also implicitly dismissing people in presuming precolonial changes to be overwhelmingly climatogenic. While this omission was justifiably informed by a) a consensus that pre-European changes were generally low-impact, and b) insufficient evidence to directly implicate Indigenous agency, this underscores the necessity for a systematic investigation of human trace proxies in order to resolve the relative influences of people on reconstructed trends. Given the cryptic expression of humans through conventional archaeological evidence across the High Country (and indeed Australia), future research should prioritise the analysis of more robust, quantitative proxies to establish more robust constraints on Indigenous population dynamics and impacts.

References

Abbas, H., Daramola, M. T. & Xu, M., 2024. Elevation-dependent warming and possible-driving mechanisms over global highlands. *International Journal of Climatology,* 44(12)**,** 4157-4177.

Adam, J. C., Hamlet, A. F. & Lettenmaier, D. P., 2009. Implications of global climate change for snowmelt hydrology in the twenty-first century. *Hydrological Processes: An International Journal,* 23(7)**,** 962-972.

AdaptNSW, 2024. *Climate change in the South East and Tablelands* [Online]. AdaptNSW, NSW Government. Available: https://www.climatechange.environment.nsw.gov.au/my-region/south-east-and-tablelands [Accessed April 2 2025].

Adhikari, S., Baral, H. & Nitschke, C., 2018. Adaptation to climate change in Panchase Mountain ecological regions of Nepal. *Environments,* 5(3)**,** 42.

Adler, C., Wester, P., Bhatt, I., Huggel, C., Insarov, G., Morecroft, M., Muccione, V., Prakash, A., Alcántara-Ayala, I. & Allen, S. K., 2023. Cross-chapter paper 5: mountains. *Climate change 2022: impacts, adaptation, and vulnerability*.

Aitchison, C., 2001. The effect of snow cover on small animals. *Snow ecology: an interdisciplinary examination of snow-covered ecosystems. Cambridge University Press, Cambridge***,** 229-265.

Albrich, K., Rammer, W. & Seidl, R., 2020. Climate change causes critical transitions and irreversible alterations of mountain forests. *Global Change Biology,* 26(7)**,** 4013-4027.

Alcock, D., 2012. Impacts of Projected Climate Change on Monaro Native Pasture Systems. NSW Department of Primary Industries. Cooma, NSW.

Allan, N. J., 1986. Accessibility and altitudinal zonation models of mountains. *Mountain Research and Development***,** 185-194.

Allen, J., 1996. *Report of the Southern Forests Archaeological Project: Site Descriptions, Stratigraphies and Chronologies*, School of Archaeology, La Trobe University. 186446111X

Anderson, D. E., 2002. Carbon accumulation and C/N ratios of peat bogs in North-West Scotland. *Scottish Geographical Journal,* 118(4)**,** 323-341.

Anderson, L., Wahl, D. B. & Bhattacharya, T., 2022. Understanding rates of change: a case study using fossil pollen records from California to assess the potential for and challenges to a regional data synthesis. *Quaternary International,* 621(26-36).

Aplin, K. P., Ford, F. & Hiscock, P., 2010. *Early Holocene Human Occupation and Environment of the Southeast Australian Alps: New Evidence from the Yarranbobilly Plateau, New South Wales*, ANU E Press.

Argue, D., 1995. Aboriginal occupation of the Southern Highlands: Was it really seasonal? *Australian Archaeology,* 41(1)**,** 30-36.

Armenteras, D., Rodríguez, N., Retana, J. & Morales, M., 2011. Understanding deforestation in montane and lowland forests of the Colombian Andes. *Regional Environmental Change,* 11(3)**,** 693-705.

Australian Bureau of Agricultural Resource Economics Sciences. 2024. Catchment Scale Land Use of Australia and Commodities – Update December 2023. CC BY 4.0. Australian Bureau of Agricultural Resource Economics Sciences -Australian Government Department of Agriculture, Fisheries and Forestry. 26 February 2024. https://www.agriculture.gov.au/abares/aclump/land-use/catchment-scale-land-use-and-commodities-update-2023.

Baiping, Z., 1995. Geoecology and sustainable development in the Kunlun Mountains, China. *Mountain Research and Development***,** 283-292.

Bakis, J., 2021. *A Holocene paleoenvironmental history of the Monaro Tablelands, NSW: Implications for future landscape response to climate.* Bachelor of Science/Advanced Studies Unpublished honours thesis, The University of Sydney.

Bakis, J., Penny, D., Hamilton, R., Hua, Q., Barry, L. & Gadd, P., 2025. Thresholds in montane sensitivity to climate and land use change over the Late Holocene: Multiproxy evidence from Snowy Mountains peat records, southeastern Australia. *Palaeogeography, Palaeoclimatology, Palaeoecology***,** Manuscript under review.

Bakis, J., Penny, D., Hamilton, R., Hua, Q., Barry, L. & Gadd, P., 2026. Asymmetric sensitivity of lake catchments to climate and land use change on the Monaro Tablelands, southeastern Australia: A multiproxy, multisite synthesis of postglacial lacustrine records. *Quaternary Science Reviews,* 373(109729). https://doi.org/10.1016/j.quascirev.2025.109729.

Bamonte, F. P., Echeverría, M. E. & Marcos, M. A., 2025. Last glacial–interglacial transition and early Holocene vegetation reconstruction: Pollen and plant macrofossil analysis from a Subantarctic forest sequence at 49°S. *Review of Palaeobotany and Palynology,* 343(105415). https://doi.org/10.1016/j.revpalbo.2025.105415.

Banks, J., 1989. A history of forest fire in the Australian Alps. *The scientific significance of the Australian Alps***,** 265-80.

Barnes, J., 1982. *The Presocratic Philosophers,* London, Routledge. 9780415050791

Barr, C., Tibby, J., Leng, M., Tyler, J., Henderson, A., Overpeck, J., Simpson, G., Cole, J., Phipps, S. & Marshall, J., 2019. Holocene el Niño–southern Oscillation variability reflected in subtropical Australian precipitation. *Scientific Reports,* 9(1)**,** 1627.

Barrows, T. T., Mills, S. C., Fitzsimmons, K., Wasson, R. & Galloway, R., 2022. Low-altitude periglacial activity in southeastern Australia during the late Pleistocene. *Quaternary Research,* 107(125-146).

Barrows, T. T., Stone, J. O. & Fifield, L. K., 2004. Exposure ages for Pleistocene periglacial deposits in Australia. *Quaternary Science Reviews,* 23(5-6)**,** 697-708.

Barrows, T. T., Stone, J. O., Fifield, L. K. & Cresswell, R. G., 2001. Late Pleistocene glaciation of the Kosciuszko massif, snowy mountains, Australia. *Quaternary Research,* 55(2)**,** 179-189.

Barrows, T. T., Stone, J. O., Fifield, L. K. & Cresswell, R. G., 2002. The timing of the last glacial maximum in Australia. *Quaternary Science Reviews,* 21(1-3)**,** 159-173.

Bassett, O. D., Prior, L. D., Slijkerman, C. M., Jamieson, D. & Bowman, D. M., 2015. Aerial sowing stopped the loss of alpine ash (*Eucalyptus delegatensis*) forests burnt by three short-interval fires in the Alpine National Park, Victoria, Australia. *Forest Ecology and Management,* 342(39-48).

Bauch, C. T., Sigdel, R., Pharaon, J. & Anand, M., 2016. Early warning signals of regime shifts in coupled human–environment systems. *Proceedings of the National Academy of Sciences,* 113(51)**,** 14560-14567. doi:10.1073/pnas.1604978113.

Beckage, B., Osborne, B., Gavin, D. G., Pucko, C., Siccama, T. & Perkins, T., 2008. A rapid upward shift of a forest ecotone during 40 years of warming in the Green Mountains of Vermont. *Proceedings of the National Academy of Sciences,* 105(11)**,** 4197-4202.

Becker, A. & Bugmann, H., 2001. Global change and mountain regions—an IGBP initiative for collaborative research. *Global change and protected areas.* Springer. 3-9

Beniston, M., 1999. Global environmental change in mountain regions: an overview. *Geographica Helvetica,* 54(3)**,** 120-124.

Beniston, M., 2003. Climatic change in mountain regions: a review of possible impacts. *Climatic Change,* 59(1)**,** 5-31.

Beniston, M., 2016. *Environmental change in mountains and uplands*, Routledge. 1315824825

Benson, J., 1994. *The native grasslands of the Monaro region: Southern Tablelands of NSW*, sn.

Benson, J. & Jacobs, S., 1994. Plant communities of the Monaro lakes. *Cunninghamia,* 3(651-76).

Benson, L., Kashgarian, M., Rye, R., Lund, S., Paillet, F., Smoot, J., Kester, C., Mensing, S., Meko, D. & Lindström, S., 2002. Holocene multidecadal and multicentennial droughts affecting Northern California and Nevada. *Quaternary Science Reviews,* 21(4-6)**,** 659-682.

Bergstrom, D. M., Wienecke, B. C., Van den Hoff, J., Hughes, L., Lindenmayer, D. B., Ainsworth, T. D., Baker, C. M., Bland, L., Bowman, D. M. & Brooks, S. T., 2021. Combating ecosystem collapse from the tropics to the Antarctic. *Global Change Biology,* 27(9)**,** 1692-1703.

Bilish, S., 2020. Snowpack processes and dynamics in the marginal snow environment of the Australian Alps.

Bilish, S. P., Callow, J. N. & McGowan, H. A., 2020. Streamflow variability and the role of snowmelt in a marginal snow environment. *Arctic, Antarctic, and Alpine Research,* 52(1)**,** 161-176.

Birks, H. H. & Birks, H. J. B., 2006. Multi-proxy studies in palaeolimnology. *Vegetation History and Archaeobotany,* 15(235-251).

Bishop, P., 1988. The eastern highlands of Australia: the evolution of an intraplate highland belt. *Progress in Physical Geography,* 12(2)**,** 159-182.

Blaauw, M., 2010. Methods and code for 'classical'age-modelling of radiocarbon sequences. *Quaternary Geochronology,* 5(5)**,** 512-518.

Blaauw, M. & Christen, J. A., 2011. Flexible paleoclimate age-depth models using an autoregressive gamma process. *Bayesian Analysis,* 6(3)**,** 457-474, 18.

Black, M. P., Mooney, S. D. & Haberle, S. G., 2007. The fire, human and climate nexus in the Sydney Basin, eastern Australia. *The Holocene,* 17(4)**,** 469-480.

Blau, M. T., Kad, P., Turton, J. V. & Ha, K.-J., 2024. Uneven global retreat of persistent mountain snow cover alongside mountain warming from ERA5-land. *npj Climate and Atmospheric Science,* 7(1)**,** 278.

Blott, S. J. & Pye, K., 2001. GRADISTAT: a grain size distribution and statistics package for the analysis of unconsolidated sediments. *Earth Surface Processes and Landforms,* 26(11)**,** 1237-1248.

Blyth, S., 2002. *Mountain watch: environmental change & sustainable developmental in mountains*, UNEP/Earthprint. 1899628207

Boland, D. J., 2006. *Forest trees of Australia*, CSIRO publishing. 0643069690

Bowler, J., 1981. Australian salt lakes: a palaeohydrologic approach. *Salt Lakes: Proceedings of the International Symposium on Athalassic (Inland) Salt Lakes, held at Adelaide, Australia, October 1979.* Springer. 431-444

Bowler, J. & Hamada, T., 1971. Late Quaternary stratigraphy and radiocarbon chronology of water level fluctuations in Lake Keilambete, Victoria. *Nature,* 232(5309)**,** 330-332.

Bowman, D. M., Murphy, B. P., Neyland, D. L., Williamson, G. J. & Prior, L. D., 2014. Abrupt fire regime change may cause landscape-wide loss of mature obligate seeder forests. *Global Change Biology,* 20(3)**,** 1008-1015.

Bradley, R. S., 2008. 10 Holocene perspectives on future climate change. *Natural Climate Variability and Global Warming***,** 254.

Brandt, J. S., Haynes, M. A., Kuemmerle, T., Waller, D. M. & Radeloff, V. C., 2013. Regime shift on the roof of the world: Alpine meadows converting to shrublands in the southern Himalayas. *Biological Conservation,* 158(116-127). https://doi.org/10.1016/j.biocon.2012.07.026.

Brereton, R., Bennett, S. & Mansergh, I., 1995. Enhanced greenhouse climate change and its potential effect on selected fauna of south-eastern Australia: a trend analysis. *Biological Conservation,* 72(3)**,** 339-354.

Brookhouse, M. T., Farrow, R., Meyer, J., McDougall, K., Ward-Jones, J. & Wright, G. T., 2024. Incidence and severity of *Phoracantha*-induced decline within high-elevation eucalypt woodlands are strongly associated with elevation and land management. *Forest Ecology and Management,* 561(121872).

Brown, J. & Ingram, L., 2021. Increased Above-Ground Biomass and Plant Species Decline Related to the Presence of *Eragrostis curvula* across Multiple Grazing Grasslands in the Snowy Monaro Region of Australia.

Brown, M., 1994. An interpretation of Tertiary landform evolution in the area of the Monaro Volcanic Province. *The Tertiary geology and geomorphology of the Monaro: The perspective in*, 30-35.

Brown, M., McQueen, K. & Taylor, G., 1992. A core through the Monaro basalt: Bega (BMR) no. 7. *Australian Journal of Earth Sciences,* 39(4), 555-559.

Brown, R. D. & Mote, P. W., 2009. The response of Northern Hemisphere snow cover to a changing climate. *Journal of Climate,* 22(8), 2124-2145.

Bryant, C., Ball, M. C., Borevitz, J., Brookhouse, M. T., Carle, H., Cunningham, P., Davey, M., Davies, J., Eason, A. & Erskine, J. D., 2024. Elevation-dependent patterns of borer-mediated snow-gum dieback are associated with subspecies' trait differences and environmental variation. *Austral Ecology,* 49(3), e13508.

Bryant, W., 1971. Deterioration of vegetation and erosion in the Guthega catchment area, Snowy Mountains, NSW. *Soil Conservation Journal,* 27(62-81.

Burdick, A. W., 2022. Reconstructing deglacial and Holocene climatic and environmental change in the Snowy Mountains of southeast Australia.

Bureau of Meteorology, 2025a. *Climate statistics for Australian locations: Cooma Visitors Centre (070278)* [Online]. Bureau of Meteorology. Available: http://www.bom.gov.au/climate/averages/tables/cw_070278.shtml [Accessed May 3 2025].

Bureau of Meteorology, 2025b. *The Southern Annular Mode in winter: Rainfall impacts* [Online]. Available: http://www.bom.gov.au/climate/sam/content/samwinter-rain.html [Accessed].

Bush, M. B., 2020. New and Repeating Tipping Points: The Interplay of Fire, Climate Change, and Deforestation in Neotropical Ecosystems1. *Annals of the Missouri Botanical Garden,* 105(3), 393-404.

Butterbach-Bahl, K., Kögel-Knabner, I. & Han, X., 2011. Steppe ecosystems and climate and land-use changes—vulnerability, feedbacks and possibilities for adaptation. *Plant and Soil,* 340(1), 1-6.

Byles, B. U., 1932. *Report on a reconnaissance of the mountainous part of the River Murray catchment in New South Wales*, Commonwealth Forestry Bureau.

Cadd, H., Sherborne-Higgins, B., Becerra-Valdivia, L., Tibby, J., Barr, C., Forbes, M., Cohen, T. J., Tyler, J., Vandergoes, M. & Francke, A., 2022. The application of pollen radiocarbon dating and bayesian age-depth modeling for developing robust geochronological frameworks of wetland archives. *Radiocarbon,* 64(2), 213-235.

Cai, W., Ng, B., Geng, T., Jia, F., Wu, L., Wang, G., Liu, Y., Gan, B., Yang, K. & Santoso, A., 2023. Anthropogenic impacts on twentieth-century ENSO variability changes. *Nature Reviews Earth & Environment,* 4(6), 407-418.

Calvo, E., Pelejero, C., De Deckker, P. & Logan, G. A., 2007. Antarctic deglacial pattern in a 30 kyr record of sea surface temperature offshore South Australia. *Geophysical Research Letters,* 34(13).

Carr, G., Yugovic, J. & Robinson, K. E., 1992. *Environmental weed invasions in Victoria: conservation and management implications*, Department of Conservation and Environment and Ecological Horticulture Pty …. 0730626512

Carré, M., Braconnot, P., Elliot, M., d'Agostino, R., Schurer, A., Shi, X., Marti, O., Lohmann, G., Jungclaus, J. & Cheddadi, R., 2021. High-resolution marine data and transient simulations support orbital forcing of ENSO amplitude since the mid-Holocene. *Quaternary Science Reviews,* 268(107125).

Carré, M., Sachs, J. P., Purca, S., Schauer, A. J., Braconnot, P., Falcón, R. A., Julien, M. & Lavallée, D., 2014. Holocene history of ENSO variance and asymmetry in the eastern tropical Pacific. *Science,* 345(6200)**,** 1045-1048.

Chape, S., Harrison, J., Spalding, M. & Lysenko, I., 2005. Measuring the extent and effectiveness of protected areas as an indicator for meeting global biodiversity targets. *Philosophical Transactions of the Royal Society B: Biological Sciences,* 360(1454)**,** 443-455.

Charman, D. J., Beilman, D. W., Blaauw, M., Booth, R. K., Brewer, S., Chambers, F. M., Christen, J. A., Gallego-Sala, A., Harrison, S. P. & Hughes, P. D., 2013. Climate-related changes in peatland carbon accumulation during the last millennium. *biogeosciences,* 10(2)**,** 929-944.

Chen, L., Wang, L., Li, T. & Liu, J., 2019. Drivers of reduced ENSO variability in mid-Holocene in a coupled model. *Climate Dynamics,* 52(9)**,** 5999-6014. 10.1007/s00382-018-4496-5.

Cheng, L. & Ye, W., 2019. Multi-proxy evidence for paleoclimate evolution performed on a paleolake sediment core in the East Asian Monsoon Region. *Environmental Earth Sciences,* 78(3)**,** 92.

Chubb, T. H., Siems, S. T. & Manton, M. J., 2011. On the decline of wintertime precipitation in the Snowy Mountains of southeastern Australia. *Journal of Hydrometeorology,* 12(6)**,** 1483-1497.

Cifuentes-Croquevielle, C., Stanton, D. E. & Armesto, J. J., 2020. Soil invertebrate diversity loss and functional changes in temperate forest soils replaced by exotic pine plantations. *Scientific reports,* 10(1)**,** 7762.

Clark, E., 1992. Alpine grazing, a tale of two states. *In:* Grenier, P. & Good, R. B. (eds.) *The Australian Alps.* Grenoble: Institut de Géographie Alpine.

Clark, P. U., Shakun, J. D., Baker, P. A., Bartlein, P. J., Brewer, S., Brook, E., Carlson, A. E., Cheng, H., Kaufman, D. S. & Liu, Z., 2012. Global climate evolution during the last deglaciation. *Proceedings of the National Academy of Sciences,* 109(19)**,** E1134-E1142.

Clement, A. C., Seager, R. & Cane, M. A., 2000. Suppression of El Niño during the mid-Holocene by changes in the Earth's orbit. *Paleoceanography,* 15(6)**,** 731-737.

Clerke, L., 2023. *Hydrological regime of Australian lakes over the Late-Quaternary and Holocene.* Thesis (Master of Research), Macquarie University, Faculty of Science and Engineering, School of Natural Sciences.

Clothier, D. & Condon, R., 1968. Soil conservation in alpine catchments. *Journal of the Soil Conservation Service of New South Wales,* 24(96-113).

Clymo, R., 1984. The limits to peat bog growth. *Philosophical Transactions of the Royal Society of London. B, Biological Sciences,* 303(1117)**,** 605-654.

Cohen, A. S., 2003. *Paleolimnology: the history and evolution of lake systems*, Oxford university press. 0195350898

Cohen, T. J. & Nanson, G. C., 2007. Mind the gap: an absence of valley-fill deposits identifying the Holocene hypsithermal period of enhanced flow regime in southeastern Australia. *The Holocene,* 17(3)**,** 411-418.

Colhoun, E. & Peterson, J., 1986. Quaternary landscape evolution and the cryosphere: research progress from Sahul to Australian Antarctica. *Australian Geographical Studies,* 24(1)**,** 145-167.

Colhoun, E. A. & Barrows, T. T., 2011. The glaciation of Australia. *Developments in Quaternary Sciences.* Elsevier. 1037-1045

Conroy, J. L., Overpeck, J. T., Cole, J. E., Shanahan, T. M. & Steinitz-Kannan, M., 2008. Holocene changes in eastern tropical Pacific climate inferred from a Galápagos lake sediment record. *Quaternary Science Reviews,* 27(11-12)**,** 1166-1180.

Cook, D. E., 2021. Anthropogenic environmental change on the frontiers of European colonisation in Australia, AD 1788–1840. A reply to comments in Woodward (2020). *Geomorphology,* 373(107234.

Coop, J. D., Parks, S. A., Stevens-Rumann, C. S., Crausbay, S. D., Higuera, P. E., Hurteau, M. D., Tepley, A., Whitman, E., Assal, T. & Collins, B. M., 2020. Wildfire-driven forest conversion in western North American landscapes. *BioScience,* 70(8)**,** 659-673.

Cooper, C. S., Porinchu, D. F., Reinemann, S. A., Mark, B. G. & DeGrand, J. Q., 2021. A lake sediment–based paleoecological reconstruction of late Holocene fire history and vegetation change in Great Basin National Park, Nevada, USA. *Quaternary Research,* 104(28-42. 10.1017/qua.2021.17.

Copernicus Data Space Ecosystem, 2025. *Copernicus Browser — Copernicus Data Space Ecosystem* [Online]. Copernicus Data Space Ecosystem / European Union Space Programme. Available: https://browser.dataspace.copernicus.eu/ [Accessed].

Cosgrove, R., 1989. Thirty thousand years of human colonization in Tasmania: new Pleistocene dates. *Science,* 243(4899)**,** 1706-1708.

Costin, A., 1955. Alpine soils in Australia with reference to conditions in Europe and New Zealand.

Costin, A., 1957. The grazing factor and the maintenance of catchment values in the Australian Alps.

Costin, A., 1989. The Alps in a global perspective. *The scientific significance of the Australian Alps,* 7(19).

Costin, A. B., 1954. *A study of the ecosystems of the Monaro region of New South Wales, with special reference to soil erosion*, AH Pettifer, Government printer.

Costin, A. B., 1972. Carbon-14 dates from the Snowy Mountains area, southeastern Australia, and their interpretation. *Quaternary Research,* 2(4)**,** 579-590.

Costin, A. B., 2000. *Kosciuszko alpine flora*, CSIRO publishing. 0643065229

Costin, A. B. & Polach, H. A., 1971. Slope deposits in the Snowy Mountains, south-eastern Australia. *Quaternary Research,* 1(2)**,** 228-235.

Costin, A. B., Wimbush, D. & Kerr, D., 1960. Studies in catchment hydrology in the Australian Alps. H. Surface runoff and soil loss.

Cresswell, I., Janke, T. & Johnston, E., 2021. Australia state of the environment 2021: overview, independent report to the Australian Government Minister for the Environment, Commonwealth of Australia, Canberra. *Australia State of the Environment*.

Cristea, G., Cuna, S. M., Fărcaş, S., Tanţău, I., Dordai, E. & Măgdaş, D. A., 2014. Carbon isotope composition as indicator for climatic changes during the middle and late Holocene in a peat bog from Maramureş Mountains (Romania). *The Holocene,* 24(1)**,** 15-23.

Critical Ecosystem Partnership Fund, 2024. *Explore the Biodiversity Hotspots* [Online]. Online: Critical Ecosystem Partnership Fund. Available: https://www.cepf.net/node/1996 [Accessed 17 September 2024].

Croudace, I. W. & Rothwell, R. G. (eds.) 2015. *Micro-XRF Studies of Sediment Cores: Applications of a non-destructive tool for the environmental sciences,* Dordrecht: Springer Dordrecht.

Cullen, B., Johnson, I., Eckard, R., Lodge, G., Walker, R., Rawnsley, R. & McCaskill, M., 2009. Climate change effects on pasture systems in south-eastern Australia. *Crop and pasture science,* 60(10)**,** 933-942.

Currie, M. J., 1825. Journal of an excursion to the southward of Lake George. *In:* Field, B. (ed.) *Geographical Memoirs of New South Wales.* London: John Murray. Quoted in Young M (2000), The Aboriginal People of the Monaro. New South Wales Parks and Wildlife Service, Jindabyne, NSW, pp. 68–71

Das, P., Behera, M. D., Roy, P. S. & Barik, S. K., 2024. Predicting tipping points of vegetation resilience as a response to precipitation: Implications for understanding impacts of climate change in India. *Biodiversity and Conservation,* 33(12)**,** 3441-3458.

Dätwyler, C., Grosjean, M., Steiger, N. J. & Neukom, R., 2020. Teleconnections and relationship between the El Niño–Southern Oscillation (ENSO) and the Southern Annular Mode (SAM) in reconstructions and models over the past millennium. *Climate of the Past,* 16(2)**,** 743-756.

Davenport, F. V., Herrera-Estrada, J. E., Burke, M. & Diffenbaugh, N. S., 2020. Flood size increases nonlinearly across the western United States in response to lower snow-precipitation ratios. *Water Resources Research,* 56(1)**,** e2019WR025571.

Davies, S. J., Lamb, H. F. & Roberts, S. J., 2015. Micro-XRF Core Scanning in Palaeolimnology: Recent Developments. *In:* Croudace, I. W. & Rothwell, R. G. (eds.) *Micro-XRF Studies of Sediment Cores: Applications of a non-destructive tool for the environmental sciences.* Dordrecht: Springer Netherlands. 189-226

Department of Climate Change, the Environment, Energy and Water. 2015a. Grasslands, Pre-Settlement, South-eastern Highlands. The Sharing and Enabling Environmental Data Portal. NSW Department of Climate Change, E., The Environment and Water. 2025-04-25. https://datasets.seed.nsw.gov.au/dataset/6f80012b-00a4-412e-9595-701dfde1e70e.

Department of Climate Change, the Environment, Energy and Water. 2015b. MonaroLakesPC_1994_E_4154. NSW Department of Climate Change, Energy, the Environment and Water. The Central Resource for Sharing and Enabling Environmental Data in NSW. 1993. https://datasets.seed.nsw.gov.au/dataset/plant-communities-of-the-monaro-lakes-vis_id-41544f966. 26 November 2023

Department of Climate Change, the Environment, Energy and Water. 2016a. NSW State Vegetation Type Map. NSW Department of Climate Change, Energy, the Environment and Water. https://datasets.seed.nsw.gov.au/dataset/95437fbd-2ef7-44df-8579-d7a64402d42d.

Department of Climate Change, the Environment, Energy and Water. 2016b. Peat-forming bogs and fens of the Snowy Mountains. NSW Department of Climate Change, Energy, the Environment and Water. Nanson, R. & Hope, G. https://datasets.seed.nsw.gov.au/dataset/06b9b7b7-4214-4d8d-b442-ec3d4d69aa85.

Department of Climate Change, the Environment, Energy and Water. 2019. Critically Endangered Ecological Community: Monaro and Werriwa Tablelands Cool Temperate Grassy Woodlands v1.4. NSW Department of Climate Change, Energy, the Environment and Water. The Central Resource for Sharing and Enabling Environmental Data in NSW. https://datasets.seed.nsw.gov.au/dataset/ceec-monaro-and-werriwa-tablelands-cool-temperate-grassy-woodlands-v1-4. 29 April 2022

Department of Climate Change, the Environment, Energy and Water. 2020. Interim Biogeographic Regionalisation for Australia (IBRA), Version 7 (Subregions). Australian Government, Department of Climate Change, Energy, the Environment and Water. https://gis.environment.gov.au/gispubmap/rest/services/ogc_services/IBRA7_Subregions/MapServer/0.

Department of Climate Change, the Environment, Energy and Water. 2023. Interim Biogeographic Regionalisation for Australia (IBRA) Version 7.0. Australian Government Department of Climate Change, Energy, the Environment and Water. 25 April 2025. https://fed.dcceew.gov.au/datasets/fa066cfb26ff4ccdb8172a38734905cc/about.

Department of Climate Change, the Environment, Energy and Water, 2024a. NARCliM2.0 NSW South East Tablelands regional climate change snapshot. 978-1-76058-804-5. NSW Department of Climate Change, Energy, the Environment and Water. Parramatta, NSW.

Department of Climate Change, the Environment, Energy and Water. 2024b. NARCliM climate projections. NSW Department of Climate Change, Energy, the Environment and Water. 2024-06-14. https://data.nsw.gov.au/data/dataset/8ef07543-174f-4bdd-bbf4-5c2e3a652802.

Department of Climate Change, the Environment, Energy and Water. 2025. National Vegetation Information System (NVIS) data products. 7.0. Australian Government, Department of Climate Change, Energy, the Environment and Water. 2025-11-13. https://www.dcceew.gov.au/environment/environment-information-australia/national-vegetation-information-system/data-products.

De Deckker, P., 2022. The Holocene hypsithermal in the Australian region. *Quaternary Science Advances,* 7(100061).

De Deckker, P., Hancock, G. J., Olley, J. M., Stanley, S. & Hope, G., 2023. The effect of the introduction of livestock on the erosion of alpine soils: a comparison of five dating techniques applied to sediments of the Australian alpine Blue Lake. *Journal of Paleolimnology,* 70(2)**,** 77-93.

De Jong, R., Blaauw, M., Chambers, F. M., Christensen, T. R., De Vleeschouwer, F., Finsinger, W., Fronzek, S., Johansson, M., Kokfelt, U. & Lamentowicz, M., 2010. *Climate and peatlands*, Springer. 904818715X

de Porras, M. E., Maldonado, A., Abarzúa, A. M., Cárdenas, M. L., Francois, J. P., Martel-Cea, A., Stern, C. R., Méndez, C. & Reyes, O., 2012. Postglacial vegetation, fire and climate dynamics at Central Chilean Patagonia (Lake Shaman, 44 S). *Quaternary Science Reviews,* 50(71-85).

de Porras, M. E., Maldonado, A., Quintana, F., Martel-Cea, A., Reyes, O. & Méndez, C., 2014. Environmental and climatic changes in central Chilean Patagonia since the late glacial (Mallín El Embudo, 44 S). *Climate of the Past,* 10(3)**,** 1063-1078.

de Villemereuil, P., Mouterde, M., Gaggiotti, O. E. & Till-Bottraud, I., 2018. Patterns of phenotypic plasticity and local adaptation in the wide elevation range of the alpine plant Arabis alpina. *Journal of Ecology,* 106(5)**,** 1952-1971.

Dearing, J. A., 1999a. *Environmental Magnetic Susceptibility: Using the Bartington MS2 System,* United Kingdom, Bartington Instruments Ltd. 0952340909

Dearing, J. A., 1999b. Holocene environmental change from magnetic proxies in lake sediments. *In:* Maher, B. A. & Thompson, R. (eds.) *Quaternary Climates, Environments and Magnetism.* Cambridge: Cambridge University Press. 231-278

Deline, P., Gruber, S., Delaloye, R., Fischer, L., Geertsema, M., Giardino, M., Hasler, A., Kirkbride, M., Krautblatter, M. & Magnin, F., 2015. Ice loss and slope stability in high-mountain regions. *Snow and ice-related hazards, risks, and disasters.* Elsevier. 521-561

Deng, K., Azorin-Molina, C., Yang, S., Hu, C., Zhang, G., Minola, L. & Chen, D., 2022. Changes of Southern Hemisphere westerlies in the future warming climate. *Atmospheric Research,* 270(106040.

Department of Customer Service Spatial Services. 2020. NSW Administrative Boundaries Theme MultiCRS - Local Government Area. NSW Government. https://www.spatial.nsw.gov.au/publications/information_sheets/data_dictionaries.

Department of Regional New South Wales. 2017. Conservation value of NSW Travelling Stock Reserves (TSRs). Department of Regional New South Wales. https://www.seed.nsw.gov.au.

Department of the Environment and Energy, 2016. Natural Temperate Grassland of the South Eastern Highlands: a nationally protected ecological community. Commonwealth of Australia, Canberra.

Department of the Environment and Heritage, 2005. Upland Wetlands of the New England Tablelands and the Monaro Plateau. Canberra, Australia.

Diaz, H. F. & Eischeid, J. K., 2007. Disappearing “alpine tundra” Köppen climatic type in the western United States. *Geophysical Research Letters,* 34(18).

Diaz, H. F., Grosjean, M. & Graumlich, L., 2003. Climate variability and change in high elevation regions: past, present and future. *Climatic change,* 59(1)**,** 1-4.

Dinerstein, E., Olson, D., Joshi, A., Vynne, C., Burgess, N. D., Wikramanayake, E., Hahn, N., Palminteri, S., Hedao, P. & Noss, R., 2017. An ecoregion-based approach to protecting half the terrestrial realm. *BioScience,* 67(6)**,** 534-545.

Ding, R., Tseng, Y. H., Di Lorenzo, E., Shi, L., Li, J., Yu, J.-Y., Wang, C., Sun, C., Luo, J.-J. & Ha, K. J., 2022. Multi-year El Niño events tied to the North Pacific oscillation. *Nature Communications,* 13(1)**,** 3871.

Dixon, B. C., Tyler, J. J., Lorrey, A. M., Goodwin, I. D., Gergis, J. & Drysdale, R. N., 2017. Low-resolution Australasian palaeoclimate records of the last 2000 years. *Climate of the Past,* 13(10)**,** 1403-1433.

Dodson, J., 1986. Holocene vegetation and environments near Goulburn, New South Wales. *Australian journal of botany,* 34(3)**,** 231-249.

Dodson, J., De Salis, T., Myers, C. & Sharp, A., 1994. A thousand years of environmental change and human impact in the alpine zone at Mt Kosciusko, New South Wales. *The Australian Geographer,* 25(1)**,** 77-87.

Dodson, J. R. & Mooney, S. D., 2002. An assessment of historic human impact on south-eastern Australian environmental systems, using late Holocene rates of environmental change. *Australian Journal of botany,* 50(4)**,** 455-464.

Doerr, S., Shakesby, R., Blake, W., Chafer, C., Humphreys, G. & Wallbrink, P., 2006. Effects of differing wildfire severities on soil wettability and implications for hydrological response. *Journal of Hydrology,* 319(1-4)**,** 295-311.

Donders, T. H., Haberle, S. G., Hope, G., Wagner, F. & Visscher, H., 2007. Pollen evidence for the transition of the Eastern Australian climate system from the post-glacial to the present-day ENSO mode. *Quaternary Science Reviews,* 26(11-12)**,** 1621-1637.

Donders, T. H., Wagner-Cremer, F. & Visscher, H., 2008. Integration of proxy data and model scenarios for the mid-Holocene onset of modern ENSO variability. *Quaternary Science Reviews,* 27(5-6)**,** 571-579.

Donders, T. H., Wagner, F. & Visscher, H., 2006. Late Pleistocene and Holocene subtropical vegetation dynamics recorded in perched lake deposits on Fraser Island, Queensland, Australia. *Palaeogeography, Palaeoclimatology, Palaeoecology,* 241(3-4)**,** 417-439.

Dorrough, J. & Ash, J., 2003. The impact of livestock grazing on the persistence of a perennial forb in a temperate Australian grassland. *Pacific Conservation Biology,* 9(4)**,** 302-307.

Dorrough, J., Ash, J. & McIntyre, S., 2004. Plant responses to livestock grazing frequency in an Australian temperate grassland. *Ecography,* 27(6)**,** 798-810.

Driscoll, D. A., Worboys, G. L., Allan, H., Banks, S. C., Beeton, N. J., Cherubin, R. C., Doherty, T. S., Finlayson, C. M., Green, K. & Hartley, R., 2019. Impacts of feral

horses in the Australian Alps and evidence-based solutions. *Ecological Management & Restoration,* 20(1)**,** 63-72.

Drollinger, S., Kuzyakov, Y. & Glatzel, S., 2019. Effects of peat decomposition on δ13C and δ15N depth profiles of Alpine bogs. *Catena,* 178(1-10.

Dyring, J., 1990. *The impact of feral horses (Equus caballus) on sub-alpine and montane environments in Australia.* University of Canberra.

Dzwonko, Z., Loster, S. & Gawroński, S., 2018. Effects of fire severity on understory community regeneration and early succession after burning of moist pine forest. *Tuexenia,* 38(

Echeverria, M. E., Sottile, G. D., Mancini, M. V. & Fontana, S. L., 2014. *Nothofagus* forest dynamics and palaeoenvironmental variations during the mid and late Holocene, in southwest Patagonia. *The Holocene,* 24(8)**,** 957-969. 10.1177/0959683614534742.

Edwards, A. C., Scalenghe, R. & Freppaz, M., 2007. Changes in the seasonal snow cover of alpine regions and its effect on soil processes: a review. *Quaternary international,* 162(172-181).

Egan, P. A. & Price, M. F., 2017. Mountain ecosystem services and climate change: A global overview of potential threats and strategies for adaptation.

Ehrlich, D., Melchiorri, M. & Capitani, C., 2021. Population trends and urbanisation in mountain ranges of the world. *Land,* 10(3)**,** 255.

Elsen, P. R., Monahan, W. B. & Merenlender, A. M., 2020. Topography and human pressure in mountain ranges alter expected species responses to climate change. *Nature Communications,* 11(1)**,** 1974.

Elsen, P. R. & Tingley, M. W., 2015. Global mountain topography and the fate of montane species under climate change. *Nature Climate Change,* 5(8)**,** 772-776.

Elumeeva, T. G., Onipchenko, V. G., Egorov, A. V., Khubiev, A. B., Tekeev, D. K., Soudzilovskaia, N. A. & Cornelissen, J. H., 2013. Long-term vegetation dynamic in the Northwestern Caucasus: which communities are more affected by upward shifts of plant species? *Alpine Botany,* 123(77-85).

Environment, D. o. & NSW, C. C., 2008. The Central Monaro Reserves – Plan of Management. Department of Environment and Climate Change NSW. Sydney, New South Wales, Australia.

Eyles, R., 1977. Changes in drainage networks since 1820, Southern Tablelands, NSW. *Australian Geographer,* 13(6)**,** 377-386.

Eyring, V., Bony, S., Meehl, G. A., Senior, C. A., Stevens, B., Stouffer, R. J. & Taylor, K. E., 2016. Overview of the Coupled Model Intercomparison Project Phase 6 (CMIP6) experimental design and organization. *Geoscientific Model Development,* 9(5)**,** 1937-1958.

Fahey, B. & Jackson, R., 1997. Hydrological impacts of converting native forests and grasslands to pine plantations, South Island, New Zealand. *Agricultural and Forest Meteorology,* 84(1-2)**,** 69-82.

Ferguglia, O., Palazzi, E. & Arnone, E., 2024. Elevation dependent change in ERA5 precipitation and its extremes. *Climate Dynamics,* 62(8)**,** 8137-8153.

Fewster, R., Swindles, G., Carrivick, J., Gałka, M., Roland, T., McKeown, M., Sutherland, J., Tweed, F., Mullan, D. & Graham, C., 2025. Climate warming and deglaciation drive new peat formation in the Southern Alps, Aotearoa/New Zealand. *Geophysical Research Letters,* 52(4)**,** e2024GL113786.

Fick, S. E. & Hijmans, R. J., 2017. WorldClim 2: new 1-km spatial resolution climate surfaces for global land areas. *International journal of climatology,* 37(12)**,** 4302-4315.

Fiddes, S. L. & Pezza, A. B., 2015. Current and future climate variability associated with wintertime precipitation in alpine Australia. *Climate Dynamics,* 44(9)**,** 2571-2587.

Field, C. B., Lobell, D. B., Peters, H. A. & Chiariello, N. R., 2007. Feedbacks of terrestrial ecosystems to climate change. *Annu. Rev. Environ. Resour.,* 32(1)**,** 1-29.

Fierro, A. O. & Leslie, L. M., 2014. Relationships between southeast Australian temperature anomalies and large-scale climate drivers. *Journal of climate,* 27(4)**,** 1395-1412.

Fink, D., Hotchkis, M., Hua, Q., Jacobsen, G., Smith, A. M., Zoppi, U., Child, D., Mifsud, C., van der Gaast, H. & Williams, A., 2004. The antares AMS facility at ANSTO. *Nuclear Instruments and Methods in Physics Research Section B: Beam Interactions with Materials and Atoms,* 223(109-115).

Fisher, G. & van Velthuizen, H., 2002. Global Agro-ecological Assessment for Agriculture in the 21st Century: Methodology and Results, IIASA, FAO. *RR-02-02, March*.

Fitzsimmons, K. E. & Barrows, T. T., 2010. Holocene hydrologic variability in temperate southeastern Australia: an example from Lake George, New South Wales. *The Holocene,* 20(4)**,** 585-597.

Flood, J., 1980. The moth hunters: Aboriginal prehistory of the Australian Alps. *(No Title)*.

Fogt, R. L. & Marshall, G. J., 2020. The Southern Annular Mode: variability, trends, and climate impacts across the Southern Hemisphere. *Wiley Interdisciplinary Reviews: Climate Change,* 11(4)**,** e652.

Fort, M., 2015. Impact of climate change on mountain environment dynamics. An introduction. *Journal of Alpine Research| Revue de géographie alpine,* 103-2).

Foster, J. R. & D'Amato, A. W., 2015. Montane forest ecotones moved downslope in northeastern USA in spite of warming between 1984 and 2011. *Global Change Biology,* 21(12)**,** 4497-4507.

Francke, A., Dosseto, A., Panagiotopoulos, K., Leicher, N., Lacey, J. H., Kyrikou, S., Wagner, B., Zanchetta, G., Kouli, K. & Leng, M. J., 2019. Sediment residence time reveals Holocene shift from climatic to vegetation control on catchment erosion in the Balkans. *Global and Planetary Change,* 177(186-200).

Franco, C., Maldonado, A., Ohlendorf, C., Gebhardt, A. C., de Porras, M. E., Nuevo-Delaunay, A., Méndez, C. & Zolitschka, B., 2024. Holocene environmental and climate evolution of central west Patagonia as reconstructed from lacustrine

sediments of Meseta Chile Chico (46.5° S, Chile). *Clim. Past,* 20(4)**,** 817-839. 10.5194/cp-20-817-2024.

Fraser, I. P., Williams, R. J., Murphy, B. P., Camac, J. S. & Vesk, P. A., 2016. Fuels and landscape flammability in an Australian alpine environment. *Austral Ecology,* 41(6)**,** 657-670.

Freeman, B. G., Song, Y., Feeley, K. J. & Zhu, K., 2021. Montane species track rising temperatures better in the tropics than in the temperate zone. *Ecology Letters,* 24(8)**,** 1697-1708.

Frei, E., Bodin, J. & Walther, G.-R., 2010. Plant species' range shifts in mountainous areas—all uphill from here? *Botanica Helvetica,* 120(117-128.

French, B. J., Hope, G. S., Pryor, L. D. & Bowman, D. M., 2016. The vulnerability of peatlands in the Australian Alps. *Australasian Plant Conservation: Journal of the Australian Network for Plant Conservation,* 24(4)**,** 16-18.

Fuentes, E. V. & Petrucio, M. M., 2015. Water level decrease and increased water stability promotes phytoplankton growth in a mesotrophic subtropical lake. *Marine and Freshwater Research,* 66(8)**,** 711-718.

Gaffney, P. P., Tang, Q., Wang, J., Zhang, C., Xu, X., Xu, X., Li, Y., Pap, S., Ratcliffe, J. L. & Li, Q., 2025. The high-altitude peatland carbon cycle: A review of the impacts of climate and land-use change. *Geography and Sustainability***,** 100353.

Gallant, J., Wilson, N., Tickle, P., Dowling, T. & Read, A., 2009. 3 Second SRTM derived digital elevation model (DEM) version 1.0. Record 1.0. *Geoscience Australia: Canberra*.

Galloway, R. Glaciation in the Snowy Mountains: a reappraisal. Proceedings of the Linnean Society of New South Wales, 1963. 180-198.

Galloway, R. W., 2003. Earth Science Values'. *An assessment of the values of Kosciuszko National Park***,** 21-26.

Garden, D., Dowling, P., Eddy, D. & Nicol, H., 2001. The influence of climate, soil, and management on the composition of native grass pastures on the central, southern, and Monaro tablelands of New South Wales. *Australian Journal of Agricultural Research,* 52(9)**,** 925-936.

Garisoain, R., Jacotot, A., Delire, C., Binet, S., Le Roux, G., Gascoin, S., Rosset, T., Gogo, S., Granouillac, F. & Payre-Suc, V., 2024. Mountain peatlands and drought: Carbon cycling in the Pyrenees amidst global climate change. *Journal of Geophysical Research: Biogeosciences,* 129(7)**,** e2024JG008041.

Gehrig-Fasel, J., Guisan, A. & Zimmermann, N. E., 2007. Tree line shifts in the Swiss Alps: climate change or land abandonment? *Journal of vegetation science,* 18(4)**,** 571-582.

Geng, T., Jia, F., Cai, W., Wu, L., Gan, B., Jing, Z., Li, S. & McPhaden, M. J., 2023. Increased occurrences of consecutive La Niña events under global warming. *Nature,* 619(7971)**,** 774-781.

Geoscience Australia 2008. GEODATA 9 second DEM and D8: Digital Elevation Model Version 3 and Flow Direction Grid 2008. Bioregional Assessment Program. 25

April 2025. https://data.gov.au/data/dataset/ebcf6ca2-513a-4ec7-9323-73508c5d7b93.

Geoscience Australia. 2012. Surface Geology of Australia 1:1 million scale dataset (2012 edition). Commonwealth of Australia. 25 April 2025. https://ecat.ga.gov.au/geonetwork/srv/eng/catalog.search#/metadata/c8856c41-0d5b-2b1d-e044-00144fdd4fa6.

Geoscience Australia, 2014. *Elevations* [Online]. Online. Available: https://www.ga.gov.au/scientific-topics/national-location-information/landforms/elevations [Accessed 26 September 2024].

Gergis, J., Neukom, R., Gallant, A. J. & Karoly, D. J., 2016. Australasian temperature reconstructions spanning the last millennium. *Journal of Climate,* 29(15)**,** 5365-5392.

Glen, R., 2013. Refining accretionary orogen models for the Tasmanides of eastern Australia. *Australian Journal of Earth Sciences,* 60(3)**,** 315-370.

Good, R., 1992. 1—Les Alpes australiennes/The Australian Alps (texte disponible en français et en anglais). *Revue de Geographie Alpine,* 80(2)**,** 39-63.

Good, R., 1995. Ecologically sustainable development in the Australian Alps. *Mountain Research and Development***,** 251-258.

Good, R. & Johnston, S., 2019. Rehabilitation and revegetation of the Kosciuszko summit area, following the removal of grazing–An historic review. *Ecological Management & Restoration,* 20(1)**,** 13-20.

Good, R., Wright, G., Whinam, J. & Hope, G. S., 2010. *Restoration of mires of the Australian Alps following the 2003 wildfires*, ANU E Press.

Gordon, J. E., Dvorák, I. J., Jonasson, C., Josefsson, M., Kociánová, M. & Thompson, D. B., 2002. Geo–ecology and management of sensitive montane landscapes. *Geografiska Annaler: Series A, Physical Geography,* 84(3-4)**,** 193-203.

Gornitz, V., 2008. *Encyclopedia of paleoclimatology and ancient environments*, Springer Science & Business Media. 1402045514

Goudie, A. S., 2002. *Encyclopedia of Global Change: Environmental Change and Human Society 2 Volumes*, Oxford University Press. 0195108256

Grabherr, G., Gottfried, M., Gruber, A. & Pauli, H., 1995. Patterns and current changes in alpine plant diversity. *Arctic and alpine biodiversity: patterns, causes and ecosystem consequences***,** 167-181.

Grabherr, G., Gottfried, M. & Pauli, H., 2001. High mountain environment as indicator of global change. *Global change and protected areas***,** 331-345.

Grabherr, G., Gottfried, M. & Pauli, H., 2010. Climate change impacts in alpine environments. *Geography Compass,* 4(8)**,** 1133-1153.

Grabherr, G., Nagy, L. & Thompson, D., 2003. *An outline of Europe's alpine areas*, Springer. 3642623875

Gray, J. M., Bishop, T. F. & Smith, P. L., 2016. Digital mapping of pre-European soil carbon stocks and decline since clearing over New South Wales, Australia. *Soil Research,* 54(1)**,** 49-63.

Green, D., Singh, G., Polach, H., Moss, D., Banks, J. & Geissler, E. A., 1988. A fine-resolution palaeoecology and palaeoclimatology from south-eastern Australia. *The Journal of Ecology***,** 790-806.

Green, K., 2009. Causes of stability in the alpine treeline in the Snowy Mountains of Australia–a natural experiment. *Australian Journal of Botany,* 57(3)**,** 171-179.

Green, K., Mansergh, I. & Osborne, W., 1992. 13—La faune des Alpes australiennes: conservation et gestion/The fauna of the Australian Alps: conservation and gestion (texte disponible en français et en anglais). *Revue de Géographie Alpine,* 80(2)**,** 381-407.

Green, K. & Venn, S., 2012. Tree-limit ribbons in the Snowy Mountains, Australia: characterization and recent seedling establishment. *Arctic, Antarctic, and Alpine Research,* 44(2)**,** 180-187.

Grose, M. & Hennessy, K., 2024. *Climate concerns: Trends in Australian snow* [Online]. Available: https://www.csiro.au/en/news/all/articles/2024/june/snow-trends-australia [Accessed].

Grover, S. & Baldock, J., 2012. Carbon chemistry and mineralization of peat soils from the Australian Alps. *European Journal of Soil Science,* 63(2)**,** 129-140.

Grover, S., McKenzie, B., Baldock, J. & Papst, W., 2005. Chemical characterisation of bog peat and dried peat of the Australian Alps. *Soil Research,* 43(8)**,** 963-971.

Grover, S. P., Baldock, J. A. & Jacobsen, G. E., 2012. Accumulation and attrition of peat soils in the Australian Alps: Isotopic dating evidence. *Austral Ecology,* 37(4)**,** 510-517.

Grover, S. P. P., 2006. *Carbon and water dynamics of peat soils in the Australian Alps.* La Trobe.

Growcock, A. J. W., 2006. Impacts of camping and trampling on Australian alpine and subalpine vegetation and soils.

Gu, D., Andreev, K. & Dupre, M. E., 2021. Major trends in population growth around the world. *China CDC weekly,* 3(28)**,** 604.

Guisan, A., Broennimann, O., Buri, A., Cianfrani, C., D'Amen, M., Di Cola, V., Fernandes, R., Gray, S., Mateo, R. & Pinto, E., 2019. Climate change impacts on mountain biodiversity. *Biodiversity and climate change: Transforming the biosphere.* Yale University Press. 221-233

Hagedorn, F., Mulder, J. & Jandl, R., 2010. Mountain soils under a changing climate and land-use. *Biogeochemistry,* 97(1)**,** 1-5.

Hagemans, K., Urrego, D. H., Gosling, W. D., Rodbell, D. T., Wagner-Cremer, F. & Donders, T. H., 2022. Intensification of ENSO frequency drives forest disturbance in the andes during the holocene. *Quaternary Science Reviews,* 294(107762). https://doi.org/10.1016/j.quascirev.2022.107762.

Hall, J., Burgess, N. D., Lovett, J., Mbilinyi, B. & Gereau, R. E., 2009. Conservation implications of deforestation across an elevational gradient in the Eastern Arc Mountains, Tanzania. *Biological conservation,* 142(11)**,** 2510-2521.

Hamilton, R., Amano, N., Bradshaw, C. J., Saltré, F., Patalano, R., Penny, D., Stevenson, J., Wolfhagen, J. & Roberts, P., 2024. Forest mosaics, not savanna corridors, dominated in Southeast Asia during the Last Glacial Maximum. *Proceedings of the National Academy of Sciences,* 121(1)**,** e2311280120.

Hamilton, R., Stevenson, J., Li, B. & Bijaksana, S., 2019. A 16,000-year record of climate, vegetation and fire from Wallacean lowland tropical forests. *Quaternary Science Reviews,* 224(105929).

Han, D., Gao, C., Yu, Z., Yu, X., Li, Y., Cong, J. & Wang, G., 2019. Late Holocene vegetation and climate changes in the Great Hinggan Mountains, northeast China. *Quaternary International,* 532(138-145.

Hancock, W. K., 1972. *Discovering Monaro : a study of man's impact on his environment* Melbourne, Cambridge University Press Cambridge.

Hansson, A., Dargusch, P. & Shulmeister, J., 2021. A review of modern treeline migration, the factors controlling it and the implications for carbon storage. *Journal of Mountain Science,* 18(2)**,** 291-306.

Haque, U., Da Silva, P. F., Devoli, G., Pilz, J., Zhao, B., Khaloua, A., Wilopo, W., Andersen, P., Lu, P. & Lee, J., 2019. The human cost of global warming: Deadly landslides and their triggers (1995–2014). *Science of the Total Environment,* 682(673-684).

Harris, L. I., Roulet, N. T. & Moore, T. R., 2020. Drainage reduces the resilience of a boreal peatland. *Environmental Research Communications,* 2(6)**,** 065001.

Harris, R., Remenyi, T. & Bindoff, N., 2016. The potential impacts of climate change on Victorian alpine resorts. A report for the alpine resorts co-ordinating council.

Harrison, S. P., 1993. Late Quaternary lake-level changes and climates of Australia. *Quaternary Science Reviews,* 12(4)**,** 211-231.

Harsch, M. A., Hulme, P. E., McGlone, M. S. & Duncan, R. P., 2009. Are treelines advancing? A global meta-analysis of treeline response to climate warming. *Ecology Letters,* 12(10)**,** 1040-1049.

Hartley, I. P., Garnett, M. H., Sommerkorn, M., Hopkins, D. W., Fletcher, B. J., Sloan, V. L., Phoenix, G. K. & Wookey, P. A., 2012. A potential loss of carbon associated with greater plant growth in the European Arctic. *Nature Climate Change,* 2(12)**,** 875-879.

Hemp, A., 2002. Ecology of the pteridophytes on the southern slopes of Mt. Kilimanjaro–I. Altitudinal distribution. *Plant Ecology,* 159(211-239).

Hemp, A., 2008. Introduced plants on Kilimanjaro: tourism and its impact. *Plant Ecology,* 197(17-29).

Hennessy, K., Fitzharris, B., Bates, B. C., Harvey, N., Howden, M., Hughes, L., Salinger, J., Warrick, R., Becken, S. & Chambers, L., 2007. Australia and New Zealand. *Climate Change 2007: impacts, adaptation and vulnerability.* Cambridge University Press (CUP). 507-540

Hennessy, K., Whetton, P., Smith, I., Bathols, J., Hutchinson, M. & Sharples, J., 2003. *The impact of climate change on snow conditions in mainland Australia*, CSIRO Aspendale.

Hennessy, K., Whetton, P., Walsh, K., Smith, I., Bathols, J., Hutchinson, M. & Sharples, J., 2008. Climate change effects on snow conditions in mainland Australia and adaptation at ski resorts through snowmaking. *Climate Research,* 35(3)**,** 255-270.

Hermann, N. W., Oster, J. L. & Ibarra, D. E., 2018. Spatial patterns and driving mechanisms of mid-Holocene hydroclimate in western North America. *Journal of Quaternary Science,* 33(4)**,** 421-434.

Heusser, C., 1998. Deglacial paleoclimate of the American sector of the Southern Ocean: Late Glacial–Holocene records from the latitude of Canal Beagle (55 S), Argentine Tierra del Fuego. *Palaeogeography, Palaeoclimatology, Palaeoecology,* 141(3-4)**,** 277-301.

Ho, J. C., Michalak, A. M. & Pahlevan, N., 2019. Widespread global increase in intense lake phytoplankton blooms since the 1980s. *Nature,* 574(7780)**,** 667-670.

Hobbs, S., Paull, D., Clarke, J. & Roach, I. C., 2016. Multi-agent gully processes: evidence from the Monaro Volcanic Province, Australia and in Terra Cimmeria, Mars. *Geomorphology,* 257(23-46.

Hock, R., Rasul, G., Adler, C., Cáceres, B., Gruber, S., Hirabayashi, Y., Jackson, M., Kääb, A., Kang, S. & Kutuzov, S., 2019. High mountain areas. *IPCC special report on the ocean and cryosphere in a changing climate.* H.-O. Pörtner, DC Roberts, V. Masson-Delmotte, P. Zhai, M. Tignor, E …. 131-202

Hodelka, B. N., McGlue, M. M., Zimmerman, S., Ali, G. & Tunno, I., 2020. Paleoproduction and environmental change at Mono Lake (eastern Sierra Nevada) during the Pleistocene-Holocene transition. *Palaeogeography, Palaeoclimatology, Palaeoecology,* 543(109565. https://doi.org/10.1016/j.palaeo.2019.109565.

Hoffmann, A. A., Rymer, P. D., Byrne, M., Ruthrof, K. X., Whinam, J., McGeoch, M., Bergstrom, D. M., Guerin, G. R., Sparrow, B. & Joseph, L., 2019. Impacts of recent climate change on terrestrial flora and fauna: Some emerging Australian examples. *Austral Ecology,* 44(1)**,** 3-27.

Hofstede, R. G., Groenendijk, J. P., Coppus, R., Fehse, J. C. & Sevink, J., 2002. Impact of pine plantations on soils and vegetation in the Ecuadorian high Andes. *Mountain Research and Development,* 22(2)**,** 159-167.

Hogg, A. G., Heaton, T. J., Hua, Q., Palmer, J. G., Turney, C. S., Southon, J., Bayliss, A., Blackwell, P. G., Boswijk, G. & Ramsey, C. B., 2020. SHCal20 Southern Hemisphere calibration, 0–55,000 years cal BP. *Radiocarbon,* 62(4)**,** 759-778.

Holtmeier, F.-K., 2009. *Mountain timberlines*, Springer.

Holtmeier, F.-K. & Broll, G., 2018. Subalpine forest and treeline ecotone under the influence of disturbances: a review. *Journal of Environmental Protection,* 9(7)**,** 815-845.

Hope, G., 2006. Histories of wetlands in the Australian Capital Territory and the bog recovery program. *Caring for Namadgi Science and People.* National Parks Association of the ACT Inc. 129-144

Hope, G. & Clark, R. A tale of two swamps: sub-alpine peatlands in the Kelly-Scabby area of Namadgi National Park. Corridors for Survival in a Changing World

Proceedings of the NPA ACT Symposium, 2008. National Parks Association of the ACT Inc., 61-76.

Hope, G., Kershaw, A. P., van der Kaars, S., Xiangjun, S., Liew, P.-M., Heusser, L. E., Takahara, H., McGlone, M., Miyoshi, N. & Moss, P. T., 2004. History of vegetation and habitat change in the Austral-Asian region. *Quaternary International,* 118(103-126.

Hope, G., Macphail, M. & Keaney, B., 2005. Snowy Flat and Ginini Bogs, Brindabella Range, Australian Capital Territory. *Unpublished report to environment ACT and Ecowise Services*.

Hope, G., Macphail, M. & Keaney, B., 2009a. Mires of the ACT Region; Mountain Occupation Project. Consultancy report. ACT Region.

Hope, G., Mooney, S. D., Allen, K., Baker, P., Keaney, B., Kemp, J., Martin, L., Pearson, S., Stevenson, J. & Zheng, X., 2019. Science through time: Understanding the archive at rennix gap bog, a sub-alpine peatland in kosciuszko national park, New South Wales, Australia. *Proceedings of the Linnean Society of New South Wales,* 141(25-47).

Hope, G. & Nanson, R., 2015. Peatland carbon stores and fluxes in the Snowy Mountains, New South Wales, Australia. *Mires and Peat,* 15(11).

Hope, G., Nanson, R. & Jones, P., 2012. Peat-forming bogs and fens of the Snowy Mountains of NSW. 9781742935584. Office of Environment and Heritage. Sydney South, NSW.

Hope, G., Stevenson, J. & Haberle, S., 2006. Palaeoecology of Blundells flat, ACT. *Unpublished Report to Ecowise Services and ACT Forests*.

Hope, G. S., Nanson, R. & Flett, I., 2009b. *The peat-forming mires of the Australian Capital Territory*, Territory and Municipal Services Canberra. 0980684811

Hotovy, O., Nedelcev, O., Seibert, J. & Jenicek, M., 2024. Rain-on-snow events in mountainous catchments under climate change. *EGUsphere,* 2024(1-29).

Hua, Q., Jacobsen, G. E., Zoppi, U., Lawson, E. M., Williams, A. A., Smith, A. M. & McGann, M. J., 2001. Progress in radiocarbon target preparation at the ANTARES AMS Centre. *Radiocarbon,* 43(2A)**,** 275-282.

Huber, U. M. & Markgraf, V., 2003. Holocene Fire Frequency and Climate Change at Rio Rubens Bog, Southern Patagonia. *In:* Veblen, T. T., Baker, W. L., Montenegro, G. & Swetnam, T. W. (eds.) *Fire and Climatic Change in Temperate Ecosystems of the Western Americas.* New York, NY: Springer New York. 357-380

Huber, U. M., Markgraf, V. & Schäbitz, F., 2004. Geographical and temporal trends in Late Quaternary fire histories of Fuego-Patagonia, South America. *Quaternary Science Reviews,* 23(9-10)**,** 1079-1097.

Hughes, A. C., Orr, M. C., Yang, Q. & Qiao, H., 2021. Effectively and accurately mapping global biodiversity patterns for different regions and taxa. *Global Ecology and Biogeography,* 30(7)**,** 1375-1388.

Hughes, P. D., 2000. A reappraisal of the mechanisms leading to ombrotrophy in British raised mires. *Ecology Letters,* 3(1)**,** 7-9.

Huss, M., Bookhagen, B., Huggel, C., Jacobsen, D., Bradley, R. S., Clague, J. J., Vuille, M., Buytaert, W., Cayan, D. R. & Greenwood, G., 2017. Toward mountains without permanent snow and ice. *Earth's Future,* 5(5)**,** 418-435.

.idcommunity, 2023. *Snowy Monaro Regional Council economic profile* [Online]. Available: https://economy.id.com.au/snowy-monaro/value-of-agriculture [Accessed October 8 2024].

Iglesias, V., Haberle, S. G., Holz, A. & Whitlock, C., 2018. Holocene dynamics of temperate rainforests in West-Central Patagonia. *Frontiers in Ecology and Evolution,* 5(177).

Iglesias, V., Markgraf, V. & Whitlock, C., 2016. 17,000 years of vegetation, fire and climate change in the eastern foothills of the Andes (lat. 44 S). *Palaeogeography, Palaeoclimatology, Palaeoecology,* 457(195-208.

Iglesias, V. & Whitlock, C., 2014. Fire responses to postglacial climate change and human impact in northern Patagonia (41–43 S). *Proceedings of the National Academy of Sciences,* 111(51)**,** E5545-E5554.

Iglesias, V., Whitlock, C., Bianchi, M. M., Villarosa, G. & Outes, V., 2012. Holocene climate variability and environmental history at the Patagonian forest/steppe ecotone: Lago Mosquito (42°29'37.89"S, 71°24'14.57"W) and Laguna del Cóndor (42°20'47.22"S, 71°17'07.62"W). *The Holocene,* 22(11)**,** 1297-1307. 10.1177/0959683611427330.

Immerzeel, W. W., Lutz, A. F., Andrade, M., Bahl, A., Biemans, H., Bolch, T., Hyde, S., Brumby, S., Davies, B. & Elmore, A., 2020. Importance and vulnerability of the world's water towers. *Nature,* 577(7790)**,** 364-369.

Inouye, D. W. & Wielgolaski, F. E., 2024. Phenology at High Altitudes. *In:* Schwartz, M. D. (ed.) *Phenology: An Integrative Environmental Science.* Cham: Springer Nature Switzerland. 281-311

Inouye, D. W. & Wielgolaski, F. E., 2025. Phenology at high altitudes. *Phenology: An integrative environmental science.* Springer. 281-311

Intergovernmental Panel on Climate Change, 2023. Climate Change 2023: Synthesis Report. Contribution of Working Groups I, II and III to the Sixth Assessment Report of the Intergovernmental Panel on Climate Change Online.

Ioan, S., Roseo, F. & Brambilla, M., 2025. Mountain ecosystem services under a changing climate: A global perspective. *Ecosystem Services,* 73(101732).

Ives, J. D., 2012. The origins of mountain ecology. *Pirineos,* 167(167)**,** 15-27.

Ives, J. D., 2019. Applied high altitude geoecology: Can the scientist assist in the preservation of the mountains? *High altitude geoecology.* Routledge. 9-45

Jacobs, P. & Anderson, G., 2016. Australian Alps Climate Futures: Taking Action Now to Strengthen Resilience – Summary Report. People in Nature; Australian Alps National Parks Cooperative Management Program. Canberra, ACT.

Jara, I. A., Moreno, P. I., Alloway, B. V. & Newnham, R. M., 2019. A 15,400-year long record of vegetation, fire-regime, and climate changes from the northern Patagonian Andes. *Quaternary Science Reviews,* 226(106005).

Jenkins, B. & Morand, D., 2002. A comparison of basaltic soils and associated vegetation patterns in contrasting climatic environments. *Regolith and landscapes in Eastern Australia (IC Roach, ed.). CRC LEME, Sydney, Australia***,** 76-80.

Jenkins, C. N., Pimm, S. L. & Joppa, L. N., 2013. Global patterns of terrestrial vertebrate diversity and conservation. *Proceedings of the National Academy of Sciences,* 110(28)**,** E2602-E2610.

Johnson, C. N. & Brook, B. W., 2011. Reconstructing the dynamics of ancient human populations from radiocarbon dates: 10 000 years of population growth in Australia. *Proceedings of the Royal Society B: Biological Sciences,* 278(1725)**,** 3748-3754.

Johnston, F. M. & Pickering, C. M., 2001. Alien plants in the Australian Alps. *Mountain Research and Development,* 21(3)**,** 284-291.

Jonas, T., Rixen, C., Sturm, M. & Stoeckli, V., 2008. How alpine plant growth is linked to snow cover and climate variability. *Journal of Geophysical Research: Biogeosciences,* 113(G3).

Jouzel, J., Masson-Delmotte, V., Cattani, O., Dreyfus, G., Falourd, S., Hoffmann, G., Minster, B., Nouet, J., Barnola, J.-M. & Chappellaz, J., 2007. Orbital and millennial Antarctic climate variability over the past 800,000 years. *science,* 317(5839)**,** 793-796.

Jouzel, J., Waelbroeck, C., Malaizé, B., Bender, M., Petit, J.-R., Stiévenard, M., Barkov, N., Barnola, J.-M., King, T. & Kotlyakov, V., 1996. Climatic interpretation of the recently extended Vostok ice records. *Climate Dynamics,* 12(513-521.

Jung, M., Arnell, A., De Lamo, X., García-Rangel, S., Lewis, M., Mark, J., Merow, C., Miles, L., Ondo, I. & Pironon, S., 2021. Areas of global importance for conserving terrestrial biodiversity, carbon and water. *Nature Ecology & Evolution,* 5(11)**,** 1499-1509.

Jurskis, V., 2016. 'Dieback'(chronic decline) of *Eucalyptus viminalis* on the Monaro is not new, unique or difficult to explain. *Australian Forestry,* 79(4)**,** 261-264.

Kapnick, S. B. & Delworth, T. L., 2013. Controls of global snow under a changed climate. *Journal of Climate,* 26(15)**,** 5537-5562.

Kaufman, D., McKay, N., Routson, C., Erb, M., Davis, B., Heiri, O., Jaccard, S., Tierney, J., Dätwyler, C. & Axford, Y., 2020. A global database of Holocene paleotemperature records. *Scientific data,* 7(1)**,** 115.

Keaney, B. & Hope, G., 2006. The Holocene vegetation history of Yaouk Swamp. *New South Wales. Unpublished manuscript*.

Kemp, J., 1993. The end of the Pleistocene in the southern tablelands, southeastern Australia. *Unpublished BA thesis, Dept geography, ANU, Australia*.

Kemp, J. & Hope, G., 2014. Vegetation and environments since the Last Glacial Maximum in the Southern Tablelands, New South Wales. *Journal of Quaternary Science,* 29(8)**,** 778-788.

Kerr, T., 2013. The contribution of snowmelt to the rivers of the South Island, New Zealand. *Journal of Hydrology (New Zealand)***,** 61-82.

Kershaw, A. P., McKenzie, G., Porch, N., Roberts, R., Brown, J., Heijnis, H., Orr, M. L., Jacobsen, G. & Newall, P. R., 2007. A high-resolution record of vegetation and climate through the last glacial cycle from Caledonia Fen, southeastern highlands of Australia. *Journal of Quaternary Science: Published for the Quaternary Research Association,* 22(5)**,** 481-500.

Kilian, R. & Lamy, F., 2012. A review of Glacial and Holocene paleoclimate records from southernmost Patagonia (49–55°S). *Quaternary Science Reviews,* 53(1-23. https://doi.org/10.1016/j.quascirev.2012.07.017.

King, H., 1959. Transhumant grazing in the snow belt of New South Wales. *Australian geographer,* 7(4)**,** 129-140.

Kirkpatrick, J. The natural significance of the Australian Alps. Celebrating Mountains Proceedings of an International Year of Mountains Conference, Jindabyne, Australia, 2002.

Knudson, K. P., Hendy, I. L. & Neil, H. L., 2011. Re-examining Southern Hemisphere westerly wind behavior: insights from a late Holocene precipitation reconstruction using New Zealand fjord sediments. *Quaternary Science Reviews,* 30(21)**,** 3124-3138. https://doi.org/10.1016/j.quascirev.2011.07.017.

Kohn, B., Gleadow, A. & Cox, S., 1999. Denudation history of the Snowy Mountains: constraints from apatite fission track thermochronology. *Australian Journal of Earth Sciences,* 46(2)**,** 181-198.

Körner, C., 2000. Why are there global gradients in species richness? Mountains might hold the answer. *Trends in ecology & evolution,* 15(12)**,** 513-514.

Körner, C., 2004. Mountain biodiversity, its causes and function. *AMBIO: A Journal of the Human Environment,* 33(sp13)**,** 11-17.

Körner, C., 2013. Vegetation of the Earth. *Strasburger's Plant Sciences.* Springer. 1217-1262

Körner, C., 2021. The alpine life zone. *Alpine plant life: Functional plant ecology of high mountain ecosystems***,** 23-51.

Körner, C., Jetz, W., Paulsen, J., Payne, D., Rudmann-Maurer, K. & M Spehn, E., 2017. A global inventory of mountains for bio-geographical applications. *Alpine botany,* 127(1-15.

Körner, C., Paulsen, J. & Spehn, E. M., 2011. A definition of mountains and their bioclimatic belts for global comparisons of biodiversity data. *Alpine Botany,* 121(73-78).

Korpak, J., 2017. Human impact on mountain streams and rivers. *Open channel hydraulics, river hydraulic structures and fluvial geomorphology.* CRC Press. 400-435

Kosolapova, A. & Altshuler, I., 2024. Effects of reduced snowpack due to climate warming on abiotic and biotic soil properties in alpine and boreal forest systems. *PLOS Climate,* 3(5)**,** e0000417.

Kotlarski, S., Bosshard, T., Lüthi, D., Pall, P. & Schär, C., 2012. Elevation gradients of European climate change in the regional climate model COSMO-CLM. *Climatic change,* 112(189-215).

Koutavas, A. & Joanides, S., 2012. El Niño–Southern oscillation extrema in the holocene and last glacial maximum. *Paleoceanography,* 27(4).

Kuhry, P. & Vitt, D. H., 1996. Fossil carbon/nitrogen ratios as a measure of peat decomposition. *Ecology,* 77(1)**,** 271-275.

Kumar, A. & Deshmukh, B., 2015. A review on 'Geo-ecological Studies'-An interdisciplinary approach for evaluation and sustainable management of 'Geo-ecosystems'. *Journal of the Geological Society of India,* 86(605-612).

Kumar, A., Kumar, S. & Deshmukh, B., 2021. Geoecological integrity index for assessment and prioritisation of watersheds in the Indian northwestern Himalayan region using geoinformatics. *Journal of Earth System Science,* 130(1)**,** 19.

Kylander, M. E., Ampel, L., Wohlfarth, B. & Veres, D., 2011. High-resolution X-ray fluorescence core scanning analysis of Les Echets (France) sedimentary sequence: new insights from chemical proxies. *Journal of Quaternary Science,* 26(1)**,** 109-117.

Lacourse, T. & Gajewski, K., 2020. Current practices in building and reporting age-depth models. *Quaternary Research,* 96(28-38. 10.1017/qua.2020.47.

Lamb, A. L., Wilson, G. P. & Leng, M. J., 2006. A review of coastal palaeoclimate and relative sea-level reconstructions using δ13C and C/N ratios in organic material. *Earth-Science Reviews,* 75(1-4)**,** 29-57.

Laskar, J., Robutel, P., Joutel, F., Gastineau, M., Correia, A. C. & Levrard, B., 2004. A long-term numerical solution for the insolation quantities of the Earth. *Astronomy & Astrophysics,* 428(1)**,** 261-285.

Last, W. M. & Smol, J. P., 2002. *Tracking environmental change using lake sediments: volume 2: physical and geochemical methods*, Springer Science & Business Media. 1402006284

Lawrence, R., Rutherfurd, I., Ghadirian, P., White, M., Coates, F. & Thomas, I., 2009. The geography and hydrology of high country peatlands in Victoria Part 1. *Geography and Classification. Arthur Rylah Institute for Environmental Research Technical Report,* 173

Lawrence, S. & Davies, P., 2011. *An archaeology of Australia since 1788*, Springer. 1441974857

Le Roux, G., Hansson, S. V., Claustres, A., Binet, S., De Vleeschouwer, F., Gandois, L., Mazier, F., Simonneau, A., Teisserenc, R. & Allen, D., 2020. Trace metal legacy in mountain environments: a view from the Pyrenees Mountains. *Biogeochemical Cycles: Ecological Drivers and Environmental Impact***,** 191-206.

Lê, S., Josse, J. & Husson, F., 2008. FactoMineR: an R package for multivariate analysis. *Journal of Statistical Software,* 25(1-18).

Le, T., 2017. ENSO response to external forcing in CMIP5 simulations of the last millennium. *Global and Planetary Change,* 148(105-112).

Lees, K., Artz, R., Chandler, D., Aspinall, T., Boulton, C., Buxton, J., Cowie, N. & Lenton, T., 2021. Using remote sensing to assess peatland resilience by estimating soil surface moisture and drought recovery. *Science of the Total Environment,* 761(143312.

Leonard, N., Welsh, K., Lough, J., Feng, Y. x., Pandolfi, J., Clark, T. & Zhao, J. x., 2016. Evidence of reduced mid-Holocene ENSO variance on the Great Barrier Reef, Australia. *Paleoceanography,* 31(9)**,** 1248-1260.

Leslie, D. M. & McGlone, M. S., 1973. Relict periglacial landforms at Clarks Junction, Otago. *New Zealand Journal of Geology and Geophysics,* 16(3)**,** 575-583. 10.1080/00288306.1973.10431380.

Leys, B. A., Commerford, J. L. & McLauchlan, K. K., 2017. Reconstructing grassland fire history using sedimentary charcoal: Considering count, size and shape. *PLoS One,* 12(4)**,** e0176445.

Lhotsky, J., 1835. *A Journey from Sydney to the Australian Alps, undertaken in the months of January, February, and March, 1834. Being an account of the geographical & natural relation of the country traversed, its aborigines, etc.[With a map and with MS. material inserted.]*, Sydney;[by commission at R. Ackerman's depository: London].

Li, L., Gou, M., Wang, N., Ma, W., Xiao, W., Liu, C. & La, L., 2021. Landscape configuration mediates hydrology and nonpoint source pollution under climate change and agricultural expansion. *Ecological Indicators,* 129(107959).

Li, X., El Solh, M. & Siddique, K. H., 2019. Mountain agriculture: Opportunities for harnessing zero hunger in Asia. *Mountain agriculture: opportunities for harnessing Zero Hunger in Asia.* Bangkok: Food and Agriculture Organization of the United Nations.

Lieber, R., Brown, J., King, A. & Freund, M., 2024. Historical and Future Asymmetry of ENSO Teleconnections with Extremes. *Journal of Climate,* 37(22)**,** 5909-5924.

Lieber, R., Gillett, Z., Taschetto, A. & King, A., 2023. El Niño's Impact on Australia's Weather and Climate. ARC Centre of Excellence for Climate Extremes. Sydney, Australia.

Liedtke, R., Barros, A., Essl, F., Lembrechts, J. J., Wedegärtner, R. E., Pauchard, A. & Dullinger, S., 2020. Hiking trails as conduits for the spread of non-native species in mountain areas. *Biological Invasions,* 22(1121-1134).

Lim, E. P., Hendon, H. H., Arblaster, J. M., Delage, F., Nguyen, H., Min, S. K. & Wheeler, M. C., 2016. The impact of the Southern Annular Mode on future changes in Southern Hemisphere rainfall. *Geophysical Research Letters,* 43(13)**,** 7160-7167.

Liu, X., Cheng, Z., Yan, L. & Yin, Z.-Y., 2009. Elevation dependency of recent and future minimum surface air temperature trends in the Tibetan Plateau and its surroundings. *Global and Planetary Change,* 68(3)**,** 164-174.

Loarie, S. R., Duffy, P. B., Hamilton, H., Asner, G. P., Field, C. B. & Ackerly, D. D., 2009. The velocity of climate change. *Nature,* 462(7276)**,** 1052-1055. 10.1038/nature08649.

Loeffler, J., Anschlag, K., Baker, B., Finch, O.-D., Diekkrueger, B., Wundram, D., Schroeder, B., Pape, R. & Lundberg, A., 2011. Mountain ecosystem response to global change. *Erdkunde***,** 189-213.

Loisel, J. & Bunsen, M., 2020. Abrupt fen-bog transition across southern Patagonia: Timing, causes, and impacts on carbon sequestration. *Frontiers in Ecology and Evolution,* 8(273).

Loisel, J., Sarna, K., Xia, Z., Huang, Y. & Yu, Z., 2023. Concordant changes in late Holocene hydroclimate across southern Patagonia modulated by westerly winds and the El Niño–Southern Oscillation. *Geology,* 51(3)**,** 247-251.

Loisel, J. & Yu, Z., 2013. Recent acceleration of carbon accumulation in a boreal peatland, south central Alaska. *Journal of geophysical research: biogeosciences,* 118(1)**,** 41-53.

Loisel, J., Yu, Z., Beilman, D. W., Camill, P., Alm, J., Amesbury, M. J., Anderson, D., Andersson, S., Bochicchio, C. & Barber, K., 2014. A database and synthesis of northern peatland soil properties and Holocene carbon and nitrogen accumulation. *the Holocene,* 24(9)**,** 1028-1042.

Lone, A., AA, F., Shah, R. & Achyuthan, H., 2018. Reconstruction of paleoclimate and environmental fluctuations since the early Holocene period using organic matter and C: N proxy records: A review. *Journal of the Geological Society of India,* 91(209-214.

Lopes dos Santos, R. A., Spooner, M. I., Barrows, T. T., De Deckker, P., Sinninghe Damsté, J. S. & Schouten, S., 2013. Comparison of organic (UK'37, TEXH86, LDI) and faunal proxies (foraminiferal assemblages) for reconstruction of late Quaternary sea surface temperature variability from offshore southeastern Australia. *Paleoceanography,* 28(3)**,** 377-387.

López-Moreno, J. I., Beguería, S. & García-Ruiz, J. M., 2004. The management of a large Mediterranean reservoir: storage regimens of the Yesa Reservoir, Upper Aragon River Basin, central Spanish Pyrenees. *Environmental Management,* 34(4)**,** 508-515.

Lorrey, A., Williams, P., Salinger, J., Martin, T., Palmer, J., Fowler, A., Zhao, J.-x. & Neil, H., 2008. Speleothem stable isotope records interpreted within a multi-proxy framework and implications for New Zealand palaeoclimate reconstruction. *Quaternary International,* 187(1)**,** 52-75.

Love, J., Thapa, R., Drielsma, M. & Robb, J., 2019. Climate change impacts in the NSW and ACT alpine region: Impacts on biodiversity. *NSW Department of Planning, Industry and Environment www. environment. nsw. gov. au*.

Lowry, A. L. & McGowan, H. A., 2024. Insights into the Australian mid-Holocene climate using downscaled climate models. *Climate of the Past,* 20(10)**,** 2309-2325.

Lu, X., Liang, E., Wang, Y., Babst, F. & Camarero, J. J., 2021. Mountain treelines climb slowly despite rapid climate warming. *Global Ecology and Biogeography,* 30(1)**,** 305-315.

Lu, Z., Schultze, A., Carré, M., Brierley, C., Hopcroft, P. O., Zhao, D., Zheng, M., Braconnot, P., Yin, Q. & Jungclaus, J. H., 2025. Increased frequency of multi-year El Niño–Southern Oscillation events across the Holocene. *Nature Geoscience***,** 1-7.

Lyon, E. C., McGlue, M. M., Erhardt, A. M., Kim, S. L., Stone, J. R. & Zimmerman, S. R. H., 2020. Late Holocene hydroclimate changes in the eastern Sierra Nevada revealed by a 4600-year paleoproduction record from June Lake, CA. *Quaternary Science Reviews,* 242(106432. https://doi.org/10.1016/j.quascirev.2020.106432.

MacDonald, D., Crabtree, J. R., Wiesinger, G., Dax, T., Stamou, N., Fleury, P., Lazpita, J. G. & Gibon, A., 2000. Agricultural abandonment in mountain areas of Europe: environmental consequences and policy response. *Journal of environmental management,* 59(1)**,** 47-69.

Mani, M. S. & Giddings, L. E., 2012. *Ecology of highlands*, Springer Science & Business Media. 9400991746

Mansilla, C. A., McCulloch, R. D. & Morello, F., 2018. The vulnerability of the *Nothofagus* forest-steppe ecotone to climate change: Palaeoecological evidence from Tierra del Fuego (~ 53 S). *Palaeogeography, palaeoclimatology, palaeoecology,* 508(59-70).

Marchin, R. M., McHugh, I., Simpson, R. R., Ingram, L. J., Balas, D. S., Evans, B. J. & Adams, M. A., 2018. Productivity of an Australian mountain grassland is limited by temperature and dryness despite long growing seasons. *Agricultural and Forest Meteorology,* 256-257(116-124. https://doi.org/10.1016/j.agrformet.2018.02.030.

Marcos, M. A., Bamonte, F. P. & Echeverria, M. E., 2025. Holocene Paleoenvironmental Reconstruction at 47° S (Patagonia, Argentina) from Sedimentary Sequences (Fens and Lagoon) and Archaeological Sites: A Regional Synthesis. *Fossil Studies,* 3(4)**,** 15.

Markgraf, V., Bradbury, J. P., Schwalb, A., Burns, S. J., Stern, C., Ariztegui, D., Gilli, A., Anselmetti, F. S., Stine, S. & Maidana, N., 2003. Holocene palaeoclimates of southern Patagonia: limnological and environmental history of Lago Cardiel, Argentina. *The Holocene,* 13(4)**,** 581-591.

Markgraf, V. & Huber, U. M., 2010. Late and postglacial vegetation and fire history in Southern Patagonia and Tierra del Fuego. *Palaeogeography, Palaeoclimatology, Palaeoecology,* 297(2)**,** 351-366.

Markgraf, V., Iglesias, V. & Whitlock, C., 2013. Late and postglacial vegetation and fire history from Cordón Serrucho Norte, northern Patagonia. *Palaeogeography, Palaeoclimatology, Palaeoecology,* 371(109-118).

Marlon, J. R., Bartlein, P. J., Walsh, M. K., Harrison, S. P., Brown, K. J., Edwards, M. E., Higuera, P. E., Power, M. J., Anderson, R. S. & Briles, C., 2009. Wildfire responses to abrupt climate change in North America. *Proceedings of the National Academy of Sciences,* 106(8)**,** 2519-2524.

Martel-Cea, A., Abarzúa, A. M., González, M. E., Jarpa, L. & Hernández, M., 2024. Fire–climate–human dynamics over the last 1800 years in the mesic *Araucaria-Nothofagus* forests. *Journal of Biogeography,* 51(8)**,** 1490-1504.

Martin, A., 1986a. Late glacial and early Holocene vegetation of the alpine zone Kosciusko National Park. *Flora and Fauna of Alpine Australasia: Ages and Origins***,** 161-170.

Martin, A., 1986b. Late glacial and holocene alpine pollen diagrams from the Kosciusko National Park, New South Wales, Australia. *Review of palaeobotany and palynology,* 47(3-4)**,** 367-409.

Martin, A., 1999. Pollen analysis of Digger's Creek Bog, Kosciuszko National Park: vegetation history and tree-line change. *Australian Journal of Botany,* 47(5)**,** 725-744.

Martini, I. & Glooschenko, W., 1985. Cold climate peat formation in Canada, and its relevance to Lower Permian coal measures of Australia. *Earth-Science Reviews,* 22(2)**,** 107-140.

Marx, S. K., Kamber, B. S., McGowan, H. A. & Denholm, J., 2011. Holocene dust deposition rates in Australia's Murray-Darling Basin record the interplay between aridity and the position of the mid-latitude westerlies. *Quaternary Science Reviews,* 30(23-24)**,** 3290-3305.

Marx, S. K., McGowan, H. A. & Kamber, B. S., 2009. Long-range dust transport from eastern Australia: A proxy for Holocene aridity and ENSO-type climate variability. *Earth and Planetary Science Letters,* 282(1-4)**,** 167-177.

Mason, R. & Williams, J., 2013a. Climate and Weather of the Australian Alps: Education Resource. Australian Alps Liaison Committee. Canberra, Australia.

Mason, R. & Williams, J., 2013b. Soils of the Australian Alps. Australian Alps National Parks.

Mason, R. & Williams, J., 2013c. Vegetation in the Australian Alps. Parks, A. a. N., Online.

Mayr, C., Fey, M., Haberzettl, T., Janssen, S., Lücke, A., Maidana, N. I., Ohlendorf, C., Schäbitz, F., Schleser, G. H., Struck, U., Wille, M. & Zolitschka, B., 2005. Palaeoenvironmental changes in southern Patagonia during the last millennium recorded in lake sediments from Laguna Azul (Argentina). *Palaeogeography, Palaeoclimatology, Palaeoecology,* 228(3)**,** 203-227. https://doi.org/10.1016/j.palaeo.2005.06.001.

McCulloch, R. D. & Davies, S. J., 2001. Late-glacial and Holocene palaeoenvironmental change in the central Strait of Magellan, southern Patagonia. *Palaeogeography, Palaeoclimatology, Palaeoecology,* 173(3-4)**,** 143-173.

McDougall, K. L. & Broome, L. S. Challenges facing protected area planning in the Australian Alps in a changing climate. Protected Areas: Buffering nature against climate change. Proceedings of a WWF-Australia and IUCN World Commission on Protected Areas symposium, Canberra 18-19 June 2007, 2007. 73-84.

McDougall, K. L., Morgan, J. W., Walsh, N. G. & Williams, R. J., 2005. Plant invasions in treeless vegetation of the Australian Alps. *Perspectives in Plant Ecology, Evolution and Systematics,* 7(3)**,** 159-171.

McDougall, K. L., Whinam, J., Coates, F., Morgan, J. W., Walsh, N. G., Wright, G. T. & Hope, G. S., 2023. Fire in the bog: responses of peatland vegetation in the Australian Alps to fire. *Australian Journal of Botany,* 71(3)**,** 111-126.

McGlone, M., Moar, N. & Meurk, C., 1997. Growth and vegetation history of alpine mires on the Old Man Range, Central Otago, New Zealand. *Arctic and Alpine Research,* 29(1)**,** 32-44.

McGlone, M. S. & Moar, N. T., 1998. Dryland Holocene vegetation history, Central Otago and the Mackenzie Basin, South Island, New Zealand. *New Zealand Journal of Botany,* 36(1)**,** 91-111. 10.1080/0028825X.1998.9512549.

McGlone, M. S. & Wilmshurst, J. M., 1999. A Holocene record of climate, vegetation change and peat bog development, east Otago, South Island, New Zealand. *Journal of Quaternary Science: Published for the Quaternary Research Association,* 14(3)**,** 239-254.

McGowan, H., Callow, J. N., Soderholm, J., McGrath, G., Campbell, M. & Zhao, J.-x., 2018. Global warming in the context of 2000 years of Australian alpine temperature and snow cover. *Scientific Reports,* 8(1)**,** 4394.

McGowan, H., Callow, N., Soderholm, J. & Campbell, M., 2019. Alpine temperature and snowcover reconstructions for the Snowy Mountains, Australia.

McKillup, S. & Dyar, M. D., 2010. *Geostatistics explained: an introductory guide for earth scientists*, Cambridge University Press. 1139486691

McMinn, M., Kiernan, K. & Fink, D., 2008. Cosmogenic nuclide dating in the Denison range, Southwestern Tasmania.

McQueen, K., 1994. The Tertiary Geology And Geomorphology Of The Monaro: The Perspective In 1994. *Occasional Publication No*.

McWethy, D. B., Whitlock, C., Wilmshurst, J. M., McGlone, M. S., Fromont, M., Li, X., Dieffenbacher-Krall, A., Hobbs, W. O., Fritz, S. C. & Cook, E. R., 2010. Rapid landscape transformation in South Island, New Zealand, following initial Polynesian settlement. *Proceedings of the National Academy of Sciences,* 107(50)**,** 21343-21348.

Meerhoff, M., Teixeira-de Mello, F., Kruk, C., Alonso, C., Gonzalez-Bergonzoni, I., Pacheco, J. P., Lacerot, G., Arim, M., Beklioğlu, M. & Brucet, S., 2012. Environmental warming in shallow lakes: a review of potential changes in community structure as evidenced from space-for-time substitution approaches. *Advances in Ecological Research,* 46(259-349).

Mehmood, K., Anees, S. A., Rehman, A., Rehman, N. U., Muhammad, S., Shahzad, F., Liu, Q., Alharbi, S. A., Alfarraj, S. & Ansari, M. J., 2024. Assessment of climatic influences on net primary productivity along elevation gradients in temperate ecoregions. *Trees, Forests and People,* 18(100657.

Meneghini, B., Simmonds, I. & Smith, I. N., 2007. Association between Australian rainfall and the southern annular mode. *International Journal of Climatology: A Journal of the Royal Meteorological Society,* 27(1)**,** 109-121.

Mensing, S., Livingston, S. & Barker, P., 2006. Long-term fire history in Great Basin sagebrush reconstructed from macroscopic charcoal in spring sediments, Newark Valley, Nevada. *Western North American Naturalist,* 66(1)**,** 64-77.

Meredith, M. C., 1844. *Notes and Sketches of New South Wales during a residence in that Colony from 1839 to 1844*, London: J. Murray.

Messerli, B. Mountains of the world—water towers for the 21st century. This limited edition volume of proceedings from the Rosenberg Forum was prepared and distributed by Mountain Culture at The Banff Centre with funding from the Max Bell Foundation. Permission is hereby granted by the publisher to reproduce this document for non-profit and educational purposes, 2000. Citeseer.

Messerli, B., Viviroli, D. & Weingartner, R., 2004. Mountains of the world: vulnerable water towers for the 21st century. *AMBIO: A Journal of the Human Environment,* 33(sp13)**,** 29-34.

Meyers, P. A., 1994. Preservation of elemental and isotopic source identification of sedimentary organic matter. *Chemical Geology,* 114(3-4)**,** 289-302.

Meyers, P. A. & Teranes, J. L., 2001. Sediment Organic Matter. *In:* Last, W. M. & Smol, J. P. (eds.) *Tracking Environmental Change Using Lake Sediments: Physical and Geochemical Methods.* Dordrecht: Springer Netherlands. 239-269

Mickelson, E. J., 2024. Deglacial and Holocene environmental change recorded in lake sediments from the Snowy Mountains, Kosciuszko National Park, southeastern Australia.

Millar, D. J., Cooper, D. J., Dwire, K. A., Hubbard, R. M. & von Fischer, J., 2017. Mountain peatlands range from CO 2 sinks at high elevations to sources at low elevations: Implications for a changing climate. *Ecosystems,* 20(416-432).

Minasny, B., Adetsu, D. V., Aitkenhead, M., Artz, R. R., Baggaley, N., Barthelmes, A., Beucher, A., Caron, J., Conchedda, G. & Connolly, J., 2024. Mapping and monitoring peatland conditions from global to field scale. *Biogeochemistry,* 167(4)**,** 383-425.

Minckley, T. A., Whitlock, C. & Bartlein, P. J., 2007. Vegetation, fire, and climate history of the northwestern Great Basin during the last 14,000 years. *Quaternary Science Reviews,* 26(17-18)**,** 2167-2184.

Moiseev, P. & Shiyatov, S., 2003. *Vegetation dynamics at the treeline ecotone in the Ural highlands, Russia*, Springer. 3642623875

Mooney, S., 2004. Looking Back as a Way Forward Pre-Historic Fire in the High Altitude Ecosystems of Mainland South-Eastern Australia March 2004.

Mooney, S., 2012. Late Quaternary fire regimes of Australasia. *Quaternary International,* 279(334).

Mooney, S., Martin, L., Goff, J. & Young, A. R., 2021. Sedimentation and organic content in the mires and other sites of sediment accumulation in the Sydney region, eastern Australia, in the period after the Last Glacial Maximum. *Quaternary Science Reviews,* 272(107216).

Mooney, S. & Tinner, W., 2011. The analysis of charcoal in peat and organic sediments. *Mires and Peat,* 7(09).

Mooney, S., Watson, J. & Dodson, J., 1997. Late Holocene environmental change in an upper montane area of the Snowy Mountains, New South Wales. *The Australian Geographer,* 28(2)**,** 185-200.

Moore, P., 1987. Ecological and hydrological aspects of peat formation. *Geological Society, London, Special Publications,* 32(1)**,** 7-15.

Morrison, C. & Pickering, C. M., 2013. Perceptions of climate change impacts, adaptation and limits to adaption in the Australian Alps: the ski-tourism industry and key stakeholders. *Journal of Sustainable Tourism,* 21(2)**,** 173-191.

Mosley, J. G., 1989. History of conservation of the Australian Alps. *In:* Good, R. (ed.) *The scientific significance of the Australian Alps: proceedings of the First Fenner Conference.* Canberra: Australian Alps National Parks Liaison Committee. 345-356

Mottl, O., Flantua, S. G., Bhatta, K. P., Felde, V. A., Giesecke, T., Goring, S., Grimm, E. C., Haberle, S., Hooghiemstra, H. & Ivory, S., 2021a. Global acceleration in rates of vegetation change over the past 18,000 years. *Science,* 372(6544)**,** 860-864.

Mottl, O., Grytnes, J.-A., Seddon, A. W., Steinbauer, M. J., Bhatta, K. P., Felde, V. A., Flantua, S. G. & Birks, H. J. B., 2021b. Rate-of-change analysis in paleoecology revisited: A new approach. *Review of Palaeobotany and Palynology,* 293(104483).

Moy, C. M., Seltzer, G. O., Rodbell, D. T. & Anderson, D. M., 2002. Variability of El Niño/Southern Oscillation activity at millennial timescales during the Holocene epoch. *Nature,* 420(6912)**,** 162-165.

Müller, R. D., Flament, N., Matthews, K. J., Williams, S. E. & Gurnis, M., 2016. Formation of Australian continental margin highlands driven by plate–mantle interaction. *Earth and Planetary Science Letters,* 441(60-70).

Mullins, C. E., 1977. Magnetic susceptibility of the soil and its significance in soil science–a review. *Journal of Soil Science,* 28(2)**,** 223-246.

Naccarella, A., Morgan, J. W., Cutler, S. C. & Venn, S. E., 2020. Alpine treeline ecotone stasis in the face of recent climate change and disturbance by fire. *PLoS One,* 15(4)**,** e0231339.

Nanavati, W. P., Whitlock, C., Iglesias, V. & de Porras, M. E., 2019. Postglacial vegetation, fire, and climate history along the eastern Andes, Argentina and Chile (lat. 41–55°S). *Quaternary Science Reviews,* 207(145-160). https://doi.org/10.1016/j.quascirev.2019.01.014.

National Centers for Environmental Information, 2025. *Paleo Data Search* [Online]. Online: National Centers for Environmental Information. Available: https://www.ncei.noaa.gov/access/paleo-search/ [Accessed February 19 2025].

National Museum of Australia, 2024. *Snowy Mountains Hydro* [Online]. National Museum of Australia. Available: https://www.nma.gov.au/defining-moments/resources/snowy-mountains-hydro [Accessed].

Nearing, M., Pruski, F. & O'neal, M., 2004. Expected climate change impacts on soil erosion rates: a review. *Journal of soil and water conservation,* 59(1)**,** 43-50.

Newbold, T., Hudson, L. N., Arnell, A. P., Contu, S., De Palma, A., Ferrier, S., Hill, S. L., Hoskins, A. J., Lysenko, I. & Phillips, H. R., 2016. Has land use pushed terrestrial biodiversity beyond the planetary boundary? A global assessment. *Science,* 353(6296)**,** 288-291.

Newman, J., 1954. Burning on sub-alpine pastures.

Noble, P. J., Ball, G. I., Zimmerman, S. H., Maloney, J., Smith, S. B., Kent, G., Adams, K. D., Karlin, R. E. & Driscoll, N., 2016. Holocene paleoclimate history of Fallen Leaf Lake, CA., from geochemistry and sedimentology of well-dated sediment cores. *Quaternary Science Reviews,* 131(193-210. https://doi.org/10.1016/j.quascirev.2015.10.037.

Nogués-Bravo, D., Araújo, M. B., Errea, M. & Martínez-Rica, J., 2007. Exposure of global mountain systems to climate warming during the 21st Century. *Global environmental change,* 17(3-4)**,** 420-428.

Notarnicola, C., 2020. Hotspots of snow cover changes in global mountain regions over 2000–2018. *Remote Sensing of Environment,* 243(111781).

NSW Parks and Wildlife Service, 1991. *Kosciusko Grazing. A History,* Sydney, NSW Parks and Wildlife Service (NSWPWS).

NSW Threatened Species Scientific Committe. 2004. Montane Peatlands and Swamps of the New England Tableland, NSW North Coast, Sydney Basin, South East Corner, South Eastern Highlands and Australian Alps Bioregions–Endangered Ecological Community Listing. NSW National Parks and Wildlife Service. Committee, N. T. S. S. Sydney, NSW, Australia.

NSW Threatened Species Scientific Committe, 2005. Commonwealth Listing Advice on Upland Wetlands of the New England Tablelands and the Monaro Plateau. Committee, N. T. S. S.

NSW Threatened Species Scientific Committe, 2015. Windswept Feldmark in the Australian Alps Bioregion – critically endangered ecological community listing: Final Determination. NSW Office of Environment and Heritage. Committee, N. T. S. S.

NSW Threatened Species Scientific Committe, 2018. Snowpatch Herbfield in the Australian Alps Bioregion: Critically Endangered Ecological Community listing – Final Determination. NSW Office of Environment and Heritage. Committee, N. T. S. S.

NSW Threatened Species Scientific Committe, 2019. Monaro Tableland Cool Temperate Grassy Woodland in the South Eastern Highlands Bioregion – critically endangered ecological community listing. Committee, N. T. S. S., Online.

Nunes, A. N., 2012. Regional variability and driving forces behind forest fires in Portugal an overview of the last three decades (1980–2009). *Applied Geography,* 34(576-586).

Nyman, P., Rutherfurd, I. D., Lane, P. N. & Sheridan, G. J., 2019. Debris flows in southeast Australia linked to drought, wildfire, and the El Niño–Southern Oscillation. *Geology,* 47(5)**,** 491-494.

O'Dowd, D. J. & Gill, A. M., 1984. Predator satiation and site alteration following fire: mass reproduction of alpine ash (*Eucalyptus delegatensis*) in southeastern Australia. *Ecology,* 65(4)**,** 1052-1066.

O'Gorman, P. A., 2014. Contrasting responses of mean and extreme snowfall to climate change. *Nature,* 512(7515)**,** 416-418.

Office of Environment and Heritage, 2023. A survey of the wild horse population in Kosciuszko National Park October 2023. Online.

Oldfield, F., Barnosky, C., Leopold, E. & Smith, J. Mineral magnetic studies of lake sediments: A brief review. Paleolimnology: Proceedings of the Third International Symposium on Paleolimnology, held at Joensuu, Finland, 1983. Springer, 37-44.

Ollier, C., 1982. The Great Escarpment of eastern Australia: tectonic and geomorphic significance. *Journal of the Geological Society of Australia,* 29(1-2)**,** 13-23.

Ombadi, M., Risser, M. D., Rhoades, A. M. & Varadharajan, C., 2023. A warming-induced reduction in snow fraction amplifies rainfall extremes. *Nature,* 619(7969)**,** 305-310.

Orgill, S., 2016. *Soil Carbon in the Monaro Region: A report from Action on the Ground*, NSW Agriculture.

Öztürk, M., Hakeem, K. R., Faridah-Hanum, I. & Efe, R., 2015. *Climate change impacts on high-altitude ecosystems*, Springer. 3319128590

Parish, R., 2014. *Mountain environments*, Routledge. 1315837994

Parker, T. C., Subke, J. A. & Wookey, P. A., 2015. Rapid carbon turnover beneath shrub and tree vegetation is associated with low soil carbon stocks at a subarctic treeline. *Global Change Biology,* 21(5)**,** 2070-2081.

Pauchard, A., Kueffer, C., Dietz, H., Daehler, C. C., Alexander, J., Edwards, P. J., Arévalo, J. R., Cavieres, L. A., Guisan, A. & Haider, S., 2009. Ain't no mountain high enough: plant invasions reaching new elevations. *Frontiers in Ecology and the Environment,* 7(9)**,** 479-486.

Peel, M. C., Finlayson, B. L. & McMahon, T. A., 2007. Updated world map of the Köppen-Geiger climate classification. *Hydrology and earth system sciences,* 11(5)**,** 1633-1644.

Pepin, N., Bradley, R. S., Diaz, H. F., Baraer, M., Caceres, E. B., Forsythe, N., Fowler, H., Greenwood, G., Hashmi, M. Z., Liu, X. D., Miller, J. R., Ning, L., Ohmura, A., Palazzi, E., Rangwala, I., Schöner, W., Severskiy, I., Shahgedanova, M., Wang, M. B., Williamson, S. N., Yang, D. Q. & Mountain Research Initiative, E. D. W. W. G., 2015. Elevation-dependent warming in mountain regions of the world. *Nature Climate Change,* 5(5)**,** 424-430. 10.1038/nclimate2563.

Pepin, N. C., Arnone, E., Gobiet, A., Haslinger, K., Kotlarski, S., Notarnicola, C., Palazzi, E., Seibert, P., Serafin, S. & Schöner, W., 2022a. Climate changes and their elevational patterns in the mountains of the world. *Reviews of geophysics,* 60(1)**,** e2020RG000730.

Pepin, N. C., Arnone, E., Gobiet, A., Haslinger, K., Kotlarski, S., Notarnicola, C., Palazzi, E., Seibert, P., Serafin, S., Schöner, W., Terzago, S., Thornton, J. M., Vuille, M. & Adler, C., 2022b. Climate Changes and Their Elevational Patterns in the Mountains of the World. *Reviews of Geophysics,* 60(1)**,** e2020RG000730. https://doi.org/10.1029/2020RG000730.

Pepler, A. S., Trewin, B. & Ganter, C., 2015. The influences of climate drivers on the Australian snow season. *Australian Meteorological and Oceanographic Journal,* 65(2)**,** 195-205.

Pereira, P., Inacio, M., Bogunovic, I., Francos, M., Barceló, D. & Zhao, W., 2022. Ecosystem services in mountain environments. Benefits and threats.

Perner, K., Moros, M., De Deckker, P., Blanz, T., Wacker, L., Telford, R., Siegel, H., Schneider, R. & Jansen, E., 2018. Heat export from the tropics drives mid to late Holocene palaeoceanographic changes offshore southern Australia. *Quaternary Science Reviews,* 180(96-110).

Perrier, L., Garneau, M., Pratte, S. & Sanderson, N. K., 2022. Climate-driven Holocene ecohydrological and carbon dynamics from maritime peatlands of the Gulf of St. Lawrence, eastern Canada. *The Holocene,* 32(8)**,** 749-763.

Petherick, L., Bostock, H., Cohen, T. J., Fitzsimmons, K., Tibby, J., Fletcher, M.-S., Moss, P., Reeves, J., Mooney, S. & Barrows, T., 2013. Climatic records over the past 30 ka from temperate Australia–a synthesis from the Oz-INTIMATE workgroup. *Quaternary Science Reviews,* 74(58-77).

Pickering, C., 2007. Climate change and other threats in the Australian Alps. *Protected Areas: Buffering nature against climate change,* 18(28).

Pickering, C. & Green, K., 2009. Vascular plant distribution in relation to topography, soils and micro-climate at five GLORIA sites in the Snowy Mountains, Australia. *Australian Journal of Botany,* 57(3)**,** 189-199.

Pickering, C., Green, K., Barros, A. A. & Venn, S., 2014. A resurvey of late-lying snowpatches reveals changes in both species and functional composition across snowmelt zones. *Alpine Botany,* 124(2)**,** 93-103.

Pickering, C. & Hill, W., 2003. Ecological change as a result of winter tourism: snow manipulation in the Australian Alps. *Nature-based tourism, environment and land management.* CABI Publishing Wallingford UK. 137-149

Pickering, C., Hill, W. & Green, K., 2008. Vascular plant diversity and climate change in the alpine zone of the Snowy Mountains, Australia. *Biodiversity and Conservation,* 17(1627-1644).

Pickering, C., Johnston, S., Green, K. & Enders, G., 2003a. Impacts of nature tourism on the Mount Kosciuszko alpine area, Australia. *Nature-based tourism, environment and land management.* CABI Publishing Wallingford UK. 123-135

Pickering, C. & Venn, S., 2013. Increasing the resilience of the Australian flora to climate change and associated threats: a plant functional traits approach. *National Climate Change Adaptation Research Facility Publishing: Gold Coast*.

Pickering, C. M., Harrington, J. & Worboys, G., 2003b. Environmental impacts of tourism on the Australian Alps protected areas. *Mountain Research and Development,* 23(3)**,** 247-254.

Pickering, C. M., Hill, W., Newsome, D. & Leung, Y.-F., 2010. Comparing hiking, mountain biking and horse riding impacts on vegetation and soils in Australia and the United States of America. *Journal of environmental management,* 91(3)**,** 551-562.

Pickering, C. M., Rossi, S. & Barros, A., 2011. Assessing the impacts of mountain biking and hiking on subalpine grassland in Australia using an experimental protocol. *Journal of environmental management,* 92(12)**,** 3049-3057.

Pillans, B., 1987. Lake shadows: aeolian clay sheets associated with ephemeral lakes in basalt terrain, southern New South Wales. *Search (Sydney),* 18(6)**,** 313-315.

Pillans, B. & Walker, P., 1995. Landscape and Soil Development on Monaro Basalt West of Nimmitabel, New South Wales. *Australian Geographical Studies,* 33(2)**,** 193-211.

Porch, N. & Allen, J., 1995. Tasmania: archaeological and palaeo-ecological perspectives. *Antiquity,* 69(265)**,** 714-732.

Portenga, E. W., Rood, D. H., Bishop, P. & Bierman, P. R., 2016a. A late Holocene onset of Aboriginal burning in southeastern Australia. *Geology,* 44(2)**,** 131-134.

Portenga, E. W., Westaway, K. E. & Bishop, P., 2016b. Timing of post-European settlement alluvium deposition in SE Australia: A legacy of European land-use in the Goulburn Plains. *The Holocene,* 26(9)**,** 1472-1485.

Poulenard, J. & Podwojewski, P., 2006. Alpine soils. *Encyclopedia of Soil Science. New York: Marcel Dekker,* 7579

Prosser, I., 1990. Fire, humans and denudation at Wangrah Creek, southern Tablelands, NSW. *Australian Geographical Studies,* 28(1)**,** 77-95.

Quigley, M. C., Horton, T., Hellstrom, J. C., Cupper, M. L. & Sandiford, M., 2010. Holocene climate change in arid Australia from speleothem and alluvial records. *The Holocene,* 20(7)**,** 1093-1104.

R Core Team, 2020. RA language and environment for statistical computing, R Foundation for Statistical. *Computing*.

Raine, J. I., 1974. *Pollen sedimentation in relation to the Quaternary vegetation history of the Snowy Mountains of New South Wales*, The Australian National University (Australia). 1073947483

Rajczak, J. & Schär, C., 2017. Projections of future precipitation extremes over Europe: A multimodel assessment of climate simulations. *Journal of Geophysical Research: Atmospheres,* 122(20)**,** 10,773-10,800.

Rangwala, I. & Miller, J. R., 2012. Climate change in mountains: a review of elevation-dependent warming and its possible causes. *Climatic change,* 114(527-547).

Raut, B. A., Jakob, C. & Reeder, M. J., 2014. Rainfall changes over southwestern Australia and their relationship to the Southern Annular Mode and ENSO. *Journal of Climate,* 27(15)**,** 5801-5814.

Razjigaeva, N., Ganzey, L., Mokhova, L., Makarova, T., Panichev, A., Kudryavtseva, E., Arslanov, K. A., Maksimov, F. & Starikova, A., 2017. Late Holocene environmental changes recorded in the deposits of paleolake of the Shkotovskoe Plateau, Sikhote-Alin Mountains, Russian Far East. *Journal of Asian Earth Sciences,* 136(89-101).

Rees, A. B. & Cwynar, L. C., 2010. Evidence for early postglacial warming in Mount field National Park, Tasmania. *Quaternary Science Reviews,* 29(3-4)**,** 443-454.

Rehm, E. & Feeley, K. J., 2016. Many species risk mountain top extinction long before they reach the top. *Frontiers of biogeography,* 8(1).

Rein, B., Lückge, A., Reinhardt, L., Sirocko, F., Wolf, A. & Dullo, W. C., 2005. El Niño variability off Peru during the last 20,000 years. *Paleoceanography,* 20(4)**,** 1-17.

Reinfelds, I., Swanson, E., Cohen, T., Larsen, J. & Nolan, A., 2014. Hydrospatial assessment of streamflow yields and effects of climate change: Snowy Mountains, Australia. *Journal of Hydrology,* 512(206-220).

Renaut, R. W. & Owen, R. B., 2023. Lake Processes and Sedimentation. *The Kenya Rift Lakes: Modern and Ancient: Limnology and Limnogeology of Tropical Lakes in a Continental Rift.* Berlin, Heidelberg: Springer Berlin Heidelberg. 129-160

Richardson, J. & Caldwell, J., 2002. Diatom floras of Australia's alkaline Monaro lakes: a biogeographic perspective. *Internationale Vereinigung für theoretische und angewandte Limnologie: Verhandlungen,* 28(2)**,** 1076-1081.

Ride, W., Taylor, G., Walker, P. & Davis, A., 1989. Zoological history of the Australian Alps—the mammal fossil-bearing deposits of the Monaro. *The scientific significance of the Australian Alps***,** 79-110.

Roach, I., McQueen, K. & Brown, M., 1994. Physical and petrological characteristics of basaltic eruption sites in the Monaro Volcanic Province, southeastern New South Wales, Australia. *AGSO Journal of Australian Geology and Geophysics,* 15(3)**,** 381.

Roach, I. C., 1999. *The setting, structural control, geochemistry and mantle source of the Monaro Volcanic Province, southeastern New South Wales*, University of Canberra.

Robertson, G., Wright, J., Brown, D., Yuen, K. & Tongway, D., 2019. An assessment of feral horse impacts on treeless drainage lines in the Australian Alps. *Ecological Management & Restoration,* 20(1)**,** 21-30.

Roe, G. H., 2005. Orographic precipitation. *Annu. Rev. Earth Planet. Sci.,* 33(1)**,** 645-671.

Romeo, R., Manuelli, S., Geringer, M. & Barchiesi, V., 2021. Mountain farming systems–Seeds for the future.

Romeo, R., Vita, A., Testolin, R. & Hofer, T., 2015. Mapping the vulnerability of mountain peoples to food insecurity.

Ronkainen, T., McClymont, E. L., Tuittila, E.-S. & Väliranta, M., 2014. Plant macrofossil and biomarker evidence of fen–bog transition and associated changes in vegetation in two Finnish peatlands. *The Holocene,* 24(7)**,** 828-841.

Roop, H. A., Levy, R., Dunbar, G. B., Vandergoes, M. J., Howarth, J., Fitzsimons, S., Moon, H. S., Zammit, C., Ditchburn, R., Baisden, T. & Yoon, H. I., 2016. A hydroclimate-proxy model based on sedimentary facies in an annually laminated sequence from Lake Ohau, South Island, New Zealand. *Journal of Paleolimnology,* 55(1)**,** 1-16. 10.1007/s10933-015-9853-3.

Ross, C. & Brack, C., 2015. *Eucalyptus viminalis* dieback in the Monaro region, NSW. *Australian Forestry,* 78(4)**,** 243-253.

Rossignol-Strick, M., 1999. The Holocene climatic optimum and pollen records of sapropel 1 in the eastern Mediterranean, 9000–6000 BP. *Quaternary Science Reviews,* 18(4-5)**,** 515-530.

Rostami, H., Richter, T., Ruter, A. H., Azizi, G., Darabi, H. & Maleki, S., 2024. High-resolution, multi-proxy reconstruction of central Zagros paleoclimate and paleoenvironment from the Late Pleistocene to the Holocene. *Quaternary International,* 692(45-55).

Ruddiman, W. F., 2001. *Earth's climate: past and future*, Macmillan. 0716737418

Sahukar, R., Gallery, C., Smart, J. & Mitchell, P., 2003. The Bioregions of New South Wales: their biodiversity, conservation and history. *National Parks and Wildlife Service (NSW), Sydney*.

Saunders, K., Kamenik, C., Hodgson, D. A., Hunziker, S., Siffert, L., Fischer, D., Fujak, M., Gibson, J. A. & Grosjean, M., 2012. Late Holocene changes in precipitation in northwest Tasmania and their potential links to shifts in the Southern Hemisphere westerly winds. *Global and Planetary Change,* 92(82-91).

Sayre, R., Frye, C., Karagulle, D., Krauer, J., Breyer, S., Aniello, P., Wright, D. J., Payne, D., Adler, C. & Warner, H., 2018. A new high-resolution map of world mountains and an online tool for visualizing and comparing characterizations of global mountain distributions. *Mountain Research and Development,* 38(3)**,** 240-249.

Scanes, P. R., McSorley, A. & Dickson, A., 2021. Feral horses (*Equus caballus*) increase suspended sediment in subalpine streams. *Marine and Freshwater Research,* 72(9)**,** 1290-1302.

Schaefli, B., Hingray, B. & Musy, A., 2007. Climate change and hydropower production in the Swiss Alps: quantification of potential impacts and related modelling uncertainties. *Hydrology and Earth System Sciences,* 11(3)**,** 1191-1205.

Scheffer, M., Bascompte, J., Brock, W. A., Brovkin, V., Carpenter, S. R., Dakos, V., Held, H., Van Nes, E. H., Rietkerk, M. & Sugihara, G., 2009. Early-warning signals for critical transitions. *Nature,* 461(7260)**,** 53-59.

Scheffer, M. & Carpenter, S. R., 2003. Catastrophic regime shifts in ecosystems: linking theory to observation. *Trends in ecology & evolution,* 18(12)**,** 648-656.

Scheffer, M., Carpenter, S. R., Lenton, T. M., Bascompte, J., Brock, W., Dakos, V., Van de Koppel, J., Van de Leemput, I. A., Levin, S. A. & Van Nes, E. H., 2012. Anticipating critical transitions. *science,* 338(6105)**,** 344-348.

Scherrer, P. & Pickering, C. M., 2001. Effects of grazing, tourism and climate change on the alpine vegetation of Kosciuszko National Park. *Victorian Naturalist,* 118(3)**,** 93-93.

Schinner, F., 1982. Soil microbial activities and litter decomposition related to altitude. *Plant and Soil,* 65(1)**,** 87-94.

Schittek, K., Kock, S. T., Lücke, A., Hense, J., Ohlendorf, C., Kulemeyer, J. J., Lupo, L. C. & Schäbitz, F., 2016. A high-altitude peatland record of environmental changes in the NW Argentine Andes (24 S) over the last 2100 years. *Climate of the Past,* 12(5)**,** 1165-1180.

Schmeller, D. S., Loyau, A., Bao, K., Brack, W., Chatzinotas, A., De Vleeschouwer, F., Friesen, J., Gandois, L., Hansson, S. V. & Haver, M., 2018. People, pollution and pathogens–Global change impacts in mountain freshwater ecosystems. *Science of the Total Environment,* 622(756-763.

Schmeller, D. S., Urbach, D., Bates, K., Catalan, J., Cogălniceanu, D., Fisher, M. C., Friesen, J., Füreder, L., Gaube, V. & Haver, M., 2022. Scientists' warning of threats to mountains. *Science of the Total Environment,* 853(158611).

Schneider, T., Hampel, H., Mosquera, P. V., Tylmann, W. & Grosjean, M., 2018. Paleo-ENSO revisited: Ecuadorian Lake Pallcacocha does not reveal a conclusive El Niño signal. *Global and Planetary Change,* 168(54-66).

Schroeter, N., Toney, J. L., Lauterbach, S., Kalanke, J., Schwarz, A., Schouten, S. & Gleixner, G., 2020. How to deal with multi-proxy data for paleoenvironmental reconstructions: Applications to a Holocene lake sediment record from the Tian Shan, Central Asia. *Frontiers in Earth Science,* 8(353).

Schumacher, S., Reineking, B., Sibold, J. & Bugmann, H., 2006. Modeling the impact of climate and vegetation on fire regimes in mountain landscapes. *Landscape Ecology,* 21(4)**,** 539-554.

Searle, R. 2021. Australian Soil Classification Map (3" resolution) – Release 1. CSIRO (Commonwealth Scientific and Industrial Research Organisation). Accessed: 15 December 2025. https://data.csiro.au/collection/csiro:55695.

Shandra, O., Weisberg, P. & Martazinova, V., 2013. Influences of climate and land use history on forest and timberline dynamics in the Carpathian Mountains during the twentieth century. *The Carpathians: integrating nature and society towards sustainability.* Springer. 209-223

Sharp, K., 2004. Cenozoic volcanism, tectonism and stream derangement in the Snowy Mountains and northern Monaro of New South Wales. *Australian Journal of Earth Sciences,* 51(1)**,** 67-83.

Sharples, J. J., 2020. Foehn winds. *Encyclopedia of Wildfires and Wildland-Urban Interface (WUI) Fires.* Springer. 490-496

Shulmeister, J., 1999. Australasian evidence for mid-Holocene climate change implies precessional control of Walker Circulation in the Pacific. *Quaternary International,* 57(81-91).

Shuttleworth, E., Evans, M., Hutchinson, S. & Rothwell, J., 2015. Peatland restoration: controls on sediment production and reductions in carbon and pollutant export. *Earth Surface Processes and Landforms,* 40(4)**,** 459-472.

Siles, J. A., Cajthaml, T., Filipova, A., Minerbi, S. & Margesin, R., 2017. Altitudinal, seasonal and interannual shifts in microbial communities and chemical composition of soil organic matter in Alpine forest soils. *Soil Biology and Biochemistry,* 112(1-13).

Silveira, F. A., Barbosa, M., Beiroz, W., Callisto, M., Macedo, D. R., Morellato, L. P. C., Neves, F. S., Nunes, Y. R., Solar, R. R. & Fernandes, G. W., 2019. Tropical mountains as natural laboratories to study global changes: a long-term ecological research project in a megadiverse biodiversity hotspot. *Perspectives in Plant Ecology, Evolution and Systematics,* 38(64-73).

Singh, G. & Geissler, E. A., 1985. Late Cainozoic history of vegetation, fire, lake levels and climate, at Lake George, New South Wales, Australia. *Philosophical Transactions of the Royal Society of London. Series B, Biological Sciences*, 379-447.

Slattery, D., 2015. *Australian Alps,* Clayton South, Victoria, Australia, CSIRO Publishing. 978-1-4863-0173-7

Slatyer, R., 2010. Climate change impacts on Australia's alpine ecosystems. *The ANU Undergraduate Research Journal,* 2(81-97).

Slatyer, R. A., Umbers, K. D. & Arnold, P. A., 2022. Ecological responses to variation in seasonal snow cover. *Conservation Biology,* 36(1), e13727.

Slee, A. & Shulmeister, J., 2015. The distribution and climatic implications of periglacial landforms in eastern Australia. *Journal of Quaternary Science,* 30(8), 848-858.

Snethlage, M. A., Geschke, J., Ranipeta, A., Jetz, W., Yoccoz, N. G., Körner, C., Spehn, E. M., Fischer, M. & Urbach, D., 2022. A hierarchical inventory of the world's mountains for global comparative mountain science. *Scientific data,* 9(1), 149.

Snowy Monaro Regional Council, 2018. Snowy Monaro Regional Economic Development Strategy 2018–2022. NSW Department of Premier and Cabinet. Sydney, NSW.

Somers, L. D. & McKenzie, J. M., 2020. A review of groundwater in high mountain environments. *Wiley Interdisciplinary Reviews: Water,* 7(6), e1475.

Sottile, G. D., Bamonte, F. P., Mancini, M. V. & Bianchi, M. M., 2012. Insights into Holocene vegetation and climate changes at the southeast of the Andes: *Nothofagus* forest and Patagonian steppe fire records. *The Holocene,* 22(11), 1309-1322. 10.1177/0959683611405082.

Soudzilovskaia, N. A., Elumeeva, T. G., Onipchenko, V. G., Shidakov, I. I., Salpagarova, F. S., Khubiev, A. B., Tekeev, D. K. & Cornelissen, J. H., 2013. Functional traits predict relationship between plant abundance dynamic and long-term climate warming. *Proceedings of the National Academy of Sciences,* 110(45), 18180-18184.

Southern, W., 1982. Late Quaternary vegetation and environments of Jackson's Bog and the Monaro Tablelands. *New South Wales. M. Sc. Thesis, Monash University, Melbourne, Australia*.

Sritharan, M. S., Hemmings, F. A. & Moles, A. T., 2021. Few changes in native Australian alpine plant morphology, despite substantial local climate change. *Ecology and Evolution,* 11(9), 4854-4865.

Stanley, S. & De Deckker, P., 2002. A Holocene record of allochthonous, aeolian mineral grains in an Australian alpine lake; implications for the history of climate change in southeastern Australia. *Journal of Paleolimnology,* 27(207-219).

Starr, B., Abbott, K., Ryan, J. & Goggin, J., 1996. Bredbo and the Bidgee: management strategies for the Murrumbidgee River and its tributaries in the Bredbo district.

State Government of NSW Spatial Services. 2025. NSW Hydrography. NSW, S. G. O. & Services, S. 25 April 2025. https://data.nsw.gov.au/data/dataset/nsw-hydrography.

Steffen, W., 2009. *Australia's biodiversity and climate change*, Csiro Publishing. 0643101829

Stephens, S. L., Collins, B. M., Fettig, C. J., Finney, M. A., Hoffman, C. M., Knapp, E. E., North, M. P., Safford, H. & Wayman, R. B., 2018. Drought, Tree Mortality, and Wildfire in Forests Adapted to Frequent Fire. *BioScience,* 68(2)**,** 77-88. 10.1093/biosci/bix146.

Stephenson, B., David, B., Fresløv, J., Arnold, L. J., Land, G., Corporation, W. A., Delannoy, J.-J., Petchey, F., Urwin, C., Wong, V. N. & Fullagar, R., 2020. 2000 Year-old Bogong moth (*Agrotis infusa*) Aboriginal food remains, Australia. *Scientific reports,* 10(1)**,** 22151.

Stevenson, J. & Haberle, S., 2018. Macro charcoal analysis: A modified technique used by the Department of Archaeology and Natural History. Canberra, ACT, Australia: PalaeoWorks, Dept. of Archaeology & Natural History, Research School of Pacific & Asian Studies, The Australian National University.

Stewart, I. T., 2009. Changes in snowpack and snowmelt runoff for key mountain regions. *Hydrological Processes: An International Journal,* 23(1)**,** 78-94.

Stott, L., Cannariato, K., Thunell, R., Haug, G. H., Koutavas, A. & Lund, S., 2004. Decline of surface temperature and salinity in the western tropical Pacific Ocean in the Holocene epoch. *Nature,* 431(7004)**,** 56-59.

Stromsoe, N., Marx, S. K., Callow, N., McGowan, H. A. & Heijnis, H., 2016. Estimates of late Holocene soil production and erosion in the Snowy Mountains, Australia. *Catena,* 145(68-82).

Stromsoe, N., Vernon, J., Marx, S., Woodward, C. & Saunders, K., 2018. Late Holocene climate variability in the Australian Alps: can sedimentary and geochemical tracers track fine scale paleo-environment change? *AQUA Biennial Meeting 2018.* Canberra, Australia: Australasian Quaternary Association (AQUA).

Stuiver, M. & Reimer, P. J., 1993. Extended 14C Data Base and Revised CALIB 3.0 14C Age Calibration Program. *Radiocarbon,* 35(1)**,** 215-230. 10.1017/S0033822200013904.

Swindles, G. T., Mullan, D. J., Brannigan, N. T., Fewster, R. E., Sim, T. G., Gallego-Sala, A., Blaauw, M., Lamentowicz, M., Jassey, V. E. & Marcisz, K., 2025. Climate and water-table levels regulate peat accumulation rates across Europe. *Plos one,* 20(7)**,** e0327422.

Swindles, G. T., Mullan, D. J., Brannigan, N. T., Sim, T. G., Gallego-Sala, A., Blaauw, M., Lamentowicz Lamentowicz, M., Green, S. M., Roland, T. P. & Fewster, R. Climate and hydrology control apparent rates of peat accumulation across Europe. EGU General Assembly Conference Abstracts, 2024. 21369.

Sydney Morning Herald. 1858. MANEROO. *Sydney Morning Herald (NSW : 1842 - 1954)*, 24 May 1858.

Tamhane, J., Thomas, Z. A., Cadd, H., Harris, M. R., Turney, C., Marjo, C. E., Wang, H., Akter, R., Panaretos, P. & Halim, A., 2023. Mid-Holocene intensification of Southern Hemisphere westerly winds and implications for regional climate dynamics. *Quaternary Science Reviews,* 305(108007).

Tansley, A. G., 1935. The use and abuse of vegetational concepts and terms. *Ecology,* 16(3)**,** 284-307.

Tate, A. M., Heile, J., Giacomo, J. & Zoppi, U., 2023. Status report: A decade of traditional radiocarbon dating applications by DirectAMS. *Nuclear Instruments and Methods in Physics Research Section B: Beam Interactions with Materials and Atoms,* 537(23-28).

Taylor, G. & Roach, I., 2003. Monaro Region, New South Wales. *Cooperative Research Centre for Landscape Environments and Mineral Exploration (CRC LEME)***,** 6.

Taylor, G. & Walker, P., 1986. Tertiary Lake Bunyan, northern Monaro, NSW, Part I: geological setting and landscape history. *Australian Journal of Earth Sciences,* 33(2)**,** 219-229.

Theden-Ringl, F., 2010. *Formation History and Past Fire Regimes at Pengillys Bog, Kosciuszko National Park.* Australian National University.

Theden-Ringl, F., 2016. Aboriginal presence in the high country: new dates from the Namadgi Ranges in the Australian Capital Territory. *Australian Archaeology,* 82(1)**,** 25-42.

Theden-Ringl, F., Keaney, B., Hope, G. S., Gadd, P. S. & Heijnis, H. Landscape change and Indigenous fire use in the Namadgi Ranges in the Australian Alps over 16,000 years. Proceedings of the Linnean Society of New South Wales, 2023. Linnean Society of New South Wales Sydney, 75-97.

Theobald, A., McGowan, H. & Speirs, J., 2016. Trends in synoptic circulation and precipitation in the Snowy Mountains region, Australia, in the period 1958–2012. *Atmospheric Research,* 169(434-448).

Thirumalai, K., DiNezio, P. N., Partin, J. W., Liu, D., Costa, K. & Jacobel, A., 2024. Future increase in extreme El Niño supported by past glacial changes. *Nature,* 634(8033)**,** 374-380.

Thomas, A., 1991. *Giandarra Bog, NSW: A Natural Record of Environmental Change*, Australian Defence Force Academy, Department of Geography and Oceanography.

Thomas, Z. A., Mooney, S., Cadd, H., Baker, A., Turney, C., Schneider, L., Hogg, A., Haberle, S., Green, K. & Weyrich, L. S., 2022. Late Holocene climate anomaly concurrent with fire activity and ecosystem shifts in the eastern Australian Highlands. *Science of the Total Environment,* 802(149542).

Thompson, R., 2012. *Environmental magnetism*, Springer Science & Business Media. 9401180369

Thorburn, D. F., 1974. The palynology of Lake Hayes, Central Otago, New Zealand.

Tito, R., Vasconcelos, H. L. & Feeley, K. J., 2020. Mountain ecosystems as natural laboratories for climate change experiments. *Frontiers in Forests and Global Change,* 3(38).

Toomey, J., Glenday, J. & Twyford, L. 2024. As Australia's ski seasons get shorter, towns and operators who rely on the snow are looking to summer to diversify. *ABC News*, 6 September.

Tozer, C. R., Risbey, J. S., Monselesan, D. P., Pook, M. J., Irving, D., Ramesh, N., Reddy, J. & Squire, D. T., 2023. Impacts of ENSO on Australian rainfall: What not to expect. *Journal of Southern Hemisphere Earth Systems Science,* 73(1)**,** 77-81.

Treby, S. & Grover, S. P., 2023. Carbon emissions from Australian *Sphagnum* peatlands increase with feral horse (*Equus caballus*) presence. *Journal of Environmental Management,* 347(119034.

Treby, S. & Grover, S. P., 2024. Carbon and nitrogen storage in Australian *Sphagnum* peatlands: The influence of feral horse degradation. *Journal of Environmental Management,* 359(121049.

Troll, C., 1971. Landscape ecology (geoecology) and biogeocenology—A terminological study. *Geoforum,* 2(4)**,** 43-46.

Threatened Species Scientific Committe, 2008. Listing Advice: Alpine *Sphagnum* Bogs and Associated Fens ecological community. Threatened Species Scientific Committee.

Threatened Species Scientific Committe, 2016. Approved Conservation Advice (including listing advice) for Natural Temperate Grassland of the South Eastern Highlands (EC 152). Department of the Environment. Committee, T. S. S., Canberra, ACT, Australia.

Tulau, M. & McInnes-Clarke, S., 2015. Fire and Soils: A review of the potential impacts of different fire regimes on soil erosion and sedimentation, nutrient and carbon cycling, and impacts on water quantity and quality. *Spanish Journal of Soil Science,* 34(12)**,** 12-19.

Turner, J. N., Holmes, N., Davis, S. R., Leng, M. J., Langdon, C. & Scaife, R. G., 2015. A multiproxy (micro-XRF, pollen, chironomid and stable isotope) lake sediment record for the Lateglacial to Holocene transition from Thomastown Bog, Ireland. *Journal of Quaternary Science,* 30(6)**,** 514-528.

Turney, C., Becerra-Valdivia, L., Sookdeo, A., Thomas, Z. A., Palmer, J., Haines, H. A., Cadd, H., Wacker, L., Baker, A. & Andersen, M. S., 2021. Radiocarbon protocols and first intercomparison results from the Chronos 14Carbon-Cycle facility, University of New South Wales, Sydney, Australia. *Radiocarbon,* 63(3)**,** 1003-1023.

Turney, C. S., M c Glone, M., Palmer, J., Fogwill, C., Hogg, A., Thomas, Z. A., Lipson, M., Wilmshurst, J. M., Fenwick, P. & Jones, R. T., 2016. Intensification of Southern Hemisphere westerly winds 2000–1000 years ago: evidence from the subantarctic Campbell and Auckland Islands (52–50 S). *Journal of Quaternary Science,* 31(1)**,** 12-19.

Upper Snowy Landcare, 2015. Background on Monaro Dieback. New South Wales Soil Knowledge Network.

Vandergoes, M. J. & Prior, C. A., 2003. AMS dating of pollen concentrates—a methodological study of late Quaternary sediments from south Westland, New Zealand. *Radiocarbon,* 45(3)**,** 479-491.

Veevers, J., Conaghan, P., Powell, C. M., Cowan, E., McDonnell, K. & Shaw, S., 1994. Eastern Australia.

Vernon, J., 2017. *Identifying the impacts of climate change and human activity in Kosciuszko National Park.* University of Wollongong.

Villa-Martínez, R. & Moreno, P. I., 2007. Pollen evidence for variations in the southern margin of the westerly winds in SW patagonia over the last 12,600 years. *Quaternary Research,* 68(3)**,** 400-409. 10.1016/j.yqres.2007.07.003.

Vitense, K., Hanson, M. A., Herwig, B. R., Zimmer, K. D. & Fieberg, J., 2018. Uncovering state-dependent relationships in shallow lakes using Bayesian latent variable regression. *Ecological Applications,* 28(2)**,** 309-322.

Viviroli, D., Kummu, M., Meybeck, M., Kallio, M. & Wada, Y., 2020. Increasing dependence of lowland populations on mountain water resources. *Nature Sustainability,* 3(11)**,** 917-928.

Viviroli, D. & Weingartner, R., 2004. The hydrological significance of mountains: from regional to global scale. *Hydrology and earth system sciences,* 8(6)**,** 1017-1030.

Voigt, I., Chiessi, C. M., Prange, M., Mulitza, S., Groeneveld, J., Varma, V. & Henrich, R., 2015. Holocene shifts of the southern westerlies across the South Atlantic. *Paleoceanography,* 30(2)**,** 39-51.

Wahl, D., Starratt, S., Anderson, L., Kusler, J., Fuller, C., Addison, J. & Wan, E., 2015. Holocene environmental changes inferred from biological and sedimentological proxies in a high elevation Great Basin lake in the northern Ruby Mountains, Nevada, USA. *Quaternary International,* 387(87-98).

Walker, S., Lee, W. G. & Rogers, G. M., 2003. The woody vegetation of Central Otago, New Zealand: its present and past distribution and future restoration needs. *Science for Conservation,* 226(4.1).

Wan, L., Li, D., Zhu, C., Liu, Z., Zhang, S., Lin, X. & Lu, J., 2025. Antarctic circumpolar current evolution and its relation to southern hemisphere westerly winds during the holocene. *Climate Dynamics,* 63(8)**,** 331.

Wang, R., Dearing, J. A., Langdon, P. G., Zhang, E., Yang, X., Dakos, V. & Scheffer, M., 2012. Flickering gives early warning signals of a critical transition to a eutrophic lake state. *Nature,* 492(7429)**,** 419-422.

Wang, Y., Sun, J., He, W., Ye, C., Liu, B., Chen, Y., Zeng, T., Ma, S., Gan, X. & Miao, C., 2022. Migration of vegetation boundary between alpine steppe and meadow on a century-scale across the Tibetan Plateau. *Ecological Indicators,* 136(108599).

Wanner, H., Beer, J., Bütikofer, J., Crowley, T. J., Cubasch, U., Flückiger, J., Goosse, H., Grosjean, M., Joos, F. & Kaplan, J. O., 2008. Mid-to Late Holocene climate change: an overview. *Quaternary Science Reviews,* 27(19-20)**,** 1791-1828.

Ward-Jones, J., 2021. Spotting snow-gum dieback: Guide for recording incidental observations of snow-gums exhibiting dieback symptoms using the ArcGIS Survey123 application. Fenner School of Environment and Society, The Australian National University. Canberra, ACT.

Wasson, R., Mazari, R., Starr, B. & Clifton, G., 1998. The recent history of erosion and sedimentation on the Southern Tablelands of southeastern Australia: sediment flux dominated by channel incision. *Geomorphology,* 24(4)**,** 291-308.

Way, A. M., Piper, P. J., Chalker, R., Wilkins, D., Wilkins, E., Watson Redpath, L., Glass, P., Carroll, M. R., Nutman, E. & Kononenko, N., 2025. The earliest evidence of high-elevation ice age occupation in Australia. *Nature Human Behaviour***,** 1-9.

Wearne, L. J. & Morgan, J. W., 2001. Recent forest encroachment into subalpine grasslands near Mount Hotham, Victoria, Australia. *Arctic, Antarctic, and Alpine Research,* 33(3)**,** 369-377.

Webb, J., 2017. Denudation history of the Southeastern Highlands of Australia. *Australian Journal of Earth Sciences,* 64(7)**,** 841-850.

Webber, P. J., 2019. *High altitude geoecology*, Routledge. 0429727356

Wesche, K., Ambarlı, D., Kamp, J., Török, P., Treiber, J. & Dengler, J., 2016. The Palaearctic steppe biome: a new synthesis. *Biodiversity and conservation,* 25(12)**,** 2197-2231.

West, A., Arnold, M., Aumaître, G., Bourlès, D., Keddadouche, K., Bickle, M. & Ojha, T., 2014. High natural erosion rates are the backdrop for enhanced anthropogenic soil erosion in the Middle Hills of Nepal. *Earth Surface Dynamics Discussions,* 2(2)**,** 935-969.

White, S. M., Ravelo, A. C. & Polissar, P. J., 2018. Dampened El Niño in the early and mid-Holocene due to insolation-forced warming/deepening of the thermocline. *Geophysical Research Letters,* 45(1)**,** 316-326.

Whitlock, C., Bianchi, M. M., Bartlein, P. J., Markgraf, V., Marlon, J., Walsh, M. & McCoy, N., 2006. Postglacial vegetation, climate, and fire history along the east side of the Andes (lat 41–42.5°S), Argentina. *Quaternary Research,* 66(2)**,** 187-201. 10.1016/j.yqres.2006.04.004.

Whitlock, C. & Larsen, C., 2001. Charcoal as a Fire Proxy. *In:* Smol, J. P., Birks, H. J. B., Last, W. M., Bradley, R. S. & Alverson, K. (eds.) *Tracking Environmental Change Using Lake Sediments: Terrestrial, Algal, and Siliceous Indicators.* Dordrecht: Springer Netherlands. 75-97

Wilkins, D., Gouramanis, C., De Deckker, P., Fifield, L. K. & Olley, J., 2013. Holocene lake-level fluctuations in Lakes Keilambete and Gnotuk, southwestern Victoria, Australia. *The Holocene,* 23(6)**,** 784-795.

Williams, J. W., Grimm, E. C., Blois, J. L., Charles, D. F., Davis, E. B., Goring, S. J., Graham, R. W., Smith, A. J., Anderson, M. & Arroyo-Cabrales, J., 2018. The Neotoma Paleoecology Database, a multiproxy, international, community-curated data resource. *Quaternary Research,* 89(1)**,** 156-177.

Williams, J. W., Post*, D. M., Cwynar, L. C., Lotter, A. F. & Levesque, A. J., 2002. Rapid and widespread vegetation responses to past climate change in the North Atlantic region. *Geology,* 30(11)**,** 971-974.

Williams, M., Cook, E., van der Kaars, S., Barrows, T., Shulmeister, J. & Kershaw, P., 2009a. Glacial and deglacial climatic patterns in Australia and surrounding regions from 35 000 to 10 000 years ago reconstructed from terrestrial and near-shore proxy data. *Quaternary Science Reviews,* 28(23-24)**,** 2398-2419.

Williams, R. J., Bradstock, R. A., Cary, G. J., Enright, N. J., Gill, A. M., Leidloff, A., Lucas, C., Whelan, R. J., Andersen, A. N. & Bowman, D. J., 2009b. Interactions

between climate change, fire regimes and biodiversity in Australia: a preliminary assessment.

Williams, R. J. & Wahren, C.-H., 2005. Potential impacts of global change on vegetation in Australian alpine landscapes: Climate change, landuse, vegetation dynamics and biodiversity conservation. *Global Change and Mountain Regions: An Overview of Current Knowledge***,** 401-408.

Williams, R. J., Wahren, C.-H., Tolsma, A. D., Sanecki, G. M., Papst, W. A., Myers, B. A., McDougall, K. L., Heinze, D. A. & Green, K., 2008. Large fires in Australian alpine landscapes: their part in the historical fire regime and their impacts on alpine biodiversity. *International Journal of Wildland Fire,* 17(6)**,** 793-808.

Williams, W., Walker, K. & Brand, G., 1970. Chemical composition of some inland surface waters and lake deposits of New South Wales, Australia. *Marine and Freshwater Research,* 21(2)**,** 103-116.

Wilmking, M., Harden, J. & Tape, K., 2006. Effect of tree line advance on carbon storage in NW Alaska. *Journal of Geophysical Research: Biogeosciences,* 111(G2).

Wilmshurst, J. M., McGlone, M. S. & Charman, D. J., 2002. Holocene vegetation and climate change in southern New Zealand: linkages between forest composition and quantitative surface moisture reconstructions from an ombrogenous bog. *Journal of Quaternary Science: Published for the Quaternary Research Association,* 17(7)**,** 653-666.

Wilson, B. R., Tulau, M., Kuginis, L., McInnes-Clarke, S., Grover, S., Milford, H. & Jenkins, B. R., 2022. Distribution, nature and threats to soils of the Australian Alps: a review. *Austral Ecology,* 47(2)**,** 166-188.

Wimbush, D. & Costin, A., 1979. Trends in vegetation at Kosciusko. II. Subalpine range transects, 1959-1978. *Australian Journal of Botany,* 27(6)**,** 789-831.

Winkler, K., Fuchs, R., Rounsevell, M. D. & Herold, M., 2020. HILDA+ Global Land Use Change between 1960 and 2019. *PANGAEA https://doi. org/10.1594/PANGAEA,* 921846(

Wohl, E., 2006. Human impacts to mountain streams. *Geomorphology,* 79(3-4)**,** 217-248.

Woltering, M., Atahan, P., Grice, K., Heijnis, H., Taffs, K. & Dodson, J., 2014. Glacial and Holocene terrestrial temperature variability in subtropical east Australia as inferred from branched GDGT distributions in a sediment core from Lake McKenzie. *Quaternary Research,* 82(1)**,** 132-145.

Woodward, C. & Gadd, P., 2019. The potential power and pitfalls of using the X-ray fluorescence molybdenum incoherent: coherent scattering ratio as a proxy for sediment organic content. *Quaternary International,* 514(30-43.

Woodward, C., Shulmeister, J., Bell, D., Haworth, R., Jacobsen, G. & Zawadzki, A., 2014a. A Holocene record of climate and hydrological changes from Little Llangothlin Lagoon, south eastern Australia. *The Holocene,* 24(12)**,** 1665-1674.

Woodward, C., Shulmeister, J., Zawadzki, A. & Jacobsen, G., 2014b. Major disturbance to aquatic ecosystems in the South Island, New Zealand, following human settlement in the Late Holocene. *The Holocene,* 24(6)**,** 668-678.

Worboys, G. & Pulsford, I., 2013. Observations of Pest horse impacts in the Australian Alps. *Canberra. Available at: www. mount ains-wcpa. org*.

Worboys, G. & Roger, B., 2011. *Caring for our Australian Alps catchments: summary report for policy makers*, Department of Climate Change and Energy Efficiency Canberra. 1921299606

Worboys, G. L., 2015. Protected areas and water catchments: The Australian Alps. *Valuing Nature: Protected Areas and Ecosystem Services***,** 90.

World Database on Protected Areas, 2025. *Protected Planet: The World Database on Protected Areas (WDPA),* Cambridge, UK, UNEP-WCMC and IUCN.

Wulf, H., Bookhagen, B. & Scherler, D., 2010. Seasonal precipitation gradients and their impact on fluvial sediment flux in the Northwest Himalaya. *Geomorphology,* 118(1-2)**,** 13-21.

Xu, T. & Hutchinson, M. F., 2013. New developments and applications in the ANUCLIM spatial climatic and bioclimatic modelling package. *Environmental Modelling & Software,* 40(267-279).

Yang, Q., Liu, Z. & Bai, E., 2023. Comparison of carbon and nitrogen accumulation rate between bog and fen phases in a pristine peatland with the fen-bog transition. *Global Change Biology,* 29(22)**,** 6350-6366.

Yang, T., Sun, J., Li, Y., Wang, M., Li, H., Wang, S., Xia, Z. & Yu, Z., 2025. Impact of climate-induced water-table drawdown on carbon and nitrogen sequestration in a Kobresia-dominated peatland on the central Qinghai-Tibetan Plateau. *Communications Earth & Environment,* 6(1)**,** 188.

Yao, Y., Liu, Y., Wang, Y. & Fu, B., 2021. Greater increases in China's dryland ecosystem vulnerability in drier conditions than in wetter conditions. *Journal of Environmental Management,* 291(112689).

Young, D. M., Baird, A. J., Charman, D. J., Evans, C. D., Gallego-Sala, A. V., Gill, P. J., Hughes, P. D., Morris, P. J. & Swindles, G. T., 2019. Misinterpreting carbon accumulation rates in records from near-surface peat. *Scientific reports,* 9(1)**,** 17939.

Young, D. M., Baird, A. J., Gallego-Sala, A. V. & Loisel, J., 2021. A cautionary tale about using the apparent carbon accumulation rate (aCAR) obtained from peat cores. *Scientific Reports,* 11(1)**,** 9547.

Young, M., 2005. *The Aboriginal people of the Monaro : a documentary history,* Sydney, Dept. of Environment and Conservation. 1741222079

Zhang, D. & Feng, Z., 2018. Holocene climate variations in the Altai Mountains and the surrounding areas: A synthesis of pollen records. *Earth-Science Reviews,* 185(847-869).

Zhang, D., Xu, Z., Liu, Q., Li, Y., Duan, J. & Liu, J., 2024. Late-Holocene environment evolution revealed by multi-proxy analyses of peat sequence in the Sawuer Mountains, northern Xinjiang of China. *Quaternary Science Reviews,* 338(108836).

Zhao, B., Russell, J. M., Blaus, A., Nascimento, M. d. N., Freeman, A. & Bush, M. B., 2024. Tropical Andean climate variations since the last deglaciation. *Proceedings of the National Academy of Sciences,* 121(34)**,** e2320143121.

Zhou, H., Wang, D., Guo, M., Yao, B. & Shang, Z., 2020. Promoting Artificial Grasslands to Improve Carbon Sequestration and Livelihood of Herders. *Carbon Management for Promoting Local Livelihood in the Hindu Kush Himalayan (HKH) Region***,** 211-228.

Zhu, Q., Yang, X., Ji, F., Liu, D. L. & Yu, Q., 2020. Extreme rainfall, rainfall erosivity, and hillslope erosion in Australian Alpine region and their future changes. *International Journal of Climatology,* 40(2)**,** 1213-1227.

Zimmerman, S. R. H., Hemming, S. R. & Starratt, S. W., 2021. Holocene sedimentary architecture and paleoclimate variability at Mono Lake, California. *In:* Starratt, S. W. & Rosen, M. R. (eds.) *From Saline to Freshwater: The Diversity of Western Lakes in Space and Time.* Geological Society of America.

Zylstra, P., 2006. *Fire history of the Australian Alps: prehistory to 2003*, Department of the Environment and Water Resources.

Zylstra, P. J., 2018. Flammability dynamics in the Australian Alps. *Austral Ecology,* 43(5)**,** 578-591.

Appendix A

Supplementary Information for Chapter 2

Section A1: Site selection method

Selection of lake sites for sampling was informed by the key environmental criteria detailed along with in Table A1. Bias emerging from potential spatial autocorrelation of proximal sites was mitigated by a) ensuring a minimum inter-site distance of 20 km, and b) subdividing the region into five user-defined subregions (northern, southern, eastern, western and central). For each subregion, sites were considered if they satisfied the criteria in Table A1; this was assessed with spatial overlay analysis and Boolean logic in ArcGIS using site data digitised from Benson and Jacobs (1994) (DCCEEW, 2015b). From the final candidates, one was prioritised based on secondary considerations such as basin morphology and land use, with a range of bedrock types targeted to evaluate the relationship between lithology and accumulation.

Table A1. Summary of key site selection criteria, justifications and data used to evaluate criterion satisfaction.

Criterion	Details and justification	References and data sources
Site intersection with at least one threatened ecological community (TEC)	Catchment must coincide with the boundaries of Natural Temperate Grassland and/or Monaro Tablelands Cool Temperate Grassy Woodland. Upland Wetlands of the Monaro Plateau not considered as all lakes are members of this community. Presence of a TEC in a catchment is diagnostic of European degradation, rendering these catchments high priority for assessing sensitivity and future systemic change.	(DCCEEW, 2015a, DCCEEW, 2019)
Lakes between 5-25 ha	Lake floor areas must be > 5 ha as these are more likely to be mature basins with sufficiently thick and old sequences. Lakes must also be < 25 ha as these are more likely to have a more discrete depocenter conducive to sediment focusing, while also exhibiting small fetches to minimise the effect of wave action and sediment remobilisation.	(Benson and Jacobs, 1994, Pillans and Walker, 1995, DCCEEW, 2015b)
Moderate to high lake permanence	Ephemeral lakes must be removed from consideration, as more permanently inundated systems are likely to host longer, more continuous records due to their reduced	(Benson and Jacobs, 1994, Pillans and Walker,

susceptibility to lakebed exposure and hiatuses/deflation.	1995,	DCCEEW, 2015b)

Section A2: ^{14}C sample preparation method

A2.1. Bulk sediment pretreatment

1. Load 7-8 g sediment (wet mass) onto a petri dish and dry in an oven (105 ^{o}C) for 24 hours.
2. Measure stable dry mass and crush to a uniform powder using a clean mortar and pestle.
3. Load into aluminium foil for external ABA treatment and analysis.

A2.2. Sporopollenin pretreatment

1. Load ~3 g sediment (wet mass) into a clean 15 ml centrifuge tube.
2. For disaggregation, add 10 ml 5% sodium hexametaphosphate; ('Calgon' or similar) to the centrifuge tube and stir with a vortex mixer. Heat in a hot water bath (80 ^{o}C) for 20 minutes, centrifuge at 3000 rpm for 5 minutes and decant supernatant.
3. For silicate digestion, add 10 ml of lithium heteropolytungstate (LST; 'heavy liquid') to the tube, diluted/concentrated to a specific gravity of 2 g/ml and centrifuge at 1600 rpm.
4. Pipette the organic float produced after centrifuging and transfer to a new 15 ml centrifuge tube ('secondary sample').
5. Repeat steps 3-4 until sample ceases yielding organic material. Once this occurs, top up secondary sample with 15 ml distilled water, centrifuge at 3000 rpm for 10 minutes and decant.
6. For carbonate digestion, add 5 ml of 10% w/w hydrochloric acid to the tube and stir with a vortex mixer. Heat in a hot water bath (80 ^{o}C) for 20 minutes, centrifuge at 3000 rpm for 3 minutes and decant supernatant.
7. Add 10 ml distilled H_2O, stir with vortex mixer, centrifuge at 3000 rpm for 3 minutes and decant supernatant.

8. For cellulose and charcoal digestion, add 2 ml of 2.5% w/v sodium hypochlorite and heat in water bath at 90 ºC for 3 minutes.
9. Add 10 ml of distilled water, centrifuge at 3000 rpm for 3 minutes then decant supernatant. Repeat thrice.
10. Using a glass pipette, transfer the material from the 15 ml tube to a 1.5 ml micro-centrifuge tube, then centrifuge at 1500 rpm for 3 minutes and decant. If not all material is transferred at once, repeat centrifugation and decanting until this is achieved.

Section A3: Mineral grain size preparation method

1. Load ~0.5 g sediment (wet mass) into a 50 ml centrifuge tube.
2. For carbonate digestion, add 5 ml of 5% w/v hydrochloric acid to tube and heat in a water bath (80 ºC) until reaction ceases. Remove sample, top up with distilled water and stir with vortex mixer. Centrifuge at 3000 rpm for 5 minutes and decant supernatant.
3. For organic matter digestion, add 10 ml of 10% w/v hydrogen peroxide to tube and heat in water bath (80 ºC) until reaction ceases. Remove sample, top up with distilled water and stir with vortex mixer. Centrifuge at 3000 rpm for 5 minutes and decant supernatant.
4. For clay deflocculation, add 20 ml of 5% w/v sodium hexametaphosphate and place on a rotary tube mixer for two hours.
5. Dispense into dispersion unit immediately for analysis.

Section A4: Total organic carbon, total nitrogen and $\delta^{13}C$ preparation method

1. Load 2 cm^3 wet sediment into a 50 ml centrifuge tube, measure wet mass, freeze at -80 ºC overnight, then freeze dry with lid ajar for 24 hours.
2. After freeze drying, measure dry mass to calculate moisture content and dry bulk density.
3. For carbonate digestion, add 5 ml of 10% w/w hydrochloric acid to tube and heat in a water bath (80 ºC) for 2 hours.

4. Top up with distilled water, centrifuge at 3000 rpm for 5 minutes and decant supernatant liquid. Repeat 3x.
5. Freeze at -80 ºC overnight then freeze dry with lid ajar for 24 hours.
6. Crush dried sample to a uniform powder and transfer to a plastic container.
7. Depending on sample C%, transfer 100-200 mg for TOC-TN and 0.4-10 mg for $\delta^{13}C$ into a tin foil capsule, enclose and load onto relevant instrument for analysis. For $\delta^{13}C$, duplicate samples of roughly equal mass must be loaded to calculate standard deviation.

Section A5: Macrocharcoal preparation method

1. Load 1 cm^3 wet sediment into a 50 ml centrifuge tube.
2. For sample disaggregation, add 20 ml of 5% w/v sodium hexametaphosphate to the tube and place on a rotary tube mixer for two hours.
3. Empty sample through a 125 μm sieve, retaining only the coarser fraction. Use high pressure tap water to ensure removal of all finer material.
4. Empty residual fraction into a plastic container and preserve in distilled water.

Section A6: Input records for paleoclimate reconstructions

Table A2. Summary of the paleoclimate proxy data collated to construct average changes in hydroclimate and temperature for southeastern Australia (see Chapter 2 for definition) and proximal regions.

Site name	Location	Units	Inversion applied	Justification for use and inversion (if applied)	Source
Hydroclimate					
Swallow Lagoon	North Stradbroke Island (-27.50, 153.45)	Mean annual precipitation (mm/yr)	No	Within southeastern Australia; within influence of ENSO and SAM	Barr et al. (2019)
Rebecca Lagoon	Northwest Tasmania (-41.18, 144.68)	Precipitation (mm/yr)	No	Within southeastern Australia; within influence of ENSO and SAM	Saunders et al. (2012)
Laguna Llaviucu	Ecuador (-2.84, -79.1453)	δ^2H	Yes	Within influence of ENSO; Holocene-spanning record. Inverted due to opposite hydroclimatic expression of ENSO in eastern Pacific. Inverted due to δ^2H being inversely related to hydroclimate	Zhao et al. (2024)
Upper Snowy	Upper Snowy Mountains (-36.46, 148.30)	Dust flux ($g/m^2/yr$	Yes	Within southeastern Australia; within influence of ENSO and SAM. Inverted due to dust flux being negatively correlated with coastal climate.	Marx et al. (2011)
Southeastern Australian lakes	Southeastern Australia	Lake level (dimensionless)	No	Clerke (2023) identifies southeastern Australian lake levels as being strongly driven by precipitation. Only southeastern Australian lakes (n. 31) were included in aggregation, using R code shared by the source author.	Clerke (2023)

Temperature					
MD03-2611	Murray Canyons (-36.73, 136.55))	Sea surface temperature (ºC)	No	Proximal to southeastern Australia; within influence of SAM	Calvo et al. (2007)
MD03-2607	Southern Ocean (-36.96, 137.41)	Sea surface temperature (ºC)	No	Proximal to southeastern Australia; within influence of SAM	Lopes dos Santos et al. (2013)
MD98-2170	Indian Ocean (-10.60, 125.38)	Sea surface temperature (ºC)	No	Proximal to southeastern Australia; within influence of ENSO	Stott et al. (2004)
MD98-2176	Indian Ocean (-5, 133.45)	Sea surface temperature (ºC)	No	Proximal to southeastern Australia; within influence of ENSO	Stott et al. (2004)
Vostok	Vostok Station (-78.47, 106.83)	Air temperature (ºC)	No	Proximal to southeastern Australia; Holocene-spanning record	Jouzel et al. (1996)
EPICA	EPICA Dome C (-75.1, 123.4)	Air temperature (ºC)	No	Proximal to southeastern Australia; Holocene-spanning record	Jouzel et al. (2007)
Yarrangobilly Caves	Yarrangobilly (-36.04, 148.37)	Air temperature (ºC)	No	Within southeastern Australia; within influence of ENSO and SAM	McGowan et al. (2019)
Lake Mackenzie	Fraser Island (-25.45, 153.05)	Air temperature (ºC)	No	Within southeastern Australia; within influence of ENSO and SAM	Woltering et al. (2014)
Platypus Tarn	Mount Field (-42.67, 146.59)	Air temperature (ºC)	No	Within southeastern Australia; within influence of ENSO and SAM	Rees and Cwynar (2010)

Eagle Tarn	Mount Field (-42.68, 146.59)	Air temperature (ºC)	No	Within southeastern Australia; within influence of ENSO and SAM	Rees and Cwynar (2010)

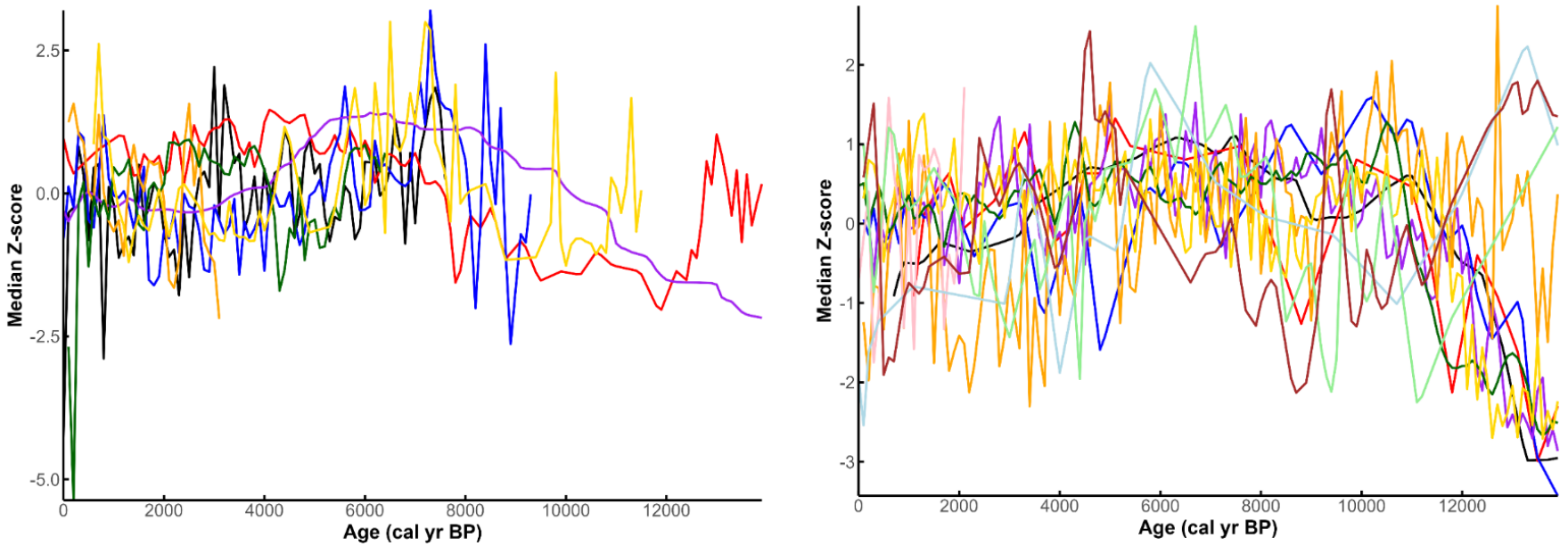

Figure A1. Time series overlays of the Z-scored hydroclimate (left) and temperature (right) records from Table A2.

Section A7: Details of selected sampling sites

Table A3. Summary of lakes selected for sampling and key physical attributes.

Site name	Latitude, longitude	Subregion	Elevation (m)	Lake area (ha)	Hydrology	Major lithologies	Intersecting TECs	Known land uses
Arable	-36.346, 149.030	North	985	16	Permanent	Basalt	UWM, NTG	Grazing, cropping
Black	-36.843, 149.313	South	815	36	Permanent	Basalt, sandstone	UWM, NTG	Fishing, grazing
Jillamatong	-36.347, 149.271	West	1085	37	Permanent	Granite	UWM, NTG, CGW	Grazing, residential conservation
Maffra	-36.545, 148.991	Central	875	23	Ephemeral	Basalt, granite	UWM, NTG	Grazing, residential, conservation, cropping
Racecourse	-36.497, 149.271	East	1100	6	Permanent	Basalt	UWM, NTG, CGW	Grazing, infrastructure

Section A8: Core details

Table A4. Lengths and locations of all sampled cores. Asterisks denote cores that were selected for multiproxy analysis.

Core ID	Lake name	Length (cm)	Longitude	Latitude
ARA*	Arable	28	149.0311	-36.3444
BLA-A1*	Black	28.5	149.3141	-36.8414
BLA-A2	Black	19	149.3141	-36.8414
JIL-A1*	Jillamatong	38	149.2708	-36.4962
JIL-A2	Jillamatong	24.5	149.2708	-36.4962
MAF-A	Maffra	29.5	148.9917	-36.545
MAF-B*	Maffra	47.5	148.9917	-36.545
RAC*	Racecourse	29	149.2708	-36.4962

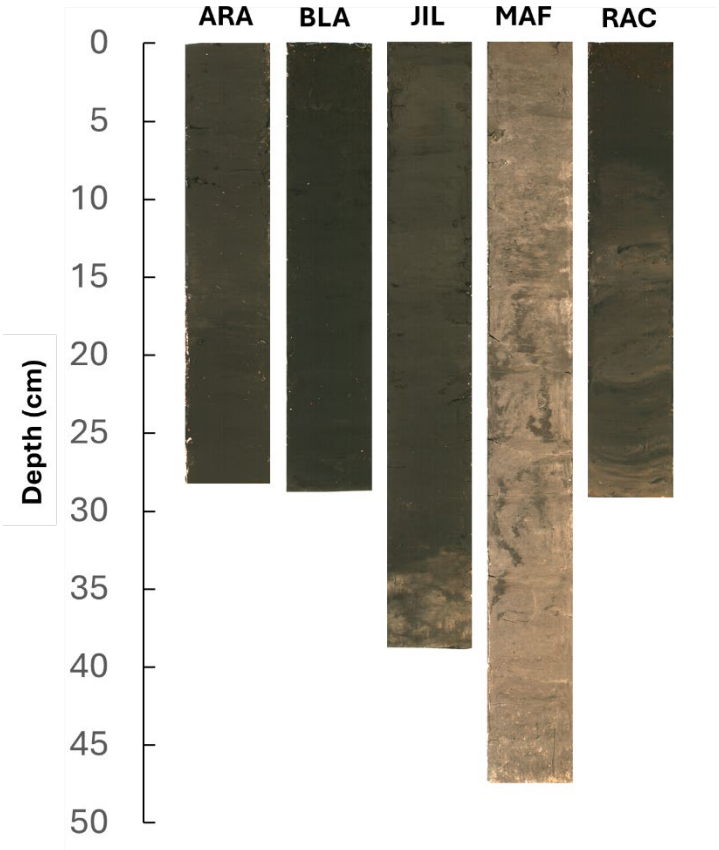

Figure A2. Optical scans of selected cores against depth. Depth markings are limited in their accuracy given optical scans were taken for replicate core halves, which experienced minor rebound of their upper sections once core caps were removed.

Section A9: Age calibration and chronological modelling outputs

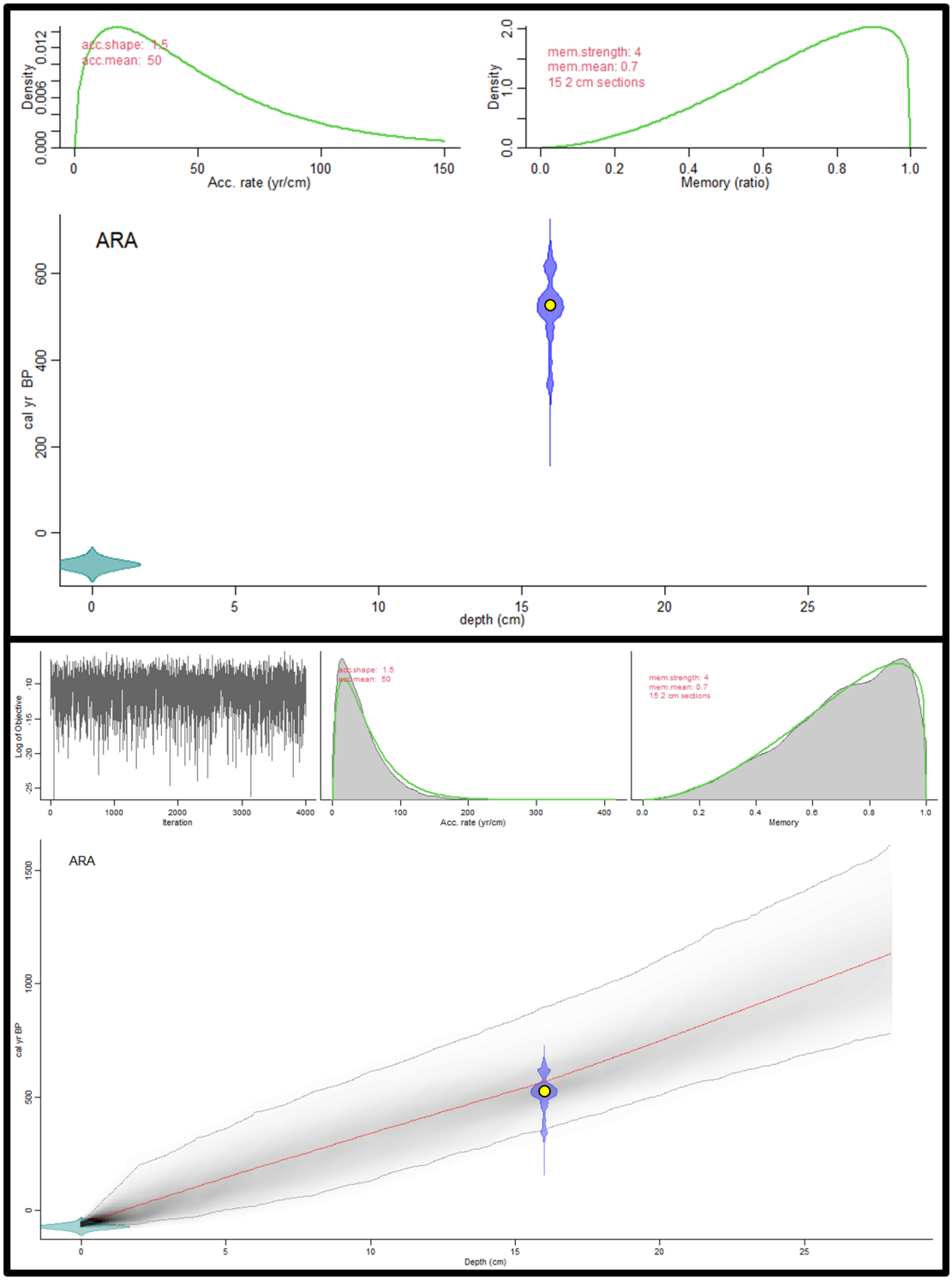

Figure A3. Outputs of age calibration (top) and age-depth modelling (bottom) for ARA. Yellow and red ages are derived from pollen and bulk sediment samples, respectively.

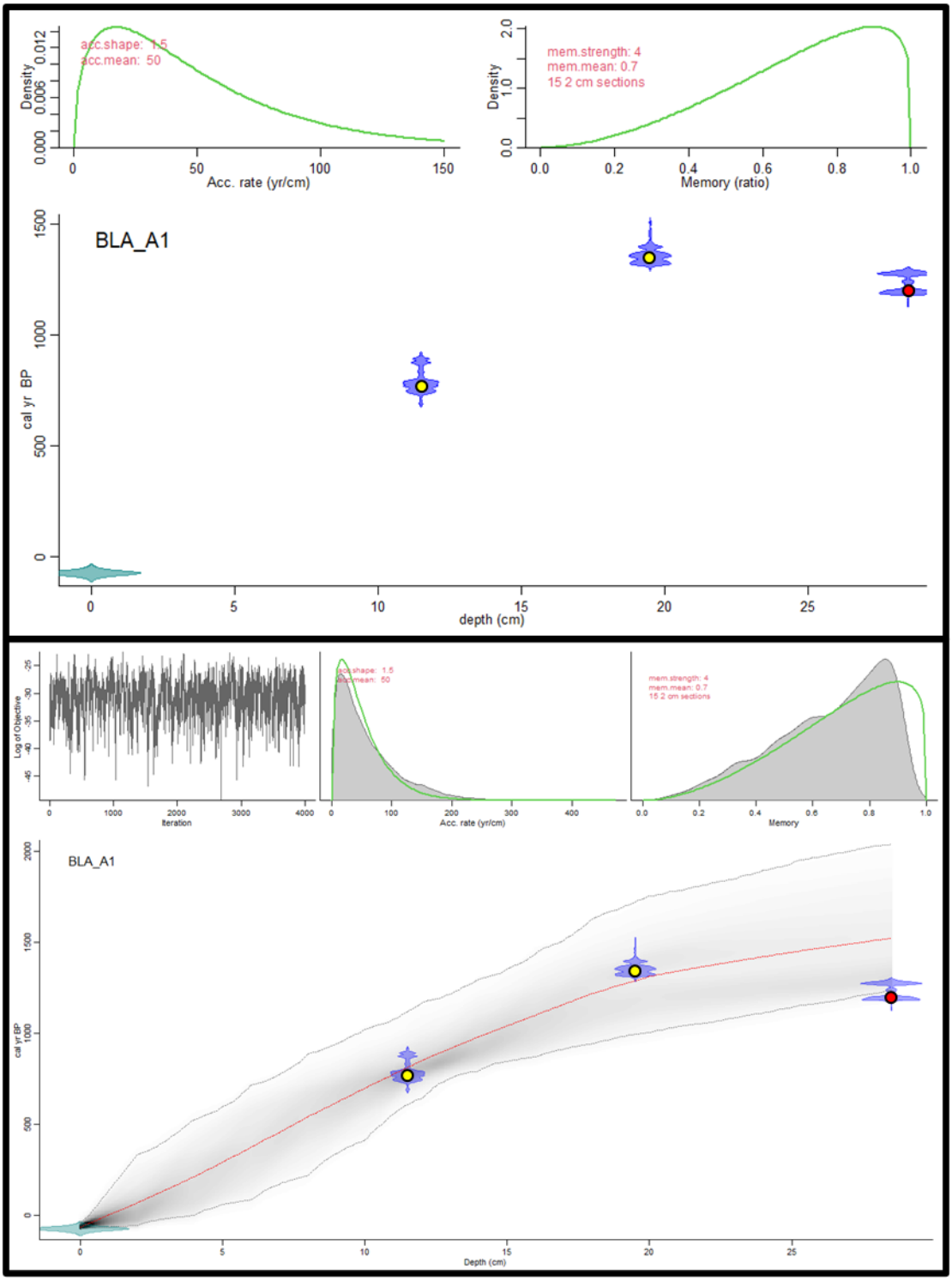

Figure A4. Outputs of age calibration (top) and age-depth modelling (bottom) for BLA. Yellow and red ages are derived from pollen and bulk sediment samples, respectively.

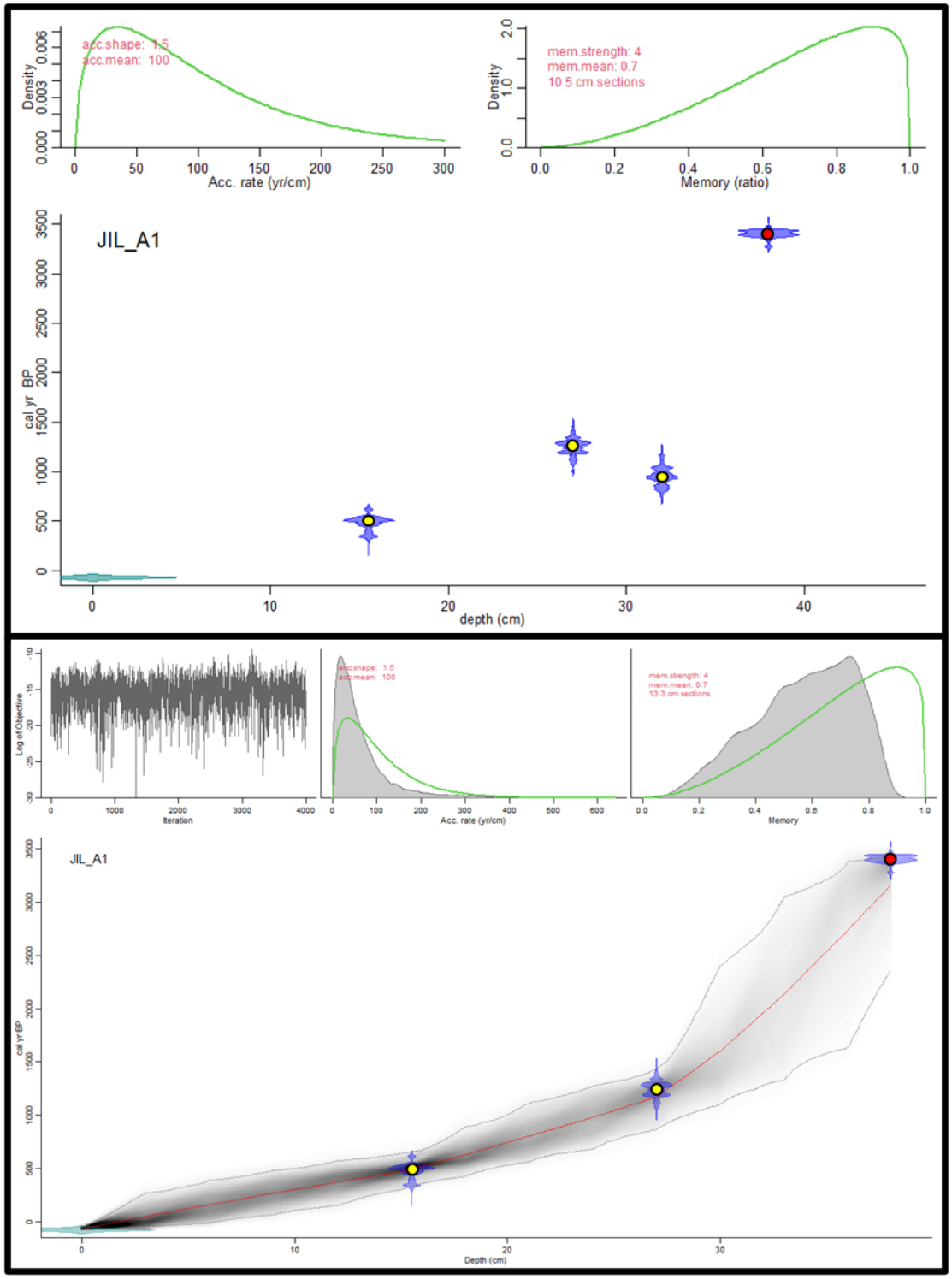

Figure A5. Outputs of age calibration (top) and age-depth modelling (bottom) for JIL. Yellow and red ages are derived from pollen and bulk sediment samples, respectively.

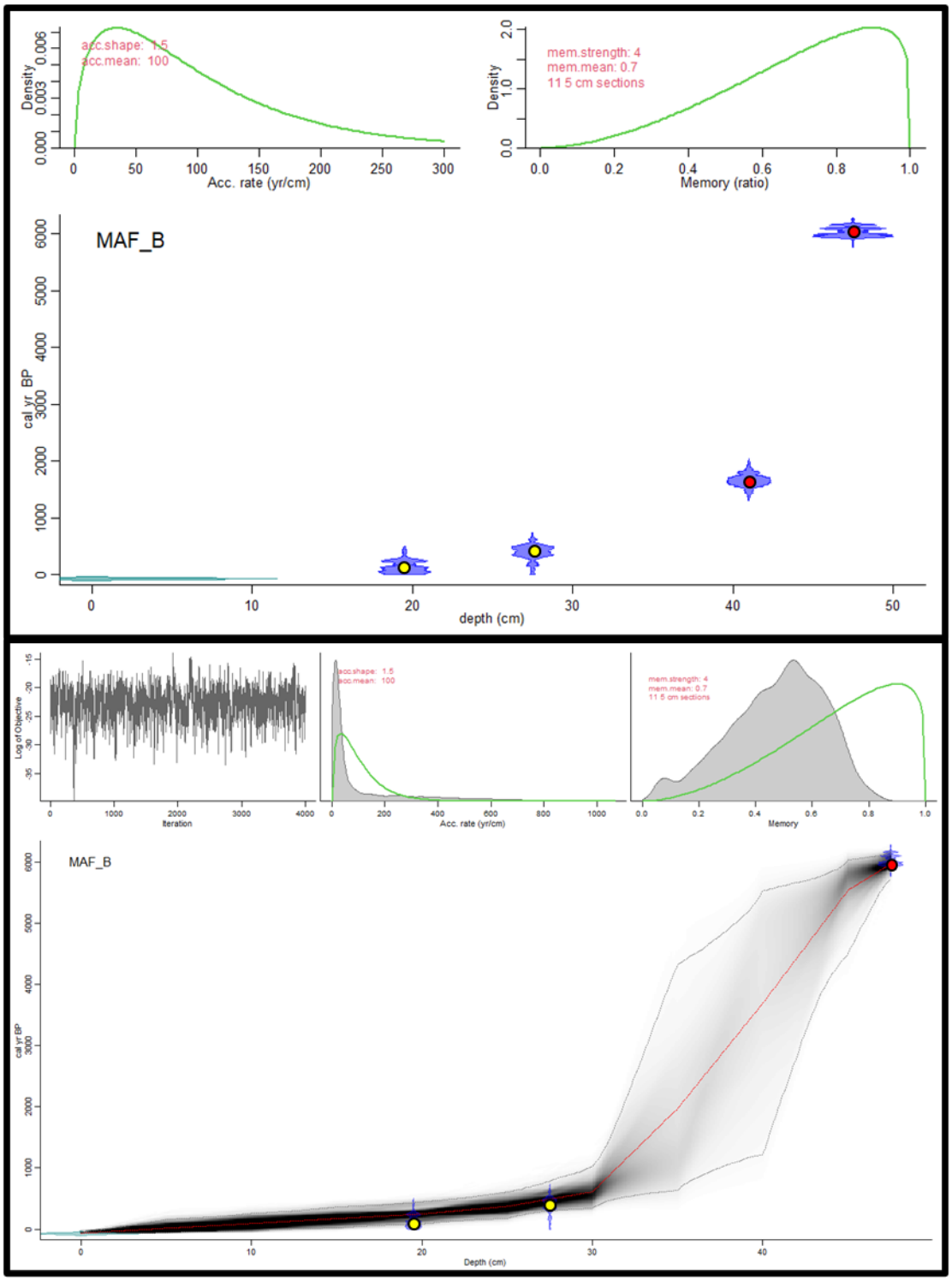

Figure A6. Outputs of age calibration (top) and age-depth modelling (bottom) for MAF. Yellow and red ages are derived from pollen and bulk sediment samples, respectively.

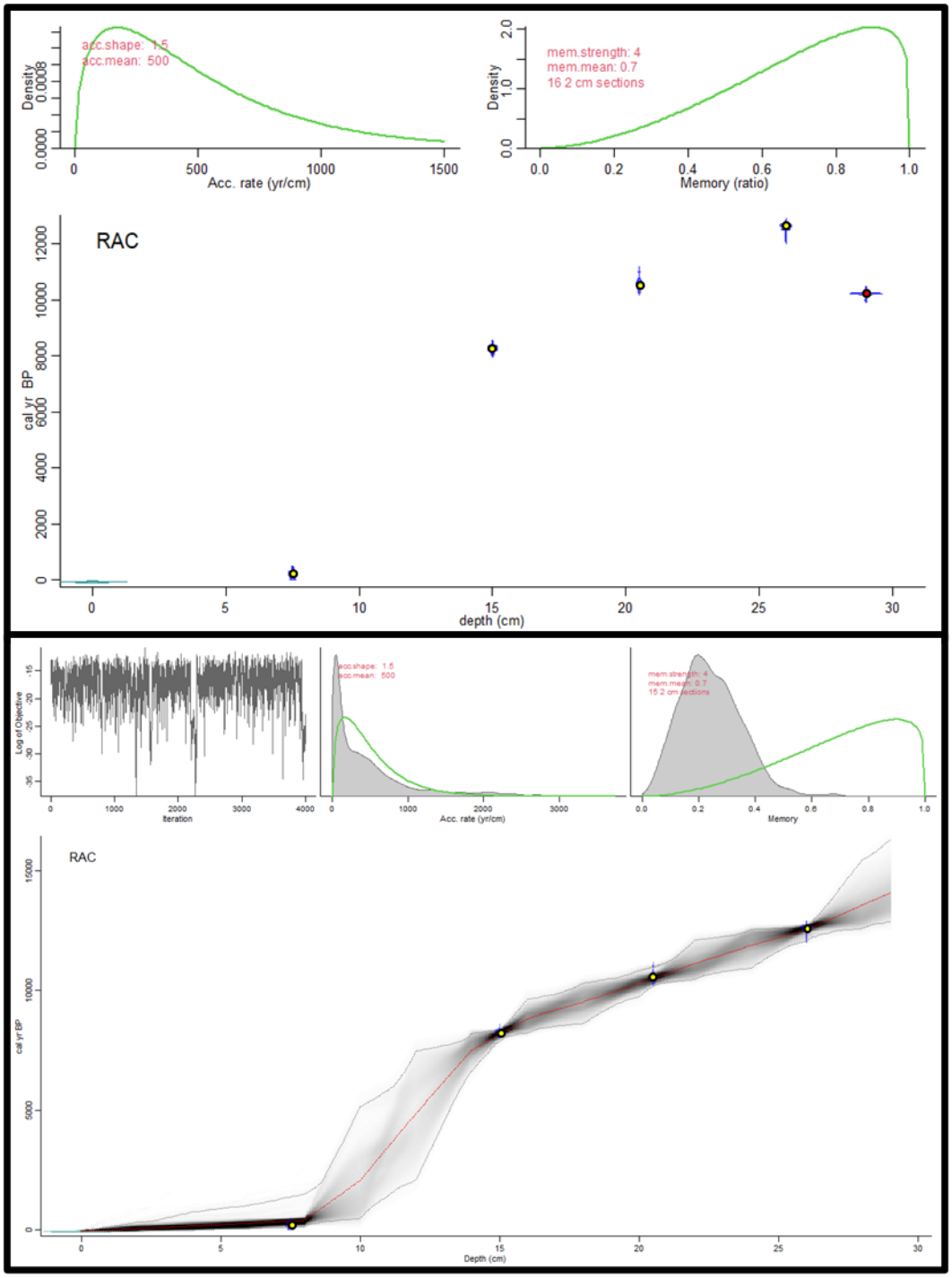

Figure A7. Outputs of age calibration (top) and age-depth modelling (bottom) for RAC. Yellow and red ages are derived from pollen and bulk sediment samples, respectively.

Section A10: Principal component analysis of XRF data

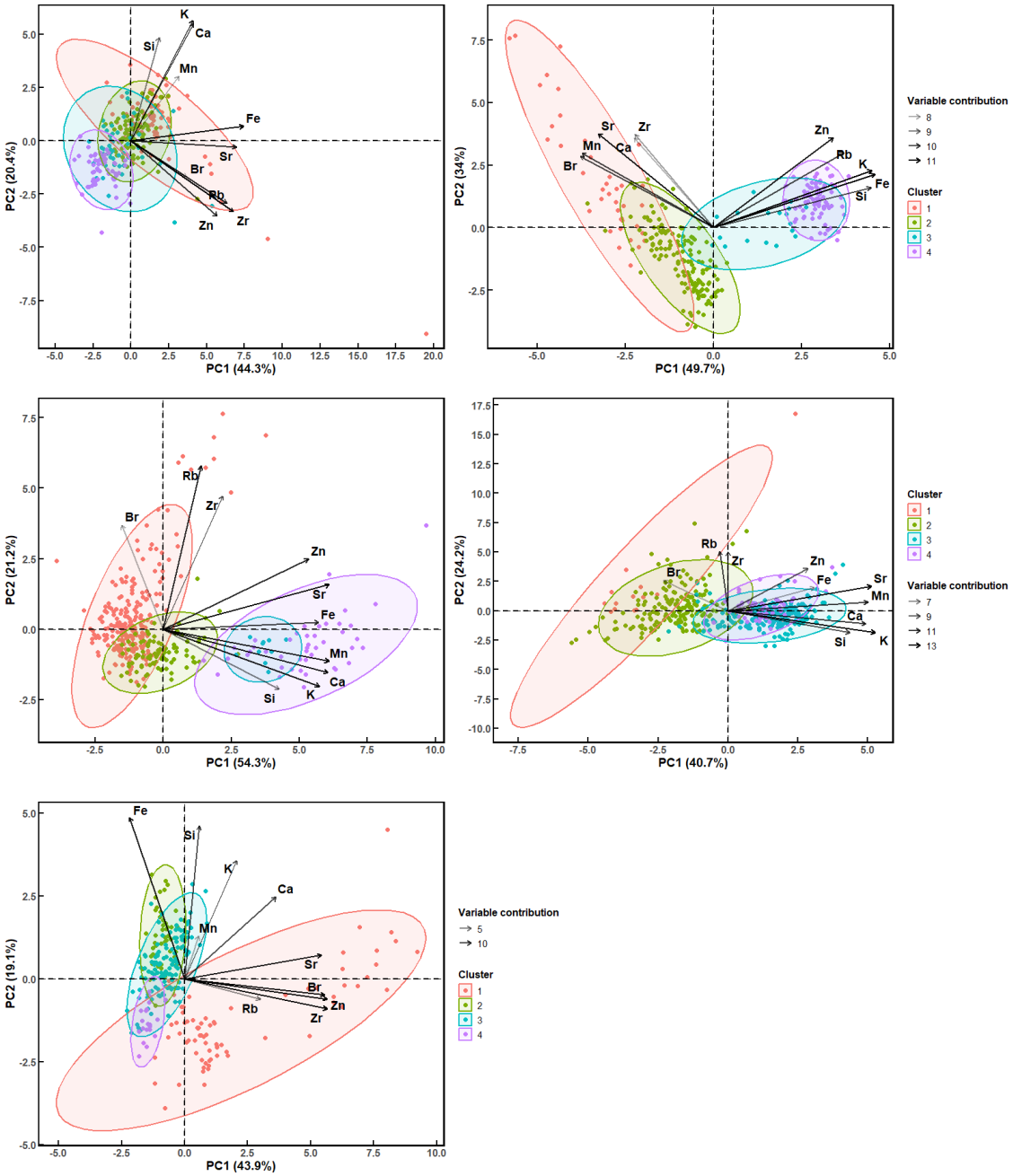

Figure A8. Principal component analysis biplots of the Ti-normalised XRF data for, from left to right, (top row) ARA, BLA, (middle row) JIL, MAF and (bottom row) RAC.

Section A11: Principal component analysis of proxies used in hydrological reconstructions

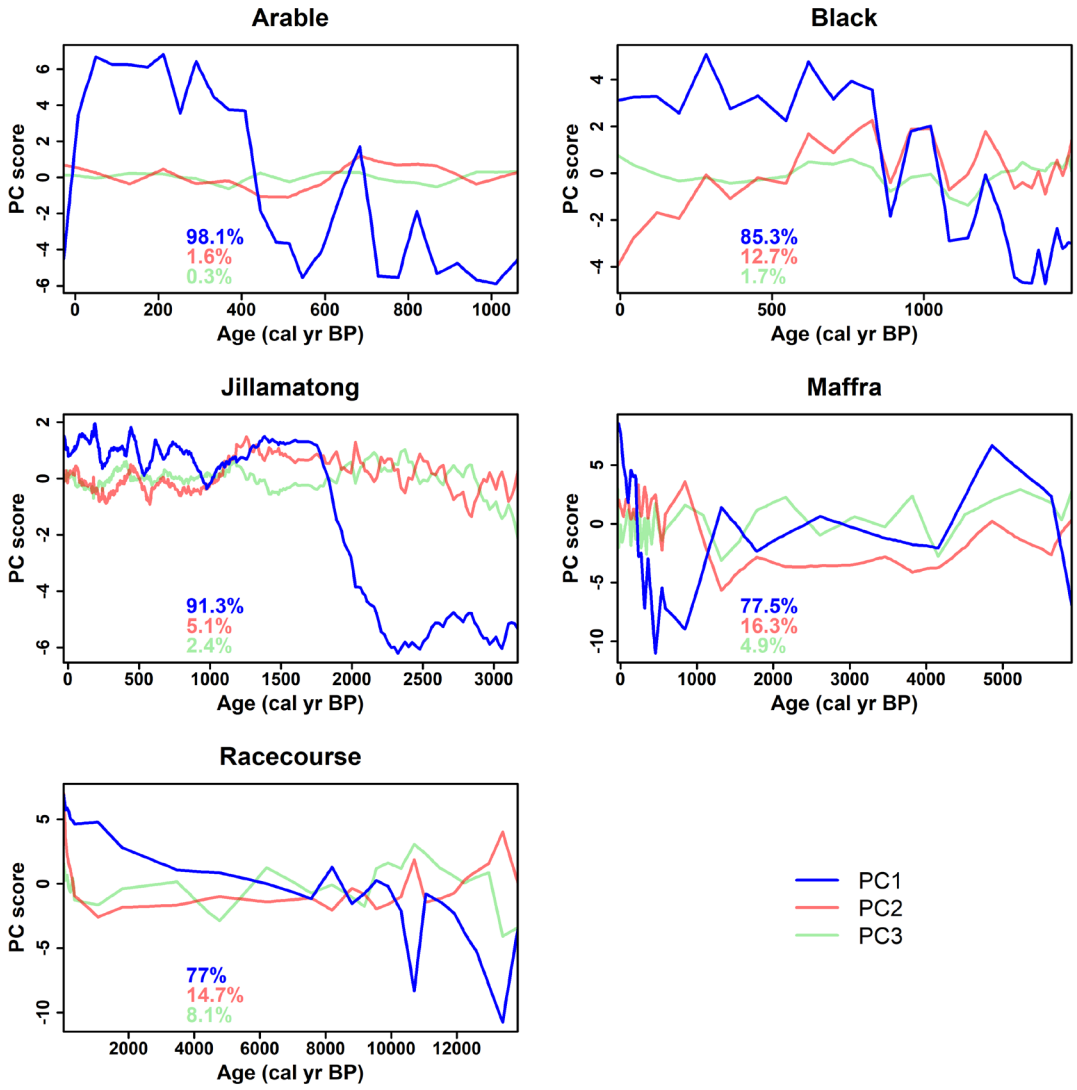

Figure A9. Time series plots of three main principal components generated by principal component analysis of the same proxies used for the site hydrological reconstructions (see Table 2.2). Inversions have been preserved for relevant proxies to assist with visual comparison between principal component 1 (the dominant mode of variability) and Z-score trends (main paper).

Section A12: Time series comparisons between site hydrology and paleoclimate records

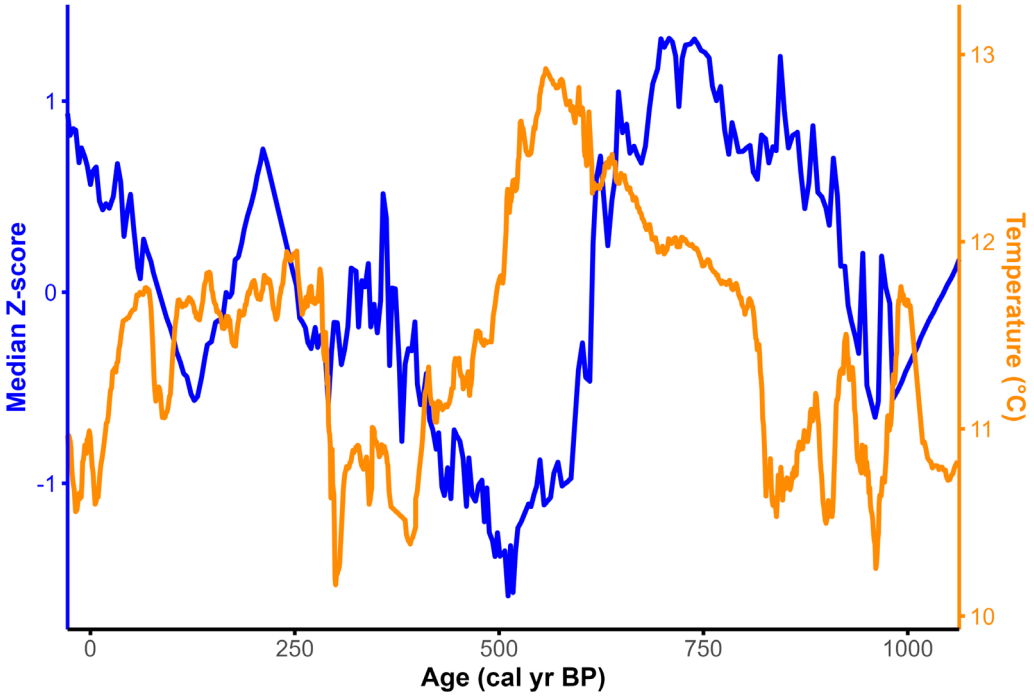

Figure A10. Time series overlay for the Arable hydrology record (blue) and the Yarrangobilly speleothem temperature reconstruction from McGowan et al. (2019) (orange).

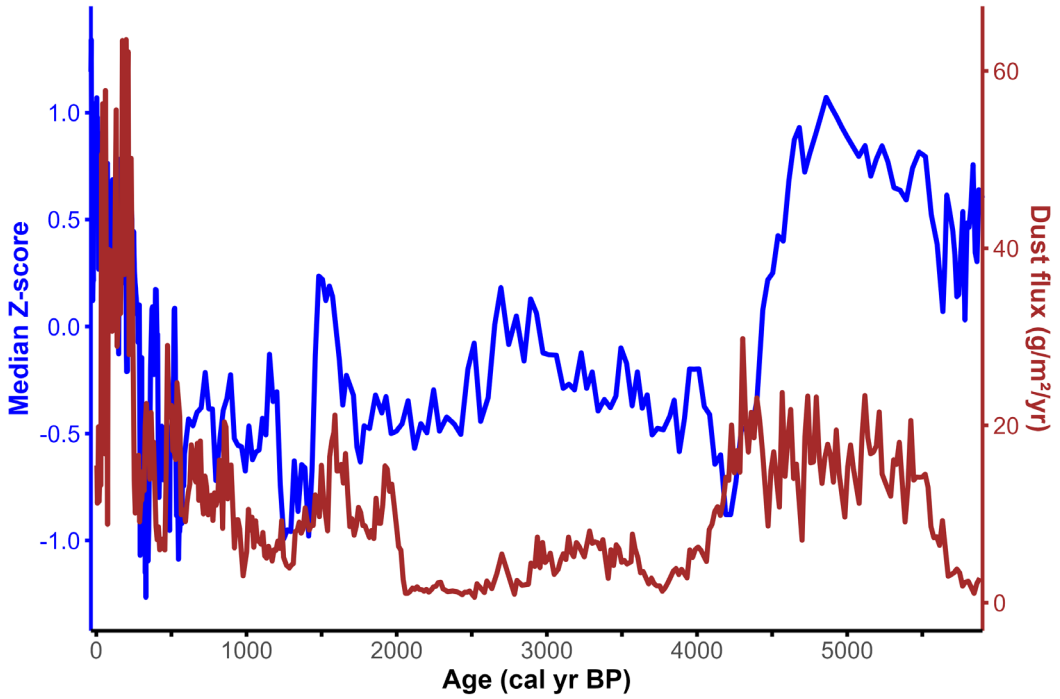

Figure A11. Time series overlay for the Maffra hydrology record (blue) and the Upper Snowy peat dust flux reconstruction from Marx et al. (2011) (brown).

Appendix B

Supplementary Information for Chapter 3

Section B1: Sampling site details

Table B1. Mires selected for sampling, including key physical attributes.

Site name	Latitude, longitude	Elevation (m ASL)	Mire area (ha)	Observed anthropogenic impacts
Delaneys Creek	-35.9100, 148.561	1355	3.78	Highway intersecting tributary upstream
Botherum Plain	-36.262, 148.565	1305	14.27	Feral horse grazing

Section B2: ^{14}C sample preparation method

B2.1. Bulk sediment pretreatment

1. Load 7-8 g sediment (wet mass) onto a petri dish and dry in an oven (105 ºC) for 24 hours.
2. Measure stable dry mass and crush to a uniform powder using a clean mortar and pestle.
3. Load into aluminium foil and send to either DirectAMS or ANSTO for ABA pretreatment and AMS ^{14}C analysis.

B2.2. Sporopollenin pretreatment

1. Load ~3 g sediment (wet mass) into a clean 15 ml centrifuge tube.
2. For disaggregation, add 10 ml 5% sodium hexametaphosphate; ('Calgon' or similar) to the centrifuge tube and stir with a vortex mixer. Heat in a hot water bath (80 ºC) for 20 minutes, centrifuge at 3000 rpm for 5 minutes and decant supernatant.
3. For silicate digestion, add 10 ml of lithium heteropolytungstate (LST; 'heavy liquid') to the tube, diluted/concentrated to a specific gravity of 2 g/ml and centrifuge at 1600 rpm.
4. Pipette the organic float produced after centrifuging and transfer to a new 15 ml centrifuge tube ('secondary sample').

5. Repeat steps 3-4 until sample ceases yielding organic material. Once this occurs, top up secondary sample with 15 ml distilled water, centrifuge at 3000 rpm for 10 minutes and decant.
6. For carbonate digestion, add 5 ml of 10% w/w hydrochloric acid to the tube and stir with a vortex mixer. Heat in a hot water bath (80 ºC) for 20 minutes, centrifuge at 3000 rpm for 3 minutes and decant supernatant.
7. Add 10 ml distilled H_2O, stir with vortex mixer, centrifuge at 3000 rpm for 3 minutes and decant supernatant.
8. For cellulose and charcoal digestion, add 2 ml of 2.5% w/v sodium hypochlorite and heat in water bath at 90 ºC for 3 minutes.
9. Add 10 ml of distilled water, centrifuge at 3000 rpm for 3 minutes then decant supernatant. Repeat thrice.
10. Using a glass pipette, transfer the material from the 15 ml tube to a 1.5 ml micro-centrifuge tube, then centrifuge at 1500 rpm for 3 minutes and decant. If not all material is transferred at once, repeat centrifugation and decanting until this is achieved.
11. At ANSTO, treat with 2M HCl at room temperature for 2 hr, then oven-dry at 60 ºC overnight.

Section B3: Micro-X-ray fluorescence analysis method

1. Cores are scanned using a 0.1 cm resolution using an Itrax core scanner fitted with a Mo tube.
2. Raw concentrations for 33 major, minor and trace elements are reported as relative counts per second (kcps).
3. Raw kcps data are normalised to the incoherent/coherent scattering ratio to remove the effect of light elements in the matrix due to high organic matter and moisture content (Woodward and Gadd, 2019). Data are cleaned by removing clear core-edge scanning artefacts.
4. Elements deemed to be environmentally significant and with a high signal-to-noise ratio (Table B4) are subject to cluster analysis using the R package rioja and Principal Component Analysis using the R package 'FactoMineR' (Lê et al., 2008, McKillup and Dyar, 2010, R Core Team, 2020).

Section B4: Mineral grain size preparation and analysis method

1. Load ~0.5 g sediment (wet mass) into a 50 ml centrifuge tube.
2. For carbonate digestion, add 5 ml of 5% w/v hydrochloric acid to tube and heat in a water bath (80 ºC) until reaction ceases. Remove sample, top up with distilled water and stir with vortex mixer. Centrifuge at 3000 rpm for 5 minutes and decant supernatant.
3. For organic matter digestion, add 10 ml of 10% w/v hydrogen peroxide to tube and heat in water bath (80 ºC) until reaction ceases. Remove sample, top up with distilled water and stir with vortex mixer. Centrifuge at 3000 rpm for 5 minutes and decant supernatant.
4. For clay deflocculation, add 20 ml of 5% w/v sodium hexametaphosphate and place on a rotary tube mixer for two hours.
5. Samples are analysed using a Malvern Mastersizer 3000 laser diffractometer equipped with a Hydro LV dispersion unit. Triplicate blue light measurements are taken per sample to calculate a mean grain size distribution, which is then decomposed into summary statistics using the 'GRADISTAT' Excel package (v. 8; Blott and Pye (2001))

Section B5: Total organic carbon/nitrogen and $\delta^{13}C$ preparation and analysis method

1. Load 2 cm^3 wet sediment into a 50 ml centrifuge tube, measure wet mass, freeze at -80 ºC overnight, then freeze dry with lid ajar for 24 hours.
2. After freeze drying, measure dry mass to calculate moisture content and dry bulk density.
3. For carbonate digestion, add 5 ml of 10% w/w hydrochloric acid to tube and heat in a water bath (80 ºC) for 2 hours.
4. Top up with distilled water, centrifuge at 3000 rpm for 5 minutes and decant supernatant liquid. Repeat 3x.
5. Freeze at -80 ºC overnight then freeze dry with lid ajar for 24 hours.
6. Crush dried sample to a uniform powder and transfer to a plastic container.

7. Depending on sample C% (verified through low-resolution test samples) transfer 100-200 mg for total carbon and total nitrogen and 0.4-10 mg for $\delta^{13}C$ into a tin foil capsule, enclose and load onto relevant instrument for analysis. For $\delta^{13}C$, duplicate samples of roughly equal mass must be loaded to calculate standard deviation.
8. Total carbon and total organic nitrogen samples are analysed with a VELP Scientifica CN802 Carbon Nitrogen Analyser.
9. $\delta^{13}C$ samples are analysed with an Elementar VarioISOTOPE Elemental Analyser coupled with an Elementar PrecisION Isotope Ratio Mass Spectrometer to measure relative isotopic abundances of C, reporting $\delta^{13}C$ as ‰.

Section B6: Macrocharcoal preparation and counting method*

* This method has been adapted from that of Stevenson and Haberle (2018).

1. Load 1 cm^3 wet sediment into a 50 ml centrifuge tube.
2. For sample disaggregation, add 20 ml of 5% w/v sodium hexametaphosphate to the tube and place on a rotary tube mixer for two hours.
3. Empty sample through a 125 μm sieve, retaining only the coarser fraction. Use high pressure tap water to ensure removal of all finer material.
4. Empty residual fraction into a plastic container and preserve in distilled water.
5. Samples are manually counted on a petri dish using a Zeiss Stemi 305 Stereo Microscope. Whole samples are counted unless macrocharcoal is extremely abundant, in which case a subset of 1 cm^2 grid cells are counted and the average count is multiplied by the petri dish area.

Section B7: Bulk mineral influx, apparent carbon accumulation rates and macrocharcoal accumulation rates calculation and aggregation method

1. Bulk mineral influx (g m^{-2} yr^{-1}) (a), apparent carbon accumulation rates (g m^{-2} yr^{-1}) (b), and macrocharcoal accumulation rates (particles cm^{-2} yr^{-1}) (c) are calculated by the following formulas:

(a) $$= SR * DBD * \left(1 - \left(\frac{TOC}{100} * 1.724\right)\right) \times 10^4$$

(b) $$= SR \times DBD \times (TOC / 100) \times 10^4$$

(c) $$= \frac{MC * 0.5}{Bottom - Top}$$

where SR is sedimentation rate (cm yr^{-1}), DBD is dry bulk density (g cm^{-3}), TOC is total organic carbon (%), 1.724 is the van Bemmelen factor, MC is macrocharcoal counts (particles cm^{-3}), and Bottom and Top are the lower and upper ages of the slice (cal yr BP).

2. For multisite synthesis, records of each metric are first divided into overlapping 200-yr windows stepped every 100 yrs, within which median values are calculated. Site-level medians are then averaged across both records to generate a composite series.

Section B8: Moisture availability computation method*

* This method has been adapted from that of Hamilton et al. (2024) using R code shared by the authors.

B8.1. Site moisture availability index construction

1. For each site, input proxy records are linearly interpolated to the maximum proxy resolution to avoid biasing the index at depths with fewer data points.
2. Proxies are inverted where necessary where they are assumed to behave inversely with moisture availability.
3. A Z-score record is computed from every proxy record, and a median Z-score is calculated for every depth interval.

B8.2. Zonal moisture availability index construction

1. Input proxy records are linearly interpolated and inverted following B5.1.
2. Proxies are Z-score standardised relative to the global mean for each proxy across both sites. A median Z-score is calculated for every depth interval.
3. Age uncertainties are propagated separately for each site using Monte Carlo resampling (10,000 iterations), where at each depth a standard deviation is estimated from the 95% confidence bounds and used to draw truncated normal ages.
4. The new random ages are used to interpolate the site MA index onto a regular 100-yr grid.
5. For each grid age for both sites, the new uncertainty bands are combined by drawing random values uniformly within each band and taking the median across sites over 10,000 iterations, yielding a regional median Z-score for each grid age with 95% uncertainty.

Table B2. Summary of input proxies for each site hydrological reconstruction, specifying where inversions have and have not been applied, with justifications. Proxies presumed to have negative correlations with wetting (N) were inverted, while those presumed to have positive correlations (P) were not. Bold text after some justifications highlights exceptions to the established relationships.

Proxy	Wetting correlation	Justification
		Delaneys Creek
Mean grain size	P	Wetting increases fluvial/slope transport energy
µXRF PC1	N	Wetting decreases the contribution of lithogenics due to dilution by organic matter
Volume magnetic susceptibility	N	Wetting decreases humification and the formation of high susceptibility secondary minerals
Carbon/nitrogen	P	Wetting increases the preservation of C relative to N due to suppressed microbial metabolisation of C
$\delta^{13}C$	N	Wetting decreases preferential microbial metabolisation of ^{12}C
Bulk mineral influx	P	Wetting increases clastic influx
Apparent carbon accumulation rates	P	Wetting increases OM accumulation and C preservation
Macrocharcoal accumulation rates	P	Wetting increases fuel loads and burning of woody vegetation
		Botherum Plain
Mean grain size	P	Wetting increases fluvial/slope transport energy
µXRF PC1	P	Wetting increases erosion and contribution of lithogenics

Volume magnetic susceptibility	P	Wetting increases the erosion of catchment soils into the mire **Pre-2800 cal yr BP, not as much soil to erode from the floodplain**
Carbon/nitrogen	P	Wetting increases the preservation of C relative to N due to suppressed microbial metabolisation of C
$\delta^{13}C$	N	Wetting decreases preferential microbial metabolisation of ^{12}C
Bulk mineral influx	P	Wetting increases clastic influx
Apparent carbon accumulation rates	P	Wetting increases OM accumulation and C preservation. **Pre-2800 cal yr BP, low CAR is due to mire inception**
Macrocharcoal accumulation rates	P	Wetting increases fuel loads and burning of woody vegetation

Section B9: Multiproxy Rate-of-Change computation method*

***** This method has been adapted from that of Mottl et al. (2021b).

1. For each site, input proxy records are linearly interpolated to avoid artefactual values arising from sampling gaps.
2. Using the R-Ratepol package, multivariate Rate-of-Change is calculated as the standardised Euclidean distance between consecutive 50-yr time bins (working units), divided by the elapsed time.
3. Step 2 is repeated 10,000 times using randomised bin representation, with the median and 2.5th and 97.5th quantiles being calculated for all randomisations.
4. A zonal Rate-of-Change record is calculated as the median of all sites for each 100-yr midpoint bin.

Due to poor multiproxy coverage at the top of each core and the necessity to calculate colonial-era values, Rate-of-Change was re-performed without CHAR between 2-4 cm depth for D-A7 and without PC1 between 8.6-4.5 cm depth for B-B. Data for this range was then appended to the whole-suite data for the underlying depth range to produce a single record. While this biases RoC over this interval to one fewer proxy for each site, it enabled data to be obtained for the colonial period.

Section B10: Method for time binning of paleoclimate records and Pearson correlation with zonal records

1. In the absence of age uncertainty data for every climate record, each is binned at 100-yr time intervals spanning every 100 cal yr from 0 cal yr BP, and a median is calculated for every interval.
2. Binned paleoclimate data are subject to Pearson correlation with zonal records for all time bins older than 200 cal yr BP, in order to remove the influence of colonial- and industrial-era anthropogenic activities on the zonal and paleoclimate records, respectively.

Section B11: Core details

Table B3. Lengths and locations of all sampled cores. Asterisks denote cores that were subject to dating and multiproxy analysis.

Core ID	Site name	Length (cm)	Longitude	Latitude	Material
D4-A1	Delaneys Creek	50	148.5611	-35.9100	Fibrous peat
D4-A2*	"	"	"	"	Sapric peat grading to sand
D4-A3	"	"	"	"	Sand
D7-A*	"	49	148.5619	-35.9100	Fibrous to sapric peat overlying silty sand
D7-B	"	40	148.5618	-35.9102	Fibrous to sapric peat overlying silty sand
D7-C	"	30	148.5619	-35.9101	Fibrous to sapric peat
B-A*	Botherum Plain	41	148.5654	-36.2617	Fibrous to sapric peat
B-B*	"	35	148.5653	-35.9618	Fibrous to sapric peat

Section B12: Core scans and stratigraphic correlation of Delaneys cores for date transfer

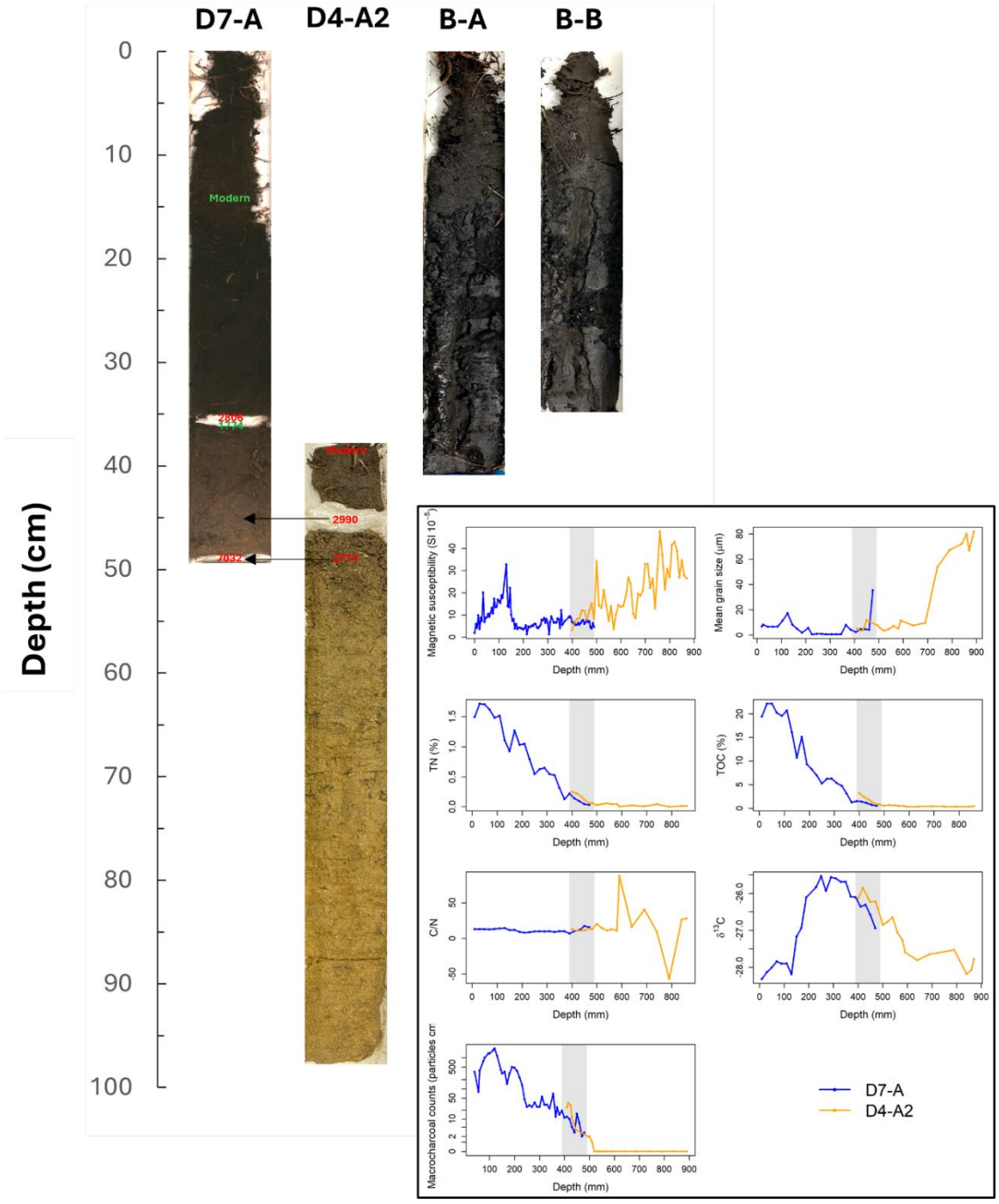

Figure B1. Optical scans of cores selected for dating and multiproxy analysis. Annotations show transfer of dates from D4-A2 to D7-A, based on visual stratigraphic correlation verified by multiproxy overlay (inset plots). Shaded region in proxy plots corresponds to the overlap presumed from lithostratigraphy alone.

Section B13: Age calibration and chronological modelling outputs

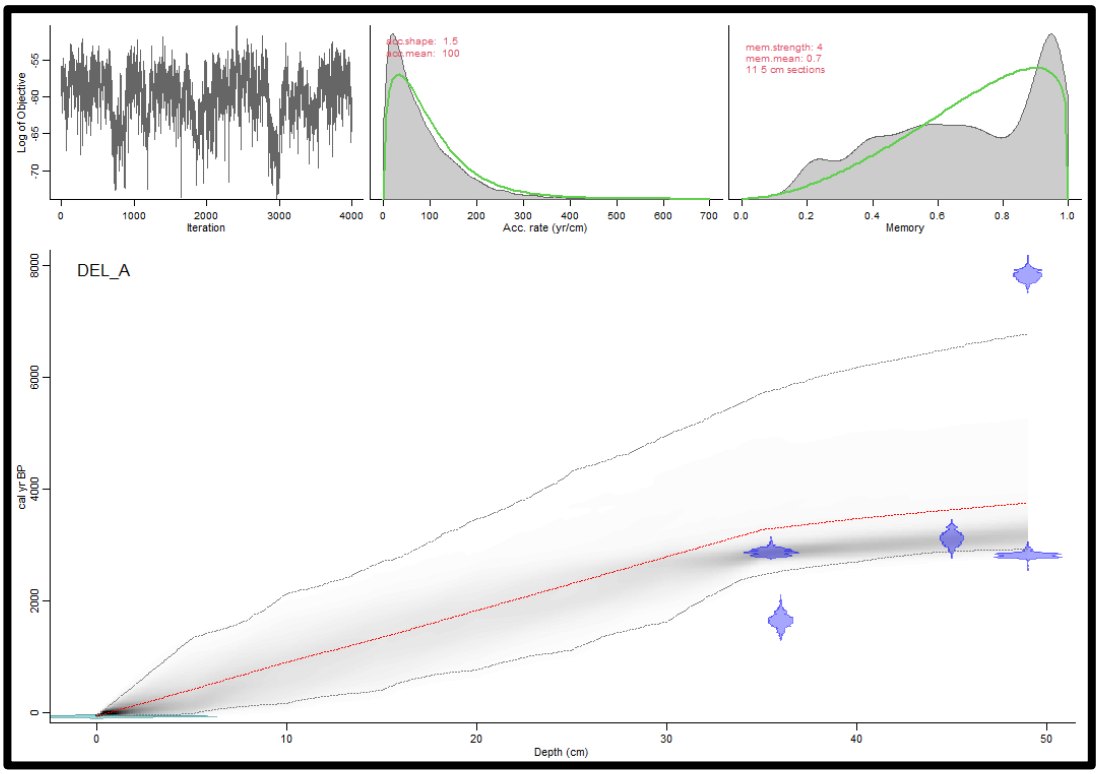

Figure B2. Output of age-depth modelling for D7-A. Blue histograms denote calibrated ages, red line denotes mean modelled age and grey gradient denotes age likelihood (darker shades being more likely) within the 95% confidence envelope (grey lines).

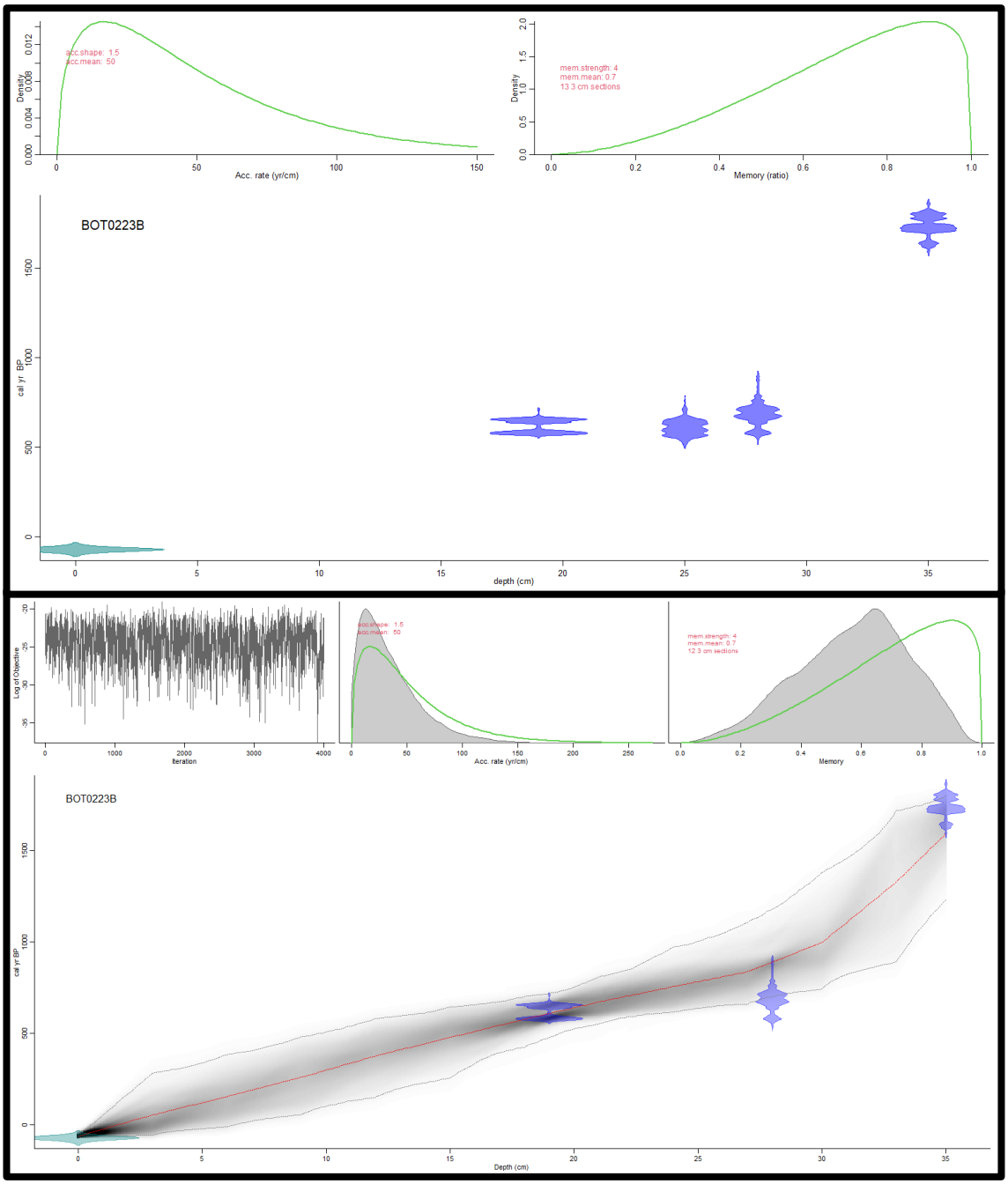

Figure B3. Outputs of age calibration (top) and age-depth modelling (bottom) for B-B. Blue histograms denote calibrated ages, red line denotes mean modelled age and grey gradient denotes age likelihood (darker shades being more likely) within the 95% confidence envelope (grey lines).

Section B14: Principal component analysis biplots of µXRF data

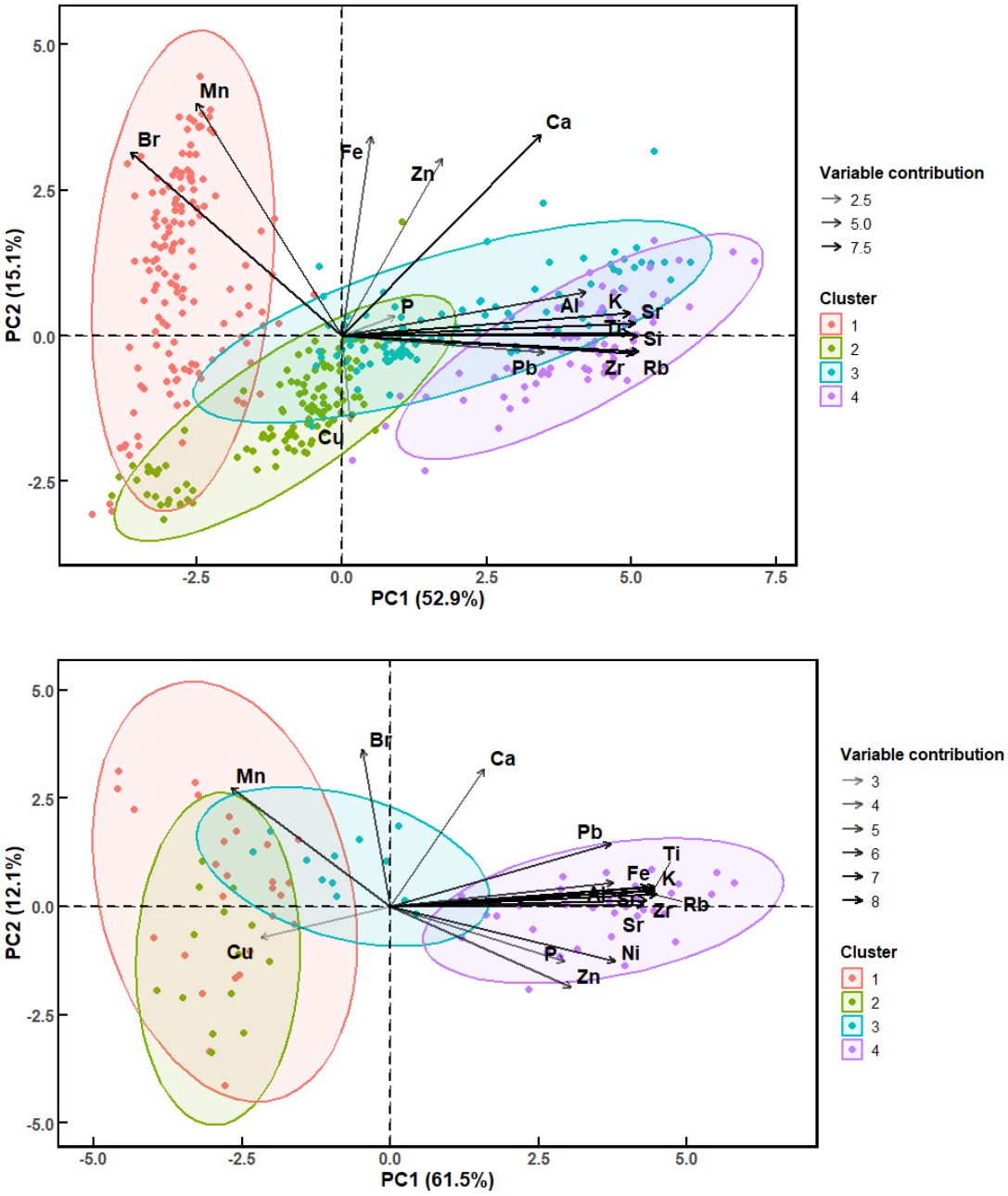

Figure B4. Principal component analysis biplots of the µXRF data for D7-A (top) and B-B (bottom; after transfer from B-A).

Table B4. PC1 variable contributions for each site.

Element	D7-A	B-B
Al	7.54	6.75
Si	11.02	9.18
P	0.38	4.11
K	10.35	9.48
Ca	4.97	1.18
Ti	10.71	9.48
Mn	2.68	3.44
Fe	0.12	8.97
Ni	7.43	6.83
Cu	0.03	2.27
Zn	1.39	4.42
Br	5.43	0.10
Rb	11.10	9.59
Sr	10.82	8.69
Zr	10.77	8.91
Pb	5.26	6.59

Section B15: Method for synthesis of montane pollen and charcoal records

1. All publicly available pollen and charcoal records from the Snowy Mountains montane zone are compiled from the Neotoma Paleoecology Database (Table B5) (Williams et al., 2018) and the Global Paleofire Database.
2. For each pollen record, total pollen counts for *Eucalyptus* and *Poaceae* are extracted, as these are respectively the dominant canopy and grassland genera. The ratio of their counts calculated as this is a proxy for the degree of landscape opening (i.e., grassland expansion) in the montane zone.
3. In the absence of age uncertainty data for every pollen record, each is simply binned at 200-yr intervals, and a median *Eucalyptus/Poaceae* ratio is calculate for each bin. A median value is then calculated for all sites at each bin.

4. Site charcoal records are synthesised following the same procedure outlined in B8.2, with each record being Z-score standardised and interpolated to a fixed 50-yr time grid, though without age uncertainty due to data unavailability.

Table B5. Details of independent Snowy Mountains montane study sites from which paleoenvironmental data were collated to produce the synthesised montane pollen and charcoal records.

Site	Data type	Latitude	Longitude	Altitude (m)	Source
Brooks Ridge Fen	Charcoal	-36.1583	148.5944	1441	(Mooney et al., 1997)
Bogong Creek Swamp	Pollen	-35.7591	148.9606	1000	(Hope et al., 2009b)
Rotten Swamp	Charcoal, pollen	-35.707	148.8864	1445	(Hope and Clark, 2008)
Nursery Swamp	Charcoal, pollen	-35.6814	148.9669	1092	(Hope et al., 2009b)
Micalong Swamp	Charcoal, pollen	-35.318	148.524	1000	(Kemp, 1993)
Tom Gregory Bog	Charcoal, pollen	-35.38	148.49	1024	(Hope, 2006)
Yaouk Swamp	Charcoal, pollen	-35.7953	148.8578	1115	(Keaney and Hope, 2006)

Section B16: Output of cross-correlation analysis

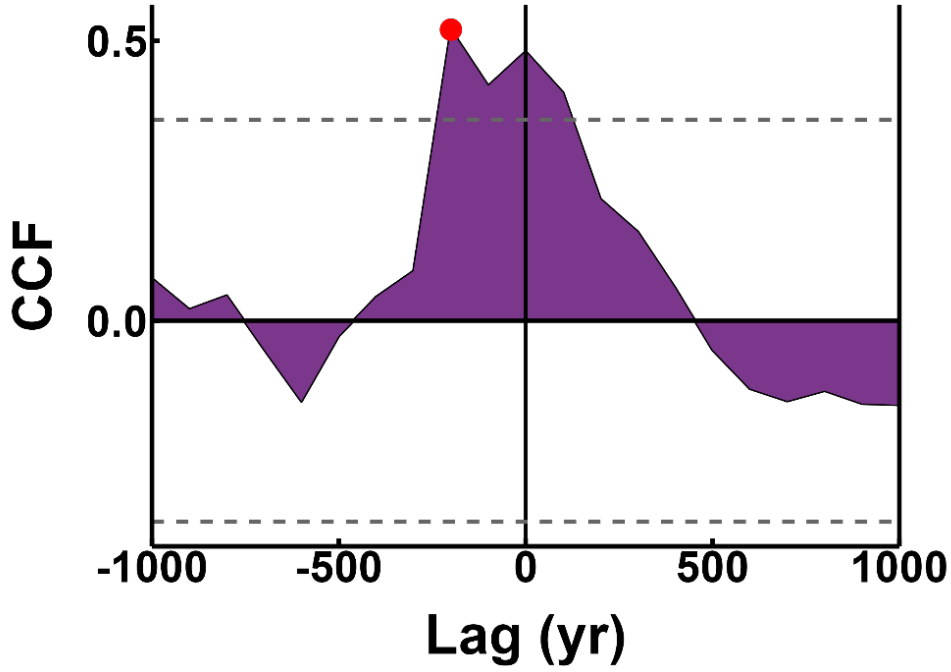

Figure B5. Output of cross-correlation analysis performed on the zonal Rate-of-Change data and the binned record of mean annual precipitation from Barr et al. (2019). Analysis performed using base R (R Core Team, 2020). 'CCF' denotes cross-correlation function, dashed lines mark the statistical significance threshold, and red marker denotes peak correlative strength.

Appendix C

Supplementary Information for Chapter 4

Section C1: Sampling site details

Table C1. Site selected for sampling, including key physical attributes.

Site name	Zone	Latitude, longitude	Elevation (m)	Bog/lake area (ha)	Observed/recorded European land uses
Diggers Creek	Subalpine	-36.3794, 148.4836	1645	2.18	Grazing, gold panning, water impoundment downstream.
Prussian Plain	Subalpine	-36.4010, 148.4413	1700	18.17	Grazing
Betts Creek	Subalpine	-36.4226, 148.3749	1745	2.16	Grazing, road constructed 290 m to the south.
Hedley Tarn (bog)	Alpine	-36.4102, 148.3205	1860	3.44	Grazing
Hedley Tarn (lake)	Alpine	-36.4115, 148.3203	1860	3.2	Grazing
Muellers Pass	Alpine	-36.4452, 148.2824	1920	0.34	Grazing

Section C2: ^{14}C sample preparation method

C2.1. Bulk sediment pretreatment

1. Load 7-8 g sediment (wet mass) onto a petri dish and dry in an oven (105 ºC) for 24 hours.
2. Measure stable dry mass and crush to a uniform powder using a clean mortar and pestle.
3. Load into aluminium foil and send to either DirectAMS, ANSTO or UNSW for ABA pretreatment and AMS ^{14}C analysis.

C2.2. Sporopollenin pretreatment

1. Load ~3 g sediment (wet mass) into a clean 15 ml centrifuge tube.

2. For disaggregation, add 10 ml 5% sodium hexametaphosphate; ('Calgon' or similar) to the centrifuge tube and stir with a vortex mixer. Heat in a hot water bath (80 ºC) for 20 minutes, centrifuge at 3000 rpm for 5 minutes and decant supernatant.
3. For silicate digestion, add 10 ml of lithium heteropolytungstate (LST; 'heavy liquid') to the tube, diluted/concentrated to a specific gravity of 2 g/ml and centrifuge at 1600 rpm.
4. Pipette the organic float produced after centrifuging and transfer to a new 15 ml centrifuge tube ('secondary sample').
5. Repeat steps 3-4 until sample ceases yielding organic material. Once this occurs, top up secondary sample with 15 ml distilled water, centrifuge at 3000 rpm for 10 minutes and decant.
6. For carbonate digestion, add 5 ml of 10% w/w hydrochloric acid to the tube and stir with a vortex mixer. Heat in a hot water bath (80 ºC) for 20 minutes, centrifuge at 3000 rpm for 3 minutes and decant supernatant.
7. Add 10 ml distilled H_2O, stir with vortex mixer, centrifuge at 3000 rpm for 3 minutes and decant supernatant.
8. For cellulose and charcoal digestion, add 2 ml of 2.5% w/v sodium hypochlorite and heat in water bath at 90 ºC for 3 minutes.
9. Add 10 ml of distilled water, centrifuge at 3000 rpm for 3 minutes then decant supernatant. Repeat thrice.
10. Using a glass pipette, transfer the material from the 15 ml tube to a 1.5 ml micro-centrifuge tube, then centrifuge at 1500 rpm for 3 minutes and decant. If not all material is transferred at once, repeat centrifugation and decanting until this is achieved.
11. At ANSTO, treat with 2M HCl at room temperature for 2 hr, then oven-dry at 60 ºC overnight.

Section C3: Micro-X-ray fluorescence analysis method

1. Cores are scanned using a 0.1 cm resolution using an Itrax core scanner fitted with a Mo tube.
2. Raw concentrations for 33 major, minor and trace elements are reported as relative counts per second (kcps).

3. Raw kcps data are normalised to the incoherent/coherent scattering ratio to remove the effect of light elements in the matrix due to high organic matter and moisture content (Woodward and Gadd, 2019). Data are cleaned by removing clear core-edge scanning artefacts.
4. Elements deemed to be environmentally significant and with a high signal-to-noise ratio (Table C4) are subject to cluster analysis using the R package rioja and Principal Component Analysis using the R package FactoMineR (Lê et al., 2008, McKillup and Dyar, 2010, R Core Team, 2020).

Section C4: Mineral grain size preparation and analysis method

1. Load ~0.5 g sediment (wet mass) into a 50 ml centrifuge tube.
2. For carbonate digestion, add 5 ml of 5% w/v hydrochloric acid to tube and heat in a water bath (80 ^{o}C) until reaction ceases. Remove sample, top up with distilled water and stir with vortex mixer. Centrifuge at 3000 rpm for 5 minutes and decant supernatant.
3. For organic matter digestion, add 10 ml of 10% w/v hydrogen peroxide to tube and heat in water bath (80 ^{o}C) until reaction ceases. Remove sample, top up with distilled water and stir with vortex mixer. Centrifuge at 3000 rpm for 5 minutes and decant supernatant.
4. For clay deflocculation, add 20 ml of 5% w/v sodium hexametaphosphate and place on a rotary tube mixer for two hours.
5. Samples are analysed using a Malvern Mastersizer 3000 laser diffractometer equipped with a Hydro LV dispersion unit. Samples containing gravel (>2 mm) are sieved as they ae emptied into dispersion unit. Triplicate blue light measurements are taken per sample to calculate a mean grain size distribution,
6. For samples containing gravel, measure dry mass of gravel fraction and calculate mass percentage of gravel fraction. Scale grain size distribution data to the residual percentage mass to obtain gravel-corrected values. Combine gravel and sub-gravel data to obtain a full corrected grain size distribution.
7. Grain size distribution data is then decomposed into summary statistics using the GRADISTAT Excel package (v. 8; Blott and Pye (2001)).

Section C5: Total organic carbon/nitrogen and $\delta^{13}C$ preparation and analysis method

1. Load 2 cm^3 wet sediment into a 50 ml centrifuge tube, measure wet mass, freeze at -80 ºC overnight, then freeze dry with lid ajar for 24 hours.
2. After freeze drying, measure dry mass to calculate moisture content and dry bulk density.
3. For carbonate digestion, add 5 ml of 10% w/w hydrochloric acid to tube and heat in a water bath (80 ºC) for 2 hours.
4. Top up with distilled water, centrifuge at 3000 rpm for 5 minutes and decant supernatant liquid. Repeat 3x.
5. Freeze at -80 ºC overnight then freeze dry with lid ajar for 24 hours.
6. Crush dried sample to a uniform powder and transfer to a plastic container. Samples containing gravel (>2 mm) are sieved out and retained prior to crushing of the sub-gravel fraction.
7. Depending on sample C% (verified through low-resolution test samples) transfer 100-200 mg for total carbon and total nitrogen and 0.4-10 mg for $\delta^{13}C$ into a tin foil capsule, enclose and load onto relevant instrument for analysis. For $\delta^{13}C$, duplicate samples of roughly equal mass must be loaded to calculate standard deviation.
8. Total carbon and total organic nitrogen samples are analysed with a VELP Scientifica CN802 Carbon Nitrogen Analyser.
9. For samples containing gravel, measure the dry mass of the gravel fraction and calculate its mass percentage. Scale TOC to the remaining percentage mass to obtain gravel-corrected values.
10. $\delta^{13}C$ samples are analysed with an Elementar VarioISOTOPE Elemental Analyser coupled with an Elementar PrecisION Isotope Ratio Mass Spectrometer to measure relative isotopic abundances of C, reporting $\delta^{13}C$ as ‰.

Section C6: Macrocharcoal preparation and counting method*

* This method has been adapted from that of Stevenson and Haberle (2018).

1. Load 1 cm^3 wet sediment into a 50 ml centrifuge tube.

2. For sample disaggregation, add 20 ml of 5% w/v sodium hexametaphosphate to the tube and place on a rotary tube mixer for two hours.
3. Empty sample through a 2 mm and 125 μm sieve, retaining both fractions and discarding the <125 μm fraction. Use high pressure tap water to ensure removal of all finer material.
4. Empty ≥ 125 μm fraction into a plastic container and preserve in distilled water. Retain gravel (2 mm) fraction.
5. Samples are manually counted on a petri dish using a Zeiss Stemi 305 Stereo Microscope. Whole samples are counted unless macrocharcoal is extremely abundant, in which case a subset of 1 cm^2 grid cells are counted and the average count is multiplied by the petri dish area.
6. For samples containing gravel, counts are corrected by determining the dry-mass percentage of the gravel fraction and scaling counts to the remaining fine-fraction mass to obtain gravel-corrected macrocharcoal abundances.

Section C7: Bulk mineral influx, apparent carbon accumulation rates and macrocharcoal accumulation rates calculation and aggregation method

1. Bulk mineral influx (g m^{-2} yr^{-1}) (a), apparent carbon accumulation rates (g m^{-2} yr^{-1}) (b), and macrocharcoal accumulation rates (particles cm^{-2} yr^{-1}) (c) are calculated by the following formulas:

(a) $$= SR * DBD * \left(1 - \left(\frac{TOC}{100} * 1.724\right)\right) \times 10^4$$

(b) $$= SR \times DBD \times (TOC \,/\, 100) \times 10^4$$

(c) $$= \frac{MC * 0.5}{Bottom - Top}$$

where SR is sedimentation rate (cm yr^{-1}), DBD is dry bulk density (g cm^{-3}), TOC is total organic carbon (%), 1.724 is the van Bemmelen factor, MC is macrocharcoal counts (particles cm^{-3}), and Bottom and Top are the lower and upper ages of the slice (cal yr BP).

2. For multisite synthesis, records of each metric are first divided into overlapping 200-yr windows stepped every 100 yr, within which median values are calculated. Site-level medians are then averaged across both records to generate a composite series.

Section C8: Moisture availability computation method*

* This method has been adapted from that of Hamilton et al. (2024) using R code shared by the authors.

C8.1. Site moisture availability index construction

1. For each site, input proxy records are linearly interpolated to the maximum proxy resolution to avoid biasing the index at depths with fewer data points.
2. Proxies are inverted where necessary where they are assumed to behave inversely with moisture availability.
3. A Z-score record is computed from every proxy record, and a median Z-score is calculated for every depth interval.

C8.2. ASA moisture availability index construction

1. Input proxy records are linearly interpolated and inverted following C5.1.
2. Proxies are Z-score standardised relative to the global mean for each proxy across both sites. A median Z-score is calculated for every depth interval.
3. Age uncertainties are propagated separately for each site using Monte Carlo resampling (10,000 iterations), where at each depth a standard deviation is estimated from the 95% confidence bounds and used to draw truncated normal ages.
4. The new random ages are used to interpolate the site MA index onto a regular 100-yr grid.

5. For each grid age for both sites, the new uncertainty bands are combined by drawing random values uniformly within each band and taking the median across sites over 10,000 iterations, yielding a regional median Z-score for each grid age with 95% uncertainty.

Table C2. Summary of input proxies for each site moisture availability reconstruction, specifying where inversions have and have not been applied, with justifications based on multiproxy triangulation, *a priori* assumptions and site observations. Proxies deduced to have negative correlations with wetting (N) were inverted, while those presumed to have positive correlations (P) were not.

Proxy	Wetting correlation	Justification
		Diggers Creek
Mean grain size	P	Wetting increases fluvial and slope transport energy
µXRF PC1	N	Wetting decreases relative lithogenic contribution due to dilution by organic matter
Volume magnetic susceptibility	P	Wetting increases erosion of catchment soils
Carbon/nitrogen	P	Wetting increases the preservation of C relative to N due to suppressed microbial metabolisation of C
$\delta^{13}C$	N	Wetting decreases preferential microbial metabolisation of ^{12}C
Bulk mineral influx	P	Wetting increases detrital influx
Apparent carbon accumulation rates	P	Wetting increases OM accumulation and C preservation
		Prussian Plain
Mean grain size	P	Wetting increases fluvial and slope transport energy
µXRF PC1	P	Wetting increases erosion and relative lithogenic contribution
Volume magnetic susceptibility	N	Wetting decreases peat humification and formation of high-susceptibility secondary minerals
Carbon/nitrogen	P	Wetting increases the preservation of C relative to N due to suppressed microbial metabolisation of C
$\delta^{13}C$	N	Wetting decreases preferential microbial metabolisation of ^{12}C

Bulk mineral influx	P	Wetting increases detrital influx
Apparent carbon accumulation rates	P	Wetting increases OM accumulation and C preservation
Macrocharcoal accumulation rates	N	Wetting decreases woodland flammability and burning
		Betts Creek
Mean grain size	N	Wetting decreases fluvial and slope transport energy due to trapping by denser alpine meadow
µXRF PC1	N	Wetting decreases relative lithogenic contribution due to dilution by organic matter
Volume magnetic susceptibility	N	Wetting decreases peat humification and formation of high-susceptibility secondary minerals
Carbon/nitrogen	P	Wetting increases the preservation of C relative to N due to suppressed microbial metabolisation of C
$\delta^{13}C$	N	Wetting decreases preferential microbial metabolisation of ^{12}C
Bulk mineral influx	P	Wetting increases detrital influx
Apparent carbon accumulation rates	P	Wetting increases OM accumulation and C preservation
		Hedley Tarn (bog)
Mean grain size	P	Wetting increases fluvial and slope transport energy
µXRF PC1	P	Wetting increases erosion and relative lithogenic contribution
Volume magnetic susceptibility	N	Wetting decreases peat humification and formation of high-susceptibility secondary minerals
Carbon/nitrogen	P	Wetting increases the preservation of C relative to N due to suppressed microbial metabolisation of C
$\delta^{13}C$	N	Wetting decreases preferential microbial metabolisation of ^{12}C
Bulk mineral influx	P	Wetting increases detrital influx

Apparent carbon accumulation rates	N	Wetting decreases peat accretion at river mouth complex due to increased fluvial erosion by enhanced outflow down Blue Lake blockstream
		Hedley Tarn (lake)
Mean grain size	P	Wetting increases fluvial and slope transport energy
µXRF PC1	P	Wetting increases erosion and relative lithogenic contribution
Volume magnetic susceptibility	N	Wetting increases supply-limited conditions and thus depletes cirque soil mantle. **Major exception:** soils are only delivered to tarn after late Holocene establishment
$\delta^{13}C$	N	Wetting decreases preferential microbial metabolisation of ^{12}C
Bulk mineral influx	P	Wetting increases detrital influx
Apparent carbon accumulation rates	P	Wetting increases OM accumulation and C preservation
Macrocharcoal accumulation rates	N	Wetting decreases woodland flammability and burning
		Muellers Pass
Mean grain size	N	Wetting decreases fluvial and slope transport energy due to trapping by denser alpine meadow
µXRF PC1	N	Wetting decreases relative lithogenic contribution due to dilution by organic matter
Volume magnetic susceptibility	N	Wetting decreases peat humification and formation of high-susceptibility secondary minerals
Carbon/nitrogen	P	Wetting increases the preservation of C relative to N due to suppressed microbial metabolisation of C
$\delta^{13}C$	N	Wetting decreases preferential microbial metabolisation of ^{12}C
Bulk mineral influx	P	Wetting increases detrital influx
Apparent carbon accumulation rates	P	Wetting increases OM accumulation and C preservation

Section C9: Multiproxy Rate-of-Change computation method*

***** This method has been adapted from that of Mottl et al. (2021b).

1. For each site, input proxy records are linearly interpolated to avoid artefactual values arising from sampling gaps.
2. Using the R-Ratepol package, multivariate Rate-of-Change is calculated as the standardised Euclidean distance between consecutive 50-yr time bins (working units), divided by the elapsed time.
3. Step 2 is repeated 10,000 times using randomised bin representation, with the median and 2.5th and 97.5th quantiles being calculated for all randomisations.
4. A zonal Rate-of-Change record is calculated as the median of all sites for each 100-yr midpoint bin.

Due to the μXRF for the MB1 core having poor depth coverage towards core top (see Fig. 4.2), and the necessity to calculate colonial-era values, Rate-of-Change was re-performed without the μXRF PC1 data between 3.5-7.2 cm for MB1. Data for this depth range was then appended to the whole-suite data for the underlying depth range to produce a single record. While this biases RoC over this interval to one fewer proxy for MB1, it enabled data to be obtained for the colonial period.

Section C10: Core details

Table C3. Lengths and locations of all sampled cores. Asterisks denote cores that were selected for multiproxy analysis.

Core ID	Site name	Length (cm)	Longitude	Latitude	Material
DA1	Diggers Creek	43	148.48367	-36.37891	Peat
DA4*	"	48	"	"	"
DB	"	38	148.48401	-36.37923	"
DD1	"	21	148.48637	-36.37966	"
DD2	"	42	"	"	"
PA	Prussian Plain	50	148/44127	-36.40099	"
PB*	"	50	148.44135	-36.40120	"
PC	"	38	148.44176	-36.40091	"
BA1*	Betts Creek	26	148.37468	-36.42287	"
BA2*	"	50	"	"	"
BB	"	31	148.37547	-36.42274	"
BC	"	39	148.37453	-36.42258	"
BD	"	25	148.37445	-36.42282	"
HA1	Hedley Tarn (bog)	20.5	148.32024	-36.40959	"
HA2	"	30.5	"	"	"
HC1	"	29	148.32042	-36.40982	"
HC2	"	27	"	"	"
HD1	"	29.5	148.32062	-36.41037	"
HD2*	"	32	"	"	"
HA*	Hedley Tarn (lake)	92	148.32106	-36.41113	Gravel
HB	"	69	148.32030	-36.41162	"
MB1*	Muellers Pass	39	148.28252	-36.44509	Peat
MB2	"	31	"	"	"

Section C11: Optical core scans

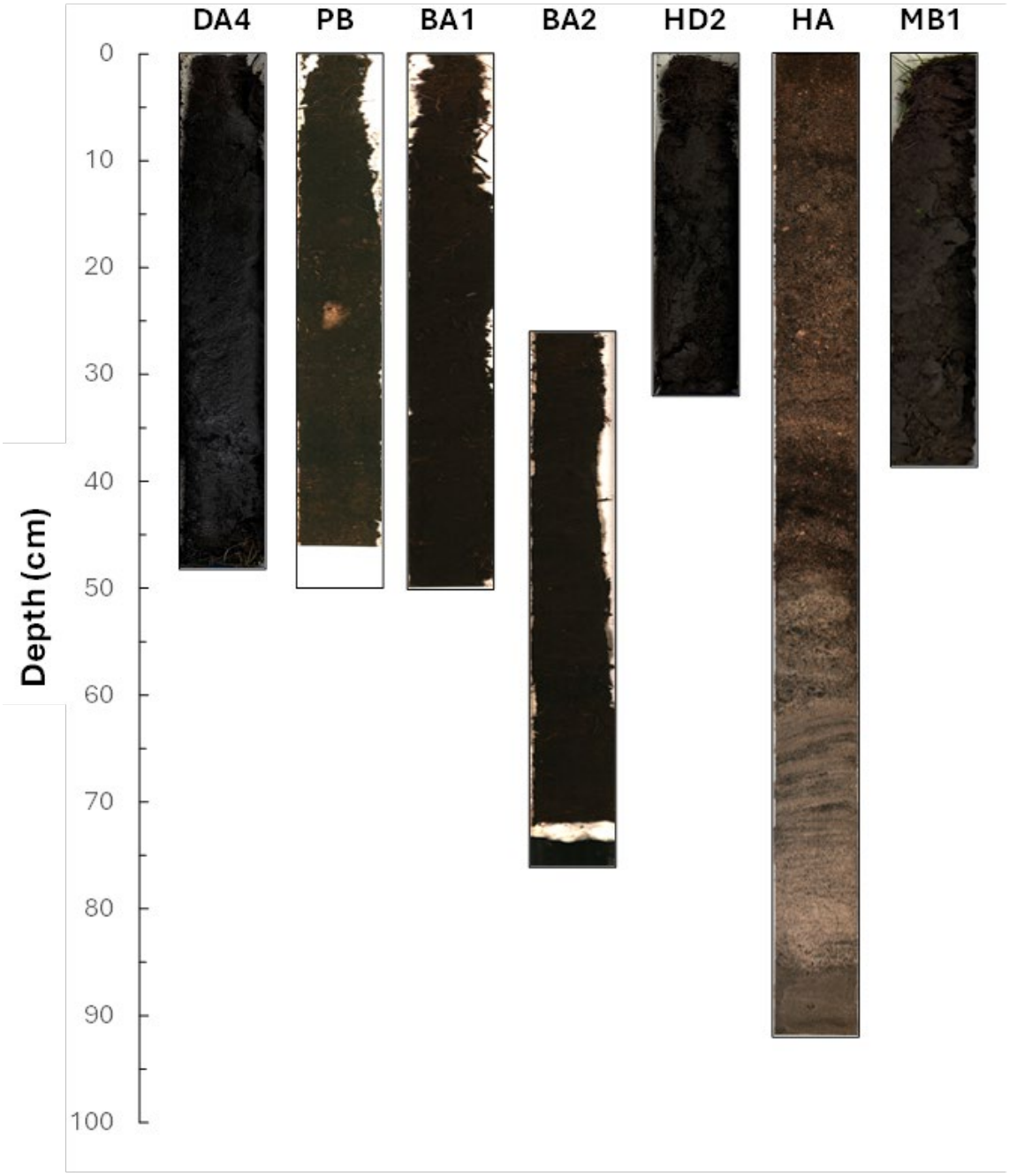

Figure C1. Optical scans of cores selected for multiproxy analysis. Blank sections correspond to ^{14}C samples that were removed prior to scanning.

Section C12: Age calibration and chronological modelling outputs

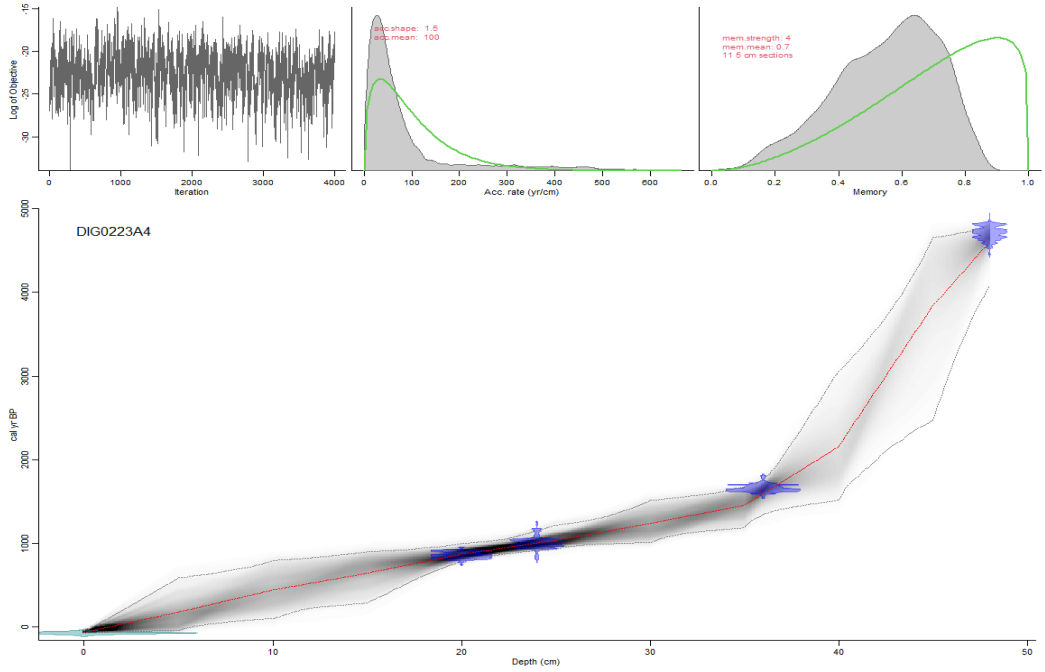

Figure C2. Output of age-depth modelling for DA4. Blue histograms denote calibrated ages, red line denotes mean modelled age, and grey gradient denotes age likelihood (darker shades being more likely) within 95% confidence envelope (grey lines).

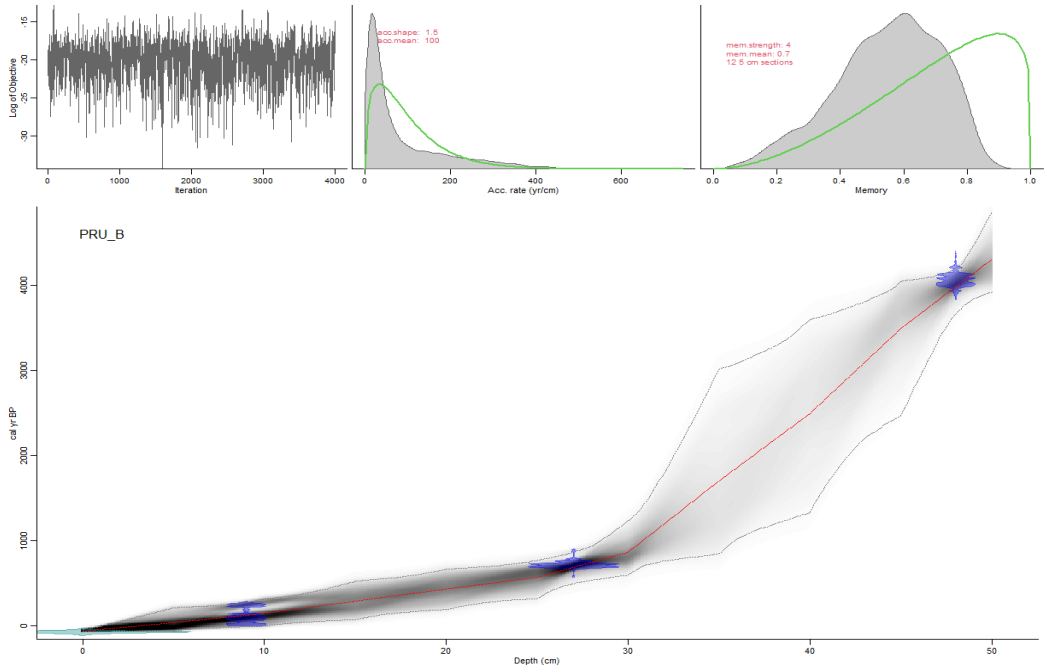

Figure C3. Output of age-depth modelling for PB.

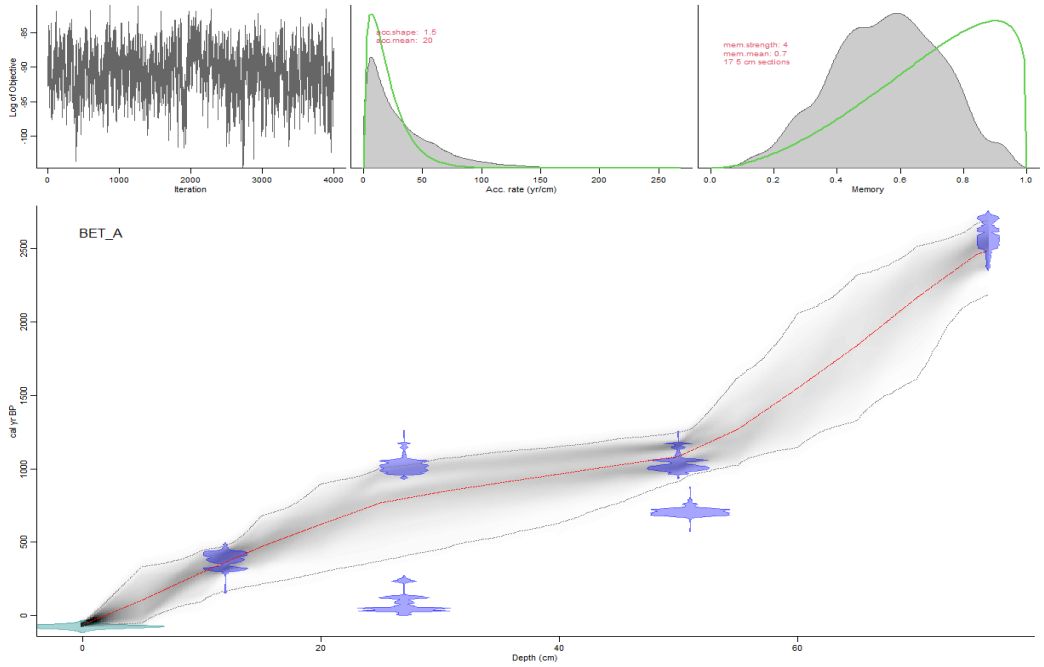

Figure C4. Output of age-depth modelling for BA.

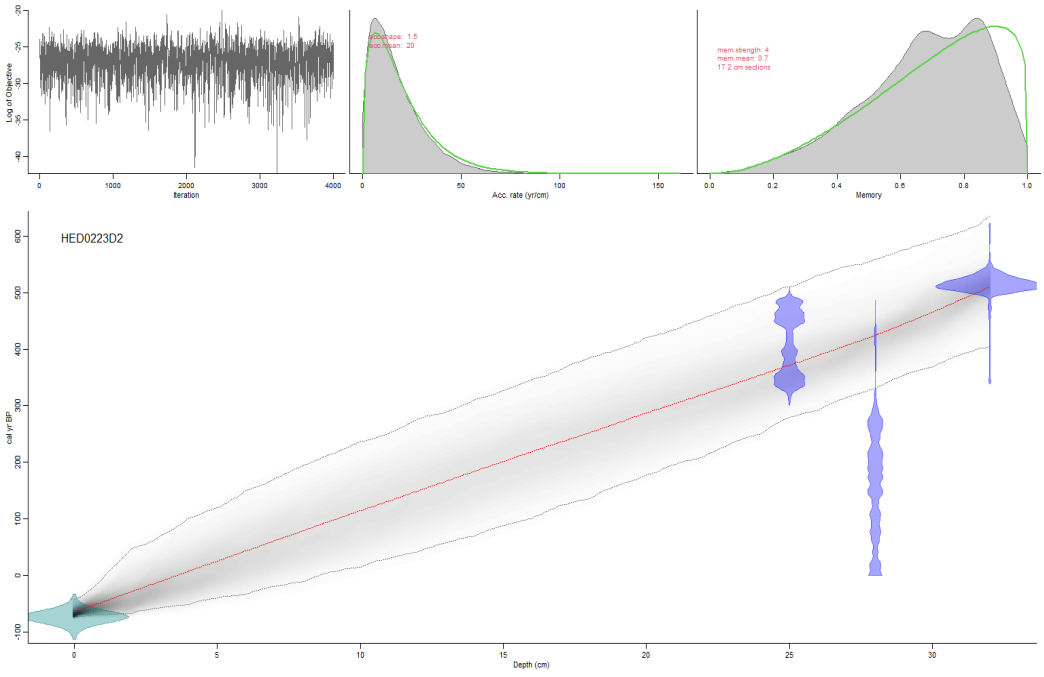

Figure C5. Output of age-depth modelling for HD2.

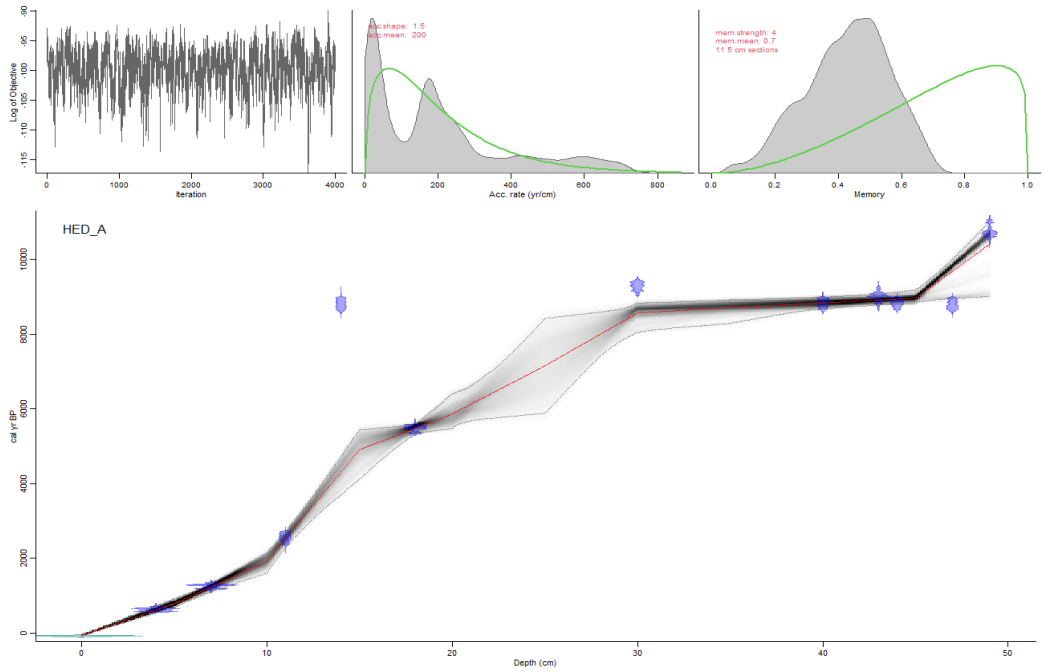

Figure C6. Output of age-depth modelling for HA.

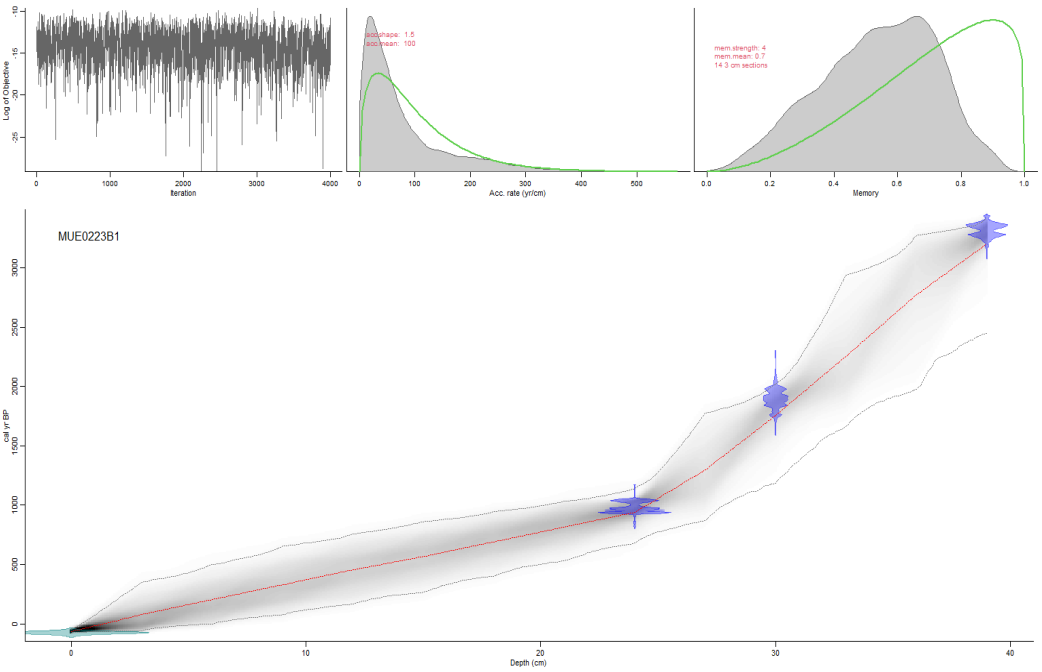

Figure C7. Output of age-depth modelling for MB1.

Section C13: Principal component analysis of µXRF data

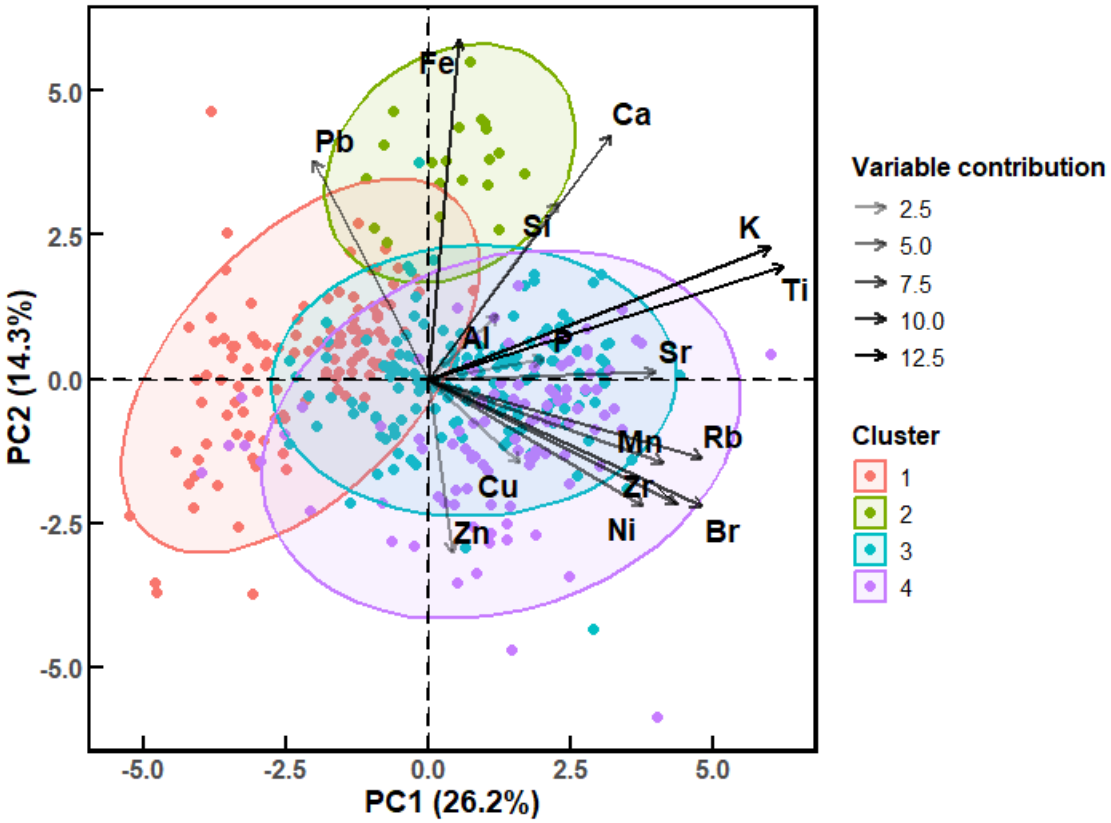

Figure C8. PCA biplot for DA4.

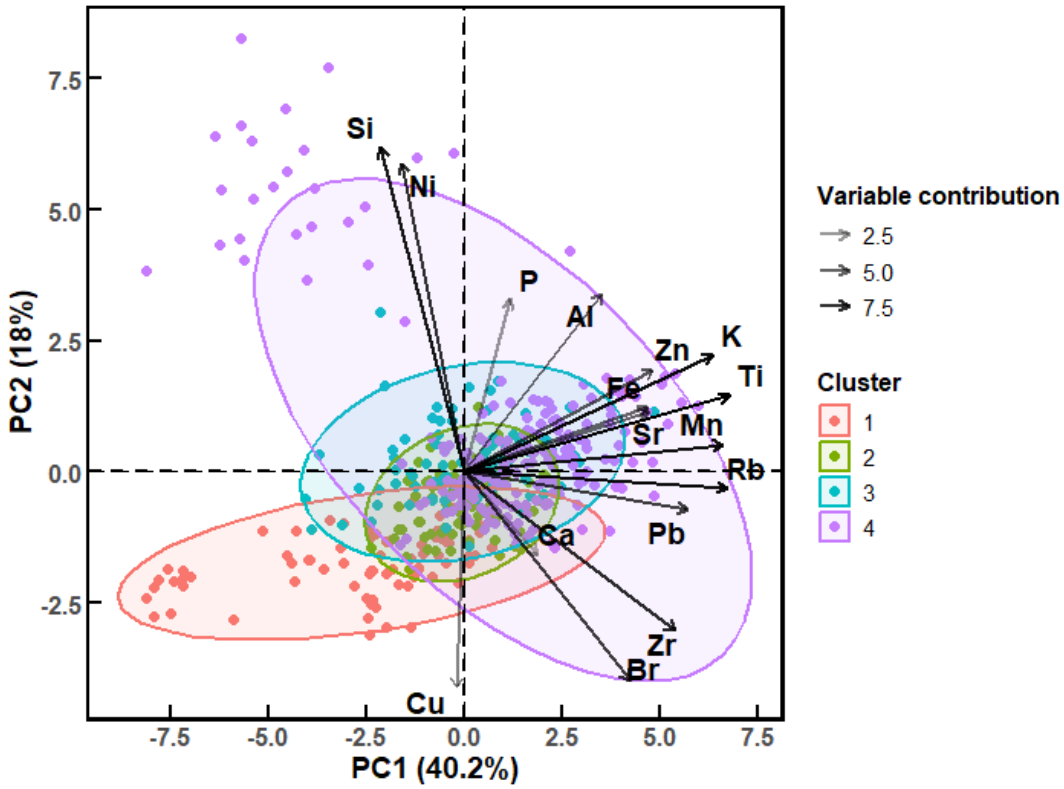

Figure C9. PCA biplot for PB.

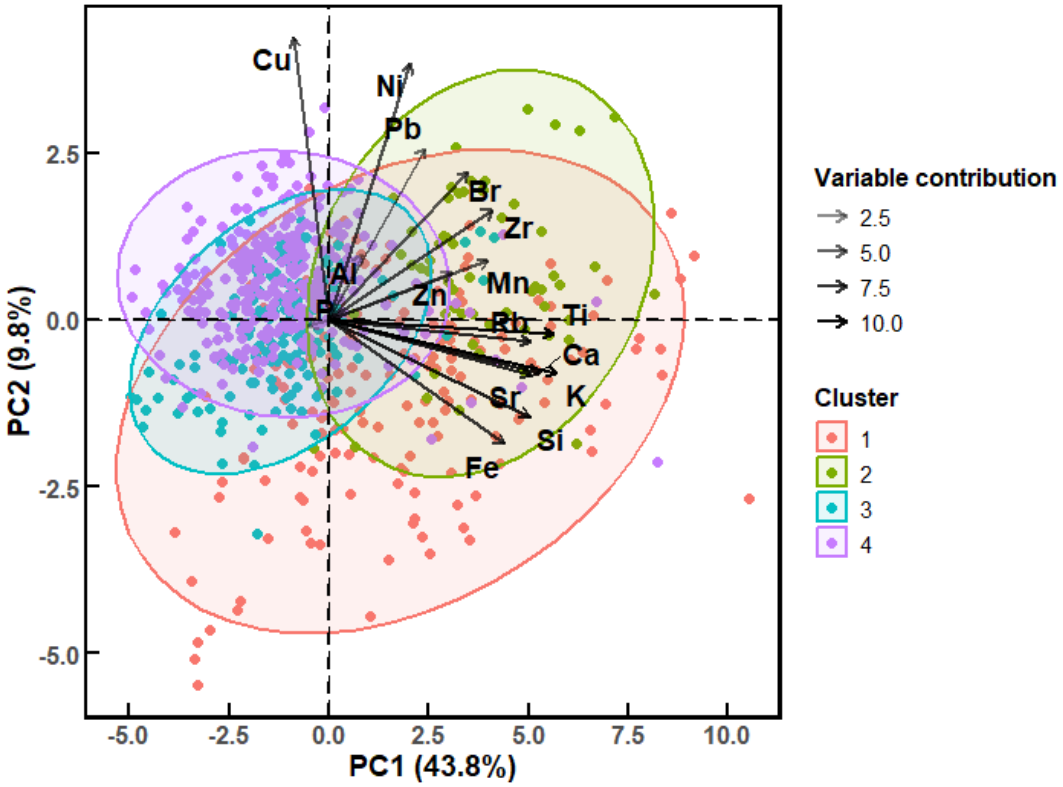

Figure C10. PCA biplot for BA.

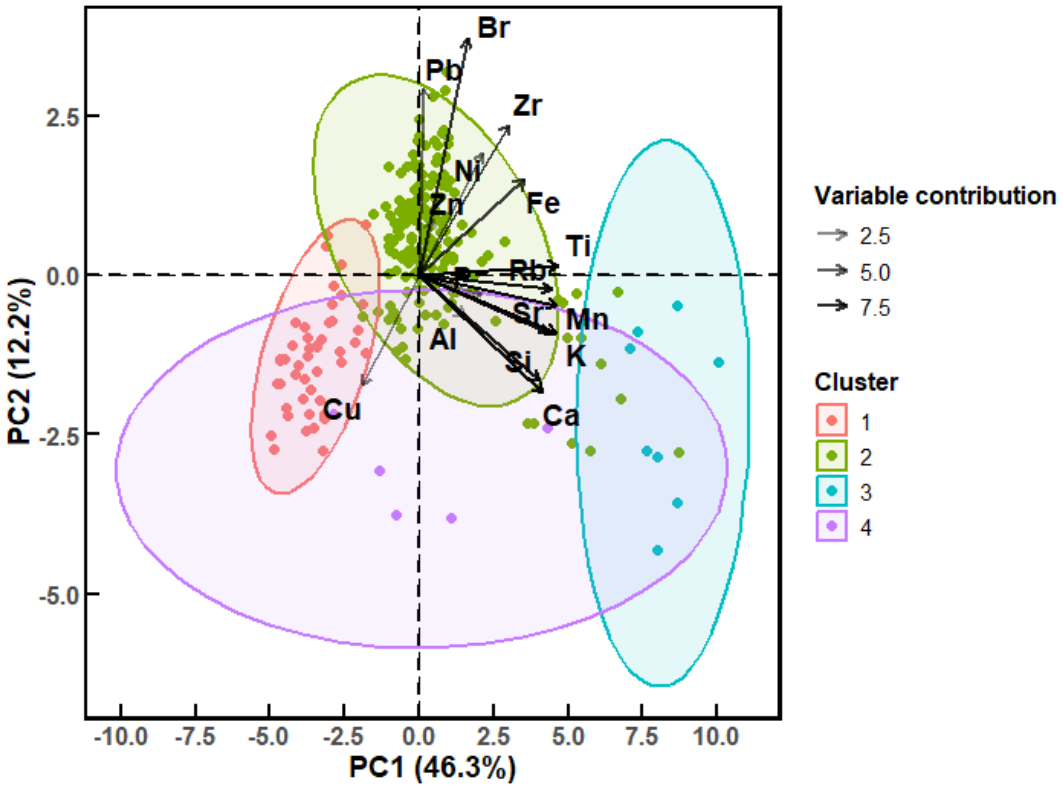

Figure C11. PCA biplot for HD2.

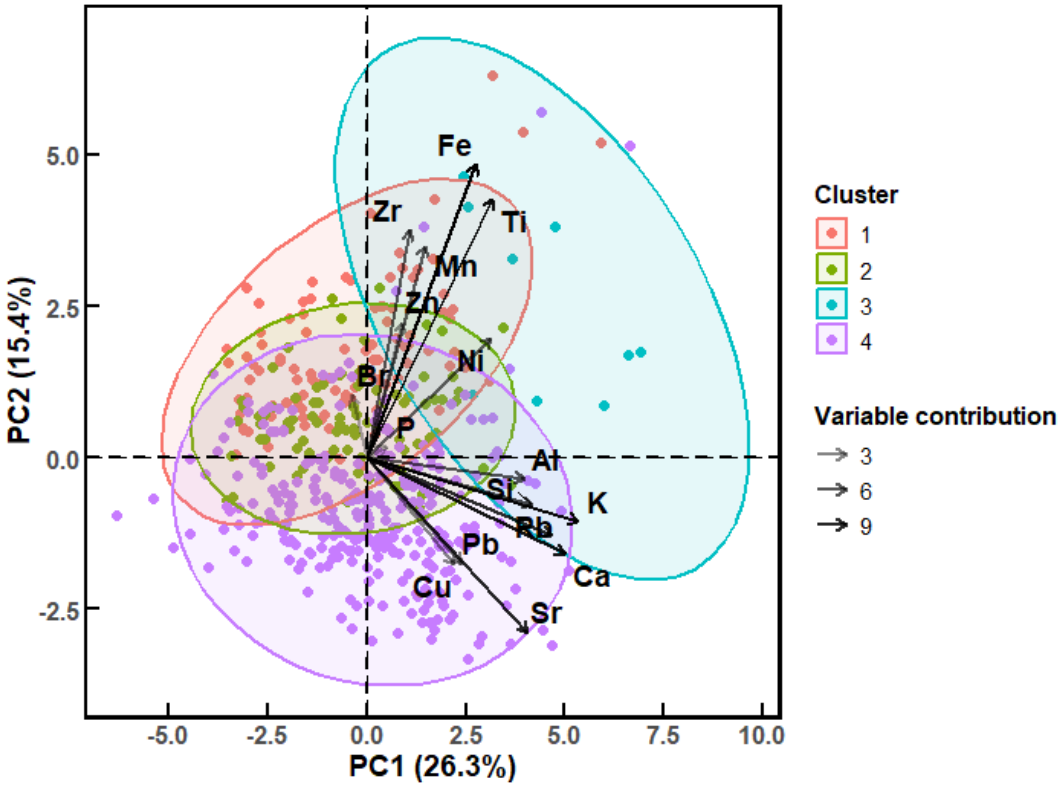

Figure C12 PCA biplot for HA.

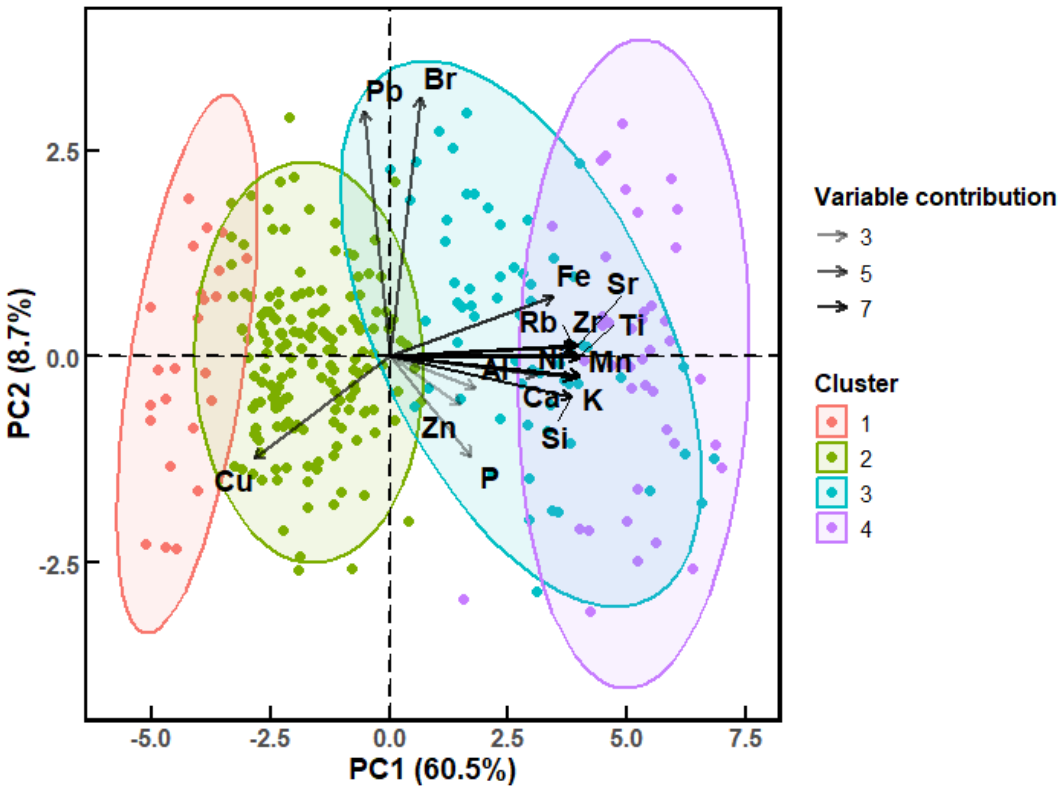

Figure C13. PCA biplot for MB1.

Table C4. μXRF PC1 element contributions (%) for each core.

Element	DA4	PB	BA	HD2	HA	MB1
Al	0.7	3.5	0.3	1.3	9.5	2.0
Si	2.4	1.3	10.0	9.2	10.4	9.1
P	1.9	0.4	0.1	2.5	0.2	1.8
K	16.7	11.6	12.9	12.0	16.9	9.9
Ca	4.8	1.0	10.9	9.8	14.9	9.2
Ti	18.1	13.3	12.5	12.4	6.0	9.9
Mn	7.9	12.6	6.3	12.1	1.3	9.8
Fe	0.1	6.4	7.6	7.1	4.5	7.4
Ni	6.6	0.7	1.6	2.6	5.8	5.9
Cu	1.2	0.0	0.3	2.0	2.9	5.0
Zn	0.1	6.7	3.8	0.1	0.5	1.4
Br	10.7	5.2	4.8	1.5	0.1	0.3
Rb	10.7	13.0	10.1	11.3	13.0	9.3
Sr	7.4	6.4	10.1	10.8	9.8	9.6
Zr	8.9	8.4	6.6	5.2	0.7	9.4
Pb	1.9	9.4	2.3	0.0	3.4	0.2

Section C14: Method for synthesis of alpine-subalpine pollen and charcoal records

1. All publicly available pollen and charcoal records from the Snowy Mountains alpine-subalpine complex are compiled from the Neotoma Paleoecology Database (Table C5) (Williams et al., 2018) and the Global Paleofire Database.
2. For each pollen record, total counts for *Pomaderris* and total pollen were extracted, and their ratio calculated.
3. In the absence of age uncertainty data for every pollen record, each is binned at 200-yr intervals, and a median *Pomaderris* / total pollen ratio is calculate for each bin. A median value is then calculated for all sites for each bin.
4. Site charcoal records are synthesised following the same procedure outlined in C8.2, with each record being Z-score standardised and interpolated to a fixed 100-yr time grid, though without age uncertainty due to data unavailability.

Table C5. Details of independent Snowy Mountains alpine and subalpine study sites from which paleoenvironmental data were collated to produce the synthesised alpine-subalpine pollen and charcoal records.

Site	Data type	Latitude	Longitude	Altitude (m)	Source
Blue Lake	Pollen, charcoal	-36.4036	148.3158	1854	(Raine, 1974)
Club Lake	Pollen	-36.4132	148.2912	1951	(Martin, 1986b)
Cotter Source Bog	Charcoal	-35.9667	148.8167	1720	(Hope and Clark, 2008)
Diggers Creek	Pollen	-36.3877	148.47959	1690	(Martin, 1999)
Pengillys Bog	Pollen	-36.3793	148.414	1617	(Theden-Ringl, 2010)
Rennix Gap	Charcoal, pollen	-36.3641	148.5055	1575	(Kemp, 1993)
Snowy Flats	Charcoal, pollen	-35.5655	148.8642	1618	(Hope et al., 2005)

Section C15: Method for time binning of non-composite paleoclimate records and Pearson correlation with zonal records

1. In the absence of age uncertainty data for every climate record, each is binned at 100-yr time intervals spanning every 100-cal yr from 0 cal yr BP, and a median is calculated for every interval.
2. Binned paleoclimate data are subject to Pearson correlation with zonal records for all time bins older than 200 cal yr BP, in order to remove the influence of colonial- and industrial-era anthropogenic activities on the zonal and paleoclimate records, respectively.

Section C16: Input records for composite paleoclimate reconstructions

Paleoclimate records listed in Table C6 and shown in Figure C14 were selected based on prioritisation of independent records that a) exhibited significant temporal overlap with our regional record, b) derived from southeastern Australia (defined here as being south of 23.5° S and east of 130° E), and c) quantitatively reconstructed hydroclimate or temperature. These criteria significantly reduced the number of records that could be collated, forcing inclusion of some records that did not satisfy all three criteria. Record-specific justifications are outlines in Table C6. 4.

Records were synthesised into composite hydroclimate and temperature records following the same procedure outlined in C8.2, with each record being Z-score standardised and interpolated to a fixed 100-yr time grid, though without age uncertainty due to data unavailability

Table C6. Summary of the paleoclimate proxy data collated to construct average changes in hydroclimate and temperature for southeastern Australia and proximal regions.

Site name	Location	Units	Inversion applied	Justification for use and inversion (if applied)	Source
Hydroclimate					
Swallow Lagoon	North Stradbroke Island (-27.50, 153.45)	Mean annual precipitation (mm/yr)	No	Within southeastern Australia; within influence of ENSO and SAM	Barr et al. (2019)
Rebecca Lagoon	Northwest Tasmania (-41.18, 144.68)	Precipitation (mm/yr)	No	Within southeastern Australia; within influence of ENSO and SAM	Saunders et al. (2012)
Laguna Llaviucu	Ecuador (-2.84, -79.1453)	δ^2H	Yes	Within influence of ENSO; Holocene-spanning record. Inverted due to opposite hydroclimatic expression of ENSO in eastern Pacific. Inverted due to δ^2H being inversely related to hydroclimate	Zhao et al. (2024)
Upper Snowy	Upper Snowy Mountains (-36.46, 148.30)	Dust flux ($g/m^2/yr$	Yes	Within southeastern Australia; within influence of ENSO and SAM. Inverted due to dust flux being negatively correlated with coastal climate.	Marx et al. (2011)
Southeastern Australian lakes	Southeastern Australia	Lake level (dimensionless)	No	Clerke (2023) identifies southeastern Australian lake levels as being strongly driven by precipitation. Only southeastern Australian lakes (n. 31) were included in aggregation, using R code shared by the source author.	Clerke (2023)
Temperature					

MD03-2611	Murray Canyons (-36.73, 136.55))	Sea surface temperature (ºC)	No	Proximal to southeastern Australia; within influence of SAM	Calvo et al. (2007)
MD03-2607	Southern Ocean (-36.96, 137.41)	Sea surface temperature (ºC)	No	Proximal to southeastern Australia; within influence of SAM	Lopes dos Santos et al. (2013)
MD98-2170	Indian Ocean (-10.60, 125.38)	Sea surface temperature (ºC)	No	Proximal to southeastern Australia; within influence of ENSO	Stott et al. (2004)
MD98-2176	Indian Ocean (-5, 133.45)	Sea surface temperature (ºC)	No	Proximal to southeastern Australia; within influence of ENSO	Stott et al. (2004)
Vostok	Vostok Station (-78.47, 106.83)	Air temperature (ºC)	No	Proximal to southeastern Australia; Holocene-spanning record	Jouzel et al. (1996)
EPICA	EPICA Dome C (-75.1, 123.4)	Air temperature (ºC)	No	Proximal to southeastern Australia; Holocene-spanning record	Jouzel et al. (2007)
Yarrangobilly Caves	Yarrangobilly (-36.04, 148.37)	Air temperature (ºC)	No	Within southeastern Australia; within influence of ENSO and SAM	McGowan et al. (2019)
Lake Mackenzie	Fraser Island (-25.45, 153.05)	Air temperature (ºC)	No	Within southeastern Australia; within influence of ENSO and SAM	Woltering et al. (2014)
Platypus Tarn	Mount Field (-42.67, 146.59)	Air temperature (ºC)	No	Within southeastern Australia; within influence of ENSO and SAM	Rees and Cwynar (2010)

Eagle Tarn	Mount Field (-42.68, 146.59)	Air temperature (ºC)	No	Within southeastern Australia; within influence of ENSO and SAM	Rees and Cwynar (2010)

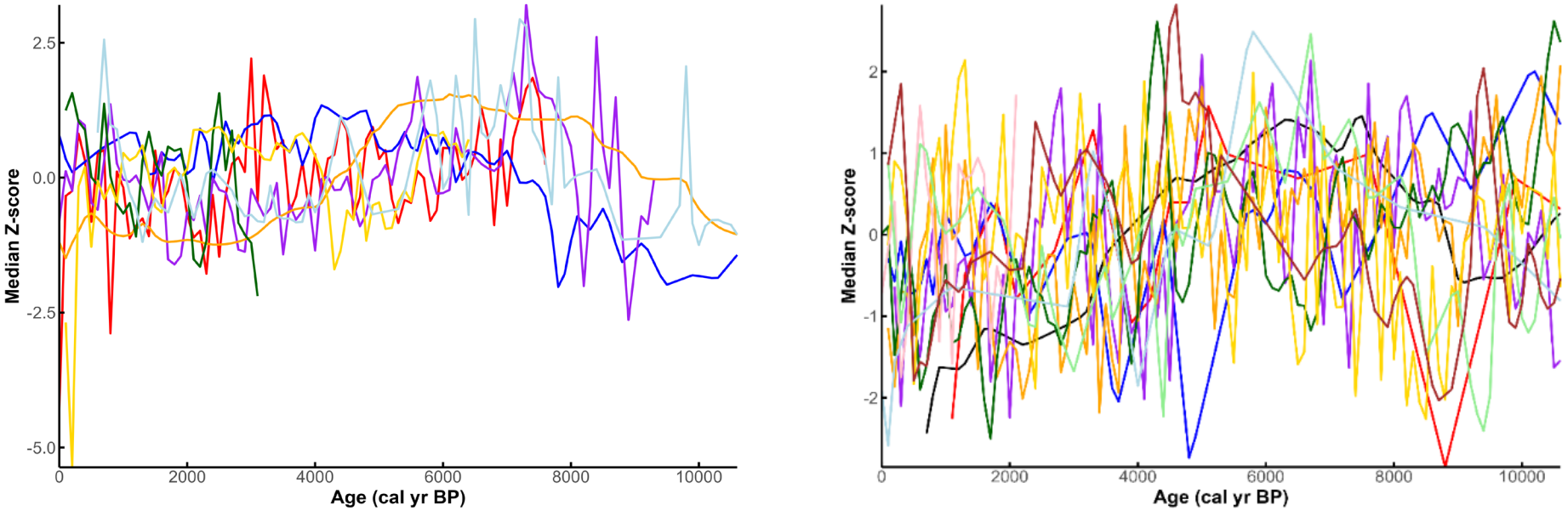

Figure C14. Time series overlays of the Z-scored hydroclimate (top) and temperature (bottom) records from Table C2.

Section C17: µXRF wavelet analysis

1. µXRF PC1 data series are truncated to the maximum age range over which sampling resolution remains sufficient to resolve the 2–7 yr band of interest.
2. The median sampling interval (dt) is calculated for each data series to define the natural sampling interval for each record. Data are then linearly interpolated to dt ensure a regular age grid while preserving the local structure of the data series. Data are then detrended and Z-standardised prior to transformation.
3. Using the R 'biwavelet' package, continuous wavelet transforms are computed using the Morlet wavelet with standard settings for the scale resolution (1/12) and minimum periodicity of detection (2·dt). Significance is tested against a red-noise background at the 95% level and the cone of influence is recorded.
4. Wavelet power between 2–7 yr periods is isolated, and median power across this band calculated for every time step.

Appendix D

Generic R script workflows for construction of moisture availability and Rate-of-Change indices

```
  ################################################################
##################
  # GENERIC MULTI-RECORD COMPOSITE + AGE-UNCERTAINTY MC + REGIONAL
TREND
  ################################################################
##################
  suppressPackageStartupMessages({
    library(dplyr)
    library(readr)
  })


  # USER INPUT ------------------------------------------------
  records <- list(
    list(record_id      =      "RECORD_1",      proxy_file      =
"path/to/proxy1.csv", age_file = "path/to/age1.csv")
    #    ,    list(record_id    =    "RECORD_2",    proxy_file    =
"path/to/proxy2.csv", age_file = "path/to/age2.csv")
  )


  age_col <- "age"; min_col <- "min"; max_col <- "max"
  comp_out_col <- "com"


  proxies_used <- list(
    RECORD_1 = c("proxyA","proxyB","proxyC")
  )
  dirs <- list(
    RECORD_1 = c(proxyA =  1, proxyB = -1, proxyC =  1)
  )


  agest       <- seq(0, 10000, 100)
  iter_site   <- 10000
  iter_region <- 1000


  out_dir <- "composite_outputs"
  dir.create(out_dir, showWarnings = FALSE, recursive = TRUE)
  write_site_csv   <- TRUE
  write_region_csv <- TRUE


  # HELPERS ---------------------------------------------------
```

```
  read_csv_stop <- function(path){
    if(!file.exists(path)) stop("File not found: ", path)
    readr::read_csv(path, show_col_types = FALSE)
  }

  get_num <- function(df, col){
    if(col %in% names(df)) as.numeric(df[[col]]) else
rep(NA_real_, nrow(df))
  }

  row_median <- function(m){
    apply(m, 1, median, na.rm = TRUE)
  }

  build_signed <- function(df, rec_id){
    use <- proxies_used[[rec_id]]
    mul <- dirs[[rec_id]]
    X <- sapply(use, function(p) mul[[p]] * get_num(df, p),
simplify = "matrix")
    colnames(X) <- use
    X
  }

  pooled_stats <- function(X_list){
    all_p <- sort(unique(unlist(lapply(X_list, colnames))))
    mu  <- setNames(numeric(length(all_p)), all_p)
    sdv <- setNames(numeric(length(all_p)), all_p)
    for(p in all_p){
      vals <- unlist(lapply(X_list, function(X) if(p %in%
colnames(X)) X[, p] else NULL))
      mu[p] <- mean(vals, na.rm = TRUE)
      s <- sd(vals, na.rm = TRUE)
      sdv[p] <- ifelse(is.finite(s) && s != 0, s, NA_real_)
    }
    list(mean = mu, sd = sdv)
  }

  zs <- function(X, mu, sdv){
    p <- colnames(X)
```

```
    sweep(sweep(X, 2, mu[p], "-"), 2, sdv[p], "/")
  }


  sd_from_bounds <- function(age, minv, maxv){
    mean(c(maxv - age, age - minv), na.rm = TRUE) / 1.96
  }


  mc_record <- function(df, iter, agest, age_col, min_col,
max_col, comp_col){
    itdiv <- max(1, floor(iter / 10))
    nA <- length(agest)

    valapproxmat <- matrix(NA_real_, nrow = iter, ncol = nA)
    valzmat      <- matrix(NA_real_, nrow = iter, ncol = nA)
    valscmat     <- matrix(NA_real_, nrow = iter, ncol = nA)
    valrmat      <- matrix(NA_real_, nrow = iter, ncol = nA)

    for(i in seq_len(iter)){
      age_it <- numeric(nrow(df))

      for(t in seq_len(nrow(df))){
        sds <- sd_from_bounds(df[[age_col]][t], df[[min_col]][t],
df[[max_col]][t])
        a <- rnorm(1, mean = df[[age_col]][t], sd = sds)
        age_it[t]     <-     pmax(pmin(a,     df[[max_col]][t]),
df[[min_col]][t])
      }

      ap <- approx(x = age_it, y = df[[comp_col]], xout = agest)
      valapproxmat[i, ] <- ap$y

      valzmat[i, ]   <- as.numeric(scale(ap$y, center = TRUE,
scale = TRUE))
      valscmat[i, ] <- as.numeric(scale(ap$y, center = FALSE,
scale = TRUE))

      v <- valzmat[i, ]
      rr <- rep(NA_real_, length(v))
      rr[2:length(v)]    <-    rev(log(rev(v)[2:length(v)]    /
rev(v)[1:(length(v) - 1)]))
```

```
      valrmat[i, ] <- rr

      if(i %% itdiv == 0) message("  iter ", i, "/", iter)
    }

    q <- function(m, p) apply(m, 2, quantile, probs = p, na.rm =
TRUE)

    out <- data.frame(
      agest = agest,
      val.md = apply(valapproxmat, 2, median, na.rm = TRUE),
      val.up = q(valapproxmat, 0.975),
      val.lo = q(valapproxmat, 0.025),
      z.md   = apply(valzmat,      2, median, na.rm = TRUE),
      z.up   = q(valzmat,      0.975),
      z.lo   = q(valzmat,      0.025),
      sc.md  = apply(valscmat,     2, median, na.rm = TRUE),
      sc.up  = q(valscmat,     0.975),
      sc.lo  = q(valscmat,     0.025),
      r.md   = apply(valrmat,      2, median, na.rm = TRUE),
      r.up   = q(valrmat,      0.975),
      r.lo   = q(valrmat,      0.025)
    )

    out$r.md[is.infinite(out$r.md)] <- NA_real_
    out$r.up[is.infinite(out$r.up)] <- NA_real_
    out$r.lo[is.infinite(out$r.lo)] <- NA_real_
    out
  }

  mc_region <- function(val_lo_df, val_up_df, iter, agest){
    itdiv <- max(1, floor(iter / 10))
    trend_mat   <-   matrix(NA_real_,   nrow   =   iter,   ncol   =
length(agest))

    for(i in seq_len(iter)){
      comb  <-  matrix(NA_real_,  nrow  =  length(agest),  ncol  =
ncol(val_lo_df))
      for(t in seq_along(agest)){
```

```
        for(r in seq_len(ncol(val_lo_df))){
          lo <- val_lo_df[t, r]
          up <- val_up_df[t, r]
          comb[t,  r]  <-  if(is.finite(lo)  &&  is.finite(up))
runif(1, lo, up) else NA_real_
        }
      }
      trend_mat[i, ] <- apply(comb, 1, median, na.rm = TRUE)
      if(i %% itdiv == 0) message("  region iter ", i, "/", iter)
    }

    data.frame(
      agest         = agest,
      trend_mean_md = apply(trend_mat, 2, median,  na.rm = TRUE),
      trend_mean_lo = apply(trend_mat, 2, quantile, probs = 0.025,
na.rm = TRUE),
      trend_mean_up = apply(trend_mat, 2, quantile, probs = 0.975,
na.rm = TRUE)
    )
  }

  # 1) LOAD + COMPOSITES ------------------------------------
  proxy_list <- list()
  X_list <- list()

  for(rec in records){
    rid <- rec$record_id

    proxy_df <- read_csv_stop(rec$proxy_file)
    age_df   <- read_csv_stop(rec$age_file)

    proxy_df[[age_col]] <- as.numeric(age_df[[age_col]])
    proxy_df[[min_col]] <- as.numeric(age_df[[min_col]])
    proxy_df[[max_col]] <- as.numeric(age_df[[max_col]])

    X_list[[rid]] <- build_signed(proxy_df, rid)
    proxy_list[[rid]] <- proxy_df
  }
```

```
  stats <- pooled_stats(X_list)

  for(rid in names(proxy_list)){
    Z <- zs(X_list[[rid]], stats$mean, stats$sd)
    proxy_list[[rid]][[comp_out_col]] <- row_median(Z)
    proxy_list[[rid]] <- proxy_list[[rid]] %>%
      filter(is.finite(.data[[age_col]]),
is.finite(.data[[min_col]]), is.finite(.data[[max_col]])) %>%
      filter(is.finite(.data[[comp_out_col]]))
  }

  # 2) MC PER RECORD ----------------------------------------
  site_out <- list()

  for(rid in names(proxy_list)){
    message("Record: ", rid)
    out   <-   mc_record(proxy_list[[rid]],   iter_site,   agest,
age_col, min_col, max_col, comp_out_col)
    site_out[[rid]] <- out
    if(isTRUE(write_site_csv)){
      write.csv(out,        file.path(out_dir,        paste0(rid,
"_site_mc.csv")), row.names = FALSE)
    }
  }

  # 3) REGIONAL TREND ---------------------------------------
  val_md_mat   <-   as.data.frame(lapply(site_out,   function(x)
x$val.md))
  N <- apply(val_md_mat, 1, function(x) sum(is.finite(x)))

  val_lo_mat   <-   as.data.frame(lapply(site_out,   function(x)
x$val.lo))
  val_up_mat   <-   as.data.frame(lapply(site_out,   function(x)
x$val.up))

  message("Regional combine")
  trend <- mc_region(val_lo_mat, val_up_mat, iter_region, agest)
%>% mutate(N = N)

  if(isTRUE(write_region_csv)){
```

```
    write.csv(trend,  file.path(out_dir,  "regional_trend.csv"),
row.names = FALSE)
  }
  ################################################################
##################
```

```
  ################################################################
##################
  # GENERIC RoC WORKFLOW (RRatepol)
  ################################################################
##################
  suppressPackageStartupMessages({
    library(RRatepol)
    library(dplyr)
    library(readr)
  })

  # USER INPUT ------------------------------------------------
  records <- list(
    list(
      record_id = "RECORD_1",
      proxy_file = "path/to/proxy.csv",
      age_file   = "path/to/age.csv",
      key_col    = "sample_id",
      age_col    = "age"
    )
  )

  out_dir <- "ROC_outputs"
  dir.create(out_dir, showWarnings = FALSE, recursive = TRUE)

  write_per_record_csv <- TRUE
  write_compiled_rds   <- TRUE
  compiled_rds_name    <- "ROC_compiled_records.rds"
```

```
  # SETTINGS ------------------------------------------------
  n_randomisations          <- 10000
  smooth_method             <- "m.avg"
  dissimilarity_coefficient <- "euc.sd"
  tranform_to_proportions     <- FALSE   # note: arg name is
misspelled in RRatepol
  working_units             <- "bins"
  bin_size                  <- 60
  peak_selection_method     <- "trend_non_linear"
  sigma_threshold           <- 2

  do_bin_summaries <- TRUE
  time_bin         <- 100
  group_cols       <- character(0)  # e.g. c("REGION") if present

  # HELPERS -------------------------------------------------
  read_csv_stop <- function(path){
    if(!file.exists(path)) stop("File not found: ", path)
    readr::read_csv(path, show_col_types = FALSE)
  }

  compute_bin_center <- function(age, width){
    hb <- width / 2
    floor((age - 1e-9 + hb) / width) * width
  }

  pick_col <- function(df, candidates){
    nm <- names(df)
    hit <- candidates[tolower(candidates) %in% tolower(nm)]
    if(length(hit) == 0) return(NA_character_)
    nm[match(tolower(hit[1]), tolower(nm))]
  }

  # PER-RECORD RoC ------------------------------------------
  roc_dfs <- vector("list", length(records))

  for(i in seq_along(records)){
```

```
    rec <- records[[i]]

    proxy_tbl <- read_csv_stop(rec$proxy_file)
    age_tbl   <- read_csv_stop(rec$age_file)

    proxy_tbl[[rec$key_col]]                                    <-
as.character(proxy_tbl[[rec$key_col]])
    age_tbl[[rec$key_col]]                                      <-
as.character(age_tbl[[rec$key_col]])
    age_tbl[[rec$age_col]]                                      <-
as.numeric(age_tbl[[rec$age_col]])

    roc_obj <- RRatepol::estimate_roc(
      data_source_community      = proxy_tbl,
      data_source_age                = age_tbl[, c(rec$key_col,
rec$age_col)],
      age_uncertainty            = NULL,
      smooth_method              = smooth_method,
      dissimilarity_coefficient  = dissimilarity_coefficient,
      tranform_to_proportions    = tranform_to_proportions,
      working_units              = working_units,
      bin_size                   = bin_size,
      rand                       = n_randomisations
    )

    roc_peaks <- RRatepol::detect_peak_points(
      data_source  = roc_obj,
      sel_method   = peak_selection_method,
      sd_threshold = sigma_threshold
    )

    roc_df <- as.data.frame(roc_peaks)
    roc_df$record_id <- rec$record_id

    if(isTRUE(write_per_record_csv)){
      write.csv(
        roc_df,
        file.path(out_dir,                paste0(rec$record_id,
"_roc_peaks.csv")),
```

```
        row.names = FALSE
      )
    }

    roc_dfs[[i]] <- roc_df
  }

  compiled_roc <- dplyr::bind_rows(roc_dfs)

  # nested RDS (optional) ----------------------------------
  if(isTRUE(write_compiled_rds)){
    split_list <- split(compiled_roc, compiled_roc$record_id)
    compiled_nested <- tibble(
      dataset.id = seq_along(split_list),
      record_id  = names(split_list),
      ROC_MAIN   = unname(split_list)
    )
    saveRDS(compiled_nested,                  file.path(out_dir,
compiled_rds_name))
  }

  # OPTIONAL BIN SUMMARIES ---------------------------------
  if(isTRUE(do_bin_summaries) && nrow(compiled_roc) > 0){

    age_col_out  <- pick_col(compiled_roc, c("Age","age","AGE"))
    roc_col_out  <- pick_col(compiled_roc, c("RoC","ROC","roc"))
    peak_col_out           <-            pick_col(compiled_roc,
c("Peak","PEAK","peak"))

    if(anyNA(c(age_col_out, roc_col_out, peak_col_out))){
      stop("Expected  columns  not  found  in  RoC  output  (need
Age/RoC/Peak-like columns).")
    }

    half_bin <- time_bin / 2

    Data_RoC <- compiled_roc %>%
      mutate(
```

```
        BIN          = compute_bin_center(.data[[age_col_out]],
time_bin),
        BIN_lower = BIN - half_bin,
        BIN_upper = BIN + half_bin,
        BIN_range = sprintf("%d-%d", BIN_lower, BIN_upper)
      ) %>%
      select(any_of(group_cols),  record_id,  BIN,  BIN_lower,
BIN_upper, BIN_range,
             all_of(age_col_out),          all_of(roc_col_out),
all_of(peak_col_out))


    write.csv(Data_RoC,  file.path(out_dir,  "roc_binned.csv"),
row.names = FALSE)


    group_vars  <-  c(intersect(group_cols,  names(Data_RoC)),
"BIN")


    Data_RoC_sum <- Data_RoC %>%
      group_by(across(all_of(group_vars))) %>%
      summarise(
        N_samples  = sum(is.finite(.data[[roc_col_out]])),
        ROC_mean   = mean(.data[[roc_col_out]], na.rm = TRUE),
        ROC_median = median(.data[[roc_col_out]], na.rm = TRUE),
        ROC_97.5   = quantile(.data[[roc_col_out]], 0.975, na.rm
= TRUE),
        ROC_2.5    = quantile(.data[[roc_col_out]], 0.025, na.rm
= TRUE),
        ROC_sd     = sd(.data[[roc_col_out]], na.rm = TRUE),
        .groups    = "drop"
      )


    write.csv(Data_RoC_sum,                   file.path(out_dir,
"roc_summary.csv"), row.names = FALSE)
  }
  ##################################################################
##################
```